PROJECT AHT

JAMES E. CRAWFORD
EARL G. BLACKWELL

FOREWORD

The design study reported herein was conducted under Contract AF 33(615)-3469 BPSN6(638170 62405214) to establish a detail configuration design of a set of two expandable structure experiments for use on an orbiting manned space laboratory. This work was a continuation of Contract AF 33(615)-2728. The objectives of this program were to modify and finalize the design configuration of the experiments, which has been studied under Contract AF 33(615)-2728.

The study was conducted in the period from 14 December 1965 to 14 December 1966 by Space-General Corporation in El Monte, California, under the direction of Mr. J. E. Crawford, Program Manager, and Mr. E. G. Blackwell, Project Engineer. This work was performed for the Air Force Aero Propulsion Laboratory, Research and Technology Division, Wright-Patterson Air Force Base, Ohio.

The Air Force Project Director for this contract was Mr. Fred W. Forbes (APFT) and associate project team personnel were Capt. J. N. Schofield and Lt. Anthony Zappanti.

A subcontract was issued to the General Electric Company, Valley Forge, Pennsylvania for the conduct of neutral buoyancy testing. Mr. Fred Parker was the GE Project Engineer.

Space-General Corporation wishes to acknowledge and express appreciation for the valuable assistance and consultation provided to Space-General during the conduct of this program by the subcontractor and:

- AFAPL, Research and Technology Division
  M. Adam Cormier
  Mr. Steve Shook
  Mr. Chester E. May
  Capt. John B. Catiller

- USAF, Aeromedical Research Laboratory
  Capt. Jack N. Schofield

This report was submitted by the authors, March 1967.

This technical report has been approved for publication by the Air Force Project Director.

Fred W Forbes

FRED W. FORBES
Actg Chief, Space Tech Branch
Support Technology Division

ABSTRACT

Existing launch vehicles provide a capability to orbit heavy payloads, but the payload compartment geometries are restricted in configuration and dimension. To fully exploit this payload capability, for manned or unmanned applications, dimensionally large structures that exceed the volume or geometric limitation of the payloads are required. Such structures can be obtained by deploying or erecting expandable materials in space, using systems that have been developed through Air Force contracts and private industry during the past few years. This contract centered on the application of these expandable materials in two particular types of space structures: a parabolic structure of high dimensional accuracy that could be used as an antenna, a solar collector or an illuminator; and an airlock for use on manned space laboratories. The primary objectives of this study were to define in depth space experiments using the most practical expandable structure system studied, to finalize the design configuration of these experiments, and to evaluate potential subcontractors for the candidate expandable materials systems. The requirements for integrating the airlock and parabola into an effective experiment were identified for applications to several manned space laboratories including the Saturn SIVB SSESM. The experiments were found to be fully feasible and could be undertaken without the necessity for additional exploratory or basic development effort. The airlock and parabola experiments were designed to permit full astronaut mobility and participation in the experiment, without requiring unusual or excessive activity. The full range of operational requirements were examined and the experiments were defined to be compatible with these requirements. The design studies defined an airlock and a parabola for use in those experiments, that could be achieved using existing materials, processes and equipments. A 5.5-foot diameter spherical airlock experiment was designed using an elastic memory composite structural-material system, fully meeting the packaging, deployment, and operational requirements for demonstrating this expanding material system. A prototype airlock was constructed and tested under Space-General sponsorship which experimentally demonstrated the efficiency of the SGC material selection and design approach. A 10-foot diameter, 45° rim angle parabola, constructed of precontoured modular honeycomb panels, was designed for use as a space experiment to be manually assembled by the astronaut. The technological concepts employed in this experiment design reflect structural and task characteristics for similar structures up to 100 feet in diameter. The assembly concept and task requirements were demonstrated in neutral buoyancy tests by a pressure-suited test subject. The elastic memory system design was found to be most applicable to an expandable airlock experiment for the currently planned missions. The chemically rigidized methods require further exploratory development; however, these methods offer many potential advantages for other mission applications.

CONTENTS

CONTENTS (Continued)

CONTENTS (Continued)

CONTENTS (Continued)

CONTENTS (Continued)

ILLUSTRATIONS

ILLUSTRATIONS (Continued)

ILLUSTRATIONS (Continued)

ILLUSTRATIONS (Continued)

ILLUSTRATIONS (Continued)

TABLES

SYMBOLS

A	orifice area
C_D	orifice discharge coefficient
CG	center of gravity
D_t	discharge time
E	modulus of elasticity of energy
f_{CR}	critical stress
f_T	total stress
h	enthalpy
I	area moment of inertia
L	lumens
m	projectile (meteoroid) mass
M	mass
M.S.	Marmon strap
N_{CR}	critical load
P	pressure or penetration
P_V	flow work energy
R	radius
T	temperature
U	internal energy
v	impact velocity
V	volume
Γ	gamma function for oxygen
ρp	projectile (meteoroid) density

Section 1

INTRODUCTION

The technological development of candidate material systems for such expandable structures has been pursued in the past few years on a broad front, through industry-sponsored research and under Air Force contracts. As these developments proceeded, it became apparent that a space orbiting experimental evaluation of these material systems, in terms of specific applications, was required. This task was undertaken by Space-General under Contract AF33(615)-2728 which was the predecessor contract to the contract work reported herein.

Under Contract AF33(615)-2728, candidate material systems using chemical rigidization, urethane, vinyl-acrylic, and gelatin impregnated structures were evaluated. Subcontracts were let and the test specimens that were developed were examined in laboratory tests and analytically evaluated relative to operational requirements. Also, initial preliminary design study of an experiment suitable for integration on manned space laboratories was conducted. The experiment configuration and plan evolved proposed to evaluate a 10-foot diameter parabolic solar collector and a 4-foot diameter by 8-foot-long pressure vessel on each of three manned orbiting flights. During the latter phase (Contract AF33(615)-2728) studies were initiated for the extension of the experiment to demonstrate an operational airlock and a search and tracking aid illuminator.

The present contract AF33(615)-3469, was established to define these experiments in detail, and to finalize the design of an airlock configuration. Work was required to complete the evaluation of candidate materials and to evaluate potential subcontractors for this experiments application.

The early phases of the contract effort were directed towards several manned space laboratory applications. However, as the space program evolved, it became evident that the Saturn SIVB SSESM program would be the most immediate application. Also, since the requirements were well defined, this program was used as a basis for defining the experiment in the latter portion of the contract. Consequently, data for both the MSL-type and SIVB SSESM versions of the experiment are presented in this report.

Section 2

SUMMARY

2.1 PROGRAM SCOPE

The primary objectives of this contract were to define in depth the experiment identified in the preceding contract, to integrate and finalize the design configuration of these experiments into one which would evaluate the expandable structure technology for application to airlocks, and to evaluate potential subcontractors for the fabrication of the candidate expandable materials systems. These experiments, which consist of a cylindrical airlock 4 feet in diameter by 7 feet long, and a 10-foot diameter parabola, are proposed to be flown on a manned space laboratory, for deployment and testing by an astronaut. The experiment package is to be a high density, low-weight design which, subsequently, can be deployed and erected in space.

The study was initiated for integration into a specific manned space laboratory vehicle, but approximately mid way through the program the project was reoriented to the Saturn SIVB SSESM as it became apparent that this system would offer first opportunity to evaluate these experiments in space. In the course of these efforts, it was found that the application of these experiments to an MSL, or the Saturn SIV SSESM, have the same basic requirements. The work performed early in the contract on the MSL application, and the later work on the SSESM, were generally mutually applicable; therefore, each section of this report discusses the experiment characteristics that are unique to each application.

These design studies concluded that the basic experiment concepts are feasible and are within the present state-of-the art. An airlock constructed of expandable materials can be achieved from existing materials and processes.

No technological break through is needed, and the restraints of the space operation, mission requirements, and astronaut interface can be achieved in a straightforward manner. Furthermore, the feasibility of constructing an airlock using elastic memory composite was demonstrated in a prototype unit in a parallel Space-General sponsored effort.

A lightweight, large, antenna or solar collector modular structure of high contour accuracy and up to 100 feet diameter can be manually assembled in space by an astronaut. This structural system concept was demonstrated in neutral buoyancy tests by a 10-foot diameter mock-up, which showed that the astronaut can be highly effective, and that the tasks required are simple and easily accomplished.

Parallel experiment definition studies indicated the feasibility of orbital tests of an airlock and parabola on either an MSL-type vehicle or the Saturn SIV SSESM, are within the known and predictable physical and operational environmental limitations.

2.2 SELECTION AND EVALUATION OF MATERIALS

Various candidate material systems have been selected and laboratory evaluations have been conducted on these candidate chemically rigidized systems. The emphasis in this contract was placed on selecting specific design solutions for the expandable material system selected in support of the design studies. Limited laboratory tests were made on adhesives to provide sufficient data to verify the design choice and to permit the development of a finalized configuration of the airlock experiment. Additional laboratory evaluations were made on chemically rigidized specimens to conclude the work conducted in the preceding contract. These samples were improved versions, and served to support the contract requirements of evaluating the industrial capability to successfully develop expandable structural material systems.

The candidate material systems considered in this contract are summarized below:

a. Chemically Rigidized Systems - These systems are based on the pre impregnation of a flexible material composite by a chemical resin formulation which, upon deployment in space, can subsequently be rigidized to form a serviceable structure with mechanical and geometric integrity.

(1) The three primary approaches are as follows:

(a) An urethane resin impregnated fluted core or drop-thread fabric systems, which is rigidized upon deployment by the circulation of a water vapor catalyst through the structural composite.

(b) A gelatin impregnated fluted core or drop-fabric system which becomes rigid upon subsequeny exposure to the space vacuum through the evaporation of a water-solvent flexibilizing medium.

(c) A vinyl-acrylic resin impregnated polyurethane-foam structural composite which, on thermal/catalytic command, initiates a sustaining exothermic rigidizing reaction.

b. Elastic Memory System - Expanded foam is used to provide the capability to package the structure which subsequently can be deployed in space into the preselected configuration. Structural integrity is achieved by incorporating the foam into a composite of appropriate layers of load carrying fabrics, non permeable liners, coatings, and adhesives.

c. Modular Construction - Precontoured panels of aluminum honeycomb are employed which can be assembled into the desired structure, through simple interconnecting joints.

The work done to evaluate each of these systems, and the selected approach for the airlock and parabolic structures is reviewed in the sections below.

2.2.1 CHEMICAL SYSTEMS

A parabolic test specimen of acrylic impregnated polyester foam, provided by National Cash Register Company, was tested in vacuum deployment and rigidization test. The cure and general contour of the surface were good, but the specular surface exhibited "orange-peel" effects with radial wrinkles. The resin used for impregnation was too fluid and tended to settle to yield a nonuniform distribution.

Two specimens were supplied by Geophysics Corporation of America, Viron Division of a gelatin impregnated nylon cylinder and a drop-thread fabric parabola. The cylinder incorporated an internal thin mylar bladder. The cylinder showed good internal geometry when inflated and rigidized, but the flutes were only about 50% deployed. The gelatin failed to wet the fabric totally, and tended to flake off where surplus gelatin accumulated. Distribution of the gelatin was uneven. The parabola showed several large wrinkles and 75% of the surface showed an orange-peel effect.

Two samples, a fluted core cylinder and a drop-thread disc supplied by Goodyear Aircraft Company employing urethane vapor set resin impregnation were tested during the final phase of the prior contract, and are reviewed here for reference. The disc showed fair resin distribution, but the surface did not exhibit characteristics desirous of a parabolic structure in that it was not totally flat, showed waviness and no attempt was made to provide a specular surface so that anti markoff layers could be evaluated. Resin distribution in the cylinder was not uniform, and the ports for the water-vapor catalyst became blocked during the rigidization tests.

Based on the laboratory and design evaluation, additional development is needed on chemically rigidized structures to achieve good, expandable parabolic structures for use as mirrors or solar collectors. Pressure vessel-type structures, such as an airlock can be developed using gelatin, vinyl or

urethane materials. Gelatin rigidized fabric will cure slowly, but reliably (fail-safe), and produce moderate strengths. Vinyl impregnated urethane foam and fabric will cure rapidly and reliably (fail-safe), and produce low strength structures. Urethane impregnated fabric structures are not cure fail-safe, but will achieve satisfactory reliability with high strength and moderate cure-times - if further development is accomplished. In general, the chemical systems require additional development before an experiment can be undertaken with a high degree of certainty and on a short development schedule.

A critique of industrial capability was provided to the Air Force under separate cover early in the contract.

2.2.2 ELASTIC MEMORY SYSTEMS

Polyurethane foam was selected as the best elastic memory material for a deployment mechanism for use in the airlock in previous contracts. It was not considered for the parabola because no developmental effort has considered this application. The material study effort in this contract considered the selection of each component of the composite structure from the array of commercially available materials.

The functional criteria applied in the evaluation were as follows:

a. Flexible material composite shall exhibit structural integrity as a pressure vessel and shall operate at 3.5 psig with a safety factor of five with 100% oxygen atmosphere.

b. The structural system shall be adaptable to high density folding and packaging for transportation into near earth orbit, whereupon it must deploy to its intended configuration and function in the space environment.

c. The deployed airlock structure shall maintain pressure at a leakage rate of less than 1/2 lb of oxygen per day for 30 days.

d. The flexible composite wall shall provide micrometeoroid protection to the extent that no penetration shall occur within a 0.9999 probability factor to the standard NASA micrometeoroid environment.

e. The materials and adhesive systems shall tolerate the temperatures and radiation of a 200 nmi orbit, and be capable of exhibiting a thermal control against solar radiation.

f. The materials shall in no way endanger an astronaut through toxic outgassing or fragmentation.

g. The deployed Elastic Recovery airlock shall exhibit a maximum of geometric integrity to astronaut loads in the unpressurized condition within the limitations set forth above.

h. The materials design selected must lend itself to ease of fabrication within the state-of-the-art techniques.

The selected construction consists of the following five basic layers:

a. Outer micrometeoroid bumper fabric - (17 oz/yd^2) Dacron cloth

b. Elastic Recovery and Micrometeoroid barrier - 1.75-inch thick polyurethane foam 1.2 lb/ft^3 density

c. Structural Load Carrying Fabric - (7.84 oz/yd Dacron cloth)

d. Permeability Barrier - 2-layers of 1 mil thick Tedlar Film

e. Inner Scuff Layer - (2.02 oz/yd nylon)

Figure 2-1 illustrates the typical material composite cross section in which the various layers are identified.

Each element of the composite and the basis for selection are described below:

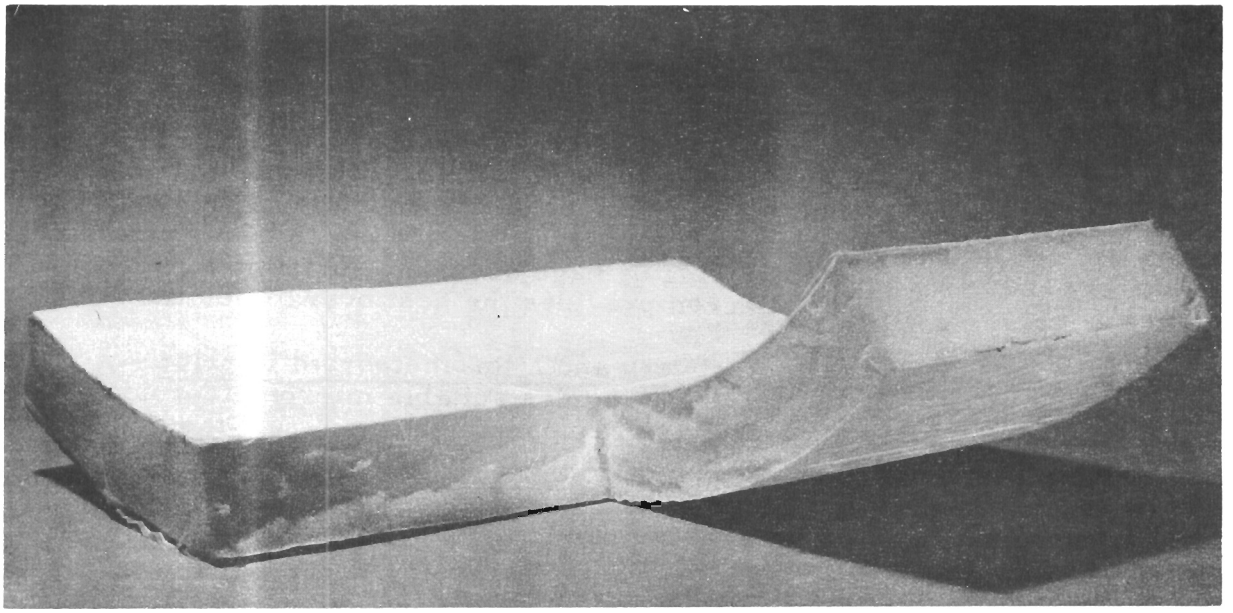

965/041

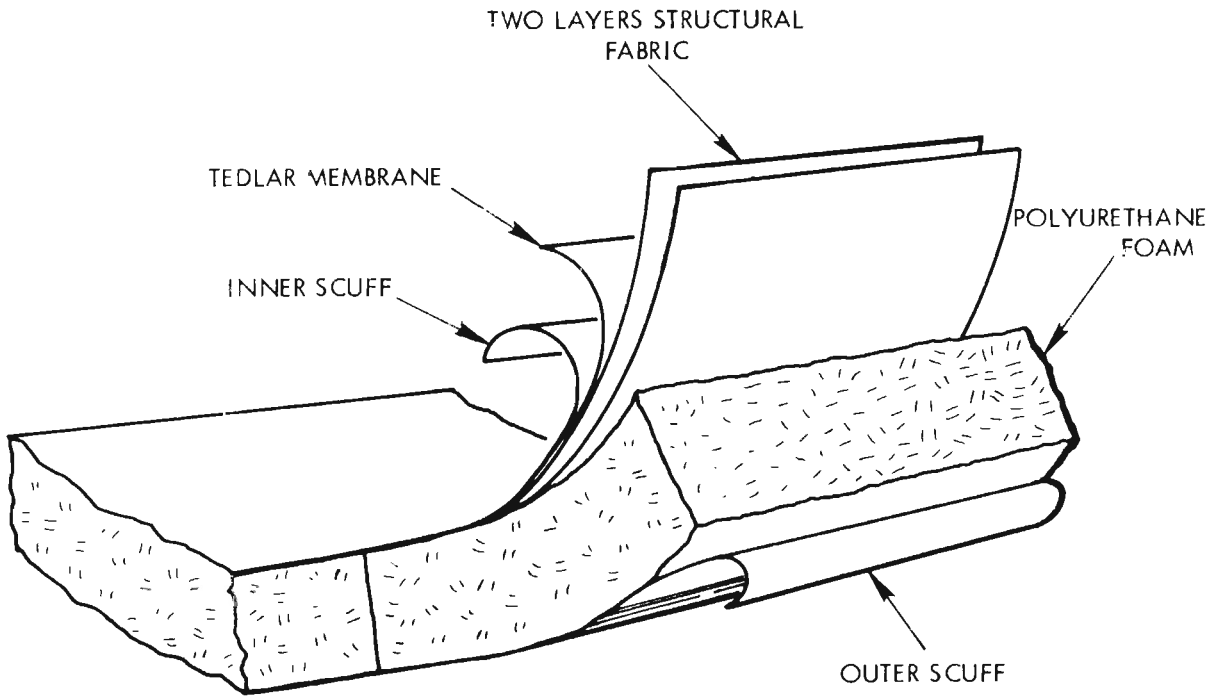

Figure 2-1. Airlock Expandable Wall Cross Section

a. Outer Micrometeroid Bumper - Fiberglass, nylon, Nomex, and Dacron were considered. Nylon does not exhibit the environmental stability shown by the others. Fiberglass possesses some desireable properties, i.e., high strength to weight rates, good compatibility with the environment, high modulus and can be bonded adequately. However, when the required high packaging density is achieved with folding, fiber crimping damage occurs. Nomex is difficult to bond. Dacron provides the best overall solution.

b. Elastic Recovery and Micrometeoroid Barrier - A density of 1.2 lb/cu ft provides suitable micrometeoroid protection, is adequately self-supporting, can accept the astronaut imposed loads, and exhibits the desired packaging characteristics and satisfactory recovery properties. Higher density foams increase weight and make packaging difficult: lower density foams provides inadequate micrometeoroid protection, poor self-supporting characteristics, and low recovery properties.

c. Structural Fabric - Fiberglass, Dacron, and nylon were considered. Dacron was selected as it provided the best overall structural characteristics, resistance to folding and environmental stability.

d. Permeability Barrier - Tedlar was chosen over Mylar and Capran as Capran loses flexibility after long exposure to vacuum and Mylar is difficult to bond, and has too high a modulus for good load transmitted to the structural fabric. Two layers were selected to preclude the possibility of pin hole leaks.

e. Inner Scuff Layer - Nylon was chosen because it has good chemical stability, low modulus, exhibits good toughness and can be fabricated easily.

A modified urethane adhesive was selected from test data. 100% join efficiencies were achieved in the structural fabric joints, flexibility was good and high lap joint strengths of 400 lb/sq in. were demonstrated.

Space-General, in addition to this contract effort, sponsored a company funded program in which an airlock structure was fabricated and tested using a similar elastic recovery material composite.

Photographs of this airlock appear in Figure 2-2. The photo in the upper left depicts the 3 ft diameter by 7 ft long structure completely retracted into its packaged condition. The lower right photo illustrates the airlock fully deployed. This structure was tested at a proof pressure 5.5 psig for a number of cycles and performed as desired. This company-sponsored effort demonstrated the basic material composite used in this experiment design. Considerable knowledge was also gained on the behavioral characteristics of this Elastic Recovery material composite in the packaging and deployment test which were performed.

2.2.3 RIGID MODULAR PANELS

Precontoured panels of aluminum honeycomb sandwich are utilized in the design of the modular parabola. A 1/8 inch Hexel core of 0.7 mil aluminum is covered with two 4 mil aluminum face skins. FM-1000 is used for the adhesive to bond these materials together. The total composite thickness is about .3 in. and gross panel weight of .36 lb per sq ft is obtained which includes all interconnecting joints and potting compound.

2.3 AIRLOCK DESIGN STUDIES

Specific experiment integration data was unavailable, therefore several key assumptions were necessarily made regarding vehicle/experiment interfaces. The major assumptions were: (1) the experiment would be mounted integral to the vehicle surface, flush and covered by pyrotechnically removable fairings, (2) the experiment location on the vehicle would be aft of the pressurized compartment and forward of the trans-stage interface, (3) this experiment would then be deployed on an extendible boom beyond the vehicle's surface, and in sequence the canister released and the structure deployed and, if chemical, rigidized. (This type of experiment integration, it was assumed, would depend on a fairly extensive remote deployment control console and attendant instrumentation and data acquisition provisions.)

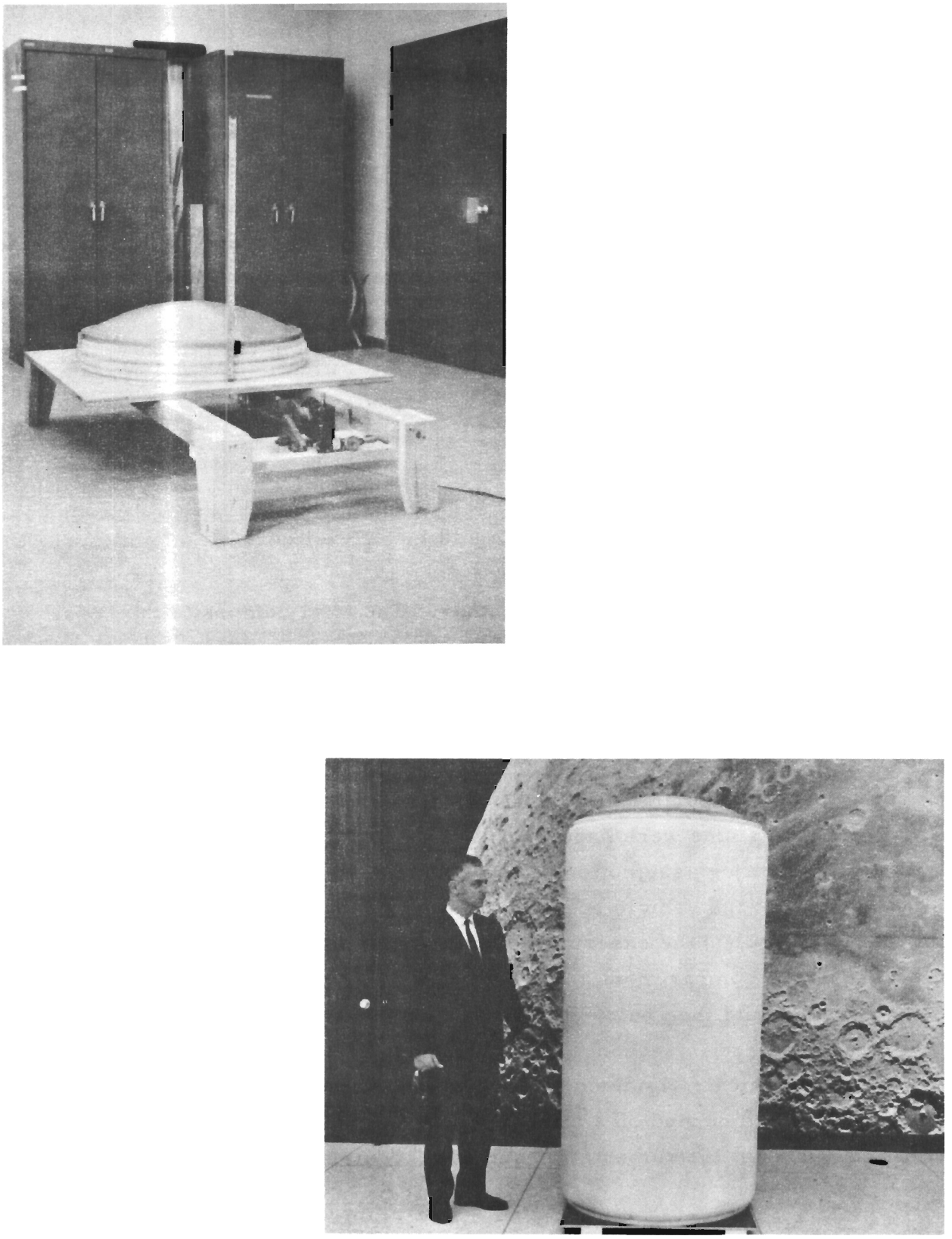

Figure 2-2. Airlock Configuration Funded by Space-General Corporation

(4) After the airlock structure deployment and testing, means were to be provided to detach the experiment from the deployment boom so that transference to an existing EVA vehicle hatch could be accomplished by the astronaut, and render the experiment into operational status for further evaluation.

As the program progressed, it became known that the first vehicle on which the Air Force may fly these expandable structures experiments would be the Saturn SIVB workshop. Consequently, the experiment design was oriented toward this specific vehicle requirement in order that the results of this work would be more pertinent to the requirements of the Air Force.

During the program, Human Factor Studies indicated that the original 4-foot diameter by 7-foot-long cylindrical airlock configuration would not allow the astronaut to turn around to reach hatches at the opposite ends. Therefore, a spherical configuration was evolved to meet the anthroprometric restraints of the astronaut, and incorporated into the SIVB experiment configuration design.

Each of these experiments for both vehicle types are described separately. However, the specific design areas discuss them concurrently because of the mutual requirements of both configurations.

2.3.1 SUMMATION OF EXPERIMENT REQUIREMENTS

The requirements of the expandable airlock experiment were to demonstrate an expandable materials technology for an application to a typical space structure, and to illustrate the practicality of an airlock design configuration for use on future manned vehicles as an operational system.

To fully demonstrate the capabilities and performance of an expandable material system for space applications, this experimental structure must exhibit a low weight, high packaging density, compatibility with the space environment, and the configurations must exhibit operational characteristics suitable for pressure-suited astronauts in zero gravity.

2.3.2 HUMAN FACTORS ANALYSIS FOR AN AIRLOCK

A Human Factors analysis was conducted as part of this study program, to define the man-machine relationships between the astronaut and the experiment hardware and insure that the experiment design and procedures represented a high level of safety and maximum utilization of man's presence. Interfaces between the astronaut and the experiment control provisions were analyzed from a functional system point of view. An example of the considerations used may be seen in Figure 2-3. Here the astronaut is integrated into the control system functional diagram, and is considered as a decision making element in the data feedback loop. Task and task time analysis were made to ascertain the detail manner and extent to which the astronaut would be involved in the experimental procedure. Considerable attention was given to the experiment design to insure that all activities were within the capabilities and anthroprometric restraints imposed on a pressure-suited astronaut in zero gravity.

This is reflected in geometric modifications introduced into the original 4-foot diameter x 7-foot-long airlock configuration. Subsequent analysis indicated that the pressure-suited astronaut would not be able to execute a turn-around maneuver which was required to gain access to the hatch and pressurization controls at opposite ends of the cylindrical structure. It was determined that a 5.5-foot spherical airlock would permit the astronaut to turn around and have access to either end of the airlock structure. This particular configuration established the baseline for the SIVB airlock experiment design presented herein.

2.3.3 MSL EXPERIMENT CONFIGURATION DESCRIPTION

The MSL airlock experiment configuration consists of a 40-inch diameter x 12-inch high canister package containing a 4-foot diameter by 7-foot-long cylindrical airlock with hemispherical end domes, into which a 34-inch diameter hatch was integrated. This hatch was included on the outer end of the tubular structure, the inboard end being used to attach the airlock experiment to the extendable boom, and later to an EVA hatch interface. A pressurization

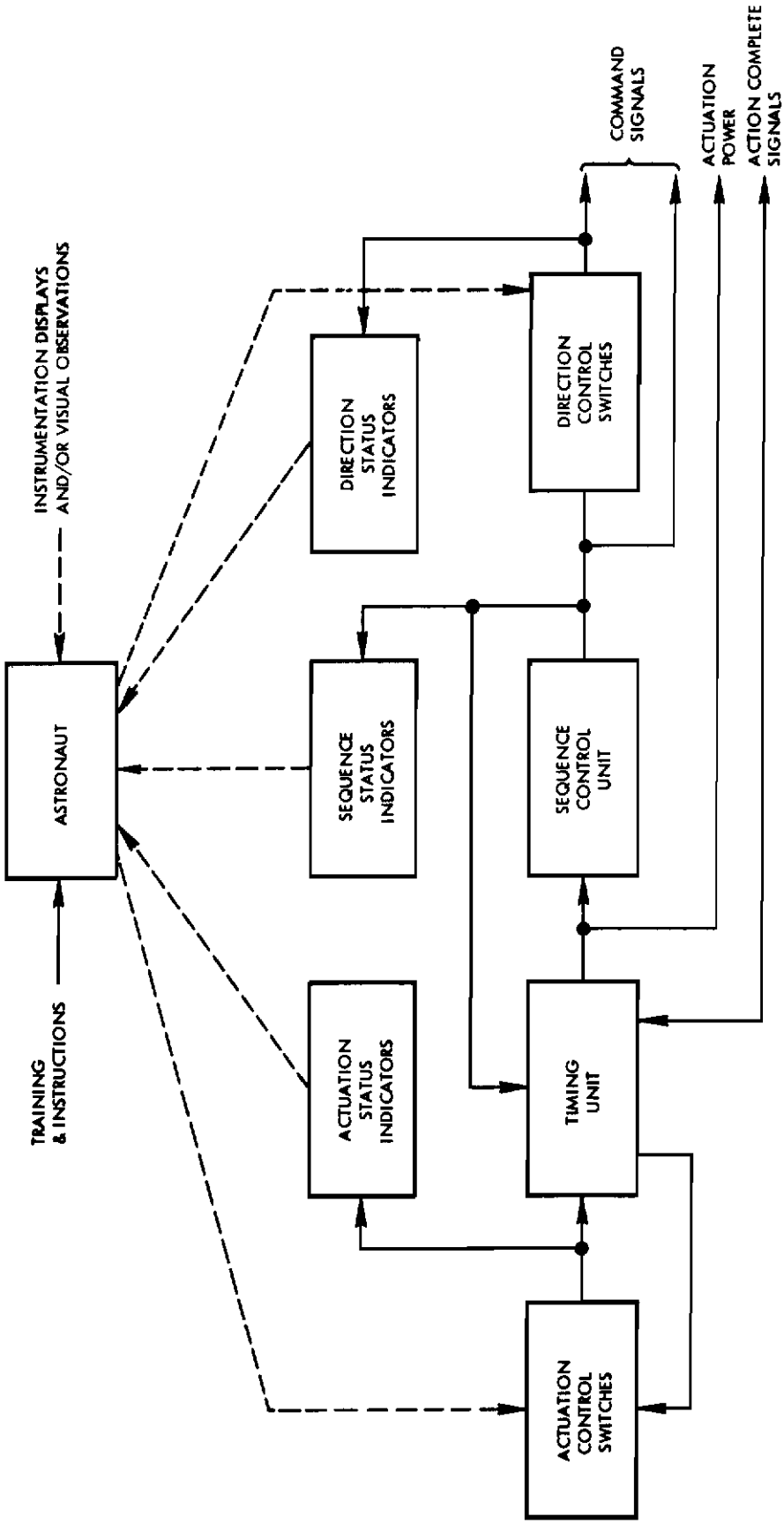

Figure 2-3. Man-Control Loop Considerations in Console Design Layout

system was to be mounted internal to the unpressurized section of the vehicle and connected to the experiment canister through a flexible umbilical. This pressurization system is controlled from the remote deployment console, and consists of a single high pressure bottle provided with suitable pressure regulator valves and instrumentation. The general preliminary MSL experiment configuration is seen in Figure 2-4.

An inward opening hatch is featured as determined by design trade-offs, and in this early design, was guided by foldable metal hinges to its internal stowage location. Labor considerations of design simplicity and Human Factor requirements led to a simple tethered means of securing the hatch vehicle open. A velcro pad is used on the outer hatch surface to effect stowage to the inner airlock wall when ingressing or egressing.

In the MSL experiment design, consideration was given to possible low orbits of 160 nautical miles, in which case considerable aerodynamic drag is encountered for any additional vehicle protruberances. In order to conserve orbit-keeping fuel, a retraction mechanism was designed for the elastic recovery airlock, which consisted of a driven hoop-type sheave about the lower end (vehicle attach end) of the structure. The airlock could then be retracted by energizing a small DC motor which drives the sheave and accumulated four retraction cables attached to the upper rigid hatch ring. This arrangement is also seen in Figure 2-4.

2.3.4 SIVB AIRLOCK EXPERIMENT CONFIGURATION

The experiment configuration for the Saturn SIVB is basically directly applicable to the MSL vehicle requirements described earlier. The major physical difference being in the spherical airlock geometry used for the SIVB rather than the cylindrical geometry, which human factor analyses had indicated as inappropriate.

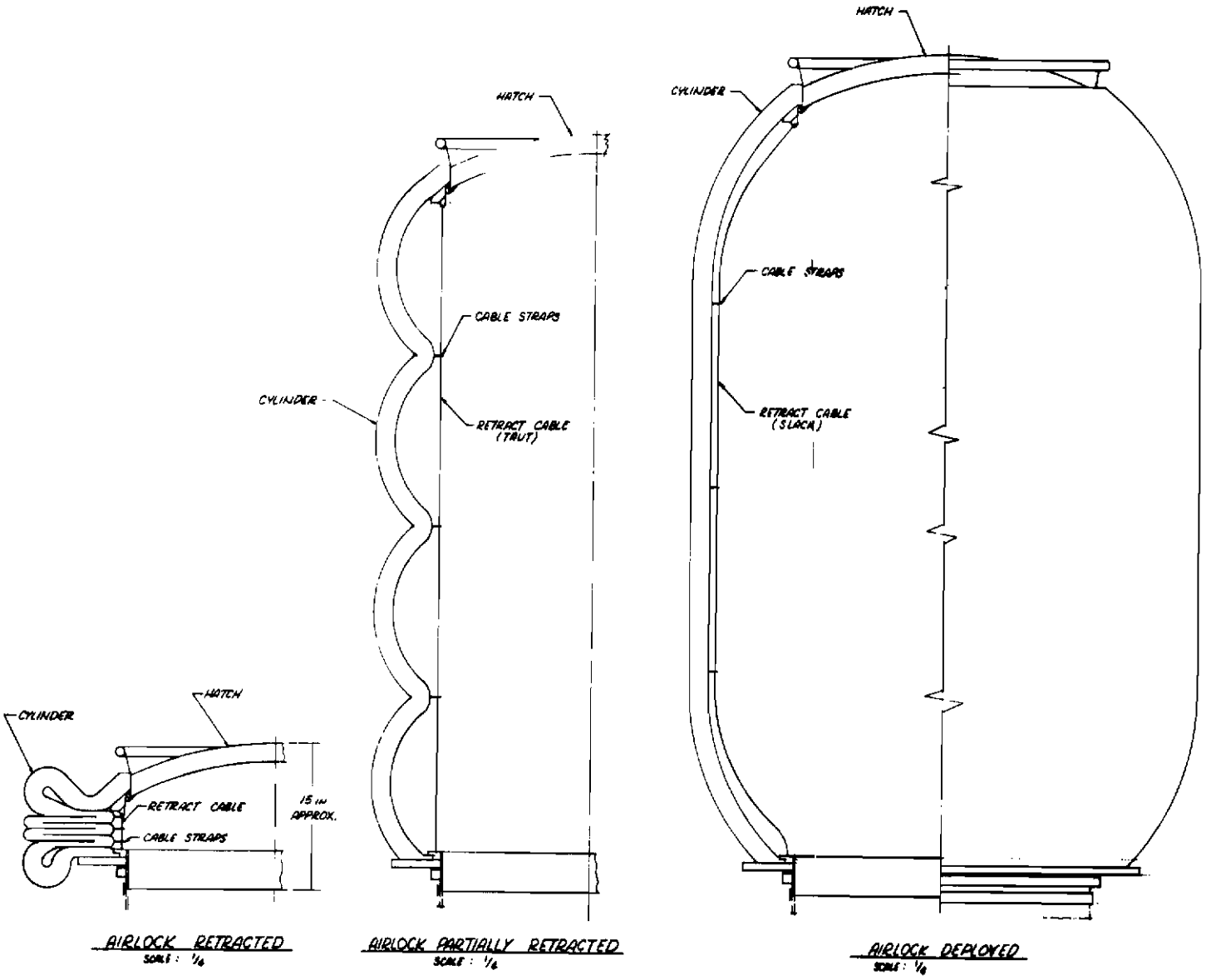

Part of Figure 2-4

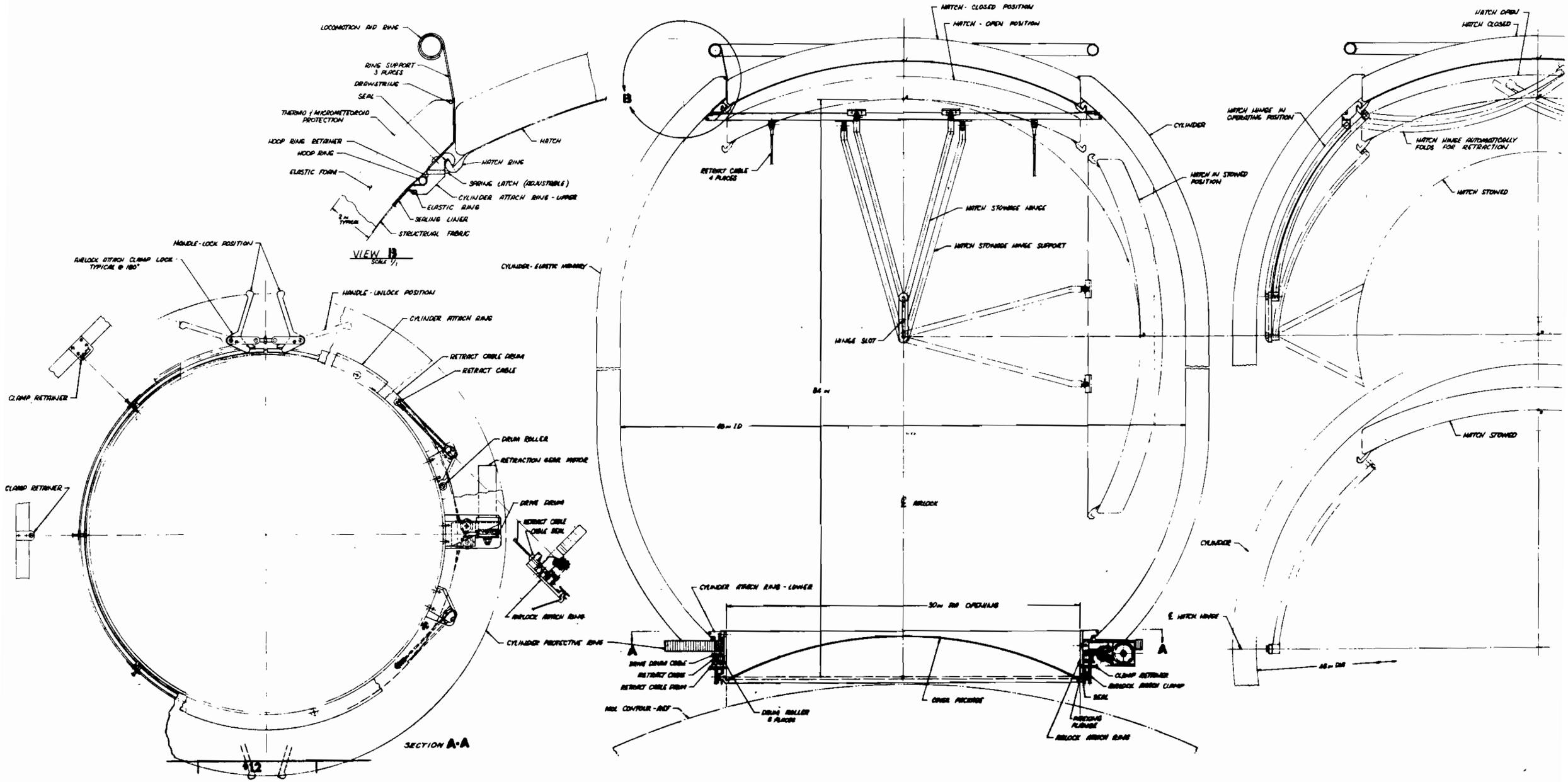

Figure 2-4 Preliminary Configuration of the Elastic Memory Airlock

For the Saturn SIVB the experiment package integrates the elastic recovery airlock canister, the pressurization system and the vehicle attachment interface into one unit. A separate remote control console is provided for the initial deployment and test phases. Figure 2-5 shows this airlock configuration.

An inward opening hatch is used with hatch latches accessible from both internal and external to the airlock. The pressurization system in the rigid base structure can be controlled from within the airlock or from the remote control console. Sufficient gas is provided for one 5.5 psig proof pressure cycle and four 3.5 psig operational pressure cycles. The operational cycles are regulated by a pressure sensor feed back system.

An emergency release device is provided at the lower airlock closure which doubles as a disconnect interface for attachment to an EVA hatch if desired. A retraction system is featured in the rigid base structure to retract the elastic recovery airlock structure once it has been deployed.

2.3.5 SUBSYSTEM DESCRIPTION

2.3.5.1 HATCH AND RING DESIGN

The hatch and fabric termination ring assembly merited considerable design attention, as the flexible structural fabric behaved in membrane tension and rigid termination ring constituted a structural perturbation which, if not carefully designed, would not react the required loads with a minimum weight metal part. Also, the hatch, the dome of which is designed of thin spun aluminum must undergo a slight buckling load until the mechanical deflection due to pressure can compress the "o" ring seal, then "bottom out" to engage the hook in the hatch ring and finally "load up" the dome in membrane tension. A hatch and hatch ring design is presented which represents a considerable improvement from a weight and structural efficiency stand over earlier designs. As the hatch design selected is inward opening, heavy latching mechanisms are avoided, however, the requirement still exists to

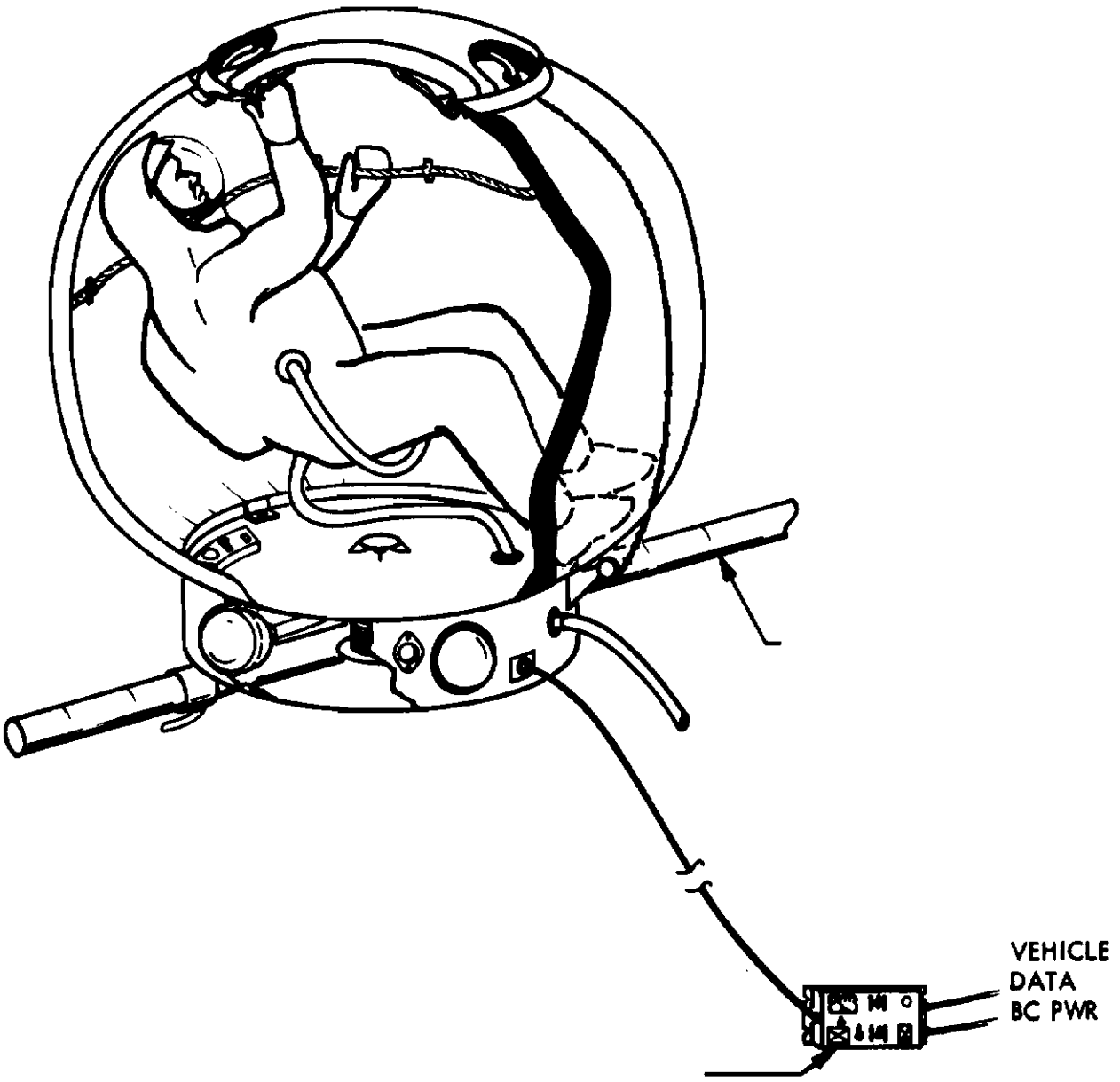

Figure 2-5. Airlock Experiment Package Configuration

secure the hatch in a closed position to initiate a seal in the pressurization phase, and to avoid inadvertent dislodgement of the hatch when the airlock is unpressurized. Two hatch latch mechanisms are provided in the lightweight dome. These latches feature large handles commensurate with the Human Factor requirement of a gloved, pressure suited astronaut. The hatch locking mechanism is accessible both internal and external to the airlock. The forces to open and close the hatch have been kept to a minimum and locomotion aids internally provide means of reacting these forces.

2.3.5.2 CANISTER AND PACKAGING CONFIGURATIONS

Various canister configurations have been studied for the airlock packaging during storage and launch. The requirements reflected in the preliminary MSL vehicle experiment canister configuration were an attempt to serve a dual function, in that either a chemically rigidized or Elastic Recovery airlock material system would interface efficiently with the rigid metal portions of the experiment hardware. For the chemically rigidized systems, a sealed canister is required, while for the elastic recovery material system sealing is not a requirement. However, one canister configuration was studied which represented a minimum package diameter specifically for an elastic recovery airlock. The minimum package diameter is determined by the largest rigid fabric ring used in terminating the flexible material at the hatch diameter of 34 inches. It should be noted that the MSL experiment configuration considered the pressurization system as a separate package and not integral with the canister package.

2.3.5.3 PRESSURIZATION SYSTEM DESIGN

The pressurization system requirements for a MSL vehicle are not specific as to configuration or quantity of gas required, therefore the basic requirements were assumed. However, in the latter portions of this

program a specific vehicle requirement was established in the Saturn SIVB. This vehicle required that the pressurization system be an integral part of the airlock canister and provide five pressurization cycles. A pressurization system design is presented which meets the requirements for such a vehicle. In order to integrate the pressure source into a minimal envelope beneath the airlock package, a number of separate steel bottles (5) were manifolded together to provide an initial deployment and proof pressure cycle at 5.5 psig, and 4 cycles at 3.5 psig, operating pressure.

A design approach was taken which isolated the 5 bottles into three groups by using burst diaphragm type valves and all welded fittings up to these valves. The object being to provide independently sealed groups of pressure sources which may be used at widely separated intervals. For example, all three subsources have high integrity seals for a long-term ground storage. The first requirement for pressure will be a combination deployment and proof cycle. The next pressure cycle may be 15 days later after the initial leak test. Conventional solenoid actuated valves would be likely to leak during this period. A final operational pressure check will be desired perhaps six months later on a revisitation by a rendezvousing Apollo vehicle.

This system features a direct blow-down from a 3000 psig bottle through a restrictor into the airlock structure for the deployment and proof pressure. For this pressure cycle, close control on the final airlock pressure of 5.5 psig is not required. The second group (three bottles) are used for the operational evaluation by the astronaut who will ingress and egress into and out of the airlock. For this pressurization sequence a closer control of airlock pressure is required in the interest of safety because of the astronaut's presence. A pressure switch feedback is sent to a control solenoid to interrupt the gas flow when the prescribed pressure is reached. Sufficient gas supply is provided for four such pressurization cycles. The lost gas reservoir is again an indirectly regulated blow-down design for the final pressurization test upon revisitation. A diagram of this system is seen in Figure 2-6.

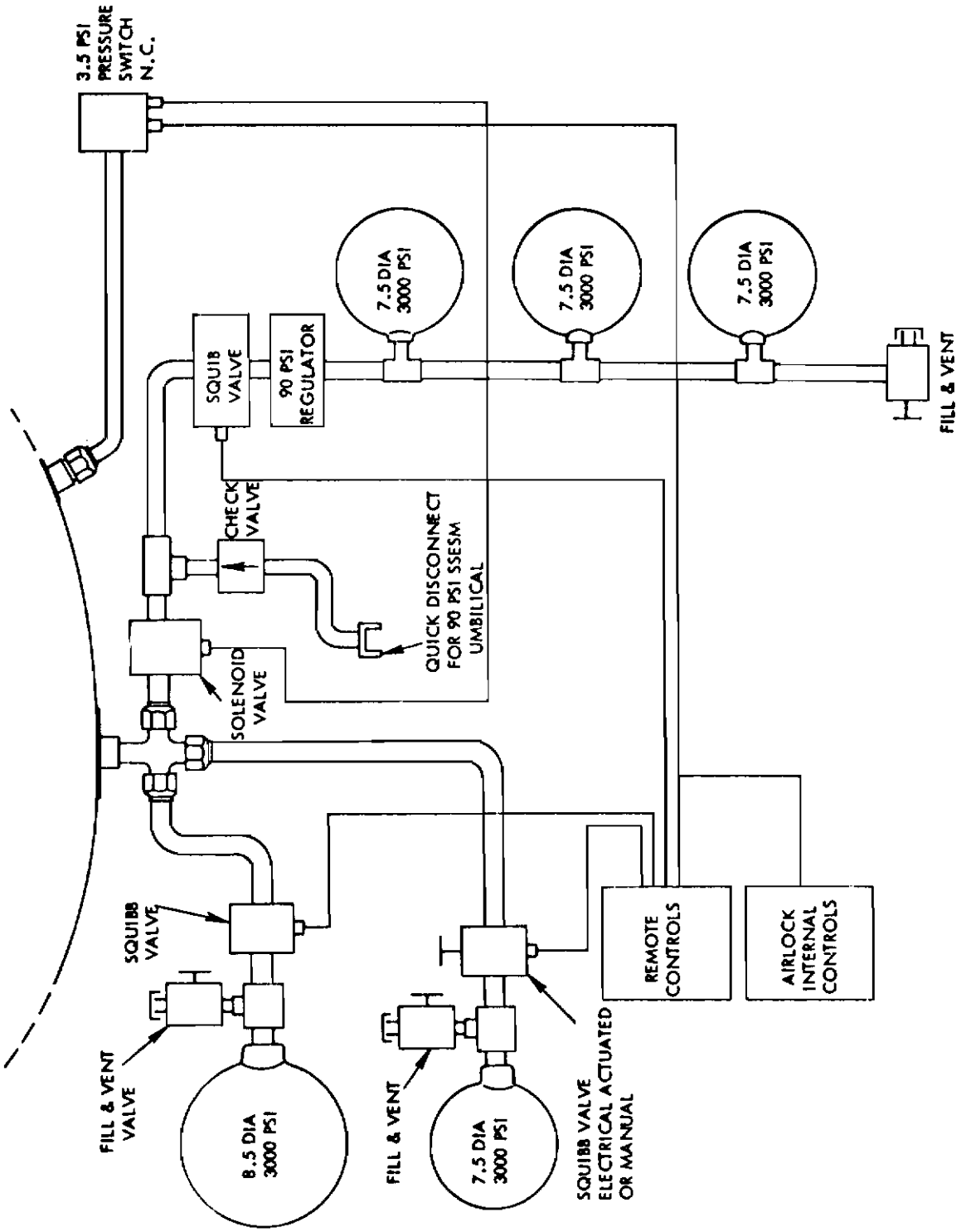

Figure 2-6. Pressurization System

This pressurization system is controlled from two locations; from a remote deployment control console and from the inside of the experimental airlock structure. A manual release valve is featured on the final pressure bottle in the event electrical power is not available upon revisitation. This pressure system weighs approximately 25 pounds.

2.3.5.4 INSTRUMENTATION AND CONTROLS

The instrumentation and controls system for the complete remote deployment and evaluation of an expandable structures experiment on a manned space laboratory was studied in detail on this program. To make maximum use of the presence of man, the experiment control system should provide means by which the astronaut may optimize the experiment procedure if unforeseen developments occur. On this program extensive studies were conducted on the design requirements for a meaningful control system which makes maximum use of man's decision making ability. The control system design incorporates sufficient data or condition feedback to the operator to allow him to control the experiment sequence with a maximum of safety and understanding.

The remote deployment control console for the MSL experiment will be operated in conjunction with an instrumentation control console from within the pressurized vehicle compartment. A signal conditioning and data scanning system is presented which features automatic sequential scanning of the data sensors or a manual step scan with a digital readout in engineering units on the Instrumentation Control Console. This will allow the astronaut the means to monitor any critical instrumented parameter, during the experiment procedure.

Instrumentation sensors and installation techniques were selected for pressure, temperature, and strain on the structural material system. Strain is one of the more difficult parameters to measure on a flexible, low

modules system, as gage attachment is difficult to provide meaningful data. A strain gage installation technique is discussed using post-yield type gages, but should be evaluated in laboratory tests to determine its actual practicality. Nickel resistance thermal sensors were selected to provide temperature profiles of the structure because of their high signal outputs and mechanical flexibility. All sensors selected for this experiment employ transduction principles which can use a common DC excitation. The output of the instrumentation system will interface with standard vehicle telemetry and is designed to utilize 28-Vdc unregulated power.

The control requirements for the Saturn SIVB are considerably simpler than those for an MSL type vehicle, as the deployment sequence does not require the release of aerodynamic fairings and extendible boom controls. The instrumentation required is also minimal and signal conditioning and recording are supplied by the SSESM. Controls for the manually assembled modular parabola, which is discussed later, are also simplified for the same reasons. Only a simple control box integral with the work station is required for the convenience of the astronaut in maneuvering the boom and hub position during the assembly task.

2.4 MODULAR PARABOLA DESIGN

The concept utilized in the design of the manually assembled modular parabola is that large precision parabolic surfaces can best be deployed in space by a man using a multiplicity of precontoured lightweight panels, affixed with simple interconnecting joints. The objective of this experiment is to demonstrate that an astronaut, when suitably restrained, can assemble accurate parabolic antennas up to 100 feet in diameter. The design of this experiment employs scalable assembly concepts by using an experimental structure of only 10 feet in diameter.

The requirements of the experiment demands a design exhibiting high packing density, low weight, and minimum overall stowed dimensions. In addition, the design must lend itself to the assembly by a pressure-suited astronaut requiring a minimum of tools, minimum of pieces to handle, involve only the simplest of assembly tasks, require only very low forces to engage the modular components, and yet be capable of exhibiting a high contour accuracy once assembled.

2.4.1 HUMAN FACTORS CONSIDERATIONS FOR THE MODULAR PARABOLA

The Human Factors considerations employed with the manually assembled modular parabola experiment were involved at the inception of the technological concept. Early in this program the problem of achieving large precision parabolic surfaces in space was analyzed from an astronaut capability standpoint, and it was determined that man could play a significant part in the deployment of expandable precision space structures. Man could assemble, adjust, repair, and correct procedures in the deployment or erection of large antennas or solar collectors, if (1) proper use was made of his presence, and (2) the hardware and deployment procedure were designed around his capabilities and limitations in the space environment.

With this goal in mind, a concept was evolved which used precision precontoured parabolic panels of lightweight aluminum honeycomb. A simple panel interconnecting joint was designed after considerable study, which met all of the criteria of the structural, mechanical, and precision requirements and was well within the astronaut's capacity of visual activity, tactility and ability to react forces.

In a subcontract to General Electric Co., Valley Forge, a full-scale neutral buoyancy mock-up of the SGC 10-foot diameter parabola design was fabricated and tested with a test subject in a Mark-4 pressure suit. A simple work station restraining device was employed and the assembly concept used,

was to keep the astronaut stationary and move the work to him. Figure 2-7 is a photograph of the neutral buoyancy test set up with the test engineer in the latter phase of the assembly task. Approximately 11 minutes were required to assemble the 10-foot parabola from 24 contoured modules. A task time analysis is presented in Section 5.3 of this report.

2.4.2 DESIGN CONCEPT

The design approach used employs 24 precurved aluminum honeycomb panels which are assembled onto a central hub into two concentric annular tiers to obtain the 10-foot diameter structure. Although the approximate size of the panels used is only 30 inches in length by 24 inches wide, panels up to 6 feet long can be used for larger structures. It obviously would have been simpler to obtain this 10-foot diameter structure with fewer panels of greater length, but scalability would not have been as well demonstrated.

A detailed configuration design was made of the aluminum honeycomb panels and manufacturing bids were sought from several local companies. The responses were good and no significant problem areas appear to be involved, as all processes appear to be within the state-of-the-art. A drawing of the panels and interconnecting joints appears in Figure 2-8. In principal, the panel joints are made of precision tapered tongue and groove members. The successive engagement of these joint pairs progressively aligns the panels until they are fully seated. At this point, a simple spring clip on the back surface of the female joint snaps into a slot provided on the male joint. The purpose of this action is to secure the panel in position, preventing it from drifting away in the weightlessness of space orbits. The amount of force required to engage this latch is only one or two pounds, which is easily reacted by the astronaut's work station.

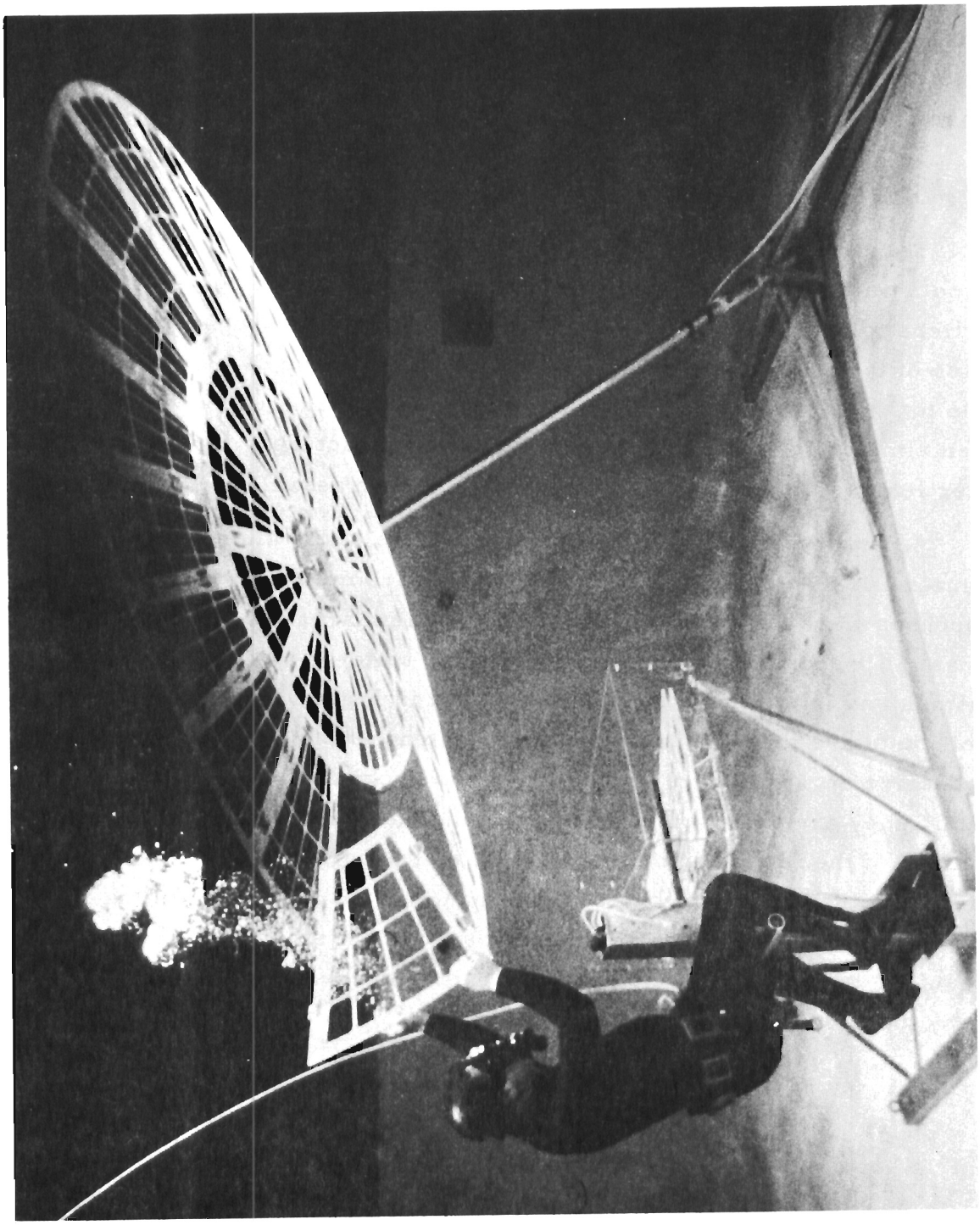

Figure 2-7. Near Completion of Outer Annulus

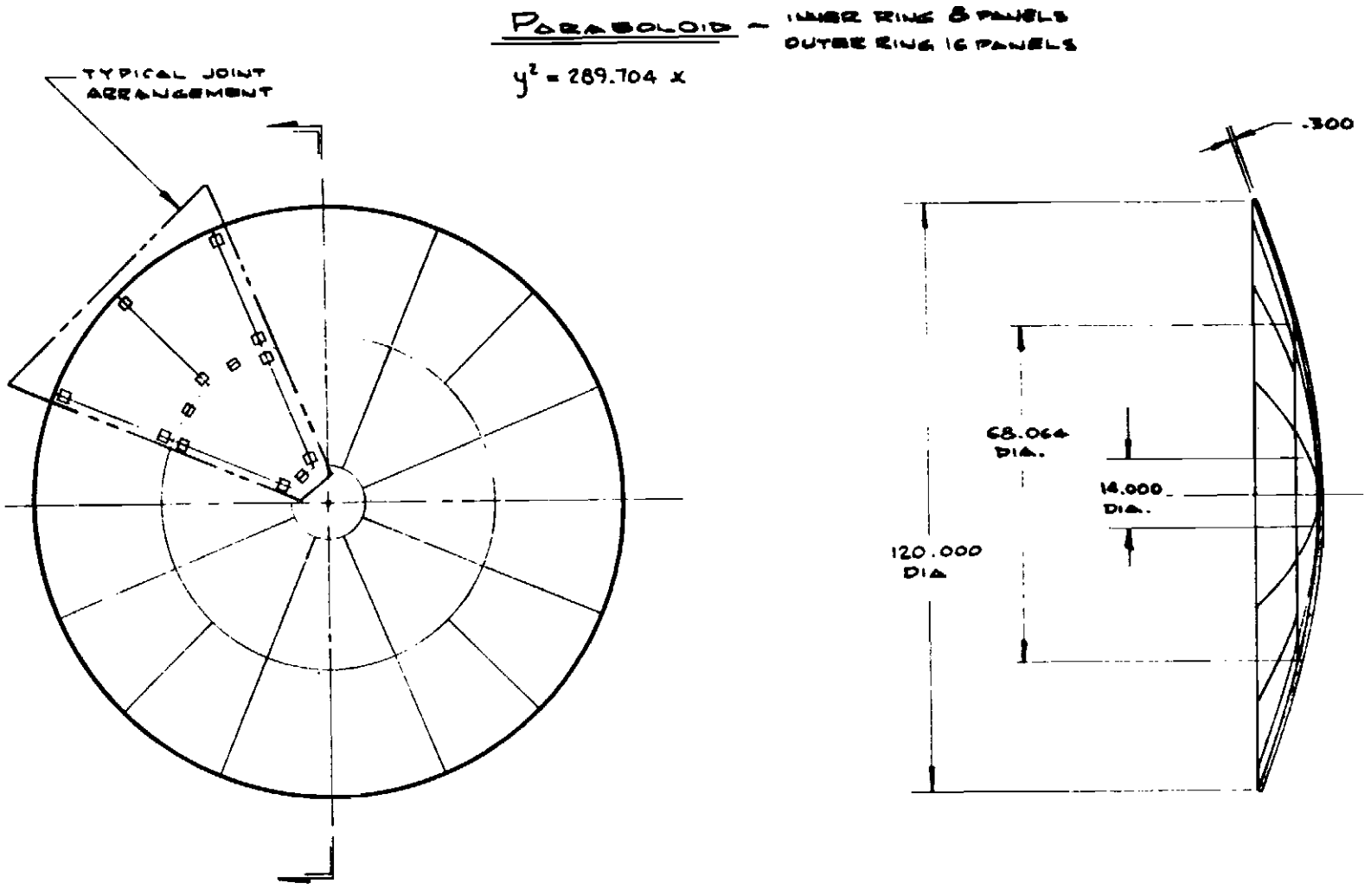

Figure 2-8. Modular Parabola Configuration Showing Optimized Joint Locations

The assembly begins with the astronaut removing the panels, one by one, from the canister and inserting them into the hub joint. A control box is provided at the work station to rotate the hub and change the boom elevation angle as the assembly proceeds. Once the panels have all been properly engaged, a simple tension bolt rope is attached about the back convex surface of the parabolic structure to place all of the tapered joints into slight compression. This action seats all joints to regain the original contour precision established in manufacturing the assembly. The total weight of this 10-foot diameter parabola is 43 pounds. The work station, canister, boom and hub drives, and peripheral equipment bring the total experiment weight up to approximately 85 pounds.

2.4.3 VEHICLE REQUIREMENTS

This experiment is designed to be used on a general MSL type vehicle, and can either be deployed from the vehicle's surface through pyrotechnically released fairings, stowed internally, or elsewhere, and manually moved to the assembly area and the assembly executed. This experiment is directly applicable to the Saturn SSESM Vehicle where it will be stowed forward of the hydrogen tank, behind the thermal curtain, retrieved by the astronaut, and taken internal to the SIVB work shop. There it can be attached to the metal tangs provided on the inner tank surface and assembled. A contour template is included with five transducers which will scan the surface of the completed structure to evaluate the surface accuracy achieved.

2.4.4 ANALYSIS AS AN ILLUMINATOR

An analysis of the performance of a 10-foot, 45° rim angle parabola as a source of illumination was conducted on this program. This analysis considered that the parabola would be provided with a xenon lamp light source of 150 to 300 watts.

This study determines the theoretical performance of this light source as: (1) its brightness appearance (in star magnitudes) to an observer at various distances from the illuminator, when used as a rendezvous aid, (2) its performance as a searchlight for distant objects of various reflectivity, (3) its ability to provide work area illumination to an EVA astronaut as a function of distance, and (4) its application of the xenon lamp.

These analyses indicate that the illuminator will be visible as a second magnitude star (polaris) up to 1000 miles away. A target with a nominal area and reflectivity can be seen (as bright as a second magnitude star) up to 1 mile away, and work area illumination can be provided to an EVA astronaut at the brightness of moonlight up to 7000 feet.

2.5 ENVIRONMENTAL ANALYSIS

An analysis of the environment to which these experiments would be exposed in a 200 nautical mile orbit was conducted and its results incorporated in the materials selction and design.

Of particular importance is a micrometeoroid analysis which calculates the shielding requirements of the elastic recovery material composite. This analysis was based on both theoretical and empirical data from micrometeoroid penetration tests. The results of the theoretical calculations were compared to actual penetration test data to validate, to some extent, the mathematical approach. These results compared very closely and indicated that a probability of no micrometeoroid penetration of 0.9999 could be achieved with 1.75 inches of 1.2 lb/cu ft polyurethane foam with an outer Dacron bumper fabric of 17 ounces per square yard.

The main reason for the high weight outer bumper is substantiated by consideration of earth orbiting low velocity, high mass particles. The interpretation of recent earth orbiting satellite data is

important in this respect and it is not too clear that even this bumper fabric will be sufficient to effect the desired degree of shielding. The theoretical mechanism used for this analysis assumes that the outer bumper fabric fragments or vaporizes the incident micrometeoroid particle which is then absorbed as an expanding gas by the polyurethane foam barrier.

A preliminary thermal analysis was conducted which predicts the expected static equilibrium temperatures for the airlock structure in a 200 nautical mile orbit. This analysis assumed that the elastic recovery airlock would be exposed to solar radiation one-half the period, in a low inclination orbit. Thermal control considerations are delineated which should be taken into account as soon as complete orbital and vehicle thermal input data is available.

An analysis of the near earth nuclear radiation environment which considered ionizing radiation from solar flares, galactic and trapped particles, indicated that there is very little concern for the problem of material degradation for the radiation which would be encountered in a 30-day mission in this type of orbit. The total radiation dosage is only at the threshold of animal effects, and constitutes no problem for the material used for this experiment.

2.6 EXPERIMENT DEFINITION SUMMARY

An experiment definition summary is presented in Section 7 of this report, and includes the preliminary summary that was done for t' .peri-ment for a MSL vehicle and the experiment definition of the revised experiment for the SIVB workshop as far as the program scope permitted.

A brief description of the elastic recovery airlock and manually assembled parabola are presented below. Although most of the final configuration and design were oriented toward the Saturn SIVB vehicle, the experiments are basically identical for applications to any MSL, the main differences being in experiment location and mechanical interfaces.

2.6.1 EXPANDABLE ELASTIC MEMORY AIRLOCK EXPERIMENT

The objective of this experiment is to demonstrate that an expandable structure concept of an elastic recovery composite may be configured into and function as an airlock for future manned space vehicles.

The total airlock experiment as designed for a Saturn SIVB vehicle can be obtained for approximately 135 pounds. The basic subsystem components included are a 5.5-foot diameter spherical airlock with a hatch at one end and a simulated hatch interface at the other; a base structure containing a pressurization system, a retraction mechanism, and required vehicle attachment provisions; a remote deployment control console; and suitable instrumentation for the experimental structures evaluation.

The experiment will be packaged into a high density configuration of 5.6 ft^3, and is of sufficient dimension to enable it to be carried through the Saturn SSESM EVA hatch in the event ingress/egress characteristics are desired to be evaluated inside the SIVB workshop.

This experiment will be stowed forward of the hydrogen tank and behind the thermal curtain of the SSESM trans-stage area. An astronaut will go EVA, and relocate the experiment for deployment, if required, and return into the SSESM vehicle. There the astronaut will deploy and pressure test the 5.5-foot diameter airlock, whereupon it may be evaluated for geometry as an airlock by several ingress/egress maneuvers by the astronaut.

Photographic film coverage will be made of the experimental procedure and retrieved by the astronaut along with instrumentation recording and material samples of the composite. This data and material will be brought back to earth for laboratory evaluation.

For an MSL vehicle, the airlock experiment configuration is essentially the same, except for the extendable boom required to position the experiment package beyond the vehicles surface, and the experiment location which will be mounted in the outer wall of an unpressurized compartment. Pyrotechnically released fairings are also employed to alleviate any aerodynamic effects during launch.

2.6.2 MANUALLY ASSEMBLED MODULAR PARABOLA EXPERIMENT

The objectives of this experiment are to demonstrate the technological concept for the manual assembly of precision precontoured modules to obtain accurately contoured parabolic structures for use as antennas, or solar collectors up to 100 feet in diameter.

This experiment consists of a 10-foot diameter parabola constructed of 24 precontoured lightweight aluminum honeycomb modules which are provided with simple interlocking joints which may be assembled by a pressure suited astronaut in a zero-gravity environment. A six-foot electrically controlled boom is provided for support of the parabolic structure. A simple work station is featured which contains the panel canister and a remote control box for positioning the boom and hub within easy reach of the work station. The total experiment weight is about 85 pounds and a volume of 5.9 cubic feet is required. The dimensions of the experiment package is commensurate with the Saturn SSESM EVA hatch size so that the experiment may be transported into the SIVB workshop.

The experiment stowage location on the Saturn SSESM will be forward of the hydrogen tank and behind the thermal curtain in the trans-stage area. In procedure, the astronaut will go EVA, retrieving the experiment package to the SIVB workshop interior, and will be attached to the inner surface of the hydrogen fuel tank via the metal tangs and tapped holes provided. The astronaut will position himself at the work station and remove the precontoured aluminum honeycomb panels and insert them singularly into the hub on the end of the boom. After the assembly of the 10-foot diameter structure is complete, a contour template may be used to evaluate the contour accuracy achieved. Motion picture coverage will be employed to study the astronaut task performance during the assembly.

The modular parabola experiment configuration for an MSL vehicle is virtually identical to that for the Saturn SIVB. The primary difference is in the storage location under aerodynamic fairings. In this experiment, the astronaut may erect the experiment from the remote control console and then proceed EVA for the manual assembly phase on the outer vehicle surface. Considerations were also given to use the finished parabola as an illuminator by the insertion of a xenon lamp string into the hub.

2.7 CONCLUSIONS AND RECOMMENDATIONS

The following conclusions and recommendations are a direct outgrowth of this study program:

2.7.1 CONCLUSION

- The Elastic Recovery material system technology is advanced to the point where an orbiting space experiment will contribute significantly to further advancement.
- It is practical to construct a lightweight expandable manned space laboratory airlock from this material system which will provide the required operational functions of an airlock and provide a substantial micrometeoroid and thermal protection from the space environment.
- A technique for the manual assembly of precision precontoured panels to obtain large, accurate parabolic structures is immediately within the state-of-the-art capability, and the assembly task is with the limitations of a pressure-suited astronaut in zero gravity. An experiment to demonstrate this technological approach has been designed and scaleability of this approach to structures up to 100 feet in diameter can be demonstrated by a 10-foot diameter model.
- An experiment to evaluate these structural systems is feasible with regard to the vehicle, human factors and mission restraints imposed by current program and technology.

- Chemically rigidized systems are very promising for expandable space structures, but require more development before they are ready for a manned space experiment.

2.7.2 RECOMMENDATIONS

- Continued development should be undertaken in the rigidizable expandable structures area for applications of future space and planetary exploration: specifically in the area of cure time, cure reliability, and uniformity of resin impregnation. More development is needed in the area of chemically rigidized parabolas regarding surface smoothness and contour accuracy.

- A prototype modular parabola should be constructed to finalize the detail design and fabrication techniques. Methods for in-orbit contour evaluation and fine figure control can be further developed with such a unit. Specific neutral buoyance and Keplerian trajectory aircraft tests need to be performed to correlate the work tasks with an actual space assembly, as considerable disagreement in comparative task difficulty of these test techniques to actual orbital conditions.

- Further analysis and design needs to be performed to optimize an airlock configuration regarding astronaut maneuverability requirements and efficient use of the structure volume to conserve gas lost per cycle.

- Continued work should be performed in the interpretation of recent micrometeoroid environment data and the mechanisms involved in proper vehicle shielding, particularly for near-earth orbiting particles.

Section 3

MATERIAL SYSTEMS

The evaluation of material systems in this contract was primarily concerned with flexible or rigidized composites for the expandable structures portion of airlocks or parabolic structures that could be used as experiments in manned orbital programs. Both design and laboratory evaluations were made to assure selection of the most suitable material system. Since the expandable structure is the key feature in these experiment concepts, and the material systems for these have not been developed yet to the same level as other elements of the design, thorough evaluation was appropriate.

The candidate material systems were evaluated using the following basic criteria:

- It must be sufficiently well developed and proven to be capable of being converted into usable hardware at an early date, and with a high probability of success.
- It must have characteristics that assure reliable and predicable performance.
- It should be "fail safe".
- It must be completely compatible with the space environment - hard vacuum, micrometeoroids, radiation, etc.
- It must be compatible with the environments associated with experiment operation such as 100% oxygen internal pressurization.
- It must be fully compatible with astronaut activities and in no way jeopardize his safety.
- It must permit design of the experiment configuration to be compatible with astronaut activities and requirements for mechanical aids, etc.
- It must not impose basic constraints or limitations on operational use.

The results of these evaluations are presented in two principal sections covering the two categories of materials systems - chemically rigidized and elastic memory.

The effort in this contract emphasized evaluation of potential subcontractors for expandable material systems and determination of design solutions in support of the design studies. The evaluations of individual materials and laboratory specimens were generally a continuation of work started in the preceding Contract (AF 33(615)-2728). For the elastic memory composite, many of the specific material-types had been selected in that earlier effort, and consequently, only the final selection of available designs was made in this program. This section of the report primarily reviews the final laboratory evaluation of chemically rigidized specimens and the design selection of the materials for the elastic memory composite. This latter effort required testing of adhesives to arrive at a suitable design and these results are also reported.

3.1 CHEMICALLY RIGIDIZED SYSTEMS

Chemically rigidized systems are potentially useful for expandable space airlocks or parabolic structures. Both design and laboratory evaluations were made for these applications.

3.1.1 LABORATORY SPECIMEN TESTS

As part of the contract effort to evaluate material systems and potential subcontractors, laboratory evaluations were made of several specimens. These evaluations were a continuation of the effort undertaken on Contract AF 33(615)-2728. The specimens tested were supplied after the preceding contract was completed which was early in this program. These were improved versions of the earlier submitted samples. The results of these tests are given in the following sections. Evaluation data on potential subcontractors was provided under separate cover to the AFAPL Project Engineer early in the contract.

3.1.2 ENVIRONMENTAL EVALUATION OF THIRD NCR TEST SPECIMEN

An inflation and rigidization test was performed on a third National Cash Register-supplied 20-inch diameter simulated parabolic test specimen. Two representatives of NCR were present for observation and consultation. This was an acrylic impregnated foam structure.

The test setup and instrumentation arrangements are shown in Figure 3-1. A resistance heater strip coated with catalyst capsules was placed mid-radius and circumferentially about the back surface of the specimen. Thermocouples were placed under the catalyst strip and at the outer rim of the back surface of the parabola to record the effects of the exothermic rigidizing reaction.

The vacuum chamber was evacuated to a pressure of 100 microns and the specimen was contoured with a pressure of 13 inches of water. The catalyst strip was energized with 3.5 amps and catalyst vapor was observed to evolve from the coated strip and disperse in the chamber. A recording of the local temperatures achieved by the exotherm is seen as a function of time in Figure 3-2. Peak exotherm was noted at 180°F at 12.5 minutes directly under the initiator strip. Approximately 11 minutes later the temperature indicated the exothermic reaction had propagated at a constant 180°F to the edge of the specimen. After a total time of 45 minutes after catalyst initiation, the specimen was removed from the vacuum chamber and inspected.

The cure and general contour of the spherical type surface were quite good. The surface was specular; however, radial wrinkles varying in length from 1/4-inch to several inches covered about 5% of the surface near the edge and the remainder of the surface had an orange-peel type effect apparently caused by a slight shrinkage of the aluminized mylar backup material. Areas under the large wrinkles were soft and uncured from an apparent lack of impregnating resin.

Figures 3-3, 3-4, and 3-5 show the back surface of the cured collector and views of the reflecting surface. A black radial line was drawn to exhibit the contour in Figure 3-4. The front surface conditions in Figure 3-5 were exaggerated by lighting and camera angle; the surface is better than

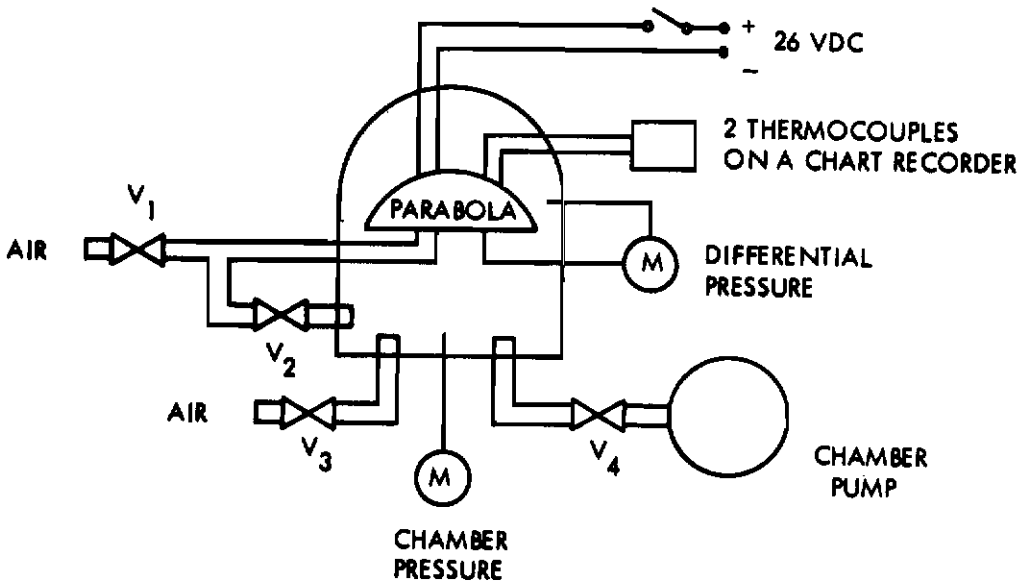

Figure 3-1. NCR Test Setup

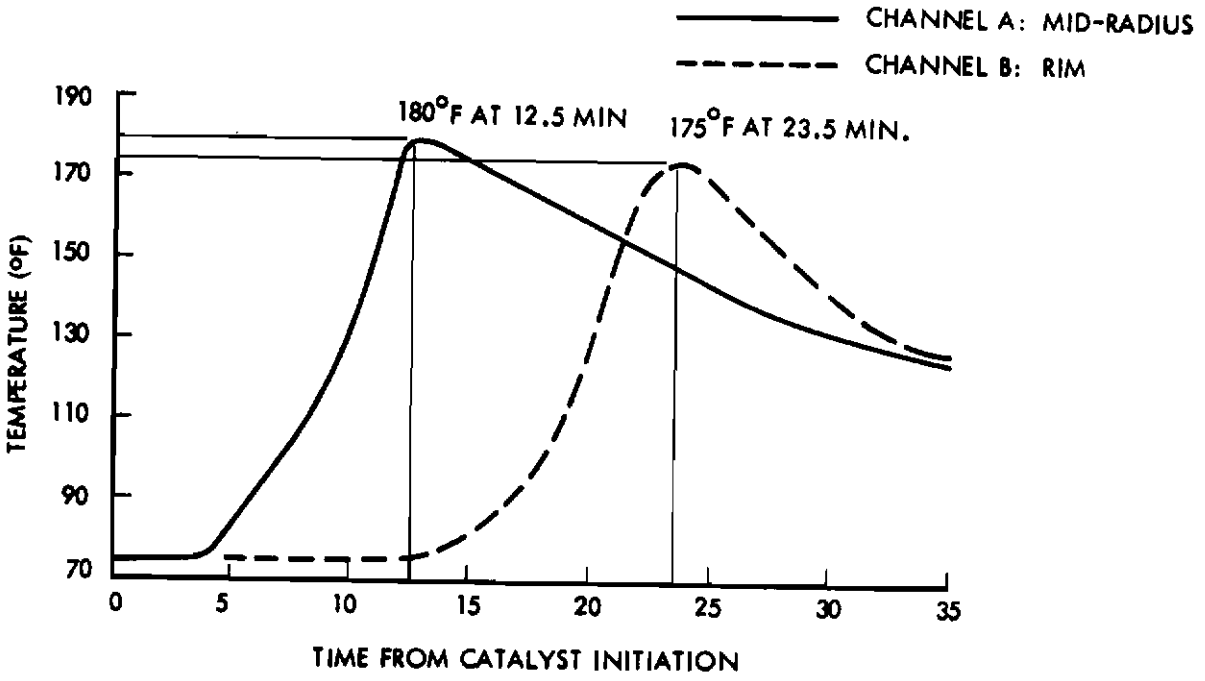

Figure 3-2. NCR Exothermic Reaction Temperatures

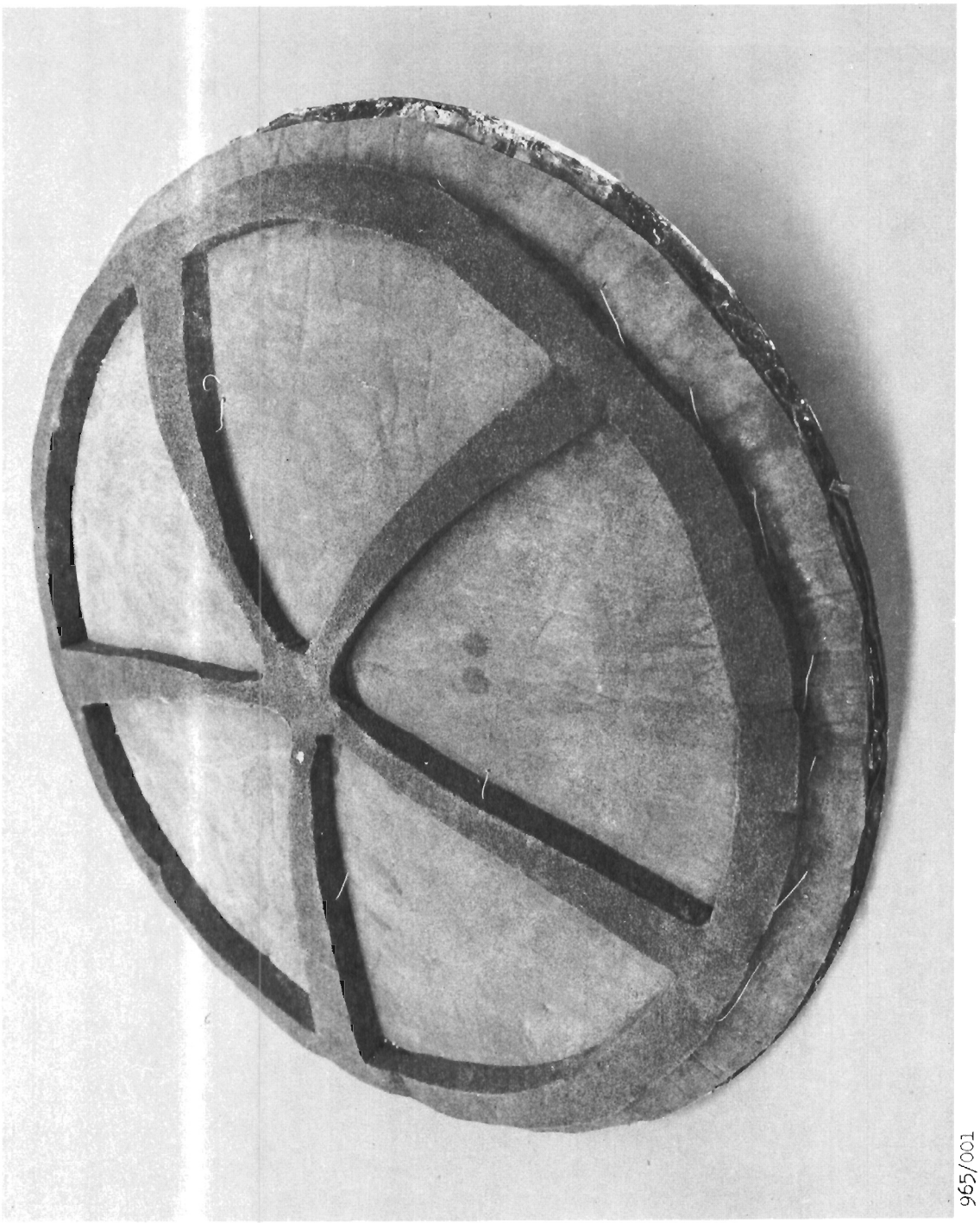

965/001

Figure 3-3. NCR Collector No. 3 After Successful Rigidization

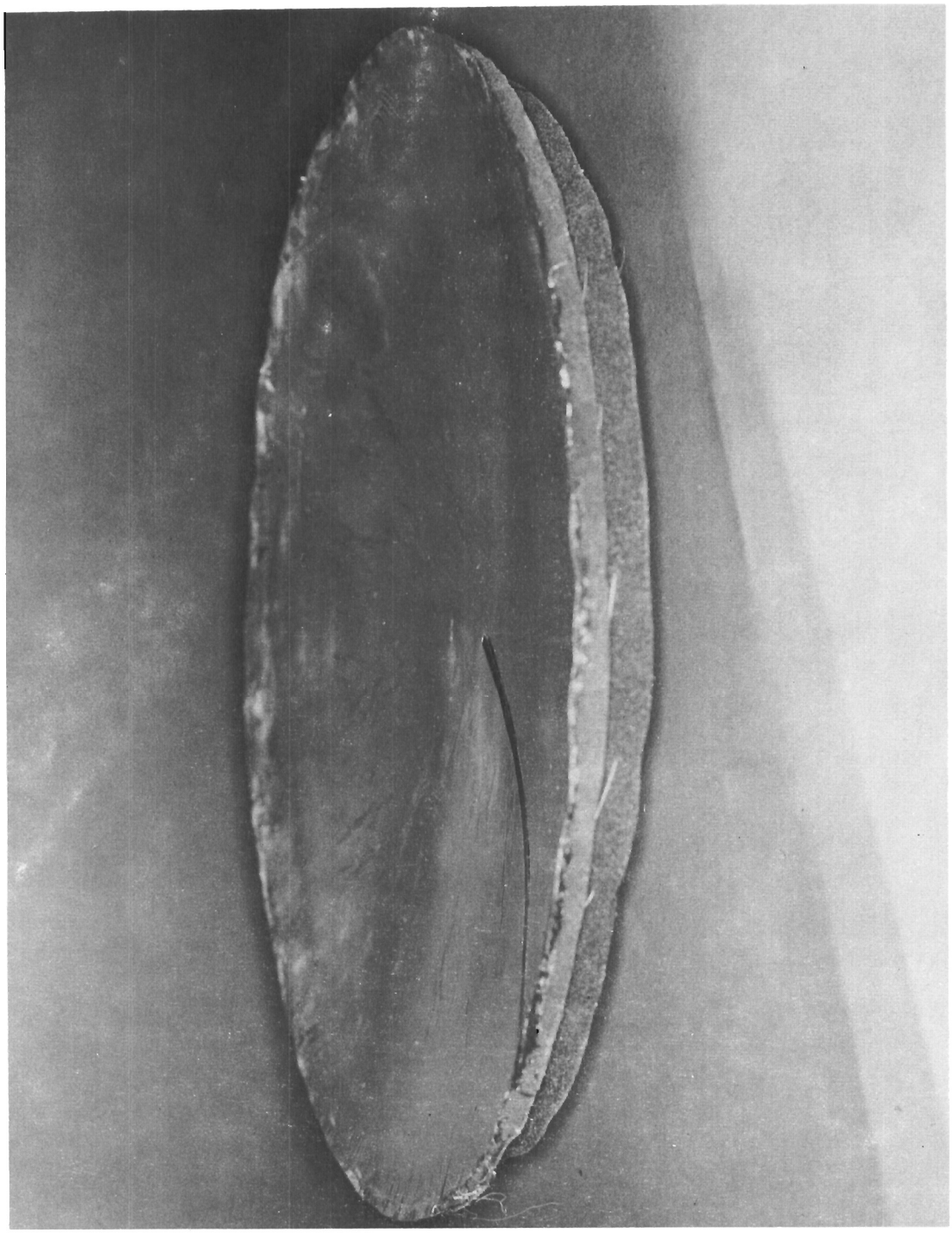

965/003

Figure 3-4. NCR Collector No. 3 Contoured Surface

965/002

Figure 3-5. NCR Collector No. 3 Surface Wrinkles and Orange Peel

the photograph would indicate. A cut was made along a radial wrinkle and the cross section in Figure 3-6 shows the uncured region. This area is painted white in the figure; depth of the uncured area is approximately 0.1 inch.

3.1.3 TEST OF GCA-VIRON SECOND GROUP OF RIGIDIZED SPECIMENS

Space environmental rigidization tests were performed on GCA-Viron specimens, consisting of a gelatin impregnated nylon cylinder and a drop-thread fabric parabola. The cylinder incorporated an internal thin mylar air bladder and the fluted core section was separately pressurized to allow for erection of the flutes. These changes were incorporated to correct inflation problems encountered in the original two cylinder specimens. The test procedures and results are summarized below.

3.1.3.1 CYLINDER

The nylon cylinder specimen test setup is shown in Figure 3-7. A bladder pressure of 4 inches of mercury was established and the flutes were erected by bleeding ambient air through an auxiliary fitting into the fluted core. This air diffused quite rapidly through the porous outer fabric, requiring a steady inlet flow to achieve partial erection pressure. This condition was maintained for 3 hours at a chamber pressure of 1 mm Hg until the end of the day. The external bleed-air valves were closed and the system was held at vacuum overnight. The specimen was then removed from the chamber and examined.

The nylon cylinder was well-inflated and rigid, with good internal geometry, but the flutes were only about 50% deployed. The gelatin had failed to totally wet the fabric and tended to flake off in some areas where surplus gelatin had accumulated. The distribution of the gelatin was uneven, especially around the end caps where it tended to bubble and congregate in patches.

Pictures of the cylinder, the fluted walls, and close-ups of special interest areas are shown in Figures 3-8 and 3-9.

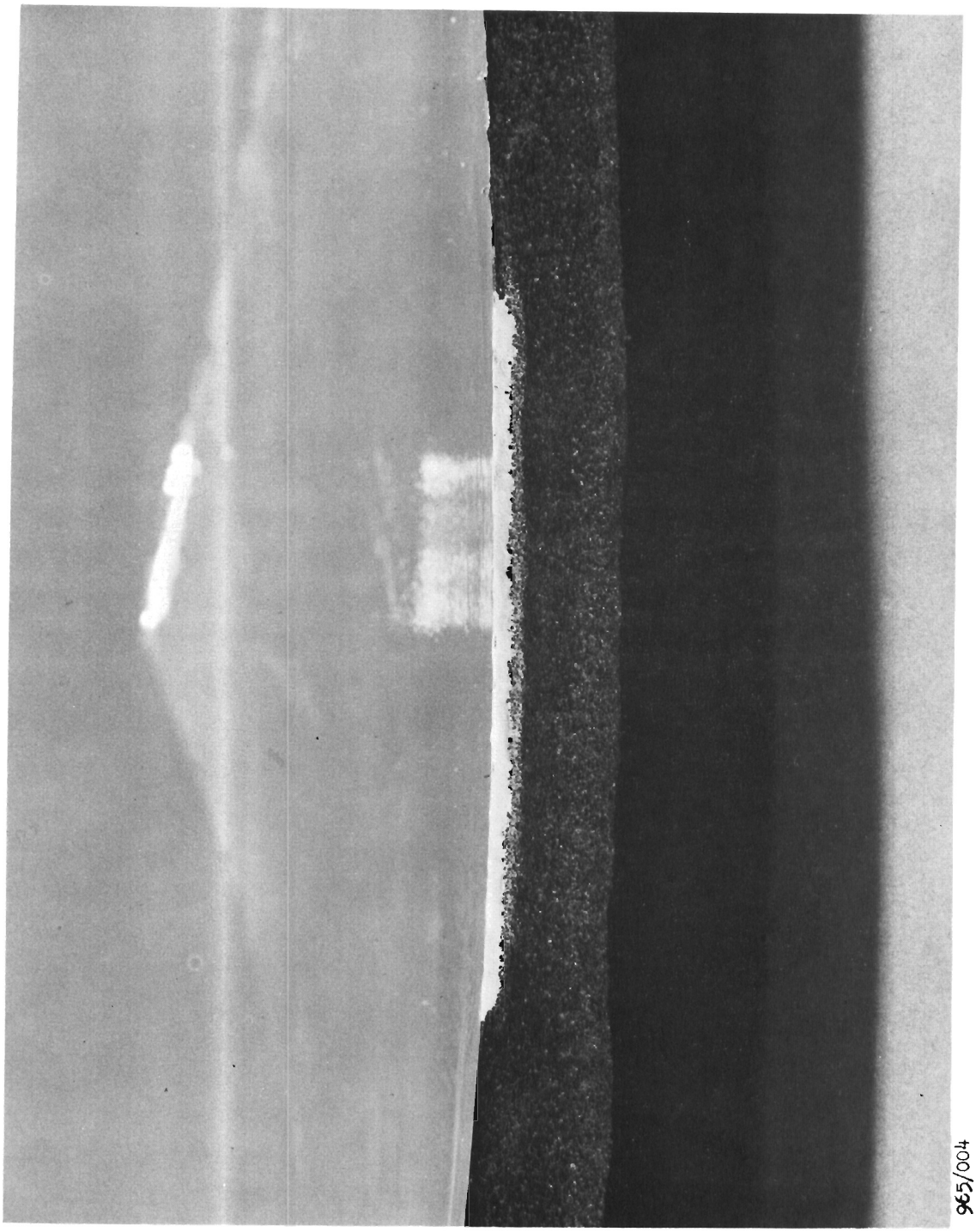

Figure 3-6. NCR Collector No. 3 Cross Section Showing Uncured Area (White Painted Area)

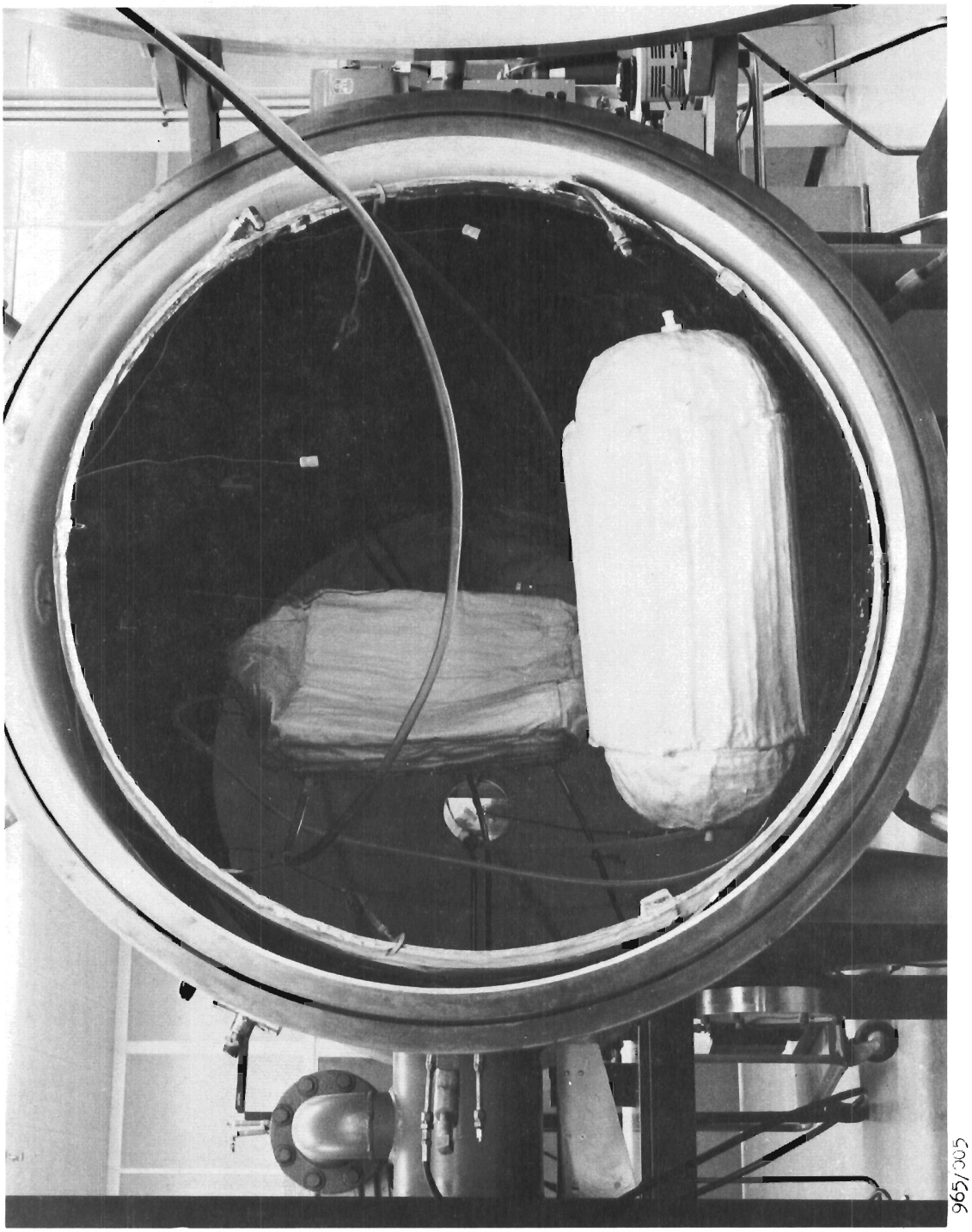

965/305

Figure 3-7. GCA-Viron Nylon Cylinder Hanging in Chamber, Fiberglass

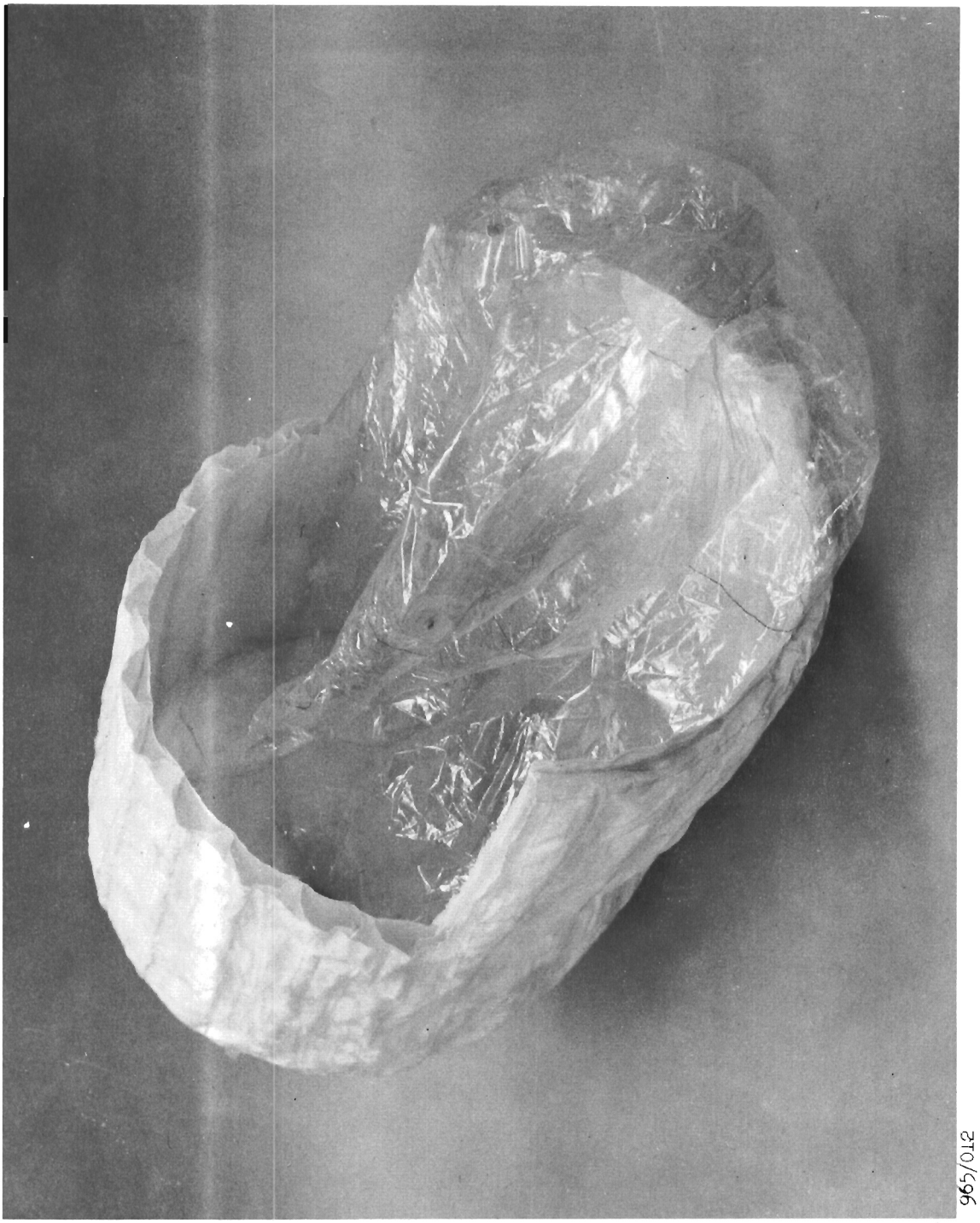

965/012

Figure 3-8. GCA-Viron Cylinder Showing Flute Cross Section and Mylar

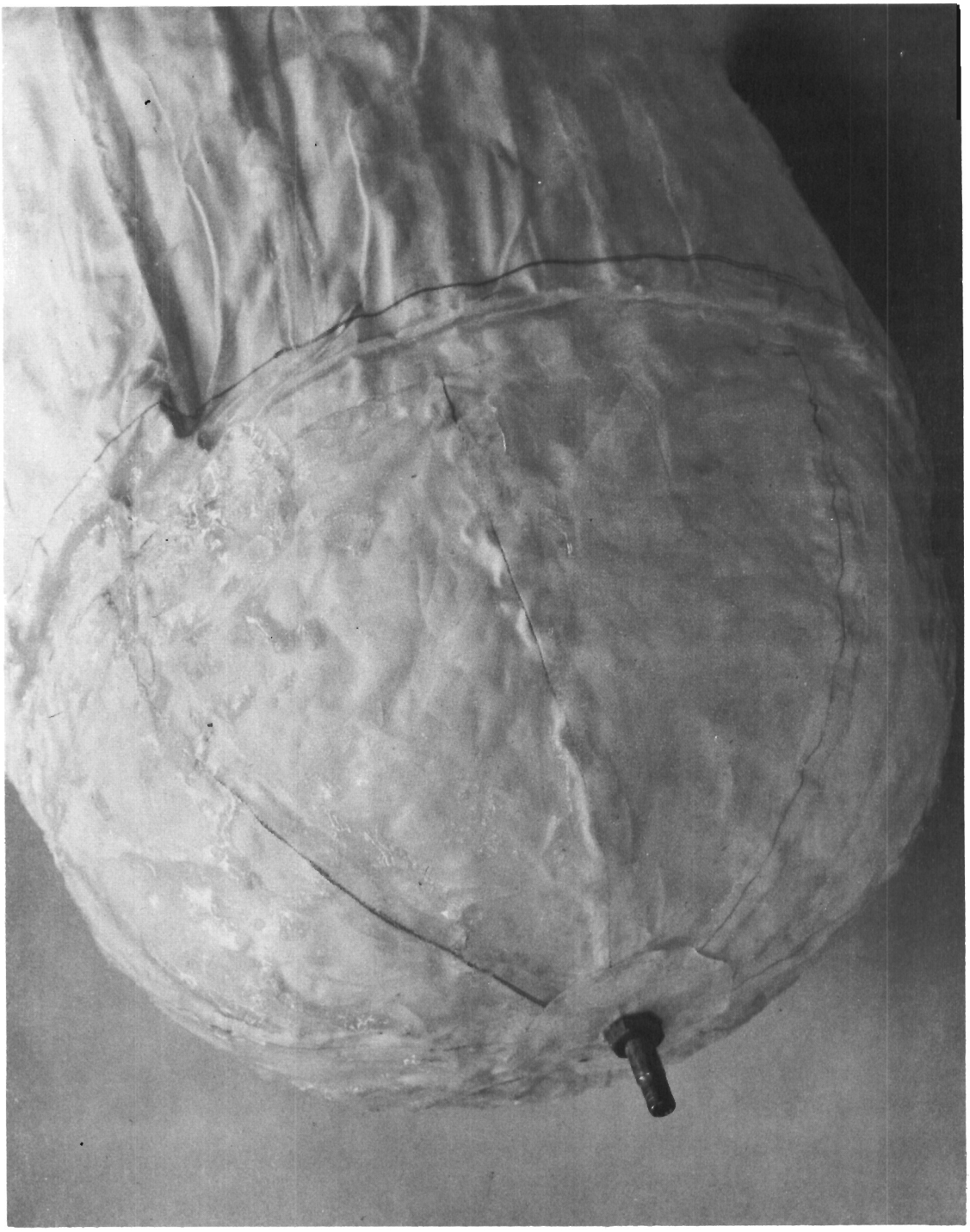

Figure 3-9. GCA-Viron Nylon Cylinder Showing Inflated End Cup with Patchy Bubbled Areas of Gelatin

3.1.3.2 PARABOLA (GELATIN IMPREGNATED DROP-THREAD SANDWICH)

The parabola was set up similarly to the cylinder and a plastic moisture barrier cover was cut away. A pressure of 10 inches of water was used to contour the reflector surface throughout the experiment. The backup drop-thread fabric was pressurized by an auxiliary fitting for one hour by bleeding in external air and then the air valve was closed, allowing the chamber vacuum to drop in pressure from 500 microns to less than one micron.

After five hours total time the parabola was removed from the chamber and cut away from the test fixture for examination. The drop-thread material seemed fully rigidized. It could be depressed with a slight hand pressure and would spring back to its original shape.

The reflective surface was slightly curved, exhibiting a 1-inch center depression for the 20-inch-diameter parabola. Several large wrinkles crossed the surface and about 75% of the surface exhibited an orange peel effect. There was no evidence of delamination of the surface material.

It was observed, upon cutting a wedge sample from the disc, that the curvature of the rigidized specimen disappeared, reducing the orange peel and wrinkling. This probably resulted from the use of a flat lay-up rather than a contoured lay-up.

3.1.4 GOODYEAR CYLINDER AND PARABOLA SPECIMEN RIGIDIZATION TESTS

These specimens consisted of the ADM vapor-set urethane resin impregnated fluted core cylinder approximately 20 inches high, and a drop-thread sandwich disc approximately 24 inches in diameter. These specimens were rigidized by the catalytic action of water vapor which was passed through the resin impregnated structures. Figures 3-10 and 3-11 illustrate these specimens.

The cylinder structure was placed in SGC vacuum chamber for the rigidization tests. The chamber was evacuated according to the experimental procedure supplied by GAC, and the inside of the cylindrical specimen was vented to a atmosphere to effect a 14.7 psi fixation pressure. The pressure for erecting the fluted core walls was provided by the water vapor carrier

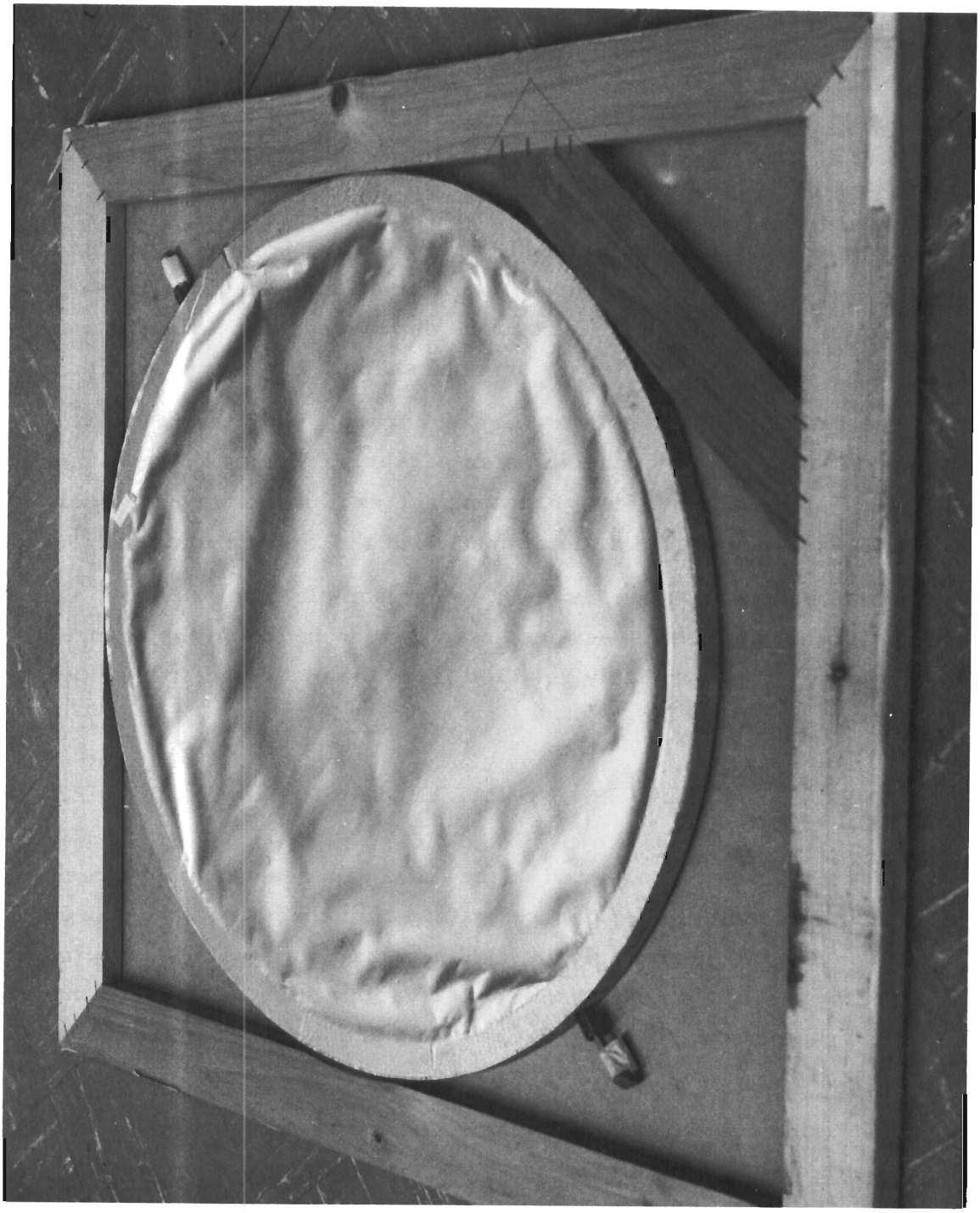

Figure 3-10. Goodyear Disc in Container

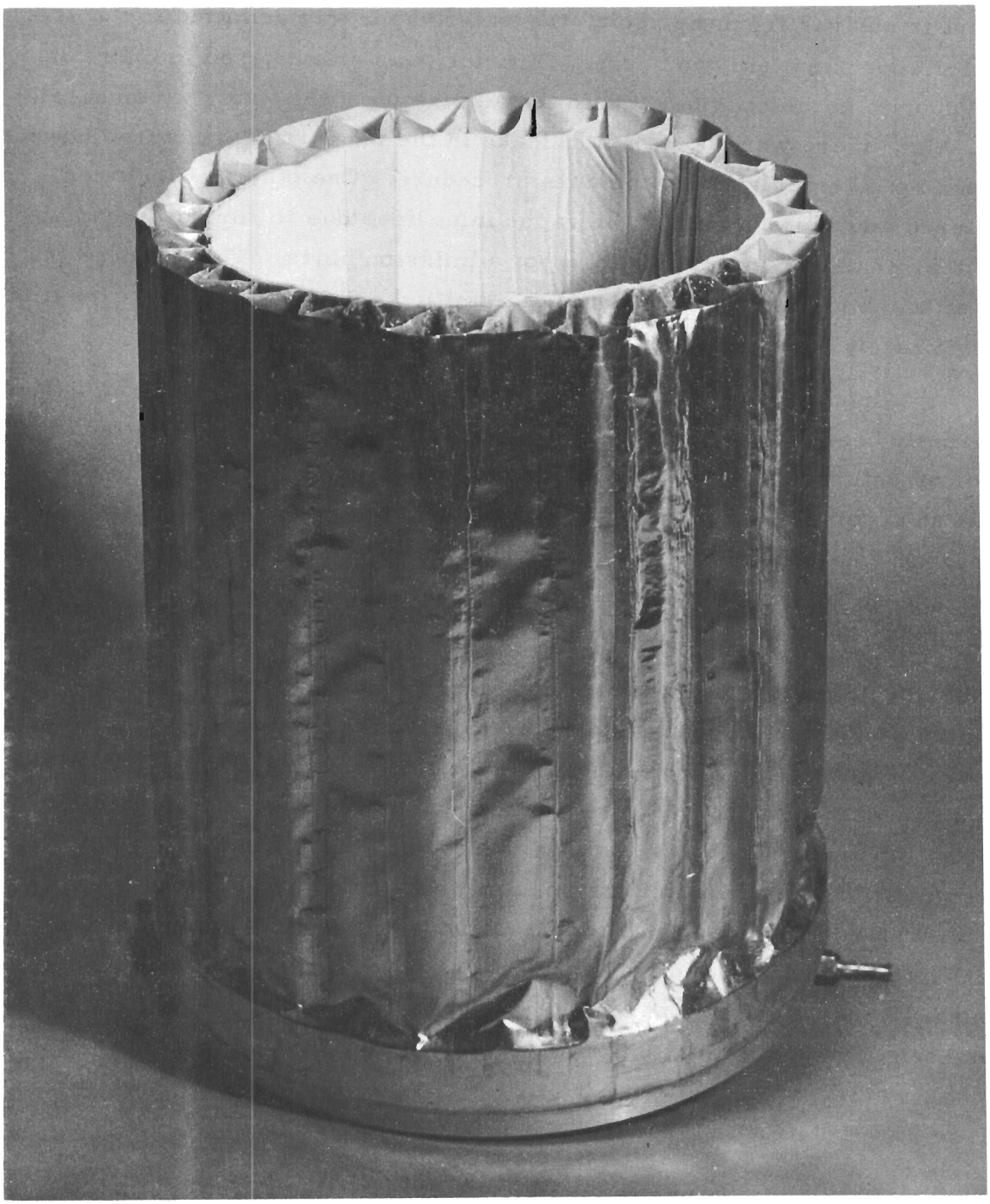

Figure 3-11. Rigidized Goodyear Cylinder

gas and was limited to 125 mm Hg differential. After allowing any remaining solvent to out-gas from the resin, the water vapor was admitted to the specimen for approximately two hours. Difficulty was encountered in maintaining a good vacuum in the chamber due to the admission of the water vapor carrier gas. Also, there were some small leaks in the inner wall structure, however, this did not adversely affect the cure procedure. One other difficulty encountered was the plugging of the vapor inlet lines due to surplus accumulation of urethane resin around the vapor admission ports. This reduced the rate at which the water vapor could be admitted and lengthened the cure time approximately 5 percent.

Upon removal of the specimen from the chamber, rigidization had apparently been affected and the specimen was cut open to examine the interior structure appearance. (This may be seen in Figure 3-12.) Cure had been accomplished in all but the heavily impregnated areas which had undergone some bubbling. The flute erection appeared to be relatively good, and the specimen exhibited good mechanical integrity.

The parabola structural specimen (flat drop-thread disc) was rigidized with the same procedure and cured properly with no severe problems. The final appearance of the rigidized drop-thread disc is shown in Figure 3-13. Drop-thread erection appeared uniform, but there was a general waviness over the surface which would not be acceptable for high accuracy parabolas, however, this could have been induced by the rigidized fixture in which the specimen was cured. Both specimens were received in the deployed configuration and it was not determined what affect high-density folding would have had on these structures. The general impression was that they were fairly stiff as received and may have been damaged if an attempt to severely fold them were made.

3.1.5 CHEMICALLY RIGIDIZED SYSTEMS EVALUATION

A review and reevaluation of the merits of the resin rigidization systems, and the experimental structures characteristics for the program experiments are summarized below.

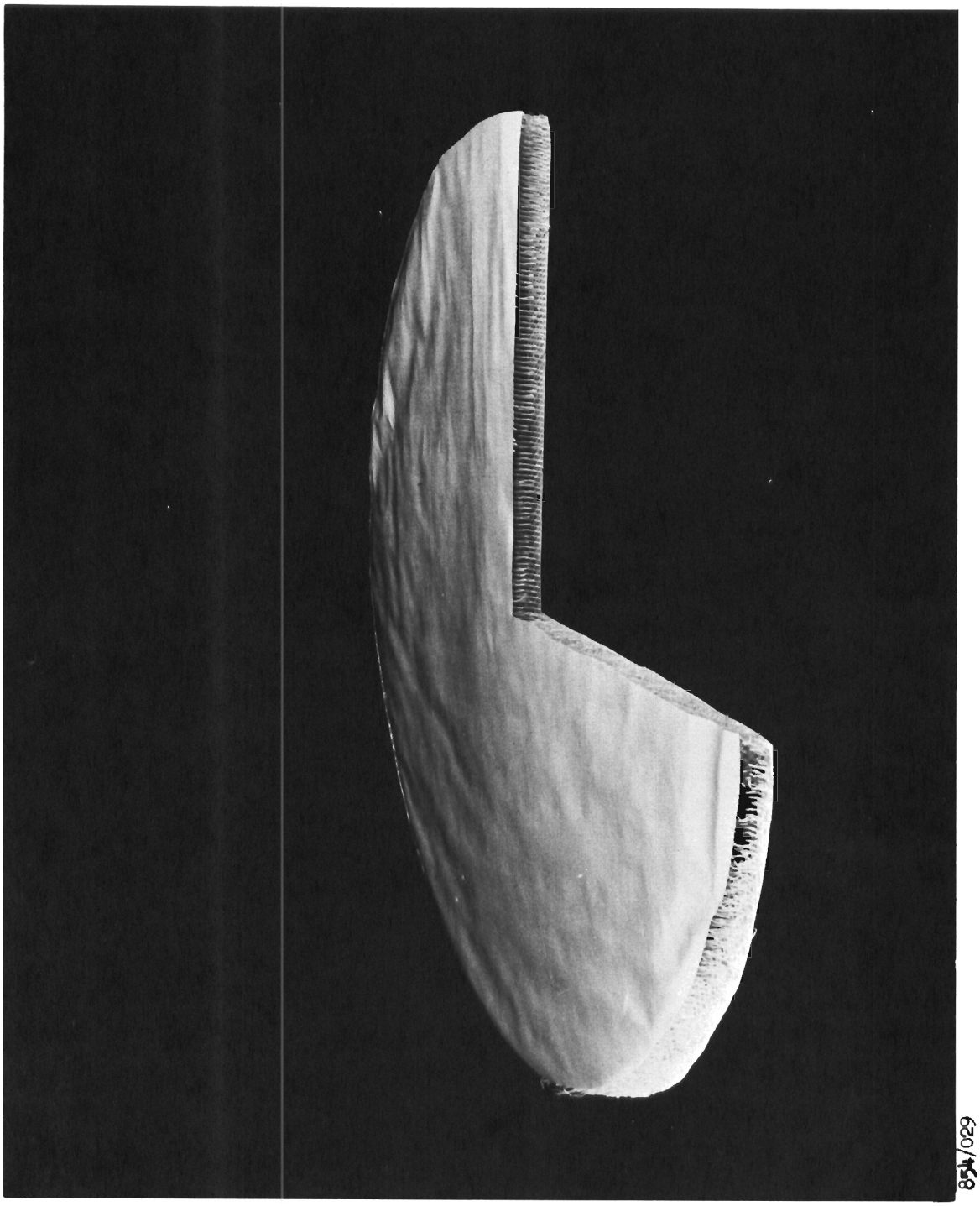

Figure 3-12. Goodyear Disc. Sectioned

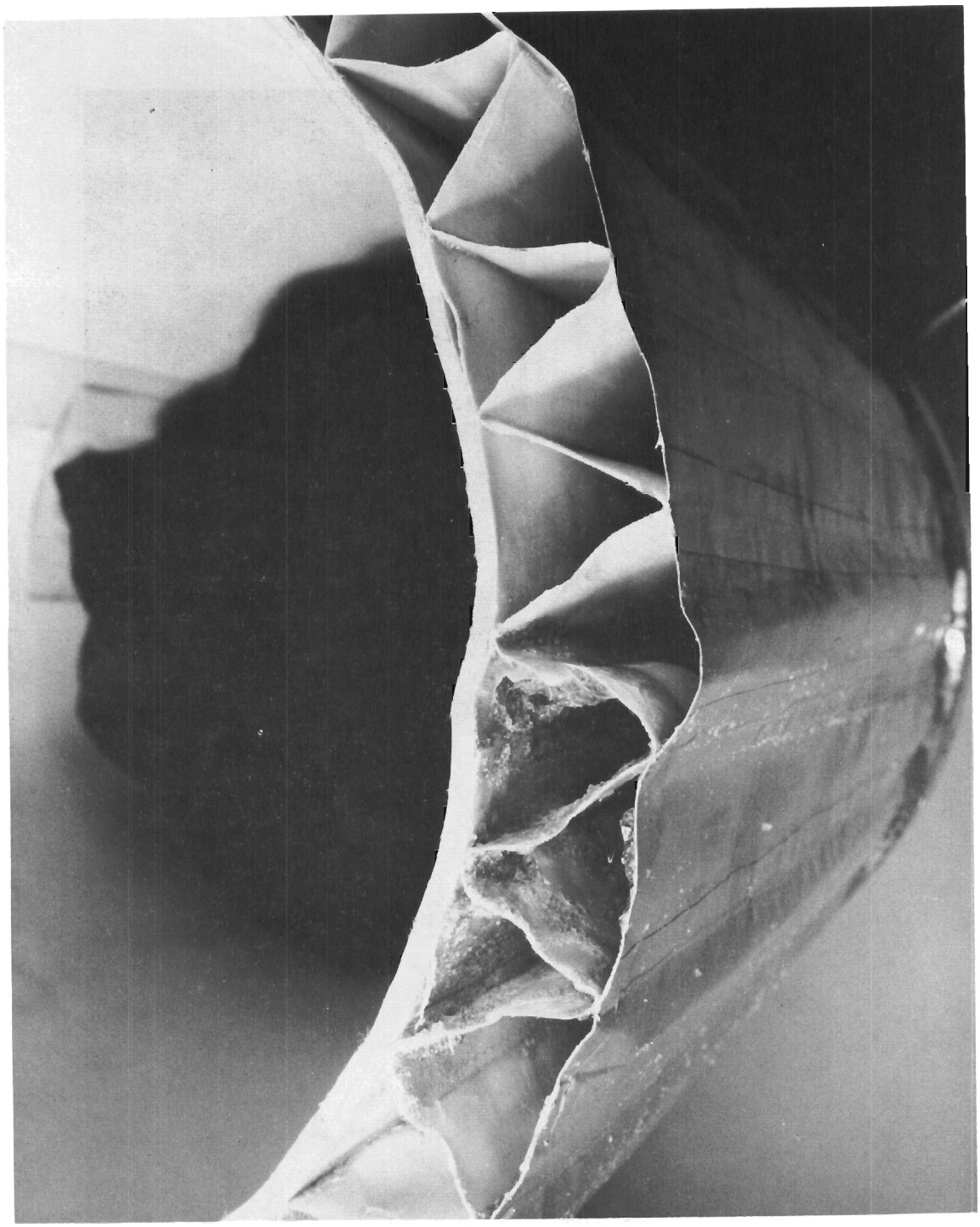

854/035

Figure 3-13. Fluted Core of Cylinder Showing Resin Accumulation

3.1.5.1 RIGIDIZATION OF STRUCTURAL SYSTEMS

Urethane, gelatin, and vinyl resin systems can be rigidized in orbit in approximately four hours, or less, to produce usable structures. The mechanical properties of each system are perhaps of less importance, at this state-of-the-art, than is the reliability of the cure system. Reliability of the cure systems is related primarily to initiation and completion of curing, uniformity of impregnation, percentage of resin content, and extrusion or settling of resin during folding and shipping. The most critical of these factors is reliability of the completion of cure, as even a local uncured area could precipitate a structural failure under the correct load.

3.1.5.2 CURE CHARACTERISTICS

The vinyl and gelatin resin systems theoretically are both chemically fail-safe cure systems in the space environment. Gelatins cure by boiling off solvents in low ambient pressures, and the acrylic resin should polymerize even in the absence of the amine catalyst by one of three mechanisms: (1) the boil-off of the inhibiting oxygen molecules dissolved in the monomer will permit the release of free radicals and the polymerization of the monomer; (2) solar heating will polymerize the resin; and (3) gamma radiation will also produce free radicals and the ultimate polymerization of the resin.

If the orbital environment and thermal characteristics of the vinyl system are such as to produce elevated resin temperatures, the system will cure; for example, at 225°F this system would cure in approximately fifteen minutes without a catalytic initiator.

The cure time of gelatin is a function of section density, thickness, temperatures, etc., but it is reasonable to assume that typical thick structural sections, properly designed, will cure in less than four hours in a 150-nautical mile equatorial orbit.

Urethane systems are not fail safe and will not cure in the absence of water vapor. However, it is believed that structural and catalytic distribution systems can be developed that will demonstrate a high degree

of reliability of cure. ADM states that both Viron and GAC have designed and developed impregnation and catalytic distribution systems that have reliably produced complete uniformity of resin distribution, proper resin content, and catalyst distribution. The specimens supplied to SGC by GAC exhibited generally excellent uniformity of impregnation, but the resin concentrated in puddles and prevented diffusion of the catalyst throughout these sections. However, it is extremely important to note that the very limited funding and schedule time permitted GAC for the analysis, design, fabrication, and testing of these specimens may have been insufficient to permit the delivery of a reliable test specimen. Viron specimens exhibited generally poor resin distribution and low resin content with local areas of resin accumulation. The resin almost totally settled out of one NCR specimen (which therefore failed to rigidize), and the several very localized resin-lean areas in the second specimentwere observed coincident with surface wrinkles.

3.1.5.3 PACKAGING CHARACTERISTICS

It can be expected that a sharp edge folding will extrude resin from the reinforcing material, causing a reduction of structural integrity in the fold line and excess resin in adjacent areas. The Viron test specimen cylinder was received in a high-density folded configuration but GAC's cylinder was received in the expanded configuration. GAC's cylinder was so relatively rigid, due to the thick material laminates, that no attempt by SGC was made to fold the cylinder due to fear of damaging the structure and aborting the entire test. All simulated parabola specimens were received mounted in a holding fixture ring, as specified by SGC, and no attempt was made to remove the specimen for simulated folding tests prior to rigidization.

It can be assumed that folding will most seriously affect the NCR material system, relative to extrusion of the resin. The urethane and gelatin systems can also be expected to be subject to some resin extrusion, but to a lesser degree.

The structural efficiency of the urethane system is potentially the highest, and that of the vinyl impregnated foam the lowest. However, resin-lean areas produced during impregnation, folding, shipping, or launch

vibration will produce local areas of low strength that may determine the maximum usable design allowables of the structure. If these low-resin-content areas are localized, and non linear, the reduction in efficiency of a structure designed for stiffness (not strength) may not be significant. This statement is also generally applicable to pressure vessels that are not subjected to shear, concentrated normal loads, or compression loads.

Continuous resin-lean cleavage planes in vinyl impregnated foam may act as barriers to the propagation of the normal exothermic cure from an initiation site, although cure will eventually be completed in a vacuum environment. These cleavage planes should not detrimentally affect the urethane or gelatin cure system cycles.

The gelatin and urethane fabric structures will both permit good packaging densities. The vinyl impregnated foam stowed volume will be at least several times greater than that of the gelatin or urethane. As the vinyl foam is presumably the most susceptible to the extrusion of resin due to folding, packaging densities will be determined by this factor rather than the compression rates of the elastic foam.

Until such time that controlled structural tests of folded, resin impregnated, typically complex structural configurations are conducted, this problem cannot be quantitatively evaluated.

3.1.5.4 THERMAL CONTROL

All three resin systems will require that the resin impregnated fabric be thermally controlled, perhaps actively, prior to deployment to prevent excessive stressing of the fabric that would result at low temperatures during deployment. The vinyl foam system should perform adequately at temperatures as low as $0^{\circ}F$ (or less). The gelatin and urethane must be maintained at temperatures above $32^{\circ}F$ to prevent freezing of the water vapors. If the structures are sufficiently flexible to permit full deployment without creating excessive stress levels, the vinyl and gelatin systems will eventually cure even at low temperatures but the urethane water catalyst will freeze and prevent circulation of the catalyst and completion of the cure process.

3.1.5.5 PARABOLIC MIRRORS

No one has as yet deployed a parabolic mirror with an end cap for shaping the structure. It is anticipated that end-cap testing will produce more new problems that may be difficult to solve. It is strongly recommended that such a test be initiated at the earliest possible date to evaluate this method of geometry control.

The method of forming a parabola from semi rigid folded gores is not considered to be an efficient approach to the solution of the problem due to the poor packaging characteristics. The automatically erected prefabricated modular concept should produce a more accurate and reliable mirror for approximately the same weight and stored volume.

An expandable parabola has been folded in a simulated stowed configuration to determine the effects of folding on the specular surface and on the resin-fabric system. Although local specularity was very good, the fold locations left creases which subtract from the effective surface area.

3.1.5.6 SUMMARY

Numerous unresolved (known and anticipated) problems exist in the development of good expandable, rigidized parabolic mirrors. Concentrated efforts should continue in order to identify and resolve these problems.

Pressure vessel type structures, such as an airlock, can be reliably developed from elastic memory, gelatin, vinyl, or urethane materials. The elastic memory material system is the most simple and predictable. Gelatin rigidized fabric will cure slowly but reliably (fail safe) and produce moderate strengths. Vinyl impregnated urethane foam and fabric will cure rapidly and reliably (fail safe) and produce low strength structures. Urethane impregnated fabric structures are not cure fail safe but will achieve a satisfactory reliability, with high strength and moderate cure times, if sufficient design development and qualification testing is accomplished.

For this contract design effort, the expandable material systems which will be used as a basis for this experimental evaluation will be the elastic recovery system for the airlock and aluminum honeycomb preformed modular panels for the parabola experiment. The airlock hardware design is also adaptable to a rigidized gelatin fluted core system with minor modifications.

The Elastic Recovery material system appears to represent the lowest technical risk for an expandable structure experiment at this time. All requirements of high packaging density, reliability astronaut safety, and structural predictability are afforded by this material system. Sufficient micrometeoroid and environmental tests have been accomplished to indicate satisfactory performance for this expandable material technology in the space and launch environments.

3.2 ELASTIC MEMORY COMPOSITE SYSTEMS

The Elastic Memory Composite Systems, which were evaluated for use in the airlock experiment design, is comprised of several functional layers. This section presents the considerations applied to the final selection of the materials for the components of the composite. The techniques for fabrication were evaluated as part of the design process and are reviewed in Section 4.0, Airlock Design and Trade-off Studies.

3.2.1 EVALUATION AND SELECTION

The candidate materials for the elastic memory composite system were evaluated based on the general requirements enumerated in the introductory portion of Section 3, and on the specific design requirements of weight, packaging, availability, and processability. The selection was based on trade-off analysis in conjunction with the design studies. The principal candidates, key factors, and the selected approach are reviewed briefly in the remaining paragraphs of Section 3.

3.2.1.1 DESIGN IMPLICATIONS OF REQUIREMENTS

The prime consideration in the design of this experiment is the safety of the astronaut. Consequently the materials used in the airlock must not present any toxic, noxious or uncomfortable effects either in its original state, or as a result of any degradation which might occur due to oxidation, radiation, micrometeoroid penetration, etc. For example: In the unlikely event of a micrometeoroid penetration, the high temperatures resulting could either effect thermal degradation with attendant noxious fumes, or conceivably trigger the inflammation of the interior airlock surface materials which are exposed to the pure oxygen atmosphere with catastrophic results. Consequently, care must be excercised in selecting inner surface and immediately adjacent materials to exclude this possibility. Another example which derives from the oxygen environment is related to the nature of the materials chosen. In the event that the materials consist primarily of plastic films, fabrics, and adhesives, the hazard of friction-generated static charges by the movement of the astronaut initiating a conflagration must be taken into consideration. In addition to these and similar unique problems deriving from the chemical nature of the materials themselves, there is the obvious requirement that the bladder and associated systems be capable of withstanding a moderate amount of mechanical deformation due to the astronauts movements without losing their functionality. Finally, the physical nature of the internal surfaces must be such that no damage can occur to them or to the astronaut or his garments during occupation.

The space environment presents special problems in the selection of suitable materials. The most obvious of these is vacuum. Obviously any materials used must not undergo any significant degradation during the anticipated exposure to the space environment. If metals and/or metal fabrics are involved, this normally presents no serious problems if care is taken to exclude the utilization of the more sublimable metals such as cadmium or zinc and their alloys. Where plastics, elastomers, and adhesives are involved, this requires the selection of materials whose final functional state contain no volatile constituents, such as solvents or plasticizers.

Another consideration is the problem of radiation. Insofar as ultraviolet and other electromagnetic radiation effects are concerned, the materials selected must obviously not suffer rapid deterioration. Whereas metallic materials present no problem, some care must be taken in selecting the more radiation resistant nonmetallic materials; especially those at the outside surface. These deleterious effects are, however, somewhat mitigated by the required thermal control surface. The other major area of concern is the thermal gradients resulting from the radiation. This is, of course, the main reason for the presence of the thermal control surface. It must be recognized, however, that there will be significant temperature gradients, especially at the outer surface of the airlock walls and the films, fabrics, elastomers, and adhesives must be capable of withstanding the gradients both with respect to inherent degradation and with respect to potentially different thermal coefficients of expansion. Another space environmental effect is the zero-g field, in which none of the solid materials should experience any measurable perturbations.

Weight is an important parameter. The choice between metallic or nonmetallic structural fabrics and the ultimate selection of resins, elastomers, adhesives, etc., must be evaluated in trade-off with strength, reliability and redundance. Within the confines of schedule, reliability, and performance requirements, the lightest package is the best. For these reasons, as much as possible, the high strength-to-weight ratio nonmetallic materials for the elastic memory airlock walls appear desirable. Also for these reasons, the use of adhesives should be restricted to providing structural integrity only where absolutely necessary.

An important requirement for the airlock is a high packaged density. This places limitations on the stiffness and density characteristics of the individual fabrication materials which ultimately determine the final composite stiffness and density. Here again, there must be a trade-off among strength, flexibility, and reliability. The nonmetallic foam/fabric/film approach provides the most likely design solution.

Although the state-of-the-art of materials and their processing techniques as applicable to the airlock is well advanced, a timely program indicates that a trade-off is necessary between the "best" choice and what can be achieved within the allowable schedule.

3.2.1.2 SELECTED STRUCTURAL COMPOSITE APPROACH

In an elastic recovery material composite a flexible structural layer is used to provide strength or primary load-carrying ability of the structural wall. The conventional approach is to employ a fabric layup technique, either by goreing or flat lay-up, curvature permitting.

Alternatives such as utilization of metallic fabrics, filament winding, integral weaving and rigid-reinforced-rib approaches are less desirable. Metal fabrics, while demonstrating high potential reliability and high temperature resistance, suffer from very high weight and high costs penalties; in addition, the very high temperature stability is not required. The personnel of Aerojet-General Corporation and Space-General Corporation, who are authorities in the field of filament winding have concluded, that while the desirability of a true isotensoidal filament wound structure would be desirable, development required to apply this technique to the airlock fabrication with any real likelihood of reliability would mitigate against its undertaking at this time. In the interest of complying with certainty to the desired schedules, the filament winding approach was abandoned. Further, recent in-house developments on resin and adhesive system in conjunction with fabric lay-up techniques have indicated that this selected fabrication process could provide equivalent stress reliability with higher probability of success within a shorter schedule. Integral weaving superficially appears attractive, but the high cost and development time far outweighs the apparent advantages of a seamless structure. Further, the bonded seam techniques have been developed to a high degree of tested reliability within the SGC in-house efforts. The hard-rib approach also appears superficially to offer isotensoidal and folding configuration advantages, but this approach was earlier discarded in favor of an all fabric/foam/film approach because of the weight penalties and packaging difficulties inherent in the former.

3.2.1.3 AIRLOCK WALL CONSTRUCTION

The construction of the airlock wall is dictated in a large part by the man-rated requirements. A leakage rate of 0.5 psi of oxygen/day against a space vacuum with an inner pressure of 3.5 psig was used as the design requirement. In addition, the problem of micrometeorite protection places additional restraints on the weight, thickness, and nature of the constituents of the composite. Finally the requirement of high density packaging with subsequent elastic memory deployment establishes certain properties that the composite must demonstrate. These and other parameters which influenced the choice of the airlock wall construction are considered below.

The wall is constructed of 5 primary layers, as illustrated in Figure 3-14, designated as follows: (1) reflective coating and inner scuff lines, (2) permeability barrier, (3) structural fabric, (4) elastic memory layer and micrometeoroid barrier, and (5) micrometeoroid bumper and thermal coating. Appropriate adhesives were selected to achieve a composite construction.

3.2.1.3.1 INNER SCUFF LAYER

Starting with the inside of the airlock, the bladder composite (consisting of the inner scuff layer, permeability barrier and reflective coating) must sustain oxygen, must present a nonabrasive surface to the astronaut, must be nonstatic charge generating, must be light colored to optimize visibility, and must be composed of materials which not only are nontoxic or nonnoxious - but also will not support combustion nor produce noxious (or toxic) fumes if an unlikely micrometeorite penetration occurs. For the inner scuff layer, a thin nylon scrim cloth which has a close weave was chosen for the following reasons: (1) light weight, (2) easily fabricated, (3) bondable to the permeability barrier bladder, (4) essentially nonflammable, (5) has an elastic modulus sufficiently less than the load bearing structural fabric so that all the load may be carried by the latter, (6) high instantaneous elongation, abrasion resistant, and (7) excellent toughness. Characteristics of various candidate fabrics are given in Table 3-1.

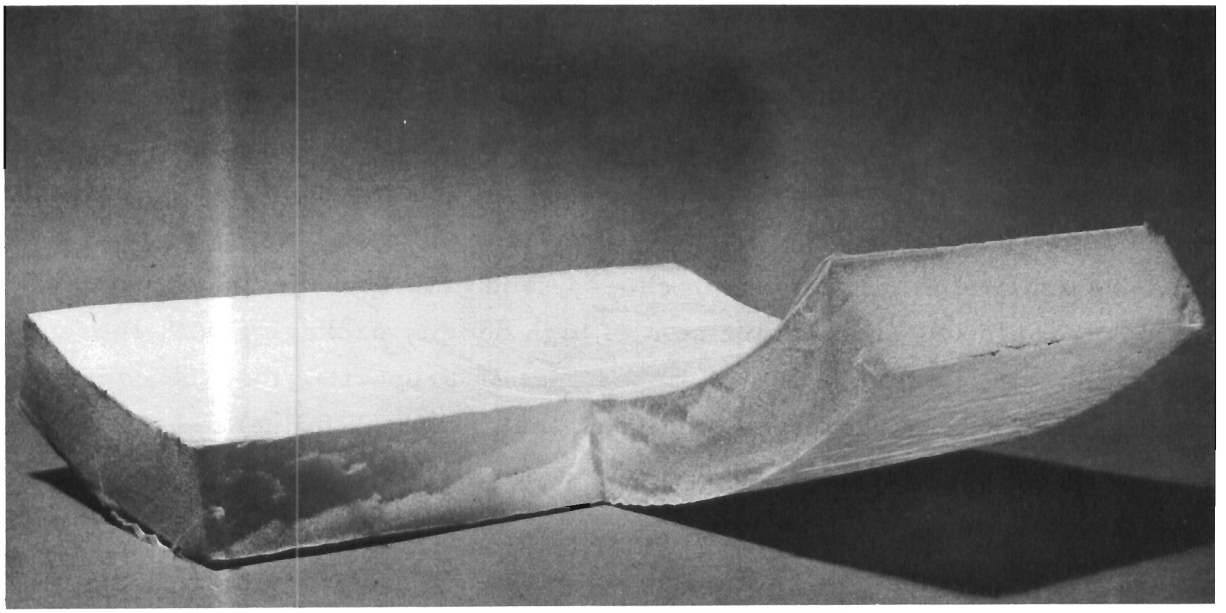

965/041

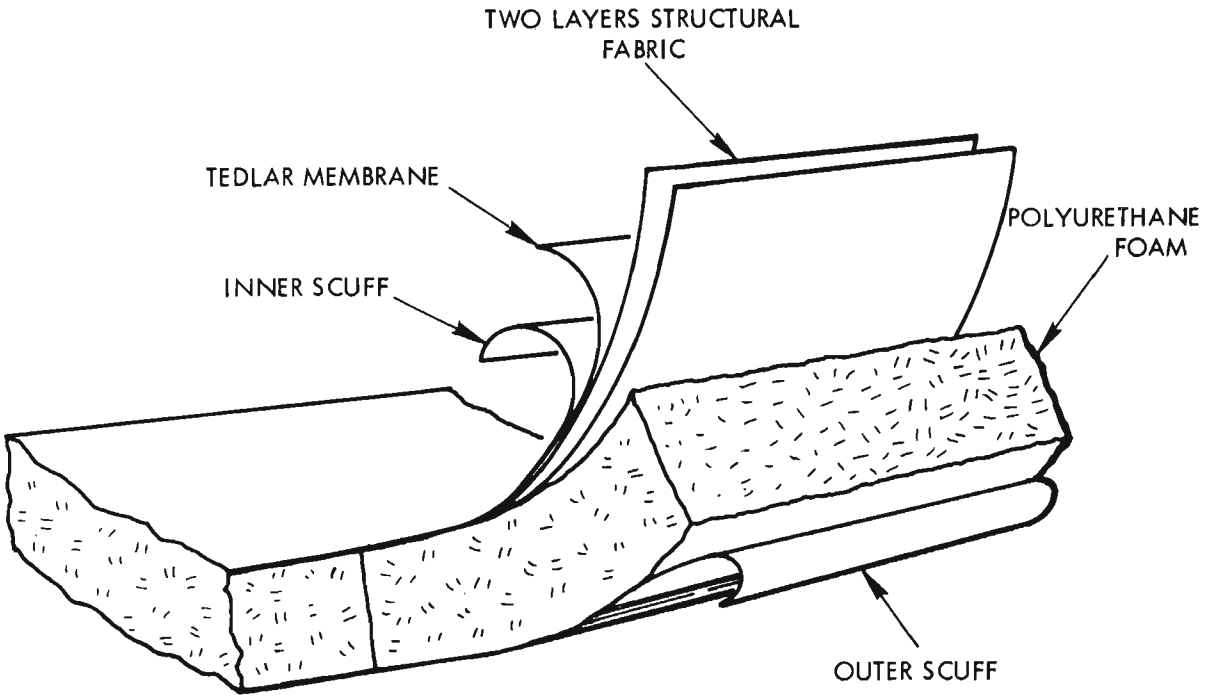

Figure 3-14. Sample Elastic Recovery Laminar Composite

Table 3-1

NYLON INNER SCUFF FABRIC

Style	Mfg.	Weight (oz/yd^2)	Tensile/Strength (lb/in.) (1) Warp	Tensile/Strength (lb/in.) (1) Fill	Elongation (%) Warp	Elongation (%) Fill	Thread Count Warp	Thread Count Fill	Gauge (in.)	Width (in.)
SN-222-ES	(3)	2.00	94 (2)	107 (2)			34	37	.0055	
SN-283-ES	(3)	2.02	134 (2)	118 (2)			38	33	.006	
N-2674-ES	(3)	2.05	142 (2)	106 (2)			40	30	.0063	
A 27 66	(4)	2.05	102	100			101	98	.005	44
SN-238	(3)	2.05	110 (2)	101 (2)			116	88	.0055	
SN-247-ES	(3)	2.05	129 (2)	114 (2)			38	34	.0061	
SN-398	(3)	2.07	80	84 (2)			72	75	.0053	
N-1605	(3)	2.10	110 (2)	76 (2)			40	28	.0055	
SN-274	(3)	2.10	110	117			77	77	.0055	
N-2615-ES	(3)	2.15	126 (2)	131 (2)			36	40	.0058	
SN-315	(3)	2.20	138 (2)	130 (2)			38-1/2	38	.006	
N-2331-ES	(3)	2.20	133 (2)	111 (2)			40	34	.0057	
N-2634-ES	(3)	2.20	116 (2)	108 (2)			40	38	.0057	
SN-87	(3)	2.20	111	114			75	77	.006	
SN-264-ES	(3)	2.20	142 (2)	124 (2)			40	34	.006	
SN-157	(3)	2.20	111	117			75	79	.0062	
SN-110	(3)	2.20	107	116			75	80	.0052	
SN-313	(3)	2.20	108	118			77	80	.0062	

(1) Ravelled Strip (1.0 in.) Method Value
(2) Ravelled Strip Method Equals 0.8 (approx.) times Grab Method Value
(3) Wellington Sears Co.
(4) Stern and Stern Textiles, Inc.

A thin nylon fabric, such as Style SN-283-ES (Wellington Sears Company) would be applicable. This fabric weighs 2.02 oz./sq yd and is 0.006-inches thick.

3.2.1.3.2 PERMEABILITY BARRIER

Permeability resistance to oxygen, high burst strength, moderate elongation, and fold endurance are required for the permeability barrier or bladder. Tedlar, Capran, and Mylar were the most suitable candidate films. Their properties are shown in Table 3-2.

Tedlar was chosen over Mylar and Capran, as a result of a trade-off evaluation of the respective properties shown in Table 3-2. Capran is considered as an acceptable alternative, except for its possible tendency upon long exposure to vacuum to lose some of its flexibility upon loss of water from its structure. Otherwise, it has the desirable properties of being self-extinguishing, has low stiffness, offers considerable elongation and has very high folding endurance characteristics.

Mylar is difficult to bond and has a high modulus. A two-layer bonded composite of 1/2 mil thickness each was chosen in order to provide redundancy against pinhole leaks in the Tedlar film material and improve the impermeability of the composite.

The bladder consists of a Tedlar-adhesive-Tedlar composite. To select the adhesive, additional materials and processes analysis effort is required. The choice appears to lie between a silicone with good non-flammability, but poor adhesion characteristics, and a polyester with the opposite characteristics. The polyester appears to be the best choice as the quantity used is too minute to constitute a flammable hazard.

3.2.1.3.3 REFLECTIVE COATING

Visual perception within the airlock can be enhanced by an inner passive coating of a passive material. The simplest solution would merely involve the use of optical brighteners on the scuff fabric. A number of

Table 3-2

PERMEABILITY BARRIER FILM

Film Class	Film Type	Tensile Strength ($\times 10^3$ psi)(1) Yield	Tensile Strength ($\times 10^3$ psi)(1) Ult.	Elong. (%) (1)	Burst Strength (psi/mil)	Tear Strength, Initial (Graves) (gm./mil)	Density (gm./cc.)	Perm. (2)	Service Temp. (°F)	Flamm.	Tensile Modulus ($\times 10^3$ psi) (1)	Impact Strength (Kg.-cm./mil)	Folding Endurance (MIT) ($\times 10^3$ cycles)	Joining (12)	Toxicity
Tedlar (3)	20	6(4)	19	110	70	452	1.38	3	-100 to 225	Slow Burn. to Self-Extng.	280	5-6	47	A(15), T	(13)
	30	5(4)	15	190	37	542	1.53	3	-100 to 225		260	4-5	5-15	A(15), T	(13)
	40	5(4)	10	260	19	634	1.38	3	-100 to 225		200	3	9	A(15), T	(13)
Capran (5)	77C(6)	?	9-12/ 10-13	350-400/ 400-500	16-18 psi(9)	500-600/ 470-520	1.13	2.6 - 4.6 (1-1/2 mil)	200	Self-Extng.	90-110/ 105-125	4.4	250/250	T	(14)
	82C(7)	?	14-18/ 11-14	250-350/ 450-550	30-32 psi(9)	950-1050/ 850-1050	1.13	?	200		95-110/ 180-200	3.6	250/250	T	(14)
Mylar (3)	A(6)	12(10)	25	120	66	600	1.395	6	-75 to 300	Slow Burn. to Self-Extng.	550	6.0	14	A(15), T(15)	(16)
	T(6)	(11)	40	50	55	450	1.377	6	-75 to 300		800	6.0	?	A(15), T(15)	(16)

(1) Machine direction (MD), except as noted to include transverse direction (TD).

(2) cc./100 in.^{2}/24 hrs./atm./mil (oxygen).

(3) E. I. Du Pont

(4) At two percent elongation.

(5) Allied Chemical Company.

(6) Thickness for data specimen: 1.0 mil.

(7) Thickness for data specimen: 1.3 mil.

(8) MD/TD

(9) Does not burst.

(10) At four percent elongation.

(11) Indeterminate.

(12) A: adhesive; T: thermal.

(13) HF is a combustion by-product or from heating near or about 400°F.; vacuum outgassing expected to be negligible.

(14) Combustion or excessive heating can generate unpleasant amide odor.

(15) Film surface must be pre-treated.

(16) No data found; not expected to be a problem.

such compounds are available commercially and can be applied from solution. Another method would utilize pigmented flexible coating on the inner side of the scuff fabric. Such a coating would have to comply with the same type. Accordingly, a titanium dioxide and aluminum or antistatic additive filled DC 92-009 silicone dispersion adhesive system has been chosen to coat the scuff surface to provide the illumination, antistatic properties and a non-flammable redundancy. This scuff surface is bonded to the bladder with unfilled DC 92-009 adhesive. See Section 3.2.2 for a detailed discussion on selection of adhesives.

3.2.1.3.4 STRUCTURAL FABRIC

The material for this layer was evaluated on the basis of strength-to-weight ratio, packaged volume, ability to be folded without property degradation, abrasion resistance, aging in the package state, thermal stability, compatibility with oxygen flammability, and availability.

Clearly, the structural requirements for the reinforcing layer is dependent upon the configuration of the expanded structure. Thus, the selection required that the basic fiber type be chosen first and then the particular fabric weave and weight selected.

The most attractive structural fabrics appear to be Dacron, Beta-fiberglass, and nylon.

Based on criteria noted above, Dacron fabric was selected as the best overall choice, with Beta-fiberglass and nylon being of lower choice in that order. This is based upon the following considerations.

a. Strength, elongation and creep.
Although Dacron, nylon, and fiberglass have high tenacity (i.e., grams per denier, hence, strength-to-weight ratio) at 75°F, the 75°F instantaneous mechanical and elevated temperature properties of nylon are significantly lower than the others. Its elongation and creep are also excessive.

b. Weight
Fiberglass has the highest strength-to-weight ratio and is the most attractive. Again, nylon is least attractive. Dacron is somewhat better than nylon but not as good as fiberglass.

c. Packaging and Folding
The self-abrasion, fold damage, and stiffness of conventional fiberglass (25.2 to 35.5 times 10^{-5} inch-diameter fiber) structural fabrics are significantly greater than with the others. Recent development of small diameter fiberglass fibers (Beta fibers - 14.5 x 10^{-5} inch-diameter fiber) reduces the above problem, but it is as yet of only limited availability.

Consequently, Dacron fabric was chosen as the most suitable overall. A selection of typical industrial Dacron constructions are shown in Table 3-3. Although the products of only two vendors is shown, Wellington Sears and Stern and Stern Textiles, similar fabrics would be available from other mills such as J. P. Stevens, and Traves Milles. Based upon primarily weight, it would appear that Style 15453 (Stern and Stern) would be a reasonable choice.

The load-carrying structure will consist of one or more layers of Dacron cloth gores and sections joined with flexible and strong polyurethane adhesive (> 400 lb/in.). The choice of one or more layers is dictated by the final design consideration and load requirements. It may be seen from Table 2.6 that several choices of structural fabric may be made depending upon the number of layers and/or the strength required. The load carrying layer(s) may be bonded to the bladder composite with the aid of an unsupported acrylic pressure sensitive transfer film adhesive. This technique provides a simplifying fabrication aid as well as composite integrity required during folding and/or deploying.

3.2.1.3.5 ELASTIC MEMORY LAYER

A flexible, open cell, polyurethane foam was found to be suitable. Although the foam's density does not appear to be critical, a lighter density foam would present less micrometeoroid protection for the same thickness and have less tensile strength (important during handling, deployment/retraction, and occupancy), and have reduced elastic memory. A thicker foam would increase micrometeoroid protection; but would represent additional weight, greater bulk, and be more difficult to fold and package. A density of approximately 1.2 lbs/cu ft, is presently considered an optimum

Table 3-3

STRUCTURAL FABRIC

Style	Mfg.	Weight (oz/yd^2)	Tensile/Strength (lb/in.) (1) Warp	Tensile/Strength (lb/in.) (1) Fill	Elongation (%) Warp	Elongation (%) Fill	Thread Count Warp	Thread Count Fill	Gauge (in.)	Width (in.)
Design			284	284						
			355 (2)	355 (2)						
FV-3696	(4)	5.10	302 (3)	303 (3)			21	23	.0102	
FV-3696-01	(4)	5.33	344 (3)	353 (3)			23	23		63
FV-2619	(4)	6.15	303 (3)	322 (3)			50	52	.0118	
15292	(5)	6.59	329.2	293.5	36.4	35.9	51-1/2	46	.0117	35-3/4
FV-1698	(4)	7.15	329 (3)	310 (3)			24	25	.0152	
15246/2	(5)	7.17	318.0	330.5			65	69-1/2	.0137	44-1/8
FV-3619	(4)	7.20	336 (3)	301 (3)			52	46	.015	
FV-3450	(4)	7.20	330 (3)	296 (3)			58	50	.014	
FV-3175	(4)	7.40	367 (3)	327 (3)			75	45	.017	
FV-3557	(4)	7.45	289 (3)	343 (3)			95	50	.0151	
FV-2994	(4)	7.50	359 (3)	398 (3)			112	63	.016	
FV-1218	(4)	7.50	290 (3)	286 (3)			27	26	.016	
FV-3745	(4)	7.51	452 (3)	322 (3)			70	42	.0161	
15, 453	(5)	7.84	343.5	288.5	45.8	48.9	56-1/2	48-1/2	.0105	32-7/8
15, 279	(5)	8.85	359.5	313.5	54.6	46.8	64	52	.0148	34-1/4
Design			568	568						
			709 (2)	709 (2)						
FV-3387	(4)	11.1	586 (3)	600 (3)	14.21 (2)	14.64 (2)	37	37	.0189	
FV-1961	(4)	12.0	570 (3)	578 (3)			35	30	.0249	
15, 141	(5)	12.57	588	596	38.8	51.5	36	36	.0246	43-1/2
FV2085-A	(4)	12.70	602 (3)	592 (3)			46	34	.0256	
FV-1794	(4)	12.90	588 (3)	612 (3)	21.68 (2)		42	36	.0253	
FV-2248	(4)	12.90	664 (3)	608 (3)			45	39	.0254	
15, 141/5	(5)	13.02	587	610	43.3	54.6	36	35	.0258	41
FV-3553	(4)	13.60	581 (3)	582 (3)			44	32	.0257	
FV3287	(4)	14.00	690 (3)	586 (3)			51	35	.026	
FV-2587	(4)	14.15	658 (3)	660 (3)			45	33	.0276	
FV-2398	(4)	14.20	598 (3)	576 (3)			46	32	.0259	
FV-2624	(4)	14.30	722	733	26.10	18.92	47	47	.0286	

(1) Ravelled Strip (1.0 in.) Method value
(2) Grab Method value
(3) Ravelled Strip Method equals 0.8 (approx.) times Grab Method value
(4) Wellington Sears Co.
(5) Stern and Stern Textiles, Inc.

choice to meet the airlock requirements. It is adequately self-supporting for handling and deployment, can accept the anticipated astronaut loads, can be packaged adequately, and has sufficient recovery characteristics under long term storage.

The elastic memory layer, as finally determined consists of a 1-3/4-inch thick, 1.24 lb/ft^3 polyurethane open cell foam, which is bonded to the structural composite with an acrylic adhesive. This foam has proved to have an excellent elastic memory retention and, in conjunction with the outer scuff and micrometeoroid bumpers described below, assures about a .9999 reliability factor against micrometeoroid penetration to conventional micrometeoroid environments. The foam layer is joined with the aid of the silicone adhesive DC 92-009.

3.2.1.3.6 MICROMETEOROID BUMPER

The material used for this outer fabric does not require high strength, as such, since hypervelocity impact does not apply a steady-state loading condition to the fabric. The primary selection criteria for this fabric are its mass and initial modulus and susceptibility to the space environment; some investigators also place limited importance to instantaneous tenacity. This suggests that bumper cloth material substitutions can be made without changing the effectiveness of the micrometeoroid protection system as long as the density per unit area is maintained. The outer fabric must also provide scuff protection to the foam portions of the composite.

The candidate materials are Dacron fabric, fiberglass, Nomex (HT-1) and nylon, and are preferred for this use in that order. This ranking is based on the following considerations.

a. The fabric should retain adequate properties at elevated temperatures in the order of 300°F which may possibly arise from solar radiation. Nylon loses strength significantly (40% of its strength at 75°F) at these temperatures, whereas the others are superior (Dacron 80%, Nomex above 90%, and fiberglass about 98%).

b. Nylon elongates and creeps excessively. Dacron and Nomex are better but not as outstanding as fiberglass.

c. The material's usefulness as a bumper is proportional to mass. The candidates would rank in accordance with their density as follows: fiberglass (2.54), Nomex (1.38), Dacron (1.38) and nylon 1.14.

d. Bonding properties are good except for Nomex.

e. Dacron, nylon, and Nomex are suitable for high density packaging, but fiberglass suffers from fiber damage with folding.

On an overall basis, Dacron is the most suitable. Beta fiberglass (fiber diameter of 14.5×10^{-5} inch compared to 25.2 to 35.5×10^{-5} of the conventional fibers) may substantially reduce the fiber damage during folding but this is to be demonstrated. Consequently, this outer layer which consists of a 17 oz per yd^2 of Dacron fabric, was selected to provide scuff protection for the foam, micrometeoroid barrier and structural integrity to the system during folding or deployment. This layer, which is bonded to the foam with the silicone adhesive DC 92-009, will be spray coated with a dispersion of Titanium Dioxide (or equivalent fillers to provide the proper α/ϵ) in DC 92-009. The final coated system will be roller-punctured (holes $\approx$ 0.1 mm diam) to permit venting of air from the open cell foam during terrestrial packaging and launch.

3.2.2 MATERIAL ADHESIVE SYSTEM EVALUATION

Numerous tensile and peel specimens have been prepared and tested to evaluate candidate adhesive systems which may be used in the fabrication of the elastic recovery laminar composite described in the previous section. The basic problem was to determine which adhesives would fulfill the structural strength and permeability requirements, and yet provide good flexibility for an expandable structure as well as permit high density packaging.

The adhesive systems fell into two basic categories; (1) structural bonds for the fabric to fabric seams, and the fabric to hatch ring

termination bonds, (2) a second type of bond is required for all of the nonstructural seams, such as Tedlar to Tedlar and foam to foam, and the interlaminar bonds such as the nonpermeable membrane to the inner scuff cloth, and the polyurethane foam to the structural fabric, etc.

The load-carrying structural fabric bonds were of primary concern as the design goal required a high strength flexible bond which could give 100 percent joint efficiency with a one inch shear lap. Several flexible epoxy and urethane adhesives were investigated for this application. A urethane adhesive system was ultimately developed which provided adequate bond efficiency while maintaining satisfactory flexibility.

The cure temperature of this adhesive is compatible with the materials and adhesives which are used in previous fabrication steps, and good stability is reported for the extremes of the space environment. The results of typical tests on flexible structural adhesives are reported in Table 3-4.

A rigid epoxy system produced the highest strength and joint efficiencies, for the structural fabric-to-metal ring bonds. Fabric to metal bonds of 600 lbs per inch were obtained, which is almost three times the margin required by the factor-of-safety design criteria. Results on three of the adhesive systems tested are given in Table 3-5.

Various silicone, polyester, and acrylic adhesives were evaluated for the nonstructural seams and the interlaminar bonds. These flexure adhesive systems were evaluated on the basis of:

a. Handleability during fabrication

b. Peel strength

c. Elongation

d. Flexibility

e. Weight

f. Stability in the space vacuum

Table 3-4

COMPARISON OF STRUCTURAL ADHESIVE SYSTEM TESTS

Type of Bond	Adhesive	Design Strength Required	Test Strength	Comments
Fabric to Fabric	"H" Epoxy	350 Lbs/In. Width	154 Lbs/In.	
Fabric to Fabric	B-9 Epoxy (Mod)	350 Lbs/In.	120 Lbs/In.	
Fabric to Fabric	M2 Epoxy	350	166 Lbs/In.	Too Rigid
Fabric to Fabric	M1 Syn Elastomer	350	109 Lbs/In.	
Fabric to Fabric	M8 Rubber	350	130 Lbs/In.	
Fabric to Fabric	U5 Urethane	350 Lbs/In.	245 Lbs/In.	Too Rigid
Fabric to Fabric	AE9 Urethane	350 Lbs/In.	315 Lbs/In.	
Fabric to Fabric	A5 Urethane/Epoxy	350 Lbs/In.	400 Lbs/In.	Marginal Flexibility
Fabric to Fabric	A1 Urethane/Spoxy	350 Lbs/In.	390 Lbs/In.	Marginal Flexibility
Fabric to Fabric	AE4 Urethane	350 Lbs/In.	380 Lbs/In.	Good Flexibility; Best-All-Round
Fabric to Metal	6010 Rigid Epoxy	215 Lbs/In.	533 Lbs/In.	Good Strength
Fabric to Metal	1838 Rigid Epoxy	215 Lbs/In.	603 Lbs/In.	Highest Strength
	AE4 Urethane	215 Lbs/In.	380 Lbs/In.	

Table 3-5

COMPARISON OF NONSTRUCTURAL ADHESIVE SYSTEM TESTS

Type of Bond	Adhesive	Primary Design Requirements	Test Strength	Comments
Bladder/Bladder (Seam)	Silicone 1	0_2 impermeability, good peel	Poor peel	Good handleability; priming improved peel strength.
Bladder/Bladder (Seam)	Silicone 2	0_2 impermeability, good peel	Poor peel	Black color considered detrimental.
Bladder/Bladder (Seam)	Silicone Pressure Sensitive	0_2 impermeability, good peel	Poor peel	
Bladder/Bladder (Seam)	Polyester 1	0_2 impermeability, good peel	Poor peel	
Bladder/Bladder (Seam)	Polyester 2	0_2 impermeability, good peel	Good peel and 0_2 impermeability	Best all-round.
Bladder/Bladder (Seam)	Polyester 3	0_2 impermeability, good peel	Good peel	
Bladder/Bladder (Seam)	Polyester 4	0_2 impermeability, good peel	Good peel	
Scuff Fabric/ Scuff Fabric (Seam)	Silicone 1	Good peel	Good peel	Good handleability; priming improved peel strength; best all-around.
Scuff Fabric/ Scuff Fabric (Seam)	Silicone 2	Good peel	Good peel	

Table 3-5 (Continued)

COMPARISON OF NONSTRUCTURAL ADHESIVE SYSTEM TESTS

Type of Bond	Adhesive	Primary Design Requirements	Test Strength	Comments
Scuff Fabric/ Scuff Fabric (Seam)	Silicone Pressure Sensitive	Good peel	Good peel	
Scuff Fabric/ Scuff Fabric (Seam)	Polyester 1	Good peel	Poor peel	
Scuff Fabric/ Scuff Fabric (Seam)	Polyester 2	Good peel	Poor peel	
Scuff Fabric/ Scuff Fabric (Seam)	Polyester 3	Good peel	Poor peel	
Scuff Fabric/ Scuff Fabric (Seam)	Polyester 4	Good peel	Poor peel	
Scuff Fabric/ Scuff Fabric (Seam)	Polyester 5	Good peel	Poor peel	
Foam/Foam (Seam)	Silicone 1	Bond Strength - Foam Tear Strength	Foam Failure	Best all-round when primer is used.
Foam/Foam (Seam)	Silicone 2	Bond Strength - Foam Tear Strength	Foam Failure	
Foam/Foam (Seam)	Silicone 3	Bond Strength - Foam Tear Strength	Foam Failure	
Foam/Foam (Seam)	Polyester 2	Bond Strength - Foam Tear Strength	Foam Failure	

Table 3-5 (Continued)

COMPARISON OF NONSTRUCTURAL ADHESIVE SYSTEM TESTS

Type of Bond	Adhesive	Primary Design Requirements	Test Strength	Comments
Foam/Foam (Seam)	Acrylic	Bond Strength - Foam Tear Strength	Foam Failure	
Outer Scuff/Foam (Interlaminar)	Silicone 1	Good peel, high elongation	Good peel and elongation	Good handleability; priming improved peel.
Outer Scuff/Foam (Interlaminar)	Silicone 2	Good peel, high elongation	Poor peel	
Outer Scuff/Foam (Interlaminar)	Silicone Pressure Sensitive	Good peel, high elongation	Poor peel	
Outer Scuff/Foam (Interlaminar)	Polyester 2	Good peel, high elongation	Good peel	
Outer Scuff/Foam (Interlaminar)	Acrylic	Good peel, high elongation	Good peel and elongation	Best all-round.
Foam/Structural Fabric (Interlaminar)	Silicone 1	Good peel, high elongation		
Foam/Structural Fabric (Interlaminar)	Silicone 2	Good peel, high elongation		
Foam/Structural Fabric (Interlaminar)	Polyester 2	Good peel, high elongation		
Foam/Structural Fabric (Interlaminar)	Acrylic	Good peel, high elongation		Best all-around.

Table 3-5 (Continued)

COMPARISON OF NONSTRUCTURAL ADHESIVE SYSTEM TESTS

Type of Bond	Adhesive	Primary Design Requirements	Test Strength	Comments
Structure/Fabric Structural Fabric (Interlaminar)	Acrylic	Good peel, high elongation	Good peel and elongation	Best all-around.
Structural Fabric/ Structural Fabric (Interlaminar)	Silicone 1	Good peel, high elongation	Good peel and elongation	
Structural Fabric/ Bladder (Interlaminar)	Acrylic	Good peel, high elongation	Good peel and elongation	Best all-around.
Structural Fabric/ Bladder (Interlaminar)	Silicone 1	Good peel, high elongation	Good peel and elongation	
Structural Fabric/ Bladder (Interlaminar)	Silicone Pressure Sensitive	Good peel, high elongation	Poor peel	
Structural Fabric/ Bladder (Interlaminar)	Polyester 2	Good peel, high elongation	Good peel	
Bladder/Inner Scuff	Acrylic	Good peel, high elongation	Good peel and elongation	Slight odor
Bladder/Inner Scuff	Silicone 1	Good peel, high elongation	Good peel and elongation	Best all-around.

Table 3-5 (Continued)

COMPARISON OF NONSTRUCTURAL ADHESIVE SYSTEM TESTS

Type of Bond	Adhesive	Primary Design Requirements	Test Strength	Comments
Bladder/Inner Scuff	Silicone 2	Good peel, high elongation	Good peel and elongation	Black color considered detrimental.
Bladder/Inner Scuff	Silicone Pressure Sensitive	Good peel, high elongation	Poor peel	
Bladder/Inner Scuff	Polyester 2	Good peel, high elongation	Good peel	

g. Thermal characteristics, and

h. Oxygen permeability (for the bladder to bladder seam).

Results of these tests are listed in Table 3-5.

Based on the results of this evaluation, a silicone adhesive was selected for bonding the inner scuff to the bladder, and a modified acrylic transfer adhesive was selected for all other interlaminar bonds.

A silicone adhesive was selected for bonding the scuff and foam nonstructural seams. A polyester adhesive was selected for the seams on the Tedlar bladders, primarily on the basis of low permeability rates in oxygen, high elongation, and excellent peel and tensile strengths.

A sample lay-up was made of the materials and adhesive systems selected for the elastic recovery airlock composite and is shown in Figure 3-14. This particular composite lay-up exhibited good overall flexibility, a weight density of 0.34 lbs/ft^2, and was representative of a section of a 48-inch diameter cylinder vessel with a 3.5 psig operating pressure. Figure 3-15 shows schematically the full system composite. Figure 3-16 shows two tensile test specimens.

To further the evaluation of this material composite design, SGC sponsored a company-funded program to fabricate a full-scale structure from this material selection. Considerable experience was obtained from the fabrication of the 38-inch-diameter x 7-foot long airlock structure, particularly in the area of the packaging and folding behavior characteristics during packaging and deployment, Figure 3-17 is a photograph of the completed structure which has been packaged into a high density configuration. Figure 3-18 shows the airlock structure fully deployed and pressurized. This elastic recovery structure has undergone numerous proof-pressure cycles at 5.5 psig and is designed to operate at 3.5 psig.

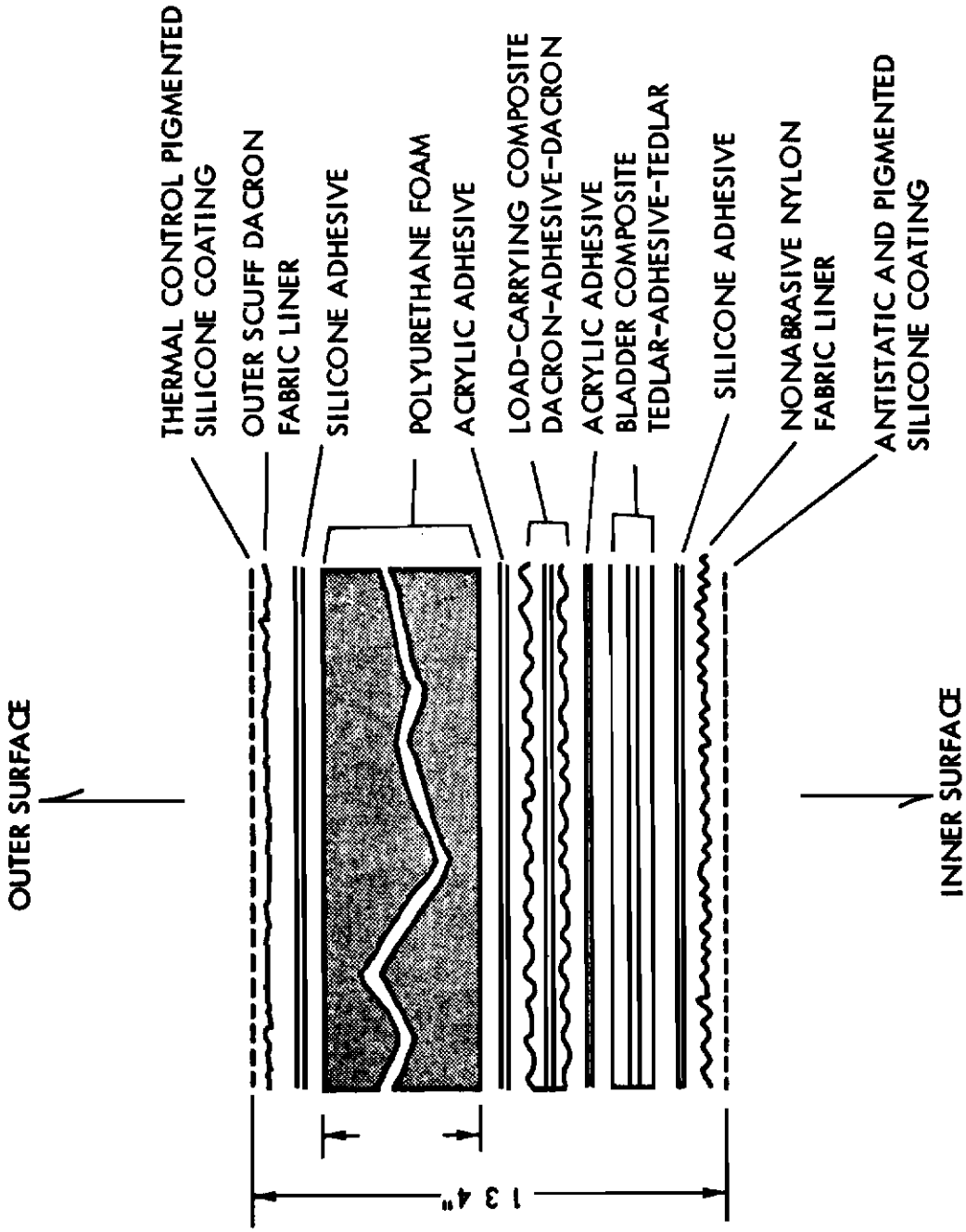

Figure 3-15. Airlock Expandable Wall Cross Section

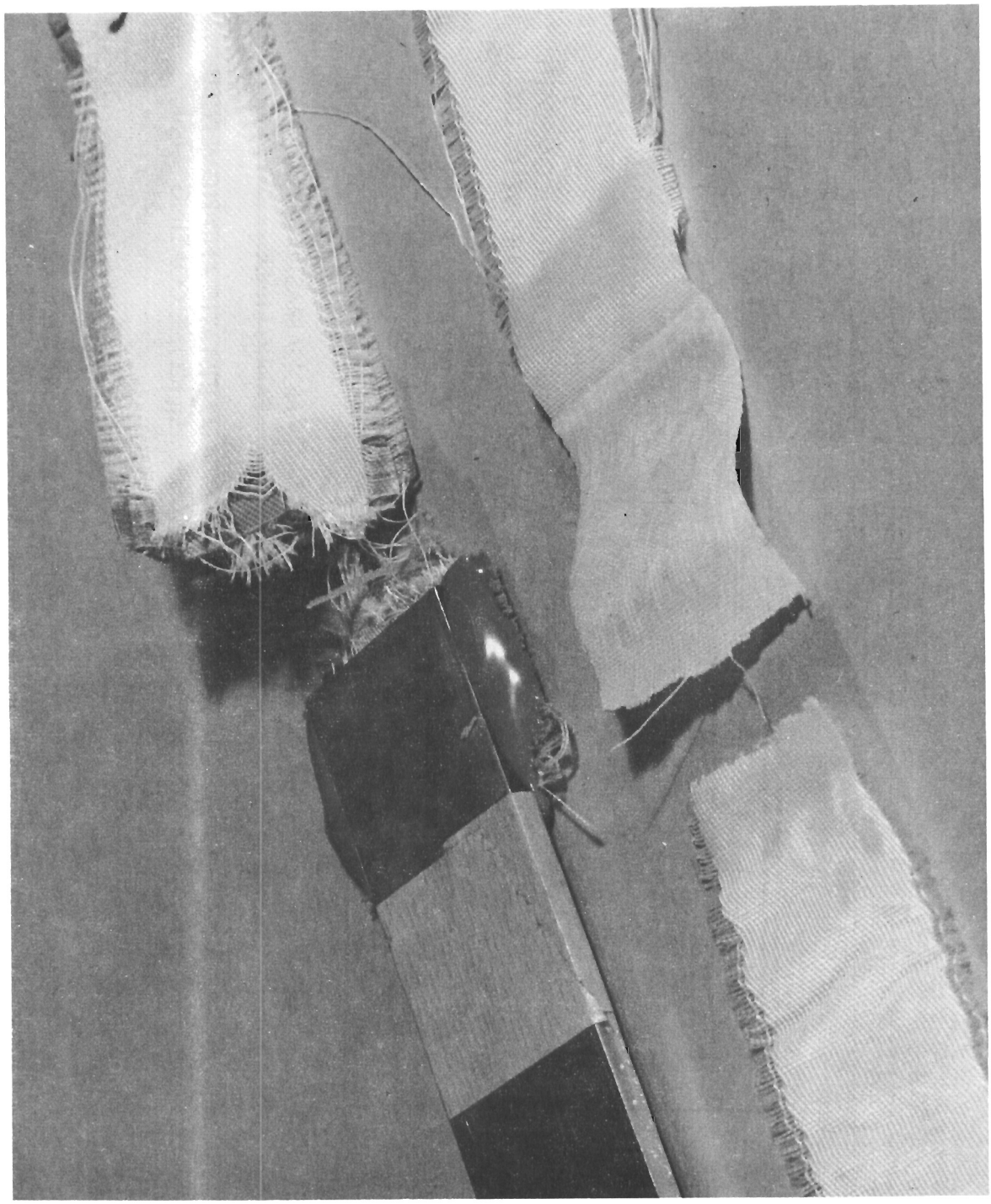

965/042

Figure 3-16. Typical Adhesive Joint Tensile Test Specimen

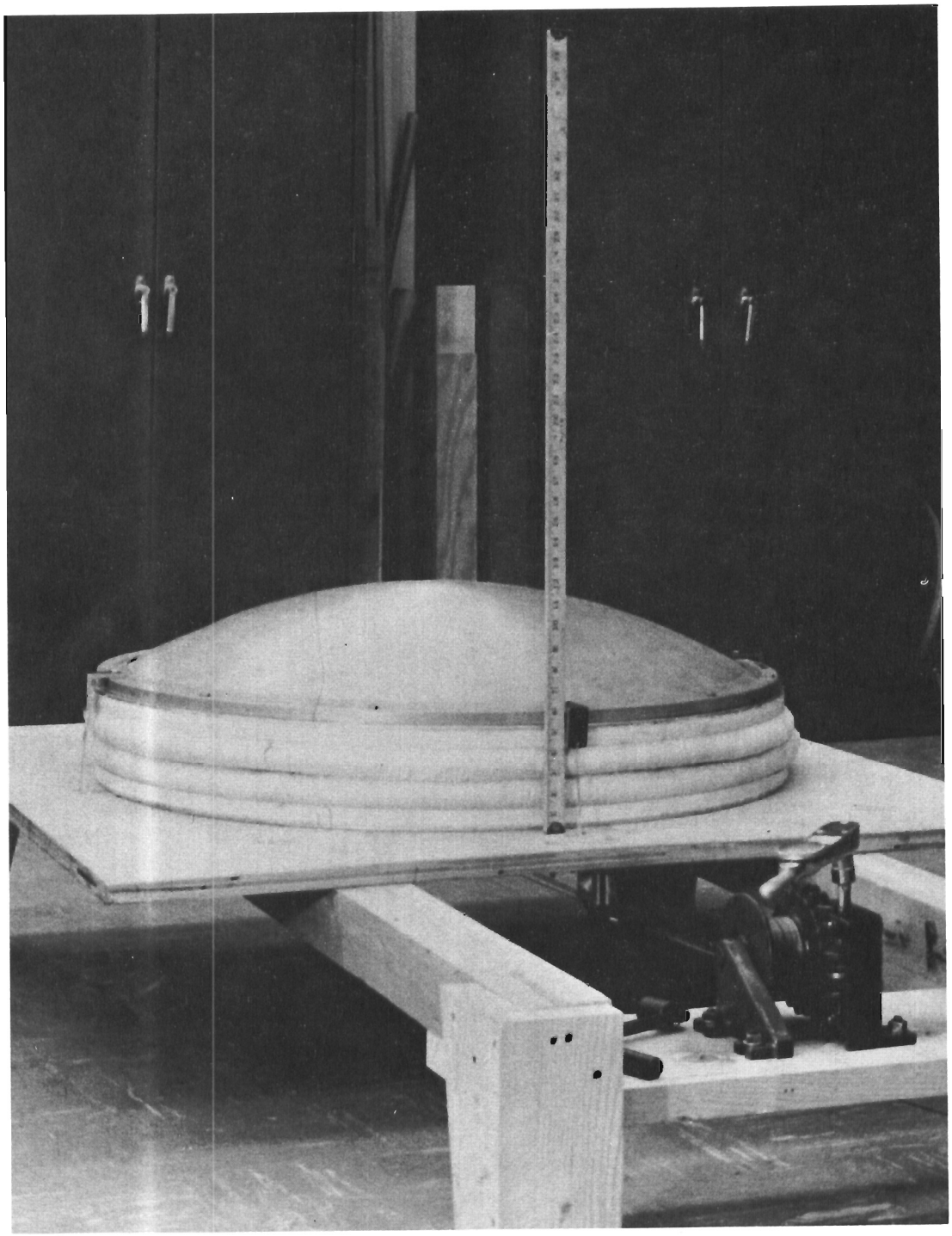

SGC/984

Figure 3-17. SGC Elastic Memory Airlock Retracted into a High Density Package

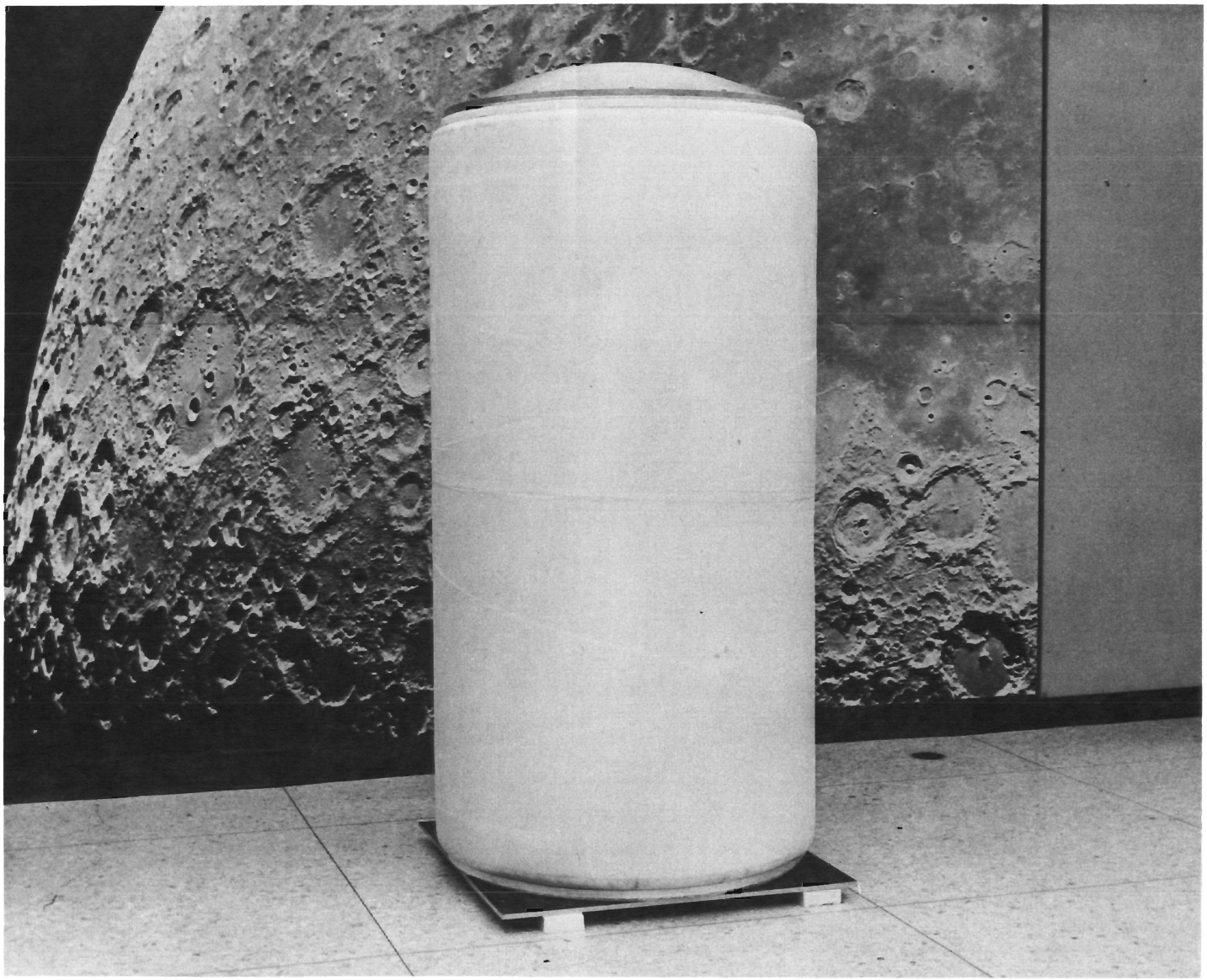

Figure 3-18. SGC Elastic Memory Airlock Fully Deployed and Pressurized

Section 4

AIRLOCK DESIGN AND TRADEOFF STUDIES

Although originally the objectives of this program were to design these experimental structures from several candidate material systems, some of which could be rigidized upon deployment in space, only the elastic recovery system appeared to exhibit sufficient technological advancement for consideration in the latter design phases. Consequently, the studies reported herein pertain primarily to an airlock design using the elastic recovery system. However, Space-General adopted the philosophy of attempting to design a basic experiment which would be capable of being adaptable to any of the candidate material systems and to any available MSL vehicle. Therefore, most of the design solution reported herein can use any material system with appropriate detail design modifications and is generally applicable to MSL-type vehicles.

During the last few months of the program, the program design effort was directed toward defining this experiment to be utilized specifically on the Saturn SIVB Spent Stage Experiment Support Module vehicle. (This vehicle was most likely to provide the first opportunity for using the experiment, and a relatively large amount of data on the vehicle was available to guide the design effort). Some design points were modified to accommodate this vehicle (such as, using a 3.5 rather than a 7.5 psig operational pressure) but these modifications only changed design details. The geometry of the airlock was also modified for the SIVB design to accommodate the results of the human factors study. These studies indicated that a 4-foot diameter by 7-foot long cylinder was not the best configuration for an operational airlock design; the geometry was modified to a spherical configuration in order to allow the astronaut sufficient room to turn around.

Both the early design results and the SIVB results are reported herein. The SIVB data is presented in greater detail in some instances because it reflects more recent and better established criteria.

4.1 GENERAL DESIGN CONSIDERATIONS AND APPROACH

The early design criteria for expandable structure airlock were:

a. Interior Geometry - diameter = 3 to 4 feet, height = 7 to 8 feet.

b. Internal Pressure - operating pressure = 7.5 psi, factor-of-safety = 5, and burst pressure = 37.5 psi.

c. Design Considerations -

(1) Astronaut safety

(2) Ease of astronaut operation

(3) Minimum stowage volume and cube

(4) Minimum weight

(5) Simplicity of installation

(6) Retractability (for low drag)

(7) Thermal control and micrometeoroid protection

(8) Hatches must be internally or externally operable

(9) Reliability

Briefly the objectives of the experiment are as follows:

a. Validate design concept of an elastic recovery airlock and establish optimum parameters for its operational use on future manned vehicles.

b. Study deployment dynamics in zero-g and space.

c. Evaluate the requirements for pressure-suited astronaut ingress and egress and simulated operational maneuvers.

d. Evaluate the expandable material system after short and long term exposure to a space environment.

The equipment is an expandable airlock constructed on an elastic recovery material system.

Launch configuration will be a package about 3 feet in diameter and 2 feet high, containing the folded airlock, its pressurization system, and suitable controls for its remote deployment and test, along with an operational control integral to the airlock for its trial operation by a pressure-suited

astronaut. The package will also contain attachment interfaces to the vehicle. System weight is estimated at 135 pounds, including a retraction mechanism.

4.1.1 AIRLOCK DESIGN

A nominal 4-foot-diameter by 7-foot-long airlock configuration was tentatively selected which could permit the rescue of an incapacitated astronaut, and for ease of ingress and egress of an astronaut equipped with an AMU and PLSS. Human factors considerations indicate that the 34-inch diameter clear hatch opening can easily accommodate the above described astronaut.

Inward and outward opening hatches were investigated and it was concluded that the inward opening configuration would be adapted to provide additional safety and reliability of sealing. The hatch may be actuated and secured from either the inside or outside to permit use by a second astronaut after the first astronaut has completed his egress. The current inward opening hatch design cannot be opened unless the differential pressure across the door has been properly vented and it is safe to do so. This is particularly important from a safety standpoint, as residual gases in the airlock could conceivably propel an untethered astronaut from the open airlock if the pressure was too high when the hatch was opened.

4.1.2 CYLINDER WALL CONFIGURATION

Two types of wall configurations using the elastic recovery material system were considered, one using straight sides and another using convoluted sides. The convolutes are preformed concentric rings and have a hoop hand at the inner apex to reinforce the structural fabric and maintain the circular shape. The convolutes provide a controlled folding schedule of the elastic walls during retraction of the airlock.

The straight-sided configuration was selected for design because it demonstrated the feasibility of folding the airlock without complicating the cylinder design and fabrication by incorporating convolutes. Also, the rigid hoops are incompatible with the requirement that the deployed diameter is larger than the packaged diameter. The multilayered composite wall construction for this design consists of an elastic-memory foam core with a

thermal-control coating on the outside and the structural fabric, sealing membranes and a scuffcoat on the inside. The total wall thickness would be approximately 1-1/2 inches. This foam thickness was coordinated with the micrometeoroid shielding criteria discussed in subsequent sections of this report.

The straight-sided cylinder has a tendency to buckle in an irregular manner during retraction, which would prevent an efficient folding schedule unless restrained or guided during folding by an external support. A study has indicated that utilization of four retraction cables could restrain the cylinder walls during retraction, and a reasonably predictable and efficient folding schedule would be obtained. This requirement is accomplished by straps which attach the structural fabric to the cables. As the cables become taut, the straps produce a radial tension load on the cylinder wall, thus initiating a fold. During retraction, the folds are stacked and compressed to the desired height. This concept is seen in Figure 4-1.

It may also be noted that, when fully extended, the wall attachment points cause the relaxed cables to lay close to the inner structural walls, providing maximum operational ingress and egress aperture, while still allowing the cables to be used for locomotion aids. The preliminary indications are that the operational retracted height will be about 15 inches.

4.1.3 RETRACT MECHANISM

The retraction of the cylindrical airlock is accomplished by the four cables attached to the upper cylinder ring and accumulated on a thin drum which revolves peripherally around the lower base of the airlock. The drum is cable-driven by a geared motor.

The retraction load is determined by the force required to compress the elastic foam walls of the cylinder. Based on Space-General experimental data, a maximum design load of 320 pounds, with a safety factor of two, was assumed to compress the cylinder. These high compressive loads occur only at the very last few inches of retraction. Intermediate compressive loads are on the order of 50 lbs.

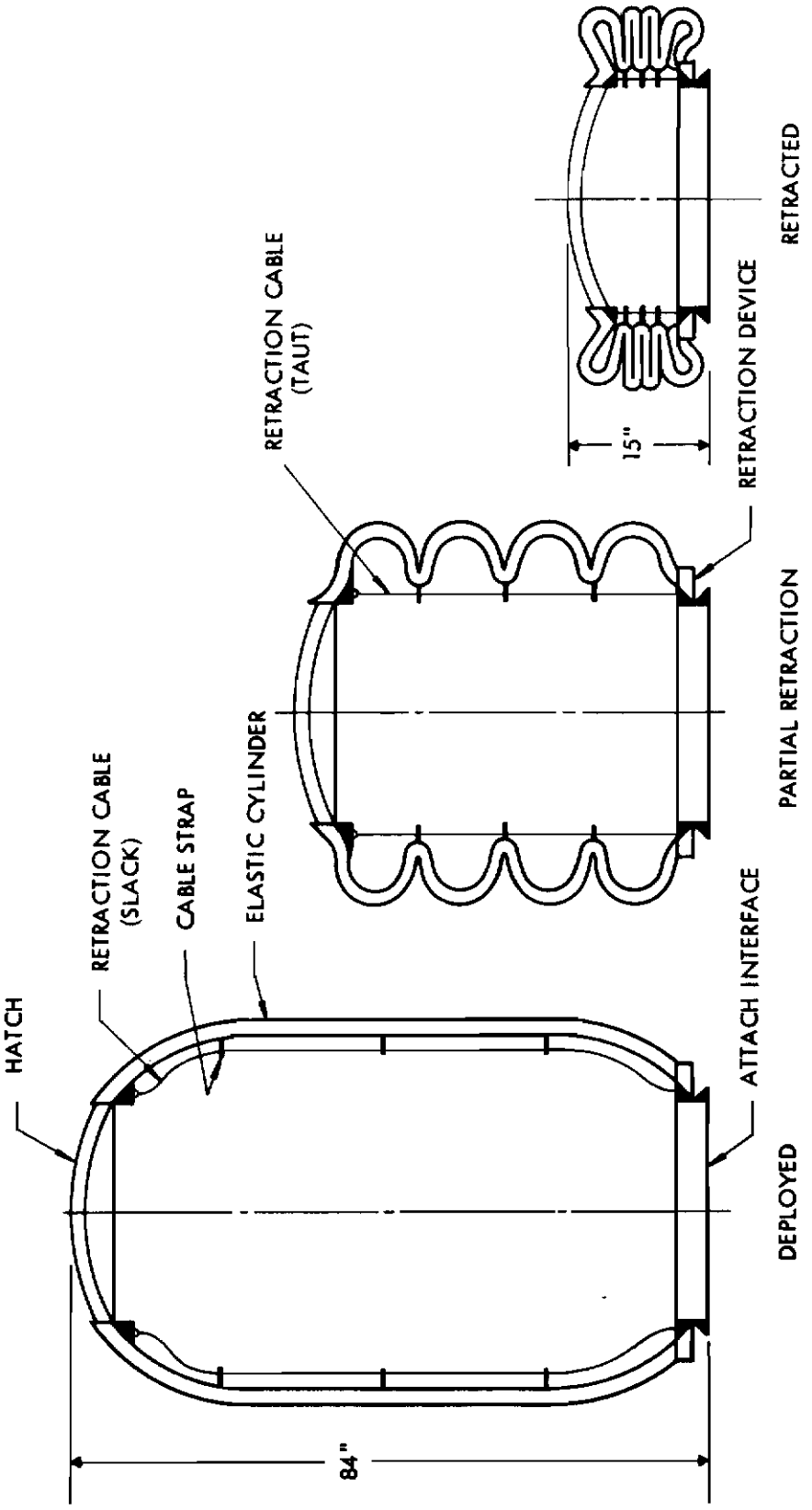

Figure 4-1. Airlock Retraction Sequence

In selecting the motor and gear ratio it was assumed that the cylinder retraction time would be 1 minute. Based on this retraction velocity, the cable drum would rotate at 0.71 rpm and require a torque of 5120 in/lb. Using a 1.4-inch driving drum, a motor torque of 0.5 lb/in with a gear ratio of 540:1 would be required to hold the airlock in the retract position.

4.1.4 THE RIGIDIZED GELATIN SYSTEM AIRLOCK

Several methods for deploying the flutes in the fabric-structural walls have been investigated. These have included the use of film and elastomeric tubes inserted into the flute and various methods for pressurizing the fluted area directly. The method which appears to offer the most possible involves direct pressurization of the flute area during rigidization, at a pressure less than the internal cylinder pressure by use of a relatively impermeable membrane of the "B" staged gelatin in the outer fabric, serving to prevent all but minor leakage through the outer fabric. Controlled venting of the pressurizing gas will permit water vapor to be removed and a reserve gas supply will supplement the water vapor boil-off, keeping the flute erection pressure constant during rigidization.

4.1.5 ADDITIONAL AIRLOCK DESIGN STUDIES

Studies and analysis of the airlock structural design were performed. After the geometry had been established it was necessary to conduct further analysis on the material strength requirements for that particular configuration as well as fabrication techniques for the application of the structural fabric. One of the analytically indeterminate factors in fabric structural systems is the percentage of load which will be shared by a fabric joint in a laminar composite when paralleled by other continuous layers. It would appear that a fabric lap joint would be stiffer than any other single layer of parallel fabric and would, therefore, load up more than other parallel joint-free layers due to the higher effective modulus of the joint. This effect is, of course, dependent on the shear transfer characteristics of the interlaminar bond, and the shear modulus of the joint adhesive.

Test results from a SGC-sponsored program on the fabrication of a similar expandable elastic recovery airlock clarified many of these indeterminate factors. The bonded seam was developed to exhibit 100% joint efficiency

from a flexible adhesive system and was shown to contribute to the overall structural behavior by acting as reinforcing bands or straps.

4.1.6 ANOMALIES OF NONRIGID STRUCTURAL GEOMETRY UNDER LOAD

Analysis of the loads in a 4-foot diameter by 7-foot-long pressure vessel with hemispherical ends shows that for an operating pressure of 5 psig, with a safety factor of 5, i.e., 25 psig ultimate, the hoop and longitudinal loads in the cylindrical section are 600 lb/in and 300 lb/in, respectively. In the hemispherical ends the stresses are equal and orthogonal at 300 lb/in. However, these stress levels will be in error by approximately 30 percent when applied to an airlock structure utilizing Dacron fabric load-carrying systems, due to the high elongation characteristic of the material which increases the effective diameter by as much as 40 percent at ultimate load or 19 inches. Figure 4-2 shows the percentage elongation versus load for a test specimen of Stern & Stern No. 15530 Dacron fabric.

An airlock design incorporating this fabric would exhibit a structural geometry change as a function of pressure as discussed above. A curve of the variation in geometry and specific stress (lb/in) as a function of pressure is seen in Figure 4-3. For reference, a dotted line is superimposed to illustrate the performance of similar vessel of a high modulus material such as steel which would not appreciably change its size. Although the fabric elongation can be coped with in a nonrigidized airlock design, the allowable fabric elongation of an impregnated rigidized system will depend on the modulus of the impregnant. This would indicate that a rigidized system design may be elongation limited, rather than stress limited, resulting in a weight penalty.

4.1.7 AIRLOCK FABRIC TERMINATION RING DESIGN

The change in geometry discussed in the foregoing section must be considered at the fabric-to-metal rings at the ends of the cylinder. Since the aluminum rings are relatively inelastic, thereby maintaining a constant diameter, a change in the stress vector angle will be incurred at the fabric/metal interface at different pressures. This phenomenon complicates the concept of

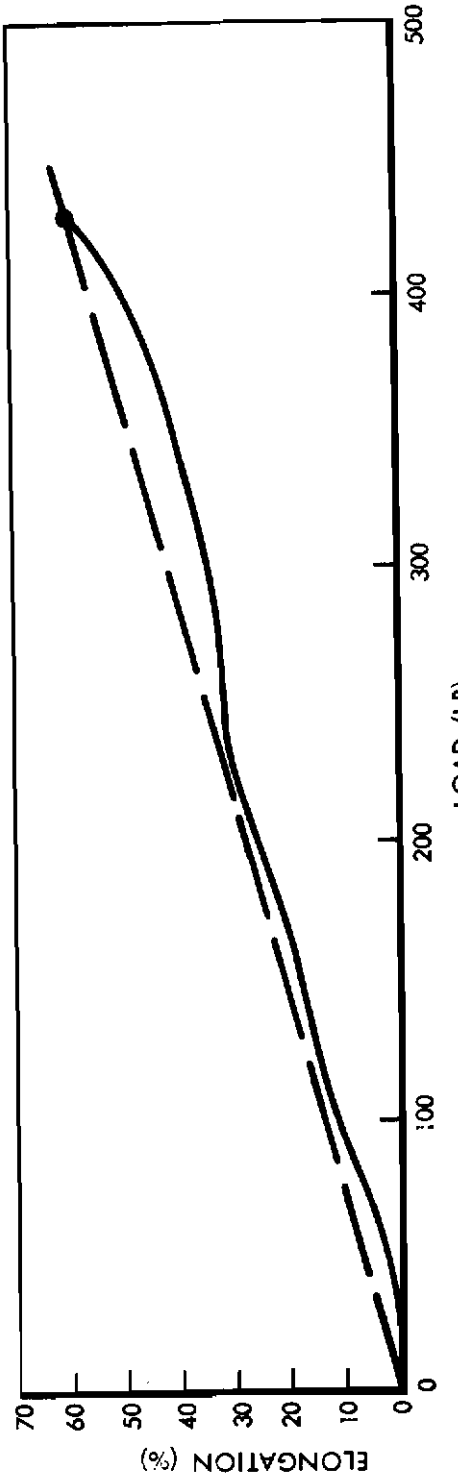

Figure 4-2. Percentage of Elongation as a Function of Load for a Sample Dacron Fabric (Stern & Stern No. 15530)

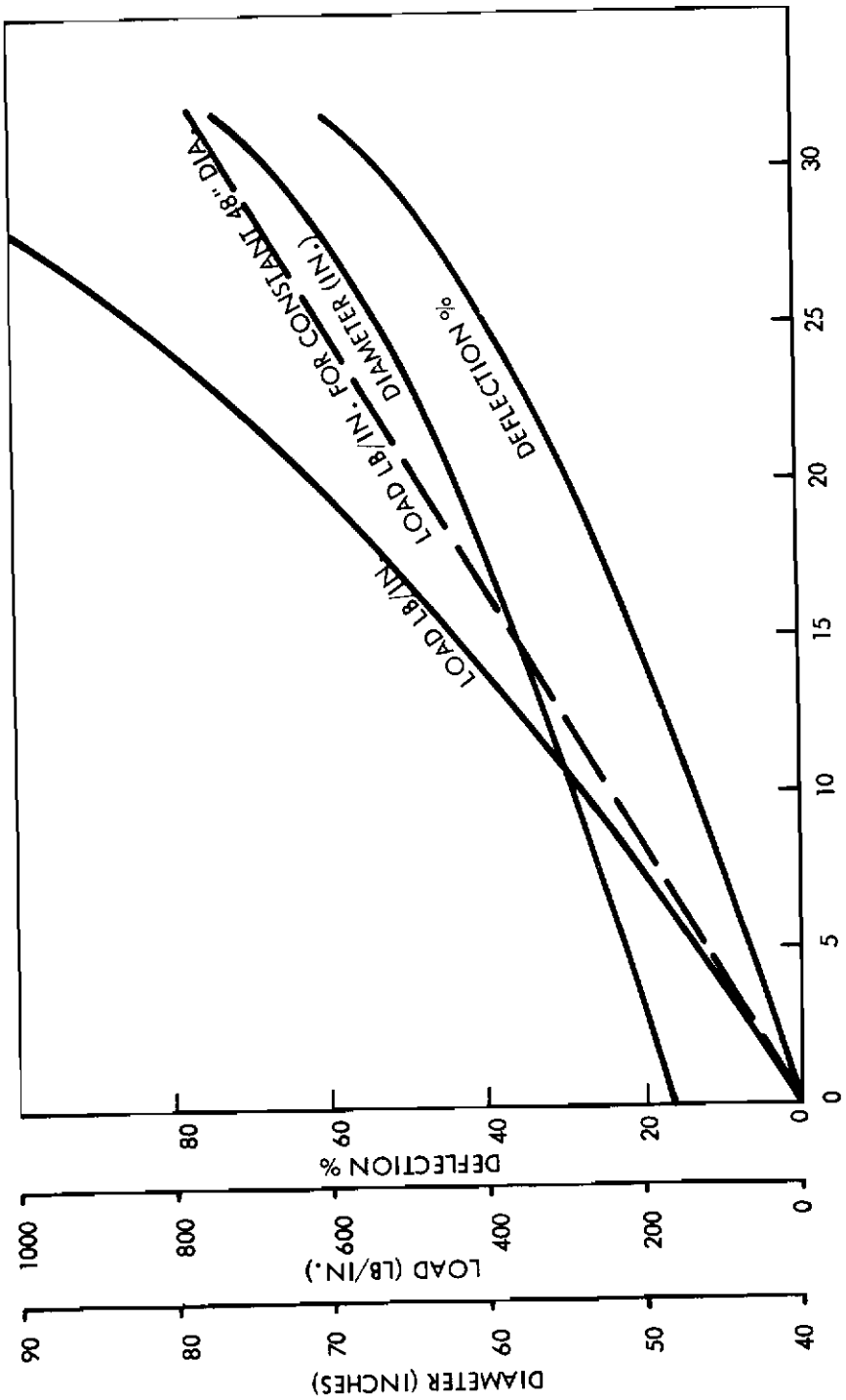

Figure 4-3. Variation in Geometry of a Dacron Fabric Pressure Level Under Load

safety factor, as the force vector of the fabric should pass through shear center of the metal ring to minimize the local bending moments. To design the ring so that no rotational moments are introduced at burst pressure compromised a weight penalty on the ring design for operational pressures, over and above a factor-of-safety of five on the stress levels occurring at operating pressures of 5 psig.

The preliminary design philosophy is to design the ring geometry so that at a proof pressure of 11.5 psig no significant rotational moments are introduced by the variation of resultant force vectors at the fabric/ring interface. Also, the ring will be sized to provide a factor-of-safety of 2.0 at a proof pressure , thus a factor-of-safety slightly greater than five is obtained at operating pressure (for the load vector orientation encountered at proof pressure), which should be the highest test loading condition applied to the structure. Eleven and one-half psig proof pressure represents approximately 150 percent of 7.5 psig which is the highest operating pressure for which the structure is designed.

Although earlier in this program the design of the fabric-to-ring interface proposed that the fabric be attached to the outside of the ring, later considerations of the diameter growth indicated an inner side termination would eliminate the peeling loads imposed by the vector rotation at the metal rings. It should be noted the actual vector rotation is not large, only 3.5^{o} at 11.5 psig relative to the load vector direction at 5 psig operating. This may be seen in Figure 4-4, showing a typical diagrammatic fabric termination and hatch seal cross section.

4.1.8 LSS CONSERVATION CONSIDERATIONS

Calculations were performed to evaluate the quantity of life support system (LSS) atmosphere saved by using an airlock of this design over that which would have to be expelled were the 5 by 10-foot-diameter pressurized section of the MSL vehicle if used as an airlock. It may be seen in Figure 4-5 that only 8 or 9 pressurization cycles would save an LSS gas weight equal to the weight of the expandable airlock.

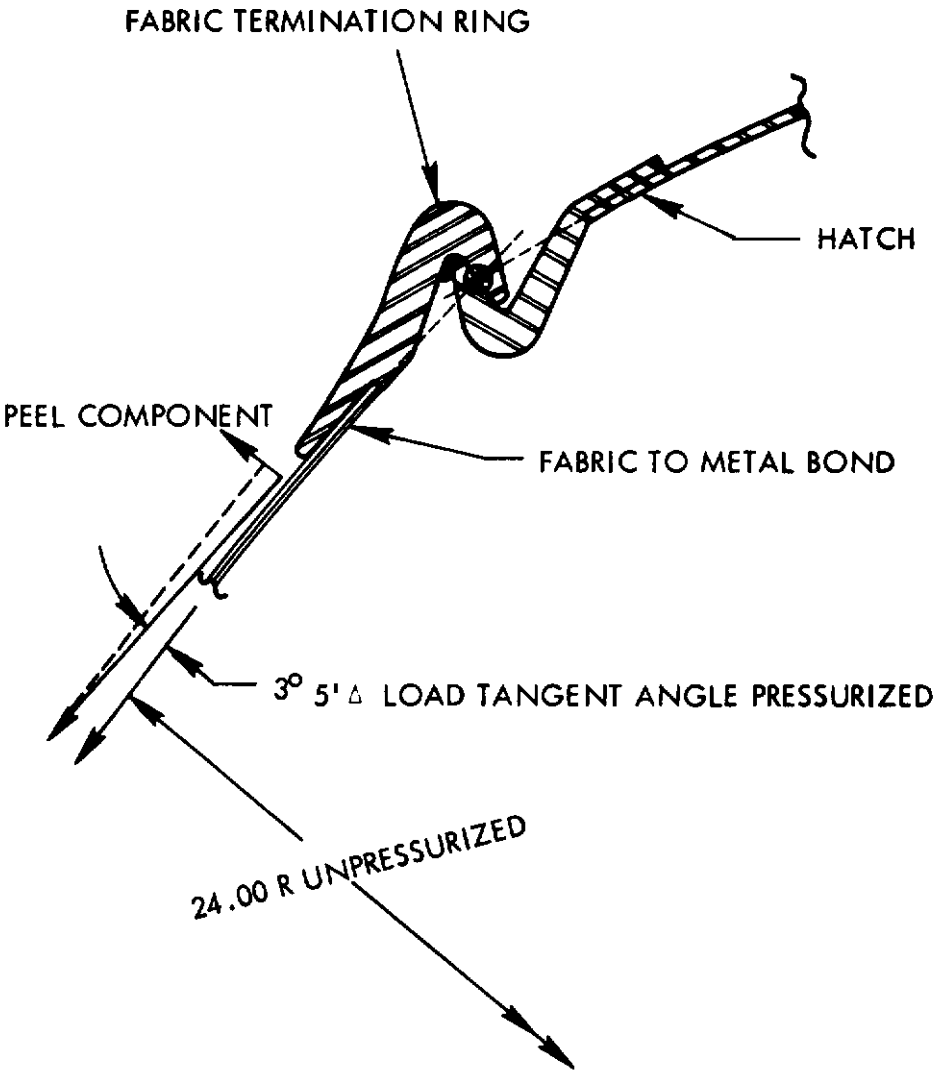

Figure 4-4. Typical Diagrammatic Crosssection of Fabric Termination Ring and Hatch Interface

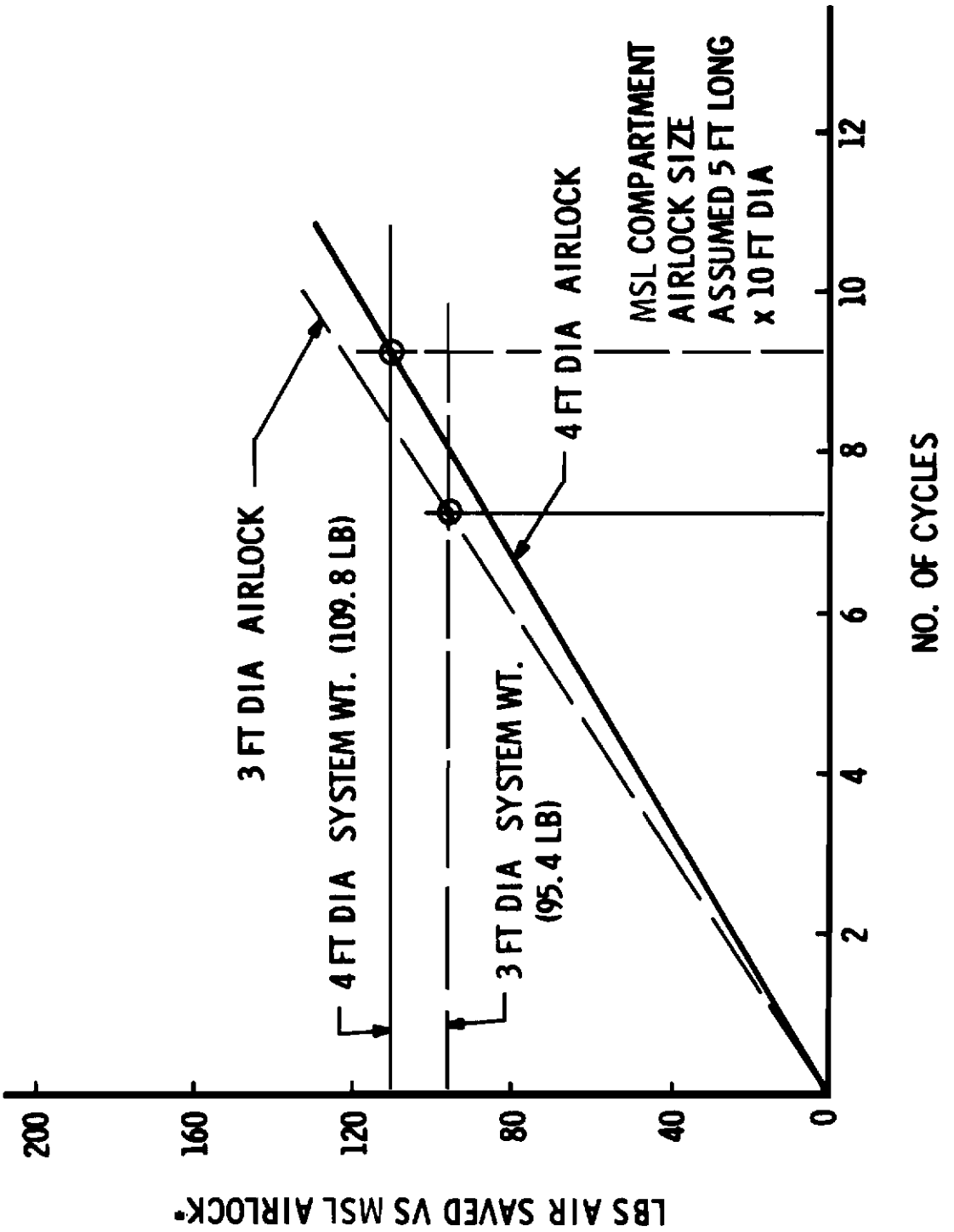

Figure 4-5. Air Weight Saved by Expandable Airlock

4.2 MECHANICAL DESIGN

4.2.1 HATCH AND FABRIC RING DESIGN AND ANALYSIS

The basic ground rules for design of the hatch subsystem are:

a. It will be capable of operation from inside or outside the airlock by an astronaut wearing an Apollo Block II pressure suit with an EVA garment and a portable life support backpack.

b. It will be as fail safe as practical for astronaut safety and should be designed to avoid jamming from cold welding or thermal distortions.

c. The sealing capability should be consistent with the airlock low-leakage requirement.

d. Weight will be minimized.

e. Materials will be protected from corrosion.

Both inward and outward opening hatch configurations have been investigated. A comparison of these two approaches is seen in Table 4-1. The inward opening hatch has been selected as the primary candidate for the baseline airlock for three reasons:

a. It is fail safe in that it cannot be opened when the airlock is pressurized.

b. The self-plugging feature for sealing.

c. The lower weight.

The results of a weight study indicate that approximately a 20 percent weight savings can be realized by the inward opening hatch design over the outward opening design in the ring weights alone. The outward opening concept would be further penalized considering a heavier hatch-locking mechanism. The basic reason for this difference is that the inward opening hatch is supported continuously about its circumferential seal, while the outward opening hatch must be supported at specific points or dogs. Weight in the hatch end closures is of particular importance since they represent a significant percentage of the airlock weights.

Table 4-1

TRADE-OFF EVALUATION OF INWARD VERSUS OUTWARD OPENING HATCH

Considerations	Inward	Outward
1. **Safety**	**Excellent (Fail-Safe)**	**Fair**
2. **Ease of operation**	**Excellent**	**Poor - locking operation difficult**
3. Stowage and swept volume	Poor	Excellent - clear of ingress or egress path
4. Weight	Low	Heavy - heavier rings and locking mechanism
5. Sealing	Excellent (operating pressure assists sealing)	Dependent upon latch mechanism integrity
6. Closing after egress	Fair	Excellent - simple
7. Opening for ingress	Good	Excellent
8. Lock mechanism	Excellent (Fail-Safe)	Complex
9. Fabrication complexity	Simple	Complex

The one disadvantage of the inward opening hatch is the requirement that it be brought inside for stowage. It is believed that the advantages outweigh the disadvantages when there is sufficient space for stowage inside. The 48-inch diameter cylinder airlock appears to provide this space.

In the preliminary MSL airlock design for a 4-foot-diameter by 7-foot airlock, the hatch is supported by a hinge structure which controls and guides the hatch during the opening, stowage, and closing operations, thus keeping the operating effort at a minimum. See Figure 4-6. The hinge structure folds during prelaunch packaging to facilitate a high packing density. This concept was abandoned in later SIVB airlock designs because of weight and design complexity.

Optimum hatch and ring design for minimum weight can be realized if discontinuities are minimized and rings are designed to be a continuation of the load-carrying fabric and dome membranes. The hook configuration shown in Figure 4-7 reflects such a minimum weight design.

Numerous methods for holding the inward opening hatch in place and for initially compressing the seal have been considered. Included were individual latches, multiple latches driven by mechanism, breech lock devices and others. The best method from a reliability, weight, and fabrication standpoint appears to be one where the hatch is snapped or plugged into place and airlock pressure is employed to compress the seal. This concept, shown in Figure 4-7, consists of a soft O-ring which is used to hold the hatch in place and, in addition, forms a secondary seal. The primary seal is a Viton or butyl O-ring which is retained in a dovetail groove. To aid the astronaut in seating the hatch, lead-in chamfers are provided on both the hatch and the fabric termination ring. The use of the secondary seal will permit the use of airlock internal pressure to force the hatch outward and compress the primary seal.

A pair of handle operated locks have been provided to prevent accidental hatch opening during launch, deployment on retraction. These locks are detented in both positions. The use of these locks would not necessarily be required for normal astronaut EVA operations. These handles may also be used by the astronaut in handling the hatch.

AIRLOCK (48" DIA)

HATCH - INWARD OPENING GEOMETRY WITH OVERHEAD DOOR TYPE HINGE

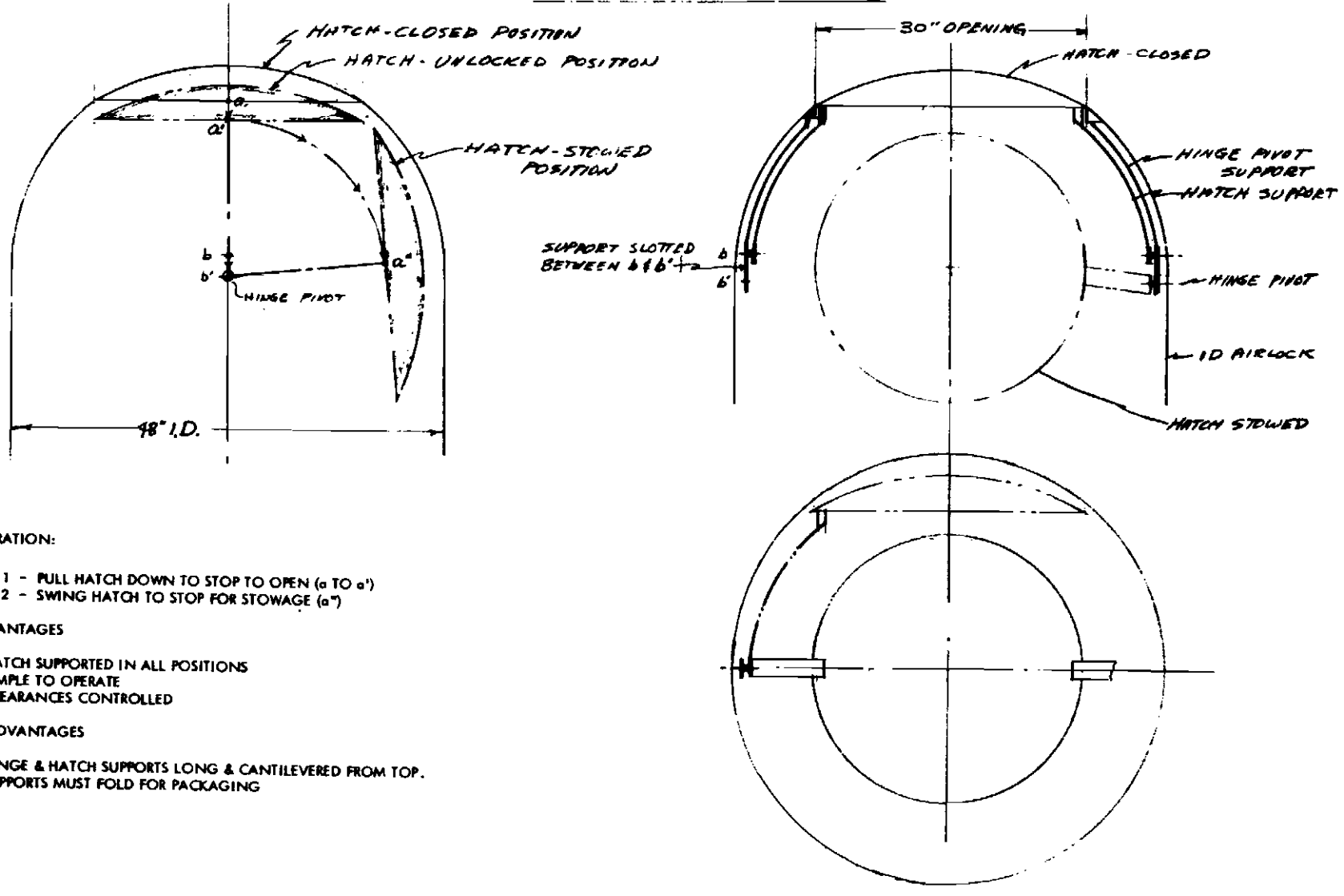

OPERATION:

STEP 1 - PULL HATCH DOWN TO STOP TO OPEN (a TO a')
STEP 2 - SWING HATCH TO STOP FOR STOWAGE (a")

ADVANTAGES

- HATCH SUPPORTED IN ALL POSITIONS
- SIMPLE TO OPERATE
- CLEARANCES CONTROLLED

DISADVANTAGES

- HINGE & HATCH SUPPORTS LONG & CANTILEVERED FROM TOP.
- SUPPORTS MUST FOLD FOR PACKAGING

Figure 4-6. Hinge structure

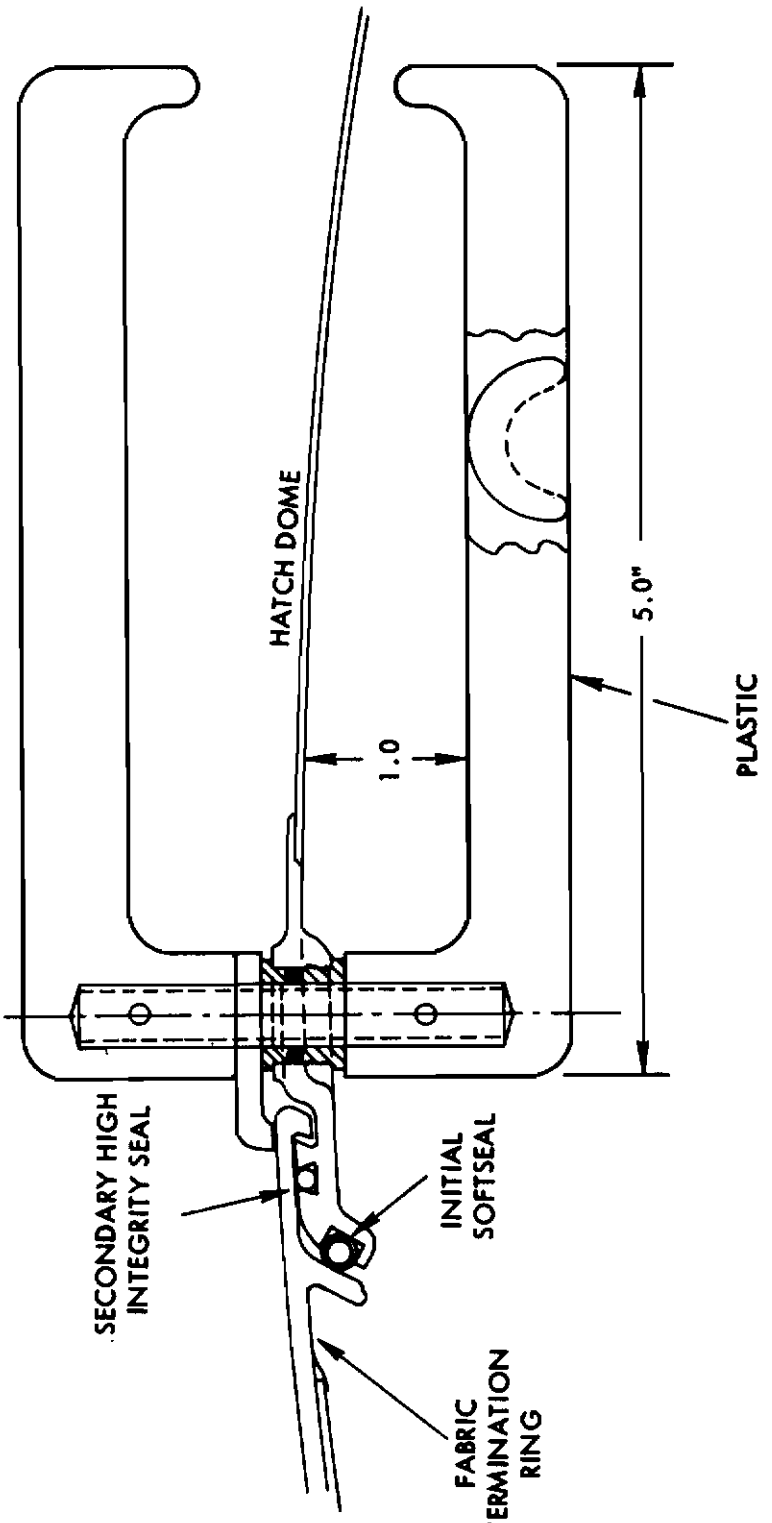

Figure 4-7. Hook Configuration

The design as shown is believed to have several significant advantages:

a. No indexing is required and it is therefore more easily installed by the astronaut particularly from the outside.

b. The hatch will stay in place and therefore does not have to be held by the astronaut for locking.

c. There are few moving parts making it very unlikely that the hatch will jam.

d. Redundant sealing is provided.

The primary material candidate for the hatch and ring is aluminum alloy. The use of reinforced plastics or fabrics for the hatch dome may also be considered. Metal parts will be coated, where required, to prevent corrosion. In addition, solid lubricants or coatings will be applied where cold welding of mating parts could occur.

Lower Structure

The lower structure consists of a fabric termination ring, vehicle attach clamp, retraction mechanism and other interface connections. For the SIVB configuration, a base assembly structure is attached to a lower dome.

A segmented V-band type clamp with two disconnect latches is utilized to provide a simple method of releasing the airlock from the deployment boom so that it may be removed and attached to the MSL EVA hatch. Each latch has two handles to provide a scissors-type action for the opening or closing operation. The clamp is attached to the airlock to prevent it from being a loose part in the open position.

Retraction for an MSL airlock will consist of a drum and drive mechanism which will be installed in a cam around the outside of the lower fabric termination ring. Figure 4-8 depicts this configuration. Retract cables will be on the outside of the airlock.

4.2.1.1 STRUCTURAL ANALYSIS

The following structural analysis was performed to adequately determine weights and to insure integrity of the design for the SIVB. The upper and lower closures are spherical segments.

SCALE: 1/1

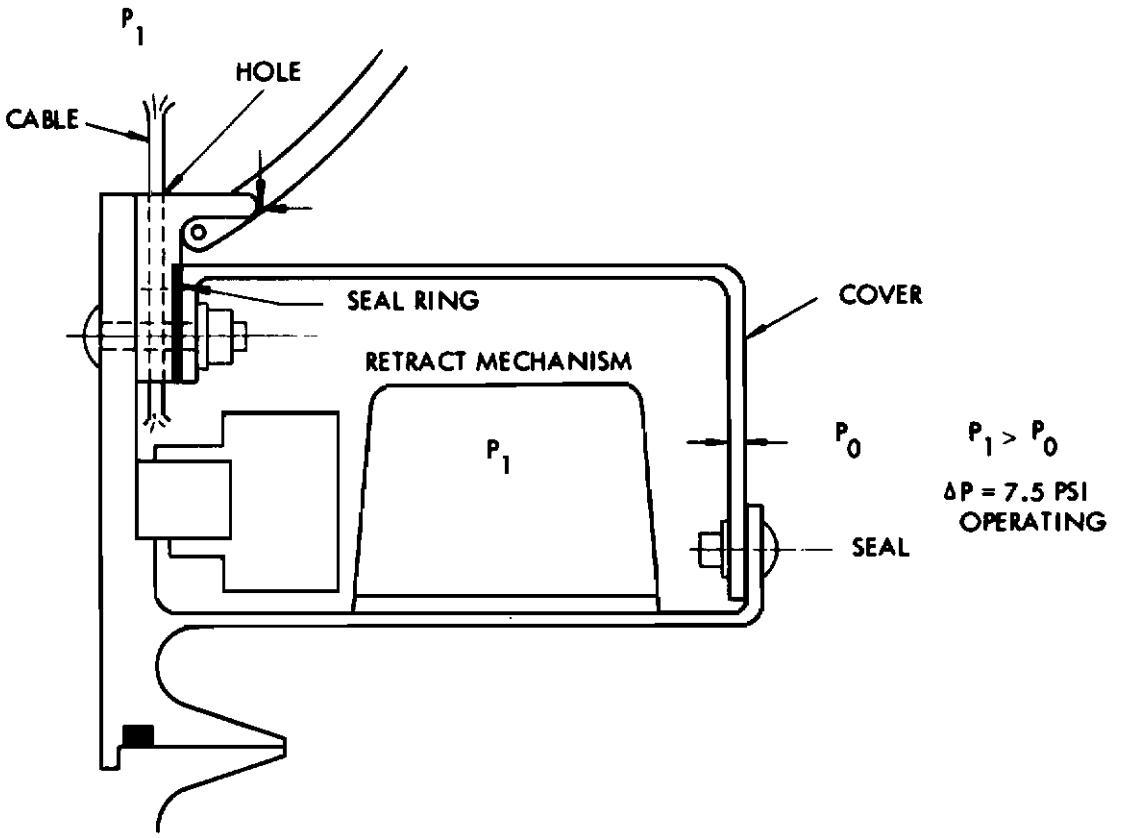

ADVANTAGES

1. SATISFIES REQUIREMENTS
2. NO CRITICAL FITS

DISADVANTAGES

1. COVER WILL DISTORT UNDER ΔP
2. COVER TO SEAL RETRACTION ASSEMBLY HEAVY
3. SEALING FAIR
4. ACCESS TO RETRACTION ASSEMBLY POOR
5. FABRICATION & ASSEMBLY POOR

Figure 4-8. Airlock Lower Attach Ring Cable Sealing Concept, Pressurized Cover

The hatch cover attach ring (6061-T6 aluminum) is subjected to an inward radial loading causing compressive stresses until this load deflects the ring inward an amount equal to the initial tolerance gap between the inner and outer ring hook. The ring is also subjected to compressive stresses due to twisting moments induced by eccentricities of the ring centroid and hatch-dome skin contour. Until the tolerance gap between the hatch ring and frame goes to zero, the dome is not in membrane tension. The critical load for the cover ring was calculated, based on the equation:

$$N_{cr} = \frac{3EI}{R^3}$$

where E is the modulus of elasticity

I is the area moment of inertia

R is the centroidal radius of the ring

The lower cover is joined to the head by a thicker cylindrical ring approximately two inches in height. The cover ring and aft end of the cylinder are machined in the form of a Marmon fitting. As in the forward cover, the aft cover ring is subjected to inward radial loads.

Based on the above equation, the critical load was calculated. The cylindrical transition ring was analyzed assuming it acts as a narrow ring under distributed torque equal to the vertical component of the meridianal load times the misalignment moment of the cover to the curvature of the head. 7075-T6 aluminum was selected as the material for this ring due to relatively high stress.

The Marmon strap was assumed to carry the longitudinal load resulting from pressure plus a moment resulting from strap eccentricity to the outer diameter of the cylinder. Material allowables were based on 301 stainless.

INWARD OPENING HATCH
SPHERICAL CONFIGURATION

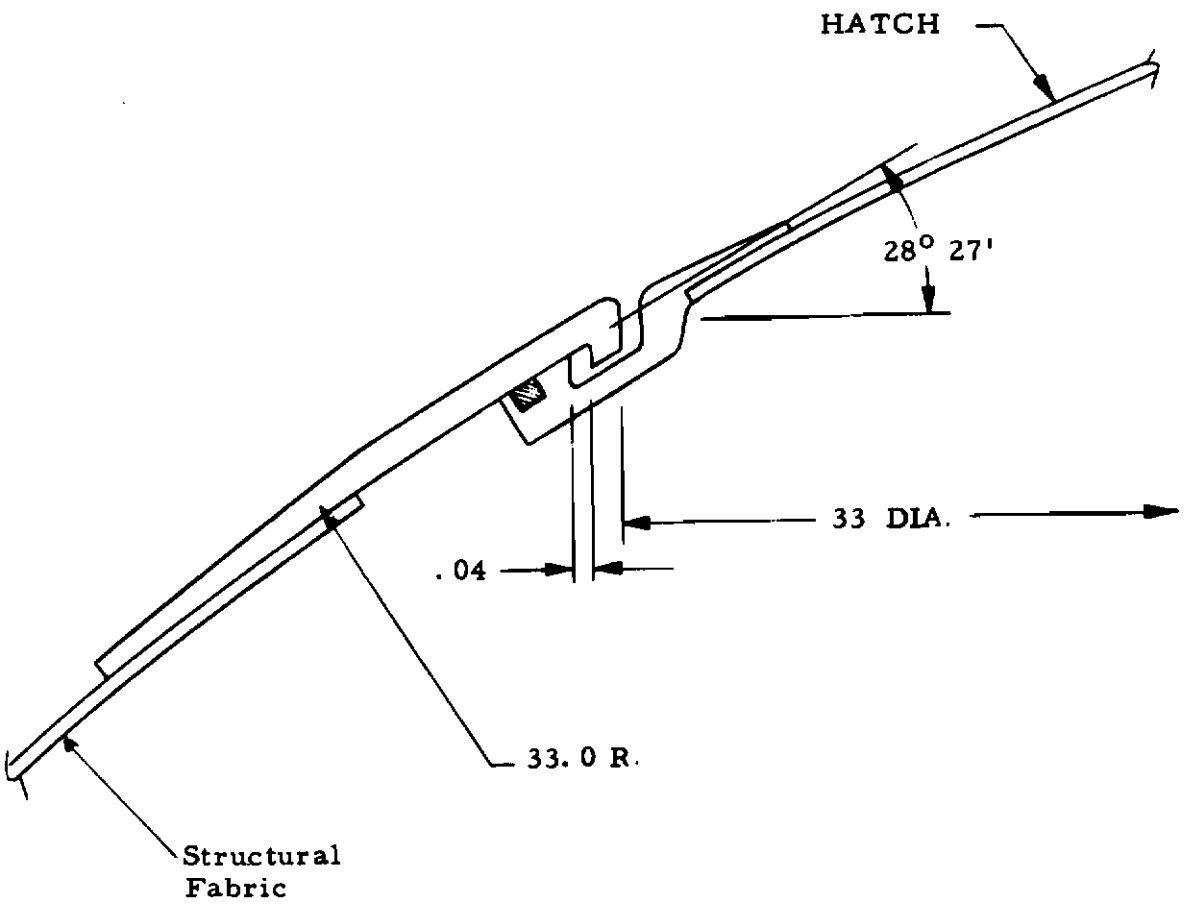

INWARD OPENING HATCH (Continued)

HATCH RING CONFIGURATION

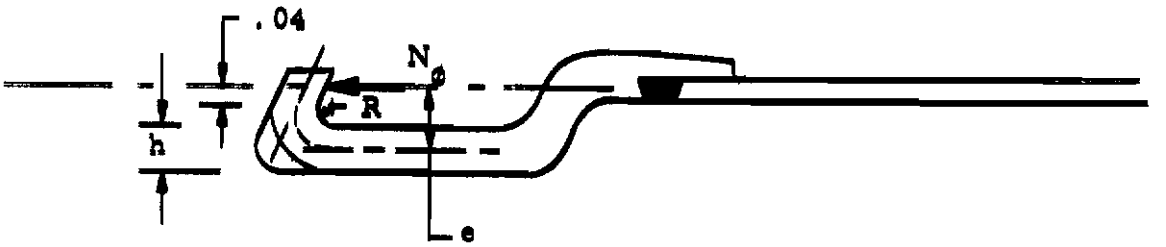

$$N_\phi = \frac{pR}{2} = \frac{3.5(33)}{2} = 57.75 \text{ lb/in.}$$

$$N_\theta = \frac{pR}{2} = \frac{3.5(33)}{2} = 57.75 \text{ lb/in.}$$

Determine h

$R = .045$ in.

$h = .09$ in.

$$e = .04 + .045 + \frac{.09}{2}$$

$$= .13 \text{ in.}$$

$b = 1.0$ in.

$$f_b = \frac{M_L}{I} K = \frac{6MK}{b h^2} = \frac{6 e N_H K}{b h^2}$$

$K = 1.51$ for $\frac{R}{h} = .5$ (Curved Beam)

$$= \frac{6 (.13) (57.75)(1.51)}{(1) (.09)^2}$$

$$= 8397 \text{ psi}$$

INWARD OPENING HATCH (Continued)

HATCH RING (Continued)

$$f_t = \frac{N_\phi}{A} = \frac{N_\phi}{b\,h} = \frac{57.75}{(1)\,(.09)}$$

$$= 642 \text{ psi}$$

Total Stress

$$f_T = 8397 + 642 = 9039$$

$$\text{M. S.} = \frac{F_{tu}}{3\,f_T} - 1 = \frac{42000}{3 \times 9039} - 1 = +.54$$

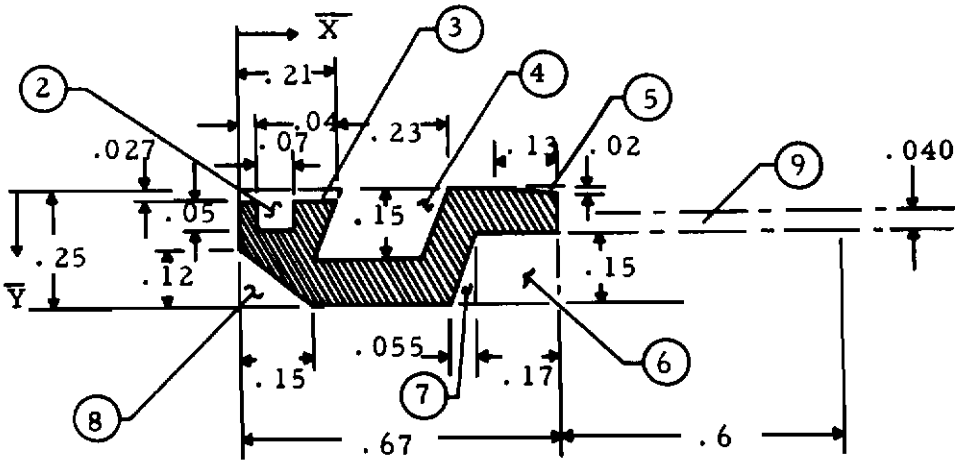

INWARD OPENING HATCH (Continued)

HATCH RING CONFIGURATION

AREA MOMENT OF INERTIA

Element	A	Y	AY	AY^2	I_{OY}	X	AX	AX^2	I_{OX}	AXY
1	1675	.125			.0008724	.335			.0062659	
2	-.0035	.052			-.0000007	.075			-.0000014	
3	-.00567	.0135			-.0000003	.105			-.0000208	
4	-.0345	.075			-.0000647	.325			-.0001521	
5	-.0013	.00667			0	.6267			-.0000012	
6	-.0255	.175			-.0000478	.585			-.0000614	
7	-.004125	.2			-.0000052	.4817			-.0000007	
8	-.009	.21			-.0000072	.05			-.0000113	
Total	.083905		.0109053	.0010693	.0007465		.0258729	.0048554		.0030436
Revised Section										
9	.024	.08	.00192	.0001536	.0000032	.97	.02328	.0225916	.000720	.0098624
Total	.107905		.0128253	.0012234	.0007497		.0491529	.0274160	.0067370	.004906

INWARD OPENING HATCH (Continued)

HATCH RING (Continued)

AREA MOMENT OF INERTIA (Continued)

$\bar{y} = \frac{\Sigma Ay}{\Sigma A} = .12997$ in

$I_x = \Sigma (I_{o_y} + Ay^2) - \Sigma Ay\bar{y}$

$= .0003989$ in^4

$\bar{x} = \frac{\Sigma Ax}{\Sigma A} = .30836$ in

$I_y = \Sigma (I_{o_x} = Ax^2) - \Sigma Ax\bar{x}$

$= .0028932$ in^4

$I_{x_y} = \bar{x}\bar{y}\Sigma A + I_{x_o y_o}$ ∴

$I_{x_o y_o} = \bar{x}\bar{y}\Sigma A - I_{xy} = xy \quad A - \Sigma A\, xy$

$= .0003191$ in^4

Revised Section

$\bar{y} = .11886$ in.

$I_x = .0004487$ in^4

$\bar{x} = .45552$ in

$I_y = .0117829$ in^4

$I_{x_o y_o} = .0009363$ in^4

INWARD OPENING HATCH (Continued)

HATCH RING (Continued)

Configuration

Scale: 2.5 to 1

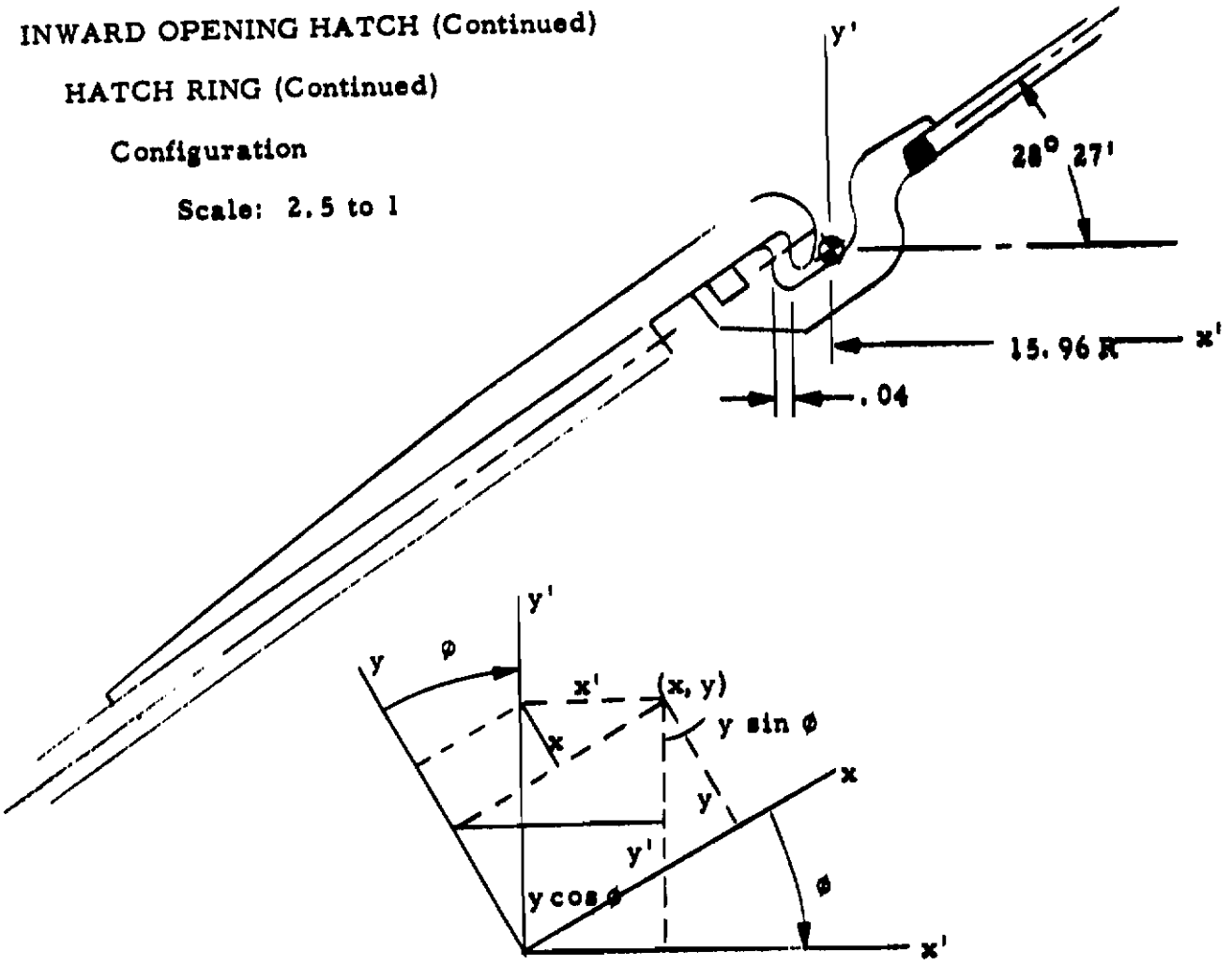

$$I_{x'} = \int y'^2 \, dA \, , \; I_{y'} = \int x'^2 \, dA$$

$$y' = y \cos\phi + x \sin\phi$$

$$x' = x \cos\phi - y \sin\phi$$

$$\phi = 23^\circ 27'$$

INWARD OPENING HATCH (Continued)

HATCH RING (Continued)

AREA MOMENTS OF INERTIA ABOUT INCLINED AXES

$$I_x' = I_x \cos^2 \phi + I_{x_c y_c} \sin^2 \phi + I_y \sin^2 \phi$$

$$= .0003989\ (.879)^2 + .0003191\ (.838) + .0028932\ (.476)^2$$

$$= .001172 \text{ in.}^4$$

$$I_y' = I_x \sin^2 \phi - I_{xy} \sin^2 \phi + I_y \cos^2 \phi$$

$$= .0003989\ (.476)^2 - .0003191\ (.838) + .0028932\ (.879)^2$$

$$= .002058 \text{ in.}^4$$

Load required to deflect ring .04 inches measured perpendicular to ring center line

$$S_R = \frac{N_{H_{CG}} R^2_{CG}}{EA}$$

$S_R = .04$ in.

$R_{CG} = 15.96$ in.

$E = 10^7$ psi

$A = .083905 \text{ in.}^2$

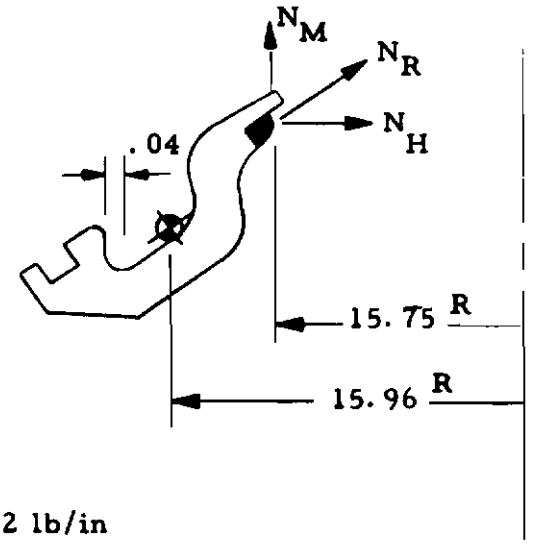

Solving for $N_{H_{CG}}$ gives

$$N_{H_{CG}} = \frac{.04\ (10^7)(.083905)}{(15.96)^2} = 132 \text{ lb/in}$$

INWARD OPENING HATCH (Continued)

HATCH RING (Continued)

CRITICAL BUCKLING LOAD

$$N_{CR} = \frac{3EI}{R_{CG}^3} = \frac{3(10^7)(.002058)}{(15.96)^3}$$

$$= 15.2 \text{ lb/in}$$

AREA MOMENTS OF INERTIA ABOUT INCLINED AXES

Revised cross section to include a 15 x t portion of the dome.

$$I_x' = I_x \cos^2 \phi + I_{x_c y_c} \sin 2\phi + I_y \sin^1 \phi$$

$$= .0004487\ (.879)^2 + .0009363\ (.838) + .0117829\ (.476)^2$$

$$= .003801 \text{ in.}^4$$

$$I_y' = I_x \sin^2 \phi - I_{x_c y_c} \sin 2\phi + I_y \cos^2 \phi$$

$$= .0004487\ (.476)^2 - .0009363\ (.838) + .0117829\ (.879)^2$$

$$= .008421 \text{ in.}^4$$

CRITICAL BUCKLING LOAD - REVISED SECTION

$$N_{CR} = \frac{3EI}{R_{CG}^3}$$

N_{CR}

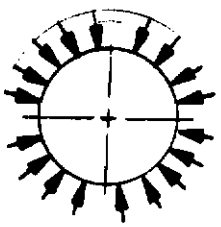

R_{CG} = 15.85 in (measured)

$$= \frac{3(10^7)(.008421)'}{(15.85)^3}$$

$$= 62.2 \text{ lb/in}$$

$$f_{CR} = \frac{N_{CR} R_{CG}}{A} = \frac{62.2 \times 15.85}{.107905} = 9136 \text{ psi}$$

INWARD OPENING HATCH (Continued)

HATCH RING (Continued)

RING ROTATION - REVISED SECTION

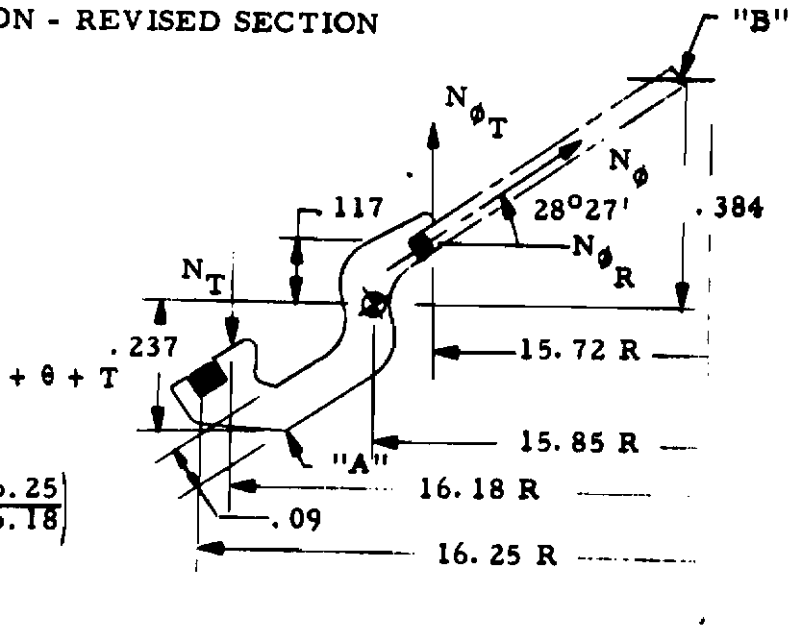

N_ϕ = 57.75 lb/in

N_{ϕ_T} = 57.75 sin 28° 27'

= 27.5 lb/in

N_{ϕ_R} = 57.75 cos 28° 27'

= 50.8 lb/in

$$N_T = \frac{pR_1}{2}\frac{R_1}{R_2} = \frac{3.5\,(16.25)}{2}\left(\frac{16.25}{16.18}\right)$$

= 28.6 lb/in

$$T_{CG} = 28.6\,(16.18 - 15.85)\left(\frac{16.18}{15.85}\right) + 27.5\,(15.85 - 15.72)\left(\frac{15.72}{15.85}\right)$$

$$- 50.8\,(.117)\left(\frac{15.72}{15.85}\right)$$

= 9.63 + 3.55 - 5.89 = 7.29 in-lb/in

$$\theta_{CG} = \frac{T_{CG}R_{CG}^2}{E\,I_x'} = \frac{7.29\,(15.85)^2}{10^7\,(.003801)}$$

= .0482 RAD

INWARD OPENING HATCH (Continued)

HATCH RING (Continued)

RADIAL DISPLACEMENT

$$S_R = \frac{N_{H_{R_{CG}}} R_{CG}^2}{EA}$$

$$N_{H_{R_{CG}}} = 57.75\left(\frac{15.72}{15.85}\right)$$

$$= 57.28 \text{ lb/in}$$

$$S_R = \frac{57.28\ (15.85)^2}{10^7\ (.107905)}$$

$$= .10133 \text{ in}$$

DIRECT COMPRESSIVE STRESS

$$f_c = \frac{N_{H_{R_{CG}}} R_{CG}}{A} = \frac{57.28\ (15.85)}{.107905}$$

$$= .8413 \text{ psi}$$

RING BENDING AT "A"

$$f_b = \frac{T_{CG} R_{CG} C}{I_x}$$

$$C = .237 \text{ in}$$

$$= \frac{7.29\ (15.85 \times .237)}{.003801}$$

$$= .7205 \text{ psi compression}$$

INWARD OPENING HATCH (Continued)

NET STRESS AT "A"

$f = 8413 + 7205 = 15,618$ (compression)

RING BENDING AT "B"

$$f_b = \frac{7.29 \times 15.85 \times .384}{.003801} = 11676 \text{ psi}$$

NET STRESS AT "B"

$f = 11,900 - 9060 = 2840$ psi

CRITICAL AT "A"

$$\text{M.S.} = \frac{f_{Lr}}{f_L} - 1 = \frac{9136}{8413} - 1 = +.08$$

$$\text{M.S.} = \frac{F_{ty}}{f_T} - 1 = \frac{35000}{15618} - 1 = +1.24$$

AFT CLOSURE

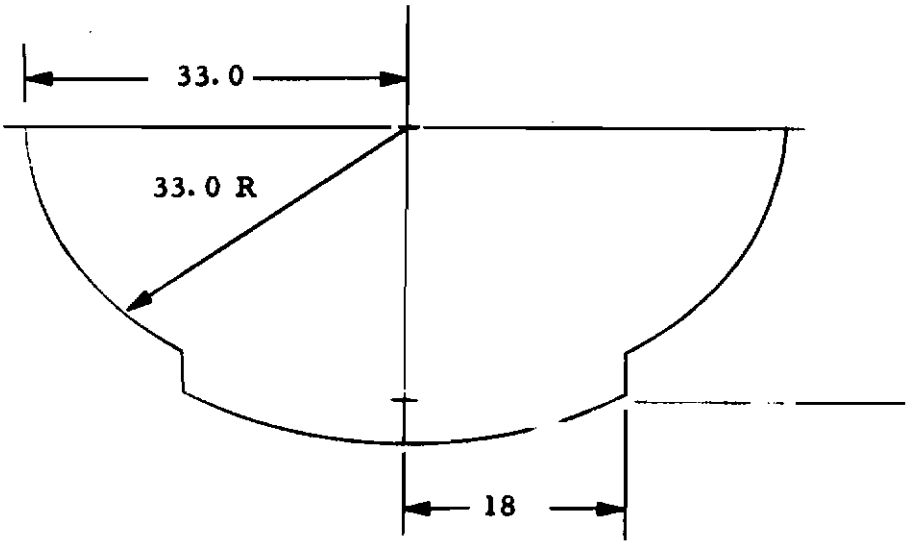

AFT CLOSURE

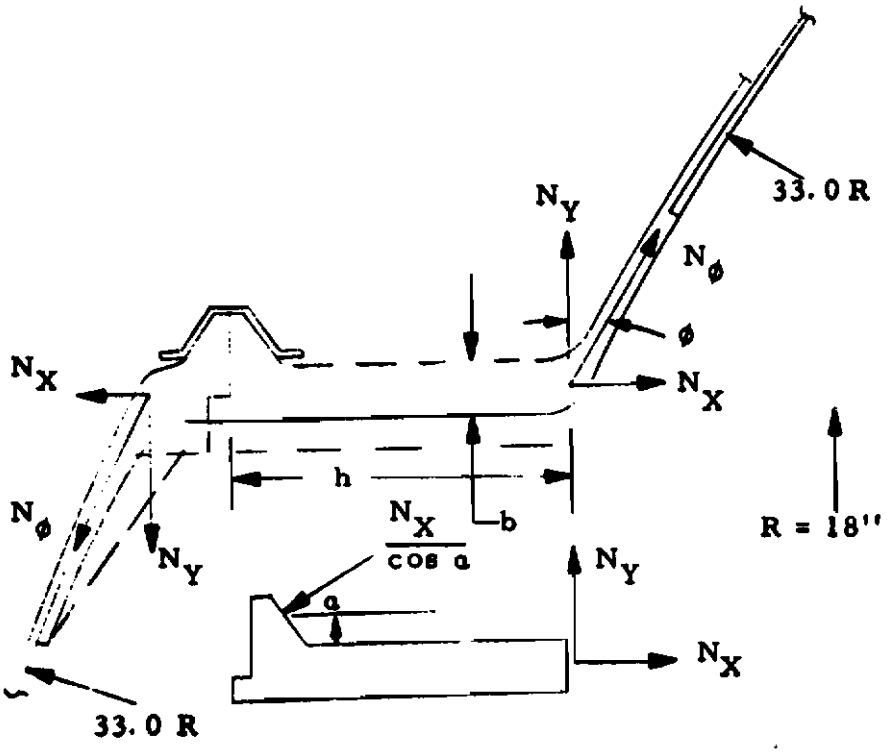

N_ϕ = 57.75 lb/in

$N_X = \frac{pR}{2}$

$= \frac{3.5 \times 18}{2} = 31.5$ lb/in

$\text{Sin } \phi = \frac{N_X}{N_\phi}$

$= \frac{31.5}{57.75} = .545$

$\text{Cos } \phi = .838$

$N_Y = N_\phi \text{ Cos } \phi = 57.75 \times .838 = 48.39$ lb/in

Assume CYl acts as a narrow ring subjected to a uniform moment = M_T

where $M \approx 2 \times N_Y = 2 \times 48.39 \approx 97$ in-lb-in

For b = .437 and h = 2.0

$I = \frac{b/4^3}{12} = \frac{.437(2)^3}{12} = .291 \text{ in.}^4$

$f = \frac{M_T R}{I/c} = \frac{M_T R\, h}{2I} = \frac{97 \times 18 \times 20}{2 \times .291} = 12000$ psi

AFT CLOSURE (Continued)

F_{tu} = 70,000 for 7075-T6

M.S. = $\frac{70,000}{3 \times 12000} - 1 = +.94$

AFT CLOSURE RING

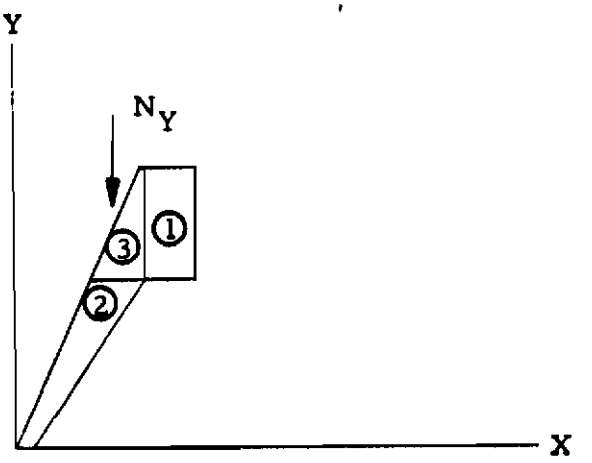

	A	Y	AY	AY^2	I_o
①	.150	1.20	.180	.216	.0018
②	.150	.55	.082	.045	.0045
③	.090	1.10	.099	.109	.0062
	.390		.361	.370	.0125

$\overline{Y} = \frac{.361}{.390} = .925$

$I = .370 + .0125 - .390(.925)^2 = .382 - .334 = .048 \text{ in}^4$

$N_{CR} = \frac{3EI}{R^3} = \frac{3 \times 10 \times 10^6 \times .048}{(18)^3} = 247 \text{ lb/in}$

M. S. = $\frac{247}{3 \times 48.39} - 1 = +.70$

MARMON CLAMP

$N_x = 31.5$ lb/in

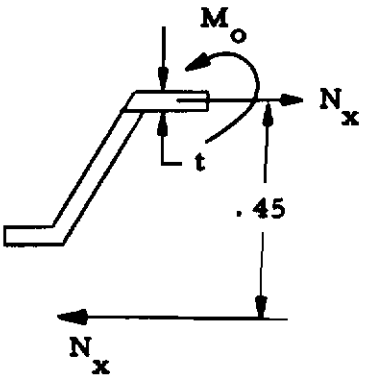

$M_o = .45 \times 365 = 14.2$ in-lb/in

$$f = \frac{6 M_o}{t^2} + \frac{N_x}{t} = \frac{85}{t^2} + \frac{31.5}{t}$$

$$t = .06 \;\; .. \;\; f = \frac{85}{.0036} + \frac{31.5}{.06} = 23,600 + 525$$

$$= 24,100 \text{ psi}$$

For 301 S. S. (annealed) $F_{tu} = 75,000$

$$\text{M. S.} = \frac{75,000}{3 \times 24,100} - 1 = +.04$$

4.2.2 PACKAGING

Methods of packaging both the elastic memory and rigidized airlocks were investigated to determine the minimum envelopes obtainable. Figures 4-9, 4-10, and 4-11 show several canister configuration concepts and their packaged dimensions. These configurations are based on a 34-inch diameter hatch opening instead of the 30-inch diameter opening. This results in a larger-diameter envelope and an increase in weight of the hardware.

Two canister configurations are shown for the elastic recovery airlock. Figure 4-10 shows a conventional canister, while Figure 4-9 shows a possible design utilizing a split ejectable cover. This design reflects an absolute minimum in diameter for the 4-foot-diameter by 7-foot-long cylindrical packaged elastic recovery airlock.

These canister and package configurations are designed for an experiment application for an MSL vehicle which requires that the airlock experiment be mounted integral with the vehicle structure and subsequently deployed through an opening which had been faired by pyrotechnically removable covers. A typical deployment sequence is seen in Figure 4-12. This sequence was planned to be controlled from a remote deployment console.

An alternate consideration, in the event that openings in the surface of the vehicle were limited to EVA hatches, is seen in Figure 4-13. In this concept the experiment package would be carried from an internally stowed position by the astronaut through an existing EVA hatch. The experiment package could then be inserted into an MSL fitting installed flush with the vehicle's surface. Connection could then be made with the experiment support subsystems for control and pressurization.

The experiment package configuration for the SIVB vehicle was designed to incorporate all of the experiment subsystems into a single package. This is accomplished by integrating the pressurization system into the experiment base structure. A remote deployment control console is still required, but is not shown in the profile of Figure 4-14. This figure depicts the SSESM Gemini EVA hatch dimensions circumscribing the experiment package envelope. This is an important canister dimensional restriction if the experiment package is required to be carried into the SIVB workshop.

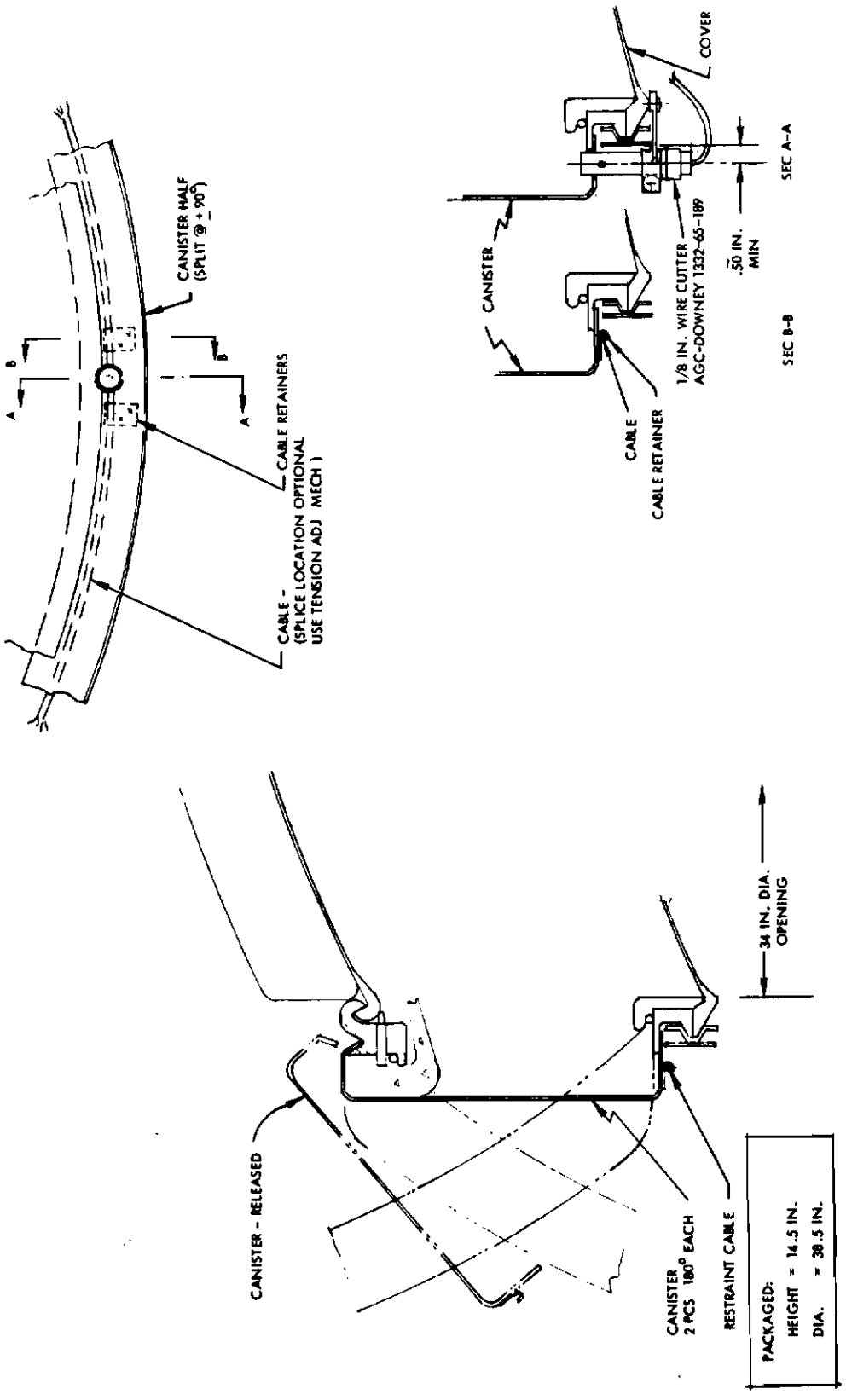

Figure 4-9. Disposable Canister Design, Elastic Memory Airlock

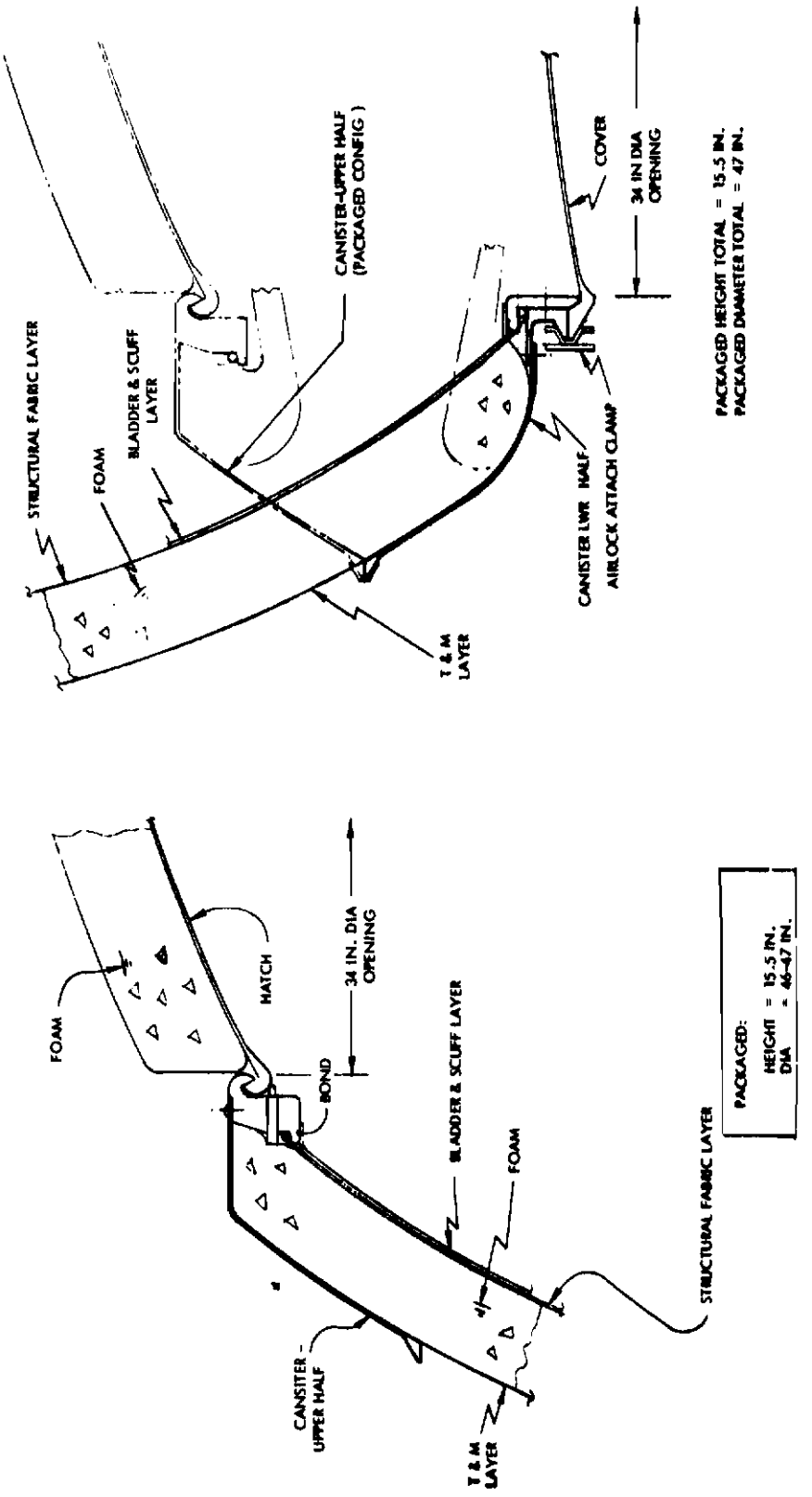

Figure 4-10. Integral Canister Design, Elastic Memory Airlock

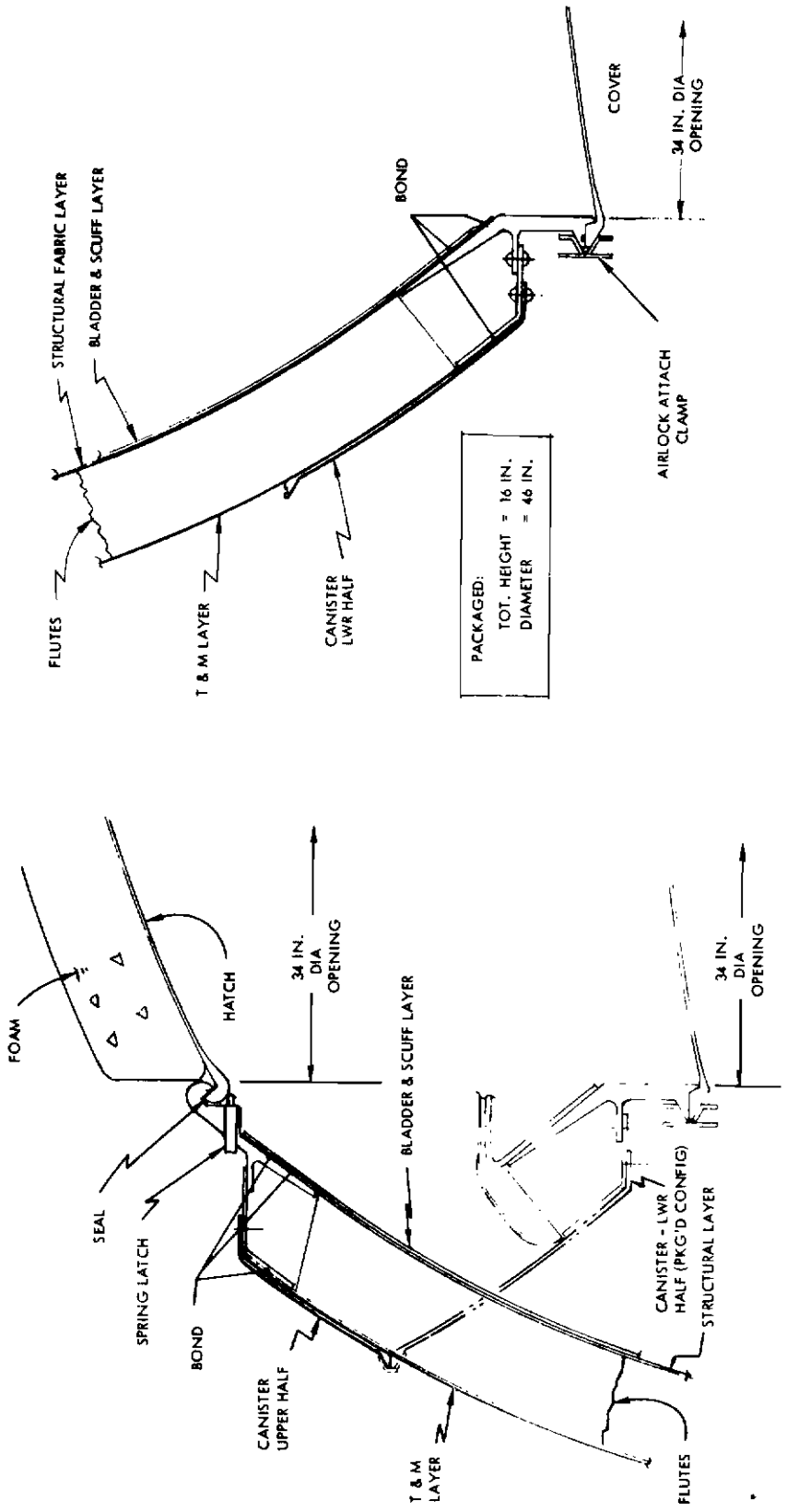

Figure 4-11. Integral Canister Design, Rigidized Gelatin Airlock

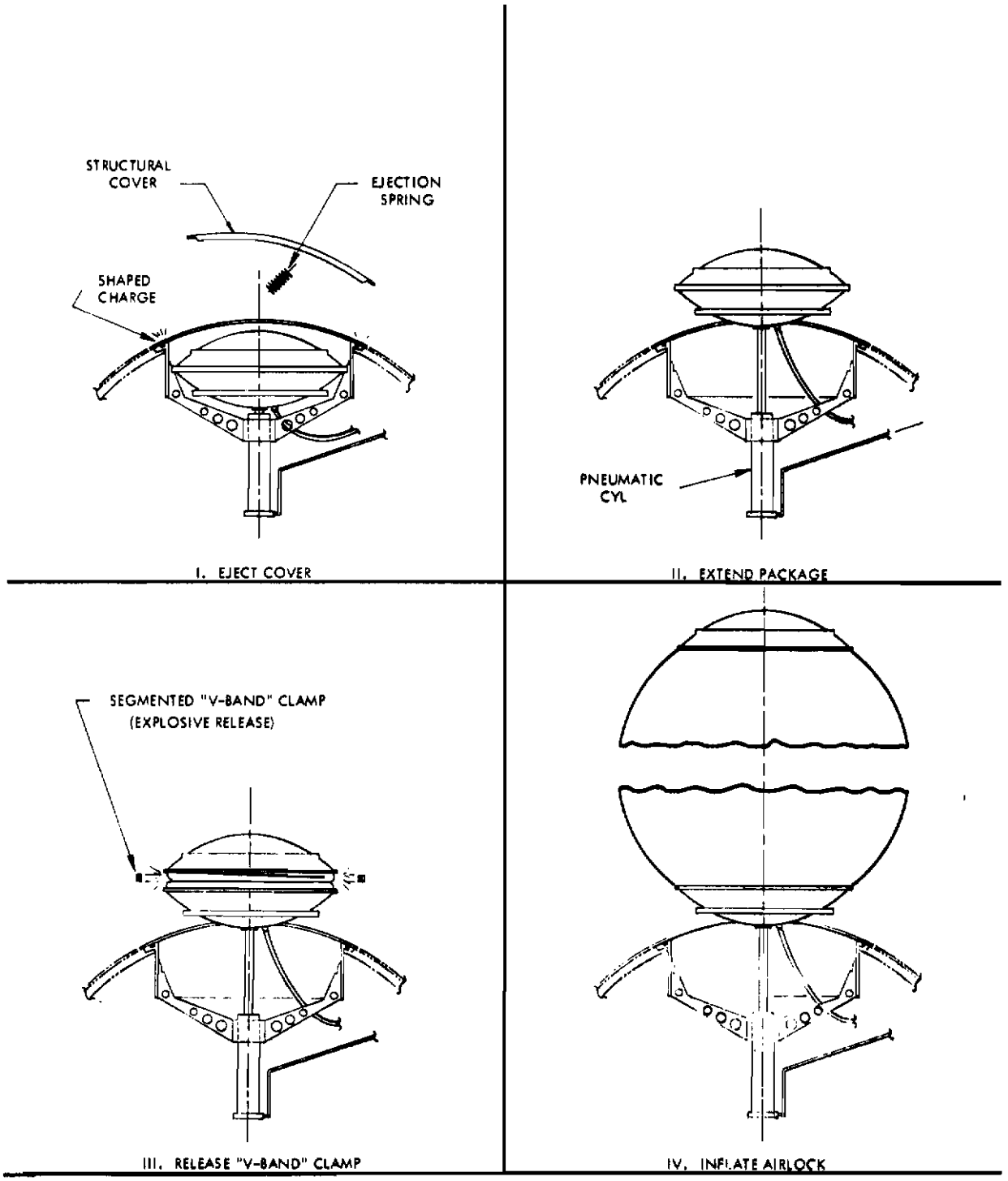

Figure 4-12. Deployment Sequence for Elastic Memory Airlock, Integral Stowage Configuration for a MST

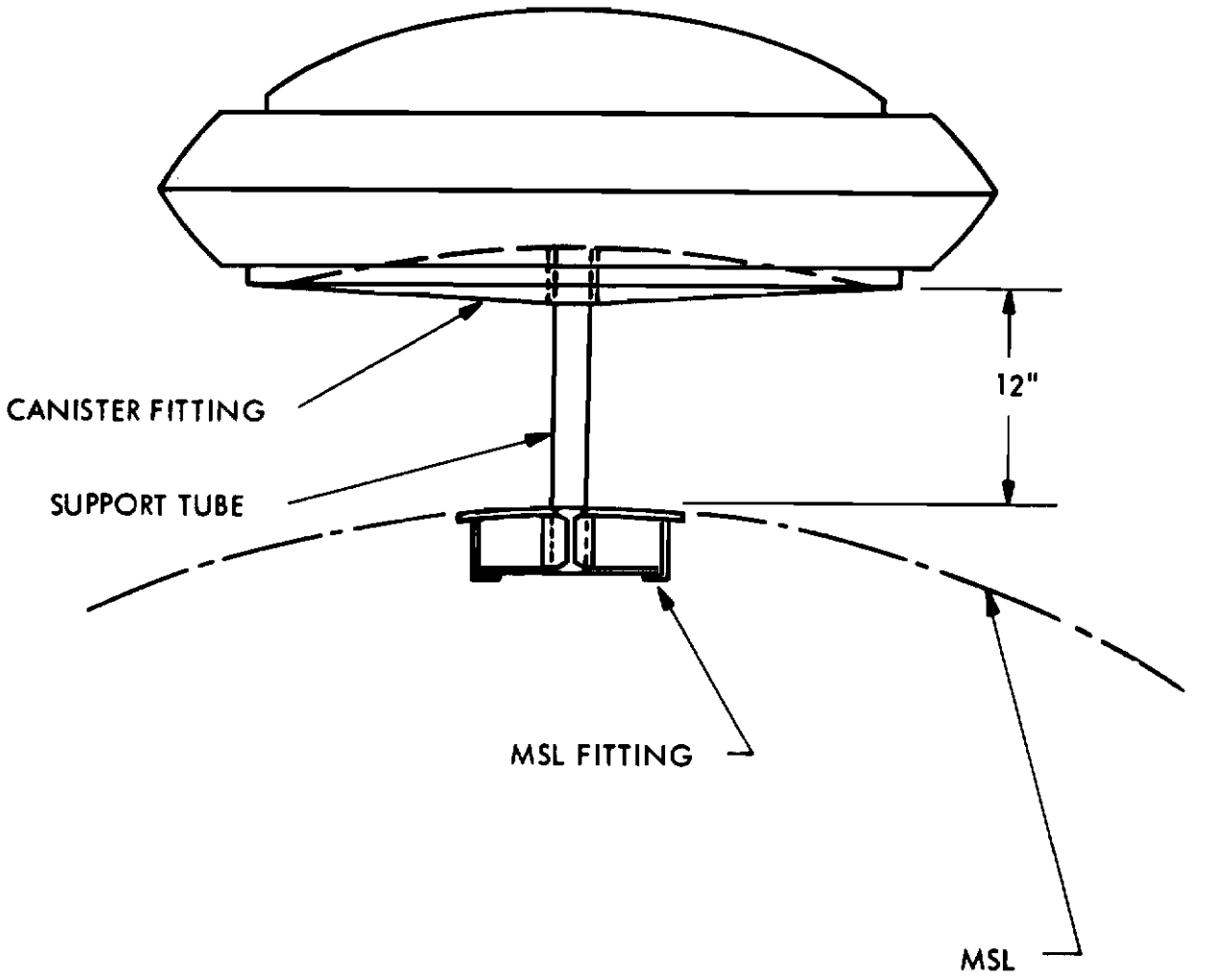

Figure 4-13. Airlock Deployment Configuration for Nonintegral (Internally) Stowed Option

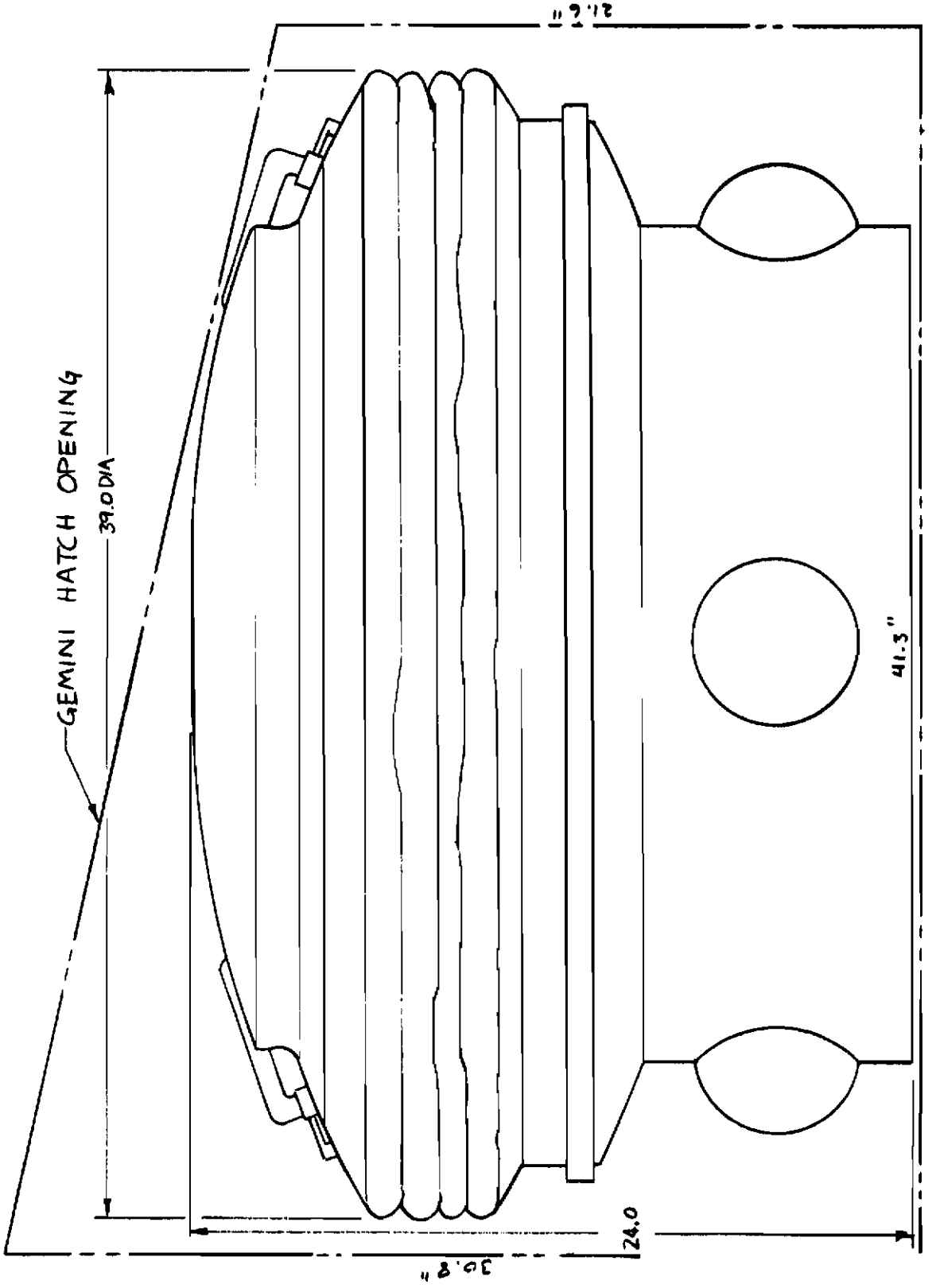

Figure 4-14. Packaged Configuration - Airlock

On a related SGC-funded program a similar elastics recovery airlock was fabricated and pressure tested. Folding and packaging tests were performed on this structure which contributed significantly to the understanding of the material behavior characteristics for high density packaging and canister design. A packaged and fully deployed view of this structure is seen in Figure 4-15. This study demonstrated the high packaging densities obtainable from structural material systems of this type. A more detailed presentation of the spherical airlock package configuration may be seen in Figure 4-51 of Section 4.8.

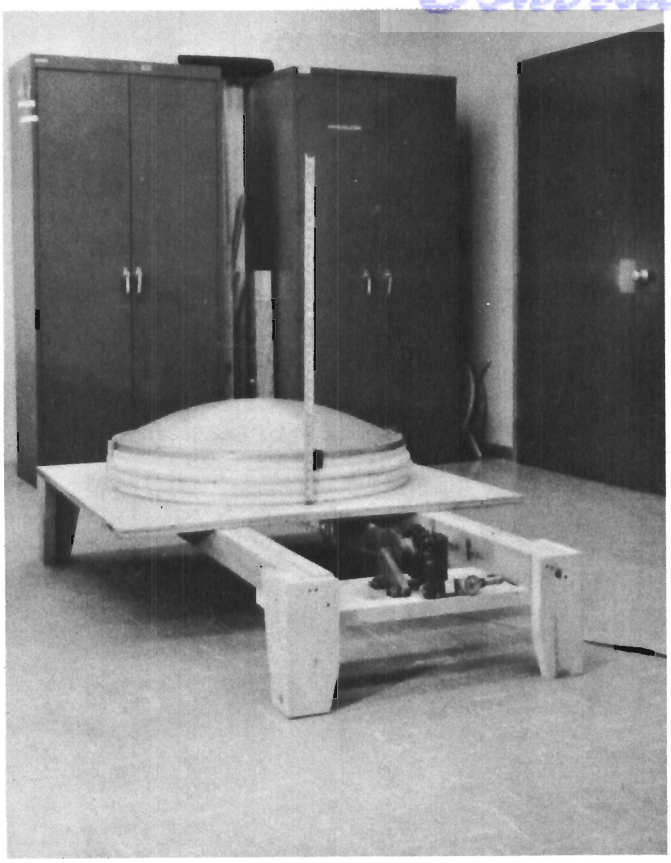

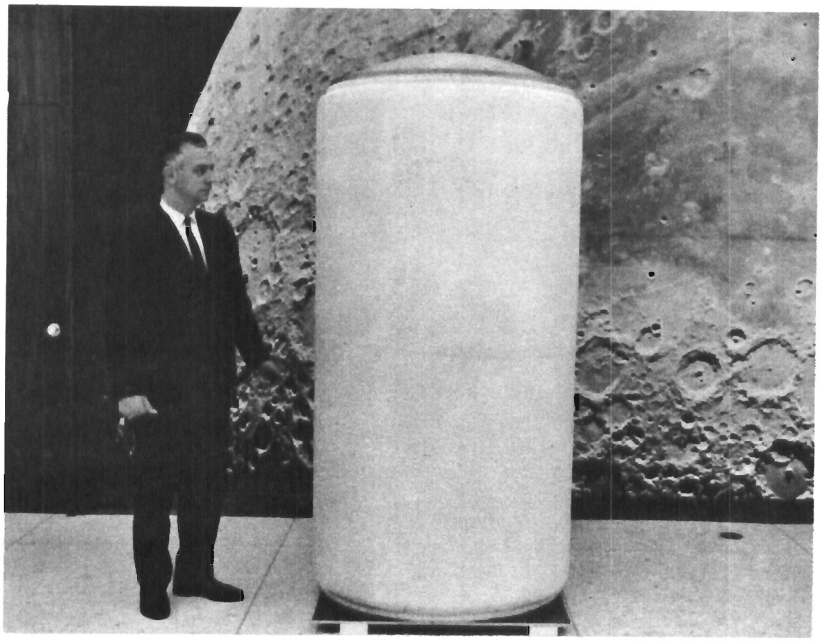

Figure 4-15. Airlock Configuration

4.3 PRESSURIZATION SYSTEM DESIGN FOR SSESM EXPERIMENT CONFIGURATION

The requirements for an Elastic Memory Airlock Experiment for the Saturn SIVB Spent-Stage Experiment Support Module are substantially different from the previous MSL which required that the experiment system be integrally mounted on external surface of the vehicle. The pressurization system is also required to be integrated as a part of the experiment package. However, the most efficient approach to pressurization of the airlock experiment would be to use the vehicle gas system. A pressurization system design is being analyzed on the basis that the experiment package must contain the integral pressurization system.

It is assumed that the airlock pressurization system will be required to provide sufficient oxygen to allow four pressurization cycles for an airlock volume of approximately 100 cubic feet. These four cycles will be required for the following functions:

a. Initial shaping and proof test (1.5 times operating)

b. Two pressurization cycles for astronaut ingress/egress operational evaluation at 3.5 psig operating pressure.

c. The fourth pressurization (at 3.5 psig) is proposed to determine long-term leakage characteristics associated with exposure to the space environment.

Since the operation and reliability of the airlock pressurization system is of prime importance for astronaut safety, attention has been concentrated on the detail design, analyses, and provisions for redundant safety of the experiment operation.

Basically, the pressurization system will consist of four spherical bottles pressurized to 3000 psig. The bottles are manifolded together and are located on the underside of the canister fairing. As the temperature of the experiment system at the time of operation is not precisely known, a pressure relief valve is employed to assure that airlock pressure does not exceed prescribed operational levels. Relief valves are also employed on the gas bottles upstream of the pressurization valve in the event that higher than anticipated temperatures are reached that could cause an increase in the reservoir pressure.

An estimate of the pressurization system weight has been made on the basis of operational airlock volume. Curves are presented for 3.5 psig and 5 psig operating pressures. These weight estimates include oxygen, pressure bottles, valves-fitting and plumbing. This data is seen in Figure 4-16.

The pressurization system will be controlled from two stations; one in the airlock itself and a second one from the remote deployment control box. It is felt that proof-pressure test should be applied to the deployed airlock with the astronaut stationed at a remote location.

4.3.1 VENTING VALVE DESIGN

Venting of the airlock is required in order to depressurize the airlock during astronaut EVA ingress and egress maneuvers. Two basic considerations are involved: first, the actual mechanics of the valve and, second, the human factors aspects. Since the EVA operation involves astronaut contact with the hatches, the hatch is considered the best location for the vent valve.

The requirements for airlock venting include:

a. The time required to pressurize or depressurize the airlock should be as short as practical to keep the loiter period to a minimum. Approximately one minute has been assumed for this task.

b. Operation of the vent should be simple and well within the dexterous capabilities of the astronaut. He should be able to open the vent and have it stay in that position, and be able to stop pressure venting at any instant during an airlock cycle (for example, to perform a suit pressure check).

c. Remote control of venting is desirable.

d. Venting should be operable from both sides of the hatch.

e. The system should include a signal device to enable the astronaut to determine the status of the pressurization process to determine when it is safe to open the outer hatch.

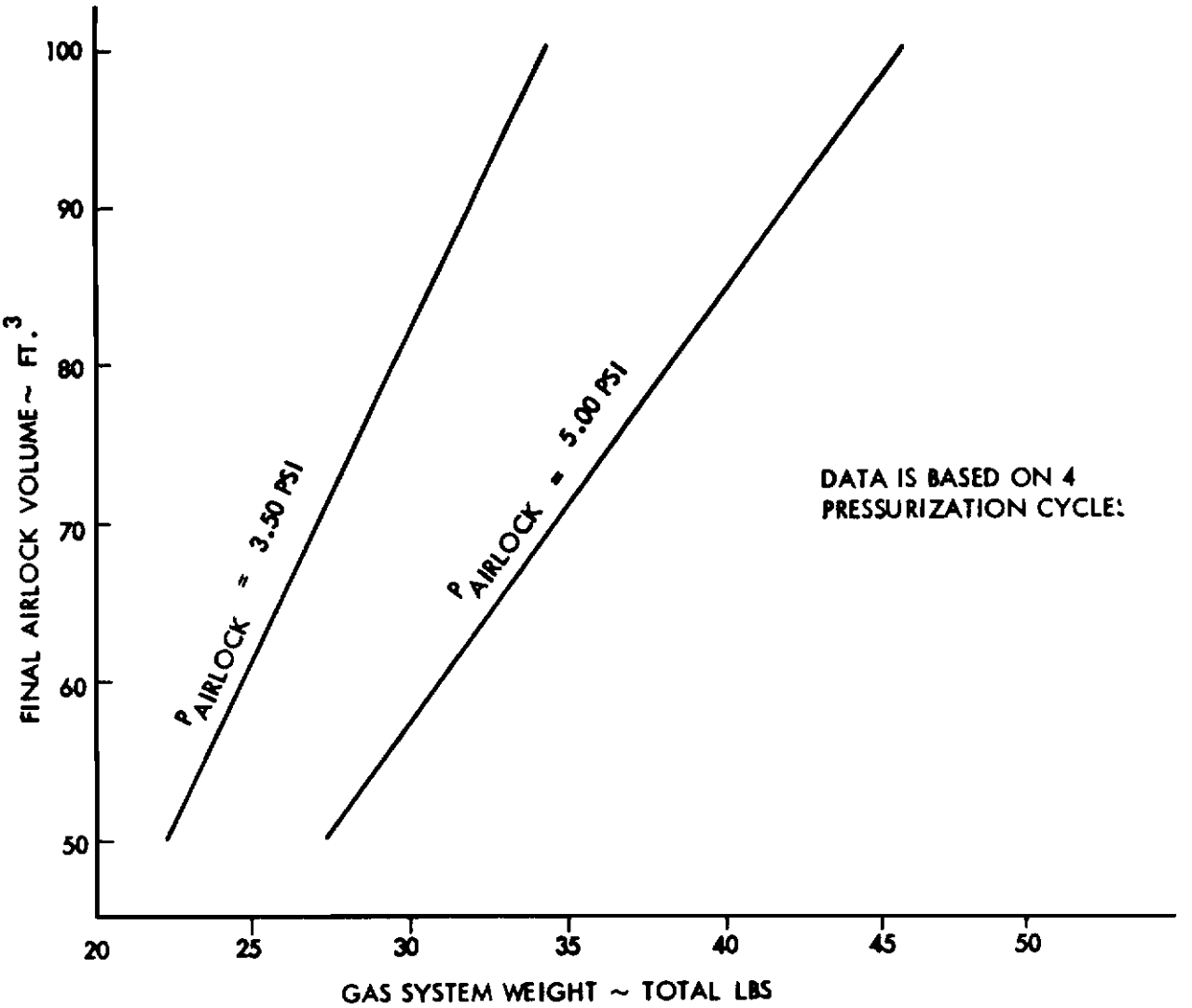

Figure 4-16. Pressurization System Weight Versus Airlock Volume

In addition to these requirements, mechanical interlocking of the vent and hatch opening controls may be desirable for an outward opening hatch. The inward opening hatch is self-interlocking.

The orifice size for the vent valve is determined by the time allowed to reduce the airlock pressure to the hatch opening level. Figure 4-17 shows the airlock pressure decay curves for various orifice diameters using the exponential decay law. This is covered more thoroughly in the pressure analysis section of this document.

Of the several basic types of valves which can be employed for venting the airlock, the diaphragm type is considered best suited for the airlock application because of its excellent sealing capability, simplicity and high reliability. Tradeoffs were conducted to ascertain this conclusion.

Signal system requirements to indicate the airlock pressure status to the astronaut were investigated. One concept consists of three colored lights operated by a pressure sensing device: a red light to indicate that the airlock is at vehicle pressure, a yellow light to indicate that the airlock is cycling, and a green light to indicate that the airlock is at space pressure. The absence of a signal light would indicate a malfunction of the lights. An additional pressure indicator (such as a dial gage or indicator) should be included to provide a backup to the system. The advantage of the colored signal light is that the astronaut would be able to determine the pressure status of the airlock from any position, without looking at the lights, by the glow color. A disadvantage is that when the yellow light is on, the astronaut cannot determine if the pressure is increasing or decreasing.

4.3.2 AIRLOCK PRESSURIZATION SYSTEM ANALYSIS

The airlock pressurization system must supply the required gas for three modes of operation. These are:

a. Deployment and proof

b. Normal operation cycles (three)

c. Final pressurization cycle

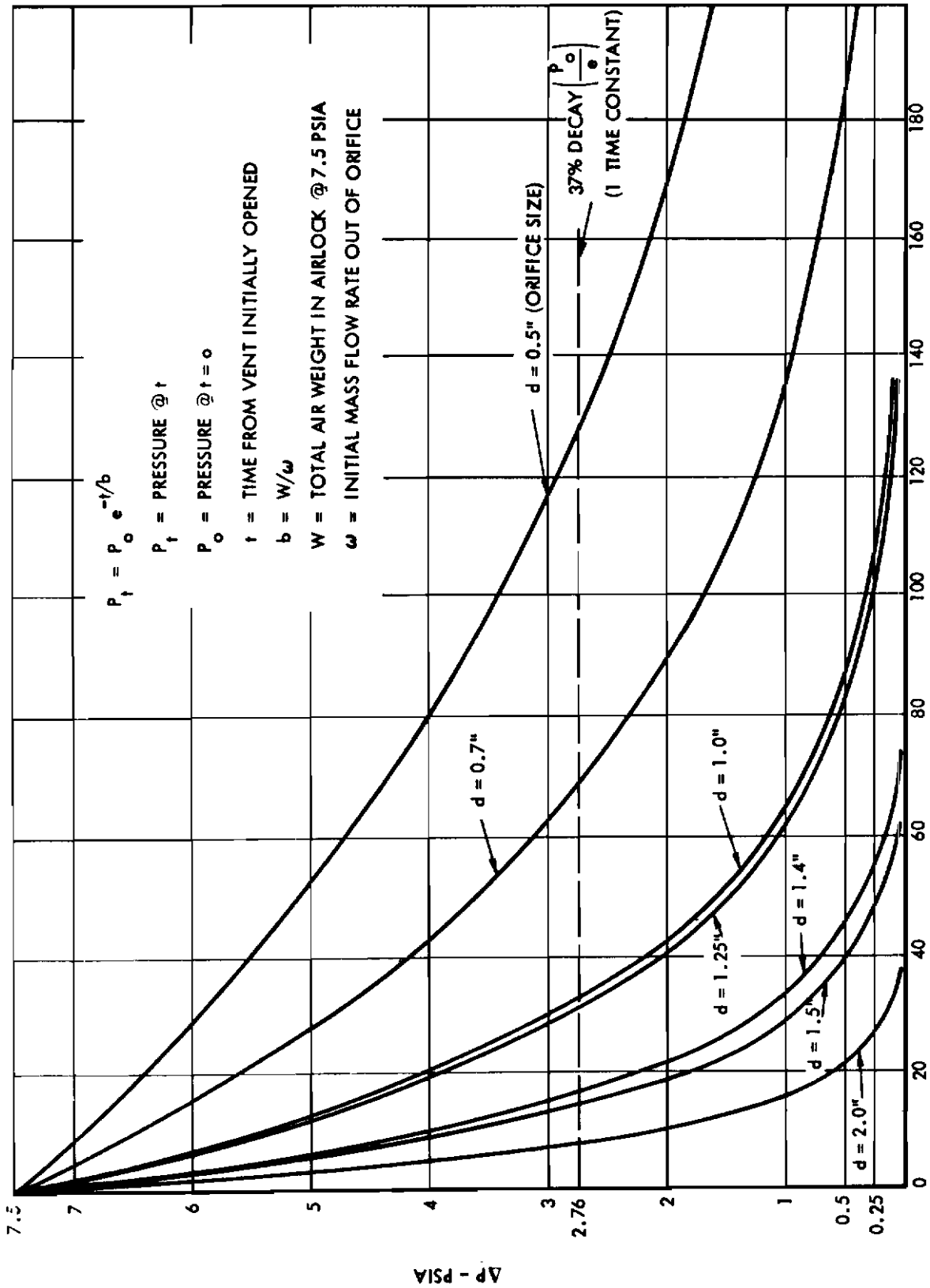

Figure 4-17. Pressure Decay Curves for Various Airlock Venting Apertures

System temperatures and pressures must be predicted for each mode of operation so that storage bottles, valves, regulators, lines and flow control orifices can be sized. These components must provide the correct airlock pressure in the selected pressurization time. These problems and related calculations are discussed in this section under the headings of thermodynamic processes, gas requirements and bottle sizes, temperature transients and, finally, orifice and component sizes.

4.3.2.1 THERMODYNAMIC PROCESSES

A number of thermodynamic processes occur during the various airlock pressurizations. In this section each of the processes is described in detail so that the calculations which follow can be better understood. A schematic diagram of the system under discussion is shown in Figure 4-18. In the schematic, station 1 is the storage bottles, station 2 is the line upstream of the pressure regulator, station 3 is upstream of the control orifice, and station 4 is inside the airlock. A squib valve and pressure-actuated solenoid valve are also located between stations 2 and 3.

During pressurization of the airlock, the gas remaining in the storage bottles undergoes an expansion. Since the total process time is short (one minute for the normal pressurizations and the final pressurization, and three minutes for the proof-pressurization) this expansion is nearly adiabatic. For an adiabatic expansion the temperature of the gas left in the bottle is related to the pressure in the bottle by:

$$\frac{T_{1t}}{T_{1i}} = \left(\frac{P_{1t}}{P_{1i}}\right)^{\frac{\gamma-1}{\gamma}}$$

where subscripts

- 1 = bottle gas condition
- t = at time t during the expansion
- i = initial condition
- f = final condition (used later)

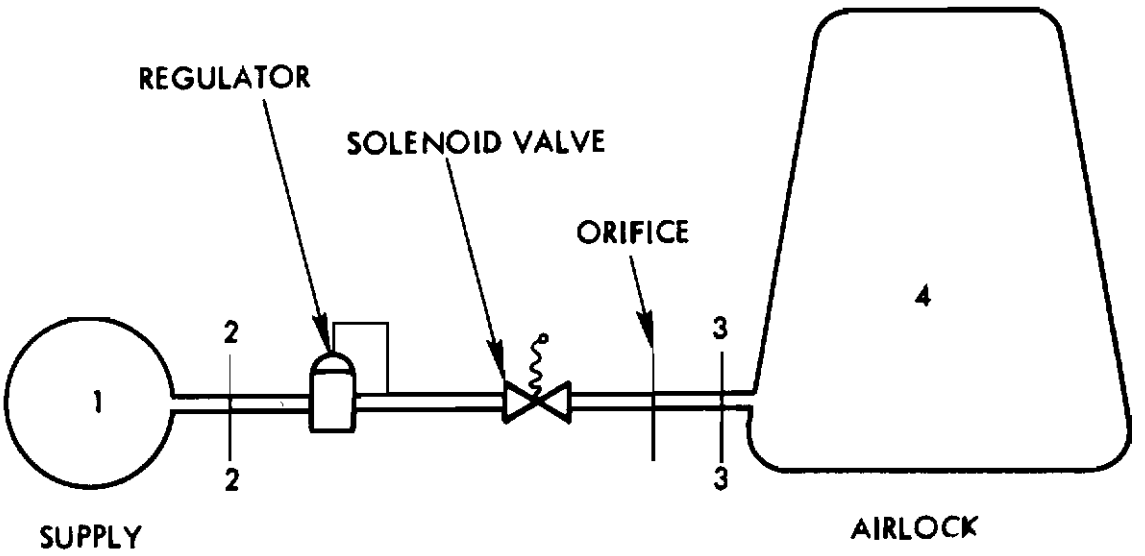

Figure 4-18. Thermodynamic Schematic

This adiabatic expansion process is very familiar and also occurs during expansion of a gas in a cylinder where a piston removes flow work (p_V) and during expansion through a turbine where the shaft removes flow work. In our expulsion flow work is removed by the gas flowing out of the bottles.

The next thermodynamic process of interest occurs as the gas flows through the regulator, valves, and flow control orifice. In this portion of the system the gas undergoes a throttling process. Again, since the process occurs quickly, heat transfer is neglected. For throttling of a perfect gas, temperature remains constant, but for real gases the temperature can increase or decrease, depending on its properties. The gas property controlling this temperature change is called the Joule-Thomson coefficient and is defined as,

$$\mu_J = \left(\frac{\partial T}{\partial p}\right) \qquad h = \text{constant}$$

For oxygen, this coefficient is positive and results in a temperature drop due to throttling.

This Joule-Thomson cooling is used in gas liquefaction processes in the manufacture of cryogenic liquids. For the expansion of oxygen from 3000 psia to 90 psia temperature drops of $60^{\circ}F$ to $83^{\circ}F$ occur with initial temperatures of $100^{\circ}F$ and $50^{\circ}F$, respectively.

Another thermodynamic process of interest occurs as the gas enters the airlock. Gas flowing in the line has flow work energy (p_V) but this energy is converted into heat as it comes to rest in the airlock. The energy of the entering gas is equal to the energy of the gas at rest in the airlock. Therefore,

$$h_3 = U_r$$

where:

h = enthalpy = $U + PV$

U = internal energy

If a perfect gas is assumed,

$$C_p T_3 = C_v T_4$$

$$T_4 = \frac{C_p}{C_v} T_3$$

or,

$$T_4 = \gamma T_3$$

For a typical entering-gas temperature of $-30^\circ F = 430^\circ R$ the final temperature of the gas at rest in the airlock, neglecting heat transfer, is

$$T_{4_f} = 1.39 \times 430 = 598^\circ R = 138^\circ F$$

This temperature is not believed to be excessive for the astronaut because of the low pressures involved and because he is protected by his space suit. The temperature will decay as heat is transferred into the airlock, hatch, and other structures.

This thermodynamic process is most commonly experienced when a gas container is pressurized but it can also be noted when vacuum chambers are opened to atmosphere or when spacecraft are pressurized after an EVA. In the case of vacuum chambers and spacecraft, a large mass of metal is available to absorb heat so that the measured temperatures may be considerably closer to ambient.

The final thermodynamic process of interest is somewhat a combination of the above processes. It is most applicable to the proof pressurization and final pressurization cycles where the mass of gas remaining in the bottles at the end of the process is small. In these cases the final temperature of the gas in the airlock is equal to its initial temperature in the bottles, except for Joule-Thomson cooling (for oxygen). The process is similar to the famous Joule experiment in which a pressurized container and an evacuated container interconnected by a valve were submerged in a water bath. The bath was insulated from the surroundings and the bath temperature observed. No noticeable change in bath temperature was noted after the interconnecting valve was opened.

In practice, some temperature change may occur depending on the gas used, pressure range,and initial temperature. The temperature change is dependent on the Joule-Thomson coefficient of the gas and is equal to the change for a throttling process described above.

This final process requires some further description. As gas flows out of the high pressure bottle the remaining gas undergoes an adiabatic expansion and is, therefore, cooled. Also, the gas entering the evacuated container is heated as flow work is converted into heat. But as the process continues cooler and cooler gas leaves the supply and flows into the initially evacuated container. The mixture temperature is thereby lowered so that the final temperature is equal to the initial gas temperature in the supply. This occurs when very little gas is left in the supply and omits the Joule-Thomson cooling effects.

In the following sections the thermodynamic processes equations are used to calculate gas requirements, bottle sizes, temperatures and flow control orifice sizes.

4.3.2.2 GAS REQUIREMENTS AND BOTTLE SIZES

The mass of gas required for a single pressurization is:

$$M_{4f} = \frac{P_{4f} V_4}{R T_{4f}}$$

In this equation the lowest final temperature which is expected should be used to give the highest gas requirement. The system temperatures are expected to be between 50 and 100°F; therefore, for normal pressurization of the 92 ft^3 airlock,

$$M_{4f} = \frac{3.5 \times 92 \times 144}{48.29 \times 510} = 1.88 \text{ lb}$$

and for three cycles the gas required is,

$$M_{4f}\Big]_{3 \text{ cycles}} = 5.65 \text{ lb}$$

For proof pressurization the temperature just after pressurization may be somewhat lower than 50°F but later rises to the equilibrium temperature range of 50 to 100°F. Using 50°F and 5.5 psia proof conditions,

$$M_{4f\ Proof} = 2.96 \text{ lb}$$

The gas required for the final pressurization is approximately equal to the gas required for a normal cycle above or 1.88 lb. These results are summarized in Table 4-2.

The bottle sizes required are dependent on the charging pressure and temperature and on the bottle temperature before and after expulsion. A charging pressure of 3000 psig and a charging temperature of 80°F will be used. These and other system input data are summarized in Table 4-3.

The required bottle volume is

$$V_l = \frac{M_{4f}\, Z\, R}{\frac{P_{li}}{T_{li}} - \frac{P_{lf}}{T_{lf}}}$$

For the normal pressurization bottles,

$$V_l = \frac{5.65 \times 1.08 \times 48.29 \times 12}{\frac{3015}{540} - \frac{90}{510}}$$

Similarly, the proof bottle volume is

$$V_{l\ Proof} = \frac{2.96 \times 1.08 \times 48.29 \times 12}{\frac{3015}{540} - \frac{5.5}{510}} = 332 \text{ in}^2$$

Again, the final pressurization bottle is equal in volume to a single normal pressurization bottle or 218 in^3.

4.3.2.3 TEMPERATURE TRANSIENTS

Temperature transients at a number of places in the system are of interest. Of particular interest are the temperature in the normal supply bottle at the end of each cycle and the airlock temperature just after a normal pressurization. Other important temperatures which were discussed previously are tabulated in Table 4-3.

Table 4-2

CALCULATED AIRLOCK PRESSURIZATION DATA

	95 ft^3 System
Gas Required for Normal Pressurization (lb)	5.65
Gas Required for Proof Pressurization (lb)	2.96
Gas Required for Final Pressurization (lb)	1.88
Bottle Volume for Normal Pressurization (in^3)(3 cycles)	655
Bottle Volume for Proof Pressurization (in^3)	332
Bottle Volume for Final Pressurization (in^3)	218
Bottle Diam for Normal Pressurization each of 3 (in)	7.48
Bottle Diam for Proof Pressurization (in)	8.60
Bottle Diam for Final Pressurization (in)	7.48
Transient Airlock Temperature - Nominal	
First Normal Cycle (^oF)	180
Proof Cycle (^oF)	75
Final Cycle (^oF)	75
Control-Orifice Diameter	
Normal Pressurization (in)	0.136
Proof Pressurization (in)	0.046
Final Pressurization (in)	0.064

Table 4-3

SYSTEM INPUT DATA

Temperature Range in Orbit	50-100°F
Pressurization Gas	Oxygen
Bottle Charging Pressure	3000 psig
Bottle Charging Temperature	80°F
Airlock Volume	92 ft^2
Number of Normal Cycles	3
Normal Cycle Pressure	3.5 psia
Proof Cycle Pressure	5.5 psia
Final Cycle Pressure	3.5 psia
Normal Pressurization Time	60 sec
Proof Pressurization Time	180 sec
Final Pressurization Time	60 sec

For the present calculation maximum and minimum initial bottle temperatures are assumed and the corresponding final conditions calculated. These calculations assume a perfect gas and adiabatic processes (omitting Joule-Thomson effects and heat transfer, respectively).

For consideration of energy,

$$M_{1i}\, C_v\, T_{1i} = M_{1f}\, C_v\, T_{1f} + M_{4f}\, C_v\, T_{4f} \tag{1}$$

For the adiabatic expansion in the bottle,

$$\frac{T_{1f}}{T_{1i}} = \left(\frac{p_{1f}}{p_{1i}}\right)^{\frac{\gamma-1}{\gamma}} \tag{2}$$

For conservation of mass,

$$M_{1i} = M_{1f} + M_{4f} \tag{3}$$

and the equations of state,

$$M_{1f} = \frac{p_{1f}\, V_1}{R\, T_{1f}} \tag{4}$$

$$M_{4f} = \frac{p_{4f}\, V_4}{R\, T_{4f}} \tag{5}$$

These five equations have five unknowns, i.e., M_{1f}, T_{1f}, M_{4f}, T_{4f}, and p_{1f}.

Replacing Equations (4) and (5) into Equation (1) gives,

$$M_{1i}\, C_v\, T_{1i} = \frac{p_{1f}\, V_1}{R\, T_{1f}}\, C_v\, T_{1f} + \frac{p_{4f}\, V_4}{R\, T_{4f}}\, C_v\, T_{4f} \tag{6}$$

Solving for p_{1f} gives,

$$p_{1f} = \left[M_{1i}\, T_{1i} - \frac{p_{4f}\, V_4}{R}\right] \frac{R}{V_1}$$

or

$$p_{1f} - p_{1i} - p_{4f} \frac{V_4}{V_1}$$

Using the 92 ft^3 airlock conditions for the first expression we have for the minimum and maximum initial bottle temperature,

$$p_{1f}\Big]_{\min T} = 2845 - 3.5 \frac{92 \times 1728}{655} \quad 1995 \text{ psia}$$

$$p_{1f}\Big]_{\max T} = 3120 - 850 = 2270 \text{ psia}$$

From Equation (2),

$$T_{1f}\Big]_{\min T} = 510 \left(\frac{1995}{2845}\right)^{\frac{0.39}{1.39}} = 462^\circ R$$

$$T_{1f}\Big]_{\max T} = 560 \left(\frac{2270}{3120}\right)^{0.28} = 513^\circ R$$

From Equation (4),

$$M_{1f}\Big]_{\min T} = \frac{1995 \times 655}{48.29 \times 462 \times 12} = 4.88 \text{ lb}$$

$$M_{1f}\Big]_{\max T} = \frac{2270 \times 655}{48.29 \times 513 \times 12} = 5.00 \text{ lb}$$

From Equation (3),

$$M_{4f}\Big]_{\min T} = 6.30 - 4.88 = 1.42 \text{ lb}$$

$$M_{4f}\Big]_{\max T} = 6.30 - 5.00 = 1.30 \text{ lb}$$

And, finally, from Equation (5),

$$T_{4f}\Big]_{\min T} = \frac{3.5 \times 92 \times 144}{48.29 \times 1.42} = 676^\circ R = 216^\circ F$$

$$T_{4f}\Big]_{\max T} = \frac{3.5 \times 92 \times 144}{48.29 \times 1.30} = 739^\circ R = 279^\circ F$$

As was mentioned previously these temperatures do not take Joule-Thomson cooling for oxygen into account nor heat transfer into the airlock and other surrounding structure. The actual temperatures will be approximately 83°F and 60°F lower for min T and max T, respectively, due to Joule-Thomson cooling. In addition, the second and third cycles will not experience as great a temperature rise because the supply bottle pressure ratio will be smaller.

4.3.2.4 ORIFICE AND COMPONENT SIZES

The selected pressurization times for each pressurization mode dictate the control orifice diameters and component sizes.

A pressurization time of 60 sec has been selected for normal operation. The flow rate required is approximately 1.35 lb/min. For sonic flow through an orifice,

$$\dot{M}_3 = \frac{p_3 A_t C_D}{\sqrt{T_3}} \Gamma$$

where

C_D = orifice discharge coefficient

Γ = gamma function for oxygen

$$\Gamma = \sqrt{\frac{\gamma g}{R} \left(\frac{2}{\gamma + 1}\right)^{\frac{\gamma+1}{\gamma-1}}}$$

$$\Gamma_{O_2} = 0.56 \frac{lb_m \ ^\circ R}{lb_f \ sec}$$

Therefore,

$$A_t = \frac{1.35 \sqrt{465}}{60 \times 90 \times 0.67 \times 0.56} = 0.0144 \text{ in}^2$$

$$D_t = 0.1355 \text{ in.}$$

A pressurization time of 3 min has been selected for the proof cycle. This is a blowdown process. The applicable equation for calculating the required orifice size is,

$$A_t = \frac{\left[\left(\frac{P_{1i}}{P_{1f}}\right)^{\frac{\gamma-1}{2\gamma}} - 1\right] \quad (V_1)}{\frac{\gamma-1}{2}\sqrt{\gamma g R T_{1i}}\left(\frac{2}{\gamma+1}\right)^{\frac{\gamma+1}{2(\gamma-1)}} C_D t}$$

where

t = required blowdown time

$$A_t = \frac{\left[\left(\frac{3000}{30}\right)^{\frac{0.39}{2.78}} - 1\right] \quad (332)}{\frac{0.39}{2}\sqrt{1.39 \times 32.2 \times 48.29 \times 535}\left(\frac{3}{2.39}\right)^{\frac{2.39}{0.78}} 0.67 \times 180 \times 12}$$

$$= \frac{\left[1.907 - 1\right] \quad (332)}{\frac{0.39}{2} \times \sqrt{1075 \times 0.338 \times 0.67 \times 180 \times 12}} = 0.001632 \text{ in}^2$$

$D_t = 0.0455$ in.

Line sizes of 1/4-inch in the high pressure portions of the system and 3/8-inch in the lower pressure portions of the system have been selected. The resulting Mach Numbers are acceptable.

The vent time requirement of approximately one minute has been established. A brief study was made to determine the size of the vent as a function of airlock volume.

An exponential decay of pressure was assumed.

$$P_T = P_o e^{-\frac{t}{b}}$$

where

P_T = final pressure (0.01 psi)

P_o = initial pressure (3.5 psi)

t = time, sec.

$$b = \frac{w}{\dot{w}} = \frac{\text{weight of oxygen}}{\text{mass flow rate}}$$

The required mass flow is found by:

$$w = A P_o \frac{2g}{RT} \Upsilon \text{ Cd.}$$

where

Cd = orifice coefficient = .70

A = orifice area (in^2)

T = ^oR = 530^oF

R = O_2 gas constant = 48.24

Υ = flow factor = .48

The results are presented in Figure 4-19.

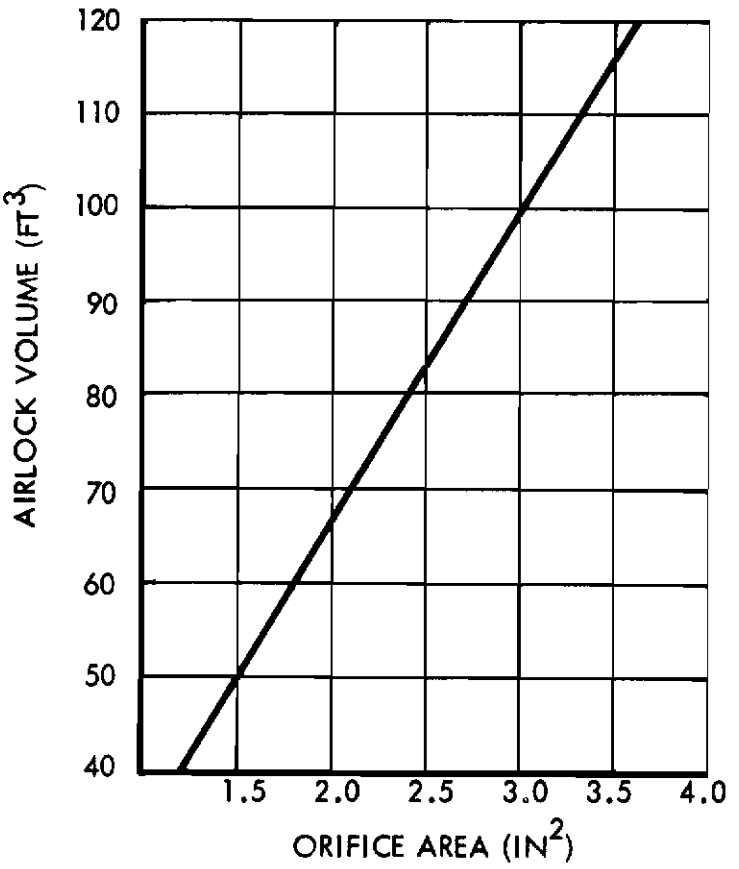

Figure 4-19. Vent Area Versus Airlock Volume for One-Minute Venting

4.4 INSTRUMENTATION AND CONTROLS

Control system studies were done with emphasis on safety of electroexplosive subsystem design, human engineering considerations, and maximum utilization of the astronaut's presence to control the experiment by man's judgment. The airlock control system incorporates the functions of interlocked switching and program status indicators to enhance crew safety and minimize task complexity and crew training requirements. It is anticipated that the circuits and control devices selected for the airlock console will be directly applicable to all other experiment control consoles.

4.4.1 DESIGN CRITERIA

Major emphasis was placed on the following design criteria.

4.4.1.1 MAXIMUM ASTRONAUT SAFETY

Since some steps in the deployment sequence of an experiment employing pyrotechnic devices could constitute a condition hazardous to the astronauts engaged in EVA, the control console must incorporate the following safety provisions:

a. All circuits must be in a safe condition when power is first applied to the console.

b. In the event of a short circuit condition, power must be removed from the console.

c. Indicators must be provided to show the deployment step, and its safe, armed, or actuated condition.

d. To initiate a deployment step, at least two switches (arm and actuate) must be thrown.

e. Deployment steps must be performed in an automatically controlled sequence; i.e., before a given actuation step can occur, all previous steps must have been performed.

f. In the event of a temporary power failure, the control sequence must automatically reset to zero, with the actuation control circuits in a safe condition.

g. A "safe" switch must be provided which will enable the console operator to interrupt power to the arming and actuation circuits at any time.

h. Controls and indicators, and the panel layout, must provide maximum information on the status of the experiment in a clear, logical manner.

i. Circuits must be simple and straightforward. If possible, failure of a given circuit element must not cause a hazardous condition or, in the event of a failure, panel indicators should provide a warning.

j. A completely automatic experiment deployment system should not be used; the astronaut should control each deployment step.

4.4.1.2 MAXIMUM UTILIZATION OF ASTRONAUT'S CAPABILITIES

Servocontrol systems should not be used in the consoles if maximum advantage is to be taken of the human operator's presence. The astronaut's ability to interpret instrumentation readouts and visual observations should be utilized to the fullest extent possible. Similarly, the console design should include a deployment step manual override provision so that the operator may progress rapidly through the deployment sequence if, in his judgment, it is safe to do so. Reliance upon the astronaut's capabilities results in increased safety and reliability, with considerable savings in equipment weight, volume, and power requirements.

4.4.1.3 MAXIMUM APPLICABILITY AND FLEXIBILITY

The airlock experiment control console design should be such that its basic circuit elements and control switching methods can be applied to the design of all of the control consoles. The design should permit a high degree of flexibility in meeting new deployment-sequence requirements as further information on experiments becomes available. Off-the-shelf components should be used in the design, with little or no modifications required to produce an operational unit.

The functional block diagram shown in Figure 4-20 illustrates the man-machine relationships and basic functional components of the control console. The actuation control switches are used to progress through the

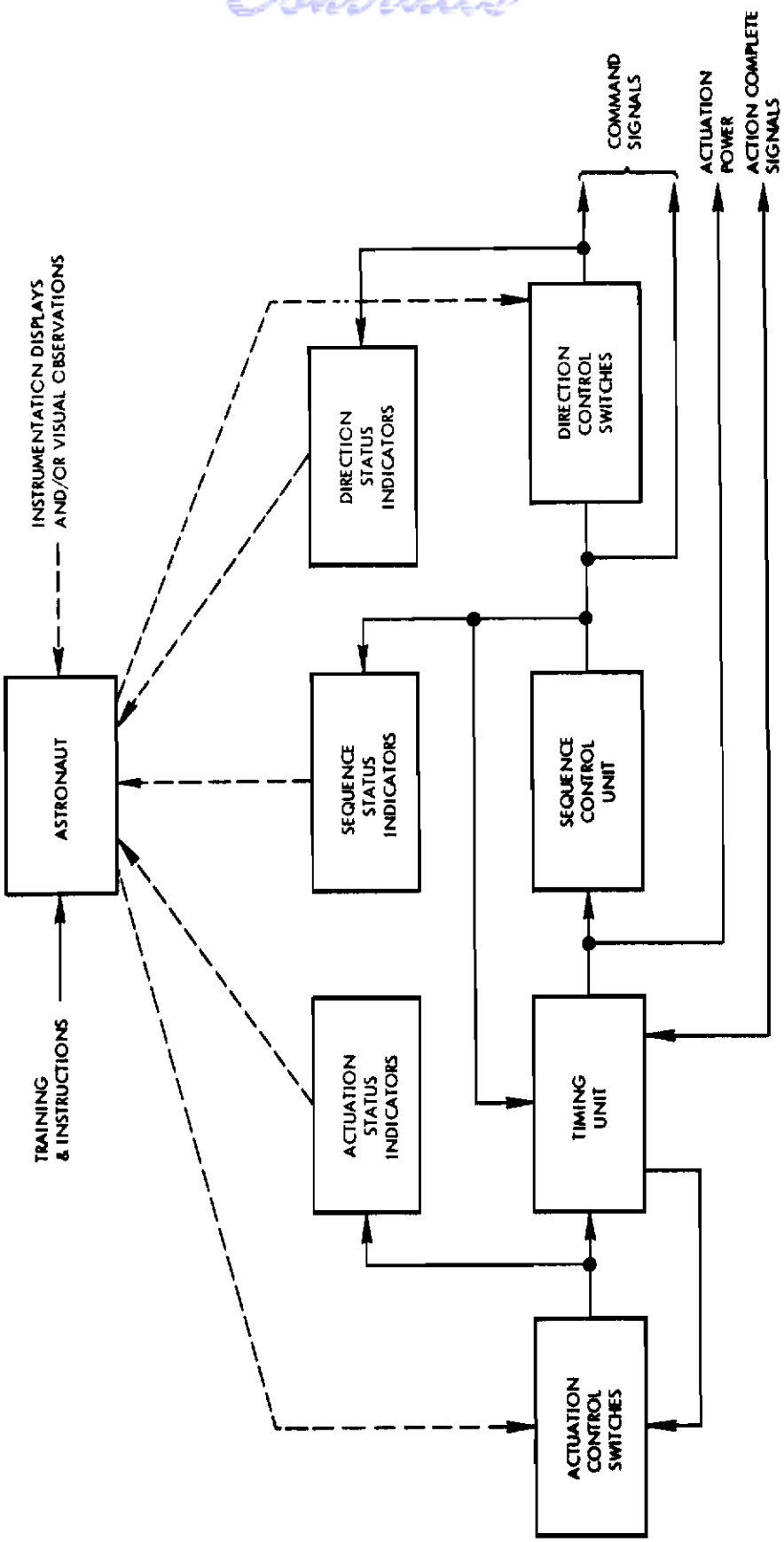

Figure 4-20. Man-Control Loop Considerations in Console Design Layout

deployment steps. Actuation status indicators show the condition of the control circuits (safe, armed, or actuated). A timing unit supplies power for a predetermined time interval to the (normally open) contacts of relays used to control electroexplosive devices, solenoid valves, and electric motors in the experiment. A sequence control unit sequentially energizes the relays; it simultaneously lights the appropriate sequence status indicator and selects the time interval required for the actuation. At points in the deployment sequence where it is desired to manually control and/or reverse an operation (for example, pressurization and venting of the structure), direction control switches are provided to route the sequence control unit output signal to the appropriate relays. The direction of the actuation is shown on direction status indicators. In cases where an "action complete" signal is available, the sequence control unit may be automatically advanced to the next step without requiring a time delay.

Lighted display pushbutton switches will be used for control switching, primarily to conserve panel space while enhancing the man-machine relationship by means of straight, in-line, sequential, visual presentations. The letters in parentheses above each block indicate the color of the lighted display.

Solenoid-hold switches will be used extensively to insure that, when power to the console is removed or momentarily interrupted, all switches will return to their OFF, or SAFE, positions. The POWER ON-OFF switch will incorporate a solid-state or electromechanical trip-free circuit breaker to interrupt power in the event of excessive current demand.

The arrangement of the controls and indicators for the chemically rigidized airlock control console is shown in Figure 4-21. The elastic memory air-lock control console is shown in Figure 4-22. Experiment status indicators are nonswitching lighted displays. Operation of the panel is as follows:

a. When the power switch is set to ON, the SAFE displays of the deployment and abort controls are lighted. The HEATER POWER indicator is ON. When the deployment control ARM switch is depressed, it is magnetically held in position, while its display is lighted and the SAFE switch goes dark. When the ACTIVATE switch is momentarily depressed, the

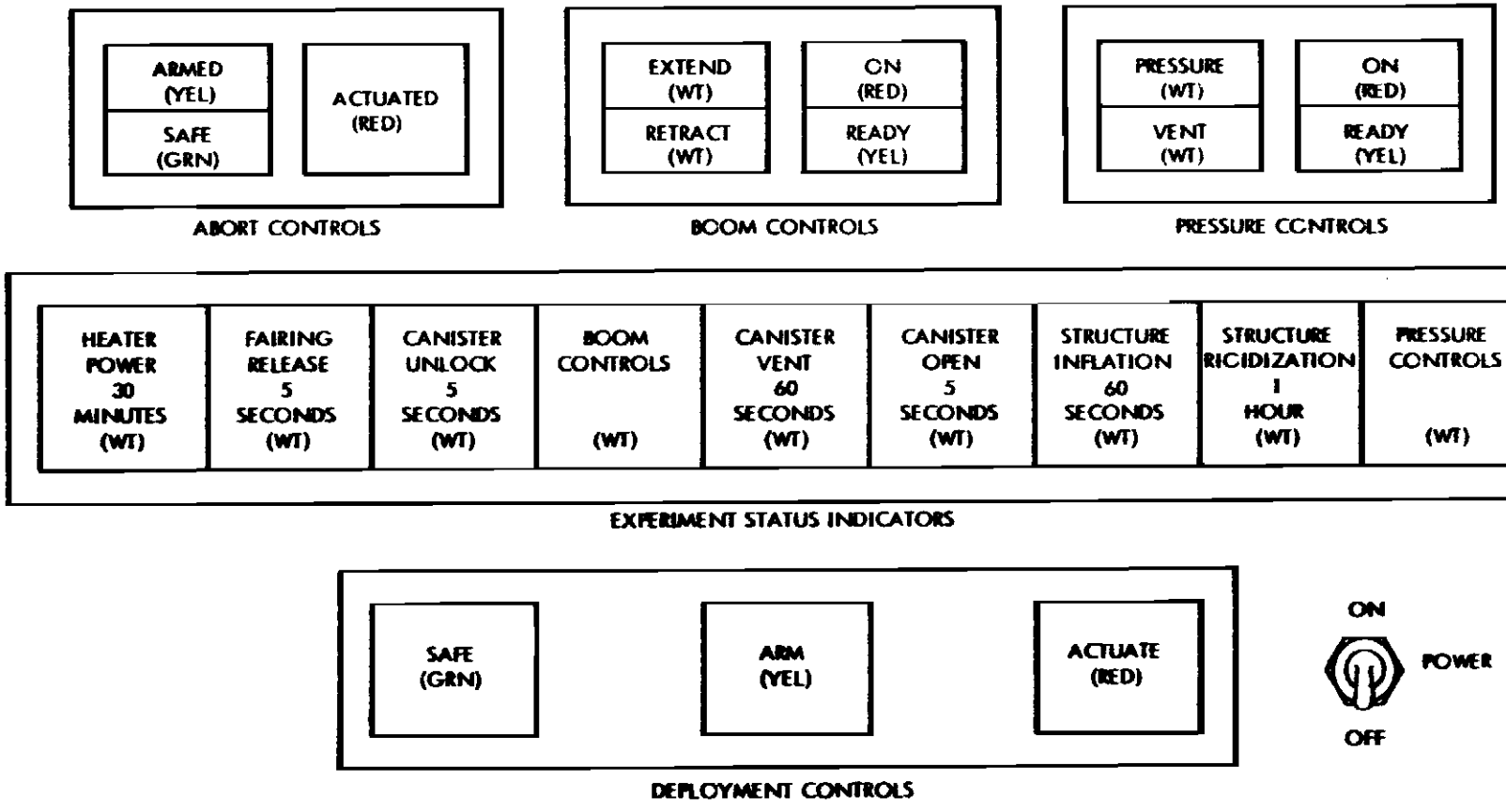

Figure 4-21. Chemical Airlock Control Console Panel Layout

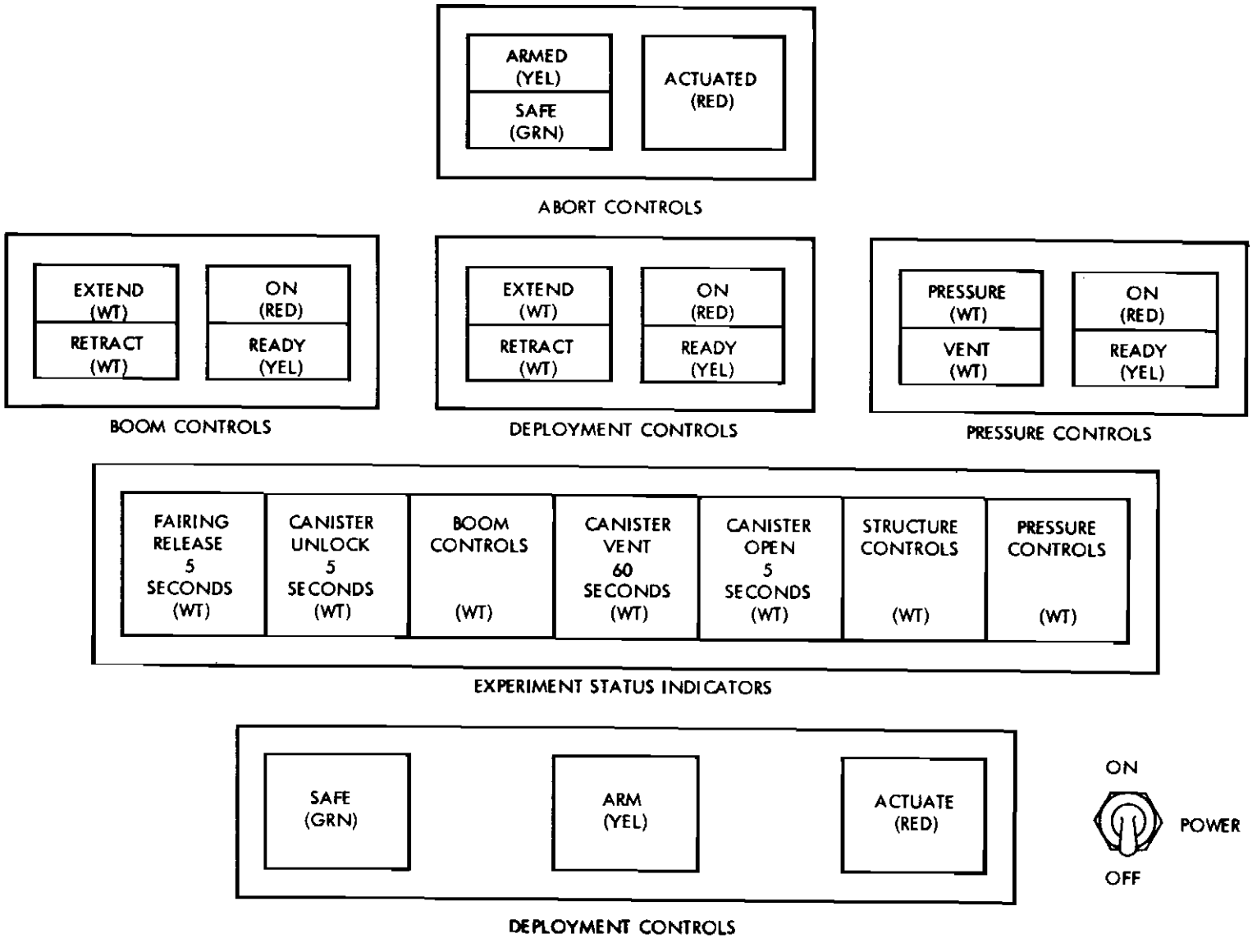

Figure 4-22. Elastic Memory Airlock Control Console Panel Layout

ARM switch is released and goes dark, while the ACTIVATE switch is lighted. This condition is maintained for the time interval indicated on the HEATER POWER display. At the end of the period, the ACTIVATE switch goes dark and the SAFE switch is lighted. Simultaneously, the HEATER POWER indicator goes dark and the FAIRING RELEASE display is lighted, indicating that this is the next step in the experiment's sequence. To activate the fairing release, the ARM and ACTIVATE switches must be operated again in the correct sequence. The ACTIVATE switch will again be lighted for the time interval noted on the FAIRING RELEASE indicator, after which the SAFE switch will be lighted.

b. The deployment sequence is continued in the above manner, until the BOOM CONTROL step is reached. At this point, when the step is actuated, the boom control READY-ON switch READY display is lighted. The EXTEND-RETRACT switch is an alternate action type and, depending on its position, controls the direction the boom will travel when the (momentary) READY-ON switch is depressed. With the EXTEND-RETRACT switch set to EXTEND and the READY-ON switch depressed to ON, the boom will extend until an (limit switch) action-complete signal is received by the console; at this time the boom control switches, ACTIVATE switch, and BOOM CONTROL indicator will go dark, while the SAFE switch and CANISTER VENT indicator will be lighted. The sequence is then continued in the usual manner. The pressure control switches are arranged in the same manner as the boom control switches, and are not energized until the last step in the sequence has been reached.

c. The armed or actuated control circuit conditions may be interrupted at any time in the deployment sequence by momentarily depressing the SAFE switch. If a deployment step has been actuated, operation of the SAFE switch will automatically advance the sequence to the next step, before the time interval is complete. This enables the console operator to progress rapidly through the deployment sequence if, in his opinion, the preceding steps have been successfully completed.

d. The abort control switches are momentary-contact, magnetically held types. To initiate jettison, the SAFE-ARMED switch must first be depressed, and then the ACTIVATE switch. The switches are held in automatically until power is removed from the console.

A simplified schematic designed to illustrate the general principles of operation of the control system is shown in Figure 4-23. A solid-state ring counter is used to control the deployment sequence, and a solid-state RC timer

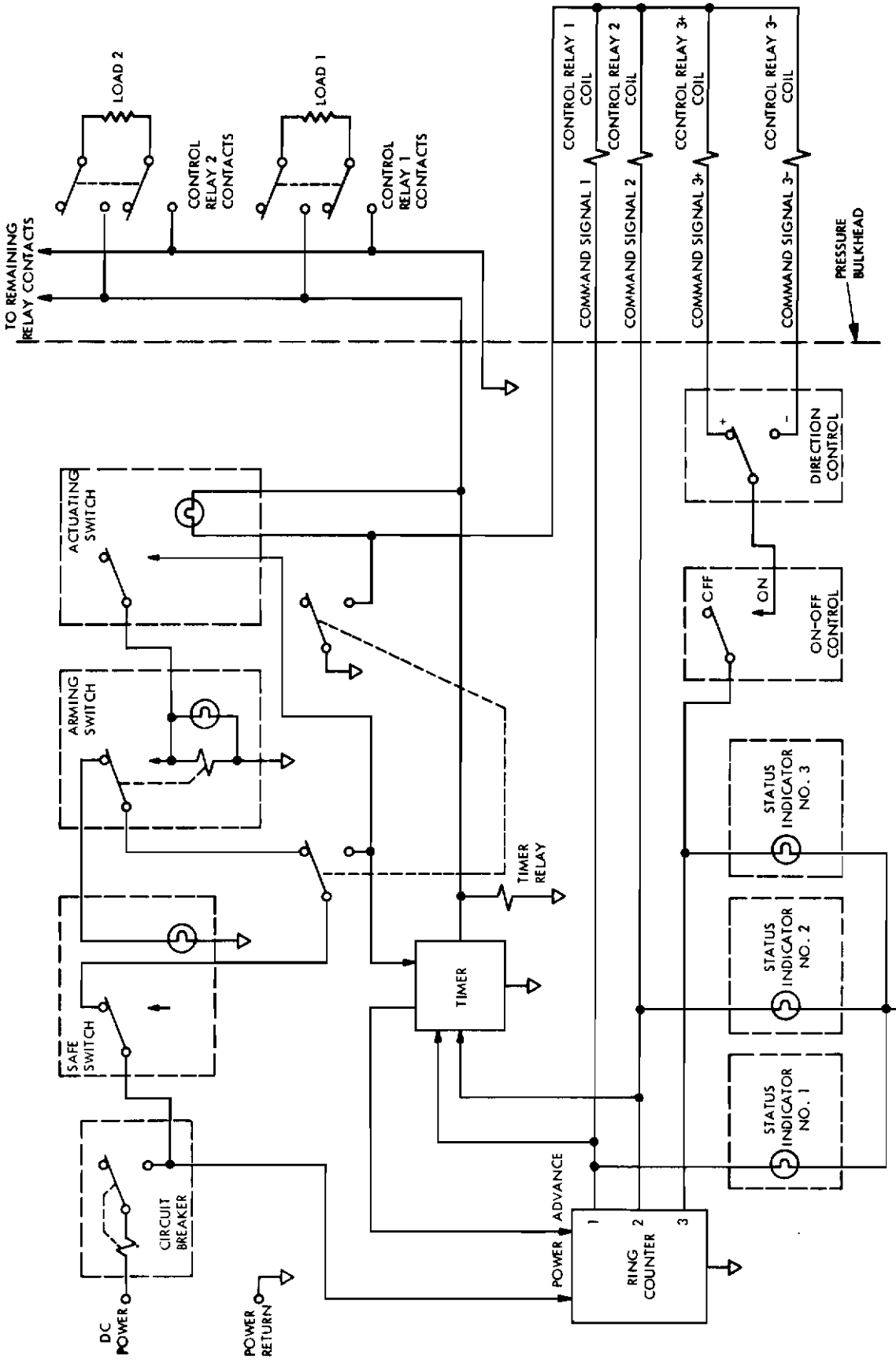

Figure 4-23. Simplified Schematic Typical of Control Console Design

is to be used to control the period during which power is applied to a control device. When the circuit breaker power switch is closed, the safe switch lamp(s) is lighted, if the timer relay is not energized and the arming switch is in a safe position. Simultaneously, the ring counter produces a voltage output at point 1 and status indicator number 1 is lighted. The output at point 1 is also connected to a circuit in the timer which will generate the necessary time interval for step 1 when power is applied to the unit.

When the arming switch is actuated, it is held in position by its holding solenoid, its indicator lamp(s) is lighted, power is removed from the safe switch lamp, and power is connected to the actuating switch. If this switch is closed momentarily, the timer produces a voltage output which energizes the timer relay. When the relay contacts transfer, power is connected directly from the safe switch to the timer, power is removed from the arming switch, and the actuating switch lamp(s) and control relay coils are grounded. The output of the ring counter actuates control relay number L, connecting the timer output to load number 1. At the end of the timing interval, the timer output falls to zero, the timer relay is released, and the circuit is returned to a safe condition. Simultaneously, an "advance" signal from the timer is used to step the ring counter output voltage to point 2, lighting status indicator number 2 for the second step in the deployment sequence. This deployment step may now be actuated in the same manner as outlined above.

At step 3 in the deployment sequence, a time interval is not programmed to permit manual control of a deployment operation. If an "action complete" signal is available, it may be used to trip the timer; otherwise, the console operator must momentarily open the safe switch to advance to the next sequence step.

The boom position and pressure controls are energized when the MANUAL CONTROL POWER switch is set to the ON position. After the experiment has been deployed, the boom may be slewed about its (nominal 90°) extended position by setting the DIRECTION switch to CW or CCW and depressing the MOTOR POWER switch. When the boom deflection exceeds a preset limit, the CW or CCW LIMIT display is lighted, and motor power is

interrupted. To restore motor power, the DIRECTION switch must be actuated to produce a motor rotation which will drive the boom away from the limit position. This feature prevents rotation of the experiment into the vehicle.

A schematic of the boom position control circuits is shown in Figure 4-24. Limit-switch-controlled relay logic circuits are employed to minimize the number of bulkhead feed-through terminations. With the boom in a stowed configuration, the cams, switches, and relays are in the positions shown. When power is applied to the control console and experiment package, relay coils K1 and K2 are energized. During the deployment sequence, power is applied to the armature of BOOM EXTEND switch S1. When S1 is set to ON, boom drive motor B1 is energized through relay contact E4 and MANUAL CONTROL POWER switch S2. As the boom is driven toward a fully extended position, cam number 1 is rotated in a (nominal) clockwise direction. After approximately 90° of rotation, a cam follower opens switch S3. Relay K1 is de-energized and power to the drive motor is interrupted.

To position the boom at various angles after deployment, MANUAL CONTROL POWER switch S2 is first set to ON. (The switch may be released by momentarily interrupting input power to the console with the circuit breaker switch.) The desired direction of rotation is selected with DIRECTION switch S4. Starting with the boom positioned at 90° (switches S3 and S6 open) and switch S4 set at CW, closure of MOTOR POWER switch S5 will produce a clockwise boom rotation until a preset limit (135° nominal) is reached. At this point switch S6 is closed and S3 is open. Relay K2 is energized, interrupting power to the drive motor and lighting CW limit indicator lamp LI1DS2. To drive the boom away from the limit, switch S4 must be set to CCW. The boom can then be driven in a counterclockwise direction until another preset limit (45° nominal) is reached. At this point, both relays are energized to apply power to CCW limit indicator lamp LI1DS1, while interrupting power to the motor. As in the CW limit case, switch S4 must be set to its alternate position to drive the boom away from the CCW limit. When the boom is between limits it can be driven in either direction.

The pressure controls will be interlocked to insure that neither pressurization or venting occurs if both controls are depressed simultaneously.

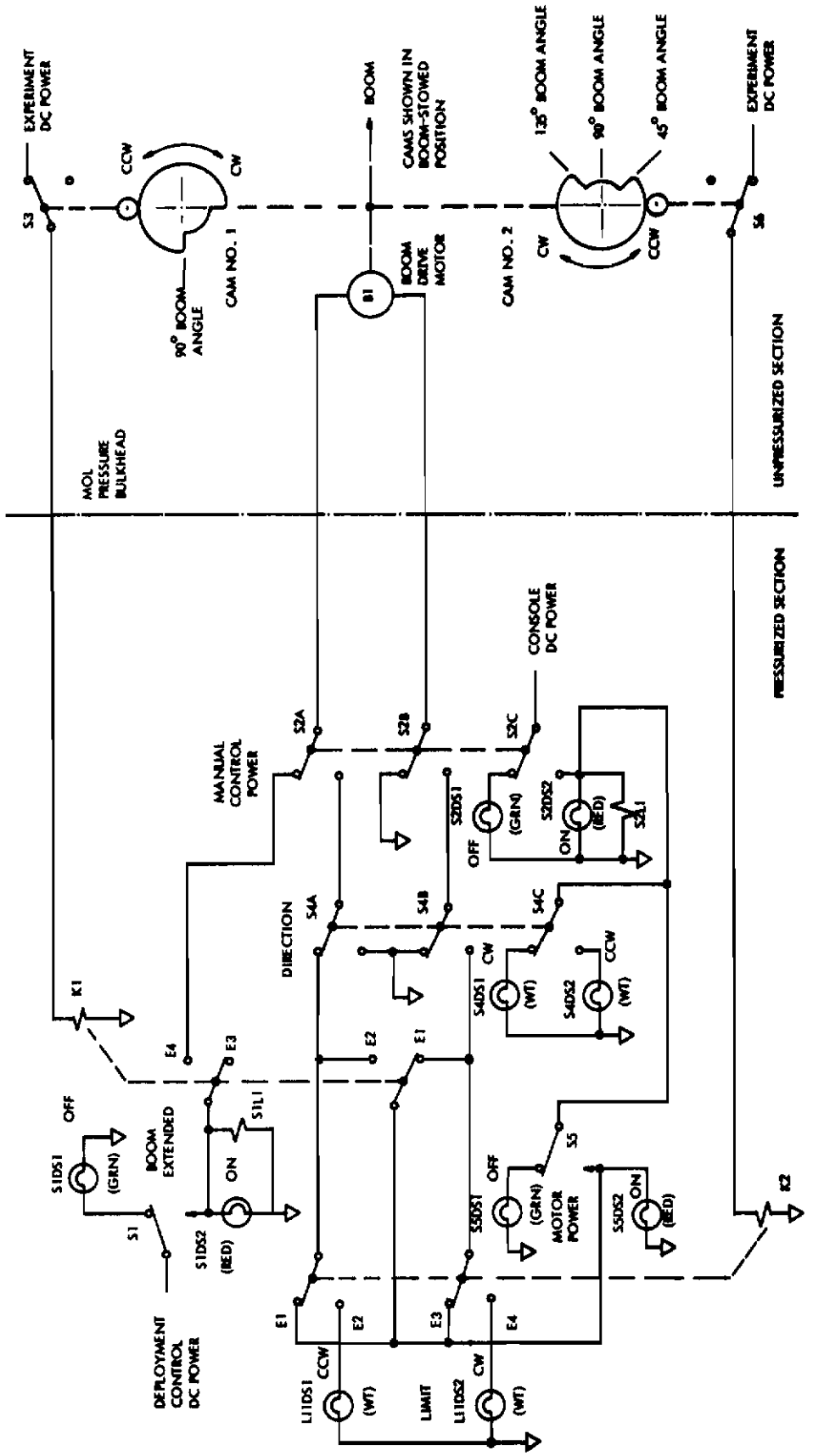

Figure 4-24. Typical Motor Control Schematic

4.4.2 ELECTROEXPLOSIVE SUBSYSTEM (EES)

Design of the electrical portion of the EES is based on the requirements of AFSCM 80-7, Part D (Reference 2, see page 4-164), as shown in a general schematic of the preliminary design in Figure 4-25. The circuit is designed to minimize the number of through-bulkhead terminations required for control functions, while providing adequate protection against RF pickup, static electricity, and spurious signal pickup hazards.

For increased reliability, electroexplosive devices (EED) will incorporate dual bridgewire initiators with no-fire characteristics of 1 watt DC/1 ampere DC for 5 minutes. A noninductive resistor (R1A, R2A, R2B, Figure 4-25) will be placed in series with initiator to impede the flow of any RF-induced currents, and will be power-limited to act as a fuse in the event activation produces a continuously shorted pyrotechnic initiator. To protect against static electricity buildup, 100,000-ohm resistors (R1B and R2C, Figure 4-25) will be connected between the firing circuits and chassis ground. Cables to the EED's will be twisted and shielded. The shields will be terminated as close to the initiators as practical, and will be insulated to prevent multiple grounding.

Each EED function will be controlled by a single relay which will be actuated by a command signal from the experiment control console. Double-pole contacts will be used to provide complete electrical isolation of the EED from the power source prior to arming and initiation

4.4.3 INSTRUMENTATION SYSTEM

The instrumentation system has been designed as an analog-to-digital type system rather than being completely analog. The instrumentation system is applicable to both the airlock and parabola experiment for a MSL vehicle. The factors that led to the design are as follows:

a. Facility of handling information

b. Predicted interface capability with mission telemetry

c. Capability to monitor any selected channel while the commutator scans all the data channels continuously

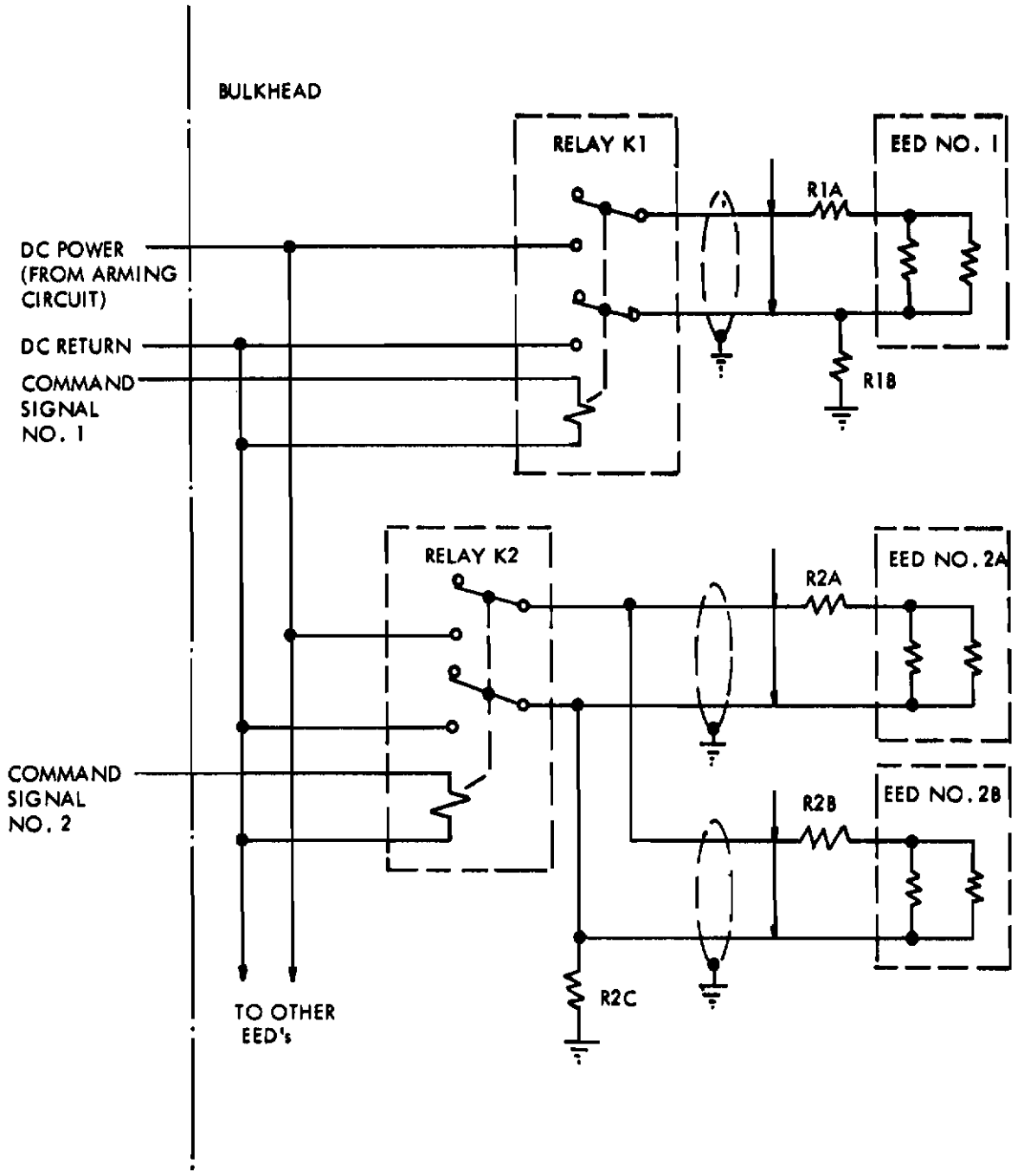

Figure 4-25. General Schematic of Electroexplosive Subsystem

The sensors will be in the configuration as seen in Figure 4-26, but will be divided into high-level sensors (potentiometer type gages) and low-level sensors (resistance thermometers and strain gages) for the purposes of commutation and amplification. All sensors will be excited with a precision regulated 5 Vdc from the experiment system power supply.

The output of each transducer will be passively filtered to eliminate unwanted noise and frequency components that cannot be handled by the sampling rate of 30 channels per second. The low-level transducers will have a balance potentiometer in their bridge network and the resistance thermometers will be resistively attenuated to a full-scale output of 50 millivolts.

As shown in Figure 4-26, the outputs of the low-level transducers are applied to a commutator which will switch the differential sensor outputs to an operational amplifier with a fixed gain of 100. This will produce a full-scale output of 5 Vdc for all the low-level transducers. The outputs of the high-level switches, at 5 Vdc full scale, are applied to a separate commutator.

A commutation switch is inserted in series with the output of the differential amplifier and is closed whenever any one of the low-level differential switches is closed. This switch is necessary to prevent the low output impedance of the differential amplifier from shorting out the input of the analog-to-digital converter at those times when high-level switch information is being read by the analog-to-digital converter.

The sequence generator shown in Figure 4-26 provides operating signals for the commutators in the proper sequence and at the rate of 30 channels per second. In addition, it supplies signals for A-to-D converter operation, differential amplifier switch operation, and a six-bit code for channel address information.

The A-to-D converter encodes the 0 to 5-Vdc input information to an accuracy of 0.1 percent. The output of the converter is in binary-coded, decimal information using a total of twelve bits. The use of binary-coded, decimal information, as contrasted to the use of straight binary coding, increases by two the total number of bits required to obtain the required accuracy, but eliminates a requirement for a binary-to-decimal converter necessary to provide readily understood information at the astronaut's control panel.

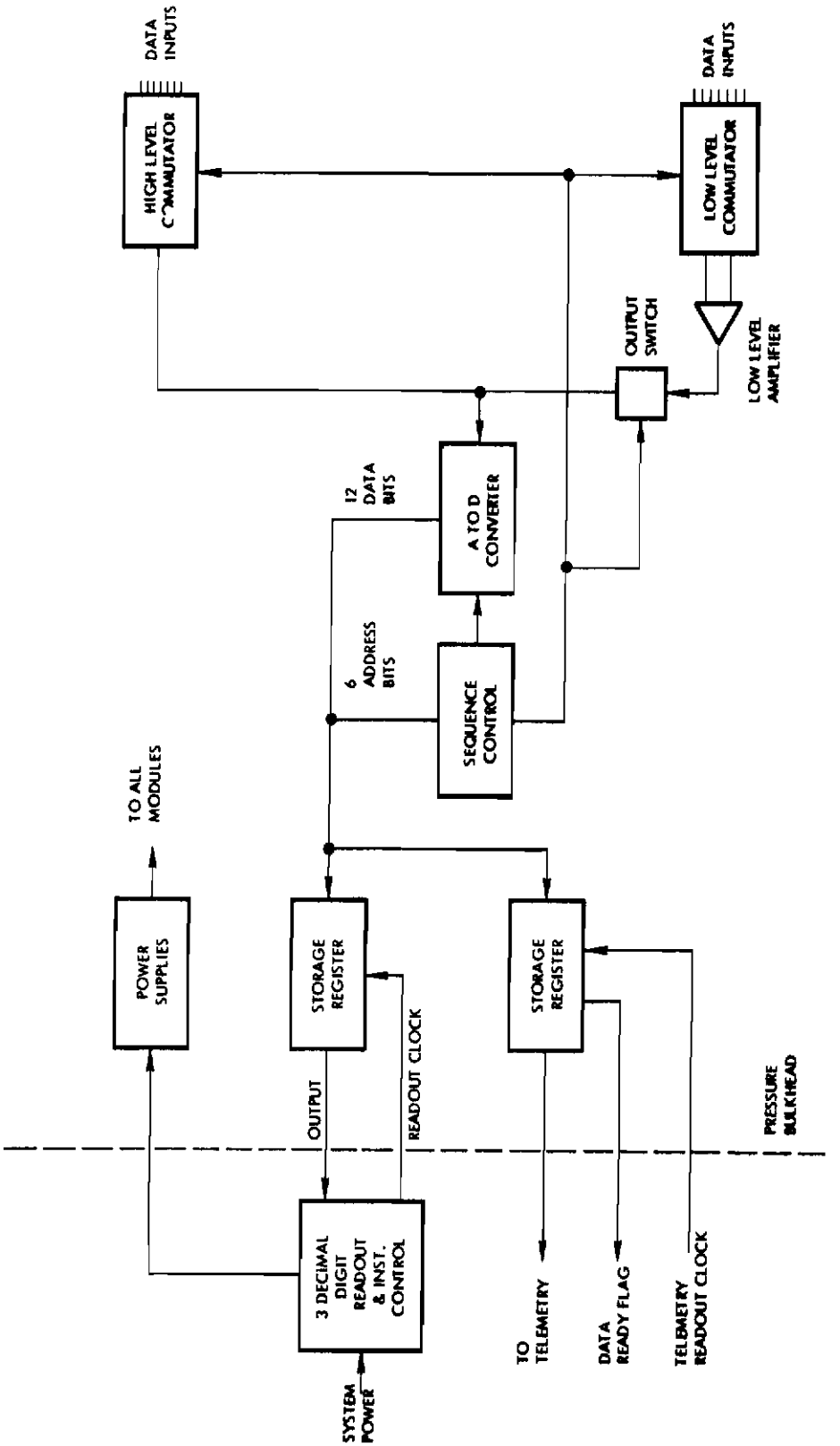

Figure 4-26. Instrumentation System, Block Diagram

Eighteen-bit output storage registers are supplied for the telemetry readout and the display panel readout. The information in the storage registers consists of the twelve-bit data information plus a six-bit binary-coded address. After the information has been transferred to the storage register from the A-to-D converter and the sequence generator, a "data ready" flag is set as an indication to the external telemetry system, which will then clock-out the information at a high rate. A "reading data" flag will be sent by the external telemetry system which will prevent the A-to-D converter from generating information during the readout operation.

A calibration signal will be placed on one channel of the system. It will be commutated on every scan cycle and fed into the low-level amplifier for amplification and encoding. This will provide for continuous system calibration and also allow the astronaut to check on system performance.

The astronaut's display panel, illustrated in Figure 4-27, will provide a three-digit decimal display of the instrumentation system readout. The astronaut will select the desired channel by means of two thumb-wheel switches, which will program a storage register to accept only data with the proper address code. The display register will then operate gates which will illuminate the proper numerals on the display screen. Display data will be updated on each scan cycle or once every second.

Controls on the display panel will include a power switch, which will supply instrumentation warm-up power and indicator power; telemetry power, which will turn on all the electronics necessary for telemetry readout; display power, which will supply power to the console readout electronics; and the experiment select switch.

There are two candidates for display numerals:

a. Gas glow tubes, which offer up to 200 ft-lambert numerals at about 0.5 watt-power per numeral.

b. Electroluminescent numerals, which offer about 15 ft-lamberts at 50 milliwatts power per numeral, which is incorporated in a compact, hermetically sealed panel.

The electroluminescent panel is attractive because of its small size and low power, but further study reveals the need for a brighter display. The

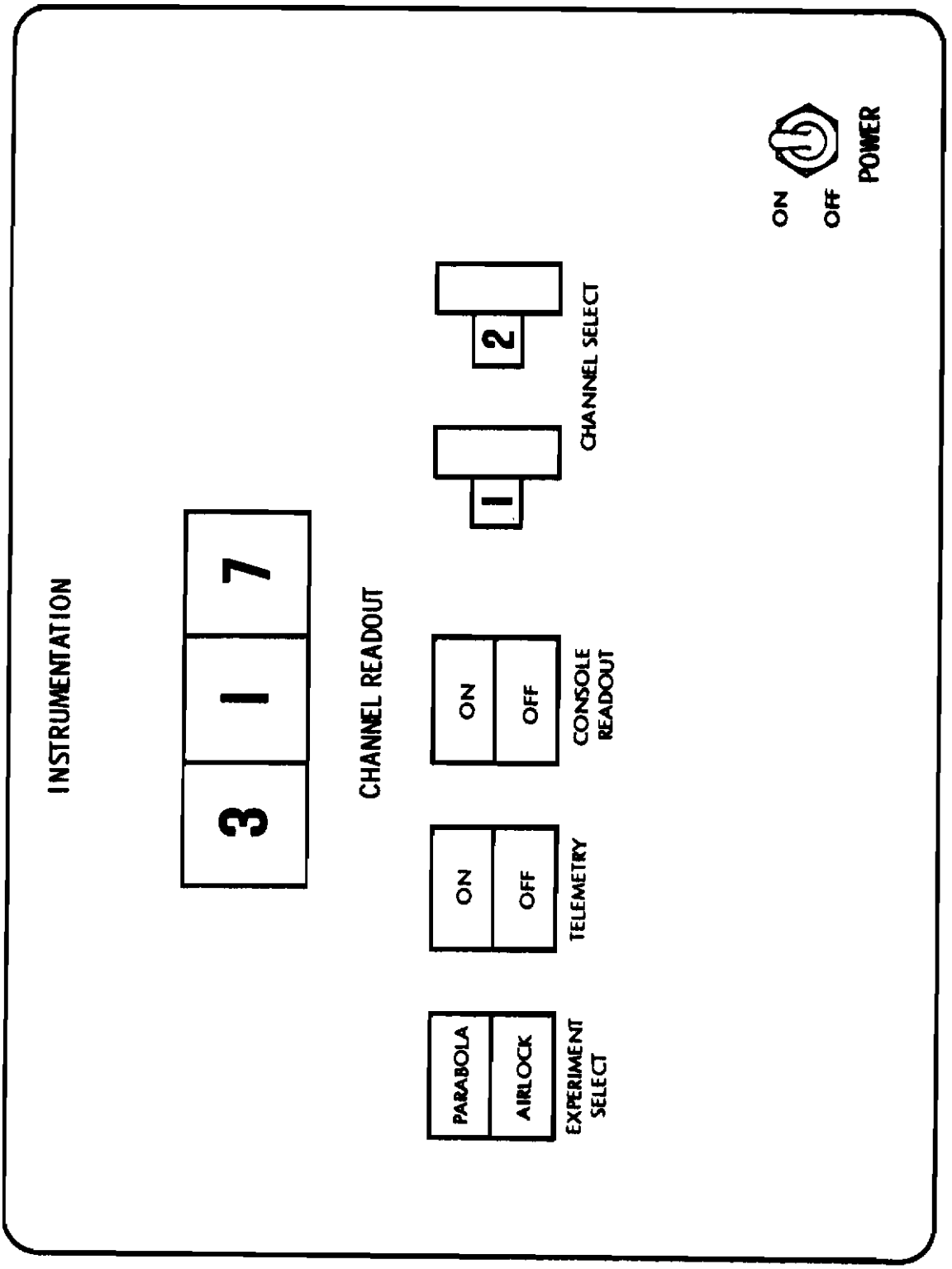

Figure 4-27. Instrumentation Control Console

display console will consume approximately 8 watts of power (using the gas glow tubes) and the scanning and encoding equipment in the unpressurized section will consume about 10 watts. The console display switch will enable the astronaut to operate the display equipment apart from the telemetry encoding and data scanning equipment for power savings when visual channel monitoring is not required. This system will require nine wires through the pressure bulkhead, including all the telemetry functions.

4.4.3.1 STRAIN MEASUREMENT

The purpose of strain measurements is to analyze the structural integrity of the chemically rigidized and elastic memory structures. Strain measurements pose a problem because of the nature of the surfaces under consideration. Conventional industrial approaches to installations of standard gages are not applicable to a flexible fabric that is subsequently rigidized. The problem in the chemical system resolves itself into attaching a limited-range strain sensor to a low-modulus flexible impregnated fabric. The elastic memory system involves the same Dacron fabric, but it will not be impregnated and rigidized, which lessens the problem somewhat compared to the chemical fabric system.

A high-elongation, post-yield type strain gage will withstand up to 10% elongation, while the standard impregnated epoxy-backed foil gages will undergo a maximum of about 5%. Semiconductor strain gages were considered but are nonlinear, very temperature-sensitive, and applicable only to strains limited to about 3% elongation. The post-yield gage will be used on the fabric surfaces, and the standard epoxy-backed gage will be used on the metal walls and hatches.

The post-yield strain gage will be used in a Wheatstone bridge circuit with an inactive gage mounted in the vicinity of the active gage in one leg for the purpose of temperature compensation. The BLH Corporation PFA-50-12 gage is a post-yield foil gage which comes in the standard 120-ohm value and is useful over the temperature range of interest.

The strain gage bridge circuit is shown below:

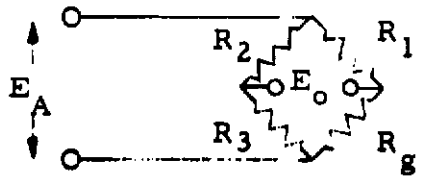

E_A = Applied voltage

R_g = Gage Resistance

E_o = Output voltage

The bridge output is given by

$$E_o = \frac{R_g R_1}{R_g + R_1} IKdS$$

I = Gage current

K = Gage factor

dS = Strain level (inches-per-inch)

For the following values of the parameters at a strain level of 6%,

R_g = 120

I = 5 ma

K = 2.1

dS = 0.06

R_1 = 880 ohms

E_o is calculated to be 67 millivolts. For compensation of the strain gage, a similar gage can be mounted in the adjacent arm of the bridge circuit. Temperature information is also available from a resistance thermometer which will be located in close proximity to the strain gage.

Changes in lead resistance due to temperature will be minimized by using equal resistance leads with the three-wire method of sensor resistance measurement.

Installation of a strain gage on a flexible fabric involves special considerations to be certain the gage receives the same strain as the fabric to which it is bonded. Also, when the fabric is under stress, the warp and fill fibers of the fabric tend to cause high, localized stresses at many points along the gage, leading to premature failure at the points of high stress.

To provide a suitable surface on which to mount the gage, a section of the fabric large enough to accommodate the gage will be stiffened with a filling compound such as Adiprene. The surface of the cured Adiprene is sanded smooth and a thin sheet of urethane film is placed on the prepared surface to act as a buffer for high point stresses. The gage is bonded to the film and fabric with post-yield cement. This method of application has given excellent results for strains up to 10% and, as Dacron will yield around 6%, there is a good margin of safety. Figure 4-28 shows a diagram of the fabric installation of the post-yield strain gage (Reference 1).

In the case of the chemically rigidized system it may prove more reliable to bond the post-yield gage, as just described, to a small section of fabric and then sew the patch to the structural fabric. The fabric will then be impregnated with the resin which will be an effective bond for the strain gage. No sewing will be subjected to stress as the rigidized resin will carry the shear loads to the patch. Tests must be conducted to establish the share of the loads seen by the strain gage, and all gage locations will be calibrated for accurate strain measurement.

Gages on any external surface of the structure will have to be covered with a sheet of aluminized mylar or other thermal control coatings to provide a thermally continuous surface, in order that accurate measurements can be made, and to eliminate thermal perturbations of the surface. The mylar or thermal patch can be mounted directly over the gage with the cement that is used to bond the gage to the fabric. Cements which do not yield with the fabric will unduly stiffen the area and lessen the effectiveness of the strain gage. These effects will be determined in hardware development phases. An alternate consideration would be the use of a circumferential pi-band provided with an extentiometer to give an average strain indication.

Tentative assignments of strain gage locations on the airlock appear in Figure 4-29. They are located on the inner wall of the structures at points that will give a maximum of information about the structural integrity of the airlock. The inner wall of both systems is the primary load-carrying surface; instrumenting the outer wall would give only low-level strain which would not provide structural strength information when the structure is loaded as a pressure vessel.

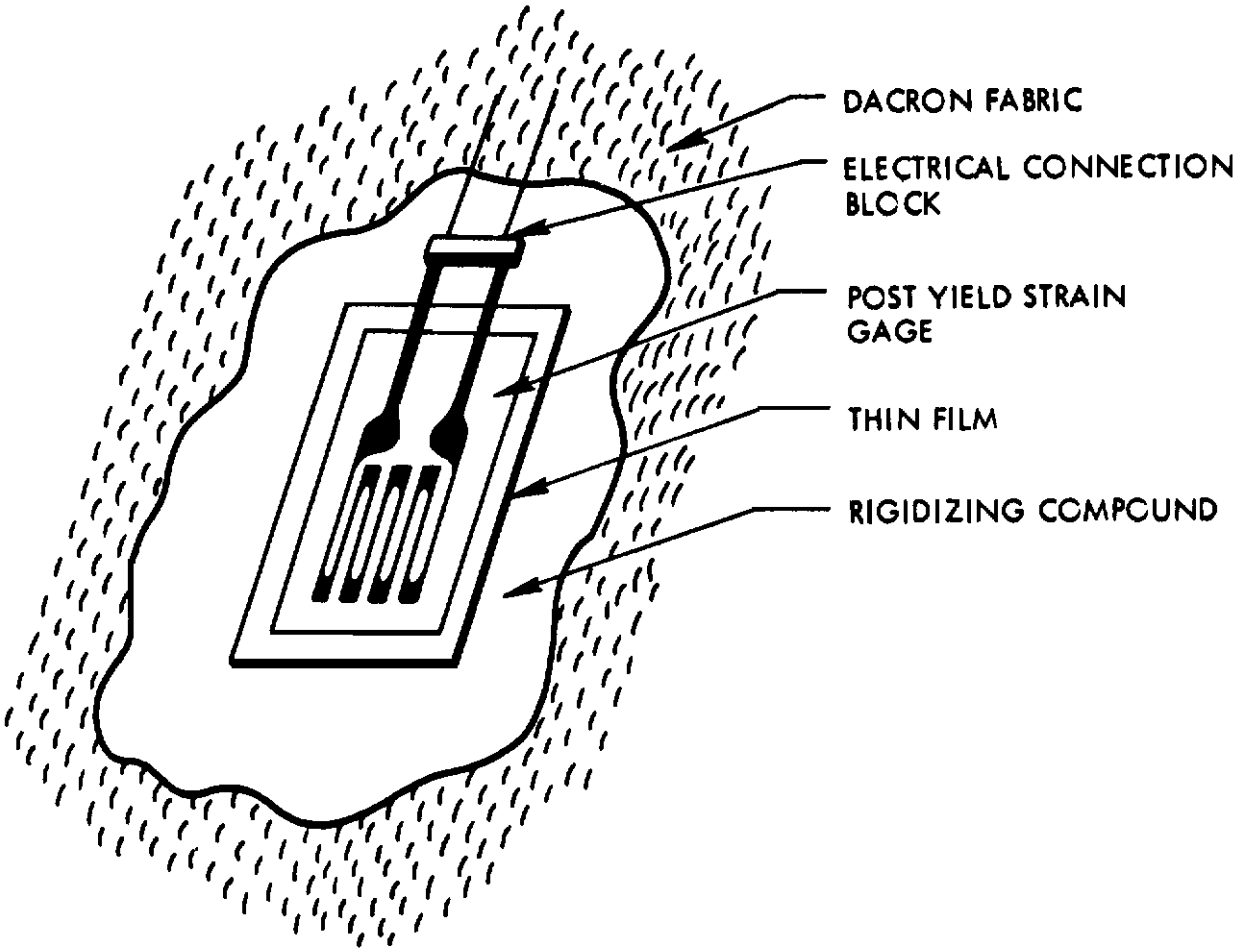

Figure 4-28. Application of a Post-Yield Strain Gage to Dacron Fabric

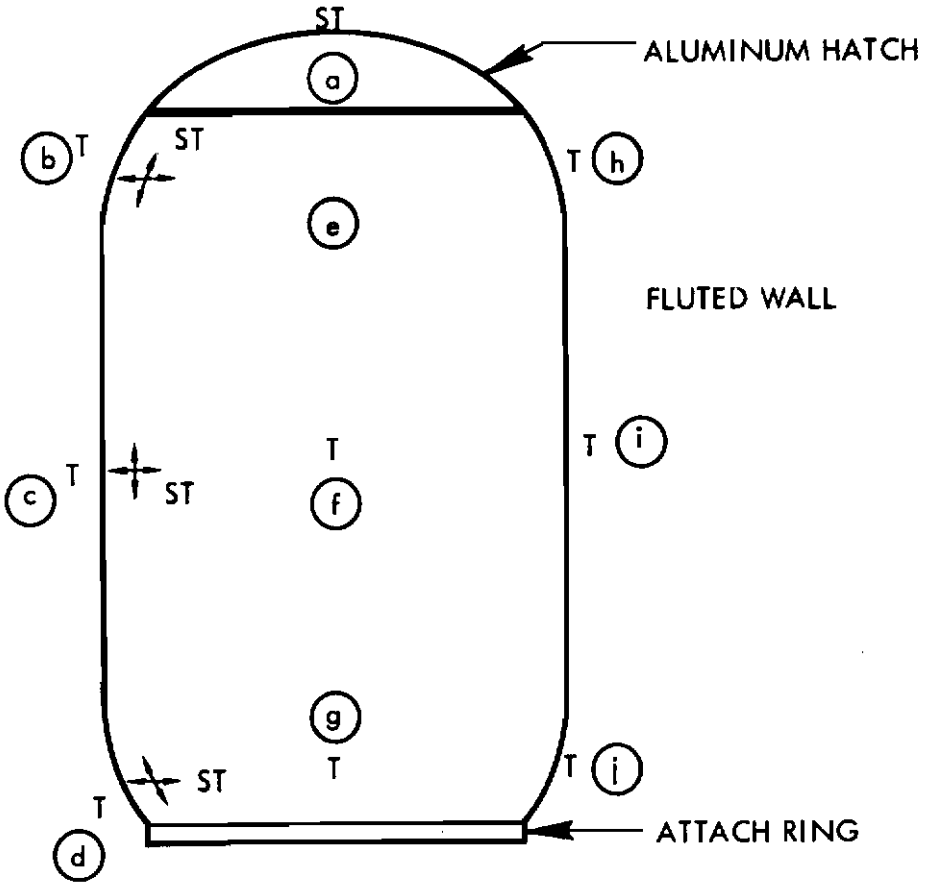

S STRAIN GAGE LOCATION

T RESISTANCE THERMOMETER LOCATION

DIRECTION OF STRAIN MEASUREMENT

1. STRAIN AND TEMP GAGES ARE ON THE INTERIOR SIDE AT (a) (b) (c) & (d) AND TEMP GAGES ONLY ARE ON EXTERIOR SIDE AT ALL OTHER LOCATIONS
2. (k) (l) & (m) ARE 180° FROM (e) (f) (g) RESPECTIVELY

Figure 4-29. Airlock Sensor Location Diagram

4.4.3.2 TEMPERATURE MEASUREMENT

Temperature measurements on the expanded structures will be made to determine several factors:

a. Extremes in surface temperatures

b. Thermal gradients in the structural walls

c. Thermal profiles along instrumented surfaces

d. Internal air temperature in the airlock

Temperature measurement locations will also be coordinated with strain measurement locations for comparative data and compensation.

The temperature transducer selected must be high in output and must lend itself to simple signal conditioning. Thermocouples require a reference junction and have low-level outputs. Thermistors are extremely nonlinear and difficult to instrument. The resistance thermometer is the best choice, as it exhibits good linearity, long-term stability, and a relatively high output.

Various metals such as platinum, nickel, copper, and several alloys are used in available resistance thermometers. Of these, the nickel thermometer, being relatively low in cost and possessing good linearity, represents the best candidate for the expandable structures system. Several backing materials are available, depending on the temperature range expected and the surface to be instrumented. A cloth backing will be used for fabric installation and the impregnated paper-backed gages will be used for metal surfaces.

RDF Corporation's BN-series nickel resistance thermometers have a continuous operating range from -100°F to +300°F, which is within the range of expected measurement. The BN-350 gage will serve as a suitable example for circuit calculations. The circuit shown in Figure 4-30 is one-half of a bridge network and the excursion of the output voltage of this leg will be examined.

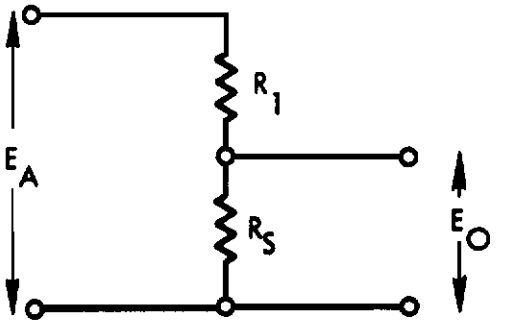

$$E_O = E_A \frac{R_S F_T}{R_1 + R_S F_T}$$

$$F_T = \frac{R_S}{R_{S_{-0}}} \quad \text{(TEMP. FACTOR)}$$

RESISTANCE THERMOMETER CIRCUIT

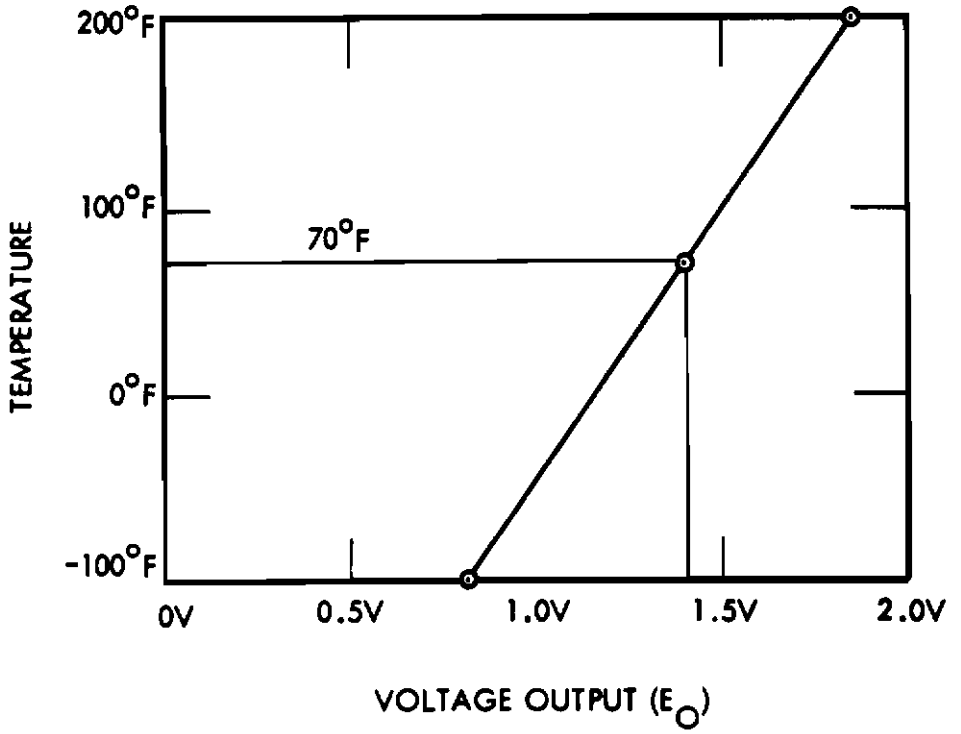

Figure 4-30. Electrical Output of Resistance Thermometer Versus Temperature

$$E_o = E_A \frac{R_s F_T}{R_l + R_s F_T}$$

E_o = Applied voltage

R_l = Series resistance

R_s = Gage resistance at 70°F

F_T = Temperature factor

R_s = 350 ohms (BN-350 gage)

R_l = $4R_s$ = 1400 ohms

I_s = 4 ma (gage current at 70°F)

E_A = 7.0 V

-100°F

F_T = .536

$$E_o = 7.0 \frac{350\ (.536)}{1400 + 350\ (.536)} = 0.83 \text{ V}$$

+70°F

F_T = 1.000

$$E_o = 7.0 \frac{350}{1400 + 350} = 1.40 \text{ V}$$

+200°F

F_T = 1.437

$$E_o = 7.0 \frac{350\ (1.437)}{1400 + 350\ (1.437)} = 1.85 \text{ V}$$

A graph of this function is shown in Figure 4-30. A value of $4R_s$ for R_l represents the closest approximation to a linear output that can be obtained from the 350-ohm gage. Values of R_l, equal to $3R_s$ or $5R_s$ will cause,

respectively, positive or negative deviations from linearity. The gage factor can lead to a $\pm$ 1°F error and deviations from linearity can lead to an additional $\pm$ 1°F error. Then, with this arrangement, a temperature measurement is accurate to within $\pm$ 2°F.

Temperature gage locations for the chemical and elastic memory airlocks are shown in Figure 4-29. Table 4-4 shows gage type and other coordinating information for each location on the elastic memory system. The chemical system has the same gage locations and data.

Figure 4-31 illustrates a technique for applying gages to fabric. The BN gage has a bakelite impregnated paper backing which can be applied to a metallic surface with bakelite cement. An epoxy cement is also under consideration. The SN gage has a glass cloth backing which can be sewn to the Dacron or, if required, a special cloth backing could be placed on the gage for sewing to the fabric system.

In the case of the rigidized system, the gages would have to be installed and the installation area impregnated with resin. For both elastic memory and chemical systems, the gage locations should be kept away from scheduled folds in the fabric to prevent damage to the gage installation.

As in the case of the strain gages, any temperature gage on an external surface will have to be covered with a thermal coating similar to that used on the structure. The gage will then be accurately measuring the temperature of the under side of the thermal coating and will not cause a thermal discontinuity across the surface of the structure.

A thermal profile will be obtained along a vertical line on four sides of the airlock at 90° intervals, as shown in Figure 4-29. This method of sensor location will give the most complete thermal profile information with a limited number of sensors. Sensors placed on the inside wall of the airlock will give added information regarding thermal gradients.

4.4.3.3 AIRLOCK PRESSURE MEASUREMENTS

The chemically regidized airlock will require a sealed canister for storage prior to its deployment. In the case of the gelatin system, an absolute

Table 4-4

ELASTIC MEMORY AIRLOCK FOR MSL VEHICLE MEASUREMENT LIST

Channel No	Function	Range of Measurement	Sensor Location	Installation Technique	Sensor Type	Manufacturer and Part No.
1	Calibrate	5.00 VDC	Ref. voltage in DATA package	N.A.	Zener Diode with Trimpot	
2	Airlock Pressure	0-7.5 psi	Base of Extension Boom	Pressure Measurement Line	Pressure Transducer	EDCLIFF 2-200
3	Airlock Temperature	-50 to +150°F	Lower Hatch Wall	Not Illustrated	Resistance Thermometer	RdF BN-350
4	Reservoir Pressure	0-4000 psi	Reservoir Pressure Line	Direct to Pressure Line	Pressure Transducer	CED 4-314A
5	Deployment Position	0-100%	Base of Airlock	Retract Cable Turns Pot	Potentiometer	Litton MD02-20
6	Hatch Strain	0-1%	Figure 9. Position (a) (Int.)	Not Illustrated	Foil Strain Gage	BLH FAB-50-12
7	Hatch Temperature	-100 to +200°F	Figure 9. Position (a) (Int.)	Not Illustrated	Resistance Thermometer	RdF BN-350
8	Fabric Strain	0-6%	Figure 9. Position (b) (Int.)	Figure 8	Post-Yield Strain Gage	BLH PFA-50-12
9	Fabric Strain	0-6%	Figure 9. Position (b) (Int.)	Figure 8	Post-Yield Strain Gage	BLH PFA-50-12
10	Fabric Temperature	-50 to +150°F	Figure 9. Position (b) (Int.)	Figure 11	Resistance Thermometer	RdF SN-350
11	Fabric Strain	0-6%	Figure 9. Position (c) (Int.)	Figure 8	Post-Yield Strain Gage	BLH PFA-50-12
12	Fabric Strain	0-6%	Figure 9. Position (c) (Int.)	Figure 8	Post-Yield Strain Gage	BLH PFA-50-12
13	Fabric Temperature	-50 to +150°F	Figure 9. Position (c) (Int.)	Figure 11	Resistance Thermometer	RdF SN-350
14	Fabric Strain	0-6%	Figure 9. Position (d) (Int.)	Figure 8	Post-Yield Strain Gage	BLH PFA-50-12
15	Fabric Strain	0-6%	Figure 9. Position (d) (Int.)	Figure 8	Post-Yield Strain Gage	BLH PFA-50-12
16	Fabric Temperature	-50 to +150°F	Figure 9. Position (d) (Int.)	Figure 11	Resistance Thermometer	RdF SN-350
17	Fabric Temperature	-100 to +200°F	Figure 9. Position (b) (Ext.)	Figure 11	Resistance Thermometer	RdF SN-350
18	Fabric Temperature	-100 to +200°F	Figure 9. Position (c) (Ext.)	Figure 11	Resistance Thermometer	RdF SN-350
19	Fabric Temperature	-100 to +200°F	Figure 9. Position (d) (Ext.)	Figure 11	Resistance Thermometer	RdF SN-350
20	Fabric Temperature	-100 to +200°F	Figure 9. Position (e) (Ext.)	Figure 11	Resistance Thermometer	RdF SN-350
21	Fabric Temperature	-100 to +200°F	Figure 9. Position (f) (Ext.)	Figure 11	Resistance Thermometer	RdF SN-350
22	Fabric Temperature	-100 to +200°F	Figure 9. Position (g) (Ext.)	Figure 11	Resistance Thermometer	RdF SN-350
23	Fabric Temperature	-100 to +200°F	Figure 9. Position (h) (Ext.)	Figure 11	Resistance Thermometer	RdF SN-350
24	Fabric Temperature	-100 to +200°F	Figure 9. Position (i) (Ext.)	Figure 11	Resistance Thermometer	RdF SN-350
25	Fabric Temperature	-100 to +200°F	Figure 9. Position (j) (Ext.)	Figure 11	Resistance Thermometer	RdF SN-350
26	Fabric Temperature	-100 to +200°F	Figure 9. Position (k) (Ext.)	Figure 11	Resistance Thermometer	RdF SN-350
27	Fabric Temperature	-100 to +200°F	Figure 9. Position (l) (Ext.)	Figure 11	Resistance Thermometer	RdF SN-350
28	Fabric Temperature	-100 to +200°F	Figure 9. Position (m) (Ext.)	Figure 11	Resistance Thermometer	RdF SN-350
29						
30						

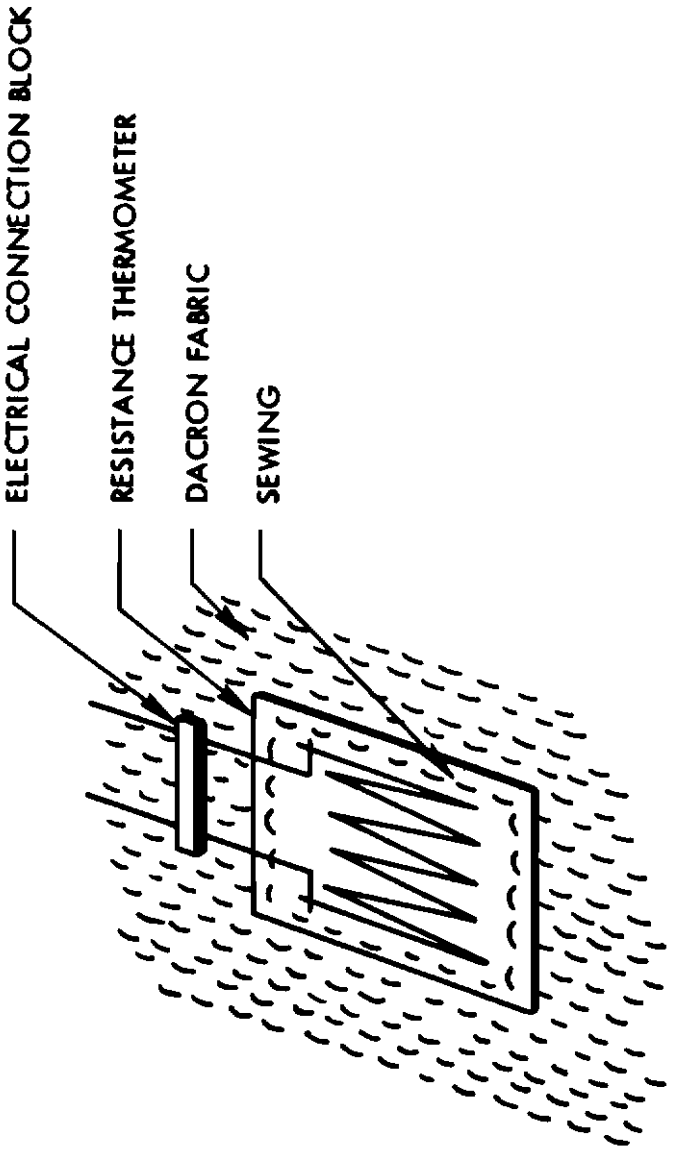

Figure 4-31. Alternate Method for Application of Resistance Thermometer to Dacron Fabric

pressure greater than 0.5 psi must be maintained inside the canister to prevent the material from prematurely rigidizing. This pressure must be consequently vented to space vacuum before deployment to prevent an explosive opening of the canister. The urethane system will not require a pressurized canister, but any residual pressure due to the outgassing of solvents will have to be vented before disengagement of the canister lid. Venting during launch may be desirable to relieve the atmospheric pressure. Canister pressure measurement is, therefore, necessary for maximum astronaut and experiment safety. An Edcliff Instrument Series 2-200 transducer, which will measure 0 to 15 psi, will be used for this measurement and the potentiometer pick-off will readily adapt to the instrumentation system signal conditioning capability.

The internal airlock pressure for both the chemical and elastic memory systems will be on the order of 7.5 to 3.5 psia. An Edcliff Series 2-200, modified for 0 to 10 psi, will provide adequate over-range protection for the application. Also, present designs for the elastic memory system do not require the pressurized canister concept, and the airlock transducer will provide measurement of predeployment pressure and subsequent test pressures applied to the structure prior to operational usage as a man-rated airlock.

The experiment pressurization system utilizes an air reservoir at 3000 psi as the supply for pneumatic requirements. A CED model 4-314A pressure transducer mounted at the inlet of the tank will be used for tank pressure measurement. The transducer uses a potentiometer pick-off and will be electrically similar to the other pressure sensors in the system.

4.4.4 INSTRUMENTATION AND CONTROLS DESIGN FOR THE SIVB AIRLOCK EXPERIMENT

4.4.4.1 GENERAL

The instrumentation and control system designs previously completed for the MSL have been reevaluated relative to the SIVB experiment and packaging requirements. The MSL design was based on complete remote deployment and control requirements, and included data scanning and signal conditioning provisions. Information available for the SIVB experiment plan and vehicle interface provisions allows for a considerably simplified control and instrumentation system. The basic control and instrumentation system design provisions are discussed in the following sections.

The provisions for instrumentation and control of the elastic recovery airlock experiment for the SSESM reflect considerations of simplicity, astronaut safety, ease of operation, and maximum assurance of experiment success. Of fundamental importance is allowance for a maximum of meaningful data to be obtained by the experiment from instrumentation sensors, film, and astronaut activity commensurate with the overall experiment objectives and system limitations.

Events which do not require the astronaut in the immediate vicinity of the experiment will be controlled from a remote console. These events include the initial deployment sequence, proof-pressurization, operational pressurization activation, venting and long term leak-check pressurization. Airlock pressure and internal temperature indications are also given on the remote console. Arm and actuate steps are required for canister release and initial pressure activation of each of the three reservoirs, since these operations are pyrotechnic in nature. The ingress/egress operational pressure reservoir requires a squib valve release before a solenoid will control air flow from the internal or remote consoles.

Integral hatch latch and vent controls are on the operational hatch as required by experiment procedure. These integral controls will be operable both internal and external to the airlock structure in the interest of operational requirements and astronaut safety redundance. An integral control panel will control operational pressure and electrically actuated venting and give indication of internal pressure. A manual vent is also provided for the astronaut for normal use. An emergency escape control is also provided to release a squib fixed clamp at the base of the airlock. This is interlocked with the vent control on the remote console.

4.4.4.2 AIRLOCK CHECKOUT PROCEDURES

Instrumentation and operational methods are being designed to ascertain the experiments' performance or status in the following functional areas:

a. Pre-installation checkout for operational condition:

   (1) Canister environment, i.e., humidity, pressure, etc.

   (2) Electrical controls and pyrotechnic-type release subsystems

   (3) Instrumentation sensor channels

   (4) Air pressurization subsystems

   (5) Electrical power sources, i.e., batteries (if used)

b. Prelaunch functional checkout:

   (1) Canister environment

   (2) Electrical control and release subsystems

   (3) Instrumentation sensor channels

   (4) Air pressurization subsystems

   (5) Electrical power sources

   (6) Vehicle system power and instrumentation interface operation

   (7) Remote control box operational condition

c. Predeployment experiment status:

(1) Canister pressure

(2) Canister temperature

(3) System electrical power

(4) Camera condition

d. Provisions for data during erection and checkout of experiment:

(1) Airlock pressure status

(2) Outer and inner surface temperature

(3) Photographic coverage of deployment and ingress/egress maneuvers (camera provided by NASA on Saturn IVB)

(4) Voice recordings of EVA astronaut during the execution of the experiment

(5) Laminar composite specimen retrieval

(6) Leakage rate of pressurized airlock through internal pressure decay and associated temperature

(7) Communication system for astronaut through umbilical connector in airlock (and/or through medical transmitter unit on PLSS)

4.4.4.3 CONTROLS

The controls which operate the airlock experiment are of three basic categories:

a. Remote deployment and pressure-test controls which will be located inside the vehicle or vehicle airlock

b. Integral controls which are on the airlock structure for normal operational functions for use by the astronaut in the performance evaluation of the airlock

c. Controls on the airlock canister base which are not required for astronaut maneuvers, such as the retract mechanism.

4.4.4.3.1 REMOTE CONTROL SYSTEM REQUIREMENTS

The remote deployment control console will allow the astronaut to erect the experiment without exposure to initial deployment and pressure-test phases. Also, the astronaut can initiate the proof pressure test, watch internal pressure and inspect it as he deems necessary. He may also vent the airlock from this position.

The remote console layout is illustrated in Figure 4-32. The following list summarizes the console's functions and indications which are necessary for all phases of airlock operation. They are arranged as close as is feasible to their operational order.

a. Experiment system power switch - turns on electrical power for all experiment operations ("on" is indicated by a red light).

b. Canister vent switch - assures the canister is vented before release of the canister cover (manual vent valve is open during launch).

c. Canister release "arm" switch - arms the canister release switch ("arm" is indicated by a red light).

d. Canister release switch - actuates the release mechanism for the canister cover.

e. Proof-pressure test switch - activates a squib valve which will allow the airlock to pressurize slowly to 5.5 psi (preceded by "arm" switch).

f. Temperature indicator - will give a reading for temperature on the internal wall of the structure.

g. Pressure indicators (2) - will indicate the airlock pressure internally and remotely.

h. Operational pressure switch - activates a squib valve which lets air flow to a solenoid valve ("arm" provision precedes squib firing switch and is indicated by a red light).

i. Ingress/egress pressure switch - turns on a solenoid valve which fills the airlock to a pressure of 3.5 psi where a pressure switch cuts off the activate signal.

j. Airlock vent switch - activates a vent valve which can be operated at any time in the procedure (internal or remote).

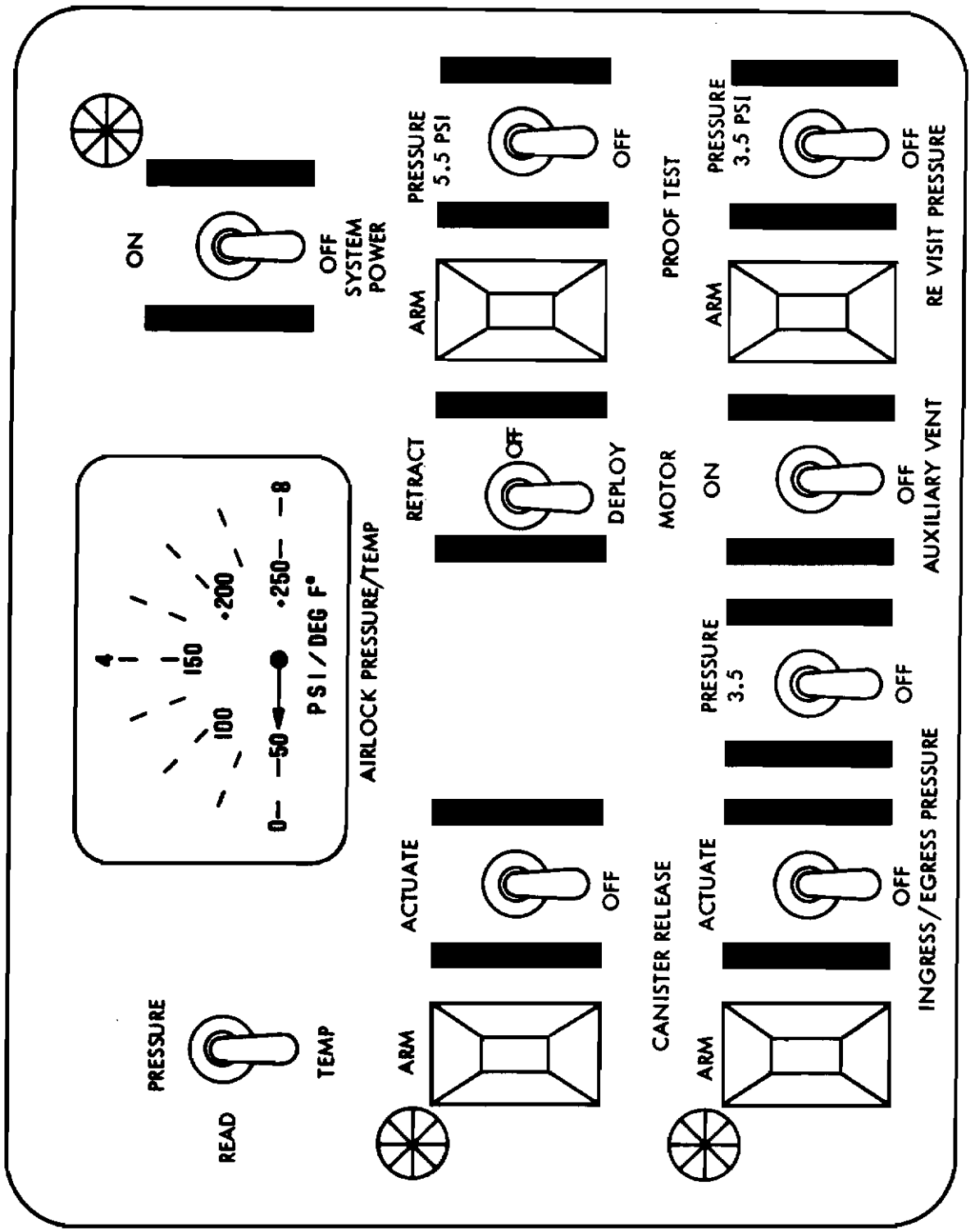

Figure 4-32. Remote Airlock Control Console

k. Revisit pressure switch - actuates a squib valve which inflates the airlock for a final leak check upon revisitation. This valve may also be manually actuated in the event DC power is not available upon revisitation.

l. Leakage will be indicated by a pressure drop in the airlock over some known period of time, over and above the pressure fluctuations due to temperature changes. Pressure and temperature data are recorded against time (during specific phases) and may be correlated accurately after the flight.

The pressurization control switches are interlocked with the canister release so that inadvertent pressurization will not be possible. When the structure has been deployed and proof-tested it will be remotely vented to vacuum. The astronaut will then go EVA to inspect the deployed airlock and prepare for the next phase of the experiment.

4.4.4.3.2 INTEGRAL OPERATIONAL AIRLOCK CONTROLS

The second phase of the experiment will be the ingress and egress trails by the pressure-switch astronaut to evaluate the structure as an operational airlock. The controls integral with the airlock which are necessary for him to accomplish the maneuvers are as follows:

a. External/internal airlock vent control - a mechanical control related to the hatch operation. (Two vent provisions are made, one manual and one electrical auxiliary.)

b. Hatch release and lock mechanism - internal and external operation of the airlock hatch.

c. Airlock operational pressure control - toggle control on the integral control panel which operates in parallel with the remote operational pressure control.

d. Airlock pressure indicator - a gage on the integral control panel which indicates internal airlock pressure.

e. Internal airlock illumination - an incandescent light is located in the airlock at a point 90° away from the control panel which provides illumination for the astronaut's activities. This light turns on when system power is turned on at the remote console.

f. **Electrical vent control** - a toggle control on the integral control panel which operates the solenoid vent valve in parallel with the remote vent control.

g. **System power indicator light** - a red light on the integral control panel indicating that the console has electrical power.

h. **Overpressure relief valve** - a relief valve which vents at 7.5 psi.

i. **Emergency release system** - actuated internal or remote, manually and/or electrically.

The integral control panel layout is illustrated in Figure 4-33.

The design of these integral controls includes consideration of the severe incumbrances offered by the fully-outfitted, pressure-suited astronaut who has very little manual dexterity and no ability to exert nonreacted forces without mechanical aids and holds. These design restraints are fully covered in the "Human Factors" section of this document.

The hatch design offers inherent safety in that it is inward opening and cannot be opened against an internal pressure, even a few-tenths of a psi. Mechanical venting is easily accomplished through a mechanism on the airlock hatch.

4.4.4.3.3 INSTRUMENTATION

Pressure indication is provided by a potentiometer-type sensor located in the lower portion of the airlock. The output of this gage is directed through an isolation amplifier to the integral and remote control consoles for an indicator readout, and to the SIVB interface for recording and telemetry readouts. A mechanical-type gage will also be placed in the airlock so that a visual indication of internal pressure can be obtained from outside the structure.

Four high-output-type nickel resistance thermometers will be located on the laminar composite walls of the airlock, one on the inside surface and one on the outside surface, with pairs being 180° apart. The output of the indicators will be available at the SIVB interface and internal temperature gage readout will be on the remote control console. A READ selection switch will allow the console readout to read pressure or temperatures.

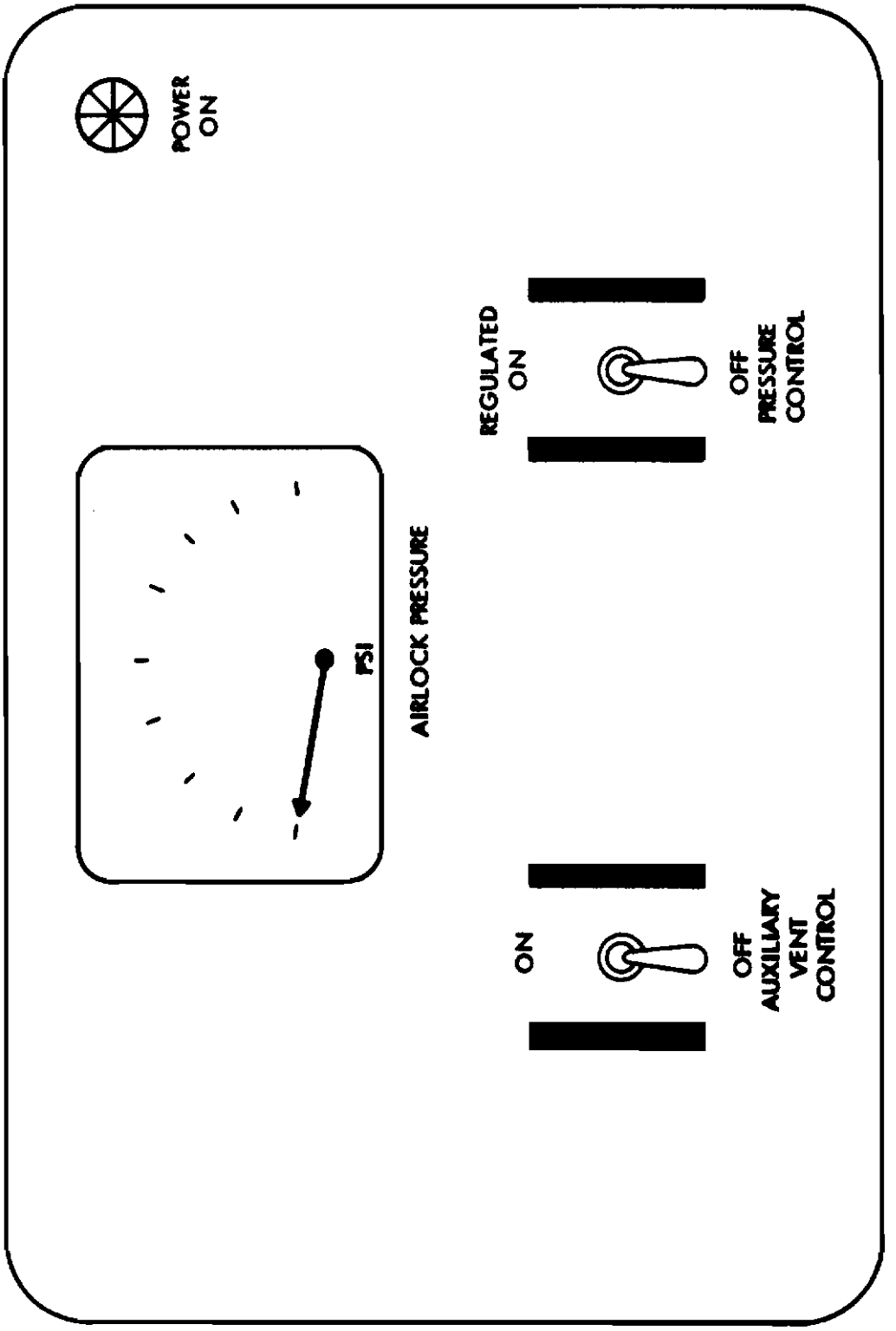

Figure 4-33. Internal Airlock Control Console

A small power conditioner will be necessary for the instrumentation sensors. A precision, 5-Vdc regulator located in the console and supplying a few milliamperes of current will handle all the instrumentation sensor power requirements.

A functional block diagram is shown in Figure 4-34.

An airlock system power demand profile is shown in Figure 4-35.

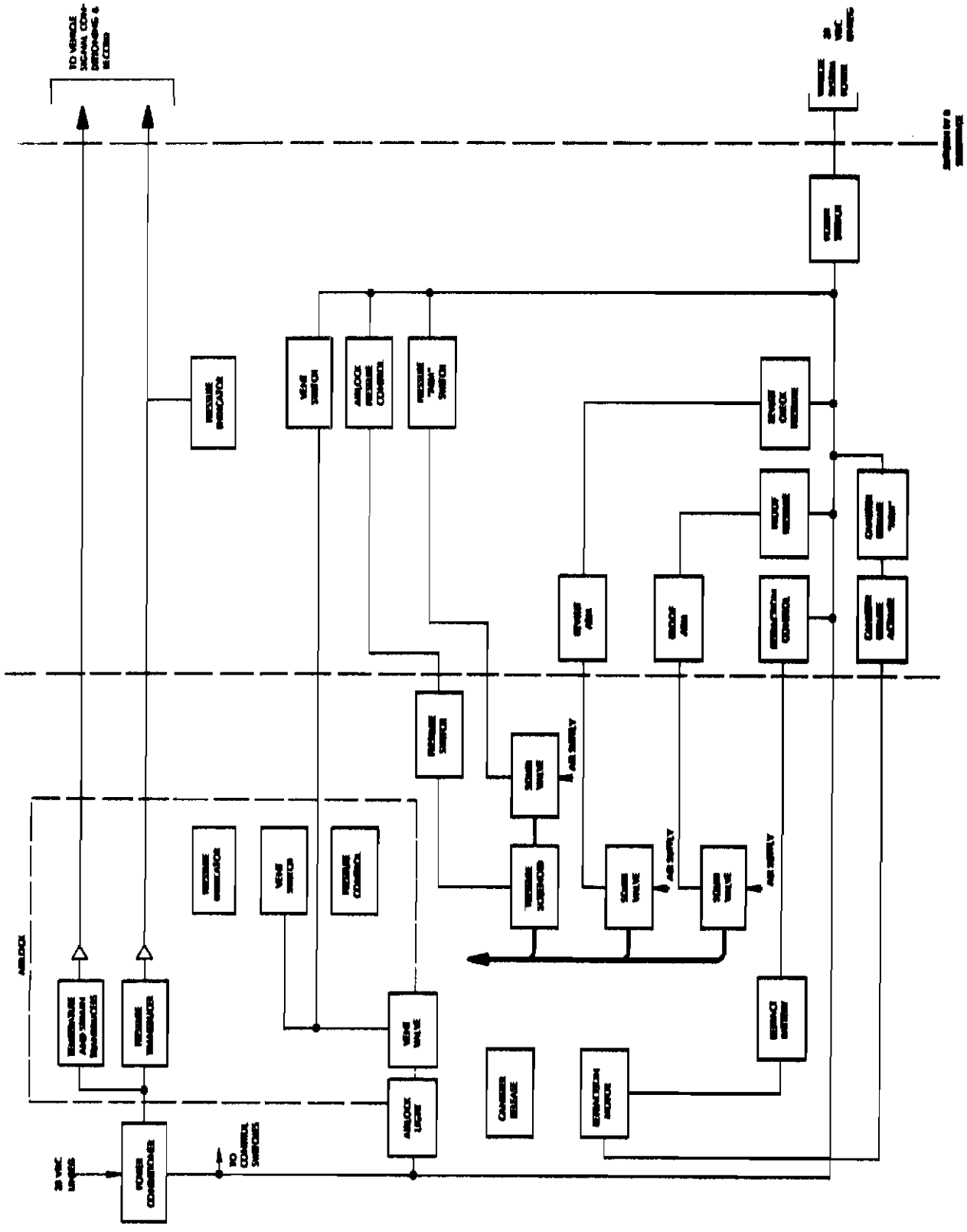

Figure 4-34. Instrumentation and Controls System, Functional Block Diagram

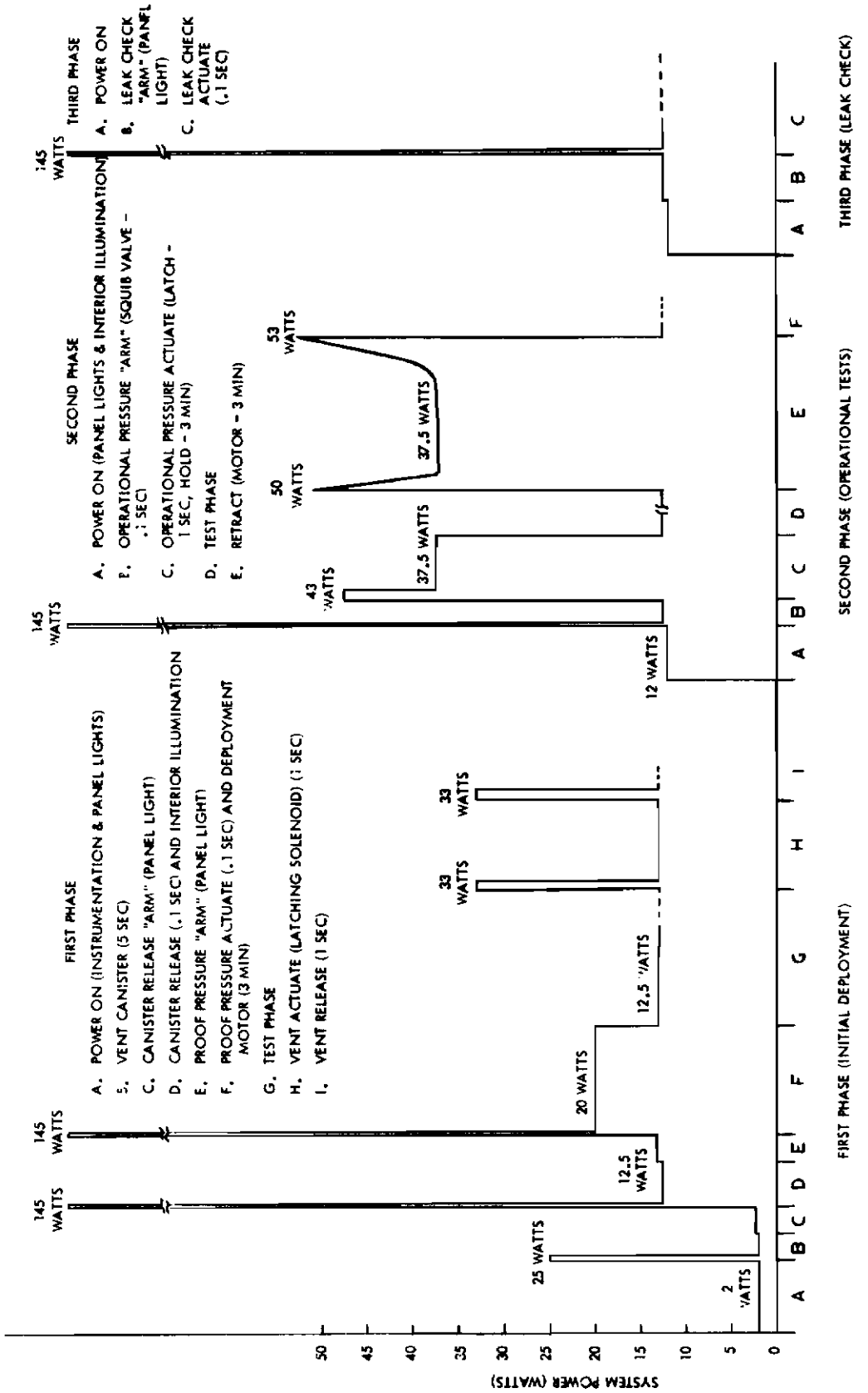

Figure 4-35. Power Demand Profile

4.5 PRELIMINARY MSL EXPERIMENT CONFIGURATION

4.5.1 AIRLOCK DESIGN STUDIES

A preliminary layout of the airlock using the elastic recovery-type material is shown in Figure 4-36. Some revisions are required due to additional design considerations, as in the area of cable seals, which will be avoided.

The design of the airlock experiment using a chemically rigidized type of material was to be virtually identical to one employing the elastic recovery material system. Two chemical systems were considered as candidates, the gelatin-impregnated and the urethane-impregnated, fluted-core fabric systems.

This airlock design will use the same hatch, upper cylinder attach ring, airlock attach clamp, and method of attaching the inner structural fabric as shown for the elastic recovery system. The lower cylinder attach ring attaches to the lower half of the canister which incorporates provisions for the airlock attach clamp, and will allow the airlock structure to be detached and moved to an operational location if desired.

The canister upper and lower shells are held together by a segmented V-clamp. A suitable, explosive-actuated device is used to release the clamp for deployment. The canister is shaped to support the inner structural fabric when deployed and is an integral part of the deployed structure. The fluted-fabric portion of the structure will be deployed between the canister halves to form the main cylindrical portion of the airlock. This experiment configuration uses a preliminary concept for a captive, inward-opening hatch, which was discussed earlier in Section 4.1.1. This concept employed the use of foldable hinges to guide the inward-opening hatch during its transient condition of opening and closing. This concept was subsequently abandoned for a tethered concept offering more simplicity and weight reduction.

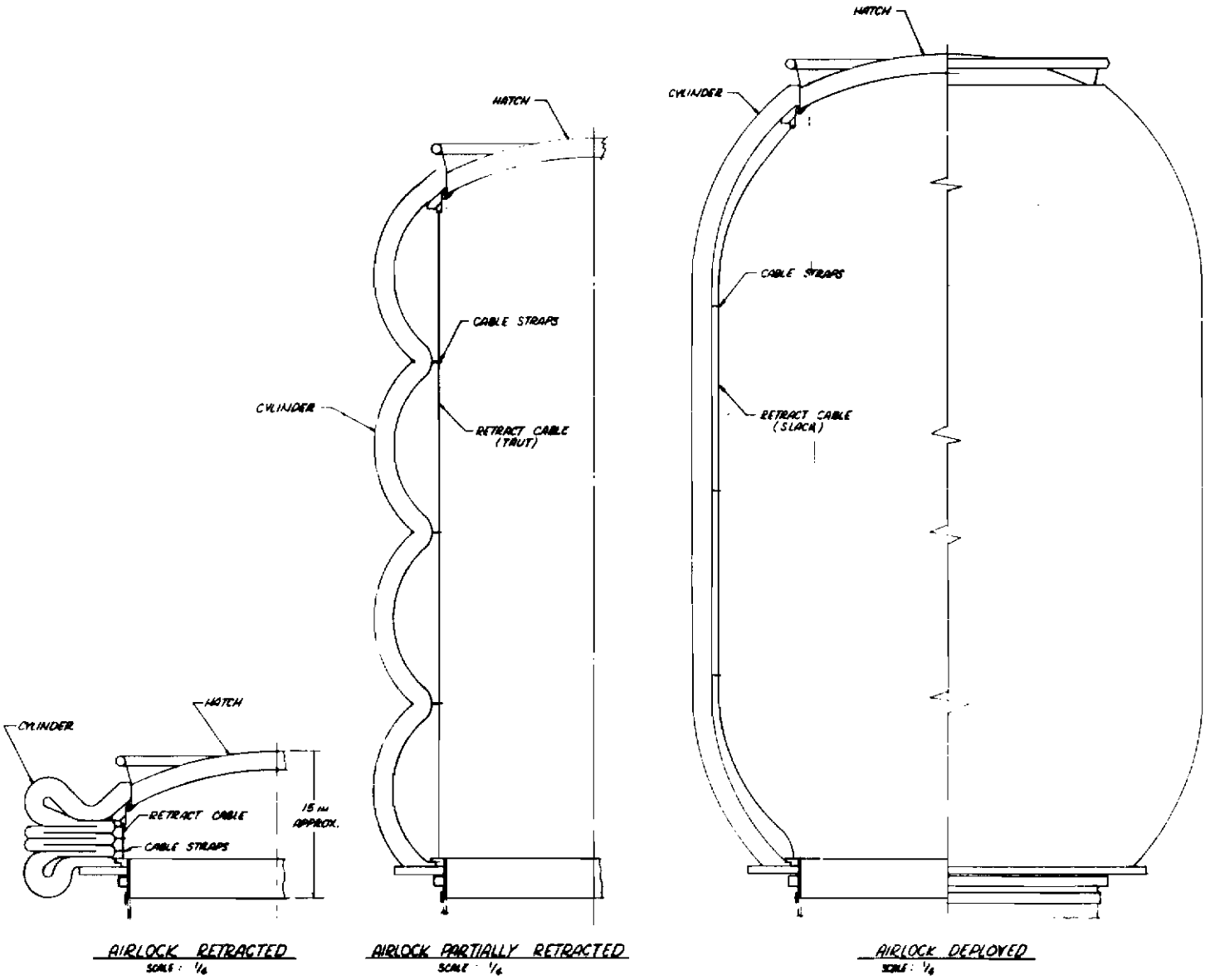

Part of Figure 4-36

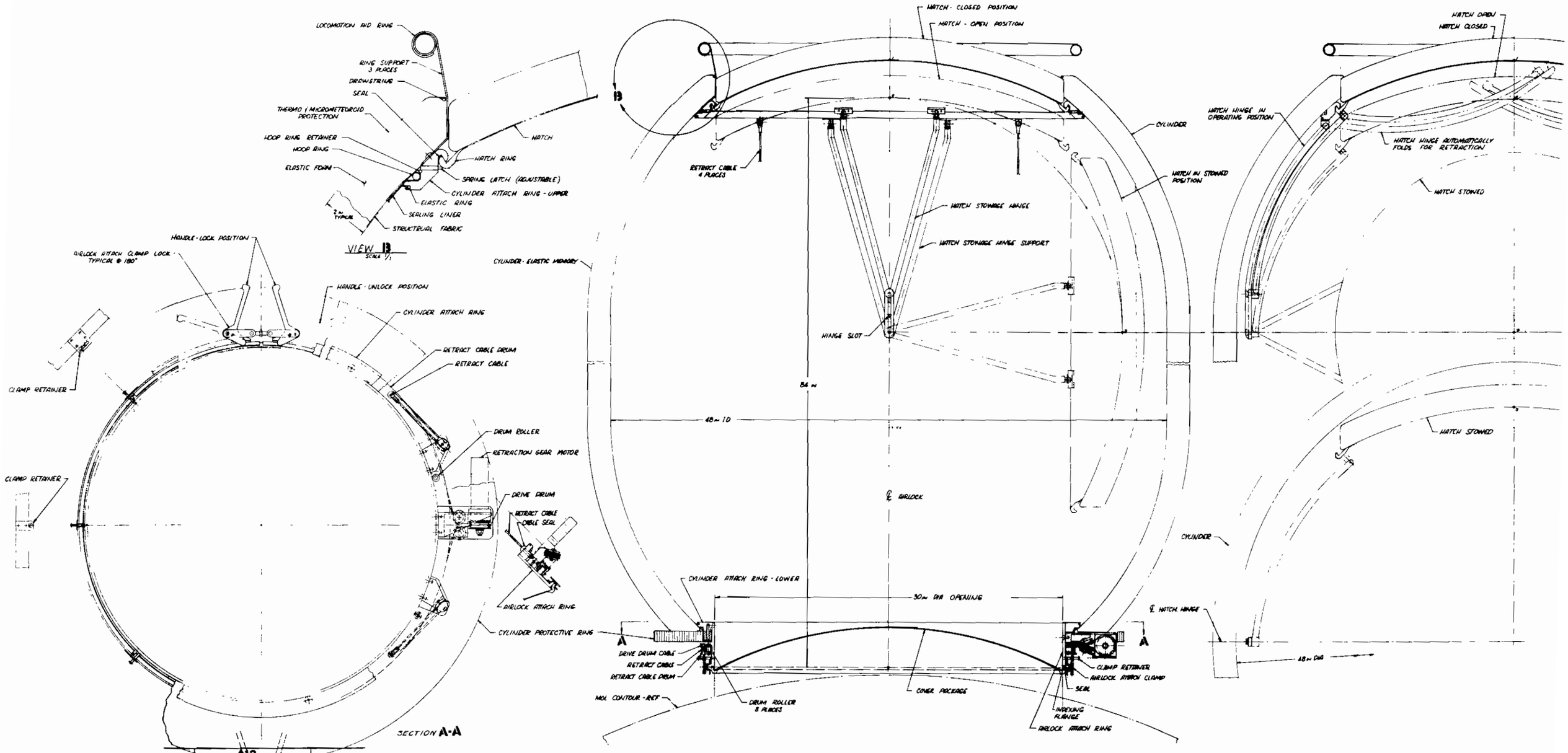

Figure 4-36. Preliminary Configuration of the Elastic Memory Airlock

4.5.2 WEIGHT AND VOLUME STATEMENT (MSL)

I. Airlock Experiment for a MSL

(A) Weight Breakdown

Item	Elastic Recovery Airlock	Gelatin Airlock
Hatch	10.43 lbs	10.43 lbs
Rings (upper & lower)	18.20	18.20
Composite	36.00	84.00
Canister	3.70	3.70
Canister Clamp	1.40	1.40
Lower Airlock Clamp	5.12	5.12
Retraction	24.00	–
Lower Closure	7.00	7.00
Water	–	49.00
Pneumatic Syst	13.40	13.40
Controls & Instrument	25.00	25.00
	147.25	221.25

(B) Volume

Item	Elastic Recovery	Gelatin
Canister	7.46 ft^3	5.28 ft^3
Control & Instrum.	1.8	1.8
Pneumatic Syst.	.8	1.1
	10.06 ft^3	8.18 ft^3

4.6 HUMAN FACTORS ANALYSES

This experiment is designed to provide a high degree of experiment reliability while still incorporating maximum astronaut control and participation in the events. Crew safety is of primary importance in the man-machine system plan. Experiment simplicity is emphasized to maximize system reliability and minimize crew training and critical task demands.

4.6.1 THE CREW AND EXPERIMENT

The scientific community has had little opportunity, to date, to experiment with dynamic structural material systems in the environment of space. The systems under study offer many extremely useful applications and solutions to space vehicle system problems. The presence of man during the experiment can greatly accelerate the development demonstration and validation of these experimental structural-material systems.

As many phenomena may occur in this foreign environment, instrumentation alone cannot be totally relied upon if the experimental procedure and data are to be optimized. Here, man becomes an irreplaceable element in the exploration of the unknown. Instruments can measure only what man presupposes will occur. But man is a highly adaptable, self-calibrating, computerized instrument that can measure and evaluate the unpredictable events. If the experimenter can visually observe all phases of the experiment, he also has the opportunity to adjust the events to optimize the experimental results.

Experiment location and orientation are being studied to insure that this visual contact, either optically or by closed-circuit TV, is available to the experimenter throughout the total cycle. Experiment malfunction during any sequenced event may not only void the experiment if the operator does not have override remote control but, equally important, other or all experiments may be blocked or aborted. Therefore, the experiment installation and deployment mechanism will provide for direct or remote visual and override control and abort-eject or fail-safe provisions to insure that unpredictable malfunctions do not negate other experimental operations.

As the experiment observer in the extravehicular mode, the astronaut will be able to inspect the experiment and the characteristics of the experimental structure in the operational environment, unhampered by the limitations of optical aids. Certain limited but critical areas of the experiment surfaces may be outside the viewing field of the ports or optical equipment, but can easily be examined by the astronaut during EVA ingress-egress experiment tasks.

The expandable airlock experiment has also been designed so that it is easily detached, if desired, for retrieval to the interior of the SIVB workshop. In the workshop environment the experiments can be conducted with a maximum of safety and at various pressure-suit differential pressures (relative to the workshop pressure) if the suit mobility should excessively complicate the ingress-egress planned tasks. However, it is believed that these tasks can be easily and successfully completed in a fully pressurized suit, as discussed in the following section.

4.6.2 HAZARD ANALYSIS

Qualification testing, large structural factors-of-safety, and proof-pressure tests in space should provide a highly predictable and reliable structural experiment. The human factors considerations are less amenable to rigorous analysis and are considered to be the first order of importance to this experiment. During current contract studies and simulated experiments for manned space programs, SGC has concentrated the program effort in this task area.

The most fundamental astronaut task-hazard is believed to be related to the mobility limitations of the pressure-suited astronaut. Therefore, the hatch opening geometry and latching mechanism, and interior configuration have received detailed analysis.

Hatch-lock actuation forces should be minimized, preferably not in excess of ten pounds of force or the equivalent. Demands for manual load application should be restricted to astronaut postures which are adaptable to these tasks and in a position to utilize adequate reaction system supports.

This is especially important in the egress hatch release task. As the airlock will be depressurized (and no longer pressure-stabilized) discrete, rigid-restraint devices must be provided for the astronaut's feet, hands, and, possibly, for the torso.

Although every precaution will be taken to avoid the possibility of cold welding of the hatch release mechanism, it is recommended that the experiment be exposed to the vacuum of space for several days prior to initiation of EVA experiments. An external pyrotechnic device (flight-qualified and nonfragmenting) has been included to release the lower "dummy" hatch should the normal hatch release mechanism fail to operate properly. As the explosive bolt is also surrounded by a steel strap this operation is not considered to be a hazard to the astronaut. In addition, an internal, manual-release mechanism is provided for release of the lower latch. Both emergency release mechanisms are interlocked with the vent system to prevent explosive decompression.

4.6.3 EXTRAVEHICULAR TASKS

During the execution of the current AHT Project, Contract AF 33 (615)-3469, Space-General conducted simulated zero-g testing of a space experiment in a neutral buoyancy facility at General Electric (as a subcontractor) as well as by SGC personnel at WPAFB. Reaction-restraint systems were evaluated as well as measurement of astronaut-applied loads. Concurrently, SGC developed the "Peter Pan" low-to-zero gravity test simulation equipment and facility (Figures 4-37 and 4-38) for evaluation of spaceflight requirements such as the Apollo Lunar Surface Experiment Package (ALSEP) (NAS 9-5182). SGC engineers, astronauts, NASA Human Factors personnel and a NASA space-suit engineer conducted extensive task experimentation in the International Latex Apollo flight suit at 1/6-g (Figure 4-39).

As a result of these extensive studies and experiments, Space-General has evaluated numerous airlock configurations in order to develop configurations that minimize the astronaut stresses and dexterity demands, as well as the envelope of manual motion.

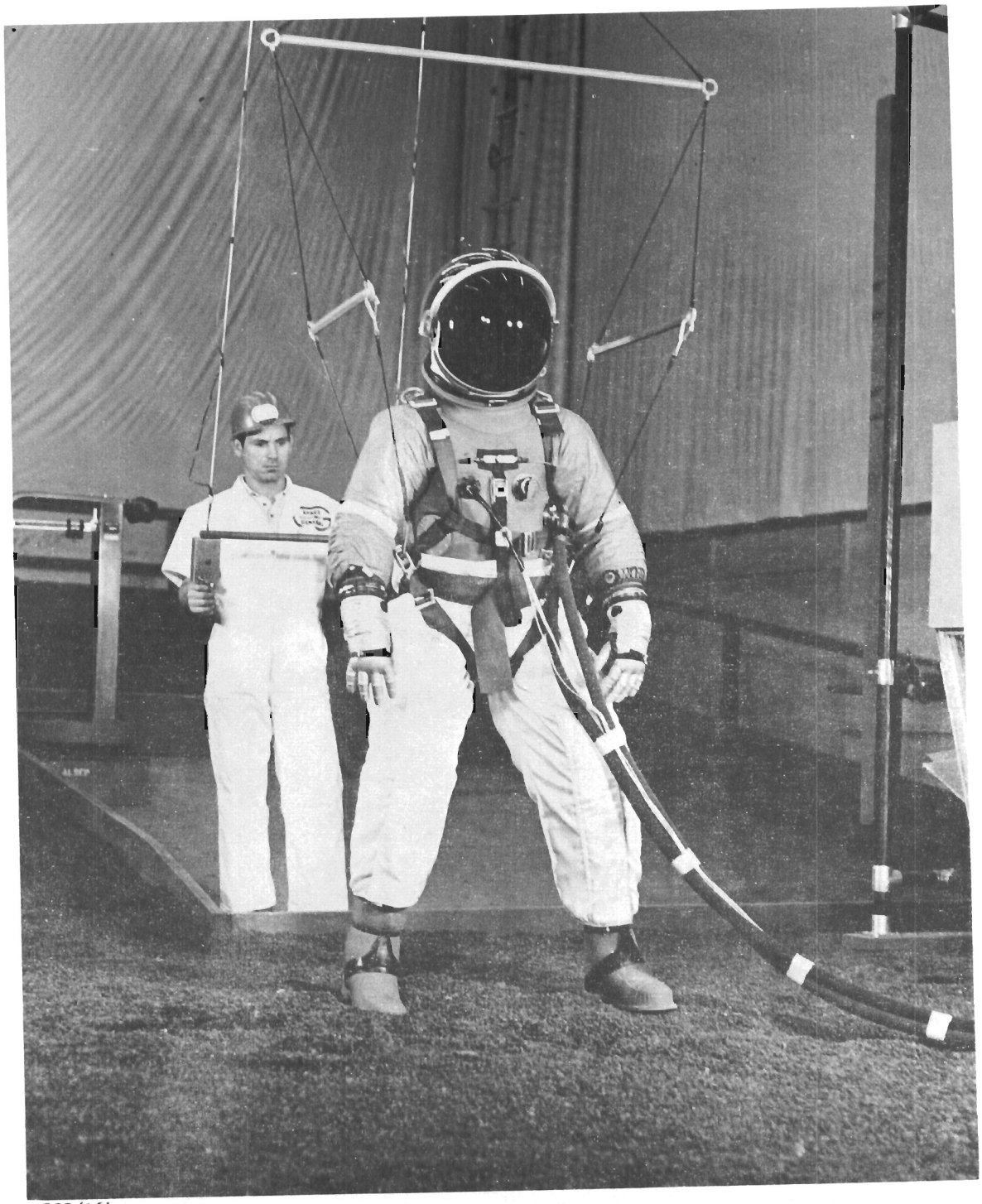

922/064

Figure 4-37. Lunar Gravity Simulation - Human Factors Testing

922-075

Figure 4-38. Lunar Gravity Simulation - Human Factors Testing

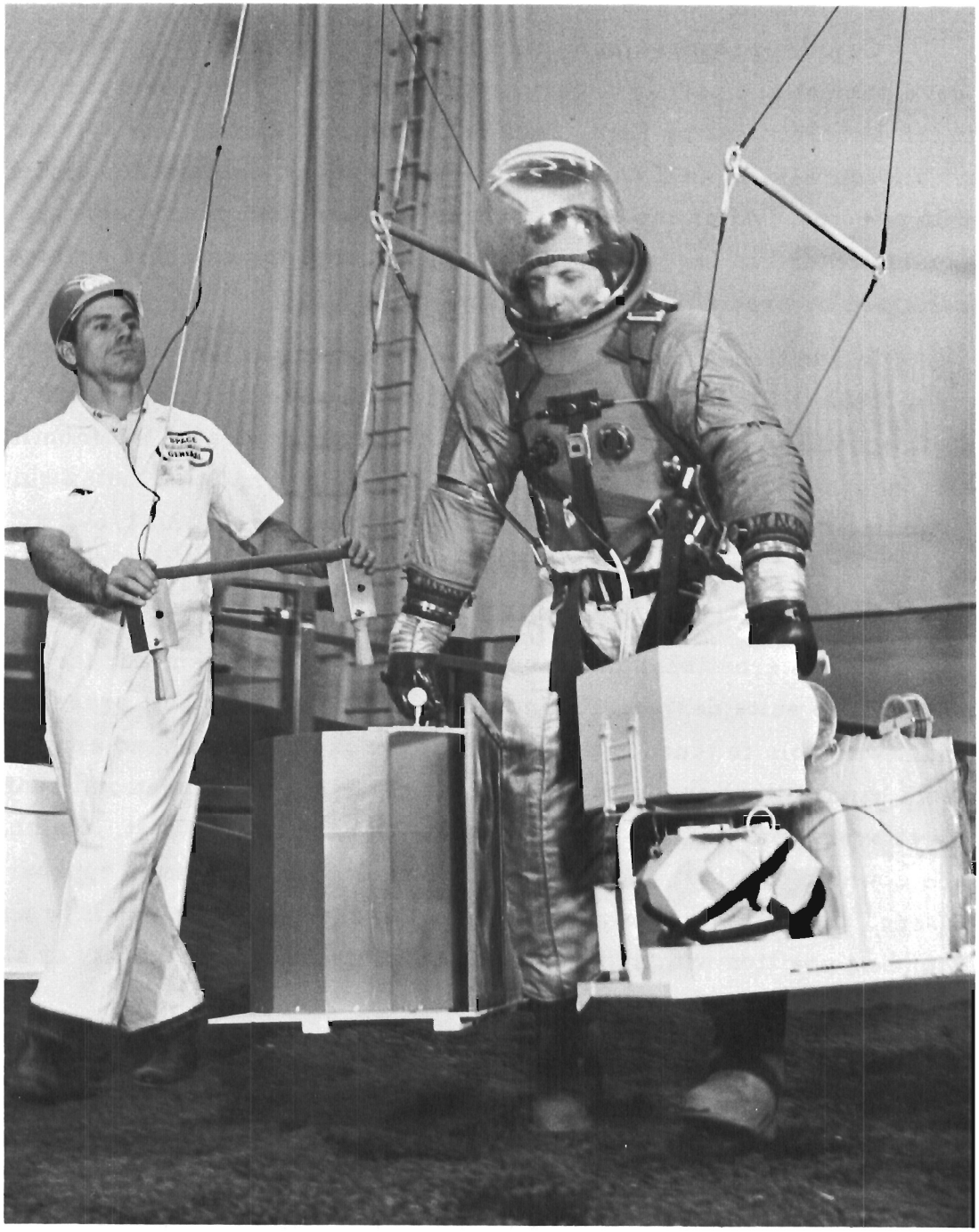

922-080

Figure 4-39. Lunar Gravity Simulation - Human Factors Testing

Current progress in Gemini EVA experiments and in pressurized suit development and zero-g experiments at the Air Force Aerospace Medical Research Laboratories by Capt. Jack Schofield indicate that the astronaut can practically operate in an EVA mode to support the experiment for periods of at least 30 minutes. After the experiment is deployed and proof-pressure tested, the experimenter can leave the SSESM and traverse the external surface of the vehicle aided by erectable cables or hand rails.

In additional mobility studies of astronaut pressure suits, SGC reviewed a NASA/MSC film of tests conducted with several Apollo-LEM suits at Bend, Oregon, and Houston, Texas. The tests demonstrated the mobility of the astronaut in Hamilton Standard-Goodrich and International Latex suits for 1-g, simulated 1/6-g (counter-balanced test rig support), and 1/6-g KC135 flight test. This was a silent film with no accompanying written discussion of the test.

The International Latex suit mobility was excellent and far superior to any previous suits designed by industry. With 3.7-psig suit pressure, the astronaut was able to touch his lower shins, back of helmet, and arm pits with both hands simultaneously, as well as raise his arms vertically with elbows at eye level, and touch his hands at the back of his waist. He could lie face down on the floor and rotate his outstretched arms over approximately a 110° arc. From the prone position he could easily erect himself to a normal standing position with apparently little effort and good stability at all times (in 1-g environment).

The astronaut demonstrated his ability to select small-diameter (1-inch to 3-inch) mineral specimens, insert specimens in a plastic bag, and insert the specimen bags into a high-density packaging arrangement in a small stowage container. He also drove nails into rock-like materials, and applied high forces with a pick-ax to chip specimens from small boulders. The latter task, however, was relatively awkward. He could easily step onto a 14-inch-high box and take strides, estimated to be 4-feet long, with ease.

The Goodrich-suited astronaut demonstrated his ability to climb volcanic rock slopes and drive nails. The mobility was fair but climbing was extremely difficult and hazardous. Tests were conducted at 1/6-g in the KC135 aircraft with a PLSS backpack attached. The astronaut hammered, jumped over obstructions approximately 30-inches high, and demonstrated his ability to remove 75-lb (1x2x2 ft) and 150-lb (2x2x2 ft) boxes from simulated LEM compartments and transport these packages the length of the KC135 compartment. All tasks were accomplished with comparative ease and good stability.

Other tests demonstrated the ability of the astronaut to remove 3/8-inch-diameter bolts with his fingers, remove equipment cover plates, and other relatively delicate tasks. These tests were conducted without thermogloves.

An outer, micrometeoroid protective garment demonstrated in some tests incorporated cutouts on the underside of the hand to permit the astronaut to manipulate tools through this cutout with his normal pressure-suited hand. This suit did not appear to significantly hamper his ability to manipulate tools although it must obstruct his vision considerably.

The results of these analyses and tests indicate that the SSESM astronaut, while performing EVA in an Apollo suit, could conduct all anticipated experiment tasks with good dexterity and safety.

4.6.3.1 EXPERIMENT CREW TASKS

The experiment is designed to incorporate prelaunch and in-space checkout systems, remote deployment with manual sequence control, and other experimental instrumentation.

At time of experiment initiation the astronaut will remotely check out the experiment-system circuit continuity, canister and experiment temperature, pressure, power source, and camera readiness. After the system checkout is complete the astronaut may arm the ordnance circuit for the canister deployment. The experiment deploy circuit can then be activated. After deployment has been initiated, the crew can control internal pressure, monitoring strain, temperature, and pressure-gage instrumentation.

It is assumed that each of the two astronauts in the SSESM will be capable of useful experimental work periods of four hours per day monitoring SSESM systems, communicating, and for vehicle control. EVA tasks will be planned for 30-minute nominal periods and 60 minutes maximum. The Apollo Block II suit is assumed to be used. In general, EVA tasks will be accomplished only during the sunlit orbital period, although the SSESM floodlights can provide adequate illumination for conduct of the experiment at any mission time desired. Internal lighting is provided in the airlock interior.

Astronaut safety will be of top priority. Tasks are planned to minimize the astronaut's required spin-of-attention and fatigue factors. Systematic and sound human engineering principles have been applied to the experiment system design from conceptual phase through design.

4.6.4 REMOTE DEPLOYMENT CONSIDERATIONS

Presence of the astronaut permits the design of a completely manually operated checkout, erection, deployment, proof-testing, and instrumentation readout system for this experiment. The experiment system is housed in the unmanned and unpressurized interstage area of the SIVB, and must, therefore, be remotely controlled for astronaut safety during initial deployment and proof-pressure testing.

If the proof-pressure test data indicates that the structural integrity of the experiment has not been degraded, the astronaut can relieve the airlock pressure and prepare for the EVA ingress/egress experiments. Optionally, the astronaut may go EVA, retract the airlock to minimum size, for retrieval of the experiment to the interior of the SIVB workshop.

4.6.5 EXPERIMENT SYSTEM DEPLOYMENT FUNCTIONS

The experiment checkout control and instrumentation system will include instrumentation and controls for the following subsystem functions:

a. Checkout

(1) Circuit continuity

(2) Safe and arm condition

(3) Canister atmosphere (pressure, temperature, etc.)

(4) System power

b. If SSESM stowage requirements necessitate experiment relocation, the astronaut must go EVA and reposition the canister.

c. Deployment and Proof Testing

(1) Canister pressure vent

(2) Canister ordnance arming

(3) Closed-circuit TV and/or motion picture camera initiation

(4) Sequence initiation

(5) Ordnance firing

(6) Experiment erection

(7) Proof pressure

(8) Record pressure leakage rates, temperature

4.6.6 INSTALLATION GEOMETRY CONSIDERATIONS

Several arrangements providing canister positions that permit the erection of the experiment in an attitude permitting visibility of the experimenter through optical port holes during the experimental periods have been studied. If optical ports are not available, closed-circuit TV would provide equally as good or better visual control by the experimenter. Camera records can be recorded by video tape systems, motion picture camera film retrieved during EVA tasks, or filmed observations through the optical ports.

4.6.7 EXTRAVEHICULAR ACTIVITIES

During EVA operations it is assumed that the workshop attitude control system will be deactivated, and the laboratory will be drifting in a random motion. Fabric loops and cables are incorporated in the experiment

structures to provide locomotion aids. With these assists the experimenter may visually examine the experiments at close visual ranges to identify and record unusual characteristics such as unbonded areas, or other conditions. A boom-mounted or hand-operated camera can also be used to photographically record these details for more rigorous study in the space or terrestrial laboratories.

A study of the events required to accomplish these tasks indicates that all the suggested tasks for the experiment can be accomplished within a 20-minute EVA excursion. If a design goal of 4 hours per task and 200 hours total mission EVA time is achieved, any EVA task presently envisioned for this experiment can be easily accomplished, with only a small demand on the total mission plan.

This task sequence includes the primary crew tasks required to visually inspect the experiments in the EVA environment, conduct ingress-egress experiments, and to retrieve material specimens and motion picture film. A study of a generalized EVA task is outlined by the General Experiment Task Descriptions section below.

4.6.8 HUMAN FACTORS SUMMARY AND PLAN

This section presents a summary of the human factors analysis and a program plan. Additional human factors analyses are presented in the form of functional flow-logic diagrams (Figure 4-40), task descriptions, work positions, basic-skill requirements, training requirements, selection criteria, and maximum work periods.

These initial analyses were based on an early preliminary version of the overall system design concept. The functions and the tasks described in this section should not be construed to be firm since they may change as a result of additions to and/or changes in requirements.

4.6.9 GENERAL EXPERIMENT TASK DESCRIPTIONS

a. Prepare for Experiment

(1) Retract any other movable structures which may interfere with or be damaged by airlock experiment erection.

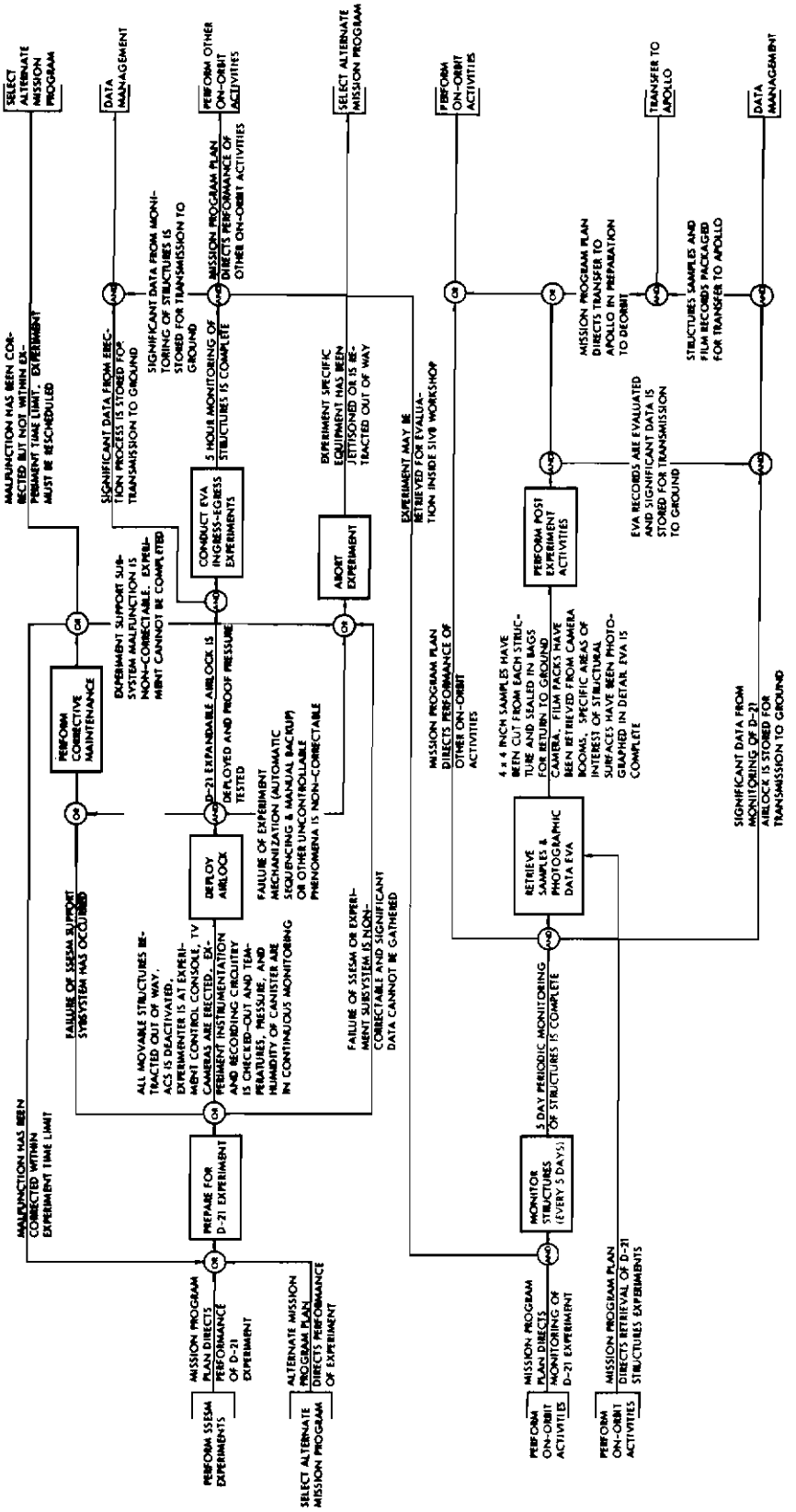

Figure 4-40. Experiment Preliminary Functional Flow Diagram

(2) Check out equipment

(a) Crewman takes place at SSESM control console.

(b) Crewman erect camera boom and/or TV cameras (if so mechanized).

(c) Check out photo and TV camera control circuitry.

(d) Check out and calibrate instrumentation and recording circuitry.

(e) Check temperature, and pressure of experiment canisters, and monitor temperature for acceptable deployment temperature zone.

NOTE 1: In event of failure of any tasks or steps, enter corrective maintenance for the appropriate SSESM subsystem. If maintenance time takes longer than allotted preparation time, the experiment may have to be rescheduled.

b. Deploy Airlock

(1) Deploy expandable airlock structure

(a) Verify that pressure in canister is safe for erection and arm canister-removal circuitry.

(b) Deactivate ACS.

(c) Activate TV cameras and adjust display for optimum picture of structure erection area (if used).

(d) Activate recording instrumentation for structure.

(e) Initiate deployment sequence and monitor erection, making verbal recording of deployment process.

(f) Photograph or video tape-record significant aspects of deployment.

(2) Proof pressurize airlock to 5.5 psi.

(a) Verify that structure is properly erected.

(b) Monitor forming process on TV display and through viewing port, making verbal recordings of forming process strains, leakage rates (if measureable), and temperatures.

NOTE 2: In the event of failure of pressurizing sequence, crewman will provide manual override to stop the sequence.

(3) Evaluate data and store significant information for transmittal to ground.

c. Monitor Structures for Five Hours (Every 90 Minutes)

(1) Monitor airlock structure during emergence into sunlight.

(a) Record temperature and pressure until stability is reached.

(b) Record time required to stabilize.

(2) Monitor leak rate of airlock.

NOTE 3: Observe slope of pressure; record mean-average line to calculate leak rate.

(3) Record temperature, pressure, and strain.

(a) Calibrate instrumentation recorders.

(b) Record parameters.

(4) Evaluate data and store significant information for transmittal to ground.

d. EVA Ingress-Egress Experiments

(1) Vent airlock

(2) Proceed EVA to experiment

(3) Visually examine structure and mechanism

(4) Operate hatch lock mechanism

(5) Ingress airlock and connect umbilical

(a) Checkout life support system communication links

(b) Inspect interior and illumination

(6) Close hatch and pressurize to 3.5 psi

(7) Rotate and depressurize airlock

(8) Release hatch and egress

(9) Inspect structure

(10) Repeat appropriate tasks for a second ingress/egress

(11) Close hatch

(12) Return to SSESM

e. Monitor Structures Every Five Days

(1) Remotely repressurize airlock to 3.5 psig

(2) Monitor experiment during emergence into sunlight

(3) Monitor leak rate of cylinder

(4) Record temperature, pressure, and strain

(5) Inspect surface of structure

(6) Evaluate data and store significant information for transmittal to ground

f. Retrieve Samples and Photographic Records at End of Mission

(1) Prepare for EVA

(a) Depressurize expandable airlock structure

(b) Deactivate ACS

(c) Proceed EVA to experiment

(2) Retrieve samples of structure

(a) Exit workshop and anchor tethers

(b) Translate to airlock

(c) Using attached locomotion aids, translate over surface of airlock to examine for degradation and verbally record condition of structure.

(d) Photograph significant areas of airlock, either on basis of own evaluation or on request from ground.

(e) Detach 4 by 4-inch material samples.

NOTE 4: Other crewman monitors performance of EVA

(3) Retrieve cameras film

(a) Translate to camera if remotely positioned

(b) Remove film and place in tethered pouch.

g. Perform Post-Experiment Activities

(1) Gather experiment data for transfer to Apollo.

(2) Evaluate data gathered during EVA and store significant information for transmittal to ground.

4.6.10 WORK POSITIONS

This experiment has been designed for one-man operation, with the exception of support of the other crewman during attitude control or orientation for experiment exposure and EVA tasks. As such, the experimenter's work station will be near the TV screen or viewing port so that he will be able to directly view the surface of the structure when erected. This may require a control console that can be connected near the viewing port during the experiment, but stowed out of the way when not in use. Since the TV system may supplement visual coverage of EVA, controls and displays should be located near the viewing port to minimize the effort required to switch from direct to remote viewing.

The support crewman's work station would be at the vehicle controls to activate and deactivate the ACS, and reorient the vehicle as required during the critical phases of the experiment.

4.6.11 BASIC SKILL REQUIREMENTS

There are no unique skills required beyond those that can be acquired during a short training period.

Alignment and calibration of the temperature, pressure, and instrumentation will be accomplished by either "marking" recording channels with standard signals prior to and following data gathering, or nulling out error signals against reference prior to data gathering and "marking" recordings with reference after data gathering. There is checkout, but no alignment and calibration, required for the displays and controls.

The displays and controls will be mechanized for simplicity of operation. Checkout is accomplished by "go-no-go" test, and operation is no more difficult than operating switches.

There is no corrective maintenance planned for this experiment. In the event of failure, the structures may be jettisoned and tethered (providing it is unable to yield significant data).

Familiarity with the information requirements of the experiment will be the basis of data analysis criteria. Most of the evaluation of data will be performed by the crewman; however, analysis of data on the ground may result in communication of new criteria to the workshop.

4.6.12 TRAINING REQUIREMENTS

The crewman should acquire sufficient knowledge of the plastics, process and fabrics used in expandable structures so he can evaluate whether the structure is performing properly. This knowledge can be gained in lecture demonstrations, using samples of properly and improperly fabricated and processed structures, and viewing operations in a vacuum chamber. The Space-General test airlock can be used for preliminary training.

He should be able to classify the anticipated characteristics such as structural characteristics of leakage and creep. The crewman should acquire proficiency in the function of the temperature, pressure, and stress instrumentation so he can evaluate the relationships between readings. This will also involve the laws of gases.

A priority of emphasis within all training requirements will be in the order of: (1) conditions and procedures related to personnel safety, (2) conditions and procedures related to the SIVB workshop mission, (3) conditions and procedures related to the airlock mission success.

It is anticipated, however, that no demanding or extraordinary training requirements will become necessary due to the experiment. Flight crews will require experiment operational fundamentals prior to simulation training tasks. Simulation training will nominally be an extension of the existing flight crew programs with direction towards experiment operation and peculiarities. Emergency operations and alternate procedures will always prevail with respect to the mission success.

Supporting activities such as the launch site crews and MSFN personnel will be definitized by the DEP in a subsequent contract.

Training should include simulation in flight-suited experiment operations; zero-g, KC-135 aircraft environments; and neutral buoyancy.

4.6.13 SELECTION CRITERIA

There are no special selection criteria for this experiment which would exceed the requirements for general space crew performance.

4.6.14 MAXIMUM WORK PERIODS

The preparation phase should not take longer than 20 minutes and is limited to one occurrence. It is principally a one-man activity.

The airlock erection will last a maximum of 3 minutes and will require constant monitoring of the deployment and forming process. During proof-pressure tests it is necessary to monitor the instrumentation for periods of 2 minutes every 20 minutes. During the second or third sunlit period, orientation, pressurizing of the airlock and photographing the structures will require approximately 30 minutes. Structure erection is principally a one-man activity; however, the other crewman may be required for SSESM attitude control and orientation for approximately 5 minutes prior to entering the second or third sunlit period. Evaluation and storage of significant data will not require more than 30 minutes.

The EVA ingress-egress experiments will require an estimated 20 minutes of EVA time.

An overall review of the recommended human factors program is presented in Figure 4-41 in the form of a functional flow-logic diagram. Blocks depicted with unbroken lines indicate activities which are considered to be primarily human factors in nature. Blocks in broken lines are those activities which are not human factors in nature but have a significant effect on human factors activities.

The purpose of the "Functions Analysis" is to initially delineate the functional configuration of the system and to define the specific requirements of individual functions. An initial "cut" of the function configuration has been determined and is presented in Figure 4-40. However, the detailed requirements supporting individual functions have not been developed to date. These requirements can be described jointly, in detail, by human factors personnel and engineering design personnel since the functions, per se, are not specifically human factors or engineering design. The requirements have not been delineated to date, since the preliminary version of the system was insufficiently defined to allow detailed derivation of tasks.

Note that the functional analysis will be conducted at varying levels of greater detail. At each level, a design concept will be established which will determine the ground rules for the next level division. This concept is compatible with the functional flow block diagramming (FFBD) concept in AFSCM 375-5. The functional flow-logic diagram presented in Figure 4-40 may be considered to be the first-level diagrams for the system. As the program continues, however, each of the blocks represented in the diagram may have to be further divided. The extent of division will be determined by the design concept which essentially will be expressed in the form of Requirements Allocation Sheet (RAS) No. 1.

The next logical step in the sequence is to define the tasks required for personnel performance. This activity can be conducted after the lowest level FFBD for the system has been derived. In the initial cut at the system, tasks have been derived for the first level FFBD depicted in Figure 4-40. This was deemed necessary to determine the basic role of personnel in the system and whether any special problems would be forthcoming. The analyses to date indicate that such special problems need not be anticipated.

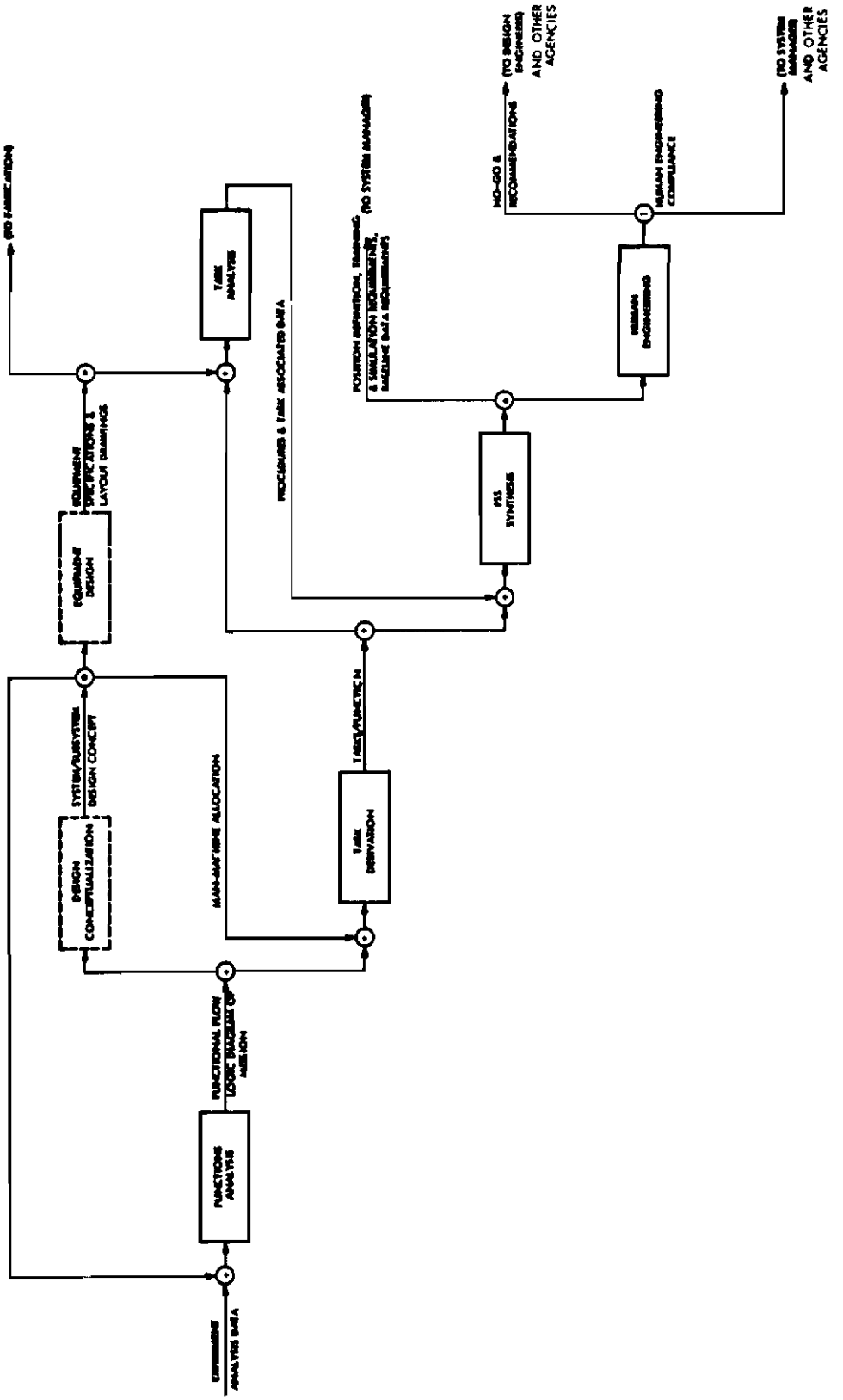

Figure 4-41. Experiment Recommended - Human Factors Program Plan

In subsequent iterations of this activity, either the RAS No. 2 or a similar form can be used. The format used is a preliminary one for the initial version of tasks to facilitate rapid derivation of the tasks. In later iterations, a tabular format such as the one used in RAS No. 2 can be used to allow an association of related data to the task of importance, e.g., personnel requirements, training requirements, procedural requirements, etc.

It is important to note that derivations of tasks do not require detailed information on equipment with which man will interface; consequently, "Task Derivation" can be continued without significant advancements in the design of the equipment. This derivation of tasks is also useful since it provides a pragmatic differentiation between tasks and steps.

The primary purpose of "Task Analysis" is to identify the steps required in implementing any given task and providing some task-associated data such as level of efforts, time, parallel efforts, etc. This activity has not been continued for the initial human factors support of the development efforts. As indicated in Figure 4-40, task analysis requires detailed information on the equipment with which the crew member will interface; consequently, it will not be possible to continue this activity until the initial version of equipment final design has been completed.

In the "Personnel Subsystem Synthesis (PSS)" activity, the varying elements relating to personnel performance would be synthesized. The outputs at this time include work positions, basic skill requirements, training requirements, selection criteria, and maximum work periods. In later iterations, the outputs will include human engineering, safety, maintainability specifications, simulation requirements (if any), and baseline data requirements.

"Human Engineering" should be conducted in conjunction with equipment design and should be based on the specifications provided in the PSS synthesis activity. This activity should consist primarily of working with the design engineers, applying human engineering principles, and reviewing equipment design for compatibility with sound human engineering principles.

4.7 HUMAN FACTORS CONSIDERATIONS ON AIRLOCK GEOMETRY

4.7.1 HUMAN FACTORS ANALYSIS

Studies of airlock configuration criteria indicate that geometry is heavily dependent on the mobility characteristics of the particular pressure suit to be used, the life support system selected, and the operational procedures specified.

Apollo, Gemini, and aircraft pressure suits are currently designed to provide maximum comfort in the seated position. Therefore, the relaxed pressure-suited astronaut position is stooped with knees bent. If a special suit is designed for EVA tasks, the mobility characteristics will differ from those of the seated-position suit. Assuming that current Gemini or Apollo suits will be used, it appears that the astronaut could not turn around in a four-foot-diameter airlock. Previous WPAFB zero-g aircraft tests on simulated crew transfer tunnels indicate that an airlock of five-foot minimum diameter cross section would be required for turnaround.

Space-General conducted 1.0 g and 1/6-g tests in the International Latex suit in the early part of 1966. Figures 4-42 and 4-43 show the astronaut in a relaxed kneeling position (1.0-g and 3.7 psig), which is probably the shortest overall height it is reasonable to assume he would attain for the purpose of turnaround. In this position he could reach and manipulate controls (e.g., hatch actuators) located 20 inches or more above the "floor." However, in a zero-g environment, 20 inches may be the lowest he could reach. These dimensional limitations will have to be verified in more realistic tests.

Figures 4-44 and 4-45 illustrate the astronaut's reach, forward and upward. The helmet is transparent over most of its area and provides almost unlimited visibility. The astronaut's head is unrestrained within the helmet, with a field of external vision of 120 degrees left and right, 85 degrees up, and 95 degrees down. The visible light transmission for the bubble helmet alone is 88 percent.

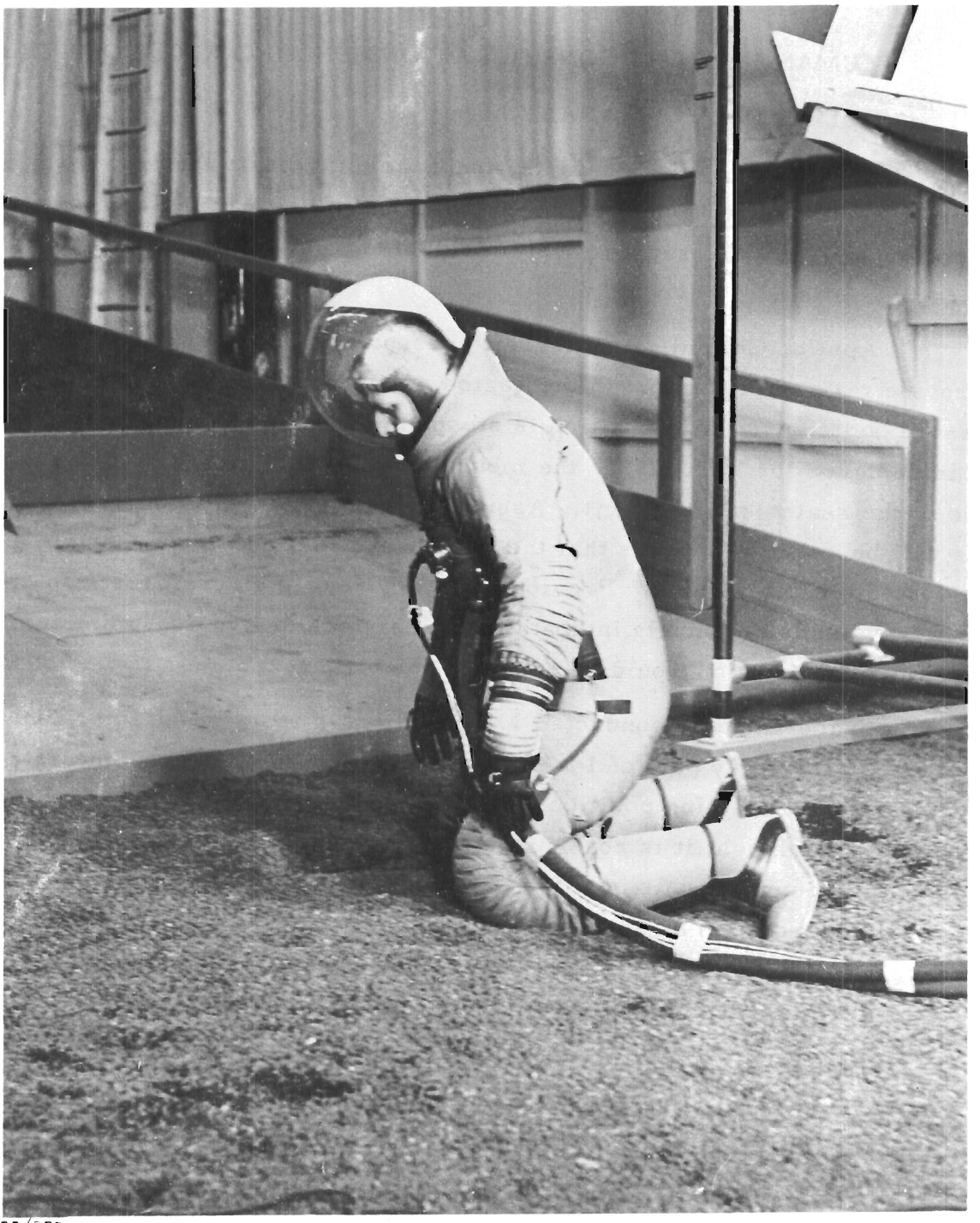

922/052

Figure 4-42. International Latex Suit, Kneeling Position (1.0-g and 3.7 psig)

922/050

Figure 4-43. International Latex Suit, Kneeling Position (1.0-g and 3.7 psig)

922/048

Figure 4-44. International Latex Suit, Overhead Reach (1.0-g and 3.7 psig)

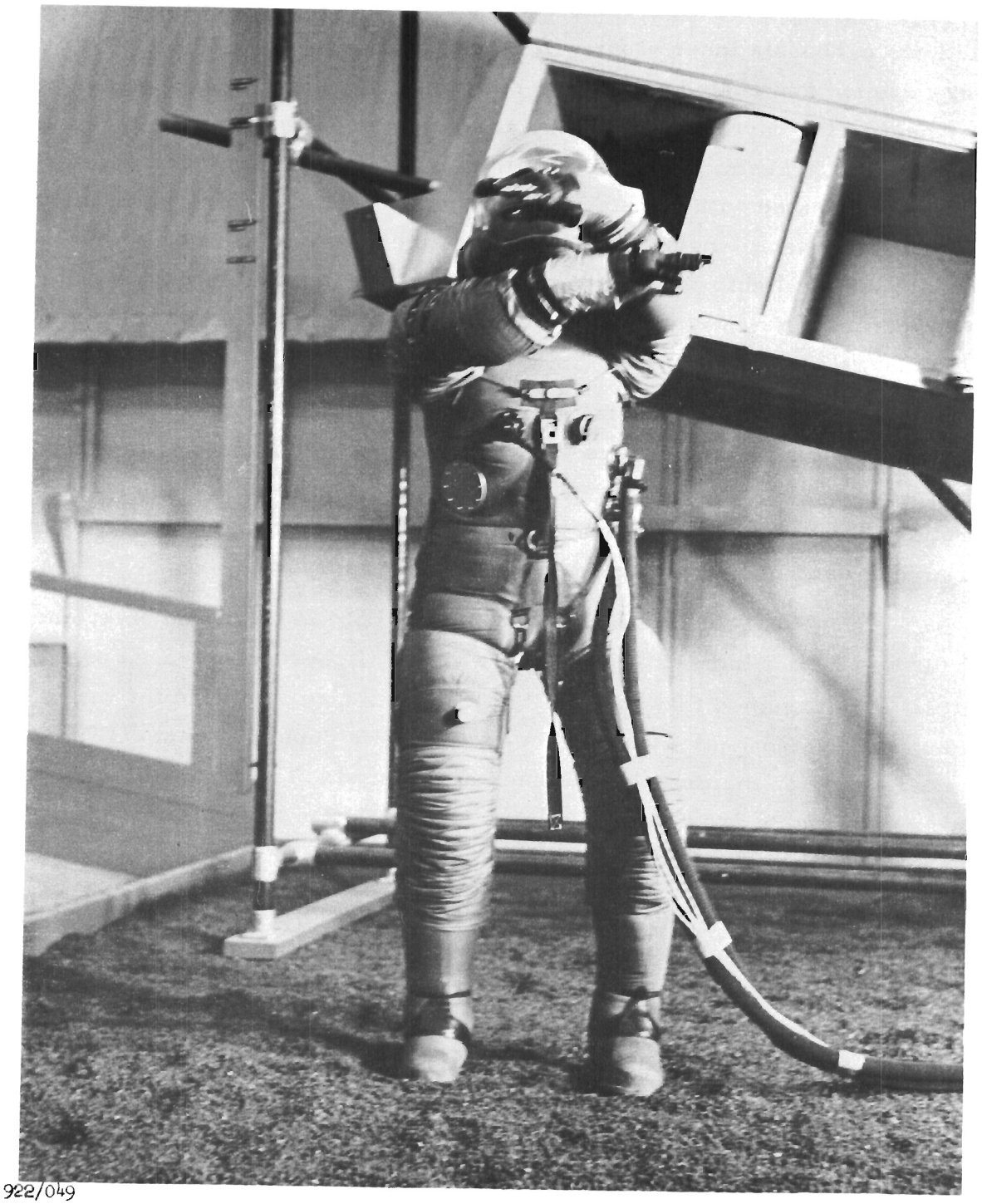

922/049

Figure 4-45. International Latex Suit, Cross Reach (1.0-g and 3.7 psig)

During EVA excursions outside the airlock it is assumed that the tinted polycarbonate inner visor will be pulled down over the face. This visor is tinted and coated with a low-emittance finish for protection against solar heat in the daytime and fogging at nighttime. The bubble helmet and this visor will transmit 60 percent of the visible light. The outer sun-visor is tinted and coated with a metallic finish to reflect solar infrared in the 0.8 to 0.5-micron wave length, to absorb or reflect ultraviolet rays, and to attenuate visible light. With both visors in place, the visible light and far infrared transmission is only 10 percent, near infrared is 5 percent, and ultraviolet is 2 percent.

Figure 4-46 shows the gloved thumb, without thermal gloves, in the relaxed position, and Figure 4-47 shows the thumb rotated toward the palm to the maximum position. The index finger is shown relaxed but can be rotated to grasp a bolt against the thumb. If the thermal gloves are required, the hand and finger dexterity is grossly reduced.

The Portable Life Support System (PLSS) is large and bulky and will further inhibit ingress, egress, and vision if chest mounted. For this analysis it is assumed that an umbilical connection will be used for the life support system with a backup Emergency Life Support System (EOS) mounted either on the chest or the back of the head. The EOS will be approximately only 2x6x8 inches in size and will not significantly inhibit astronaut mobility or vision.

Gemini and Apollo astronauts consider umbilical connections an extremely critical operation that should not be attempted in an unpressurized compartment. Therefore, unless these opinions change, it is apparent that the umbilical connection must be made on the inside of the pressurized airlock, probably on the inner hatch cover, after the astronaut has egressed into the airlock from the laboratory. The tether may also have to be carried into the airlock, which would displace additional maneuvering volume. If stowed externally to avoid congestion in the airlock, the tether should be protected from the environment of space to avoid potential cold welding or other degradation factors.

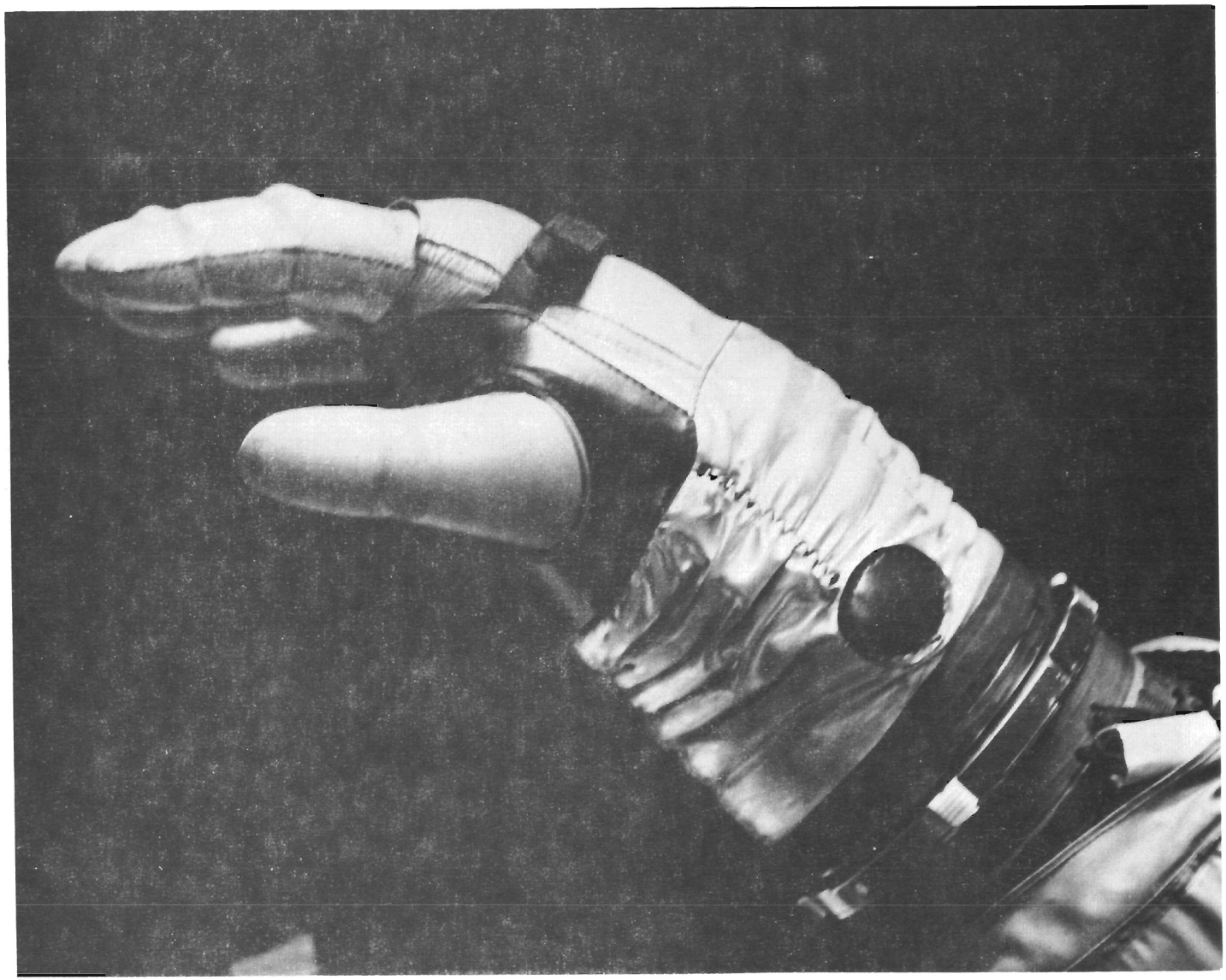

922/085

Figure 4-46. International Latex Suit, Gloved Hand, Relaxed Thumb Position

922-086

Figure 4-47. International Latex Suit, Gloved Hand, Thumb Rotated Toward Palm

In the vacuum environment, there will be an absence of aural cues, such as clanging or rasping sounds associated with the operation of hatches and mechanisms. Such cues serve as warning signals and their absence should be considered in the design of mechanisms and the assessment of operational procedures and hazards.

From this discussion it is apparent that the hatch controls, for a seven or eight-foot-long by four-foot-diameter airlock, should be located at least 20 inches from the vehicle hatch cover and be easily grasped and manipulated by the astronaut. Verification of these preliminary conclusions can be determined only by simulated zero-g, KC-135 aircraft tests scheduled to be conducted by WPAFB in the Davis Clark GC-4 suit, or zero-buoyancy testing. An illustration showing typical astronaut positions for upper and lower hatch operation is seen in Figure 4-48 for a four-foot-diameter by seven-foot-long airlock. The results of these considerations precipitated the current SIVB airlock experiments configuration of a 5.5-foot-diameter sphere. This geometry is seen in the above mentioned figure with an astronaut superimposed. The diameter for this sphere was selected based on measurements of minimal heights to which a pressure suited subject could withdraw himself in the International Latex suit. Consequently, if end-over-end turnaround is required, this is a minimum diameter circle of the maneuver. This subject is discussed further in Section 4.8 of the document.

AIRLOCK GEOMETRY STUDY

No.

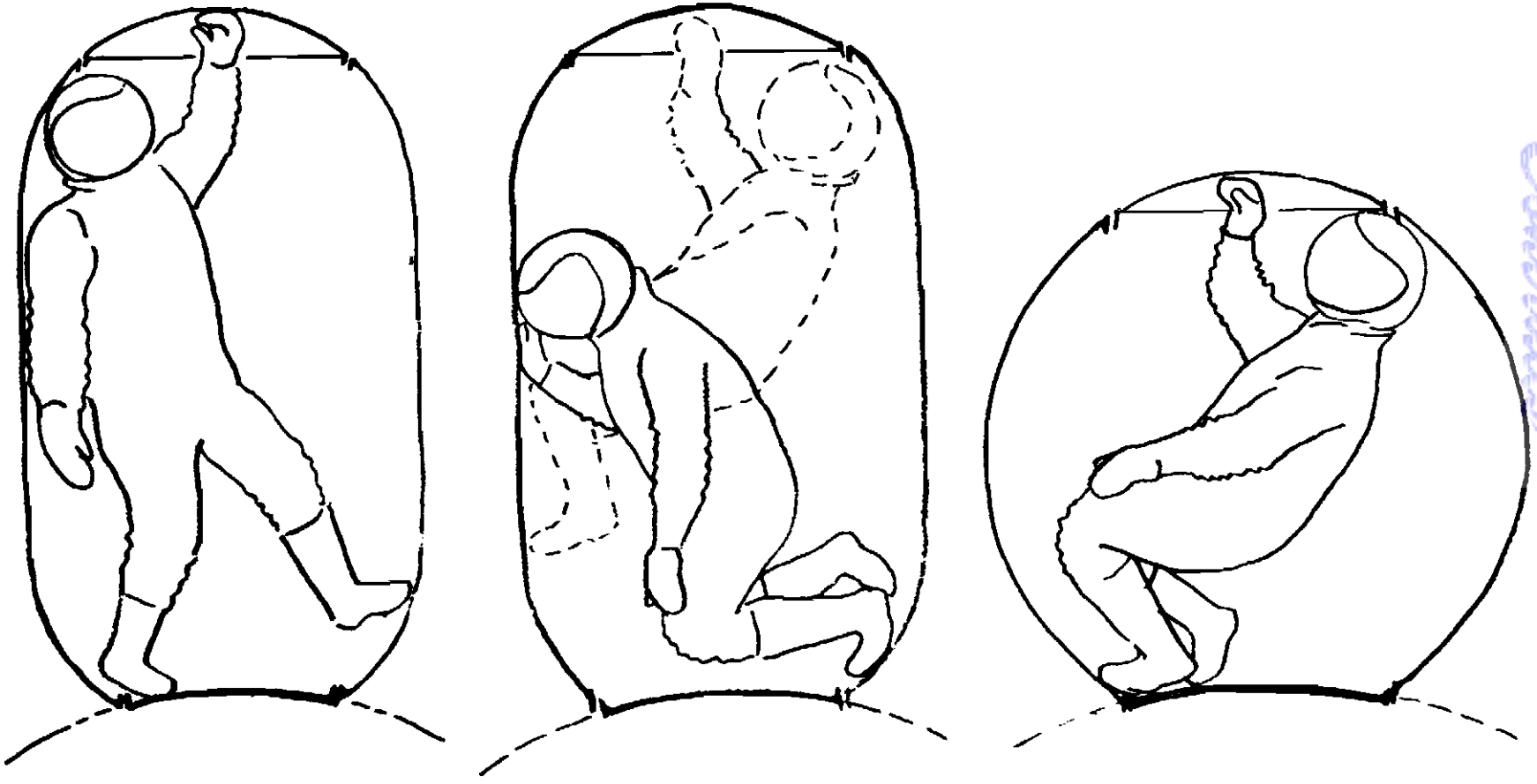

Figure 4-48. Astronaut Position for Hatch Operation

4.8 SSESM AIRLOCK CONFIGURATION

4.8.1 EXTENSION OF OPERATIONAL AIRLOCK CONFIGURATIONS

Extensive studies of numerous operational airlock configurations have been conducted. It is desirable that an SSESM experiment for the evaluation of an airlock should possess the geometry and dimensions which would be required for an actual operational airlock for an operational MSL vehicle. However, no specific MSL mission configuration or requirements are known and the vehicle interfaces can only be assumed. Also, valid zero-g anthropometric restraints must be determined by tests in order to evaluate any given airlock configuration. The problem of selection of a configuration is further compounded in that the SSESM experiment package is extremely weight critical.

The first airlock geometry considered was the four-foot-diameter by seven-foot-long cylinder with ingress/egress hatches at either end. Subsequent analysis has shown that an astronaut should be able to operate the airlock with no assistance from fellow crew members; therefore, the four-foot-diameter would have to be increased to allow a pressure-suited astronaut with a PLSS back pack to reach both end hatches and lock mechanisms. In other words, it was assumed that he would need enough room inside the airlock to completely reverse his direction end-over-end, to permit manual access to the opposite hatch mechanism.

Studies have been made to investigate other geometries which would satisfy the required maneuvers of the encumbered astronaut.

4.8.2 SPHERICAL AIRLOCKS

The rationale which was employed to obtain the spherical geometry started from the familiar four-foot-diameter by seven-foot-long cylinder. From this it can be seen that the spherical geometry is obtained by increasing the cylinder diameter to that which will just allow the astronaut to reverse direction to reach either hatch, while shortening the overall length in order to minimize volume. The operational sequency (see Figure 4-49) for the astronaut ingress from EVA is:

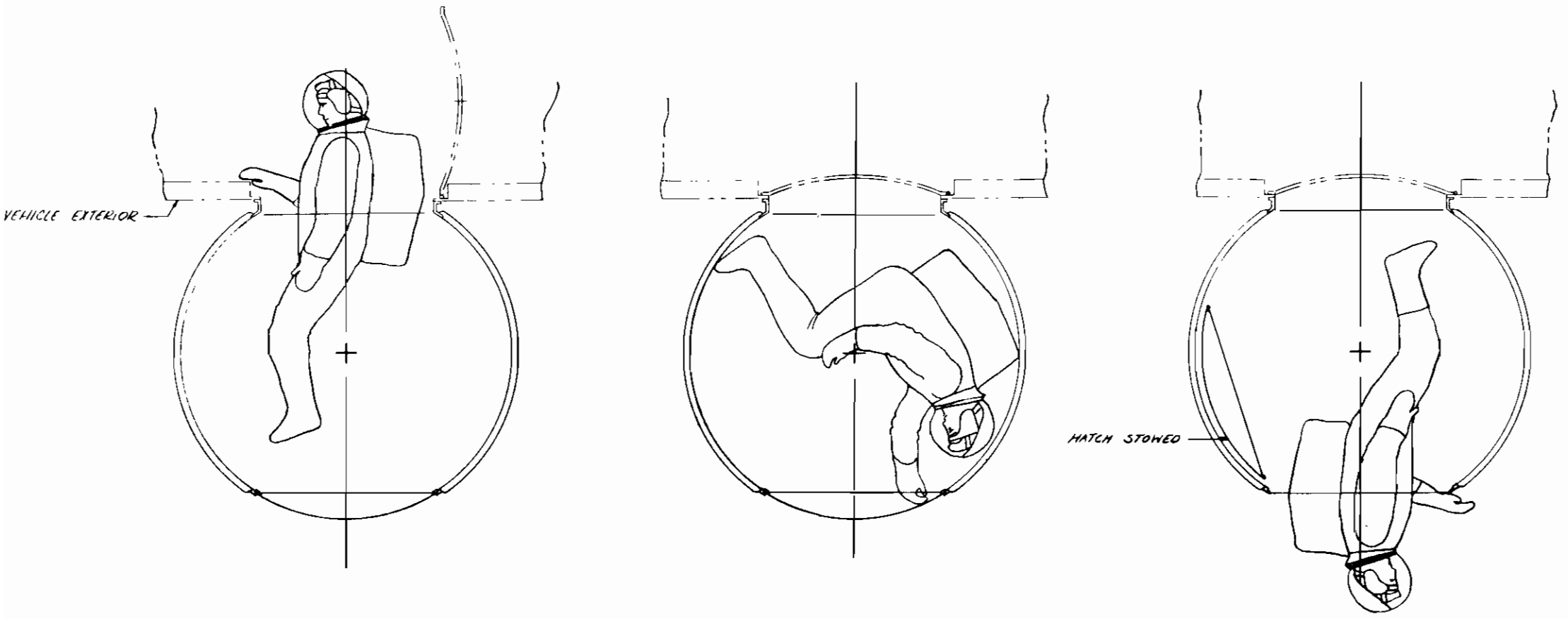

Figure 4-49. Operational Sequence Spherical Airlock

a. Release EVA hatch inward

b. Enter airlock feet first

c. Close EVA hatch and pressurize airlock

d. Somersault to face "vehicle" hatch

e. Open vehicle hatch and enter vehicle

The disadvantages of the spherical configuration is that the minimum dimension in which an astronaut can stoop to turn around is at the least 5.5 feet. This height generates a sphere of approximately 87 cubic feet. This volume can be reduced by geometrically flattening the sides, but this is difficult to fabricate, retract, and has considerable surface area (therefore it is heavier).

(See Table 4-5 for a comparison of SSESM airlocks).

4.8.3 MECHANICAL DESIGN AND ANALYSIS

The basic design requirements for the SSESM expandable airlock experiment are summarized in the following paragraphs:

a. Airlock Configuration
Inside diameter 66 inches
Inside length 65 inches
Hatch diameter 34 inches
Packaged dimensions 37 inches dia by 24 inches high
Weight 110 lb, or 135 lb with retraction
All subsystems to be contained in an integral package.

b. Experiment Hatch Subsystem - one capable of being operated by a pressure-suited astronaut with backpack.

c. Expandable Composite Subsystem - Consists of bladder, structural material, foam and thermal control coating.

- shall be capable of withstanding astronaut, pressure, and normal vehicle-maneuvering loads

- passive temperature control +50 to +100^{o}F

d. Base Assembly Subsystem - consists of rigid pressure bulkhead, skirt for mounting pressure system, retraction/deployment system, and attachments to SSESM.

- shall include emergency egress provisions

- shall be adaptable as functional airlock

Table 4-5

SSESM AIRLOCK COMPARISON CHART

	3' x 7'	4' x 7'	5' sphere	5.5' sphere
Zero psi volume (ft^3)	46.8	80.5	65.5	87.1
3.5 psi volume (ft^3) increased due to strain	65.5	112.5	91.5	122.0
Composite area (ft^2)	62.2	87.0	66.5	83.0
Composite average unit weight (lb/ft^2)	0.32	0.34	0.33	0.34
Weight Breakdown				
Composite wt (lb)	19.8	29.5	22.0	28.2
Hatch, vent, mech wt (lb)	16.1	11.3	11.3	11.3
Fabric termination ring weight (lb)	4.8	3.1	3.1	3.1
Dummy hatch wt (lb)	5.8	5.8	5.8	5.8
Canister wt (lb)	9.1	9.1	9.1	9.1
3.5 psi pressurization system wt (lb)	26.0	38.0	32.5	41.0
Instr, controls, cabling and misc wt (lb)	12.2	12.2	12.2	12.2
Retraction system wt (lb)	25.0	25.0	25.0	25.0
TOTAL WEIGHT	118.8	134.0	121.0	135.7

Table 4-5 (Continued)

SSESM AIRLOCK COMPARISON CHART

	3' x 7'	4' x 7'	5' sphere	5.5' sphere
Human Factors	Poor	Poor	Fair	Fair
Packaged Dimensions	28 x 19	40 x 20	40 x 20	40 x 20
Retraction Capability	Good	Good	Fair	Fair
Fabrication Simplicity and Cost	Good	Fair	Fair	Fair
Functional Airlock	Poor	Fair	Good	Good

e. Deployment - primary and backup

f. Retraction - to fit through Gemini hatch
- retraction time 3 minutes
- electrical operation with own power supply

g. Instrumentation - internal airlock pressure
- internal surface temperature
- external surface temperature
- strain

h. Ancillary Requirements - lighting, window, communications connection, astronaut umbilical and connection, controls

i. Human Factors - Safety
- Hand holds inside and outside
- Materials noninjurious
- Ease of operation
- Nonabrasive surfaces

j. Leakage - 0.50 lb/24 hours; prefer 0.25 lb/24 hours

k. Factors of Safety - 3.0 on hatch system
- 5.0 on composite structural fabric

l. Environment - 30 days at 200 nm orbit

Primary design emphasis was placed on astronaut and mission safety and reliability.

The airlock configuration is shown in Figure 4-50. The basic structure is a 66-inch-diameter by 65-inch-long spherical airlock. This configuration simulates a double-hatch airlock in which an astronaut will enter from one end and exit from the other. In this design it is required that the astronaut turn around in order to operate hatch and vent controls. This design can be employed as a normal straight through airlock for EVA or as a tunnel between two space vehicles.

The specific designs discussed in the following sections represent a detailed configuration for this experiment. Additional studies should be undertaken to further optimize the designs and to finalize details prior to actual hardware fabrication.

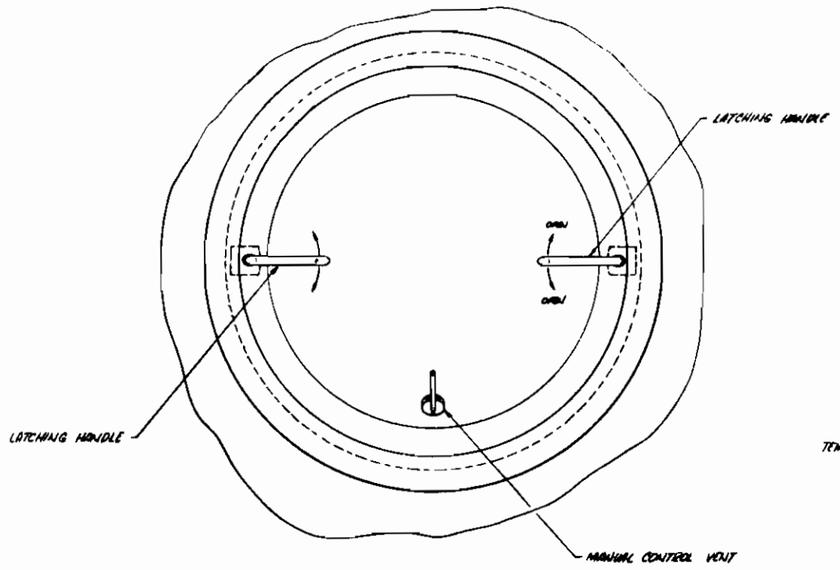

SECTION B - B

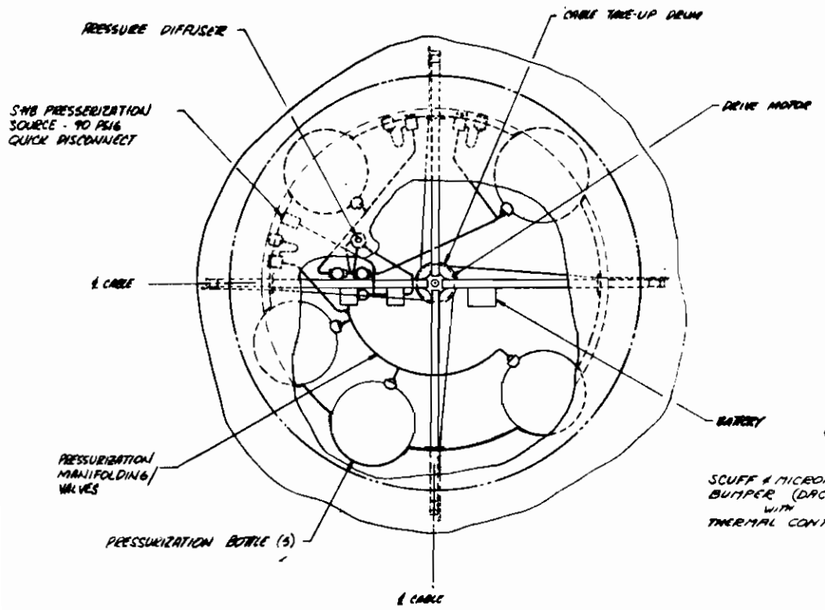

SECTION A - A

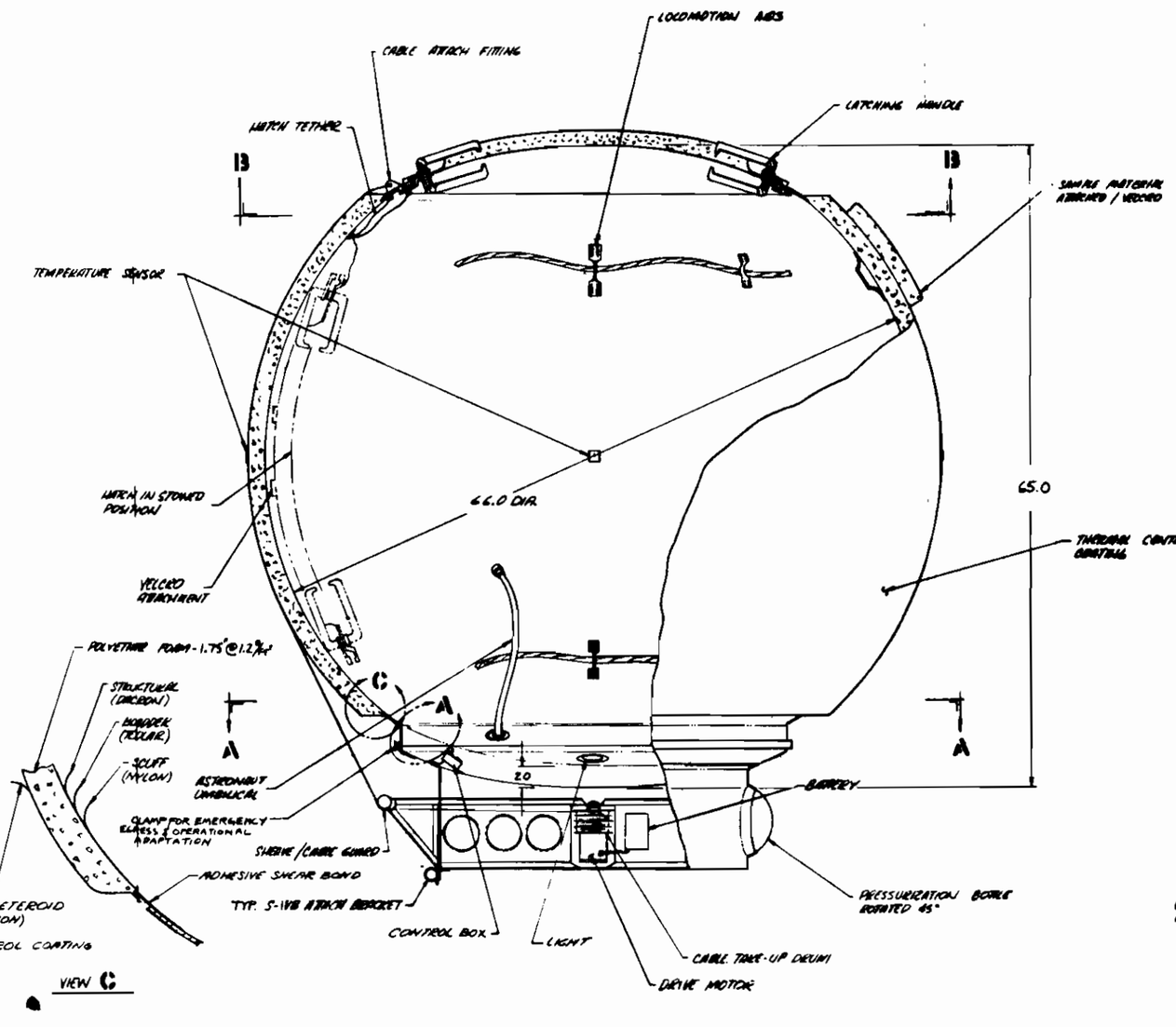

VIEW C

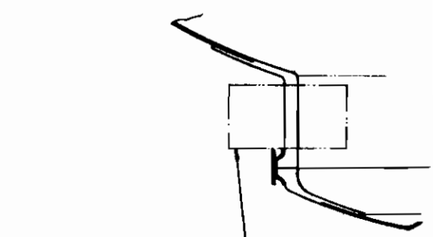

VIEW A

Figure 4-50. SSESM Spherical Airlock Assembly

4.8.4 AIRLOCK SYSTEM

4.8.4.1 SYSTEM DESCRIPTION

The airlock configuration is shown in Figure 4-50. It consists of the expandable composite material, an inward opening hatch and a fabric termination ring, a rigid bulkhead, and a base assembly structure (which houses the pressurization system, deployment and retraction mechanism), and miscellaneous subsystem attachments.

This configuration was designed to meet the dimensional and operations requirements of astronaut and SSESM vehicle interfaces. The fabric and aluminum ends of the airlock spherical in shape. Two locking handles are provided 180° apart on the hatch to prevent the hatch from accidentally opening when vented. These handles also provide the astronaut with a means for handling the hatch during stowing tasks. The manual vent is located in the hatch. A control box containing switches for electrical operation of the pressure system and for the remote vent is attached to the fabric termination ring adjacent to the hatch. An airlock pressure-indicator is also located on the control box. All controls and indicators are grouped to one side of the hatch for easy viewing and all are within reach of the astronaut. A light is located approximately 90° to these controls to provide illumination.

The rigid pressure bulkhead and base assembly consists of a lower fabric termination ring, an equipment mounting ring, a ring and dome assembly, a mounting skirt for the pressure system, retraction/deployment system and SSESM attachment brackets. The ring and dome assembly is attached to the lower fabric termination ring by means of a manually operated clamp. This clamp is utilized to provide the astronaut with an emergency egress capability and also to provide an interface for mounting the airlock as an operational system.

This provision for astronaut emergency egress and for operational adaptation of the airlock adds weight to the experiment. If this feature is not required, a design not incorporating these features could utilize a spun aluminum dome. Fabric could be bonded directly to the dome thereby decreasing the weight by approximately 18 pounds.

Suitable astronaut locomotion aids are provided inside the airlock and handling handholds can be placed on the outside of the packaged experiment.

The volume of this airlock is 91.7 ft^3 at 3.5 psig. The weight of this system is 135.3 pounds. If the airlock is used over an operational hatch, the weight will be 71.2 pounds.

4.8.4.2 EXPANDABLE COMPOSITE MATERIAL

The criteria for and the selection of the expandable composite materials is discussed in Section 4.4. As shown in Figure 4-50, it consists of an inner dacron scuff fabric, bladder, single-ply dacron structural fabric, foam, and outer dacron micrometeoroid bumper fabric with a thermal control coating.

Strength-to-weight trade-off studies have been made to determine optimum structural materials and fabrication techniques. Included have been fabric layup, filament winding and the so-called isotensoid flexible cable or strap concepts. Preliminary conclusions lead to the selection of fabric layup, with bonded seams as a first choice for this airlock configuration. The use of cables or straps will not result in lighter structural material weights on a pressure vessel of this shape, particularly when the pressure is as low as 3.5 psi. They do, however, reduce the amount of elongation of the structural material when pressurized. The flexible cables or straps are more difficult to package when the diameter of the package is to be less than the deployed diameter.

SGC studies and testing have been directed toward optimization of the dacron fabric layup concept. Tests have indicated that bonded seams can be made with strength equal to that of the fabric, making it unnecessary to add on several extra plys of fabric at seam locations. The weight of the load-carrying structural material can, therefore, be reduced. The seams have somewhat more strength in the direction of the seam than the adjacent fabric, due to the double thickness of fabric. These seams can, therefore, be used to advantage to act as flexible straps in reducing elongation or growth of the airlock.

Based on SGC studies, an approach utilizing a fabric-gored layup with eight seams appears to be optimum from weight-strength, fabrication, and packaging standpoints.

The composite layup will be accomplished on a tooling form which can be disassembled and removed through either end of the completed airlock. Form construction and the fabrication operation have been checked out on an in-house airlock fabrication program. The form surface is pressure-sealed to permit vacuum bagging operations. The inner scuff fabric is applied first, followed by each successive composite layer. Appropriate curing of adhesives is accomplished as each layer is applied. Airlock fabric termination rings are attached to the form during the fabric-to-metal bonding operation. The structural fabric is bonded to the inside of the fabric termination ring to insure that there will be no peeling loads when the airlock is pressurized. It should be noted that the lower opening is larger than the upper hatch making it possible to install the hatch after airlock fabrication is complete and, of equal importance, to be able to replace the hatch in the event of damage.

4.8.4.3 BASE STRUCTURE

The design approach for the base structure was to incorporate the pressurization system and the retraction system into one integral unit, (Figure 4-51). This design offers a minimum-weight, structurally-sound configuration which supports the entire airlock system with easy access to all components. On an operational airlock the retract system will be placed on the ring structure. This retract configuration will weigh approximately 10 pounds more.

The five spherical pressure bottles are supported about the periphery of a cylindrical skirt extending from the lower hemisphere of the airlock. This configuration allows all components to be centrally located within the periphery.

A cruciform-type structure extends through the cylindrical skirt four places at 90° for support of four pulleys which serve the retraction cables. At the apex of the cruciform structure a cable take-up drum is supported. This drum is common to the four cables providing take-up retraction at a constant rate.

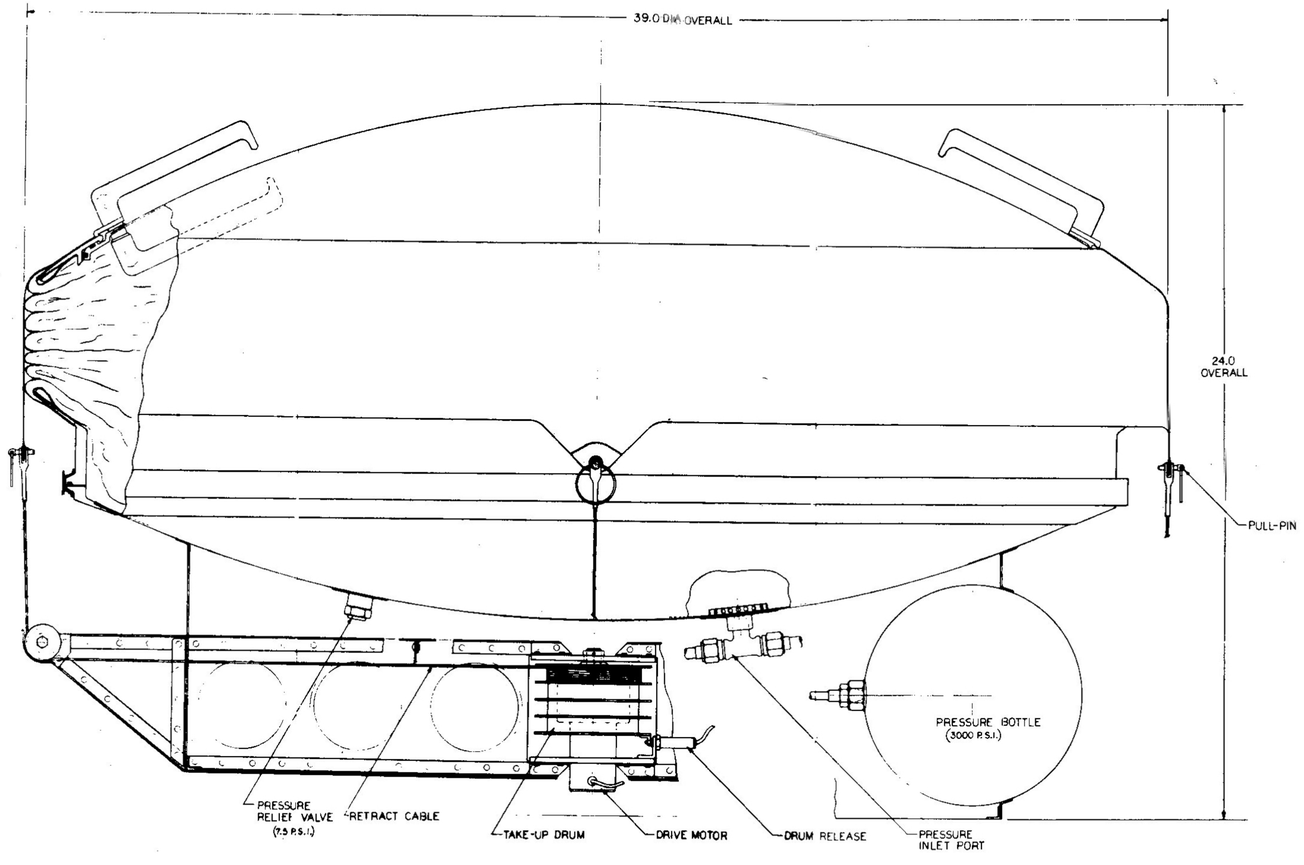

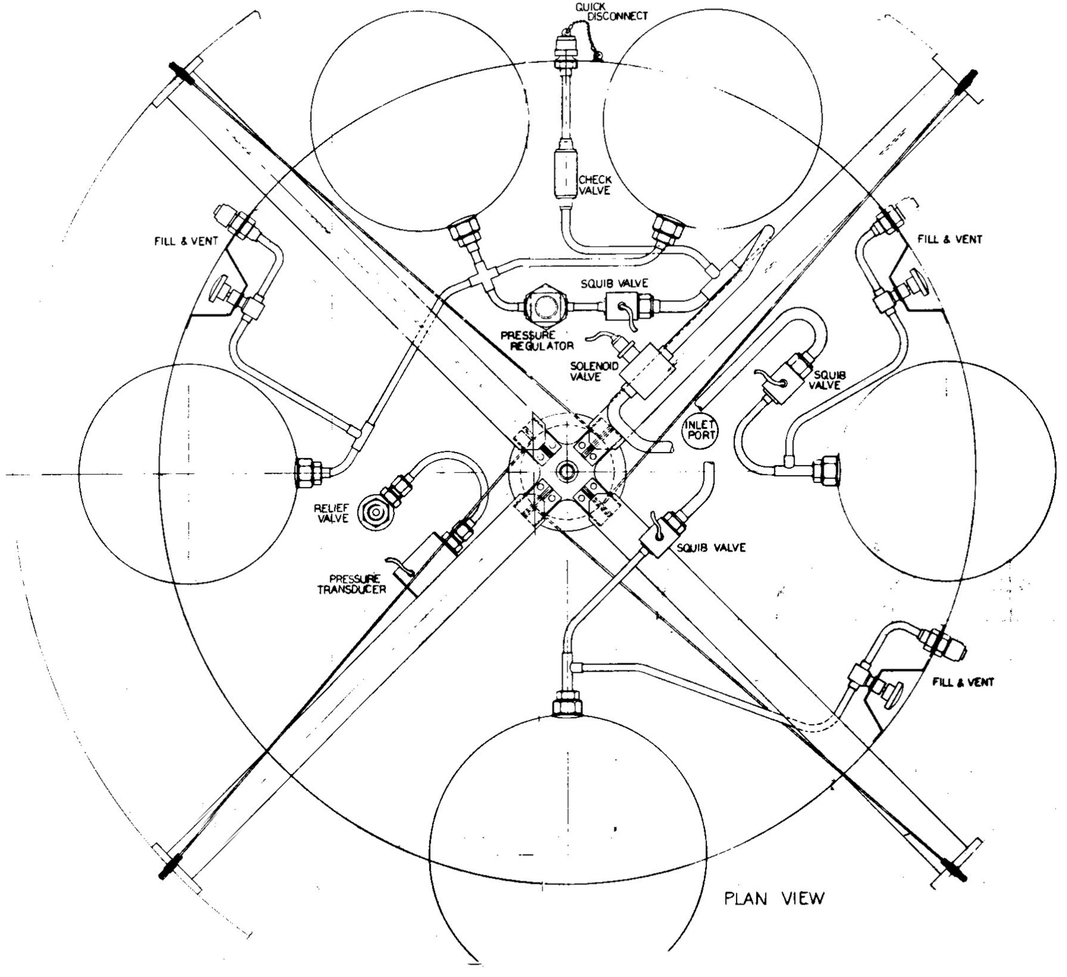

Figure 4-51. Base Structure Assembly

Driving torque for the take-up drum is supplied by a space qualified gear-head motor mounted inside the drum, thus, eliminating the requirement of a drive train operating in the space environment.

Retraction cables and attachments are aircraft-type stainless steel, cable size is 1/16-inch diameter, 7 by 7 construction with a breaking strength of 480 pounds.

The cables are attached to the airlock with lanyard pull-pins which will allow manual disconnection if for any reason the retract system should fail to function, thus, not allowing the airlock to deploy.

If retraction is not a requirement, the cable take-up drum and drive will be removed. One squib-actuated pin-puller will replace the take-up drum. Four short cables will be attached to the airlock upper dome with lanyard pull-pins (same attachment as with retraction) terminating at an eyelet engaging the pin-puller, thus, retaining the airlock as packaged.

When the squib pin-puller is activated all cables are released allowing the airlock to deploy.

The packaged configuration of the fully retracted airlock is shown in Figure 4-14. Overall dimensions of the packaged airlock are 24.0 in. high by 39.0 in. in diameter.

As shown in Figure 4-14, the packaged airlock in the proper orientation will pass through a Gemini hatch with adequate clearance.

4.8.4.4 PRESSURIZATION SYSTEM

The pressurization system, as shown in Figure 4-52, is comprised of five spherical 3000 psi pressure bottles; four 7.5-inch-diameter and one 8.6-inch-diameter, and the associated plumbing and control equipment.

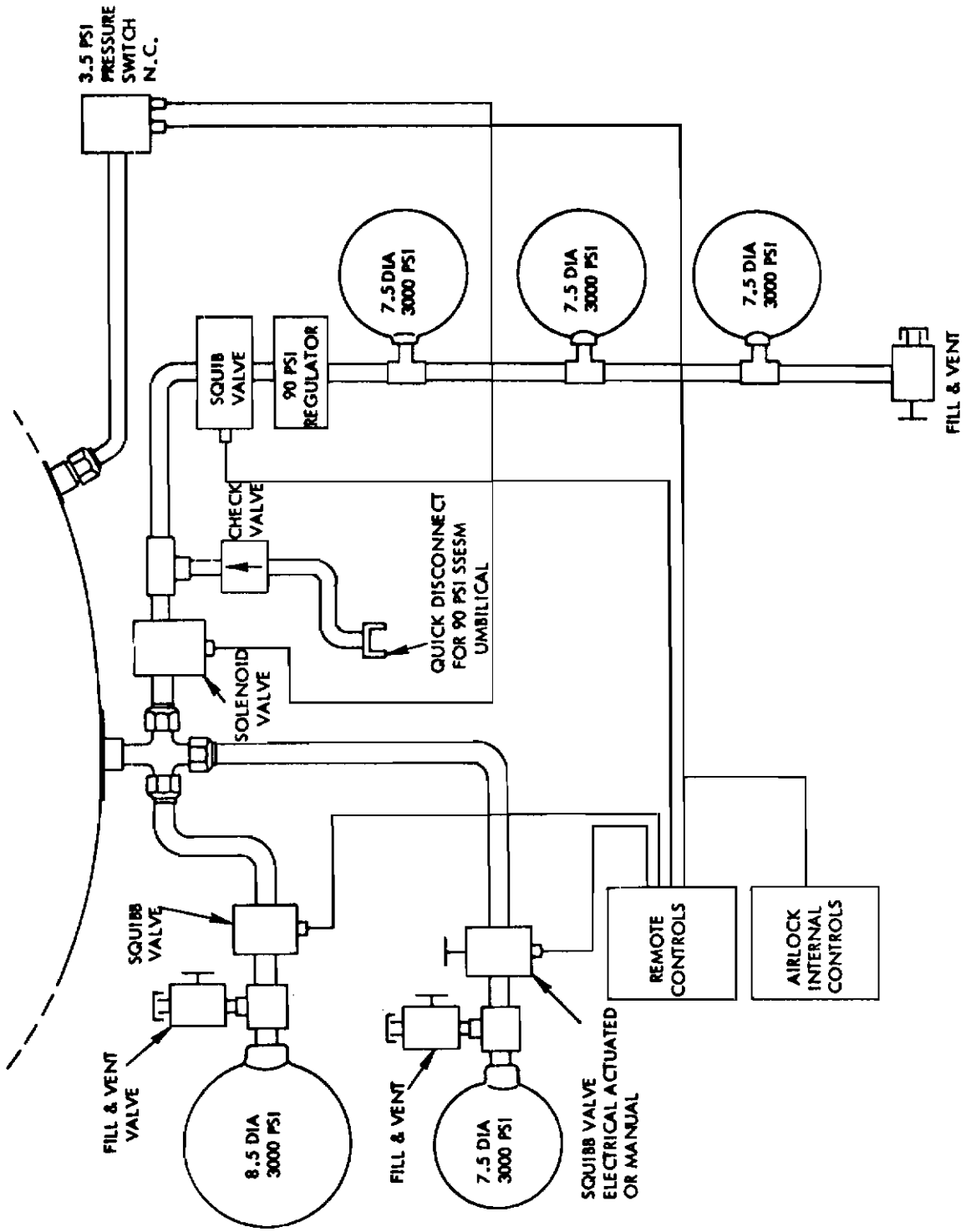

Figure 4-52. Pressurization System

4.8.4.4.1 PROOF-PRESSURE SYSTEM

The larger bottle (8.6-inch-diameter) is required for the initial deployment and pressure-proof test of 5.5 psi. This bottle is sized so that it will fully deploy the airlock within three minutes to the required internal proof pressure of 5.5 psi. There will be some press drop in time as a result of cooling.

To achieve the desired deployment rate a restricting orifice is employed in the pressure line allowing a maximum flow rate which will allow the airlock to deploy at a rate corresponding to the rate at which the retract system will allow while running in reverse without overloading the cables.

4.8.4.4.1.1 PROOF-PRESSURE SYSTEM REQUIREMENTS

The proof-pressure bottle is sized to provide the required internal pressure. A minimum of hardware is required for this system. In addition to the 8.6-inch-diameter spherical bottle one fill and vent valve (manual operating) and one explosive squib valve (with associated tubing and fittings) completes the system.

4.8.4.4.2 OPERATING-PRESSURE SYSTEM

This system is designed to allow three pressure cycles of 3.5 psi each. A simple pressure-demand system is employed giving sufficient regulation to provide correct pressure for each cycle with or without an astronaut inside the airlock.

To achieve correct pressure for all cycles three 7.5-inch-diameter spherical pressure bottles are manifolded together and pressure is controlled by one common solenoid valve activated by a 3.5 psi pressure switch series connected with the manual operating pressure switch in the control box. The 3.5 psi pressure switch is normally closed and set to open at a pressure of 3.5 psi $\pm$2%. To initiate an operating-pressure cycle the manual switch is closed activating the solenoid valve and allowing pressurant to enter the airlock. (The flow is regulated to allow a fill rate of 30 C.F.M., thus, achieving full pressurization in approximately one minute.)

When internal pressure reaches 3.5 psi ± 2% the pressure switch opens closing the solenoid valve. At this time, the manual switch may be opened and no further pressurizing will occur; if, however, the manual switch is left closed the pressure switch will command pressure and maintain airlock pressure of 3.5 psi within ± 2%.

Upstream of the solenoid valve is an explosive squib valve. This valve is a burst diaphragm-type assuring a positive leak proof system through the launch and boost phase and until just prior to the operating-pressure cycles. An arming switch at the control box is provided and must be closed prior to initiating the operating-pressure cycles.

When the arming switch is closed it fires the explosive squib valve, thus, allowing pressurant to the solenoid valve. At this time the operating pressure sequences may be initiated.

4.8.4.4.3 REVISIT PRESSURE TEST SYSTEM

This system utilizes the fifth pressure bottle (7.5-inch-diameter, 3000 psi).

This pressure bottle is sized so that the airlock will be pressurized to the required operating pressure (3.5 psi). A minimum of hardware is required for this system. In addition to the 7.5-inch-diameter pressure bottle, one explosive squib valve and a manually operated fill and vent valve, along with associated tubing and fittings, complete the system.

A restricting orifice is employed in this system allowing a maximum flow rate of 30 C.F.M.

In addition to the squib valve, a manually actuated, diaphragm-type valve will be connected in parallel with the squib valve to allow manual operation for pressurizing the airlock for a revisit-pressure test if at this time no electrical power is available.

4.8.4.4.4 PRESSURE ENTRY PORT

The pressure entry port will be welded boss with a 1/2-inch diameter through-port capped internally with a 1/4-inch thick disc approximately 2 inches in diameter. This disc will have a series of 3/16-diameter holes equally spaced radially to defuse any high-velocity pressurant.

4.8.4.5 AUXILIARY ITEMS

In this section are discussed the following:

a. Vent - manual and remote

b. Control Box

c. Instrumentation

d. Light

e. Samples

f. Hatch Stowage

h. Miscellaneous Cabling and Umbilical Connections

4.8.4.5.1 VENT-MANUAL AND REMOTE

A vent is required for depressurization of the airlock either by the astronaut from within the airlock or remotely from the SSESM. In addition, two vents are used for redundance and for emergency rapid depressurization. This requirement is met by providing one manual vent and one electrically operated vent.

A typical manual vent design is shown in Figure 4-53. Analysis of the vent size and time is presented in Section 4.8.4.6.

Several vent concepts have been investigated. These included the poppet-valve type shown in Figure 4-53, gate valves, ball valves, etc. Basically, two methods of operation can be used: lever or screw. The inward operating poppet-type valve appears to be simplest and most reliable. Pressure tends to keep it closed and sealing is simplified by the fact that an O-ring

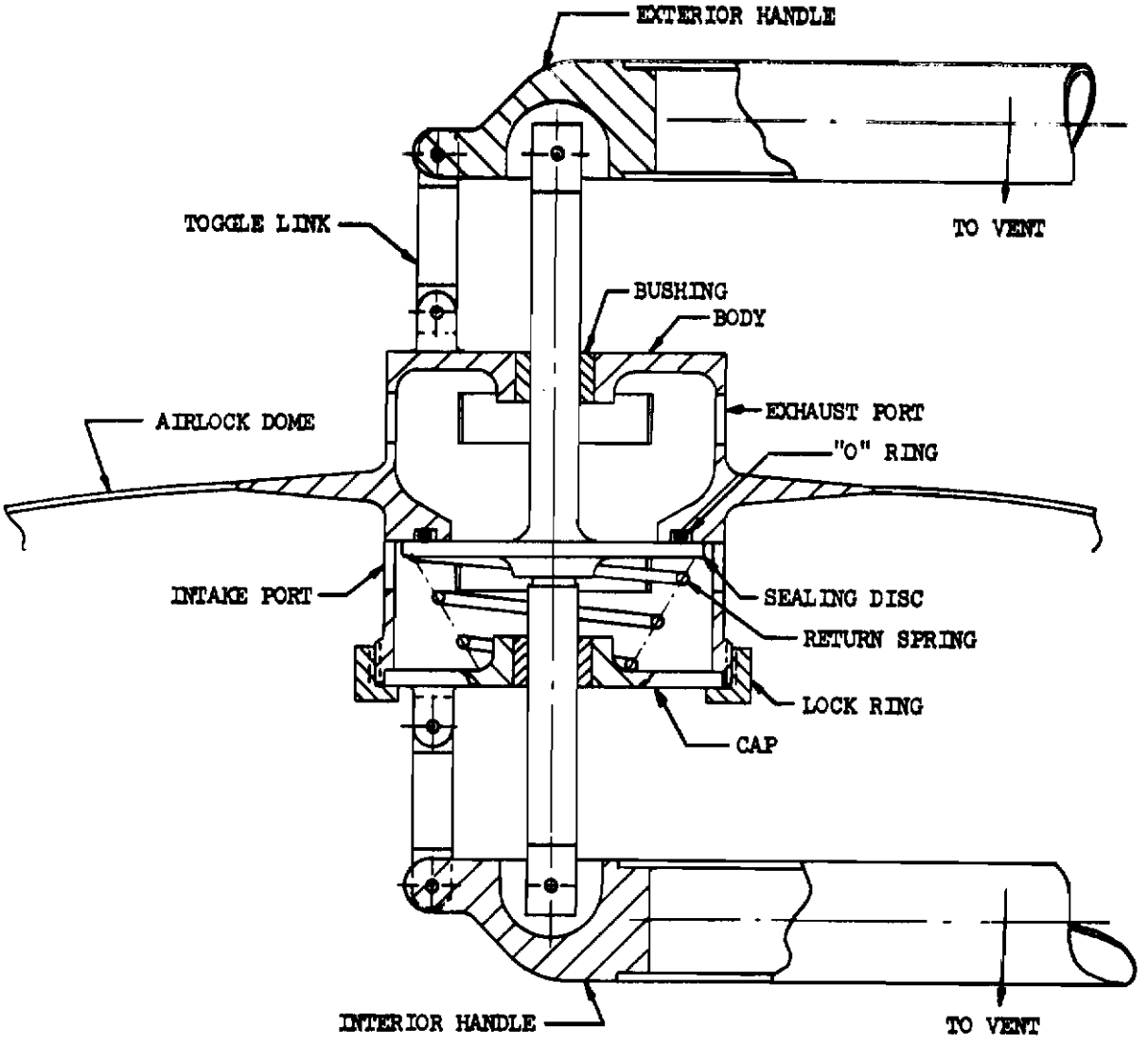

Figure 4-53. Airlock Vent Valve

seal can be employed and the fact that the operating mechanism is the valve itself. No other sealing is required. Lever operation is favored from a human factors viewpoint. If released, the vent will close automatically. Provision will be made, however, to lock the vent open. The same concept can be employed for a solenoid-operated remote vent. The same advantages of straight-through operation, self-sealing and simplicity are applicable. The remote vent will be capable of operation from the airlock control box and the SSESM control box.

The vent size for an airlock of this volume will be 2.8 square inches for a 60-second vent time.

4.8.4.5.2 CONTROL BOX

Two control boxes are required; one inside the airlock for astronaut control of operations and one inside the SSESM for remote control of operations. The control functions incorporated in the airlock control box included a power on switch, a pressurization on-off switch and a vent control switch. The SSESM control box will contain deployment and retraction controls, a switch for proof pressure initiation, and vent control switch.

In addition to the above, the airlock control box will contain an airlock internal pressure gage which can be monitored by the astronaut. The control box can be mounted to the fabric termination ring adjacent to either hatch.

4.8.4.5.3 INSTRUMENTATION

Instrumentation sensors are required to provide airlock pressure, airlock internal surface temperature, airlock exterior surface temperature, and airlock strain data for remote readout and recording within the SSESM. The pressure sensor is a qualified pressure transducer. It will be mounted in the base structure with pressure lead to the lower rigid bulkhead. Four temperature sensors will be located at 90° intervals around the circumference of airlock, inside and outside. These will be flexible nickel resistance sensors. They will be bonded inside the airlock between the inner scuff and

bladder and on the outside between the outer scuff and foam. In this manner the sensors and leads will be protected. The method of determining strain data has not been fully evaluated. It is felt, however, that a strap with a resistance strain link placed around the airlock will provide the required data.

4.8.4.5.4 LIGHT

Lighting will be required inside the airlock to permit the astronaut to see his controls and gage. The light assembly, incorporating a frosted plastic lens, will be mounted on the fabric termination ring at approximately 90^{0} to the controls and control box. The light will be on any time the power-on switch on the control box is on.

4.8.4.5.5 SAMPLES

Two 9 x 9 inch samples of the expandable composite material are required for space environment evaluation of the materials. These two samples will be stowed inside the airlock base assembly. They will be removed at the time the airlock is deployed and attached to the airlock structure or SSESM structure by means of velcro which will be bonded to the sample and the structure.

4.8.4.5.6 HATCH STOWAGE

It is envisioned that the hatch will be stowed inside the airlock to either side of the astronaut by means of velcro pads or by means of straps bonded to the inside of the airlock. In addition, the hatch will be connected to the hatch fabric termination ring by a short tether to aid in retrieval of the hatch by the astronaut.

4.8.4.5.7 MISCELLANEOUS CABLING AND CONNECTIONS

A main electrical cable between the airlock and SSESM will be provided. This cable will contain instrumentation, power, control, and possibly communication wiring. From a sealed connector in the base of

the airlock, wiring will be run to the control box, light, temperature sensors, and pressure switch. External temperature sensor wiring and wiring for the pressurization system will also terminate at a connector in the base of the airlock. Shielding practices consistent with the safety of the mission will be employed.

Two pressure connections will be provided in the base of the package. These are for the pressure link from the SSESM (90 psi) to provide oxygen addition to the umbilical connection, a short umbilical link will be provided inside the airlock.

Suitable brackets will be provided to attach the airlock to the SSESM. The design of these brackets will be determined when the location or locations of the airlock on SSESM are known. They will essentially be interface adapters and will permit the airlock and SSESM designs to proceed almost independently.

4.8.4.6 ANALYSIS

4.8.4.6.1 STRUCTURAL ANALYSIS

The spherical fabric dome is constructed of 8 gores in a rose-petal fashion. The lapped fabric seams, being of higher modulus, act in part as longitudinal and hoop straps, thereby aiding in controlling the total deflection during pressurization. The orientation of the fibers at the seam joints was estimated to be within 15° of the principal ϕ and θ axis.

Using the loads calculated for the principal axes, the fiber loads were determined using a load-transformation equation.

The maximum seam shear-load was taken as the resultant of the fabric loads.

4.8.4.6.2 FABRIC ANALYSIS

The following fabric stress analysis was performed to determine fabric requirements for the spherical airlock. One ply of fabric having approximately 290 lb/in strength appears adequate.

Configuration

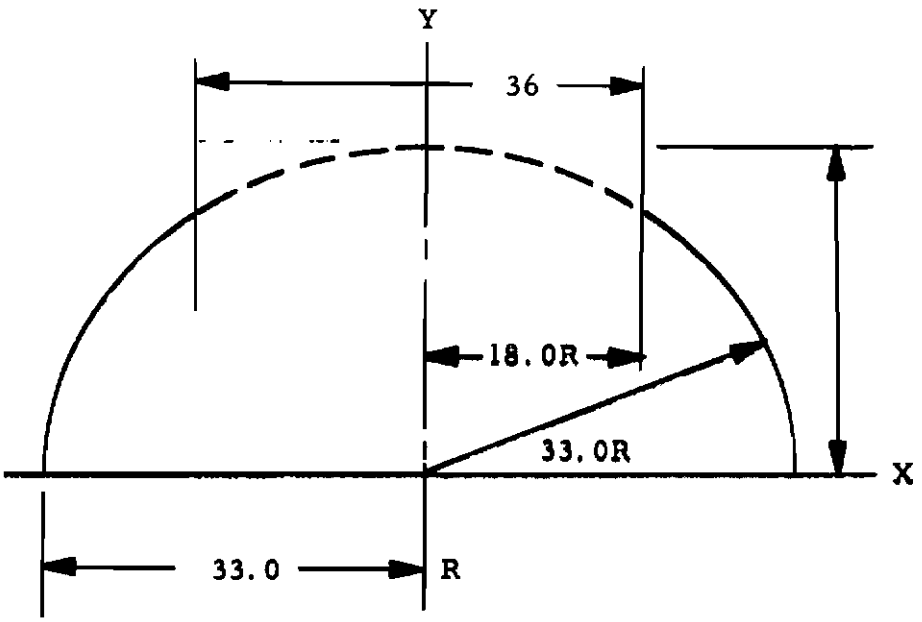

Maximum Fabric Loads @ x = $\pm$ 18 inc.

Meridinal

$$N_{\phi} = PR/_2 = \frac{3.5\ (33)}{2} = 57.75\ \text{lb/in}$$

Hoop

$$N_{\theta} = \frac{PR}{2} = 57.75\ \text{lb/in}$$

Forward Closure

Seam Configuration

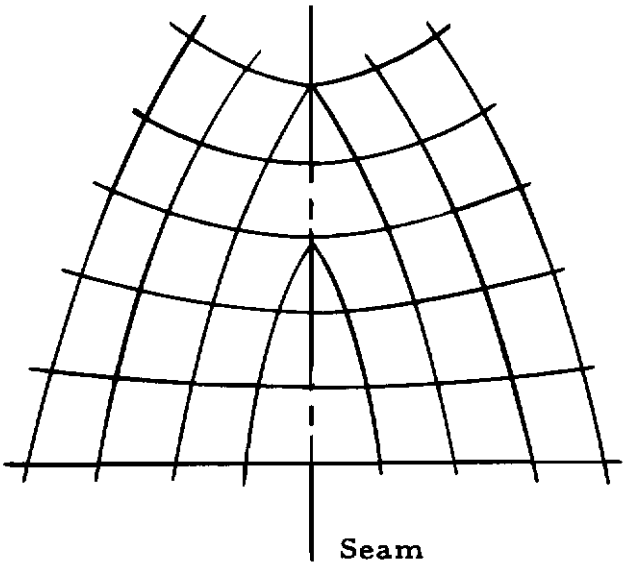

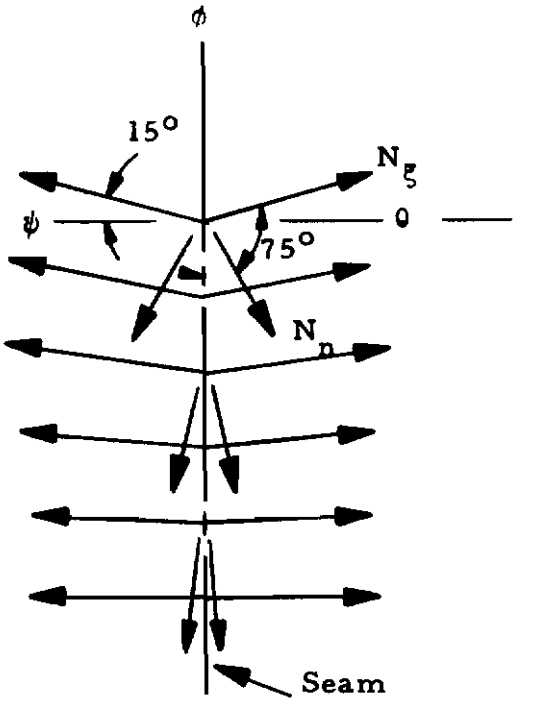

$\psi = 15^\circ$ Assumed Fiber Orientation with respect of Principal axes θ and ϕ

Fabric Loads

$$N_\eta = N_\phi \cos^2\psi + N_\theta \sin^2\psi + 2N_{\phi_\theta} \sin\psi \cos\psi$$

$$N_\xi = N_\phi \sin^2\psi + N_\theta \cos^2\psi - 2N_{\phi_\theta} \sin\psi \cos\psi$$

$$N_{\xi_\eta} = (-N_\phi + N_\theta) \sin\psi \cos\psi + N_{\phi_\theta} (\cos^2\psi - \sin^2\psi)$$

Since $N_\phi = N_\theta$ then

$$N_\eta = N_\phi = N_\theta$$

$$N_\xi = N_\phi = N_\theta$$

Fabric Loads (Continued)

Maximum Fabric Load with $P_{max} = 5(3.5) = 17.5$ psi

$$N_{\eta_{max}} = 5(N_{\eta}) = 5(57.75$$

$$= 288.75 \text{ lb/in}$$

$$N_{\phi_{max}} = 5\ N_{\phi} = 5(57.75)$$

$$= 288.75 \text{ lb/in}$$

Maximum Seam Load with $P_{max} = 5(3.5) = 17.5$ psi

$$N_J = 5(N_{\eta}^2 + N_{\phi}^2)^{1/2} = 5\ \ (57.75)^2 + (57.75)^2\ \ ^{1/2}$$

$$= 408 \text{ lb/in}$$

4.8.4.7 WEIGHT STATEMENT

WEIGHT BREAKDOWN - ELASTIC RECOVERY SPHERICAL AIRLOCK

Component		Weight (lb)
Top Hatch		
Aluminum Dome	= 2.20 lb	
Aluminum Ring	= 3.20 lb	
Latch Mech		
Shaft (2)	= .2 lb	
Handles (4)	= .5 lb	
Vents (2)	= 3.24 lb	
Total		9.85

WEIGHT BREAKDOWN - ELASTIC RECOVERY SPHERICAL AIRLOCK (Continued)

Component			Weight (lb)
Four Brackets			.1
Composite:	Foam	= 12.1 lb	
	Outer Scuff	= 8.67 lb	
	Bladder	= .93 lb	
	Inner Scuff	= 1.2	
	Adhesive	= 5.0 lb	
	Thermal	= ..67 lb	
	Fabric (2)	= 5.7 lb	
	Total		34.27
Upper Fabric Termination Ring			3.20
Lower Fabric Termination Ring			13.8
Marman Clamp			5.0
Aluminum Ring			4.4
Aluminum Dome			3.22
Seals			
	Small O-Ring (2)	= .30 lb	
	Large O-Ring (1)	= .30 lb	
	Total		.6
Pressurization System			
	4 Small Bottles	= 15.64	
	Wt of O_2	= 7.8	
	1 Large Bottle	= 5.87	
	Wt of O_2	= 2.97	
	3 Fill and Vent Valves	= .6	
	3 Squib Valves	= .9	
	1 Solenoid Valve	= .5	
	1 Check Valve	= .2	

WEIGHT BREAKDOWN - ELASTIC RECOVERY SPHERICAL AIRLOCK (Continued)

Component		Weight (lb)
1 Quick Disconnect Valve	= .2	
1 Regulator	= 1.0	
1 Press Switch	= .1	
Stainless Tubing	= .21	
Aluminum Tubing	= .05	
Manifold and Fixtures	= 1.5	
Total		37.54
Base Cruciform Structure		
Tee Sections	= 1.76	
Web	= 1.5	
Center Joint	= .1	
Structural Ring	= 4.84	
Aluminum Bottle Straps	= .324	
Hardware	= 1.0	
Total		9.52
Various Accessories		
Light	= .2	
Control Box	= 1.0	
Electric Connects	= .1	
Cabling	= 3.0	
Pressure Connects	= .2	
Umbilical Connector	= 2.5	
Relief Valve	= .1	
Pressure Transducer	= .5	
Remote Control Box	= 2.0	
Total		9.8

WEIGHT BREAKDOWN - ELASTIC RECOVERY SPHERICAL AIRLOCK (Continued)

		Weight (lb)
Retraction System		
Motor and Drive	= 1.9	
Battery	= 1.0	
Cable	= .5	
Drum	= .25	
Outer Discs	= .164	
Inner Dividers	= .11	
Shaft	= .05	
Bearings	= .1	
Total		4.07
Grand Total		135.37

4.9 ALTERNATE AIRLOCK CONFIGURATION

A brief investigation has been performed to study the integration of an expandable/retractable airlock, of the elastic memory type, directly into an existing vehicle EVA hatch design. The existing structure is assumed to be a 37-inch diameter by 48-inch-long, rigid metal cylinder provided with inboard and outboard hatches which open inward and outward, respectively. As this space is insufficient to contain a pressure-suited astronaut, an expandable elastic memory extension is considered to extend the internal dimensions of the deployed airlock to a 7-foot-long cylinder. A basic requirement of the design necessitates that during the installation of the airlock extension minimum structural modifications are incurred and limiting or interference with the clear aperture of the existing airlock does not occur. Also, when retracted, the elastic memory airlock should exhibit minimum surface protrusions, as atmospheric drag can become significant for low orbits or long missions.

These criteria may be satisfied by a design concept which involves the utilization of a toroidal canister around the periphery of the existing cylinder and recessed beneath the vehicles exterior surface. This concept is shown in Figure 4-54.

The packaging efficiency can be very good for this type of canister, as a regular folding pattern can be used (the inner opening is not included in the canister volume insomuch as the design ground rule required that this center opening be useable volume). Also, a weight advantage is gained over previous experiment configurations in that both outer and inner hatches are already included as existing hardware and the elastic memory material extensions need only provide an additional three feet of length for the overall 7-foot requirement. Although the inside dimension of the existing 4-foot cylinder is only 37 inches, the elastic memory airlock extension will be 44 inches inside diameter to provide nearly as much astronaut maneuverability as the 4-foot-diameter configuration.

4.10 REFERENCES

1. J. Q. Cragin, "Application of Post Yield Strain Gages to Nylon Tape," Society for Experimental Stress Analysis, November 1963.
"Study of Load and Life Capabilities of Purchase Tapes for Expeditionary Aircraft Arresting Gear," Final Report, Naval Air Engineering Laboratory, Contract No. N156-4152, October 1963.

2. Handbook of Instructions for Aerospace Vehicle Equipment Design (HIAVED), AFSCM 80-7, Part D, (entitled Aerospace Weapons, Electroexplosive Subsystems and Ordnance Devices) by Headquarters, Air Force Systems Command, including transmittals 1 through 5.

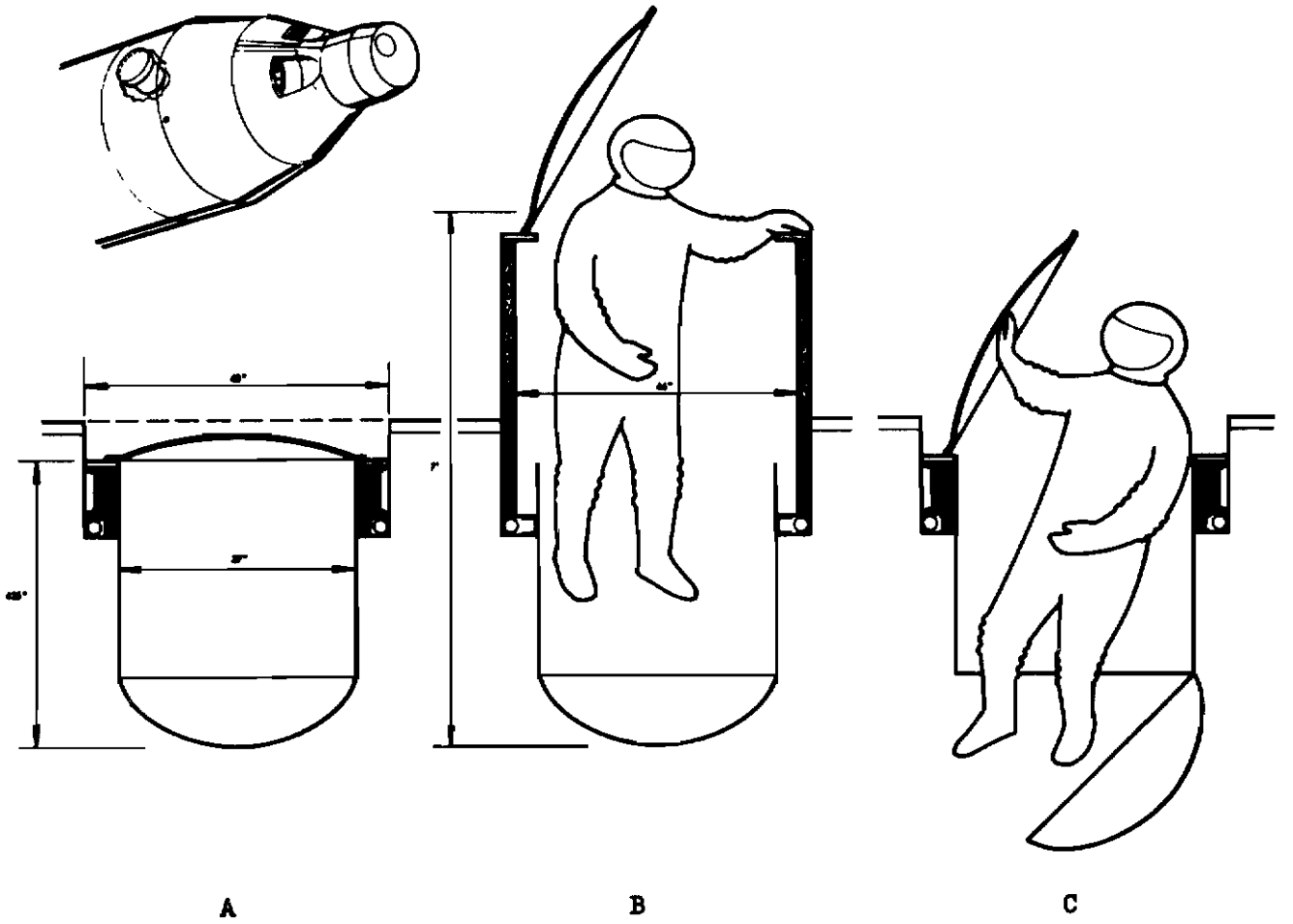

Figure 4-54. Expandable Airlock Incorporated in Existing Vehicle Hatch Structure

Section 5

EXPANDABLE PARABOLA DESIGN AND TRADEOFF STUDY

At the inception of the program two types of construction approaches were specified for study. One was to be an inflatable rigidized solar collector design, and the other was to be a modular design that could be assembled by an astronaut. Evaluation early in the program showed that the inflatable rigidized approach required further exploratory work before a design concept could be evolved that would meet the requirements. The surface condition of the samples obtained for candidate material systems was inadequate for use as a solar collector reflector, or antenna, and the accuracy of the contour was far less than the desired value. Also, the concept of using an end-cap to aid in forming the reflective surface was still to be demonstrated at any scale. For these reasons, the design study in this contract emphasized the modular concept. The concept of this type of structure reported here is termed a "Modular Parabola."

5.1 GENERAL DESIGN CONSIDERATIONS AND APPROACH

The design criteria used in the studies for the modular parabola, as well as the design approach, are reviewed in this section. The results of the design studies are given in subsequent sections.

5.1.1 MODULAR PARABOLA DESIGN CRITERIA

These criteria summarize the technical requirements for the design, development, and fabrication of a 10-foot diameter, 45°-rim-angle paraboloid collector to be assembled in orbit from prefabricated modular panel components by an astronaut working EVA in a pressurized space suit.

The natural and induced environmental conditions that may be encountered by the components and the assembled structure from pre launch to orbital flight are included for consideration in the parabola design.

5.1.1.1 BASIC DESIGN REQUIREMENTS

The design concept must be applicable and scalable to structures up to 100 feet in diameter with modular components no larger than 6 feet in length.

5.1.1.1.1 MATERIAL

The collector base material for the 10-foot-diameter collector is to be 0.300-inch-thick aluminum alloy honeycomb with 3 to 4-mil aluminum face skins. Attachment and joint mechanisms may be of aluminum, steel, or any other material as required to meet the loading conditions, the deflection and rotational constraints, and the weight limitations. Only current state-of-the-art material and mechanisms should be considered.

5.1.1.1.2 HUB SIZE

A 14-inch-diameter hub will serve as the structural attachment nucleus around which the collector is to be assembled. The hub is to be supported from the parent vehicle by a boom arrangement. The configuration is to be similar to the previous S-6 inflatable collector concept.

5.1.1.1.3 ELECTRONIC EQUIPMENT

The design, weight distribution, power requirements, and general criteria for the operational electronic equipment associated with an application of the parabola are not within the scope of this program. However, a Xenon light source sting is discussed in the section of illuminator analysis.

5.1.1.2 PHYSICAL RESTRAINTS

5.1.1.2.1 WEIGHT

The weight of the total modular panel assembly for a 10-foot, 45°-rim-angle collector, including the panels, connectors, and locking mechanisms, but excluding the weight of the hub, packaging system, and electronic equipment, shall have a design goal of 40 pounds.

5.1.1.2.2 VOLUME

The package volume of all the modular panels for the 10-foot collector shall not exceed 3.0 cubic feet. The package shall be capable of being stowed in the unpressurized locations on the vehicle.

5.1.1.2.3 MODULE DIMENSIONS

The panel module canister shall be capable of being passed through a 30-inch-diameter hatch and be of a convenient size for the astronaut to manipulate. For the purpose of the design of a 10-foot collector, the modules are assumed to be approximately 25 x 29 inches.

5.1.1.2.4 SURFACE ACCURACY

The radiation collecting surface of the assembled 10-foot collector is to be a true parabolic surface within the following tolerance. The surface deviation from a true paraboloid shall be minimal on 90% of the surface area; i.e., the combined errors in manufacturing, erection, and structural deflections shall result in deviations no larger than required to achieve the desired efficiency. The overall efficiency of the collector shall be such that 85% of the incident solar energy on the collector shall pass through a 5-inch-diameter area at the focus.

5.1.1.3 LOADING CONDITIONS

5.1.1.3.1 HANDLING IN SHOP

The panels shall be capable of being handled during the manufacturing operations, preassembled in the required configuration, disassembled, and loaded and unloaded for transportation without damage or stressing components beyond the elastic limit.

5.1.1.3.2 TRANSPORTATION

The transportation shock loadings which can be expected for the common transport systems are:

Trucks	8 g
Rail	20 g
Aircraft	5.5 g (vertical)
	1.5 g (side)
	8.0 g (longitudinal)

Shipping and packaging should be designed to attenuate the transportation shock loading as much as possible. No permanent deformations should result from loadings encountered in the transportation of the panel sections.

5.1.1.3.3 LAUNCH

The panels in their stowed positions in the launch vehicle must be capable of absorbing the following loading conditions without permanent deformations.

Acceleration	8 g
Vibration	5 to 10 g RMS

5.1.1.3.4 ORBITAL MANEUVERING

The assembled collector in space may be subjected to forces resulting from linear and angular accelerations of the following magnitudes:

Linear:	0.1 g along any axis through the center of mass
Angular:	0.1 rad/sec^2 about an axis 13 feet from the center of mass
Angular Velocity:	5.0 deg/sec maximum about an axis 13 feet from the center of mass

5.1.1.3.5 SOLAR WIND

A continuous flux of particles (protons and/or electrons) from the sun produces a phenomenon called solar winds in the vicinity of the orbit of the earth. These solar winds exert a continuous pressure in an outward direction from the sun. The strength of these solar winds at 1AU is

dependent on the activity of the sun. While the pressure during a period of quiet sun activity is as low as 1×10^{-9} lb/in^2, it may increase to 100 times this figure during severe sun storms. However, even during a sun storm, the pressure is several orders of magnitude less than those pressures produced by maneuvering. For the purpose of this design definition the effects of solar winds may be ignored.

5.1.1.3.6 AERODYNAMIC PRESSURES IN ORBIT

The proposed experimental assembly of the 10-foot collector is to take place in an earth satellite orbit of about 200 nautical miles. The density of the atmosphere at this elevation is 11.6×10^{-13} lb/ft^3 and the vehicle in this orbit would be traveling with a velocity of 25, 228 ft/sec.

Aerodynamic Pressure (P) = $1/2\ \rho V^2$

where ρ = density of the atmosphere

V = velocity of the vehicle

$P = 11.6 \times 10^{-13} \times (25,228)^2/2 = 3.7 \times 10^{-4}$ lb/ft^2

or $P = 2.57 \times 10^{-6}$ lb/in.^{2}

It should be noted that the force resulting from this pressure is only about 1% of those forces resulting from the orbital maneuvering criteria. The effects of this condition can also be neglected.

5.1.1.3.7 THERMAL STRESSES

When used as a solar collector, the efficiency is a maximum only when oriented face on to the sun. The design of the panel system shall take into account the stresses and angular rotations of the reflective surface due to the difference in temperature between the sun side and the shaded side of the collector in this orientation . Under this condition no component shall be overstressed, nor shall the deformations result in angle changes on the parabolic reflective surface of more than 0.5^o (less

manufacturing and assembly tolerances). For any other attitude, the resulting temperature stresses shall not exceed allowables, but deflection and rotations are not critical.

5.1.1.3.8 RADIATION AND METEORITIC BOMBARDMENTS

The effects of the various radiations, such as cosmic, Van Allen belt, auroral, solar flare, and nuclear, need not be considered in the panel designs. The effects of collisions with meteoritic particles and cosmic dust likewise need not be considered, except to the extent that panel replacement could be required.

5.1.1.3.9 ASTRONAUT HANDLING

During the assembly process it is assumed that the astronaut may exert a force equivalent to 10 pounds in any direction within the plane of a panel. The structural components must be capable of withstanding this load without yielding. The panel may rotate under this loading condition in excess of the 0.5^{o} criteria maximum, but it must return to the criteria configuration after the load is removed without suffering any permanent deformation. It is assumed that the astronaut is adequately restrained at a work station during parabola assembly (not on a tether) so that the probability of inadvertent overloading by the astronaut is minimized. To avoid the possibility of inadvertent astronaut suit puncture, the design should not make use of any sharp points or corners on the panel units.

5.1.1.3.10 COMBINED LOADINGS AND FACTORS OF SAFETY

All the loading conditions except Orbital Maneuvering and Thermal Stresses shall be considered uncombined with any other condition. These two conditions must be considered in the combinations which will produce the critical stresses and deflections.

The stresses resulting from criteria loadings shall not exceed either 80% of the yield strength or 2/3 of the ultimate strength of any component material.

5.1.1.4 HUMAN FACTORS CONSIDERATIONS

The design of the manually assembled modular parabola shall exhibit the characteristics necessary for assembly by a pressure-suited astronaut in zero-gravity conditions.

Consideration must be given to the limitations of manual dexterity and anthropometric restraints of the pressure-suited astronaut, in that:

a. No small parts can be handled due to tactile limitations.

b. Reach requirements and twisting of the torso shall be minimal.

c. Only light metabolic work shall be required in the assembly task.

d. Only low assembly forces can be used and these must be completely reacted by some physical restraint, as a work station.

e. The assembly task must not exceed the visual acuity limitations for the astronaut in the space lighting conditions.

f. There shall be no loose parts used which may float away if left unattended.

g. Total single task time must not exceed the limitations of the astronaut or life support system.

h. The use of tools and special equipment is not preferred if the assembly task may be efficiently accomplished without them.

i. The astronaut's location shall be fixed and the structural assembly shall move to within reach.

The conceptual design shall be evaluated by a neutral buoyancy test on a full scale mock-up of modular parabola hardware and assembly concept.

5.1.2 APPROACH

Various conceptual assembly systems and procedures were examined to determine which basic approach would most accurately meet the mission criteria of this experimental space structure.

During the initial phases of the current contract, concepts of varying mechanical and manual complexity and degrees of automatic deployment were investigated. These studies showed that more automated assembly concepts did not optimize the stowed dimension, weight, system complexity, or contour accuracy as well as the manual assembly methods. The use of the pressure-suited astronaut in a zero-g environment could more nearly optimize the man-machine and experimental structure assembly.

The primary advantages of this approach were as follows:

a. The structural contour accuracy of each rigid module can be closely controlled and tested on the ground during the fabrication process. The contour accuracy can therefore be the best rigid tooling state-of-the-art machining tolerances.

b. The assembled parabola may be tested in the laboratory prior to erection in space.

c. No exotic technological development is required.

d. No peripheral deployment mechanisms are required, and the erection is entirely independent of any auxiliary pressurization systems or chemical rigidization subsystems.

e. The manual assembly task can be made within the anthropometric and metabolic restraints imposed by a pressure-suited astronaut in zero g.

f. The design concept reflects scalability for larger structures over 100 feet in diameter.

g. After assembly, any deviations in contour oblateness may be corrected by adjustment of radial tuning wires affixed to the circumference.

h. A damaged module or section may be replaced, thereby maintaining operational integrity of the structure.

A supplementary benefit from this approach is that, since this is to be used initially as a space experiment, the astronaut's ability to erect parabolic structures of high contour accuracy in a zero-g environment, with a minimum of special tools, EVA time, and effort, will be evaluated.

A number of preliminary conceptual designs of an astronaut-assembled, modularized 10-foot parabola were evolved. Consideration was given to structural and dimensional accuracy requirements, limitations of the pressure-suited astronaut in orbital conditions, and scaling effects relative to structures larger by one order-of-magnitude. Some conceptual sketches may be seen in Figure 5-1.

The currently preferred design approach consists of the use of 24 precision contoured segmented panels, arranged to assemble annularly in two concentric parabolic sections. Each panel is provided with several interconnecting attachment devices to be engaged on assembly by the astronaut. This preliminary concept is shown in Figure 5-2 as an illustration of a design of a modular parabola and EVA assembly procedure.

A limited contract was negotiated with the General Electric Company, Valley Forge, Pennsylvania, to design and construct a simulated parabolic structure, to Space-General's specifications, for evaluation of the structural and assembly characteristics in a zero-buoyance test facility. This is reported in Section 5. 3

5.2 MODULAR PARABOLA CONFIGURATION ANALYSIS

5.2.1 GENERAL STUDY

The configuration was studied as to how it could be segmented into individual panels for stacking and packaging in a canister in the vehicle. Assembly would require the astronaut to remove the panels from the canister and assemble the modular parabola during an EVA task.

The design criteria required that the modular panels would stow in a canister whose length is no more than twice the width or depth. Modules should also be interchangeable to facilitate simplicity of assembly sequence and to minimize human errors. Perhaps of most importance, the assembly procedures must require a minimum of astronaut energy and manual dexterity. The result of this study yielded the configuration shown in Figure 5-3.

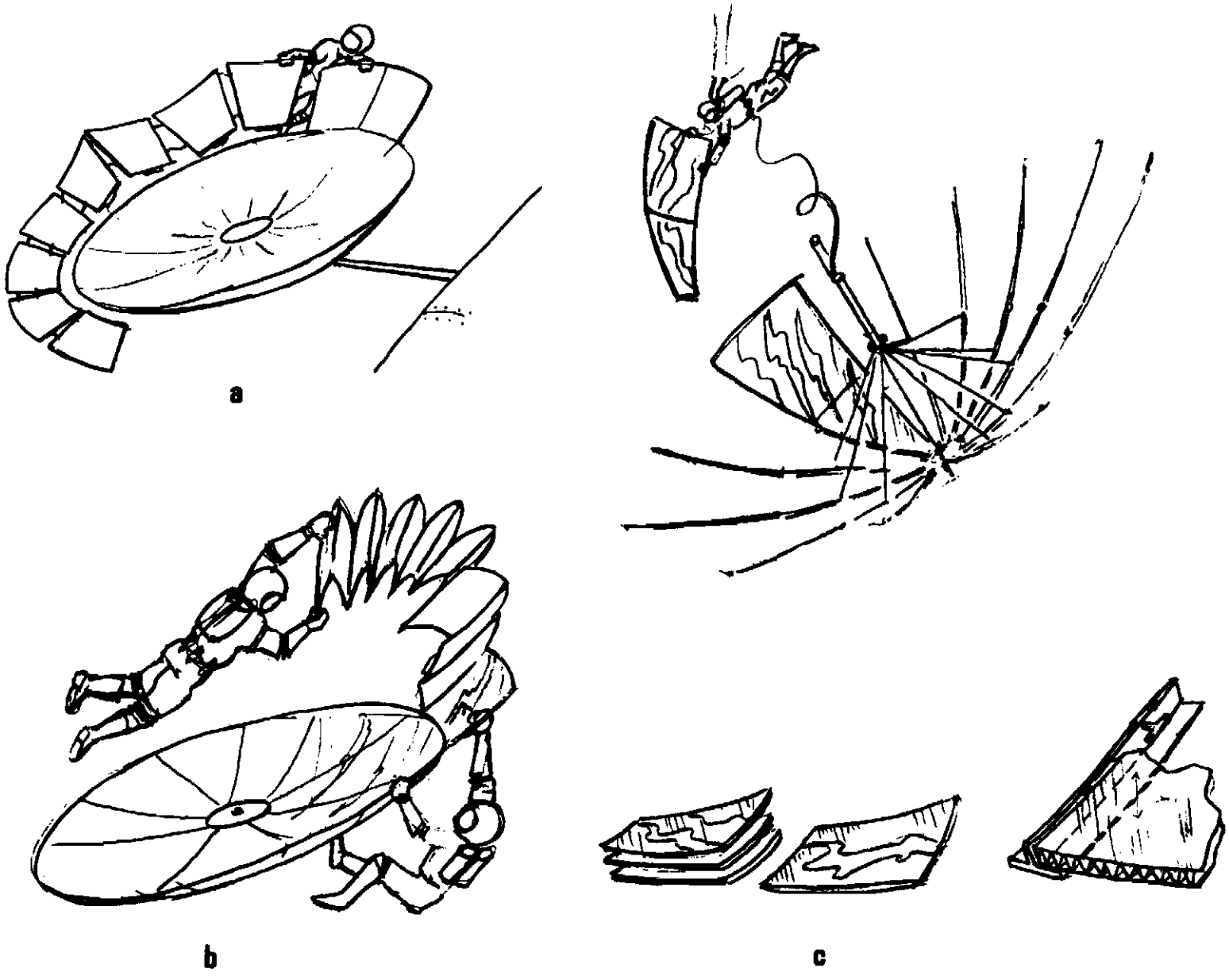

Figure 5-1. Preliminary Concepts of Modular Parabola EVA Task Requirements

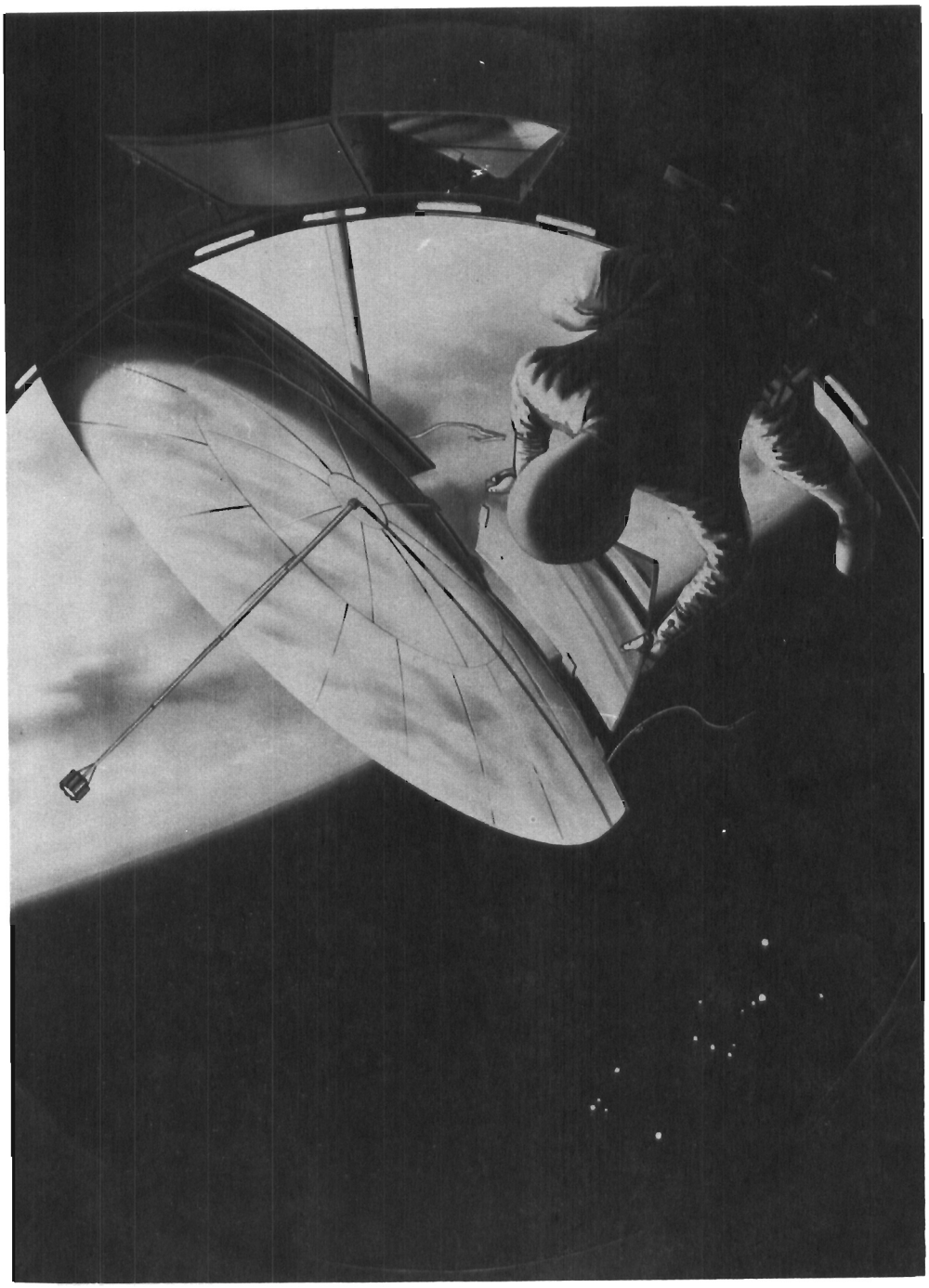

Figure 5-2. Early Concept of an EVA Astronaut at Work Station in Manual Assembly of Prefabricated Parabola

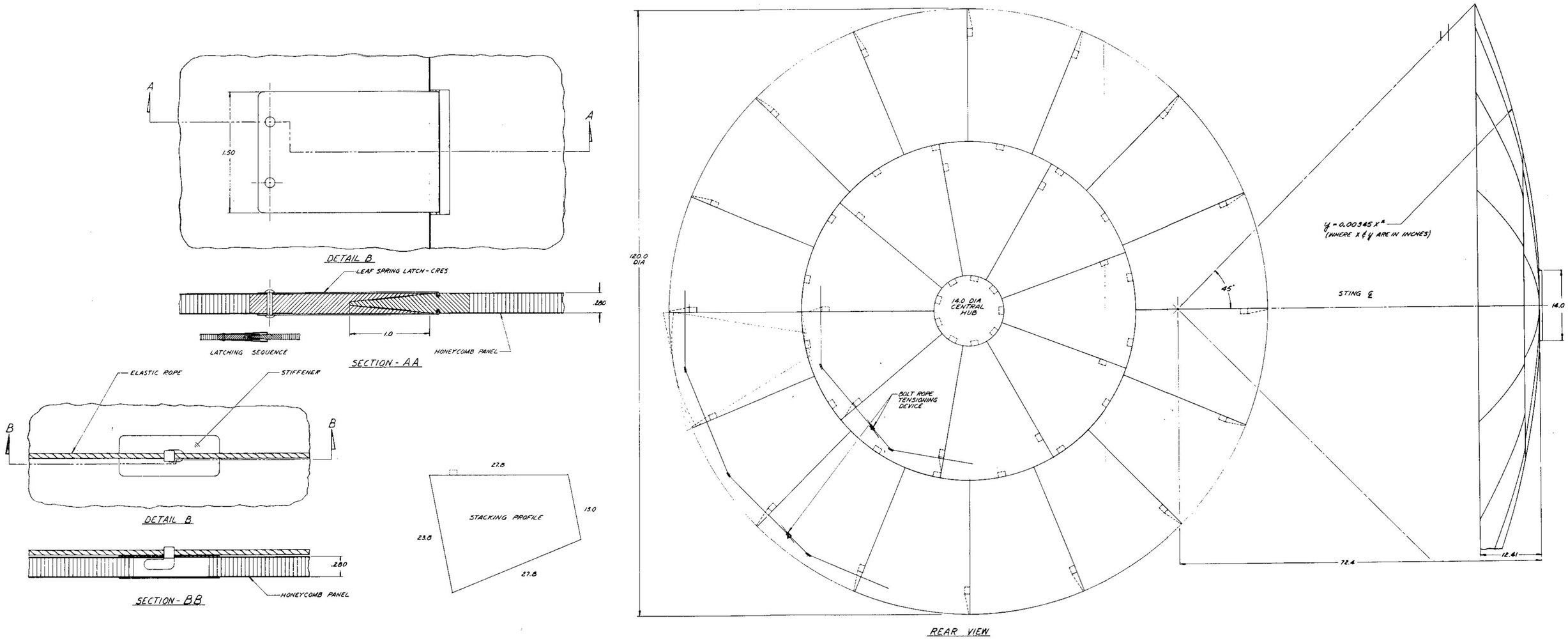

Figure 5-3. Preliminary Layout of Prefabricated Modular Parabola Design

A small central hub is provided for a structural attachment to the boom hinge. The panel configuration is divided into annular segments, approximately 18 inches wide at the base by 30 inches long. This configuration requires 24 individual panels for a 10-foot-diameter mirror, of which eight are identical in one group and 16 in the second group. The two panel configurations will stack one on the other for near-optimum high-density packaging. The maximum panel size was limited to a geometry that is convenient for the astronaut to handle, align, and assemble. Consideration was also given to flattening the flexible precontoured panels to further improve the packaging density, but little advantage from this approach was indicated.

The panel design considered is a honeycomb sandwich structure with 0.003-inch aluminum face skins and a total thickness, including core, of approximately 0.280 inch. With panel sections of these characteristics, and suitable mechanisms for joining one panel to the other, a 10-foot parabolic structure with a 45° rim angle can be assembled in a space environment. Thinner and lighter sections could be used for the 10-foot unit; however, this configuration was selected to more nearly simulate the scaling characteristics of large diameter structures.

Calculations were made on the effects of a 0.1-g axial loading condition on a one-piece parabolic structure by scaling the results of a previous similar shell computer program readout. The maximum moment (scaled) was 0.165 in.-lb/in. of panel with a maximum stress of less than 200 psi. The results of the scaled computer program were order-of-magnitude checked by a flatplate analysis which indicated moments approximately 4.0 times those found by the shell program. These calculations were consistent with expected results and the shell program scaled values are considered acceptable for these preliminary sizing analyses. The maximum rotations of a continuous shell parabola under the 0.1-g loading is approximately 2.0×10^{-4} radian which is considerably less than the maximum tangent error allowed. However, since the structure is designed with numerous panel joints, and the moment and shear forces must be transferred through these joints, the combined deflections due to elastic deformation, joint fabrication tolerances, and thermal deflections must be taken into account.

5.2.1.1 SKELETAL STUDY

To provide a geometrical frame of reference and a more stable guide for the astronaut, a ribbed or skeletal structure was investigated. In this concept the ribs would serve as the pattern or skeleton on which the concentrator panel sections would be erected.

Concept C of Figure 5-1 is a sketch of one skeletal rib concept. To permit stowage of the rib system, the individual ribs of the skeletal frame must be hinged to fold into a compact shipping package. For the 10-foot concentrator, a twelve-rib system would provide a capability of dividing the panels into sizes that satisfy the panel stowage dimensional criteria, and by using 3 hinges per rib, the ribs can fold into a package approximately 20 inches long and 14 inches in diameter.

For the 0.1-g axial loading condition, the ribs can be considered as cantilevers carrying the entire inertia loading of the structure with the panels simply supported between ribs. Deflection calculations, and considerations of practical handling and concentrator assembly requirements led to the aluminum tee shaped cross sectional configuration.

The calculations indicated that the maximum moment in the rib of the twelve-rib concept would be approximately 13.6 in.-lb and the maximum rotation of a one-piece rib section would be approximately 0.00108 radian, or 1/8 of the maximum allowed by the deflection criteria with a maximum stress in the tee of 210 psi. Calculation of the deflection characteristics of a panel simply supported between two ribs indicated that the maximum resulting stresses would be approximately 29 psi and the maximum rotation 0.0142^{o} for this loading condition. Therefore, the main technical problems for this concept are weight reduction and the development of rigid hinged joints which can be easily actuated and positioned by an astronaut in the EVA environment. The joint mechanism should be simple and rigid when closed, and should require a minimum of manual manipulations or adjustments during erection.

Hinge center-lines at the bottom of the tee web and also in the tee flange section were considered. The hinge in the bottom of the web was eliminated because of the difficulty of providing 180° of motion without the use of protruding hinge cranks which reduced packaging efficiency. The design of a latching system for each hinge to support tension, compression, shear, and moments in all axes across the joints, and to conform to the criteria of simplicity, rigidity, and minimum manual manipulations, is a problem of considerably greater difficulty. Various rib hinge lock mechanisms were investigated, including spring-actuated locks, adjustable locks and leaf springs, and over-center locks. Panel-to-rib attach devices studied included spring actuated locks, over-center mechanisms, and cam-actuated expansion bolts.

It should be noted that, in addition to these panel-to-rib joints discussed, the systems proposed for panel-to-panel connection in the ribless structural concepts may also be applicable to the rib-to-panel connections.

The approximate weights of the components of the ribbed 10-foot-diameter structure, excluding the hub section are:

a.	Panel weight	12.5 pounds
b.	Panel edges and connections	12.5 pounds
c.	Ribs and joints (12 ribs)	33.0 pounds
	Total	58.0 pounds

In summary, the study indicated that the design of a parabolic structure for assembly in space, utilizing panels attached to a skeletal rib-frame, is feasible and within the present state-of-the-art. However, design of joints which will not permit angular deflections of more than 0.5° anywhere on the structure must be carefully considered.

As the conceptual design progressed, a simple panel interconnect joint was developed which yielded a considerably lighter design than the skeletal approach.

5.2.2 PANEL CONFIGURATION AND SCALABILITY

The 10-foot-diameter modular parabola preliminary panel configuration shown in Figure 5-4 was established by assuming two basic criteria:

a. Packaging or stacking volume should be minimized

b. Scalable assembly operation should be simulated.

It was decided that scalability could be simulated by employing two annular rings of panels. These panels would be somewhat smaller than could actually be handled by the astronaut. In order that stacking volume be minimized, all panels should be equal in length and width so that, when they are nested, a minimum-sized single canister could be utilized for this experiment. By varying hub size, panel width, and number of panels per ring, a number of configurations can be established. The configuration selected consists of a 14-inch-diameter hub with eight panels in the inner ring and 16 panels in the outer ring. The panel envelope is approximately 27 x 28 inches. Addition of the tapered wedge joints increases the envelope to approximately 28 x 29 inches. Stacking height for 24 panels, each 0.30 inch thick, will be 9 to 10 inches.

As the joints in this configuration are located symmetrically in the panel and all panels within a ring are identical, the fabrication process will be simplified. The closeout panel is of a different detail design which will be determined when final preliminary design of the joints is completed. The employment of symmetrical joints and panels also produces load paths which are uniformly and radially inward when bolt-rope tensioning forces are applied to remove assembly gaps. Bolt-rope attachment points will be provided at the outer tooling hole of each panel.

Each panel will contain an inner end joint and two joints on each side. The outer end of the inner panels will contain two joints, one for each of the two outer panels which mate with it. The location of the side joints are equally spaced radially, establishing essentially four rings of joints.

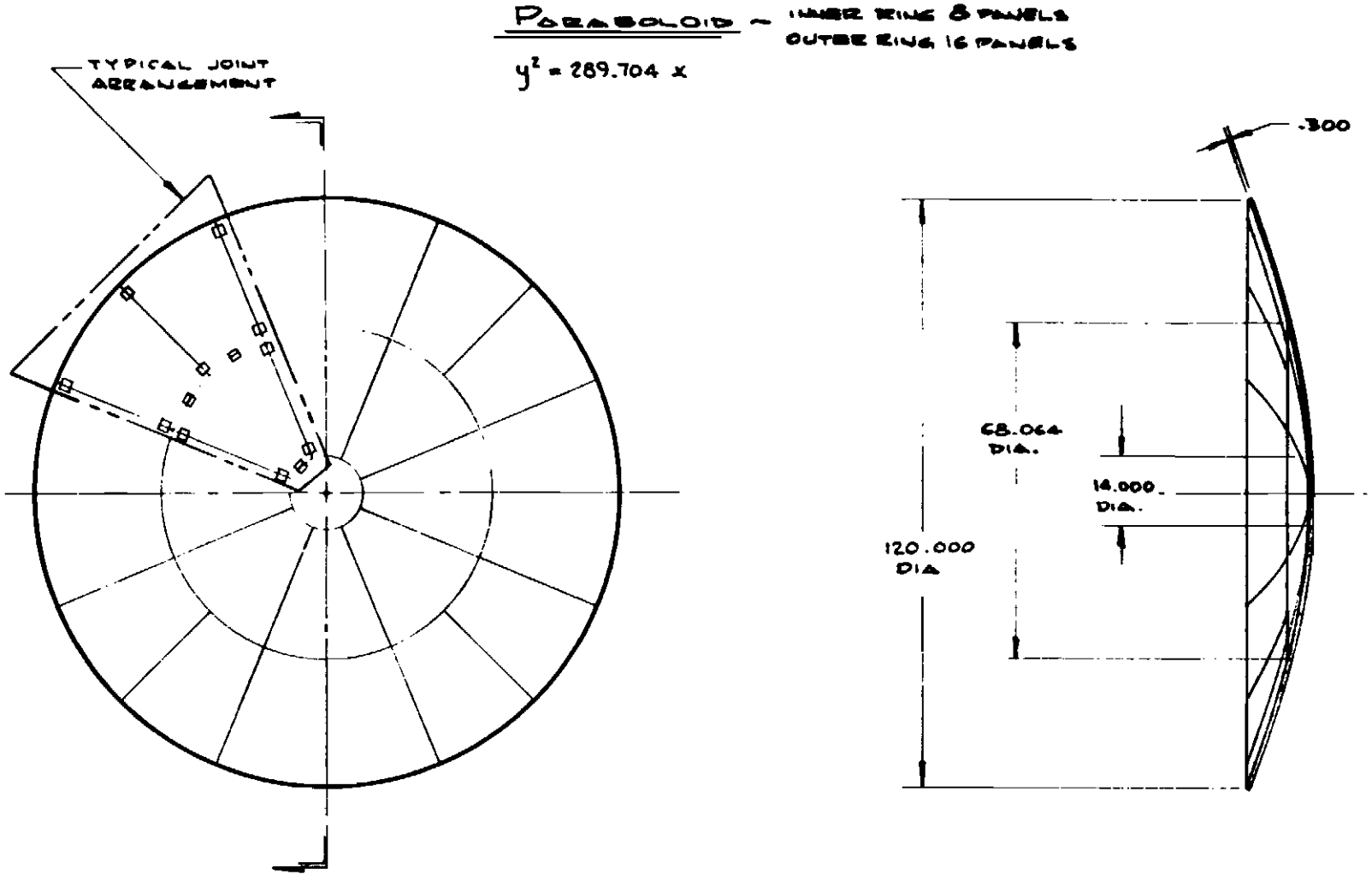

Figure 5-4. Modular Parabola Configuration Showing Optimized Joint Locations

5.2.3 JOINT STUDIES

Several joint attachment concepts were considered for joining the modular parabola panels. Several important criteria were recognized.

These were:

a. Close tolerance control would be required to maintain dimensional accuracy.

b. Structural integrity of the joint should be close to that of the panel.

c. A lead-in feature and an automatic lock-together feature would be desirable to simplify the astronaut's task.

d. The joint should be flush with the panel to promote good stacking efficiency.

The tapered tongue and groove was selected for more detailed study. Several latching mechanisms for locking the panels together were developed. These are shown in Figures 5-5 through 5-11. A trade-off study was conducted and is summarized in Table 5-1. The preferred design for each of the criteria is rated number 1, while a less preferred is rated higher. The rating method is qualitative in that it indicates preferred designs rather then acceptable or unacceptable designs.

The original conceptual design philosophy of the interconnecting panel joints required that the interpanel locks possess the integral ability to provide a preloaded compression joint by some inherent process or mechanism. To preserve the original dimensional accuracy, subsequent tests and further analysis suggested an alternate solution to this requirement.

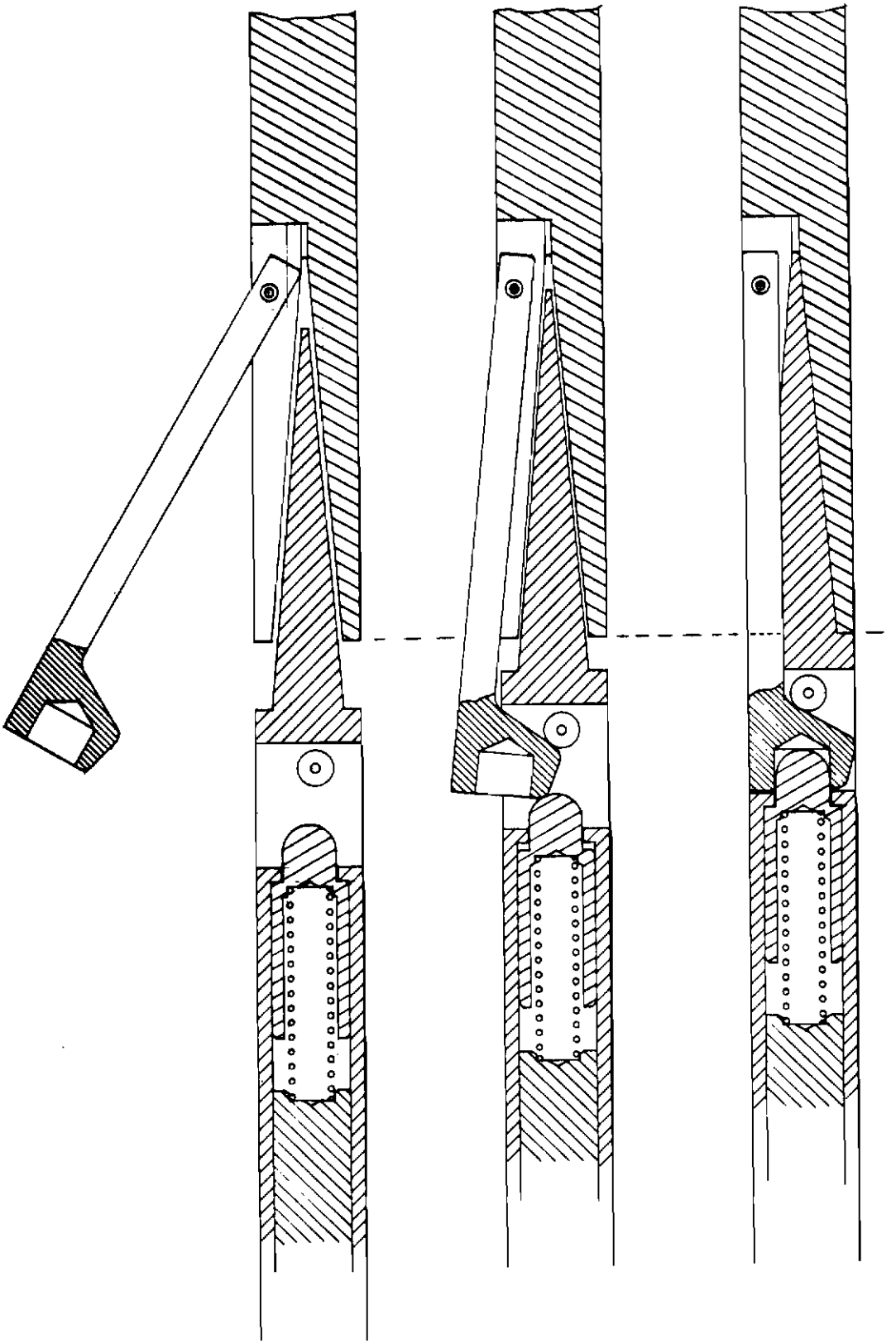

Figure 5-5. Tongue and Groove Latch Detent

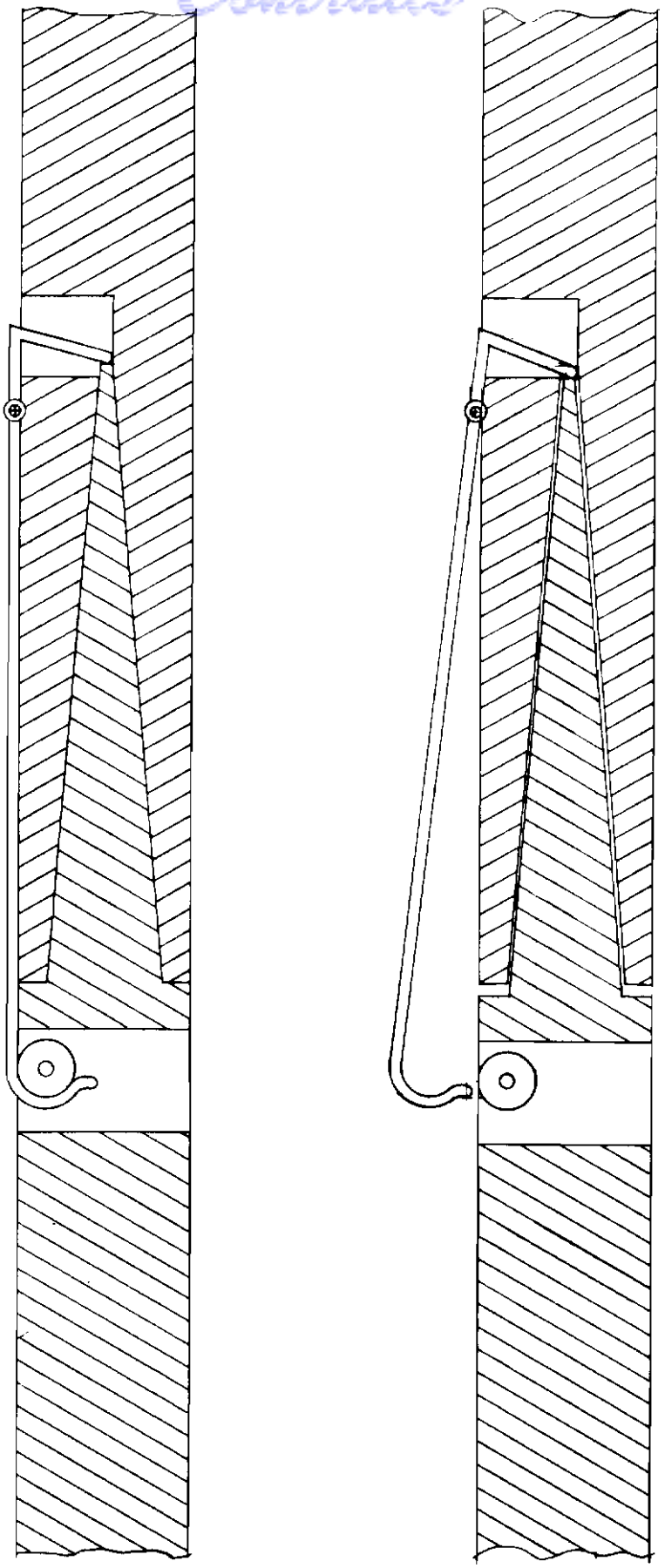

Figure 5-6. Tongue and Groove Spring Latch

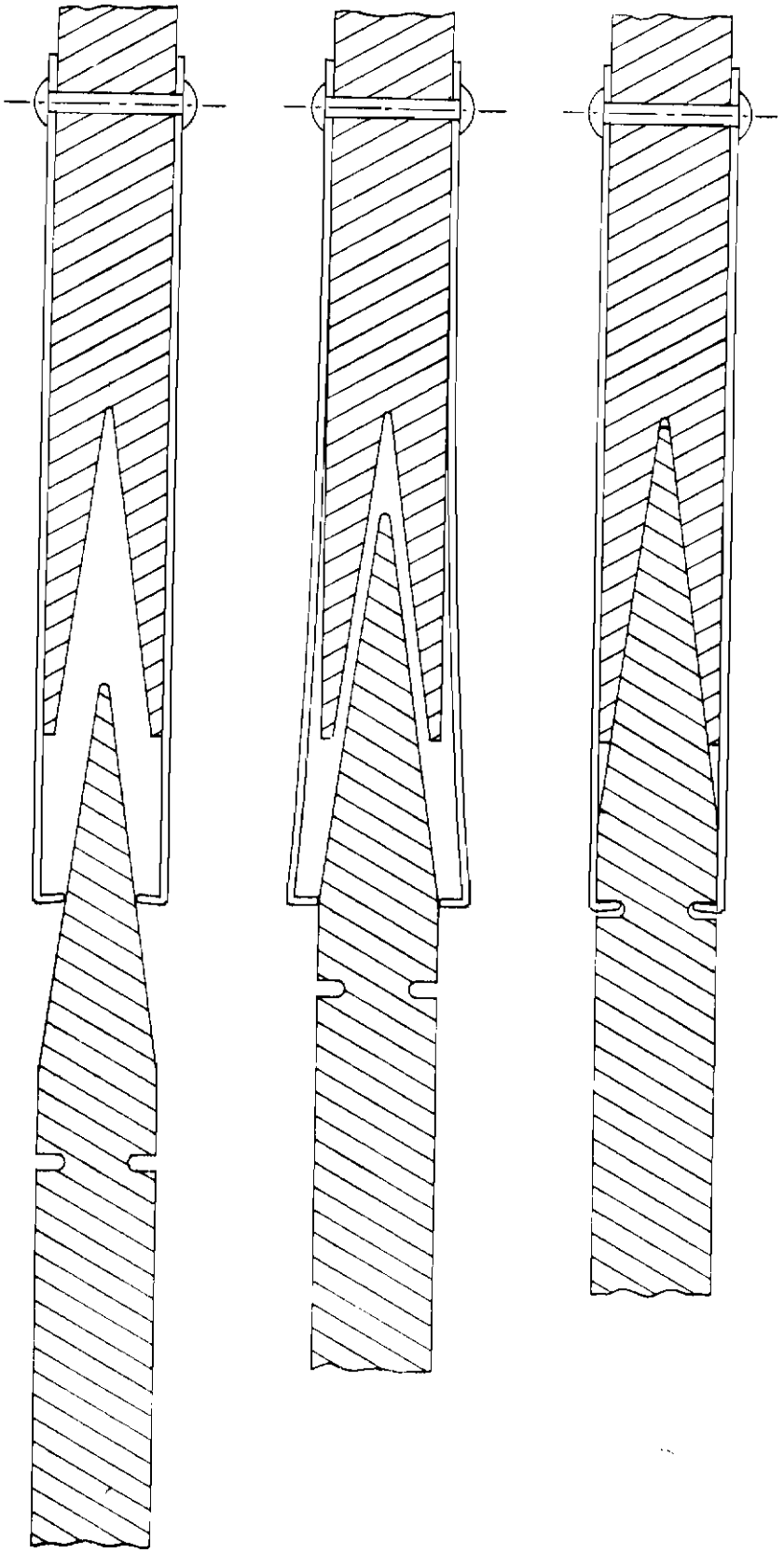

Figure 5-7. Tongue and Groove Spring Clip

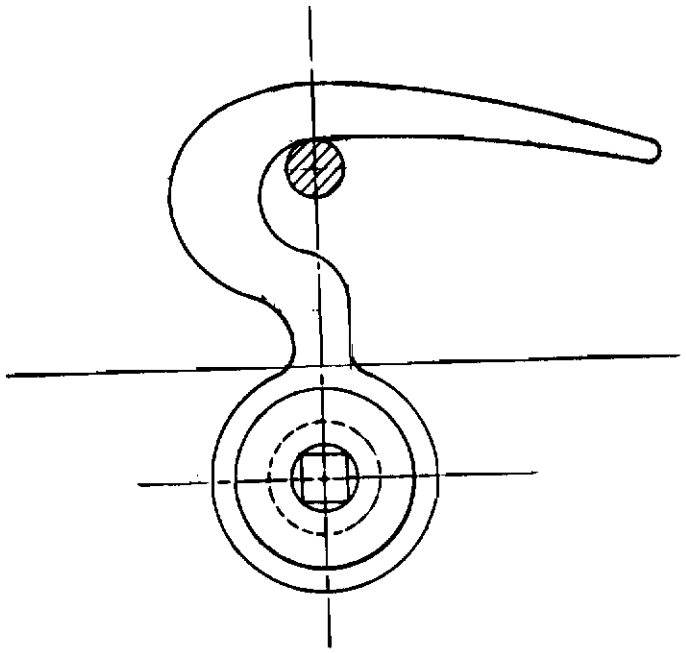

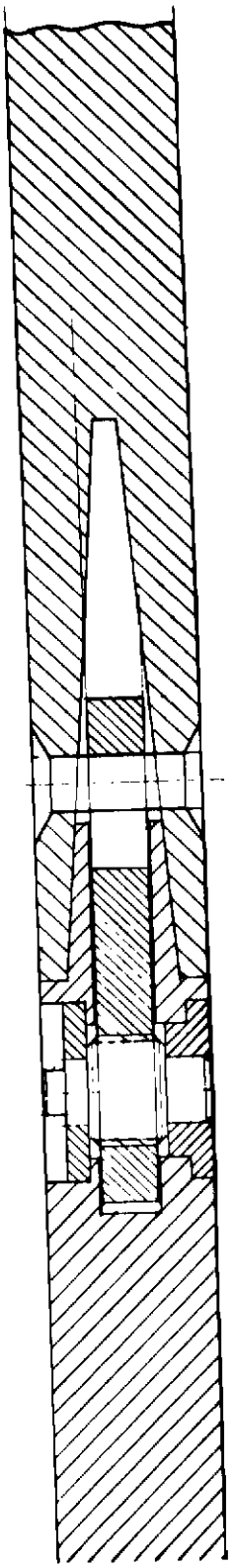

Figure 5-8. Hook Latch

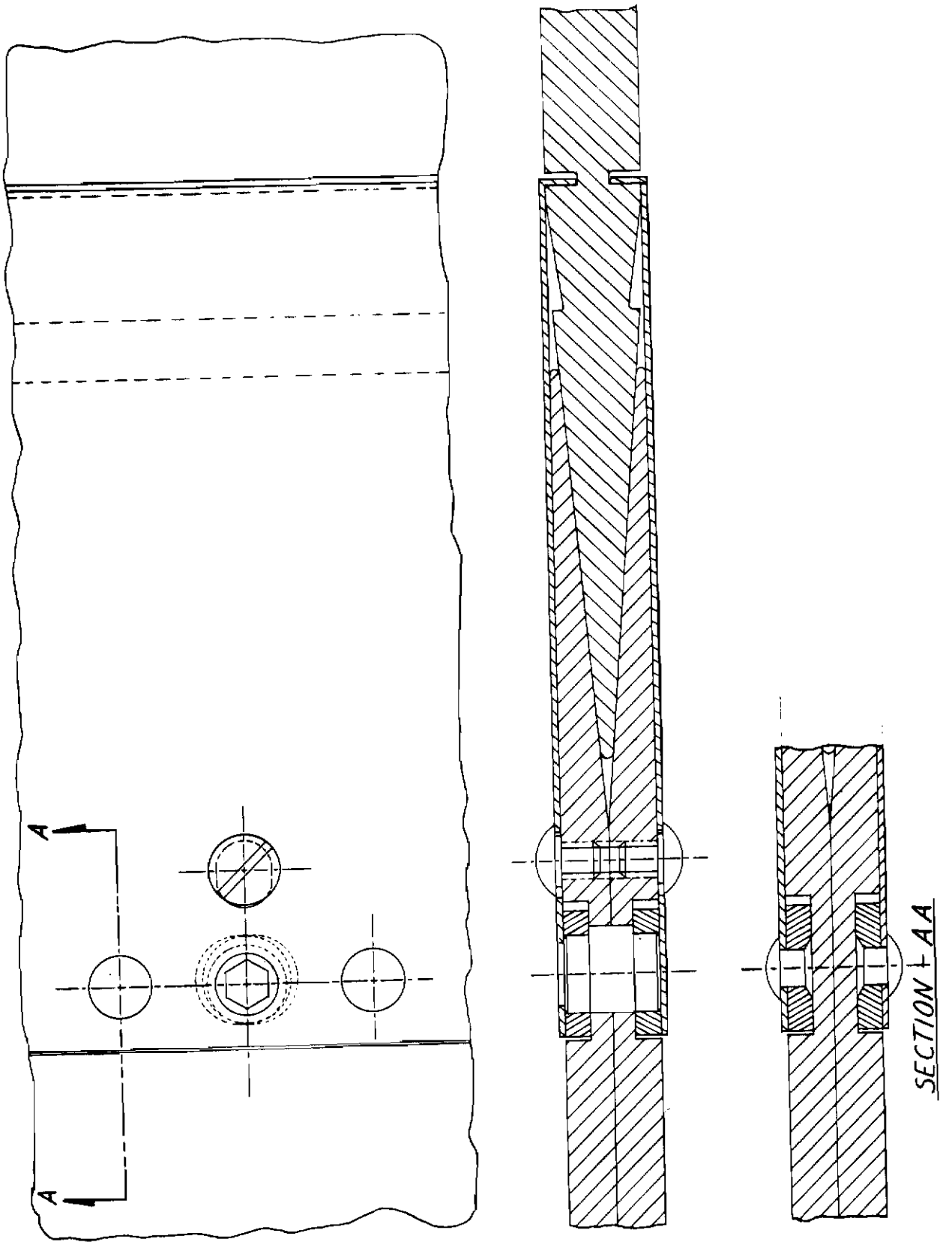

Figure 5-9. Over-Center Cam Concept

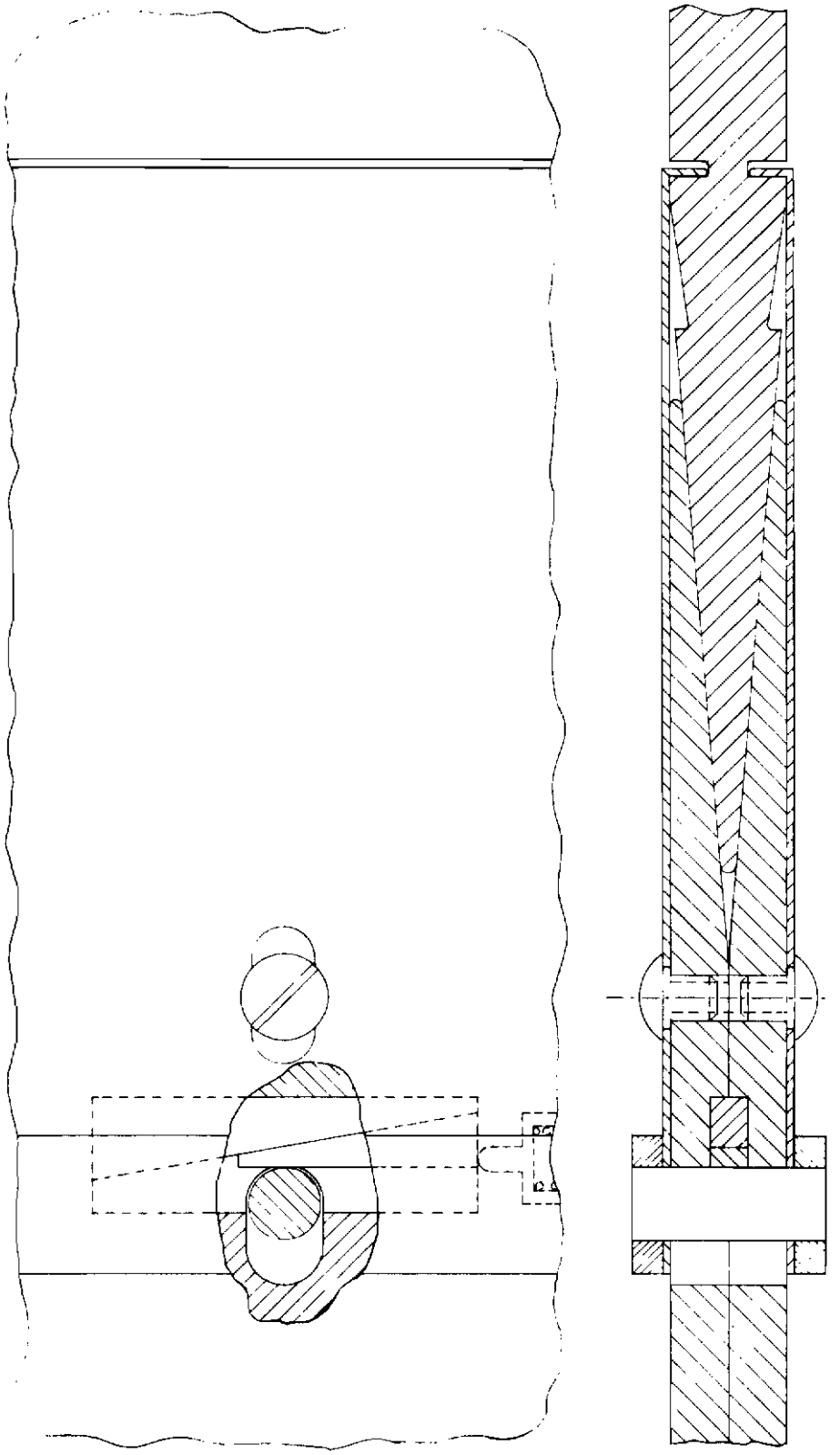

Figure 5-10. Wedge Concept

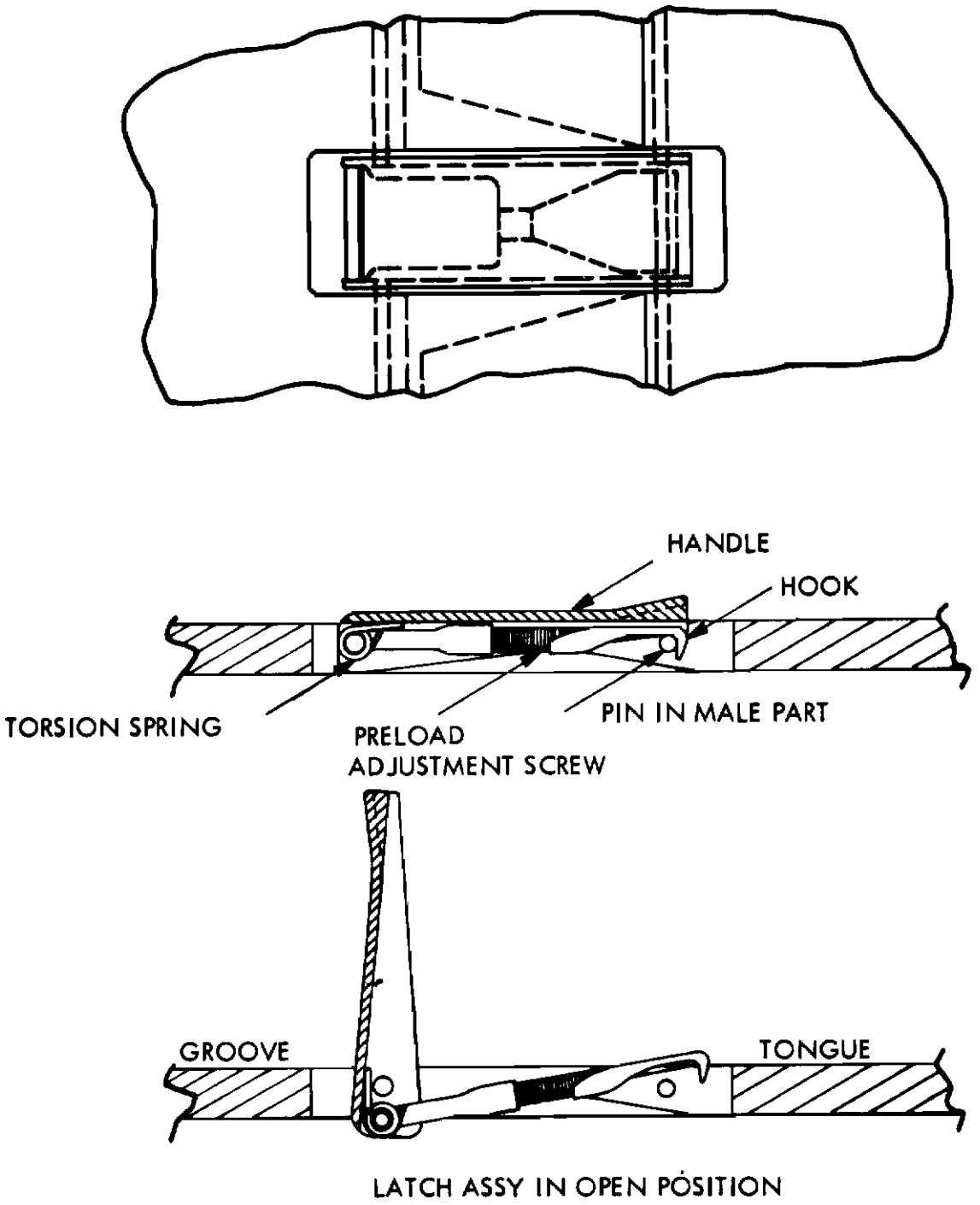

Figure 5-11. Trunk-Latch Joint

Table 5-1

PANEL ATTACHMENT TRADE-OFF CHART

Mechanism	Tension and Compression	Bending Stiffness	Stacking Efficiency	Astronaut Operation	Attachment Complexity
Latch Detent	1	1	1	4	6
Spring Latch	3	1	2	3	4
Spring Clips	2	1	2	1	1
Hook Latch	1	1	1	5	5
Cam Latch	1	1	3	5	5
Wedge Latch	1	1	3	5	5
Trunk Latch	1	1	3	3	5

Based on these studies, a tongue and groove design incorporating spring slips was selected and a prototype mock-up of the original joint design was fabricated and tested for mechanical concept and human factors considerations. The operation of this prototype panel assembly was judged to be very good and easily within the capabilities of a pressure-suited astronaut.

Demonstration of this joint model is shown in three successive stages of engagement in Figure 5-12. In the first stage the tongues are inserted between the spring clips on the groove assembly. The joint clearances are such that three such joints may be partially engaged simultaneously. Successive engagement causes the tongues to align themselves in the vee grooves until the spring clips fall into the detents provided on the tongue members. At this point the joint should be fully engaged as seen in the bottom photograph of Figure 5-12.

This method of panel attachment was also tried on the zero-buoyancy test parabola. It was observed during the first neutral buoyancy tests that some difficulty was encountered in engaging a panel joint which required sufficient force to preload the mating joint pair. In this design a 2 or 3-pound force was used to firmly seat the male and female joint components until the spring clip on the female fastener would snap into a groove

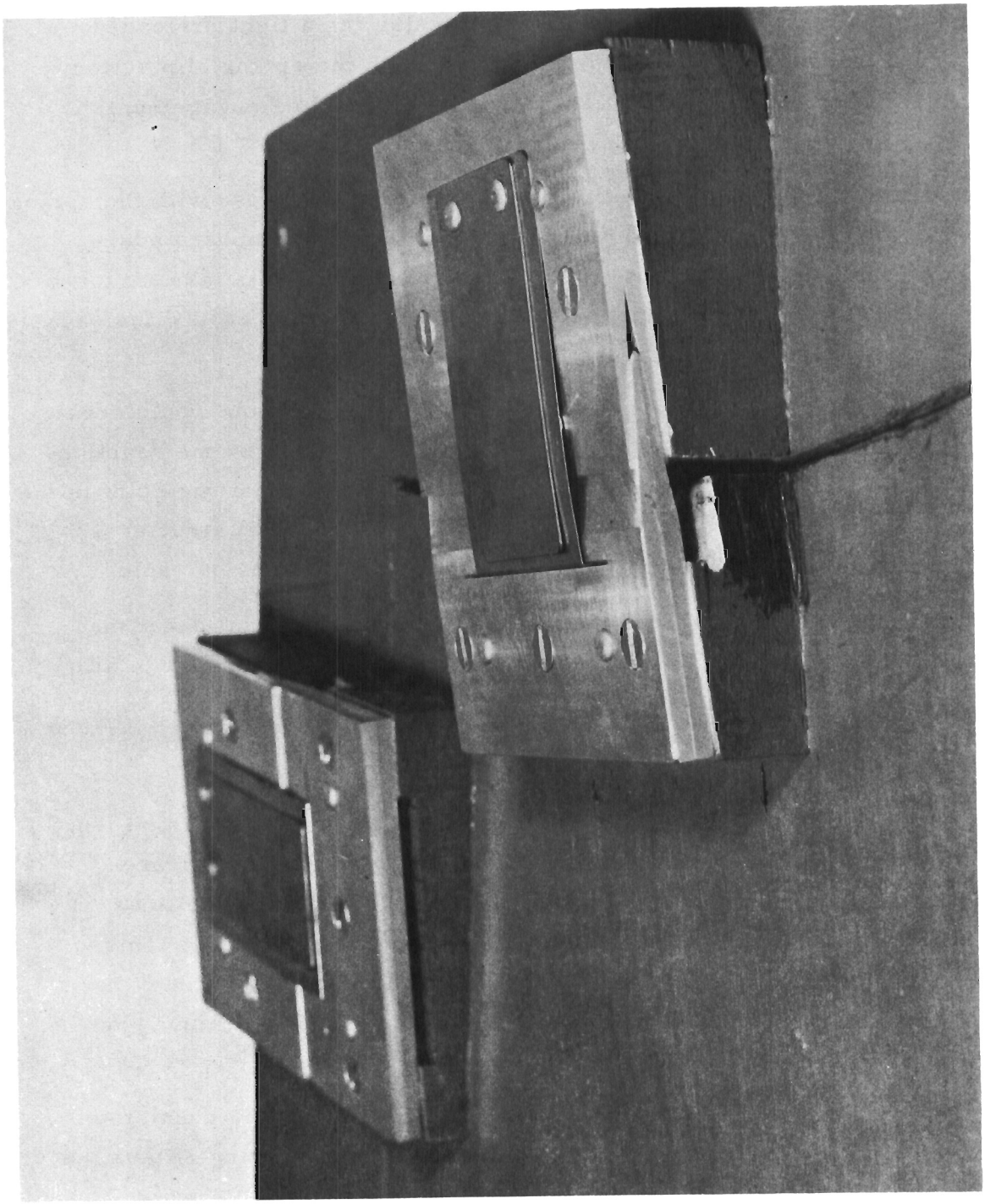

965/028

Figure 5-12. Preliminary Joint Mock-Up

provided on the male fastener, therefore, maintaining a tight preloaded joint. It was subsequently concluded that, although the spring slip action was required to prevent the panel from drifting away after engagement, it did not have to apply or retain a preload force.

Most of the latching mechanisms considered for use with the spring clip to provide take-up added complexity to the design or imposed additional workload on the astronaut. It was determined that this take-up force could be obtained by adding a circumferential tension cable around the back convex surface after the panel were assembled.

Analysis has shown that such a simple tension cable would create a compression preload on each joint in the entire structure by the reaction vectors on the curved surface at each joint. This is an important point in the structural concept, in that final contour accuracy and overall structural rigidity will be obtained with the final installation of this tension cable.

It has been recognized that, although each individual panel may possess a precise contour, a gradual accumulation of tolerance could allow the overall parabola to become slightly "out-of-round." This is an inherent problem with any large curved surface, and is not unique to the modular design. The circularity accuracy can be accomplished by a series or radially oriented wires or thin cables of precisely the same length, which attach at the outer rim of the finished parabola modules and are brought together at the center string or feed horn. Each of these lines may be adjusted in tension to bring the overall structure into "round." This feature is not a design requirement for the modular antenna, but may be considered as an additional device which can be exploited to achieve even greater surface accuracies.

The final joint configuration, shown in Figure 5-13, consists of the tapered wedge tongue and groove halves with a single spring clip on the back surface.

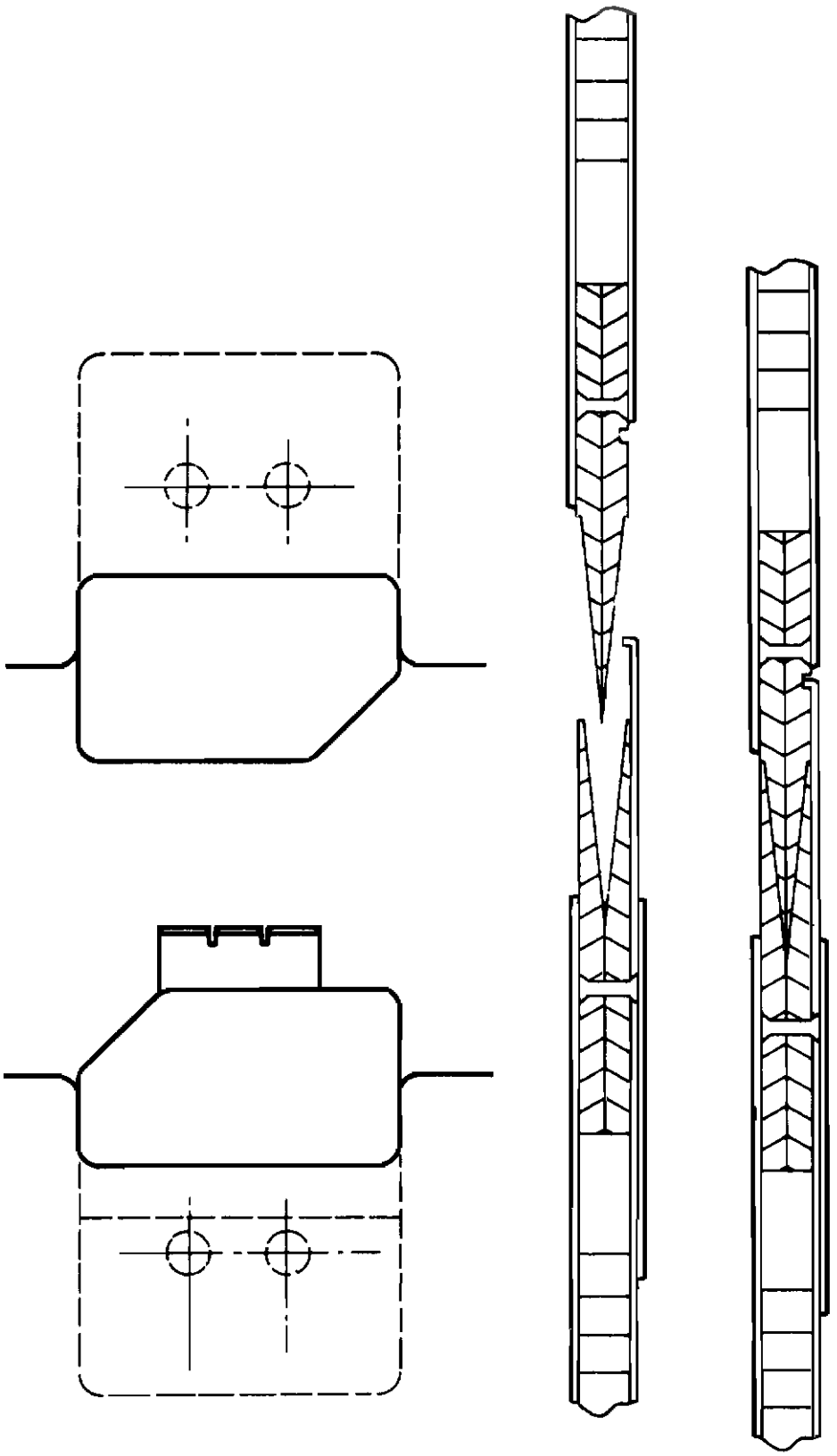

Figure 5-13. Final Joint Configuration

5.2.3.1 TRUNK-LATCH JOINT

Additional study of the tolerance take-up problem led to consideration of a concept utilizing the snap-together feature of the spring clip and a positive tightening device. The basic design shown in Figure 5-11 consists of a trunk-latch type device. A torsion spring is utilized to hold the latch handle up and the hook down. As the panels are brought together, the spring-loaded hook snaps over a pin in a manner similar to the spring clip for temporary restraint of the panels. Actuation of the cam-actuating handle by the astronaut tightens and preloads the joint to eliminate assembly tolerances.

To determine the feasibility of this concept, modification of an existing joint mock-up was made to incorporate commercially available latch assemblies. The parts were modified to accept the latch assembly in the female part and an engagement pin in the male part. The latch assembly was modified by removing the mounting bracket and by the addition of the torsion spring. Three of these latch joints were mounted on a panel and joint engagement tests were made. During joint engagement operation, several problems became evident:

a. Preload in the latch causes spreading of the tapered joint, thereby causing a loose joint. This spreading may be avoided by proper preload adjustment, by incorporating a stop in the joint, or by reinforcement of the joint.

b. Panel distortion resulted when the joints were not centered due to the inability of the joint to slide and self-center, compounded by too much slack in the take-up mechanism. A self-centering device with a much smaller take-up travel can be employed to eliminate this problem.

c. The hook of the latch assembly tended to rotate. This problem can be eliminated by inserting a pin through the hook at the time of preload adjustment.

d. This commercial latch assembly did not have sufficient over-center travel to permit the proper size torsion spring to be installed. The torsion spring which held the hook and lever apart had to be weak in order not to impose an unlatching force on the lever. At the same time the weak spring did not exert enough force to keep the hook against

the panel, causing difficulty in engagement. Proper design will eliminate this problem.

The results of this study indicate that a latch of this type, properly designed, will meet the mechanical requirements for joining the modular panels but will require that the astronaut reach out and manipulate each fastener. These results were correlated with the information received from use of a bolt-rope on the General Electric zero-buoyancy model and supplemental analysis. A determination was then made that the most efficient type of joint-tightening mechanism would be the simple spring clip on the tongue and groove joint, supplemented by a bolt-rope for the required joint payload.

5.2.3.2 TOLERANCE AND FABRICATION TECHNIQUE STUDY

Investigation of the effect of manufacturing tolerances of parabola surface accuracy indicates that a high degree of precision will be required during the fabrication of panels and joints. The problem will be compounded by any final assembly tolerances (looseness in the joints) and by thermal deflections.

An attempt was made to determine the tolerance requirements. No definite answer has been obtained because of the complexity of analyzing the effect of two-dimensional tolerances of the individual panels. The effect of edge support of the adjacent panels and the deflections of the joints must be taken into account. The amount of distortion is difficult to predict analytically and must therefore be verified on actual hardware which is built to close tolerances. Special fabrication techniques were investigated to determine the most efficient method to minimize fabrication tolerances.

5.3 HUMAN FACTORS EVALUATION

During the program human factors were continually considered in the conceptual studies and design of the prefabricated modular parabola. The resulting design concept was subsequently evaluated experimentally through a subcontract. The design considerations and the experimental program are presented in the following sections.

5.3.1 HUMAN FACTORS CONSIDERATIONS

As the experiment is planned to be flown on a manned space laboratory, the conceptual studies were directed to optimize the man and experiment system. Preliminary analysis indicated that a totally automated erection procedure would significantly increase the experiment weight, volume, mechanical complexity, and vehicle integration requirements, and would reduce the packaging and installation flexibility.

The design criteria were initially formulated as "objectives" rather than finite restraints. These human factor objectives to reflect scalability for the assembly of a modular 10-foot-diameter parabola were:

a. Maximize astronaut safety.

b. Limit EVA assembly task time to one-half hour.

c. Avoid use of the AMU or other propulsion aids.

d. Eliminate or minimize the use of special tools.

e. Minimize the variety of specialized tasks and task training requirements.

f. Minimize or eliminate the use of loose parts such as fasteners, tools, etc.

g. Eliminate tasks that require precision psychomotor control.

h. Provide rigid torso restraint to facilitate application of forces and precision assembly task motion control.

i. Minimize assembly procedure complexities.

j. Minimize reach envelope requirements (from the neutral position).

k. Minimize the normal frequency and probability of inadvertent contacts with the structural assembly.

l. Minimize tasks that require good visual acuity.

m. Avoid tasks that require torsional load applications.

n. Minimize peak and average task effort levels and metabolic rates.

5.3.1.1 SCALING CONSIDERATIONS

Mission restraints impose further limitations and certain compromises on human factors experimental parameters. As the experiment is planned to demonstrate the capability to erect very large parabolas (up to 100 to 200 feet in diameter), the design concept must reflect the characteristics of large structures. These considerations are reflected in various aspects of the design studies now in work. For example, the astronaut can probably easily manipulate modular panels up to at least 3 by 6 feet in size, which would permit the assembly of a 10-foot-diameter illuminator from a single annular ring of 10 panels. However, larger illuminators would require two or more annular rings of modules with the associated assembly problems. Therefore, the configurations studied were selected to demonstrate the characteristics and tasks representative of very large, as well as small, diameter structures.

The relatively small (24 x 30 inches) modules shown in Figure 5-2 would permit the astronaut to reach any corner of the panel to actuate a fastener or make other adjustments while restrained by a work station. However, the previously stated restraints require that the astronaut not leave his restrained work station to accomplish such tasks on large modules; therefore, the design objective in this experiment is to permit the astronaut to accomplish the assembly tasks from a fixed work station, in a manner adaptable to large modules.

5.3.1.2 HAZARDS AND FATIGUE

Astronaut safety is an overriding consideration in all design studies. Safety factors include EVA task time, task fatigue and psychological stress, span-of-attention demands, ancillary equipment or subsystem failures, work illumination, locomotion aids, etc. To be conservative, the design objective has assumed that the actual EVA assembly time will not exceed 30 minutes for one astronaut, and maximum applied forces will be less than 5 pounds. Tasks that require torsional loads will be avoided, as will tasks that require tactual discrimination such as adjusting small screw-type fasteners.

To minimize the fatigue factor, LSS demands, and crew hazards, the assembly tasks will be limited to peak metabolic work rates of less than 600 BTU/hour (light work). If the AMU and/or portable life support system (PLSS) is required, these inertial masses will also increase fatigue rates, obstruct vision, reduce mobility, and increase total task time as related to recharging of the PLSS and AMU. The tasks are planned to permit the use of an umbilical for the LSS and safety line. The fixed work station, in conjunction with provisions to rotate the parabola assembly to accommodate the astronaut tasks, obviates the need for an AMU or other propulsion device.

5.3.1.3 TOOLS AND FASTENERS

Special tools, including zero-reaction tools, have been considered for use in these assembly procedures. In general, power tools are loose equipment that require tethering and additional power. Tools create an added task complexity to the astronaut and may be difficult to manipulate. The majority of the designs studied to date have not involved the use of power or manually operated tools, as they were not required to achieve the mechanical fastener requirements.

Only fastener designs have been considered that utilize a captive fastener. Shear type fasteners, such as bolts, have been avoided due to the high degree of visual acuity, visual orientation, and manual dexterity required to insert relatively small parts in close-tolerance holes. Simple push-pull actuated latches are preferred to rotary locks.

5.3.1.4 ASSEMBLY PROCEDURES

The early structural assembly concept illustrated in Figure 5-2 optimizes the human factors characteristics of this experiment, and also satisfies most of the structural, mechanical, and integration criteria. Each panel in each annular ring is interchangeable to avoid human errors and part coding. The panels are tethered in the canister within easy reach of the astronaut. (The canister position shown would require excessive rotation of the torso and therefore will be relocated to a position within 45^{o} of the sagittal plan, for example, in front of the astronaut, waist high.)

As shown in Figure 5-14, the modules are grasped at the outer edge and installed in the assembly by a simple forward extension motion of the arms. The leaf spring latches are guided into place by the vee-shaped tongue-and-groove joint interfaces, thereby minimizing critical alignment procedural tasks. When fully engaged, the leaf springs snap into the locking detents. Safety catches similar to those on automobile door locks are featured by this concept to insure that the installed panels cannot drift away once the panel joints have been engaged. Other joint designs which are similar in assembly task definition were considered.

Assembly forces were measured in the experimental observations. Tests of the simulated panels indicate that these forces are less than 2 pounds.

After each module is installed, the astronaut manually rotates the assembly to the next module installation position. After the first annular row is assembled he repositions the boom to move the periphery 30 inches further away to facilitate the next sequence of modular installations.

Note that the astronaut-restraint mechanism and canister location depicted in this preliminary concept were modified and improved as a result of the subsequent experimental program.

5.3.1.5 WORK AREA ILLUMINATION

The illustration (Figure 5-2) of the assembly tasks shows the parabola with the reflective surface in the view of the astronaut. As this surface would be essentially invisible, it is probably desirable to rotate the assembly so that the astronaut is looking at the diffused rear surface of the structure. One or more small floodlights will be required to provide diffused lighting to enhance contour definition and depth perception. Reflective surfaces may also be employed advantageously to provide "fill" lighting at a minimum of total lamp power output. As the aluminized astronaut suit will reflect a large amount of scattered light, it is probable that only one floodlight will be required. Diffused reflective surfaces or coatings on the visible rear surface of the assembly will also assist to provide noncollinated work illumination and reduce contrast. As the work position is relatively fixed and localized, these illumination provisions should be very minimal.

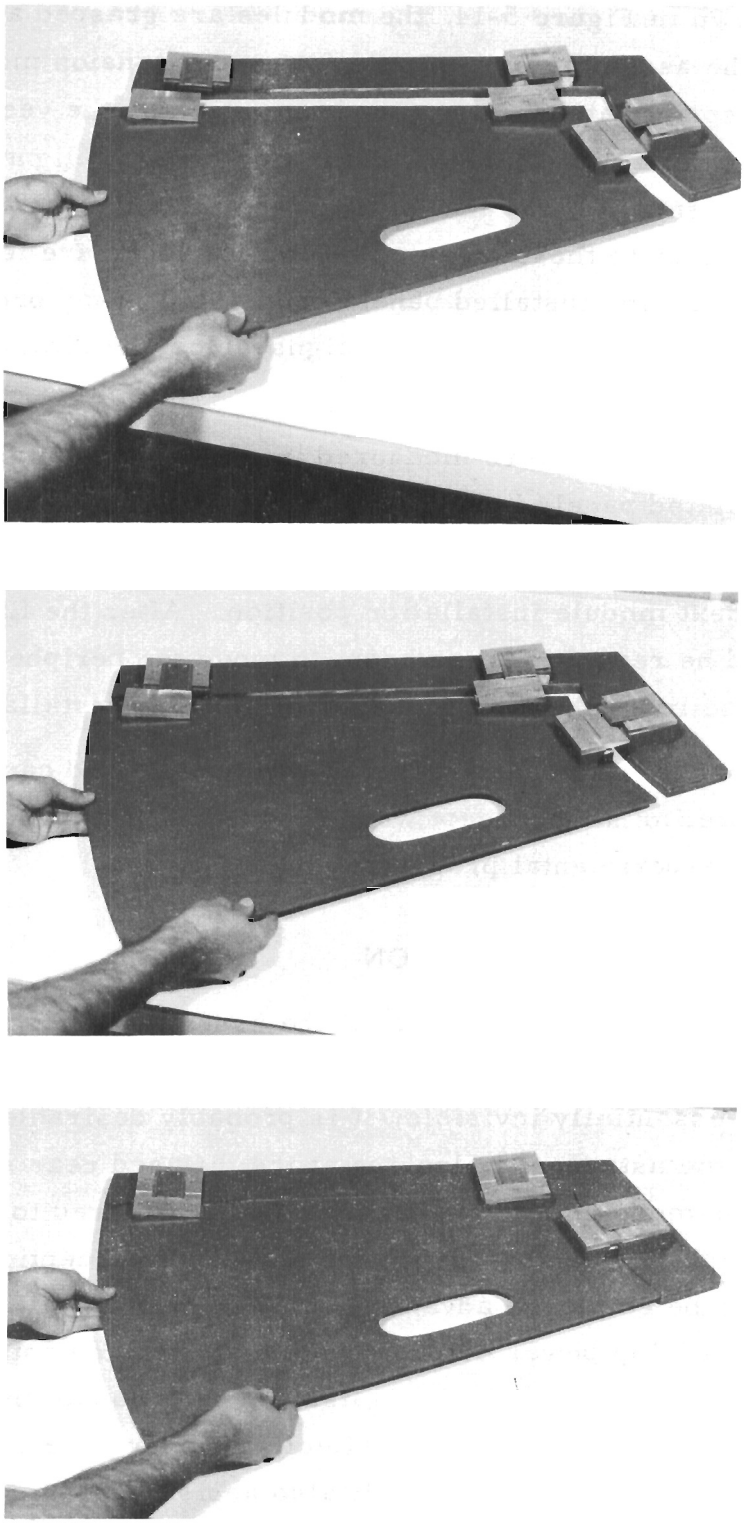

Figure 5-14. Parabola Panel and Joint Mock-Up

5.3.1.6 FIGURE CONTROL

It is anticipated that the present design approach will produce a manually assembled parabola with a contour accuracy equal to or better than that required for this system. However, the modular design concept may potentially permit the erection of highly accurate mirrors approaching the accuracy of optical surfaces. To realize this degree of contour, control devices must be incorporated that will permit adjustment of each modular panel to compensate for contour deviations caused by tolerance accumulations in the intermodular joints. If subsequent system analysis indicates that this additional contour accuracy is desired, the required geometrical surface control may be accomplished by the astronaut as discussed below.

Several methods to "figure" (adjust the contour) have been investigated. In general, a wire attached to each panel will be led radially to the sting or hub adjustment mechanism.

To figure the parabola, the astronaut will view the reflective surface through an optical device at the mean radius of curvature of the parabola. By observation of a reflected target pattern, the astronaut could determine which figure control wires must be adjusted to correct contour deviations. This technique of alignment is of course dependent on a mirror finish surface and would have to be modified to be applicable to non specular surfaces of antennae.

5.3.2 NEUTRAL BUOYANCY TEST PROGRAM

A zero-buoyancy mock-up of a simulated parabola was fabricated by the General Electric Company, based on the Space-General configuration, under subcontract to SGC, and preliminary tank testing was begun on 31 March 1966.

The simulated parabolic modules were fabricated from polypropylene plastic which has a specific gravity of 0.95 and is slightly positive-buoyant in water. The 0.22-inch-thick panels were milled in a grid frame pattern to minimize the panel area and underwater drag, as shown in Figure 5-15. The interpanel spring-lock snap fasteners shown in Figure 5-16 were constructed of aluminum alloy wedges and stainless steel spring

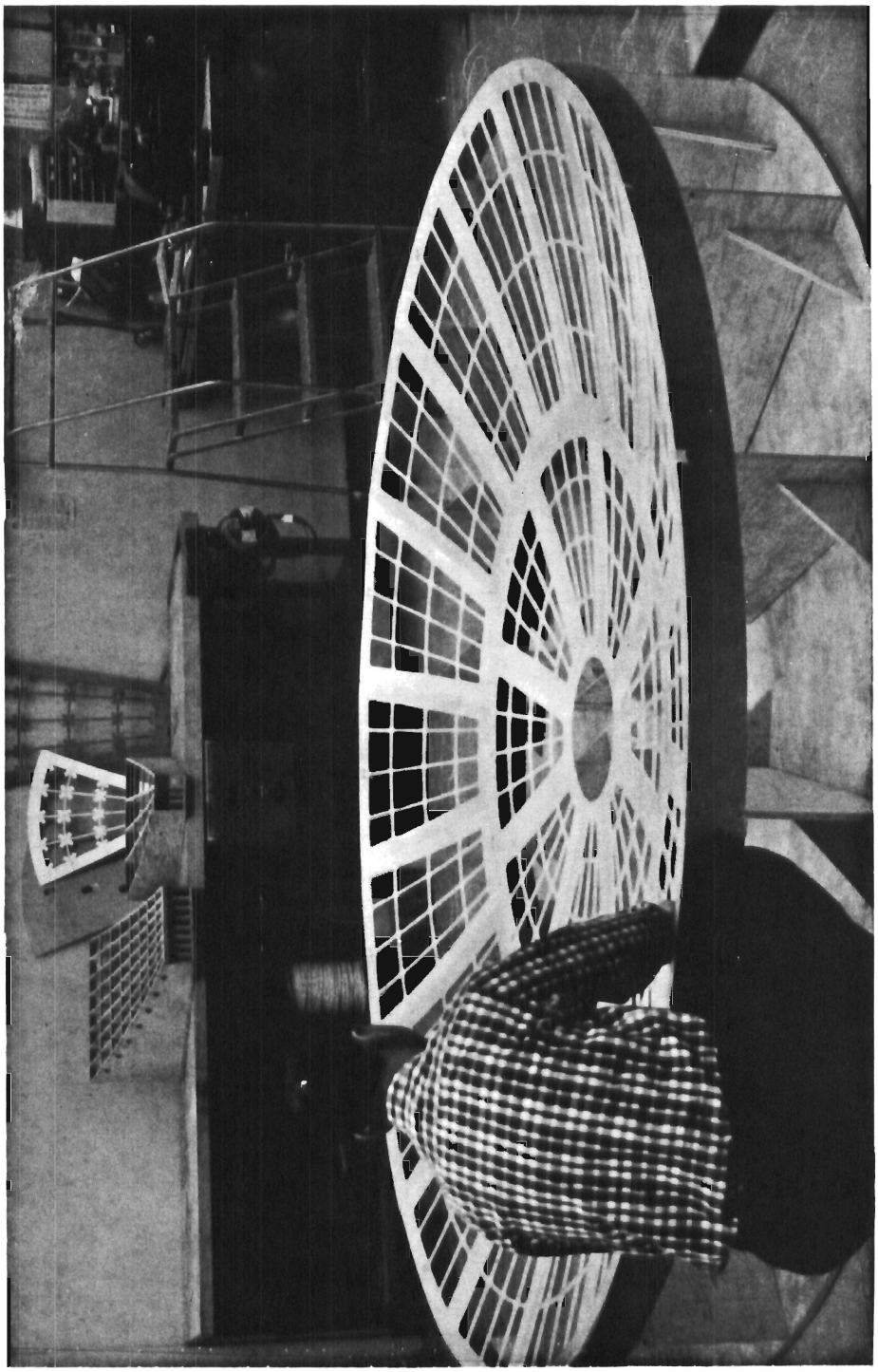

SGC/919

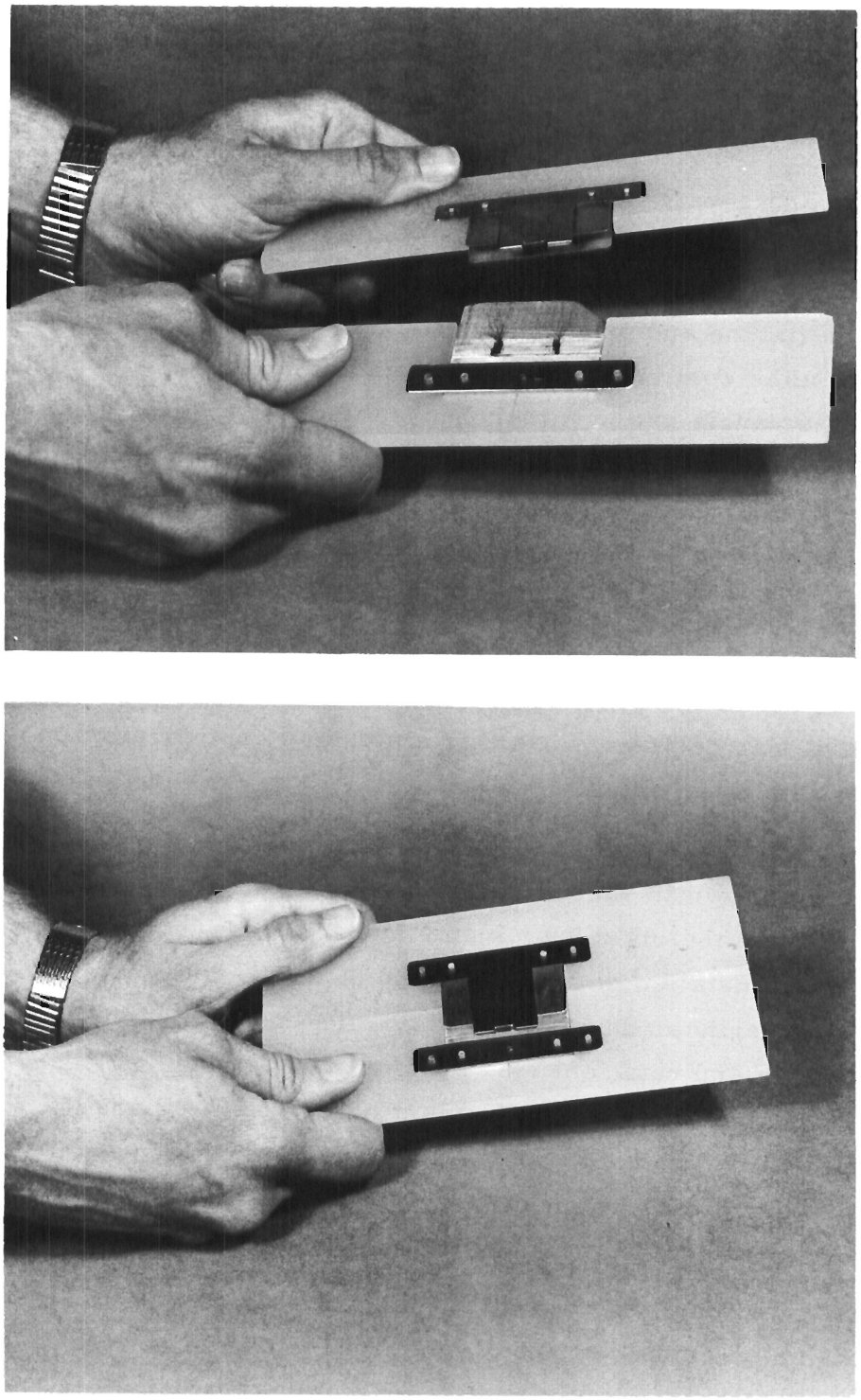

Figure 5-16. Typical Panel Joint Used on Zero-Buoyant Modular Parabola

sheet stock and were riveted to the plastic modular panels. With the additional weight of these metal fasteners the panel subassemblies were zero-buoyant.

The panels were heated and formed to contour. Due to the relatively poor dimensional stability of the plastic, the final panel contour was accurate to only approximately $\pm$ 0.1 inch. However, the fasteners were installed on assembly in the fixture and produce a relatively high accuracy of fitting interfaces. To minimize cost, no attempt was made to match-drill the fasteners and therefore the panels are not interchangeable. No attempt was made to simulate the rigidity of the flight article as prohibitive costs and schedule delays would have been incurred; therefore, the simulated panels are estimated to be considerably more flexible than the flight article hardware will be.

Joint specimen tests indicated that a leaf spring lock on only one side of the wedge fitting was sufficient to provide a tight, secure joint. As the primary purpose of this leaf spring lock is to retain the panels in position during assembly, it was decided to use this simplified configuration rather than dual leaf spring locks as originally planned.

A sketch of the underwater test fixture utilized for the zero buoyancy tests is shown in Figure 5-17. The 2.0-inch-diameter, 7.0-foot-long boom supported the rigid illuminator hub and was hinged at both ends. Strain gages were installed on the lower end of the boom to measure loads imposed by the test engineer during assembly. The boom and hub positions are controlled (in pitch and rotation) by a system of ropes, spring-loaded detent locks, and jam cleats to permit adjustment of attitude by the test engineer from the work station "control panel." The operational system attitude will be electrically controlled, which will greatly simplify this task and significantly reduce assembly time.

The illuminator lamp sting was designed with a thread-end connection rather than a quick disconnect bayonet type fitting utilized on the operational design. As the underwater test tank is only approximately eleven feet deep, the upper end of the sting projects above the surface of the water; also the upper edge of the outer annulus is just below the water surface in certain positions during the test. The surface wave action, as well as underwater

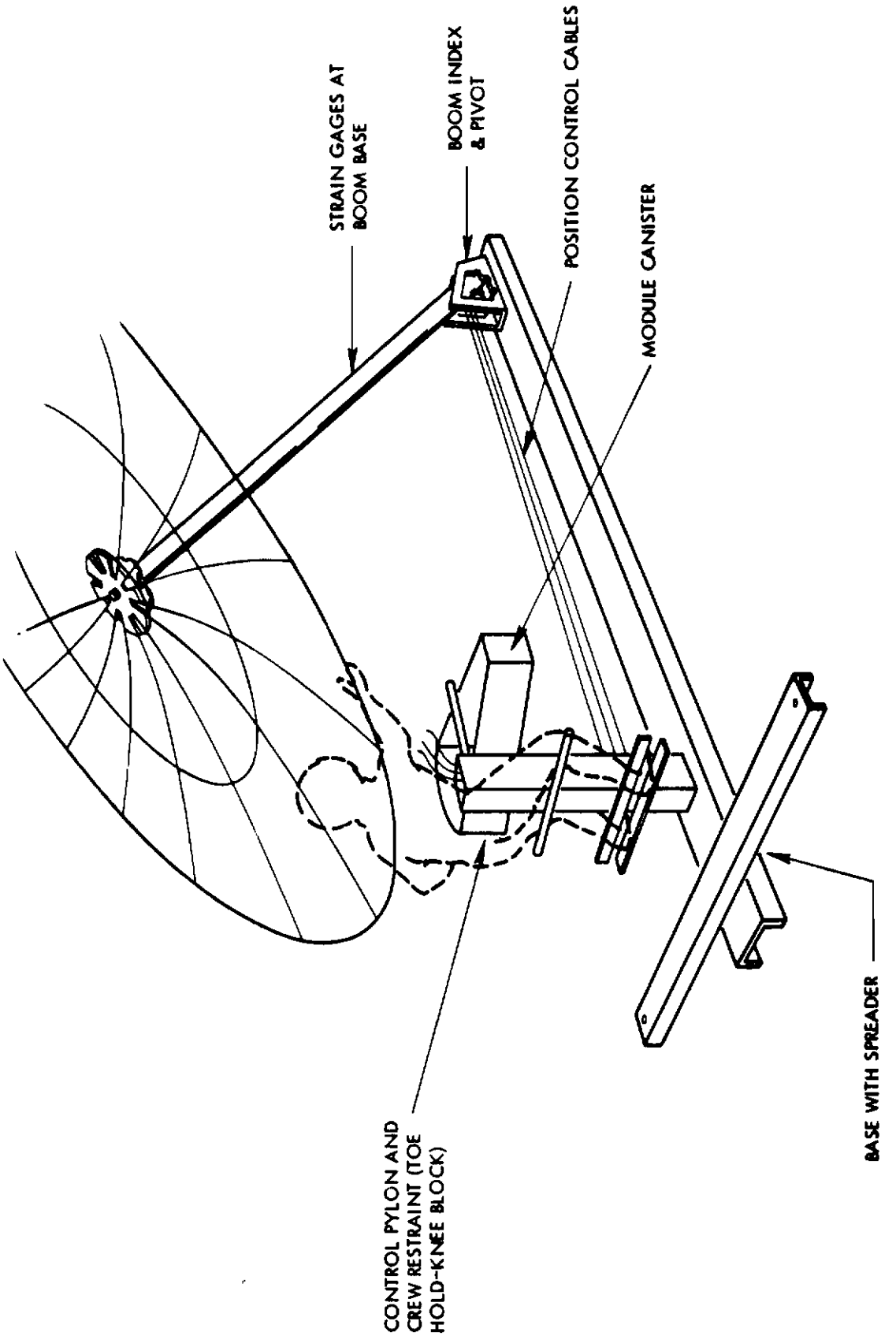

Figure 5-17. Sketch of Work Station for Test of Zero-Buoyant Modular Parabola

pressure waves, causes some oscillatory deflections of the parabolic structure during assembly as can be seen in the motion pictures of the test procedure.

A shake-down test was run by General Electric personnel on 31 March to debug the test equipment and test procedures. On 4 April the first complete test of the simulated structure assembly was conducted by a test engineer in a standard skin diver's wet suit. SCUBA gear was not used as neutral buoyancy cannot be maintained; rather an umbilical air supply line to the mouthpiece was used in all tests. The test rig was designed to permit progressive assembly of the modules with the convex surface facing "up" relative to the test engineer. This arrangement is undesirable for the assembly of specular reflective mirror modules in space as the surface would be essentially invisible in the orbital lighting conditions, but will present no such problem to antennas with nonspecular surfaces. Also, the leaf spring locks and detents were on the convex side of the modules and not visible to the test subject.

The test engineer work station was designed as shown in Figure 5-17 to provide restraint frustum points at the feet, knees, and lower torso. The restraint system provided excellent freedom on lateral and rotational motion but somewhat restricted forward reaching motions of the upper torso. The "astronaut" (test engineer) was able to maintain excellent psychomotor control and apply relatively large forces in all axes as required (these observations also apply in general to later tests in the MK-IV pressure suit).

The modular panels were stowed in a canister attached to the forward upper part of the astronaut restraint fixture. A bungee-restrained bar across the center of the canister held the panels in place and permitted easy access and removal of the panels.

Earl Blackwell, SGC Project Engineer, was provided with SCUBA gear and experimented with the underwater assembly task. He noted that when body motions were kept slow and deliberate, the presence of the water became secondary and one could get the "feel" of a simulated zero-g task. For the most part, all operations were quite effortless and the structure could be assembled with ease. The panel joints engaged very easily and

would latch with a force estimated at 1 to 5 pounds, which could be supplied by bumping with the heel of the hand or a gentle push, as the work station provided sufficient restraint to react all required forces. The polypropylene panels were quite flexible but maintained their contour even under considerable load.

The first assembly test conducted by General Electric personnel was very successful and required an average of only 15 seconds for the installation of each inner-annulus panel and 40 seconds for each outer-annulus panel. It was anticipated that difficulty would be experienced with the close-out panels in each annulus but this task was accomplished smoothly in approximately 60 seconds. The sting installed in the hub before the first annulus was complete offered little potential test data due to the nonoperational method of the threaded installation provided. In practice, such a sting would be attached by a simple twist lock fitting in lieu of the threaded base. Figures 5-18 through 5-24 show selected sequence steps in the assembly task.

The bolt-rope required for installation around the outer periphery of the outer row of interpanel fasteners was not available for this test. Therefore, the assembled panels could not be drawn together snugly and rigidly as planned. However, the parabolic contour was more accurate and symmetrical, and the structure more rigid, than anticipated. The structure was disassembled and a second assembly test conducted with similar results.

On 5 April the "astronaut" donned an MK-IV USN pressure suit with an umbilical air supply line. To achieve zero buoyancy and simulate the pressurized suit restraint, the suit was filled and pressurized with water to 1.5 psig over the water pressure (which approximates, by simulation, the mobility restraints of the new Apollo International Latex suit at 3.7 psig). The water-filled suit necessitated that a standard skin diver's face mask and air supply mouthpiece be worn inside the helmet, which significantly restricted the "astronaut's" field of vision and head motions.

The task sequences were timed after the "astronaut" was in position in his work station. The task times compiled in Table 5-2 include (1) removal of the modular panel from the canister, (2) installation of the

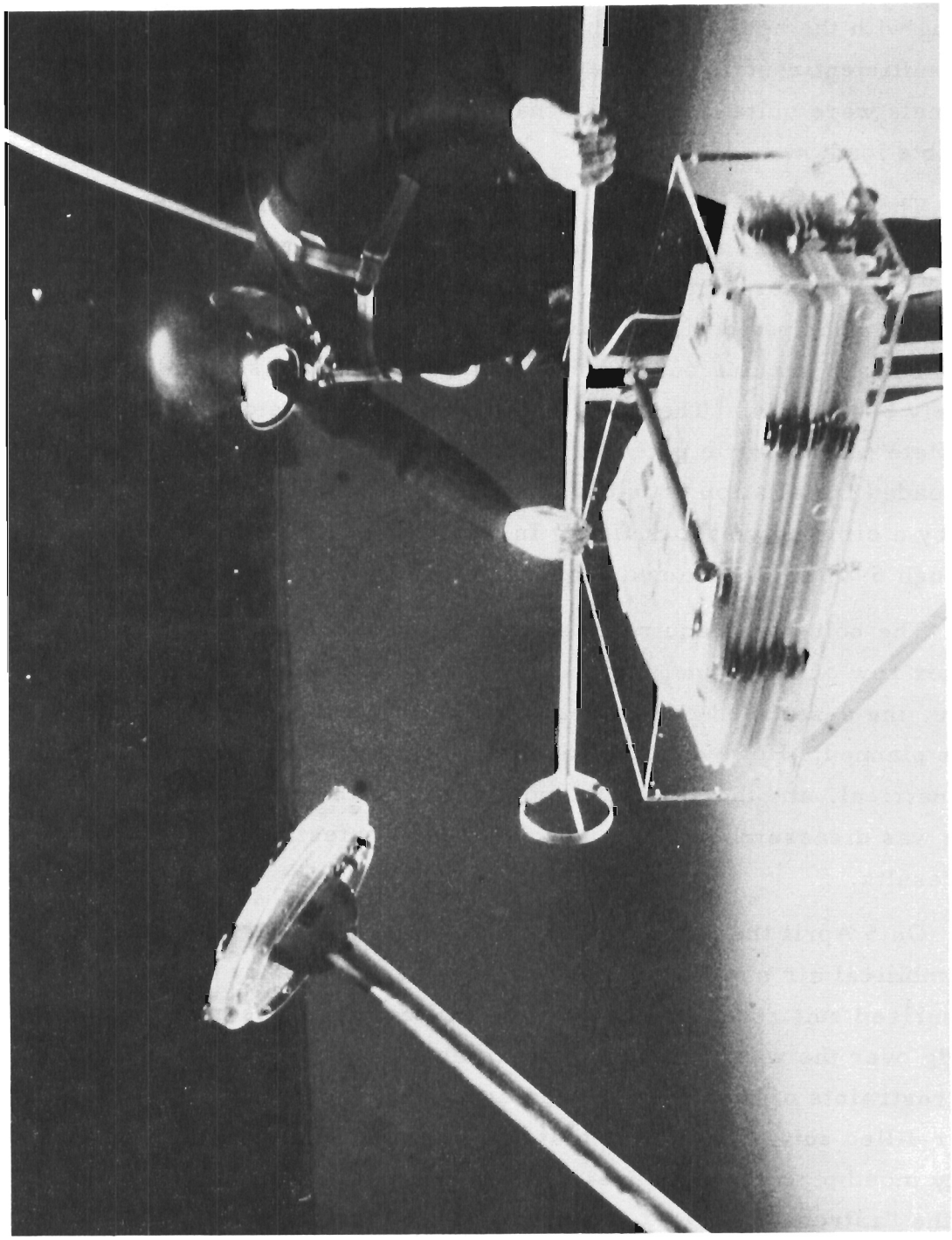

965/038

Figure 5-18. Test Engineer at Work Station

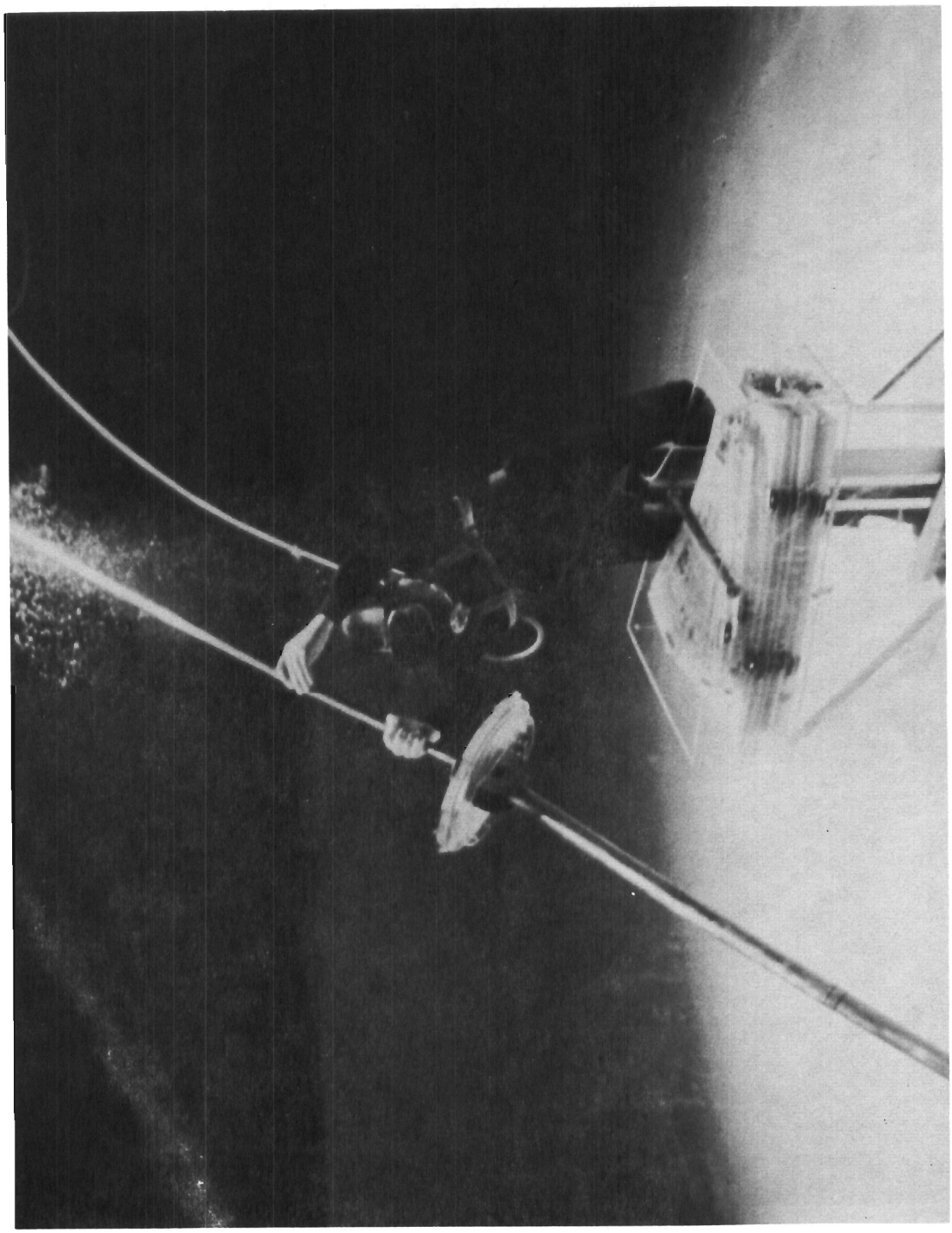

965/035

Figure 5-19. Installation of Sting

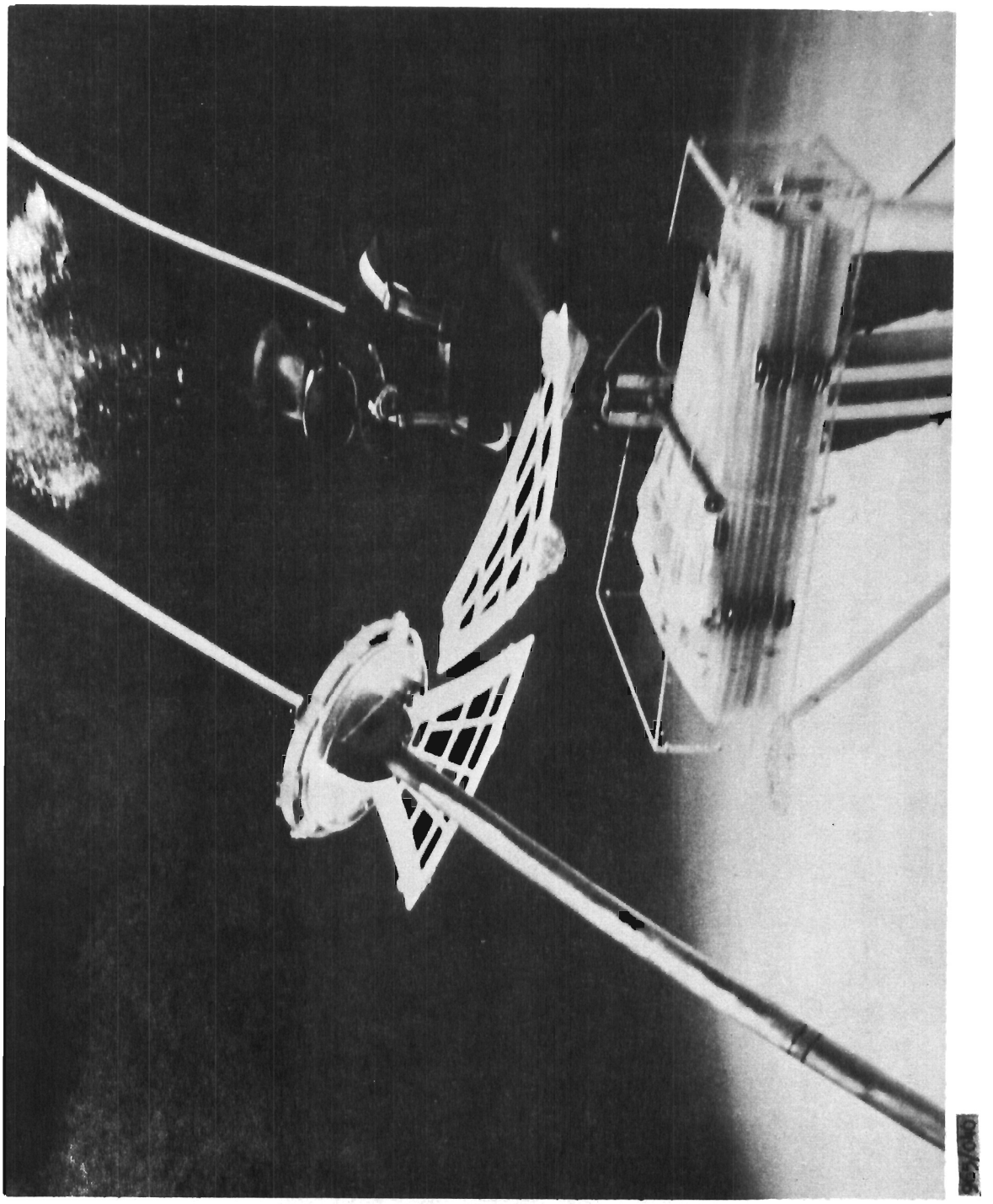

Figure 5-20. Beginning Assembly of First Annulus

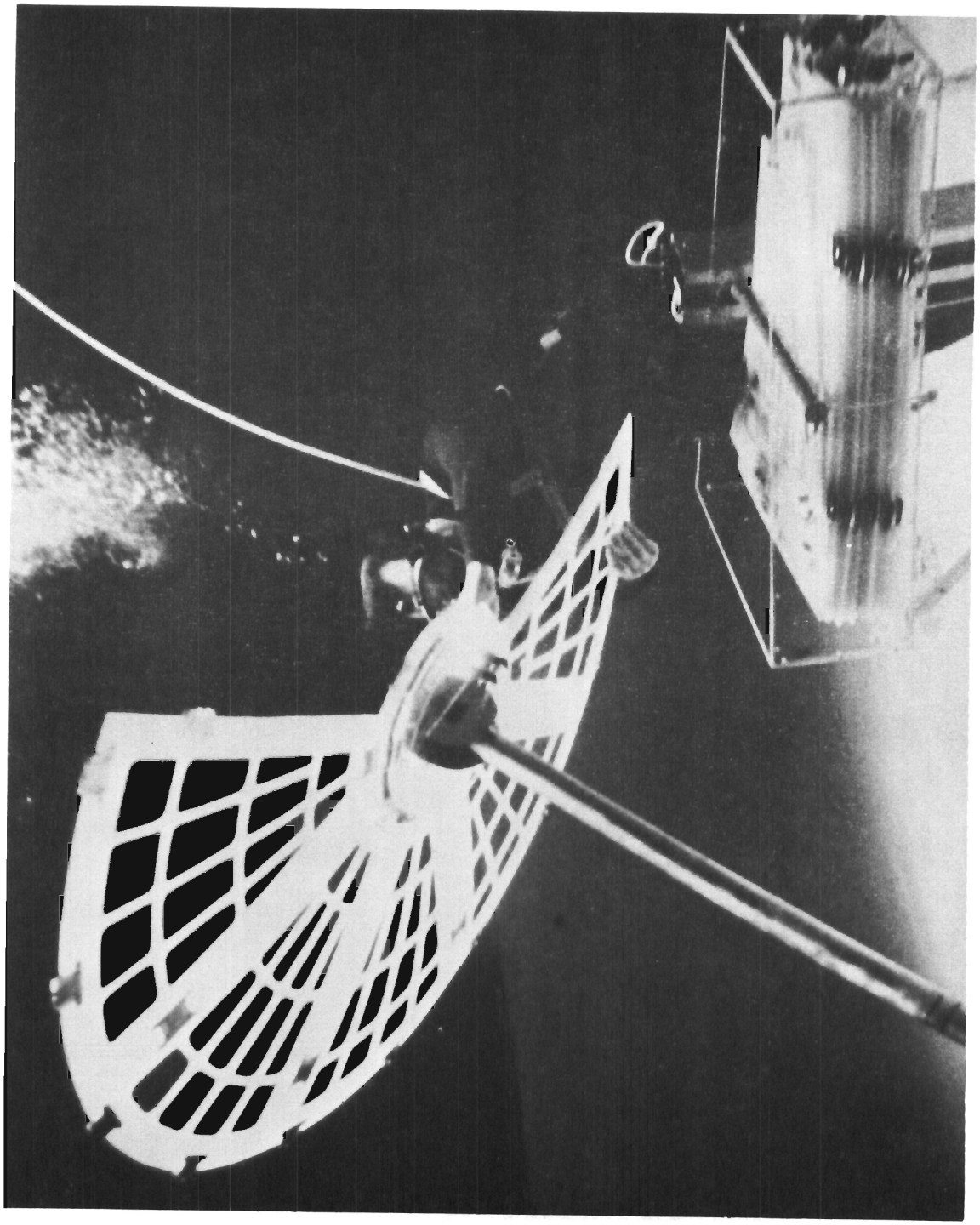

965/039

Figure 5-21. Near Completion of First Annulus

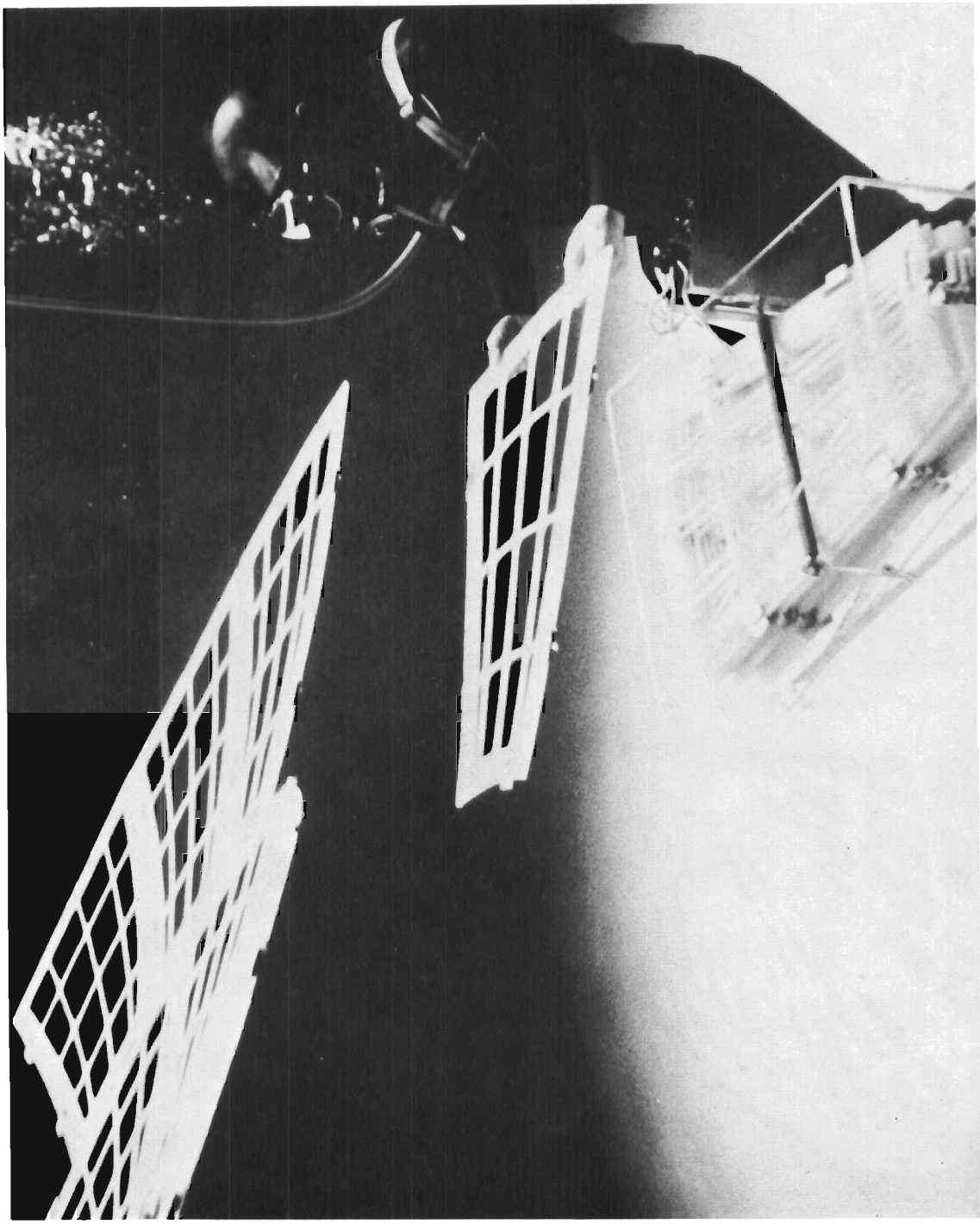

965/037

Figure 5-22. Beginning Assembly of Outer Annulus

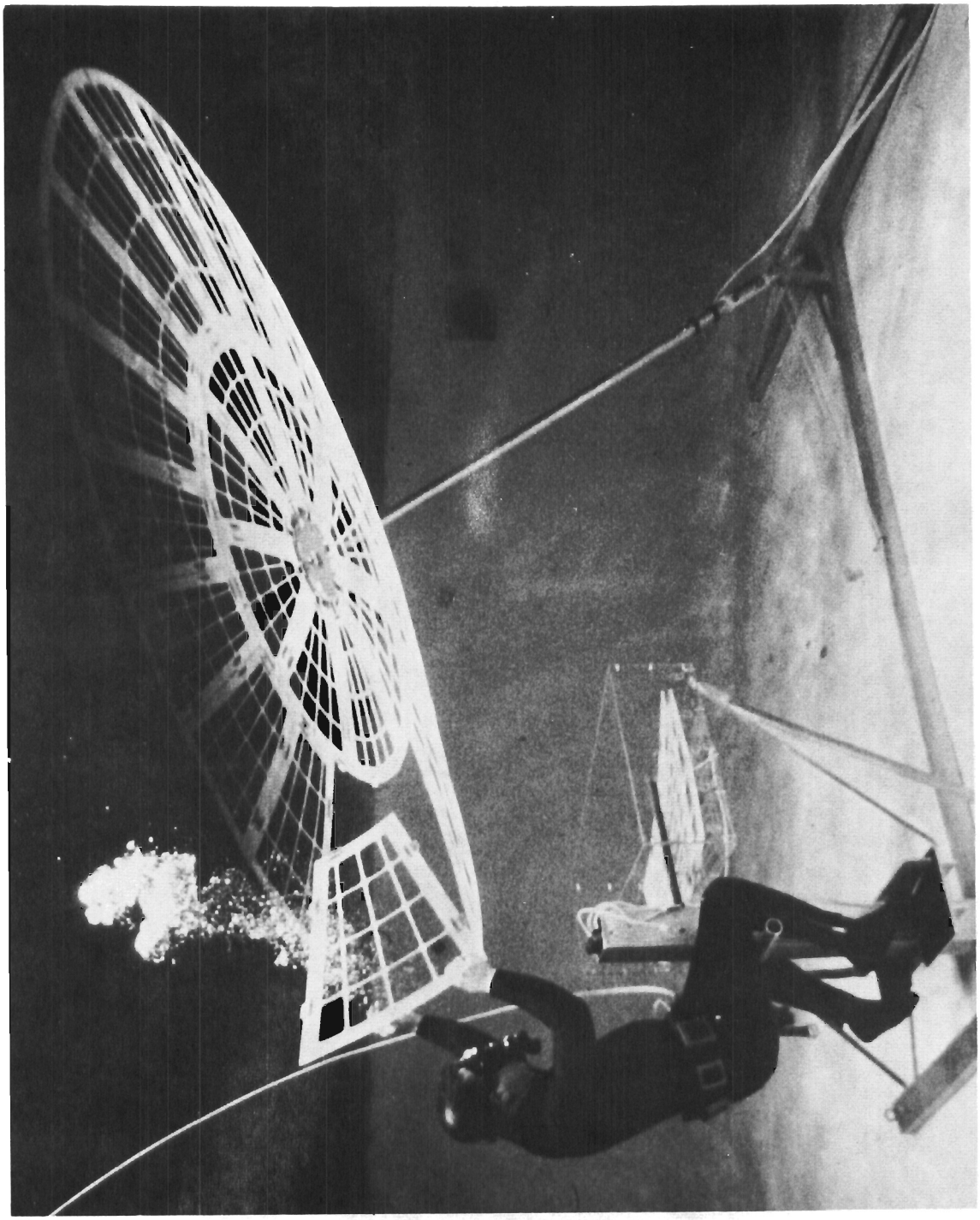

Figure 5-23. Near Completion of Outer Annulus

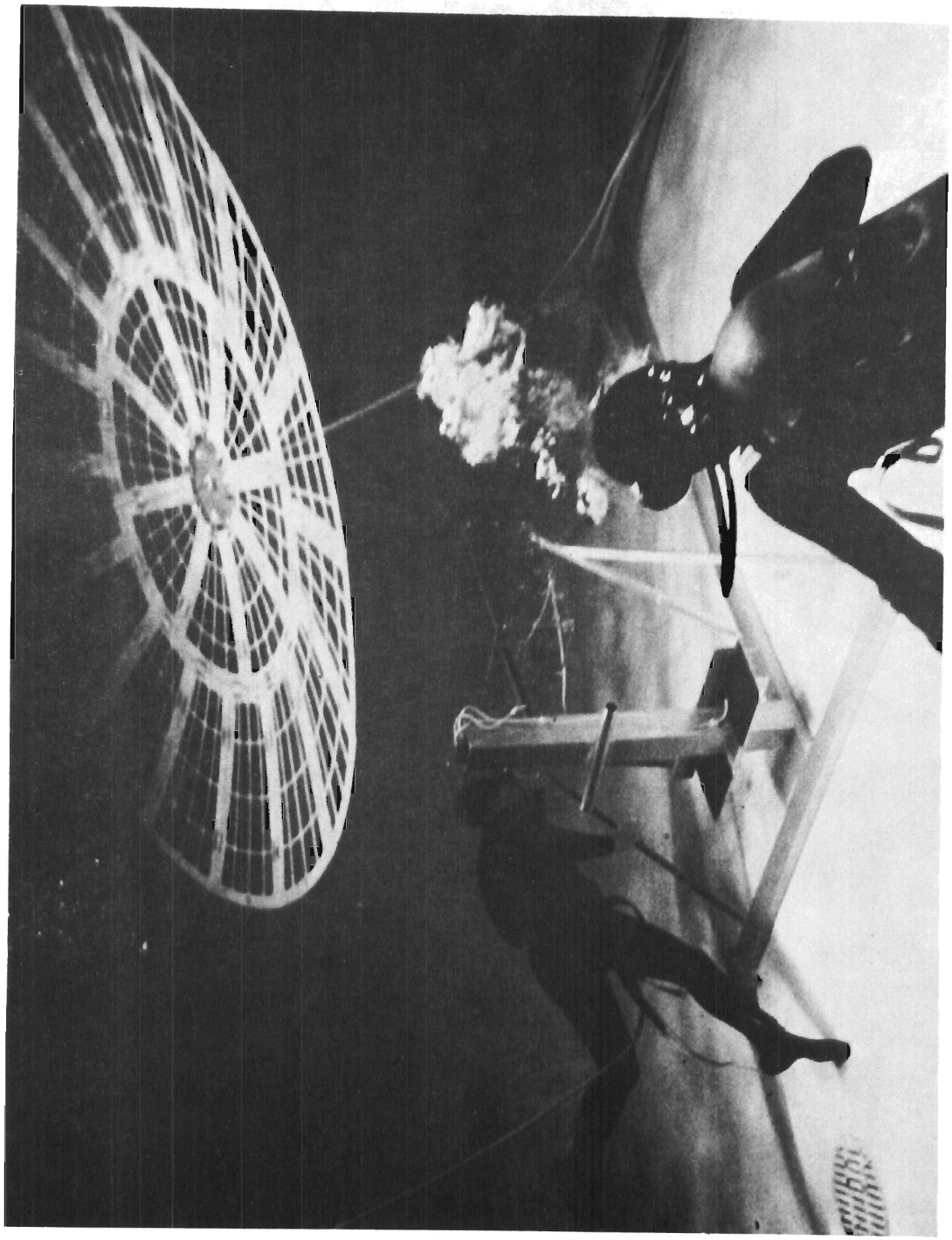

965/036

Figure 5-24. Completely Assembled Parabolic Structure

Table 5-2

ASSEMBLY TASK TIME STUDY

	Event	Time (secs) Elapsed	Incremental
Inner Annulus	Start	0	0
	Panel #1 installed	10	10
	#2	35	25
	#3	55	20
	#4	70	15
	#5	95	25
	#6	115	20
	#7	133	18
	#8 (closure)	178	45
	Readjust Boom Position	245	67
Outer Annulus	Panel #9 installed	258	13
	#10	286	28
	#11	318	32
	#12	350	30
	#13	380	30
	#14	398	18
	#15	421	23
	#16	445	24
	#17	465	20
	#18	493	28
	#19	528	35
	#20	573	45
	#21	600	27
	#22	622	22
	#23	640	18
	#24 (closure)	700	60
	Total Time = $11^{m}\ 40^{s}$		

panel in the structure, (3) visual or tactual inspection to determine if the spring leaf lock engaged in the detent, (4) release of the cleated rope to release the hub rotary lock mechanism, (5) rotation of the parabolic structure to the next work position, and (6) cleating the hub rotary lock control rope.

Rotation of the structure for each panel installation required 3.0 to 5.0 seconds, or a total of approximately 88 seconds. Adjustment of the boom to reposition the structure after completion of the first annulus required 67.0 seconds. It is conservatively estimated that the pushbutton or toggle remote controls being designed for the flight article would reduce the rotation time from 88 seconds to 30 seconds and the boom repositioning time from 67 seconds to 10 seconds; therefore, the total adjusted task time would then be 585 seconds (or 9 minutes and 45 seconds).

The test engineer moved very slowly to avoid causing pressure waves through the water and to attempt to simulate the careful, deliberate motions of an astronaut during actual EVA tasks.

It is to be noted that this was the first attempt to assemble the structure using a pressurized suit. The inspection of the position of the fasteners frequently required the test engineer to leave his normal work position to look under the structure surface to inspect the spring locks, and the manual, rope-controlled rotation and boom positioning devices required excessive task time.

It is estimated that the bolt-rope installation should require less than two minutes, and the sting installation (properly designed) less than one minute, for a combined total assembly time of approximately 13 minutes after the astronaut is in position in the work station.

The following conclusions were obtained from the General Electric neutral buoyancy tests. These data were subsequently incorporated into the final design concepts to help optimize the experiment system design.

a. The assembly preliminary concept envisioned was proven to be easily within the capabilities of a zero-g encumbered, pressure-suited astronaut.

b. A work station restraint system concept was employed which was incorporated into the experiment system design.

c. The panel interconnect joint design was refined to optimize the man-machine relationship by:

(1) Using a bolt-rope about the rear surface of the parabola to provide the required seating and alignment forces for the tongue and groove joints,

(2) Using the spring clip, previously employed to maintain the engagement force, to provide only a captive latch when a panel joint was properly engaged.

d. The assembly task times were measured and found to be less than the original estimates.

e. The assembly task proved to exhibit a short learning curve which would simplify the astronaut training requirements.

5.4 EXPERIMENT SYSTEM DESIGN

Following the initial configuration studies, and in parallel with the Human Factors Evaluation Test Program, the experiment system was defined in further detail. The data presented in this section cover this work on the modular parabola and incorporate design improvement features identified in the test program.

The results are applicable to an experiment on an MSL-type vehicle or the Saturn SIVB SSESM. The SSESM requirement is different in only two principal aspects. The attached interface is different but in no significant way. The deployment method and the associated control requirements are the major difference. For the SSESM case, the boom and hub is deployed manually compared to a fully remote operation for the MSL case. The instrumentation and remote control are thereby less complex for the SSESM case. The integral control requirements at the work station are identical for both.

This report covers the more extensive controls requirement for the MSL-type application. Both applications were examined for the attachment and stowage requirements.

The configuration of the modular parabola experiment is shown in Figures 5-25 through 5-30.

5.4.1 PARABOLA ASSEMBLY

The completed parabola assembly, individual panels, panel attachment, and bolt-rope are shown in Figure 5-26. The assembly consists of 24 panels and a hub and bolt-rope tensioning device. In addition, an illuminator sting or a contour measurement device may be installed in the central hub. The hub is attached to a flange on the boom. Panel attachments are integral parts of the panels and hub.

The panels are assembled in two annular rings. The first ring of eight panels assembles to the hub and the second ring of 16 panels assembles outside of the first ring of panels. Each panel assembly and the hub assembly consists of an aluminum honeycomb panel into which are installed the tapered wedge joints. Because of the close tolerances required across the joint, special fabrication techniques will be employed for the detail parts and for the assembly and installation of the joint into the panel.

5.4.1.1 PANELS

The honeycomb panels will consist of (1) a 0.30-inch-thick core, 1/8 cell size, 0.0007 "5052 aluminum, and (2) stretch formed 0.004" 2024 aluminum faces bonded with a suitable adhesive such as Bloomingdale FM 1000. Cutouts for the joints are formed at the time the panels are fabricated (Figure 5-27). The edges of the joint cutouts and tooling holes will be potted for increased strength. The exposed panel edges will also be potted. Corfil 615 is one of the potting candidates. The core will be perforated to allow entrapped air inside of the core to bleed out during launch. In addition, a number of small holes will be drilled in the edging material of each edge surface of the panels to allow air to bleed out during launch.

Various honeycomb sandwich structure combinations were analyzed to optimize the weight/strength/deflection characteristics of the material. The results of this study are presented in Figure 5-31, where the

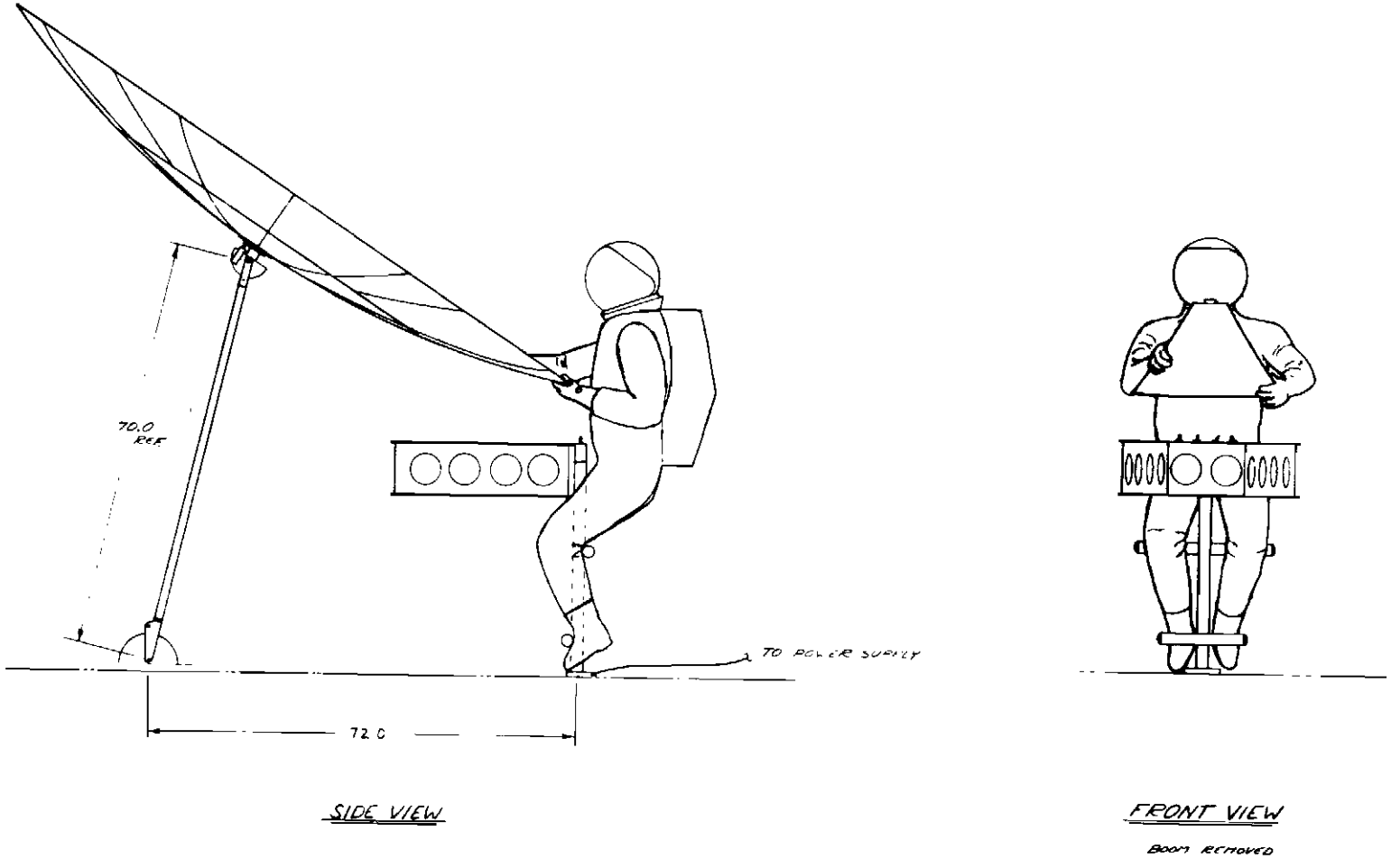

Figure 5-25. Parabola Installation Inside the SIVB

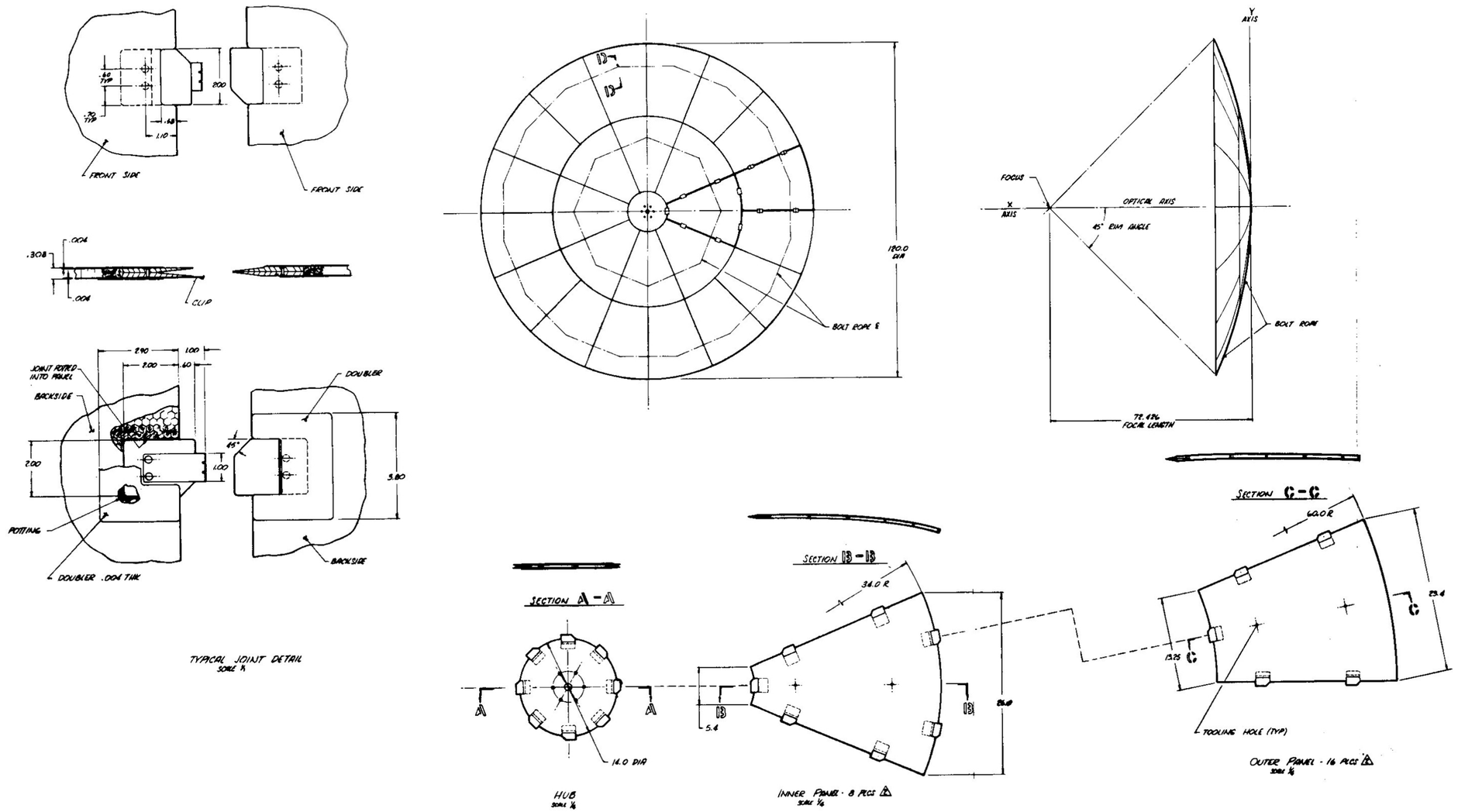

Figure 5-26. Parabola Assembly

NOTES:

1. THESE VIEWS ARE NOT PLOT PANELS
2. THE FRONT SURFACE IS DEFINED BY THE REVOLUTION OF THE PARABOLA: $Y^2 = 289.704X$ ABOUT THE X AXIS, WHERE X AND Y ARE IN INCHES

NOTES:

1. THE FRONT SURFACE IS DEFINED BY REVOLUTION OF THE PARABOLA $Y^2 = 288.796\ X$ ABOUT THE X AXIS, WHERE X AND Y ARE IN INCHES. THE PARABOLOID SHALL CONSIST OF 24 INDIVIDUAL ALUMINUM HONEYCOMB PANELS ARRANGED IN TWO CONCENTRIC ANNULAR RINGS.
2. EACH PANEL FRONT SURFACE SHALL CONFORM TO ITS SPECIFIED PORTION OF THE EQUATION $Y^2 = 288.796\ X$ WITHIN .005 INCHES TIR (TOTAL INDICATOR READING) AND THE LOCAL TANGENT ANGLE OF THE PANELS FRONT SURFACE CONTOUR SHALL NOT DEVIATE MORE THAN 7.5 MINUTES OF ARC OVER ANY 1.15 INCH DIMENSION FROM THE TRUE PARABOLIC CONTOUR. THE ACCURACY SHALL BE WITHIN THESE LIMITS OVER AT LEAST 90% OF THE TOTAL PANEL SURFACE AREA. THE ACCURACY OF THE REMAINING 10% SHALL NOT EXCEED .020 INCHES TIR AND 30 MINUTES OF ARC AND ANY ONE OF THESE AREAS SHALL NOT EXCEED 2.0 SQUARE INCHES IN AREA OR BE CLOSER THAN 10 INCHES APART.
3. PROCESSES SHALL BE IN ACCORDANCE WITH PUBLISHED RECOMMENDATIONS OF MANUFACTURERS OF MATERIALS SPECIFIED AND/OR FABRICATORS SPECIFICATIONS.
4. "PRINT THROUGH" OR "TRANSFER PATTERN" OF THE CORE CELLS ONTO THE FRONT FACE, SHALL NOT CAUSE LOCAL SURFACE TANGENT ERRORS GREATER THAN 7.5 MINUTES OF ARC FROM THE TRUE PARABOLIC SURFACE.
5. THE BACK SURFACE ACCURACY OF THE PANELS IS NOT CRITICAL. LOCAL IMPERFECTIONS WILL BE PERMITTED SUBJECT TO ENGINEERING ACCEPTANCE PROVIDING NO IMPERFECTION IS GREATER THAN .05 SQUARE INCHES OR 1.0 INCHES IN LENGTH AND DOES NOT DEGRADE STRUCTURAL INTEGRITY OF THE PANEL.
6. THE EXPOSED HONEYCOMB CORE ON THE PANEL EDGE IS TO BE FILLED WITH MATERIAL DEFINED IN NOTE 9.
7. FINISHED PANEL EDGES SHALL BE STRAIGHT WITHIN ± .010 INCHES WHEN VIEWED PARALLEL TO THE X AXIS AND SHALL BE SQUARE TO THE TRUE PARABOLIC FRONT SURFACE WITHIN THE SAME ± .010 INCHES TOLERANCE.
8. PANEL EDGES SHALL BE FREE OF SHARP CORNERS, BURRS, ETC., CUTOUTS EXCEPTS:
9. ⚠9 MATERIALS SHALL BE AS FOLLOWS:
   FRONT FACE - .004 THICK, 2024 - T6 BRIGHT SPECULAR FINISH ALUMINUM ALLOY
   BACK FACE - .004 THICK, 2024 - T6 ALUMINUM ALLOY.
   CORE — MIL-C-7438 TYPE 3.1-$\frac{1}{8}$-.07 P (5052), NO MORE THAN ONE PIECE PER PANEL. CORE 'L' DIRECTION TO BE APPROXIMATELY PARALLEL TO CENTERLINE OF EACH PANEL.
   ADHESIVE - FM - 1000 (BLOOMINGDALE DEPARTMENT, AMERICAN CYANAMID COMPANY), 0.020 LB/FT² MAXIMUM, SANDWICH PEEL 70 $\frac{LB}{IN}$, TENSILE 1200 PSI
   EDGING AND POTTING - CORREL 615 (BLOOMINGDALE DEPARTMENT, AMERICAN CYANAMID COMPANY) CURING AGENT 'Z' (BLOOMINGDALE), SHEAR 3200 PSI, COMPR 4900 PSI.
   FINAL SELECTION OF MATERIALS SHALL BE APPROVED BY SQC.
10. PROCESSING SHALL NOT CAUSE CORE DEFORMATION, CRUSHING, OR MECHANICAL STRENGTH DEGRADATION.
11. ⚠11 CORE AROUND TOOLING HOLES AND AROUND CUTOUTS TO BE POTTED TO A DISTANCE OF .38 TO .88 INCHES FROM EDGE.
12. RADIAL AND DIAMETER DIMENSIONS ARE PERPENDICULAR TO X AXIS.
13. FLEXURAL STRENGTH OF PANEL & TEST SPECIMENS TO BE 5000 PSI MIN

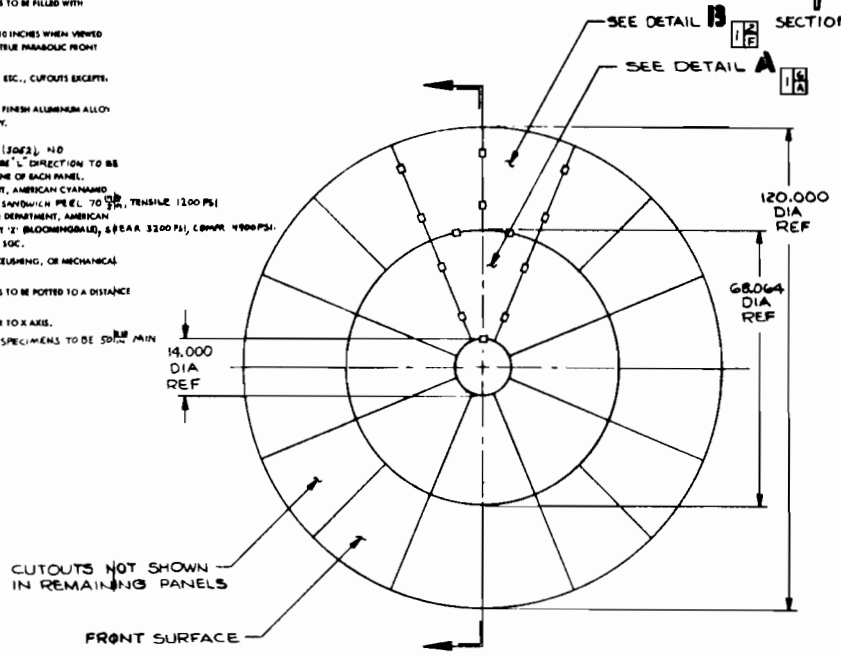

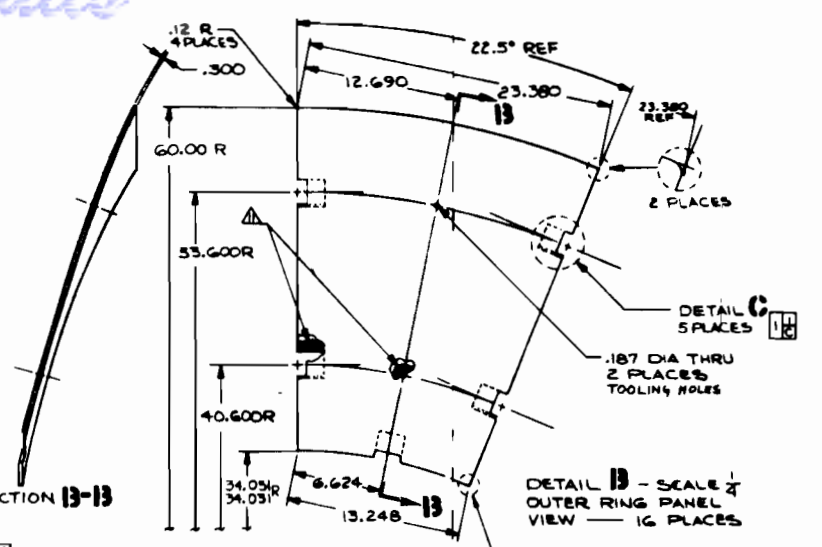

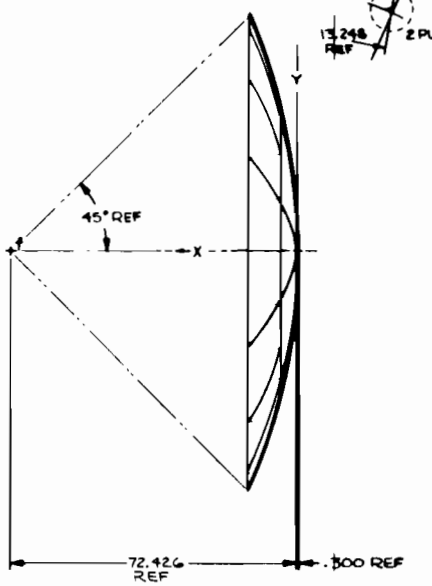

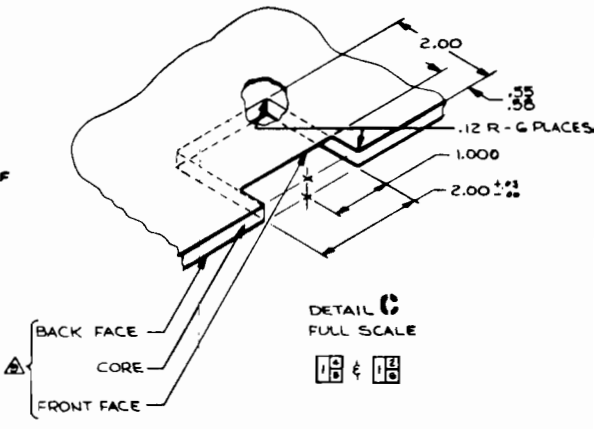

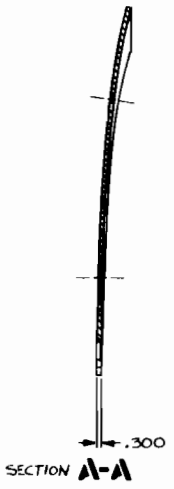

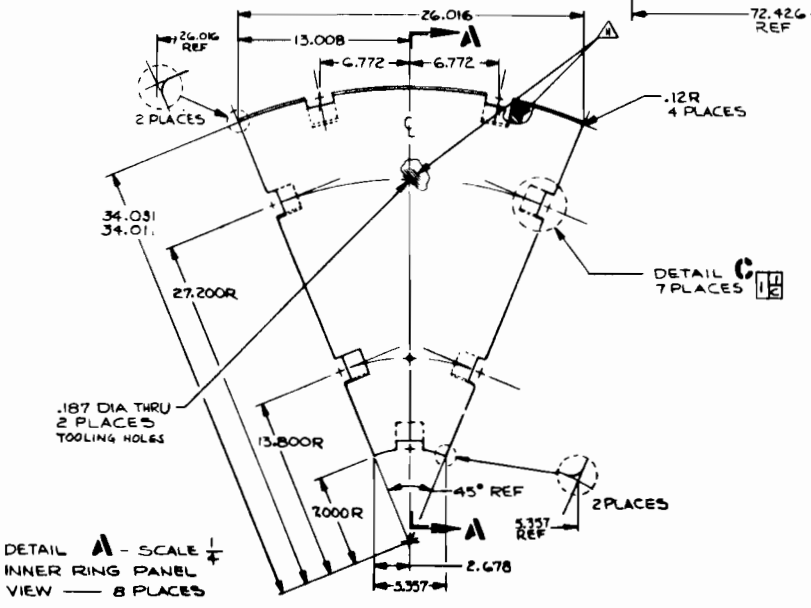

Figure 5-27. Panel Configuration

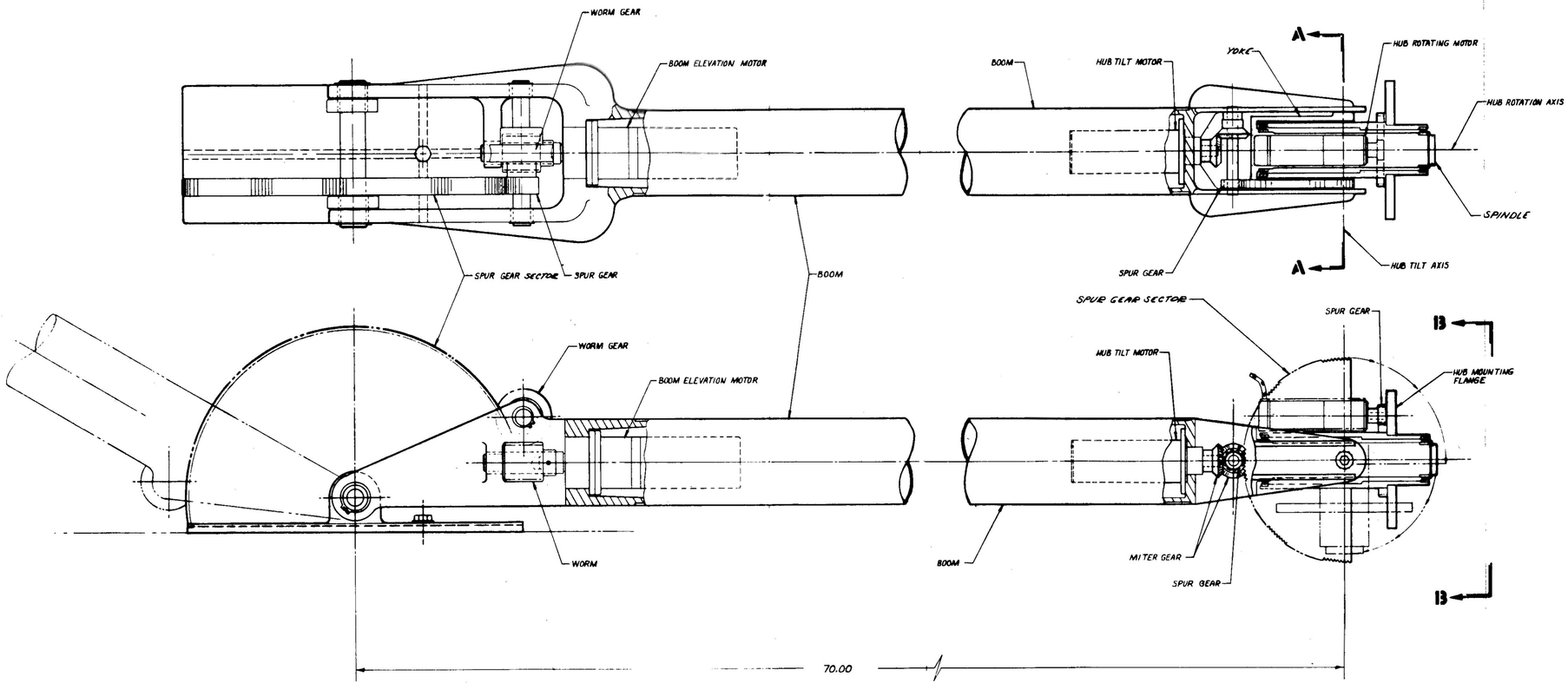

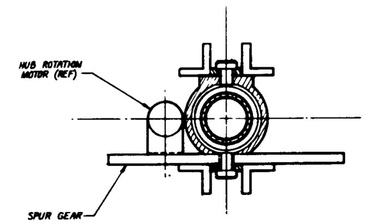

SECTION A-A

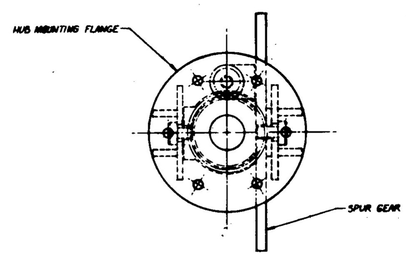

SECTION B-B

Figure 5-28. Boom Assembly

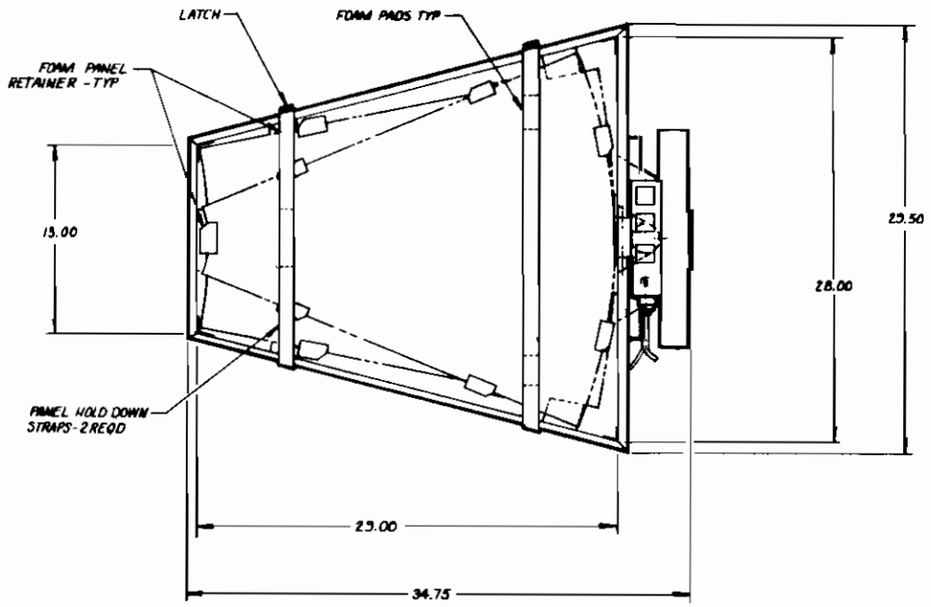

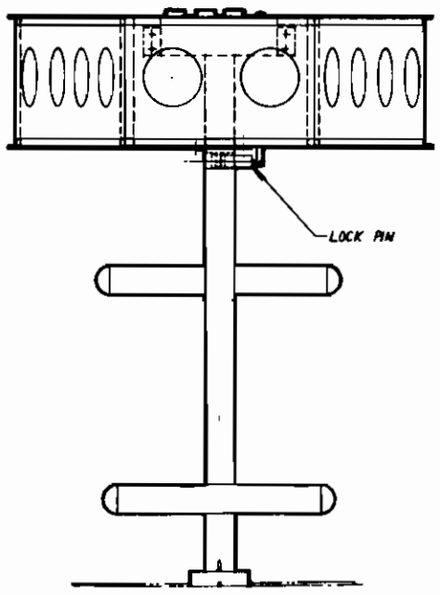

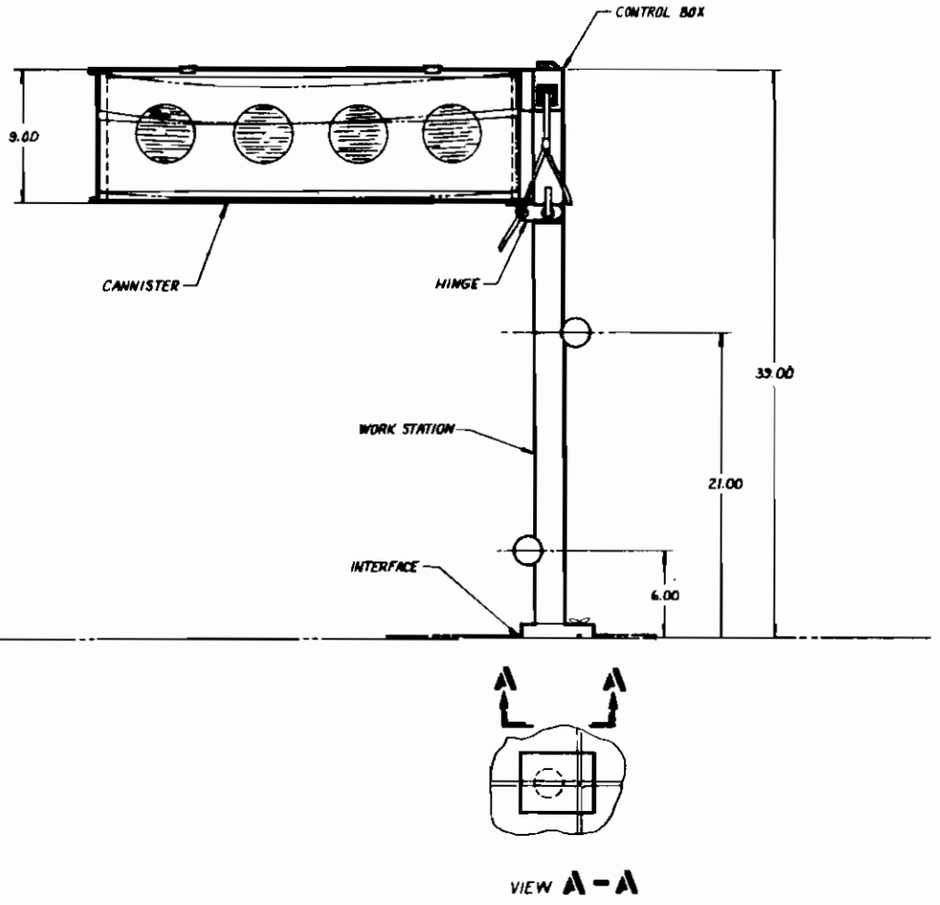

VIEW A-A

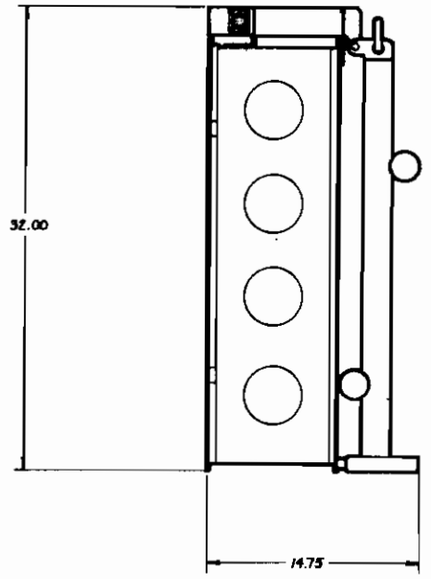

STOWED CONFIGURATION

Figure 5-29. Work Station and Canister

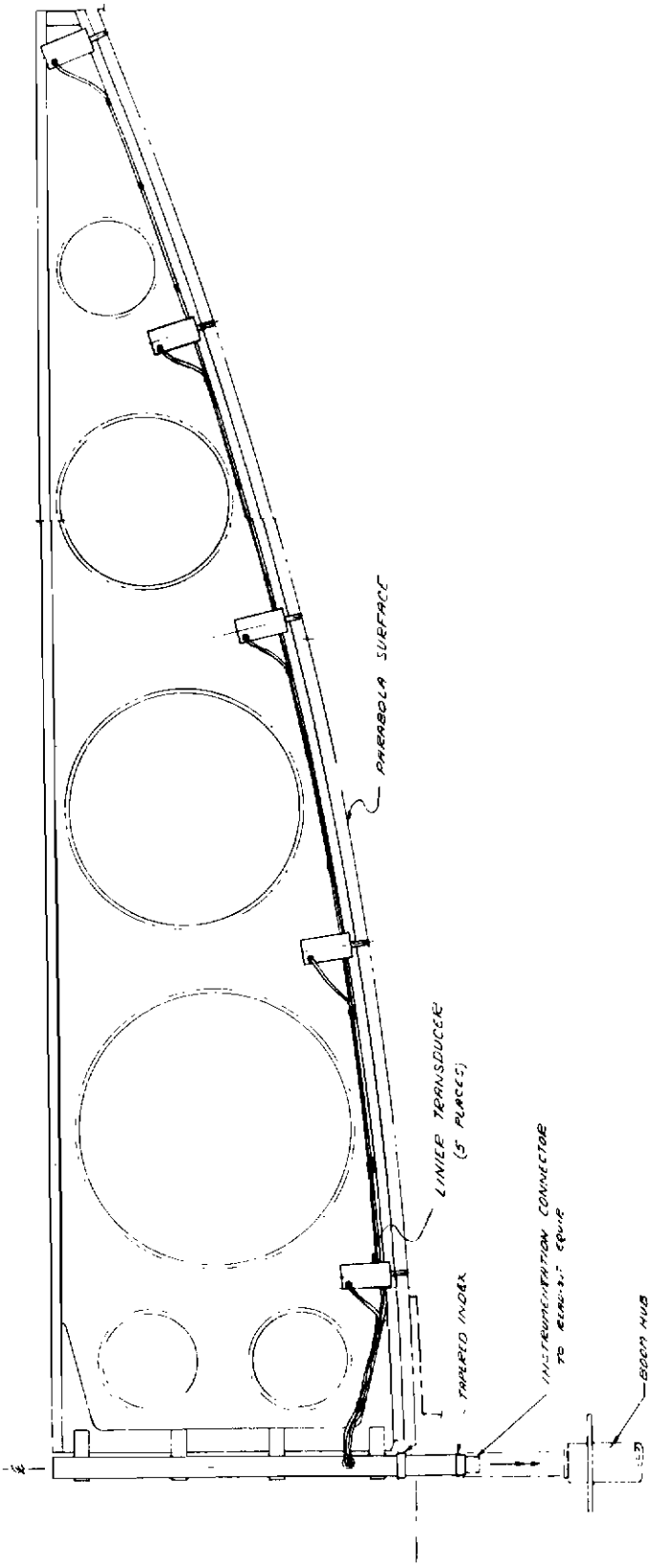

Figure 5-30. Contour Device

NOTE: CORE THICKNESS = 0.300 IN.
SKIN THICKNESS = 0.003 IN. EACH SIDE } ALL CASES

Figure 5-31. Sandwich Panel Strength Analysis

various structural loading capacities, shear, moment, and axial compression are plotted as ordinates with the panel core weight as an abscissa. The axial compression capabilities shown are based on an unsupported panel length of 36 inches; in addition, the weight of the panel (skin plus core but excluding the adhesive weights) is plotted for the various core weights. The aluminum honeycomb core dimensions and mechanical properties used in the analysis are based on data from the Hexcel products publication TSB120, dated 2-20-64.

A panel configuration drawing was prepared which defines the final modular panel dimensions and fabrication material requirements. Two local companies were contacted for fabrication cost quotations on the aluminum honeycomb panels defined by this drawing. The request did not include the interconnect joint fabrication and installation as this manufacturing task would be accomplished by SGC. The cost quotes were reasonable and neither company saw any insurmountable problems, as the dimensional accuracies and fabrication techniques required were within the state-of-the art.

5.4.1.2 JOINT HARDWARE

The joints are to be fabricated of 2024 aluminum. The most likely method for achieving the close tolerances required is the extrusion process. Each female joint and each male joint will be made up of two halves. The extruded aluminum strip will be cut into four pieces, numbered 1, 2, 3, 4. Number 1 with number 3 (reversed) will make up one female half and number 2 with number 4 reversed will make up the male half. These two sets of parts will be jig-assembled and will then be secured together to make up one complete joint. During final detail design it may be determined that lapping of these parts will be required to maintain better tolerances. At the time the female half is assembled, the spring clip will also be installed. The matched joints will be preloaded with a small axial force for the joint installation process.

5.4.1.3 JOINT INSTALLATION

Assembly of the matched joints into the panels will be accomplished on a 10-foot-diameter master parabolic (adjustable) tooling form. This convex

form will be installed on a platform and provisions will be made for optically checking panel accuracy. All 24 panels and the hub will be placed on the form, positioning being established by tooling pins. Potting material will be applied to the cutouts and the matched joints will be pressed into the cutouts. At the time of assembly, the need to precisely position the joint assembly with respect to the form will be determined. Back surface doublers will then be applied over the cutouts and bonded in place. Individual pressure pads will be employed to provide pressure for bonding and curing. Throughout this assembly operation, optical control over the panel will be maintained utilizing cut outs in the form. A check of panel positioning will be accomplished by reflection of a light pattern from the parabolic surface to the focus. Adjustments of the form and panel can be made to reduce assembly tolerances and improve parabola accuracy.

In the process of assembly, plotting material will be allowed to fill the space between adjacent panels in the area of each joint. In this way a stop is provided to prevent unequal loading and deflection of the joints during assembly. Proper release agents will be applied to the form and panel areas to prevent bonding in unwanted areas. It is envisioned that a small amount of clean-up of excess materials will be required after the curing operation is completed.

Following the curing of the assembly, the parabola will be reassembled for both optical and mechanical measurement of its accuracy. Several assembly operations will be accomplished to determine repeatability. It is at this time that the bolt-ropes will be installed and the optimum amount of tension will be determined. Since it will be impractical to submerge the parabola in water for zero-buoyancy testing, accuracy measurements will be made with the parabola upright and inverted.

5.4.1.4 BOLT-ROPE

The bolt-rope tensioning device will be installed on the parabola after assembly to remove assembly tolerances in the joints and to repeat the joint preload used in fabrication. The spring clip of each joint is used only to snap the panels together to prevent their drifting away in space. One

bolt-rope will be installed approximately 2/3 of the way out on the inner ring of panels and a second will be installed approximately 2/3 of the way out on the second ring. The tooling holes will be used for this attachment. The bolt-ropes will consist of a coated flexible steel cable with attachment hooks and a spring link to provide predetermined tension. A simple over-center latch will be employed to join the ends of the cable as a final step of assembly.

5.4.1.5 JOINT-PANEL STRUCTURAL ANALYSIS

The following preliminary analysis was conducted to ascertain the bending loads and to size the panel joint. This analysis was based on a maximum astronaut load of 10 pounds normal to the module's surface with only a single joint engaged on the opposite end of the panel.

This load, it is felt, represents a worst-case assembly-loading requirement, and should provide ample margin for the actual assembly loads encountered. The maximum load components required to engage the joints recorded by zero-buoyancy assembly test on a mock-up structure were only 5 pounds maximum and parallel, or in-line with the surface, thereby producing very little bending moment on the panel joint. The modified joint design used at present will require even less force. Therefore, this 10-pound normal design load is assumed primarily to allow for inadvertent contingencies, as the joint is designed to engage requiring only lateral forces

The main problem encountered in the modular panel design was one of load distribution into the aluminum honeycomb panel by the 2-inch-wide joints. Preliminary analysis of the load concentrations indicate that 0.004-inch aluminum face skins will be adequate for the front and back surfaces of the panels, with a 0.004-inch doubler over the rear joint skin cut-out. A doubler is not used on the front surface because the skin is not cut out so as not to interfere with the surface contour accuracy. Also, this slightly thick or front skin exhibits less tendency for "show-through" of the honeycomb core.

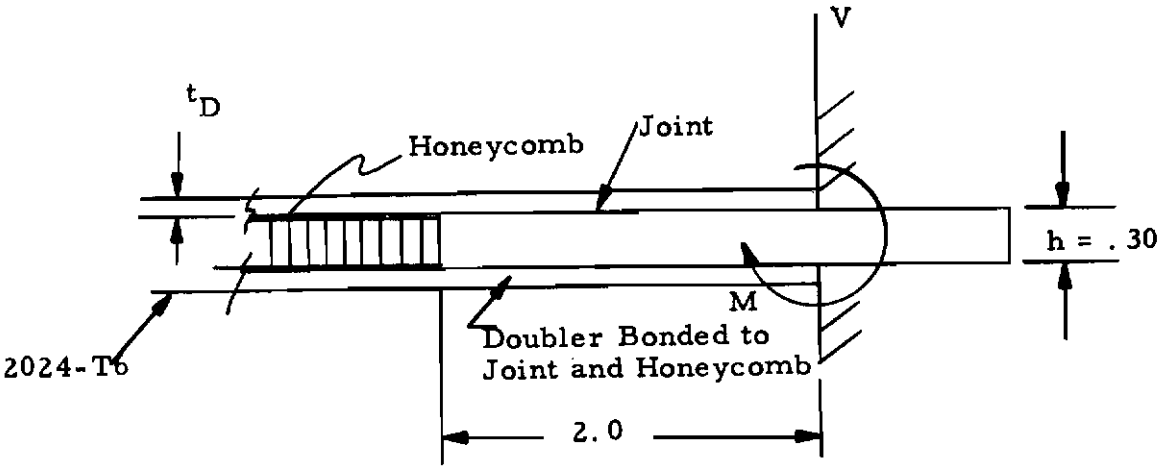

V = 10 lb

M = 10 x 28 = 280 in. -lb

Joint Load = $\frac{M}{h} = \frac{280}{.30}$ = 935 lb

Transverse Shear Area

A_t = 2 x 2 = 4 in.^{2}

$f_{st} = \frac{935}{4}$ = 234 psi

Allowable Bond Strength CORFIL615

F_s = 2715 psi

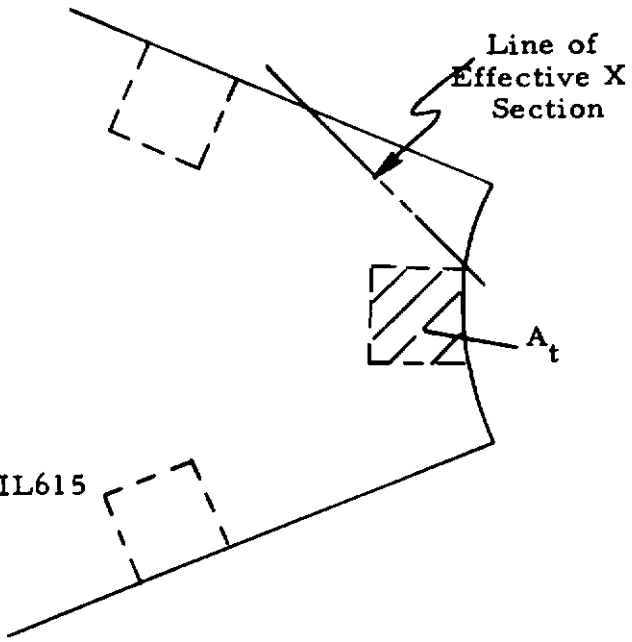

M. S. = $\frac{2715}{1.25 \times 234}$ -1 = large

Moment at Joint Runout

$$M = \frac{26 \times 10}{6} = 43.4 \text{ in.-lb/in.}$$

Sheet Load

$$q = \frac{M}{h} = \frac{43.4}{.30} = 145 \text{ lb/in.}$$

$$f = \frac{q}{t} = \frac{145}{.004} = 36,300 \text{ psi}$$

$$F_{ty} = 47,000$$

$$M.S. = \frac{47,000}{1.1 \times 36,300} - 1 = +.18$$

For Intercell Buckling

$$f_{cR} = \frac{E}{3} \left(\frac{2t}{5}\right)^{3/2}$$

$$f_{cR} = \frac{10.5 \times 10^6}{3} \times (16 \times .004)^{3/2}$$

$$= 3.5 \times 10^6 \times .016 = 56,000 \text{ psi}$$

$$M.S. = \frac{56,000}{1.25 \times 36,300} - 1 = +.23$$

Joint Loads

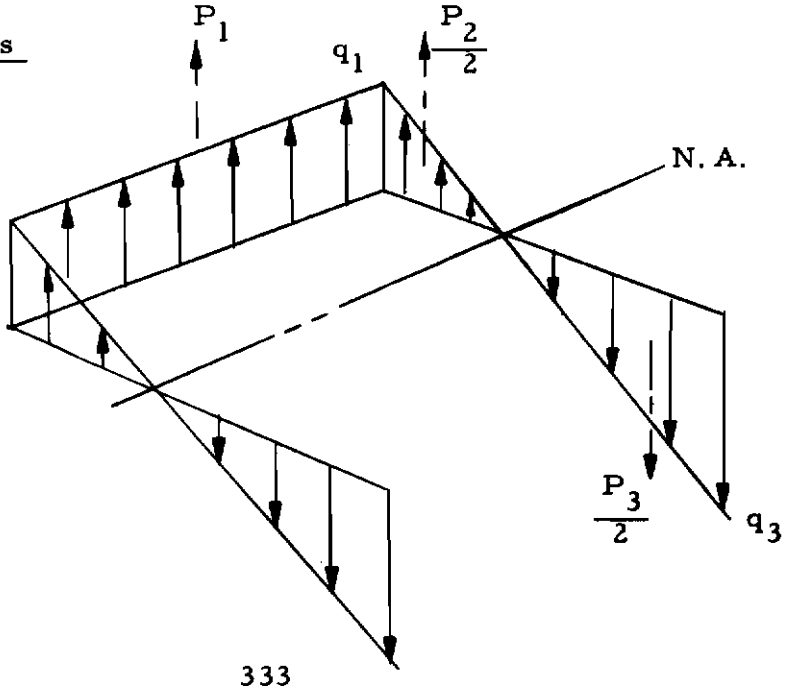

$$\text{N. A.} = \frac{(2+2) \times 1 + 2 \times 2}{6} = \frac{8}{6} = \frac{4}{3}$$

$$M_1 = P_1 \times \frac{2}{3}$$

$$M_2 = P_2 \times \frac{2}{3} \times \frac{2}{3} = P_2 \times \frac{4}{9}$$

$$M_3 = P_3 \times \frac{2}{3} \times \frac{4}{3} = P_3 \times \frac{8}{9}$$

$$P_1 \text{ , } q_1 \times 2$$

$$P_2 = q_1 \times \frac{2}{3}$$

$$P_3 = q_3 \times \frac{4}{3}$$

$$M = M_1 + M_2 + M_3 = 280 \text{ in. -lb}$$

$$q_1 \times 2 \times \frac{2}{3} + q_1 \times \frac{2}{3} \times \frac{4}{9} + q_3 \times \frac{4}{3} \times \frac{8}{9} = 280 \text{ in. -lb}$$

$$q_1 \times \frac{4}{3} + q_1 \times \frac{8}{27} + q_3 \times \frac{32}{27} = 280 \text{ in. -lb}$$

$$P_1 + P_2 - P_3 = 0 \quad \because P_3 = P_1 + P_2$$

$$q_3 \times \frac{4}{3} = q_1 \times 2 + q_1 \times \frac{2}{3}$$

$$q_3 = \frac{3}{4} \times q_1 \times \frac{8}{3}$$

$$q_3 = 2\, q_1$$

$$q_1 \times \frac{4}{3} + q_1 \times \frac{8}{27} + q_1 \times \frac{64}{27} = 280 \text{ in. -lb}$$

$$q_1 \times \frac{36 + 8 + 64}{27} = 280 \text{ in. -lb}$$

$$q_1 = \frac{27 \times 280}{108} = 70 \text{ lb/in.}$$

$$q_3 = 2 \times 70 = 140 \text{ lb/in.}$$

$$f_s = \frac{q_3}{h} = \frac{140}{.3} = 467 \text{ psi}$$

$$\text{M.S.}_{\text{Bond}} = \frac{2715}{1.25 \times 467} - 1 = \text{Large}$$

5.4.2 BOOM AND HUB MECHANISM

A layout of the modular parabola boom and hub mechanism is shown in Figure 5-28. This design concept allows fully remote adjustment at the work station for raising or lowering the boom, changing the hub tilt angle, and rotating the hub to allow the astronaut to achieve any work position desired during the manual assembly of the modular structure. The strength criteria imposed on the actuation motors and gearing were primarily determined by the accelerating moments produced during boom actuation, and vehicle ACS operation. The manual forces exerted by the astronaut on the structure during assembly were also included. These particular loads were determined during the zero-buoyancy human factors tests.

The reversible DC motors were selected for size, torque, and history of successful space vehicle operation.

Electrical cabling will be routed, for the most part, inside the boom's tubular structure. Provisions for the insertion of a contour measurement template shaft are made in the hub joint assembly by two bearings. These bearings have been spaced as far apart as practical to insure maximum alignment accuracy for the template bearing shaft.

The boom assembly consists of a section of 2-1/2-inch OD x 0.065-inch wall aluminum tubing with welded end fittings which support the boom and hub drive mechanisms.

The boom assembly boom elevation drive is attached to the vehicle by means of a flat plate with simple bolting. Attached to the plate are bearing supports which allow the boom to be elevated 150° through one axis only. A sector of a spur gear is attached to the plate with the mating gear (driven gear) attached to the boom end fitting. When the driven gear is rotated it climbs the fixed sector, thus pivoting the boom assembly.

Power is provided by a gear head motor with a worm/worm/gear drive to the driven spur gear.

The worm/worm/ gear has been chosen because of its characteristic not to "coast-through." This feature allows infinite positioning of the boom without the need of detent or brake mechanisms. Boom positioning may be accomplished by simply switching power to the drive motor, allowing the boom to elevate to the desired position. When power is "off", the boom will remain fixed in position until drive power is again applied.

5.4.2.1 HUB TILT DRIVE

The hub is supported in a yoke which is pivoted about a axis mid way between the hub rotation bearings, allowing hub tilting of 180°.

Tilt drive power is provided by a gear head motor driving a spur gear, engaging a gear sector attached to the hub support yoke.

5.4.2.2 HUB ROTATION DRIVE

The hub rotates on a spindle which extends from a yoke supported by the boom end fittings, two bearings sufficiently spaced to maintain proper alignment tolerance are employed to allow hub rotation. A small gear head motor drives the hub through a spur gear reduction.

5.4.3 WORK STATION AND CANISTER

The work station and canister for the parabola experiment are shown in Figure 5-29. The work station consists of an aluminum tubular post with cross bars positioned so that the astronaut can lock himself into the work station by his legs. The parabola panel canister is permanently mounted on the work station as is the control box for positioning the boom assembly. The whole assembly can be folded into a 29.5 x 32.0 x 14.75-inch rectangular package.

The work station concept was developed during the zero-buoyancy tests described elsewhere in this report. It provided the astronaut with an exceptionally functional, yet simple, work station. The astronaut locks

himself into the stand by placing his ankles behind the lower cross bar and his knees in front of the upper bar. A forward pitching moment is reacted by his stomach at the control box. No straps are involved.

The work station is designed to be attached to the inside of the SIVB tank by means of a single 10-32 stud or bolt through a plate. The plate is grooved to match the waffle pattern of the SIVB wall, thereby reacting any twist of the stand. Preliminary analysis shows that the work station post can be designed to bend before failure of the single bolt attachment will occur. This will provide considerable restraint capability for the zero-g astronaut.

The canister consists of a light sheet-aluminum box. Dimpled cut-outs are employed to decrease weight and at the same time improve rigidity. The parabola panels are retained during launch by two straps. Open cell foam pads have been added to partially retain the individual panels during parabola assembly operations. These parts will also protect the panels during the launch environment.

The control box on the work station contains a power switch as well as individual switches to control boom elevation, hub tilt, and hub rotation. Electrical cabling for connecting the boom to the control box will be stowed with the canister.

Suitable interface attachments for tying the stowed package to the SIVB can be provided when specific location on the SIVB, or any other vehicle, is known.

5.4.4 CONTROLS AND INSTRUMENTATION STUDIES

5.4.4.1 MODULAR PARABOLA CONTROLS FOR MSL EXPERIMENT CONFIGURATION

The modular parabola will require sequenced controls similar to the airlock controls on the MSL vehicle requirements. The control requirements are as follows:

Performed by the Astronaut Prior to EVA

a. Deployment sequence

(1) Boom fairing release (pyrotechnic)

(2) Boom release (pyrotechnic)

(3) Boom control motor

(4) Panel canister release (pyrotechnic)

(5) External console power-on

Performed by the Astronaut while EVA at the Work Station Control Console

b. Boom raise and lower controls

c. Hub tilt controls

d. Hub rotate controls

e. Abort arm and actuate controls

The control console in the pressurized section of the vehicle will incorporate all the above functions except the hub rotate controls, which will not have to be used after the parabola is assembled. The panel layout is illustrated in Figure 5-32.

The deployment sequence, item "a" in the above list of requirements, will be stepped through using arm and actuate pushbuttons for each step. The pyrotechnic functions will incorporate a timed delay of 5 seconds before allowing the "safe-indicator sequencer" to proceed to the next step. The boom control will have an action-complete signal from a boom position limit switch, which will advance the sequencer. The last item of the sequence, the external console power position, will remain active until the power switch is turned off.

The internal hub and boom controls will have an alternate-action pushbutton switch for direction control and a momentary contact pushbutton to supply power to the appropriate motor. Angular position indication will be provided for both functions as a readout on the instrumentation console. The abort control will use a solenoid-hold momentary contact switch for arming the control and a momentary contact pushbutton for actuation of the pyrotechnic if, after the completion of the experiment, it is desired to jettison.

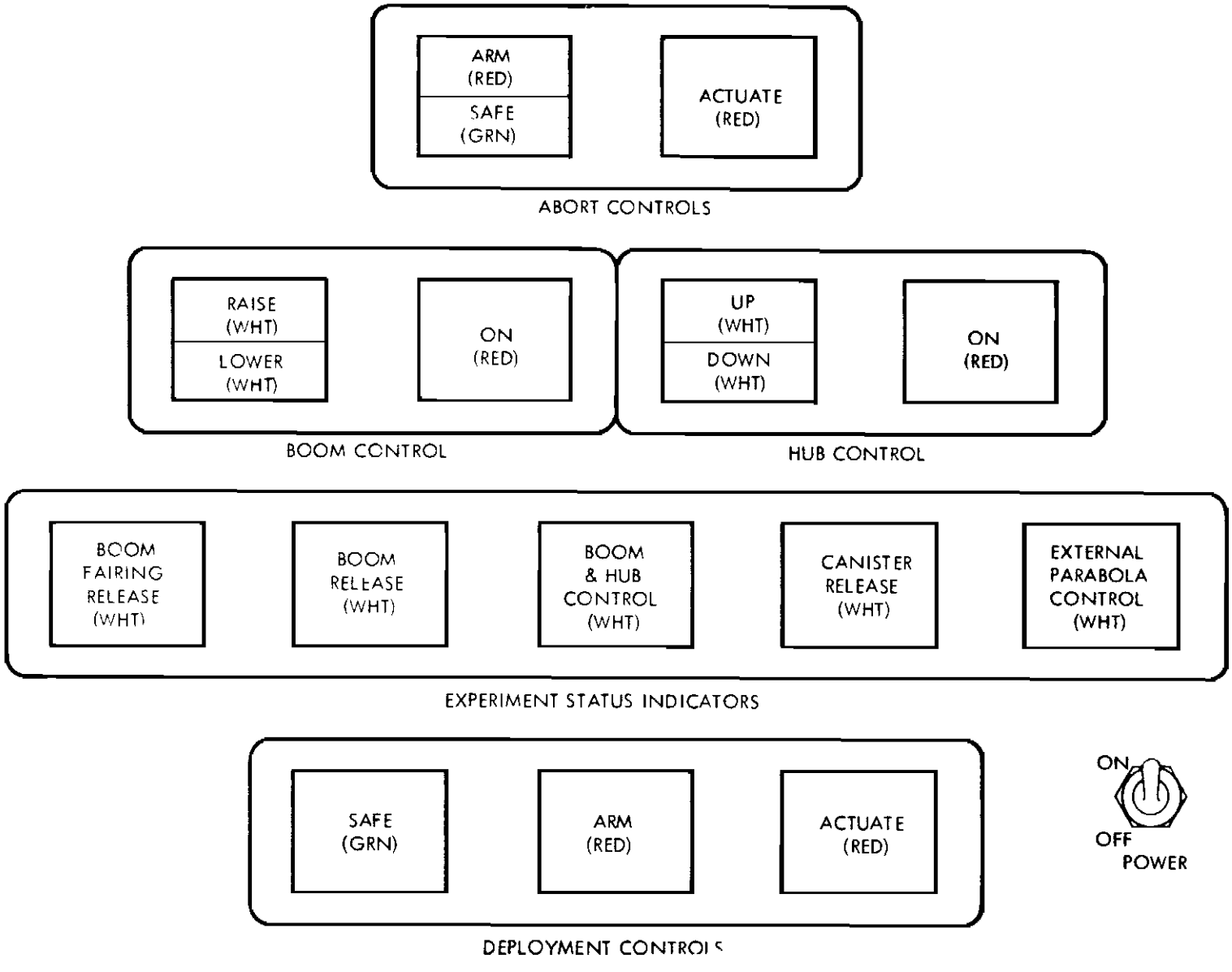

Figure 5-32. MSL Vehicle Internal Control Console for Initial Deployment of Modular Parabola

The external control box, which will be used by the astronaut in the manual assembly of the parabola, will incorporate boom erection controls, hub tilt controls, hub rotate controls, and a power-on indicator light. The position controls will be spring-return, three-position toggle switches which have one-to-two-inch handles for ease of operation. The panel layout is illustrated in Figure 5-33.

As shown on the panel layout, the switches will be operated by pushing them in the direction in which the parabola itself will move, giving the astronaut considerable "feel" for switch operation. The boom erection and the hub tilt controls will be moved vertically and the hub rotate control will be moved to one side or the other depending on which way the astronaut wants the hub to rotate. Since the astronaut will use the rotate control most frequently during assembly, it is located on the extreme right of the panel.

An intercabling diagram is shown in Figure 5-34.

5.4.4.2 SIVB MODULAR PARABOLA CONTROLS AND INSTRUMENTATION

The controls for the modular parabola for the SSESM vehicle are considerably more simple than those described for a general MSL-type vehicle. The basic reason for this is that the MSL installation considers the experiment integrated into vehicle structure and remotely erected, ready for manual assembly. For the SIVB mission plan, the experiment is stowed forward in the transtage area and manually retrieved, and is set up in the interior of the SIVB living quarters.

The integral controls requirement on the work station for moving the boom and hub are identical to those described for the MSL vehicle installation. Refer to the discussion on work station control console in the prior section.

The instrumentation requirements for the SIVB experiment were simplified by the data acquisition support on the SSESM and the scope of the measurements to be made. The contour measurement template constitutes the major instrumentation provisions for the SIVB mission plan.

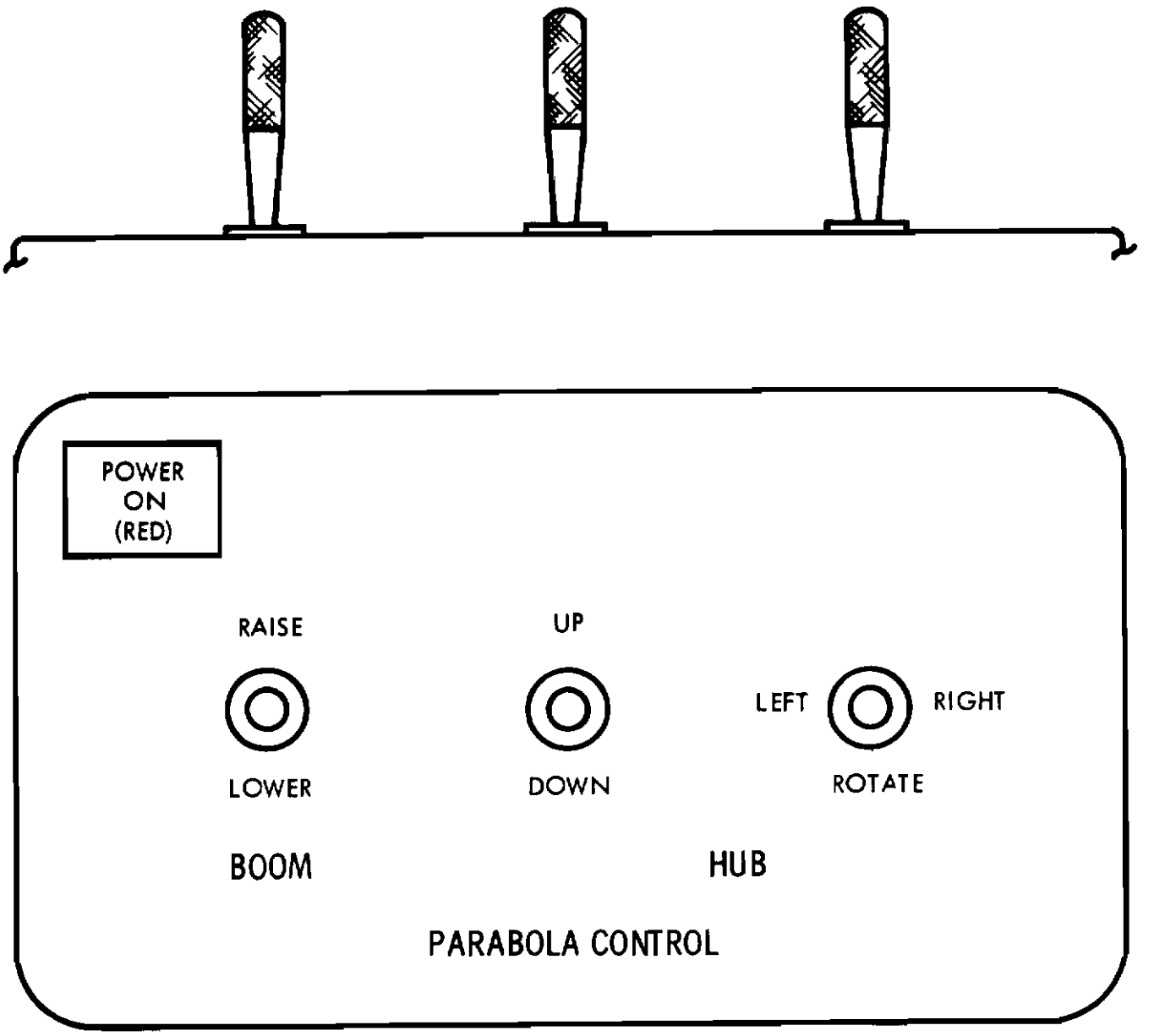

Figure 5-33. Work Station Control Console

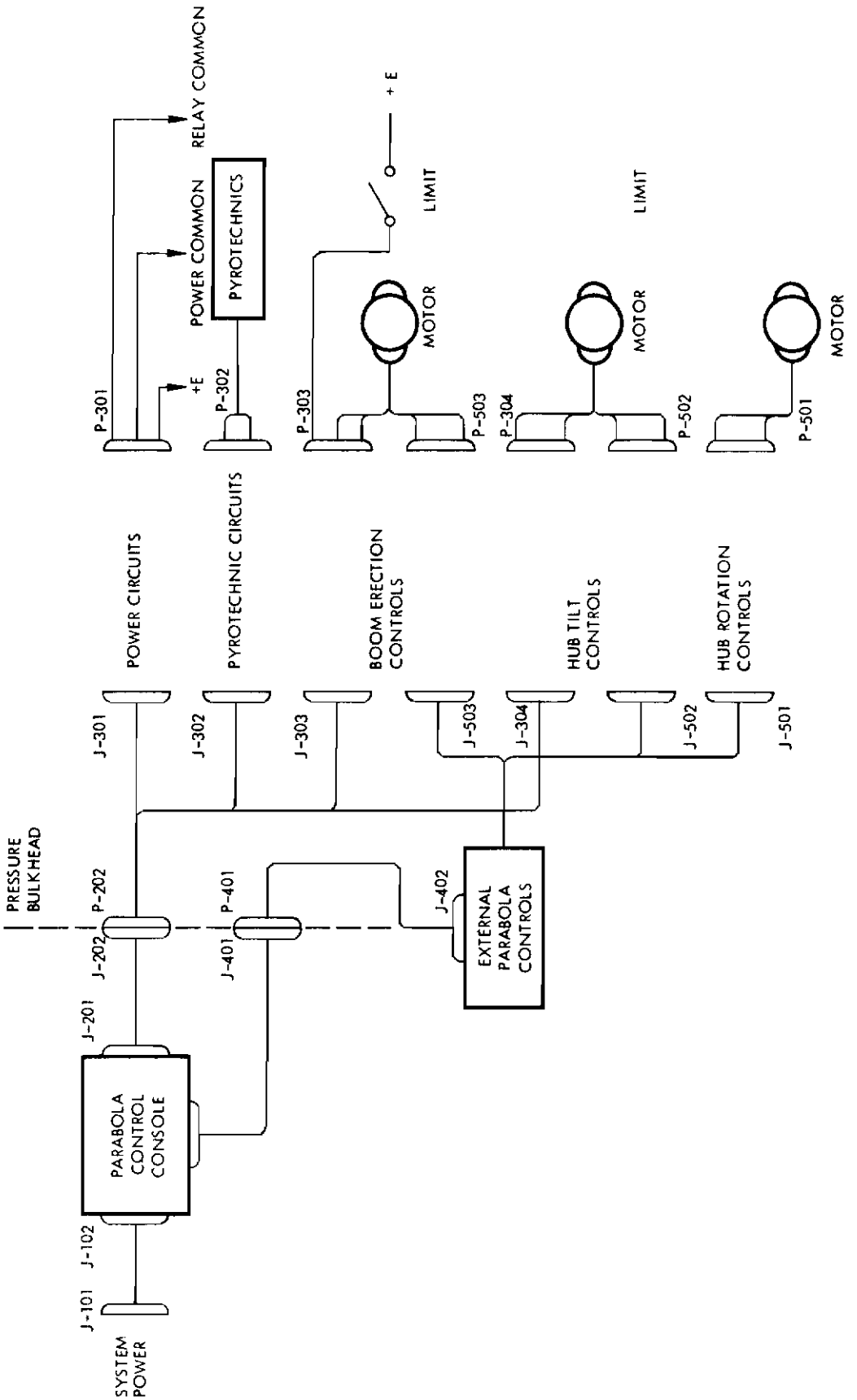

Figure 5-34. Intercabling Diagram for Modular Parabola Experiment

5.4.5 MODULAR PARABOLA CONTOUR MEASUREMENT TEMPLATE AND ILLUMINATOR STING

A parabolic reference template and extensiometer probes shown in Figure 5-30 are designed for the contour accuracy measurement of the assembled modular parabola. The lightweight template supports electronic extensiometers positioned to scan the surface of the parabola as the hub motor rotates the structure about the parabola's optical axis.

The bearings in the hub will be required to keep the parabola within the tight angular tolerance in relation to the template so that measurement errors will not be caused by template position.

q The sketch below illustrates the method used for error calculations:

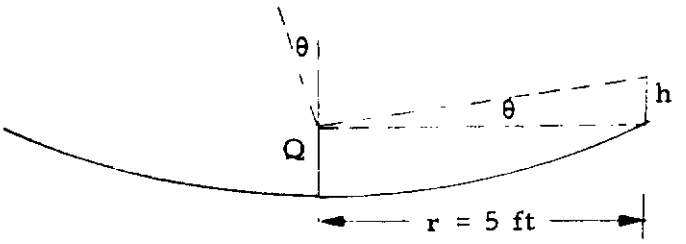

θ = angle between the axis of the parabola and the rotational axis of the measurement template

h = measurement error at the rim of the parabola caused by angular deviation

r = radius of parabolic structure

$$\tan \theta = \frac{0.005 \text{ in.}}{60 \text{ in.}} = 8.3 \times 10^{-5}$$

$\theta = \sim 0.005^{\circ}$ or 0.3 minutes of arc

If the acceptable error is less than 0.005 inch, θ must be less than 0.005°. This may be interpreted as a 0.001-inch bearing tolerance for bearings with a 12-inch separation at the hub attach point.

A conceptual design of a collapsible sting for a Xenon light source is shown in Figure 5-35. This can be plugged into the assembled parabola by the astronaut using the bayonet type attachment. Electrical connection is automatic. Further discussion of the Xenon sting is presented in Section 5.5.

5.4.6 PARABOLA INSTALLATION

Concepts for MSL stowage and installation and for SIVB installation are discussed in this section.

5.4.6.1 MSL VEHICLE

The MSL experiment system consists of the 10-foot-diameter modular parabola, a 7-foot boom/hub assembly which connects the parabola to the space vehicle, a work station which is utilized during parabola assembly, and a canister which serves as a container for the parabolic precontoured panels and a parabola contour measuring device. This system configuration and installation are shown in Figure 5-36.

The design concept provides flexibility for the vehicle installation requirements. Two preferred methods of stowing the experiment are discussed, one internal and one external, flush with the vehicle surface. In both installations the boom and hub assembly is mounted externally with a low profile fairing, parallel to the longitudinal axis of the vehicle.

In this installation, the experiment package (panel canister, work station, etc.) is stowed external to the vehicle recessed under a secondary fairing integral with the boom/hub fairing. The fairings are released and the boom is raised by remote control. The work station and canister assembly are raised manually from the exposed recess in the vehicle structure.

The deployment of the externally stowed experiment begins with the remotely controlled removal of the experiment's aerodynamic fairing. The boom assembly erection motor is then actuated to erect the boom to a suitable position. This drive mechanism is capable of moving the boom/hub assembly through a 160° arc in a plane parallel to the longitudinal axis of the space vehicle. At the outer hub end of the boom there are two drive

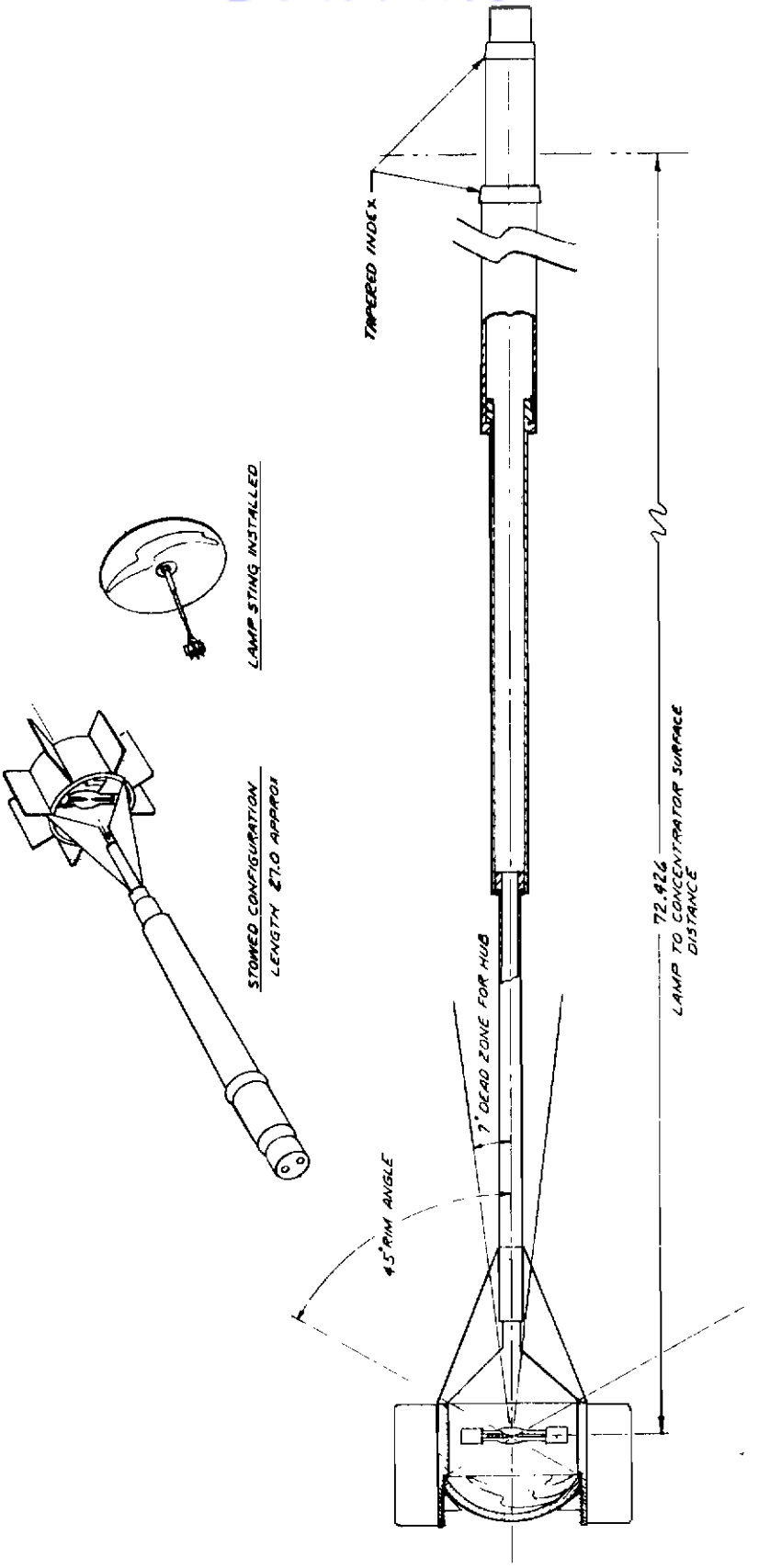

Figure 5-35. Xenon Lamp Sting

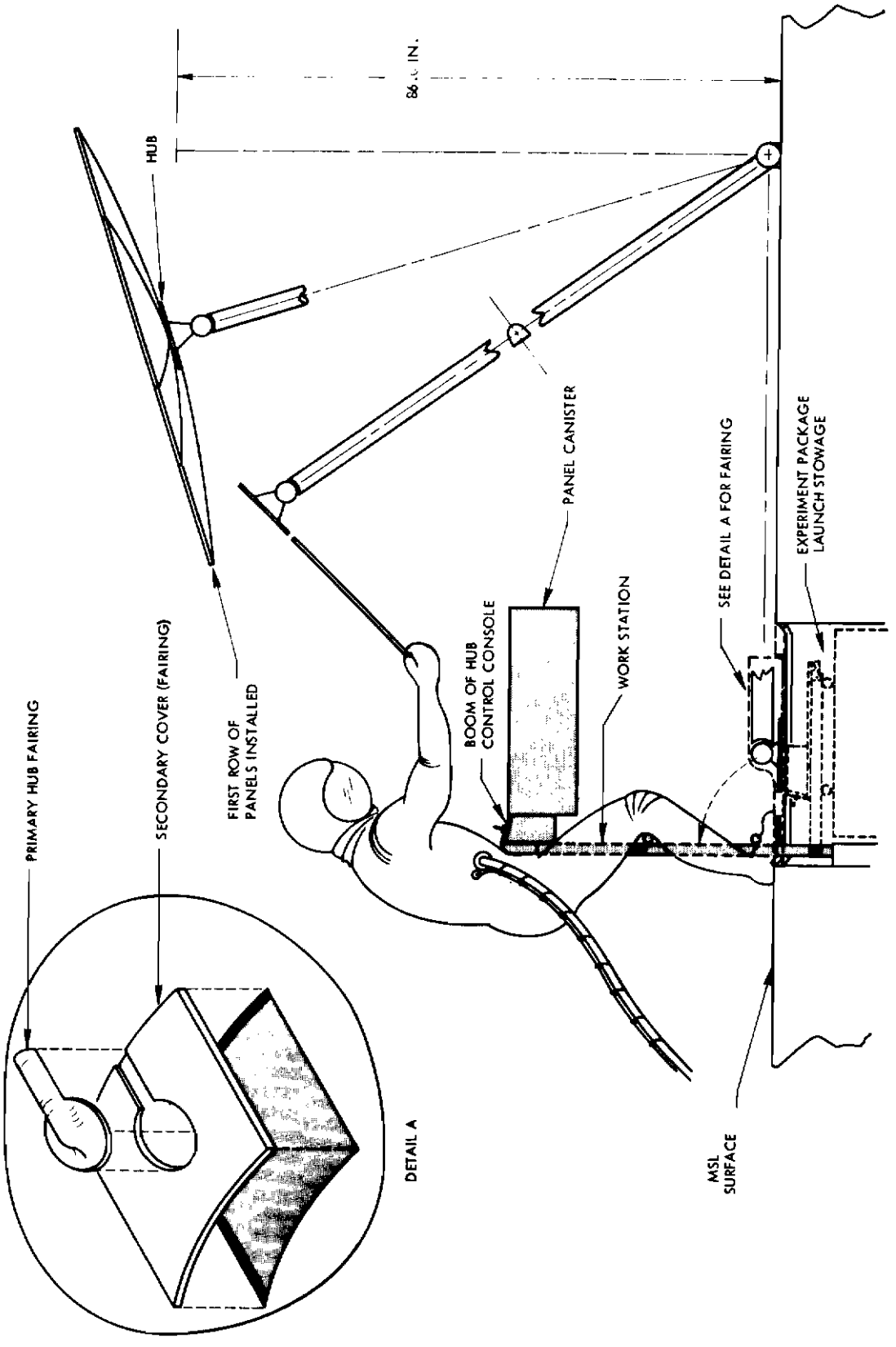

Figure 5-36. Modular Parabola Experiment Configuration and Assembly on the Vehicle External Surface

mechanisms which are capable of rotating the hub 360° about the boom axis, and which also move the hub through a 180° arc in the same plane as the boom movement. These features enable the astronaut to position the structures for greatest convenience during the manual assembly operation.

The work station is deployed manually, at or near the edge of the cutout, by raising the assembly which unfolds the station into the required configuration. The work station provides (1) the necessary reaction support for the astronaut during assembly of the parabola, (2) a control console which enables the astronaut to move the boom/hub assembly into a favorable position for easy reach of the work, and (3) a support for the panel canister. The panel canister is automatically positioned during erection of the work station.

For an internal stowage option, the canister, contour measuring device, and work station are stowed on the inside of the space vehicle in the unpressurized compartment and may be removed through an existing hatch of 34 inches or larger and carried to the assembly area by the astronaut.

For internal stowage, the deployment of the boom is the same as in the first case, except that, instead of a package cutout fairing, only a boom and hub fairing is required. The work station will be manually attached to the space vehicle, and all of the system components (except the boom and hub) will be carried to the assembly area. The major difference between the two installations is the 36 x 30-inch recessed storage compartment, attendant structural reinforcement, and cover pyrotechnic release device required by the integral installation.

The assembly of the parabola takes place after the work station has been set up. The astronaut may then position himself at the work station and adjust the boom/hub assembly position for ease of installation of the pre contoured parabolic panels. The panels of the first ring are attached to the hub by rotating the hub about its own axis as each panel is inserted; the same procedure is followed for the second annular ring of panels after the first ring is completed.

After the last panel has been inserted, a contour measuring device is inserted into a fitting in the center of the hub.

The contour measuring device consists of a beam template and probes attached to a short mast at the hub. The beam has transducers placed along its length which, as the parabola is revolved under the stationery beam, transmit the contour deviation data which can then be compared to the theoretical shape coordinates of the parabola.

5.4.6.2 SIVB VEHICLE

The parabola installation, Figure 5-25, shows the experiment components as they would be mounted inside the SIVB. The parabola is mounted on an 80-inch boom which is attached at its base to the SIVB. The astronaut work station is attached at its base to the SIVB at a distance of 72 inches from the boom attachment. It is intended that the parabola boom and work station be located along an axial line inside the SIVB tank.

Basic dimensions for the boom length and work station-to-boom spacing were determined so that the parabola boom can be positioned for the astronaut to reach the hub and any row of panels for assembly of the parabola, the back of the panels for disassembly, and the hub center for sting installation when parabola is fully assembled. Further, the parabola and boom can be positioned for contour measurement checks.

The boom and hub, by means of three electric drive motors, can be controlled by the astronaut from a control box on the work station. The boom elevation drive rotates the boom with respect to the SIVB. The hub tilt drive positions the hub about an axis parallel to the boom elevation axis. The hub rotation drive positions the hub and parabola in azimuth for installation of the parabola panels and attachment of the bolt rope. The control box contains individual switches for each drive system.

The parabola panels are contained in a canister attached to the work station and are within easy reach of the astronaut when assembling the parabola. The parabola weight and volume breakdown is given in Table 5-3.

Table 5-3

MODULAR PARABOLA EXPERIMENT WEIGHT & VOLUME BREAKDOWN FOR A MSL

(A) Weight

Item	Weight in Lbs.
Parabola (24 panels)	43.20
Boom & Drives	16.70
Work Station	4.75
Cableing & Connections	4.10
Canister	7.60
Control Boxes (2)	6.00
Miscellaneous	3.00
Total	85.35
Contour	11.95
Signal Cond	3.00
Total	14.95
Grand Total	100.00

(B) Volume

Item	Volume in ft^3
Canister	5.50
Boom & Drives	.16
Work Station	.08
Control Boxes	.03
Contour Template	.20
Total	5.97

5.4.6.2.1 SIVB WEIGHT SUMMARY

	Pounds
Dish	43.0
Boom and Drives	16.7
Work Station	3.0
Canister	7.0
Cable and Connections	3.0
Control Box	2.0
Mounting	5.0
	80.3
Contour Template	11.90
Total	92.2

5.4.6.2.2 SIVB VOLUME SUMMARY

	Volume	(inches) Dimensions
Canister	5.50 ft^3	32 x 25 x 12
Boom and Drives	.16 ft^3	72 x 2 x 2
Work Station	.08 ft^3	36 x 2 x 2
Miscellaneous	.05 ft^3	6 x 6 x 3
	5.79 ft^3	

5.5 ANALYSIS OF EXPERIMENT APPLICATIONS AS AN ILLUMINATOR

Analyses were performed for a 10-foot-diameter parabola used as an illuminator and as an aid for rendezvous, tracking and EVA task illumination. For these applications, the light source would be fixed to the central hub.

The evaluations included examination of the illuminator contributed to remote work areas, the appearance of the illuminator from large distances (as a rendezvous aid), and the beam candlepower of the light source for the contour accuracy that can be achieved.

5.5.1 VISIBLE BEACONS

The physiological considerations of visibility are not included in this preliminary analysis. Some basic ground rules which are used in this topic are summarized below:

The terms luminous, luminosity, etc., are all considered to describe that property of light which stimulates the human eye to evoke the sensation of brightness.

It is recognized that the eye's sensitivity to various wavelength shifts from the 0.55-micron peak at normal light levels toward the blue end of the spectrum (0.507) at subdued levels of illumination*.

Luminous flux is defined as radiant power evaluated with respect to the standard visibility function:

$$L = K \int_0^\infty \nu J_\lambda \, d\lambda \text{ lumens/cm}^2$$

where J_λ is the radiosity function of the source in watts per wavelength interval, and ν is the visibility function of the eye. K is a constant of 621 lumens/watt.

For a light source to be visible against a star field requires that suitable physical information be present in the source to allow observer to physiologically distinguish it from its background, in addition to his knowing where to look. At this point, some preliminary calculations are presented to illustrate the appearance of an artifically illuminated parabola by a typical 150-watt Xenon lamp if it were brough to the attention of an observer by flashing or prior knowledge as to its whereabouts.

---

*The Purkinje effect

The following criteria are used in these computations:

a. Parabolic 10-foot-diameter mirror: 60^{o} rim angle.

b. Surface reflectance is specular and 85% efficient.

c. Surface contour errors.

d. Light source is 2 mm x 2 mm and diffuse Xenon arc.

e. Visibility reference is a second magnitude star $\sim 3.3 \times 10^{-11}$ lumens/cm^2.

The emergent beam intensity of a searchlight may be expressed in terms of the luminosity of the source and the ratio of solid angels W_1 and W_2:

$$I_e = K\ I_s\ \frac{W_1}{W_2} \qquad (1)$$

where W_1 is the solid angle intercepted by the mirror from the focus and W_2 is the solid angle subtended by the area of the arc source from the surface of the mirror. K is the efficiency of the reflecting surface.

To determine the angles W_1 and W_2, we will examine the parabola in question. The diameter of 10 feet and rim angle of 60^{o} sufficiently define the subject parabola. By referring to the standard form of the equation of a parabola,

$$y^2 = 2\ px$$

and differentiating with respect to x, we have:

$$\frac{dy}{dx} = p/y$$

when y = 5 feet, the slope of the curve is 60^{o}; therefore

$$\frac{P}{y} = \tan 60^{o} \Big|_{y = 5}^{\text{or}} \qquad P = 8.65$$

and the focal length f = P/2 = 4.33 feet. See figure below.

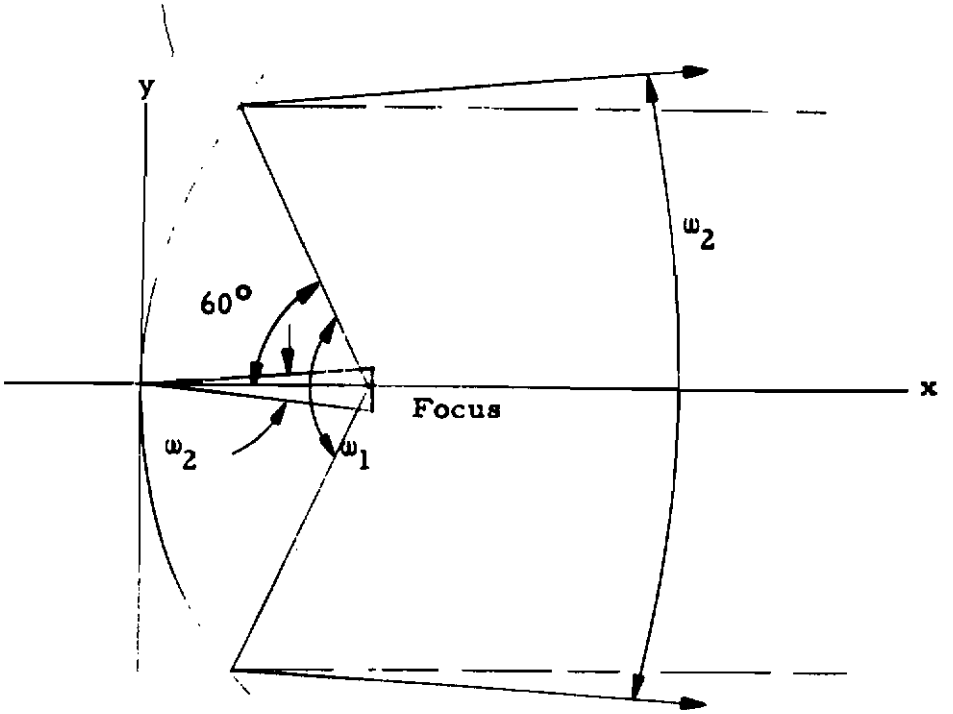

W_1 may be calculated from the conic plane angle 60° by

$$W_1 = 4\pi \sin^2 \frac{\theta}{2}$$

$$W_1 = 4\pi \sin^2 30^\circ = 4\pi (.25)$$

$$W_1 = 3.15 \text{ steradians}$$

Now, for W_2 we must consider the surface contour errors which are assumed distributed. Then the small point arc (2 mm) would appear, if viewed via the imperfect mirror, as extended source. Then W_2 becomes

$$W_2 = 4\pi \sin^2 \left|\frac{1}{2}\right| \cong 10.2 \times 10^{-4} \text{ steradians per } 1/2 \text{ degree error.}$$

Using a surface specular reflectance of 85%, and a typical Xenon 150-watt arc with a luminosity of 3.5×10^2 lumens/steradian, the output beam luminosity I_e becomes, by Equation (1):

$$I_e = .85\,(3.5 \times 10^2)\ \frac{3.14}{10.2 \times 10^{-4}}$$

$I_e = 9.16 \times 10^5$ lumens/steradian, i.e., beam candle power

With this information we now may calculate that distance from the source for which the illumination will decrease to that produced by various familiar sources, such as Polaris, a star of the second visual magnitude.

A standard reference for visual magnitude is a standard candle at a distance of 1 meter which has a visual magnitude of -14.2 and produces an illuminance of 10^{-4} lumens/cm^2 at 1 meter. To calculate the illumination produced by a second magnitude star, considered a nominally acceptable visual object well within the visual threshold, the following relationship between visual magnitude and illumination may be used:

$$n - m = 2.512 \log \left(\frac{L_m}{L_n}\right)$$

where n and m are the visual magnitudes in question and L_m and L_n are their respective illuminances. Solving this for L_n, we obtain

$$L_n = L_m\ 10^{-\left(\frac{n-m}{2.512}\right)} = L_m\ 10^{\left(\frac{m-n}{2.512}\right)}$$

Using n = 2, m = 14.2, and $L_m = {}^{10-4}$ lumens/cm^2, we obtain $L_n = 3.3 \times 10^{-11}$ lumens/cm^2 for the illumination produced by a second magnitude visual object.

The illumination E produced by a source of luminance L_s at distance D is given by the following relation:

$$E = \frac{L_s}{D^2} \qquad (2)$$

The inverse square law, shown above, may be used, provided the largest dimension of the source is less than 1/5 the distance D, without introducing errors in excess of 1%. For our 10-foot diameter parabola, this role would be acceptable for distances greater than 50 feet.

In our case, Equation (2) is rearranged to give D:

$$D = \sqrt{\frac{L_s}{E}} = \sqrt{\frac{9.16 \times 10^5}{3.3 \times 10^{-11}}} = 1.67 \times 10^6 \text{ meters}$$

or

$D \cong 1,000$ miles

It might be pointed out that this figure includes the effects of collector efficiency and surface contour accuracy.

A plot of visual magnitude as a function of distance is shown in Figure 5-37. Plots were made for 150-watt and 500-watt Xenon lamps with parabolas of two different values of surface reflectivity. To provide an approximate reference for the appearance of the reflector at various distances, within the diverging beam, points are marked on the curve corresponding to several familiar sky objects.

These calculations give appearance of the subject source provided the observer is located within the divergent beam, which in this case is about a 2^o cone. An observer outside this cone of light would see only the unreflected arc which would appear about 3000 times dimmer than the "collimated" beam and would probably be indistinguishable, even if pointed out at these distances. Some of this back radiation may be utilized if reflected by a small secondary mirror. A conceptual design of a collapsible sting for a Xenon source is shown in Section 5.4.5. A spherical retro mirror conserves luminance and a finned shield eliminates unwanted glare.

As an aid to the observer in locating and recognizing the beacon, various methods of flashing the beam have been studied. Studies indicate that a flashing rate of 4 cps or less is a definite benefit in locating and keeping continual visual contact with a very low-level light source.* Methods of amplitude modulation initially considered are as follows:

---

*Keesey, U. T., "Visibility of a Stabilized Target as a Function of Luminous Variation," Journal of the American Optical Society, Nov., 1965.

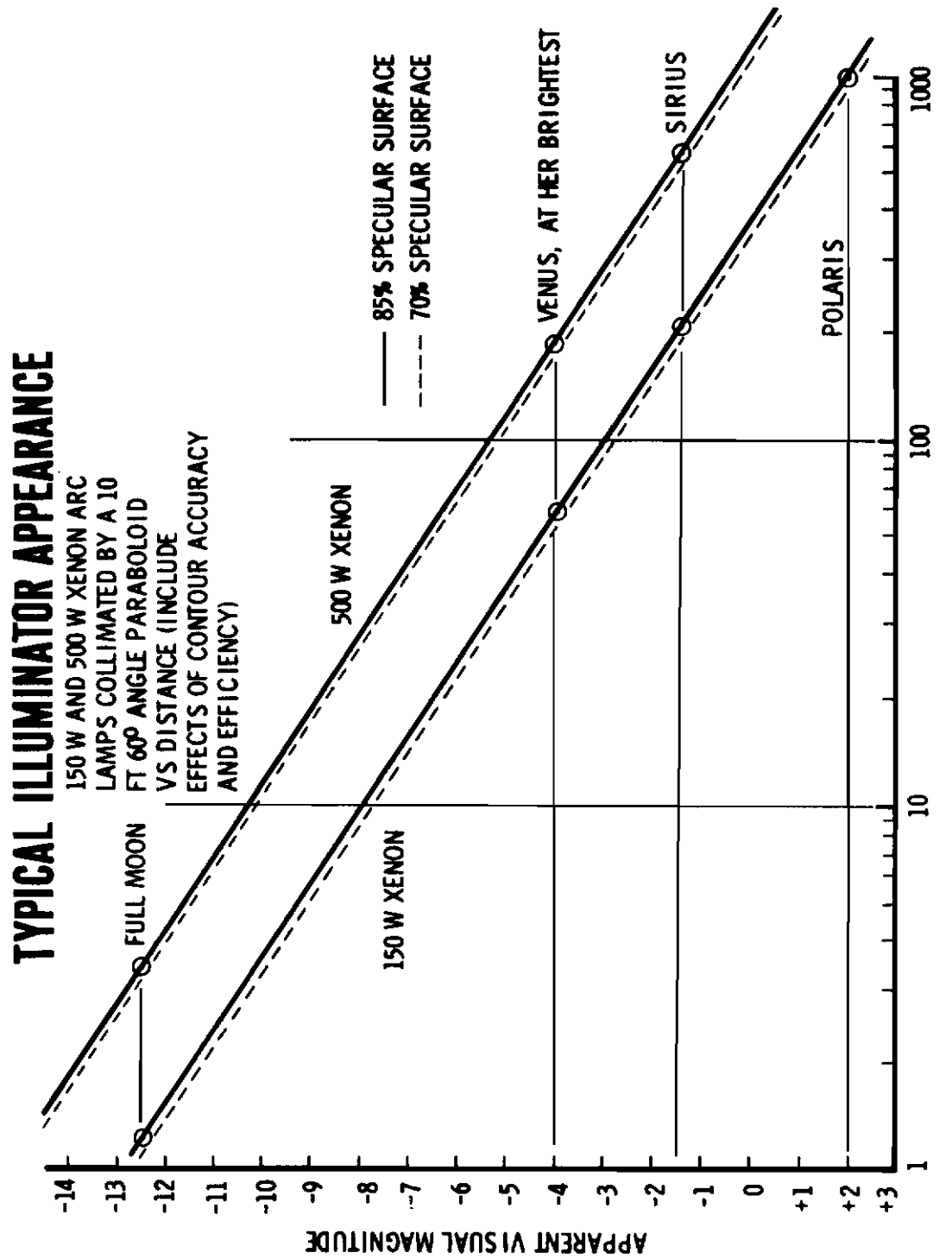

Figure 5-37. Visual Magnitude Versus Distance

a. A lamp that is moved in and out of the focal point along the axis of the parabola will produce a beam that will alternately diverge between a narrow cone and a wide cone and will appear to flash to an observer located within either cone. However, an observer in the wide cone will see a much dimmer light than an observer located in the narrow cone at an equal distance from the reflector. This can be accomplished by mechanizing the collapsible sting shown in Figure 5-35 so that the sting can be retracted and extended at a rate of one or two cycles per second.

b. A mechanical shutter between the lamp and the parabola which will open and close at the proper rate will produce a flashing beam. A plate can be made to move in and out of the optical path, or a cylinder with beam openings cut into it can rotate around the bulb and cause the light to flash.

c. Xenon short arc lamps can operate between a low power "simmer mode" and full power for flashing operation. This is easily accomplished by placing a small resistor in the lamp power line for "simmer" power and shorting around it for full power. Operation in this mode will not affect the life of the bulb. Mercury lamps cannot operate in this mode and neither Mercury nor Xenon lamps will operate in flashing schemes completely turning them off between flashes without greatly reducing the life of the bulb.

At the present time the latter appears to be the best alternative because of the ease with which it can be implemented. Methods (a) and (b) require comparatively large mechanical moving components, while (c) only requires a high current switch such as a transistor and an electronic timing device.

5.5.2 COMMUNICATION LINK

Once another vehicle or station has acquired optical contact with the beacon, and if it is maintained, voice or other information may be used to modulate a Xenon lamp of the type in this discussion. Modulation rates of up to 10 kc are reported possible by various manufacturers.

If the Xenon source is properly shielded to prevent stray light, this mode of communication is limited to receivers within the optical beam axis of the carrier. Optical communications have been experimentally tested on Gemini. Additional electronic circuitry would also

be required to effect the modulation of the lamp, as well as some means of of maintaining proper beam orientation.

Modulation of 95% of the light output is easily accomplished by incorporating an amplifier into the lamp power supply which will control the lamp current at audio frequencies by means of transistors in series with the power line. Several transistors may be placed in parallel (because of the high currents involved), the number depending on rated lamp power.

5.5.3 AUXILIARY SOURCE OF ILLUMINATION

During dark portions of an orbit it may become desirable to have a source of light external to the vehicle for EVA tasks or object identification.

The 10-foot parabola, if artificially illuminated with a Xenon arc lamp, could provide satisfactory light levels up to considerable distances for such applications. Many physical as well as physiological factors must be considered in order to calculate these illumination levels; however, one may examine Figure 5-38 and see that, for the 150-watt lamp at 1.2 miles, the illuminator can produce light levels approximating moonlight. Figure 5-38 also shows the light level produced at different working distances from the collector by the two lamps under consideration.

As EVA tasks will not probably exceed a few hundred feet of range, this illumination source should be quite adequate for simple tasks. Table 5-4 illustrates current good lighting practice under some general working conditions. These values may be compared with Figure 5-38 to evaluate at what range a task of given complexity may be performed if the general conditions are applicable. However, much more study of the problems of lighting work areas in a space environment needs to be done before an accurate evaluation of task complexity against an illumination level given by the reflector can be made. Figure 5-39 shows the minimum size which can be detected for work area objects of varying contrasts as a function of the illumination level.

Recent publications (References 1 and 2) in the field of extra-vehicular task illumination further confirm the necessity of using artificial lighting for continuous illumination of an EVA work area. Natural sources

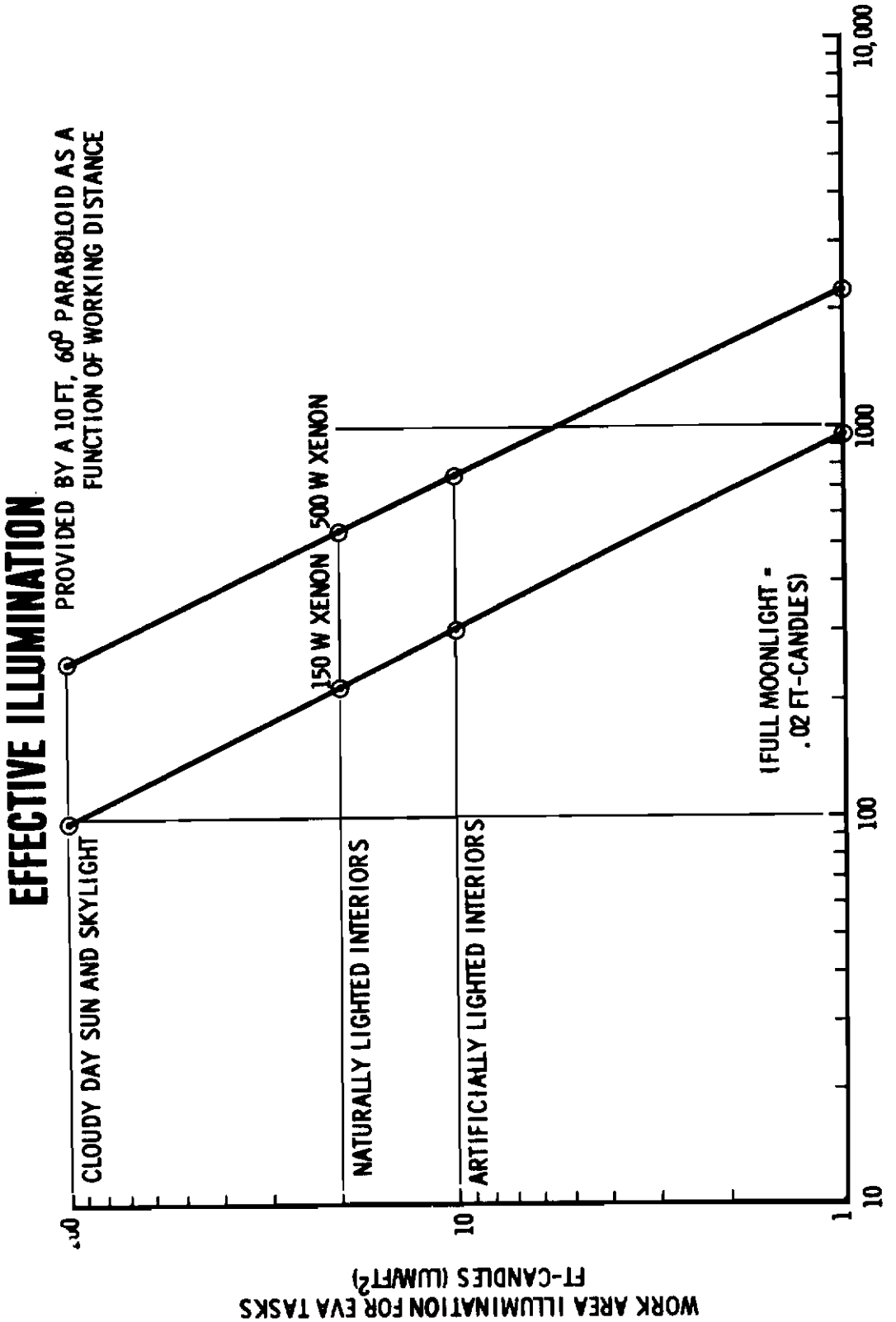

Figure 5-38. EVA Work Area Illumination Versus Distance

Table 5-4 *

RECOMMENDED ILLUMINATION LEVELS FOR GOOD CURRENT LIGHTING PRACTICE

Work Area	Illumination (foot-candles)
Machine Shop	
Rough Bench Work	20
Medium Bench Work, Rough Grinding	30
Fine Machine Work, Buffing, Polishing	100
Extra Fine Machine Work	200
Homes	
Prolonged Study	40
Sewing (medium)	80
Shaving	40
Outside Protective Lighting	0. 2-5

*I. E. S. Lighting Handbook, 1952

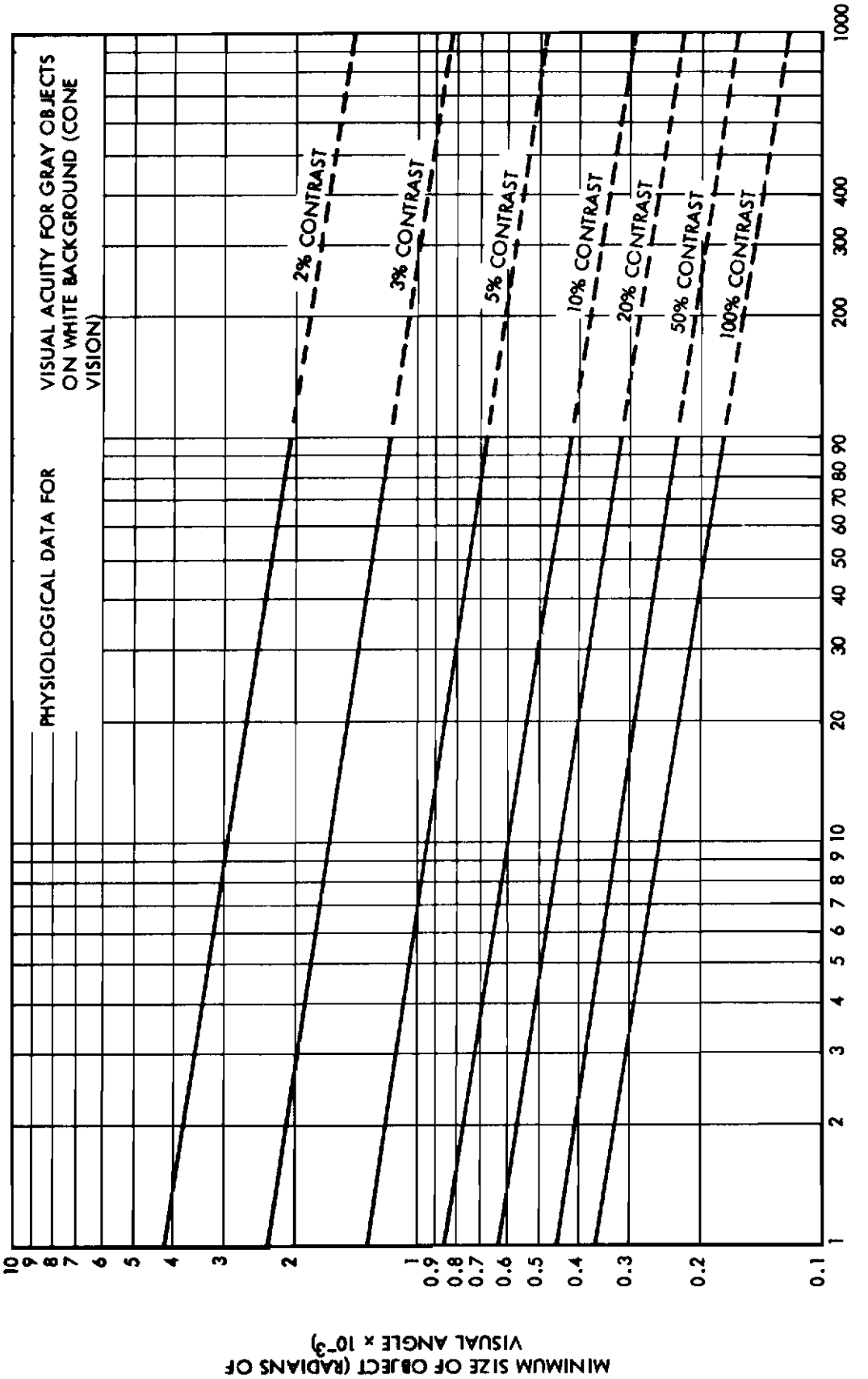

Figure 5-39. Visual Acuity as a Function of Subject Brightness

of light such as the sun, earth, and moon may be too harsh, too weak, or in the incorrect position for proper lighting. Studies by Douglas Aircraft indicate that diffuse lighting is helpful in the recognition of objects and the performance of work under space environment conditions. Reflectors and translucent shades would be especially useful with the Xenon lamp illuminator under consideration for this experiment. Other methods of achieving diffuse lighting, such as a cloud of minute particles and self-luminous surfaces, have been rejected at the present time as being unmanageable or too low-level for this purpose.

5.5.4 PASSIVE DESTRUCTION APPLICATIONS

If the 10-foot paraboloid is affixed with a remote controlled AMU, one may maneuver the AMU to direct the intense heat of the mirror at any desired object by causing the object to pass into the focal point of the mirror. There is immediately a fundamental limit to the size target which may be between the mirror and the sun because of shadowing. One may suggest an alternate surface curvature to circumvent this limitation. Such a configuration might take the form of Hershelean optics, that is, an off-axis paraboloid. With this approach, object targets up to a certain size will in no way eclipse the sun, but a size limitation would still exist unless the basic form of retro-optics was abandoned and straight-through concepts were employed.

The Fresnel zone lens, which suffers from transmission loss and chromatic aberrations for low "f" numbers, is the next logical candidate for this problem. Based on a solar constant of 1.94 cal/cm^2-min, and an 85% efficiency factor, a 10-foot-diameter parabola would deliver approximately 140,000 cal/min into a 1.0-inch-diameter spot at its focus. The thermal damage this would inflict on an object is highly dependent on many factors and cannot be discussed here.

5.5.5 SEARCH

The illuminator may be used for the illumination and location of objects at a distance from the vehicle. As shown in Figure 5-40, even a target of low reflectivity illuminated by the 150-watt Xenon lamp will appear as bright as a second magnitude star at a distance of one-half mile. Studies

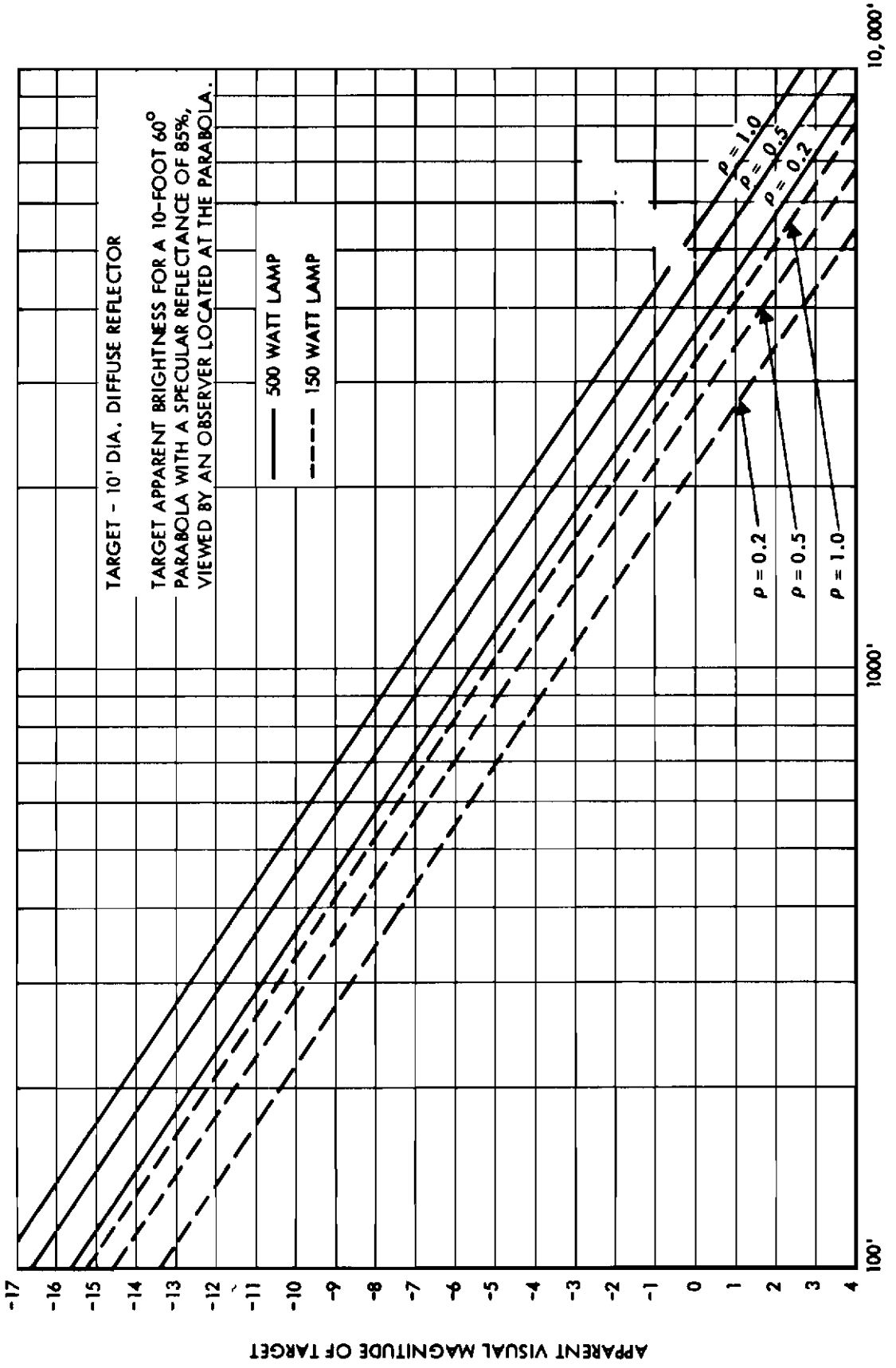

Figure 5-40. Target Brightness Versus Distance

for the 500-watt lamp and targets of various reflectivities are also illustrated in the figure.

Further analysis will be made for specular targets, moving targets, and targets which may be rolling in such a manner as to present only flashes of reflecting light back to the observer. A 100% specular flat target oriented to reflect light back to the observer will appear to be as bright as the parabola viewed at a distance equal to twice the distance between the parabola and the target; but if the target were oriented at a different angle the observer would not be able to detect it.

5.5.6 LAMP SELECTION

Several lamps have been considered for use with the parabola. The types that appear to be the most useful are the Xenon short arc lamps, the Mercury vapor short arc lamp, and the Xenon flash lamp. Each lamp must be examined for its optical properties, luminous properties, operating characteristics, and environmental requirements.

5.5.6.1 XENON SHORT-ARC LAMP

The Xenon short-arc lamp is available in sizes from 35 watts up to several kilowatts. The arc area is well within the one-degree cone which defines the parabola beam spread, it is very stable under continuous operation, and wanders only slightly under modulation or pulsing. Luminous efficiency averages about 20 lumens per watt and 90% of the total flux is contained within a 100° radial cone around the lamp.

The lamp operates on about 20-Vdc only, can be modulated in the audio range, and can be flashed or pulsed from a low-power "simmering" mode. The starting voltage varies from 15 to 30 kilovolts and the base temperature must be kept below 200°C for proper operation.

5.5.6.2 MERCURY VAPOR LAMP

The Mercury vapor lamp is also available in many wattages and the arc areas are well within the cone that defines beam spread for the 10-foot parabola. The arc is stable and the luminous efficiency is about twice that of

the Xenon lamp. The 200-watt and 500-watt lamps will operate on AC or DC, but AC operation shortens the life and affects the arc stability. DC operation varies from 50 to 86 volts.

The starting voltage varies from 5 to 10 kilovolts. The lamp can be modulated only at very low frequencies and cannot be pulsed or flashed. The average life is several times shorter than the Xenon lamp. Cooling and mounting provisions are about the same as the Xenon.

5.5.6.3 XENON FLASH LAMP

The Xenon flash lamp will give high brightness pulses which might be suitable for tracking or modulation. However, the luminous path is 2 inches or longer, making the optical properties poor for reflector applications. Even the helical configuration of the lamp falls outside the cone, making the beam spread rather large. Each pulse requires a high start voltage, which increases the complexity of the power supply.

A continuous wave version of the lamp is available, but the luminous path is also 2 inches or longer, making it also optically poor for use with the parabola.

5.5.6.4 TRADE-OFF ANALYSIS

The Xenon flash lamp is discarded almost immediately because of the long luminous path which produces poor optical source properties.

The Xenon short-arc and the Mercury short-arc lamps are about optically equal when considered for use with the parabola. The luminous efficiency of the Mercury lamp is better by a factor of 2, but since visual magnitude is a function of the log of the candlepower, this factor is diminished.

The Mercury lamp operates at three to four times the DC voltage of the Xenon lamp and thus lowers the current requirement, which might be significant if long lines are necessary.

However, the Xenon lamp is more versatile in that it can be flashed, pulsed, and modulated at audio frequencies. The life expectancy is greater and it can be operated in a reduced power mode. The selection of the Xenon lamp

for a light source makes the parabola useful as an illuminator, rendezvous aid, and searching and communications device without changing the lamp.

Studies indicate that a lamp size in the order of 150 to 500 watts will supply the most useful illumination and, when further studies are made and more information is available about the system power capabilities, the optimum lamp power selection can be made.

5.5.7 LAMP POWER SUPPLY

If 400-cycle power is available, the lamp power conditioner will include a transformer, rectifier circuit, filter, ballast resistor, and starting transformer as shown in Figure 5-41. The power supply load line is equivalent to that which is required by the lamp for proper operation and is also illustrated in Figure 5-41. It will be noted that the peak rectified voltage appears across the lamp before starting and assists start up during the initial breakdown period. A series resistor is also included in the figure; this resistor places the lamp in the "simmer" mode of operation. Alternately opening and closing S2 will produce flashing of the lamp. The modulation circuitry is not shown but can be added by putting an audio amplifier in control of a series transistor in the power supply circuit. The addition of a saturable reactor and a control circuit in the primary of the power transformer would eliminate much of the power loss across the ballast resistor, but would add a weight factor which might be prohibitive.

Operation of the lamp from vehicle DC power would result in a weight savings because the power transformer would be unnecessary, but the control circuit to supply the proper impedance to the lamp becomes complicated if power is to be conserved.

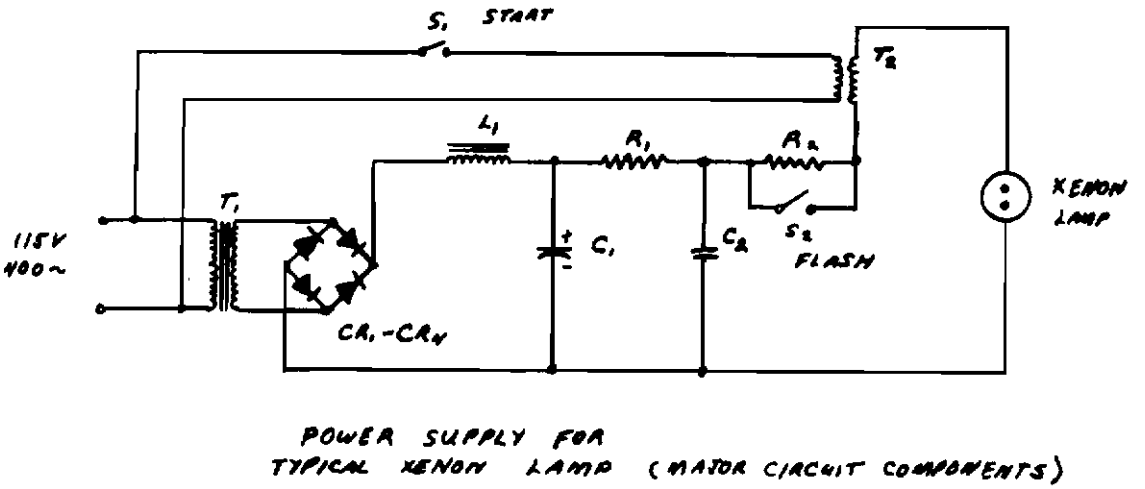

POWER SUPPLY FOR TYPICAL XENON LAMP (MAJOR CIRCUIT COMPONENTS)

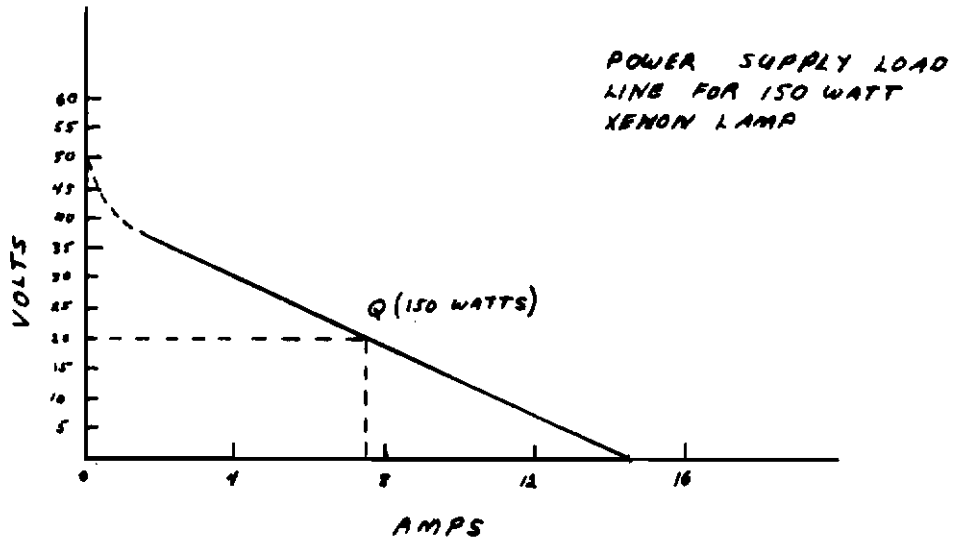

Figure 5-41. Xenon Power Conditioner Schematic and Lamp Power Load Line

Section 6

ENVIRONMENTAL ANALYSIS

The space environment was an important consideration throughout the design study. Some aspects of it are so closely related to specific design areas that they are included there. For example, hard vacuum is a key consideration in the selection of materials and is reflected accordingly in Section 3. Also, zero-g is a fundamental consideration in the Human Factors Analysis and is reflected appropriately in Sections 4.6 and 5.3 of this report. This section covers analyses which can be discussed separately from the detailed design study and includes Thermal, Micrometeoroid, Radiation, and Vacuum Cold Welding.

6.1 THERMAL ANALYSIS

Thermal analyses were made to evaluate the scope of the problem and to indicate where design solutions or direction detailed analysis should go. Both the airlock and parabola were examined in broad terms, with the airlock studied in greater depth. Extensive analyses were not made because they require detailed definition of the design configuration, and therefore were beyond the scope of this contract.

6.1.1 AIRLOCK THERMAL ANALYSIS

The following preliminary analyses and problem evaluations were made.

a. Steady-state temperatures, inside and outside, for a non-rotating cylinder in a circular 200-nautical mile day-night orbit.

b. Evaluation of probable temperatures if the airlock is shaded by the MSL for an extended period of time.

c. Evaluation of heat addition required to maintain the 50°F interior wall temperature under the most adverse conditions.

d. Evaluation of the use of radiation shields as a combined thermal control aid and meteoroid shield.

e. Evaluation of the thermal problem when the airlock houses the astronaut.

The results of these evaluations bound the problem, define potential problem areas, and suggest possible solutions. First, if the airlock were to orbit alone, as evaluated by (b) above, it is anticipated that a passive system for thermal control would be adequate. Temperature limits of -105° to 250°F outside and 50° to 100°F inside could be maintained by proper selection of surface (α/ϵ ratios). However, the airlock is attached to the MSL, and this fact must be included in the thermal evaluation. An accurate numerical evaluation cannot be accomplished without either a great deal of knowledge of the MSL thermal history, or some rather extensive assumptions. However, from an examination of previous experience with the OV3 satellites, it is clear that the lower temperature limits could be exceeded. That is, if the airlock is shaded from the sun by the main vehicle, and there are no internal heat inputs, then the internal temperature will soon fall below 50°F. Its steady-state temperature would probably be below -50°F.

Under the most adverse conditions of space exposure (minimum solar and planetary heat input), the interior of the airlock could be maintained above 50°F with about 100 watts of heating. This might be accomplished with a lamp of either visual or infrared wave length. If radiation shields were incorporated into the meteoroid bumper-shield, a reduction in heat loss would be realized and the required heat addition under the most adverse conditions would be reduced to 50 watts or less. Two to four aluminized mylar barriers would be adequate to accomplish this objective.

At the other extreme, when the airlock is in full sun and an astronaut is using it for its intended purpose, then care must be taken to avoid excessive temperatures because of the additional heat from the human body. Temperature rise rates might be between 2 and 8°F per minute depending on astronaut exertion (i. e., metabolic rate), pressure status, volume, and wall construction.

From the preliminary analysis, it is clear that if orbits and orientations are used that are equivalent to unshaded solar exposure, then the thermal control problem is one of determining the surface coatings. This would be accomplished (and the limits of solar exposure defined) using the orbital and transient nodal digital program.

If the condition where the spacecraft shades the airlock cannot be ruled out, then consideration must be given to:

a. Performing the experiment behind the MSL.

b. Some active heat addition, e.g., IR lamp.

In addition, care must be taken to evaluate the relation with the astronaut heat rejection system.

The purpose of the preliminary analysis was to verify that a chamber of this type and shape could be maintained within the temperature limits of -150° to 250°F outside and 50° to 100°F inside, and to show the general effect of surface finishes on the temperature ranges. The airlock was considered to be a nonrotating cylinder in a circular, 200-nautical mile day-night orbit. The presence of the MSL was ignored, since the orientation and hence the shading effect was not known at this time and could not be reasonably approximated. Figure 6-1 shows the vehicle and orbit relationship. The thermal inputs to the chamber (solar, albedo, and earth shine) were obtained from Reference 1. Using these thermal inputs, a steady-state heat balance was calculated for various points in the orbit considering re-radiation and conduction through the fabric-foam composite wall. Heat capacity and circumferential and longitudinal conduction were not considered in this analysis. Two α/ϵ ratios were investigated. The temperature histories are shown in Figure 6-2 for both α/ϵ ratios. It can be seen that all the temperatures follow the orbit period. This is due to the "steady-state" type of analysis and to the fact that heat storage ability of the wall was not considered. As expected, the α/ϵ of 1.000 produced higher temperatures than the α/ϵ of 0.333. The results show that the outside temperatures are well within the limits for both ratios and the inside temperatures are near the upper and lower limits of 100°F and 50°F, respectively. This indicates that more sophisticated analysis can determine an α/ϵ ratio that would produce outside and inside temperatures safely within the specified limits.

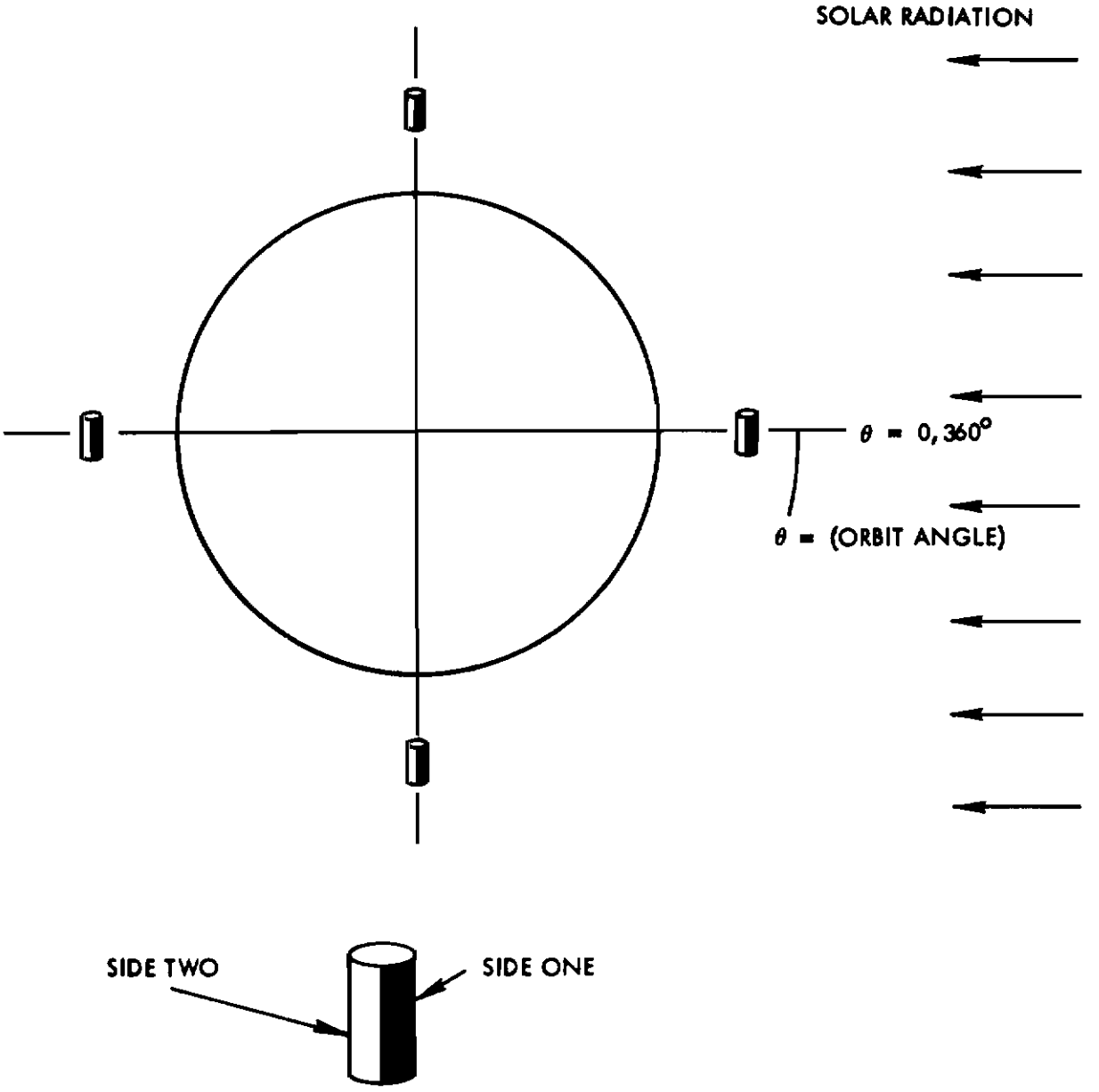

Figure 6-1. Orbit Orientation for Preliminary Analysis

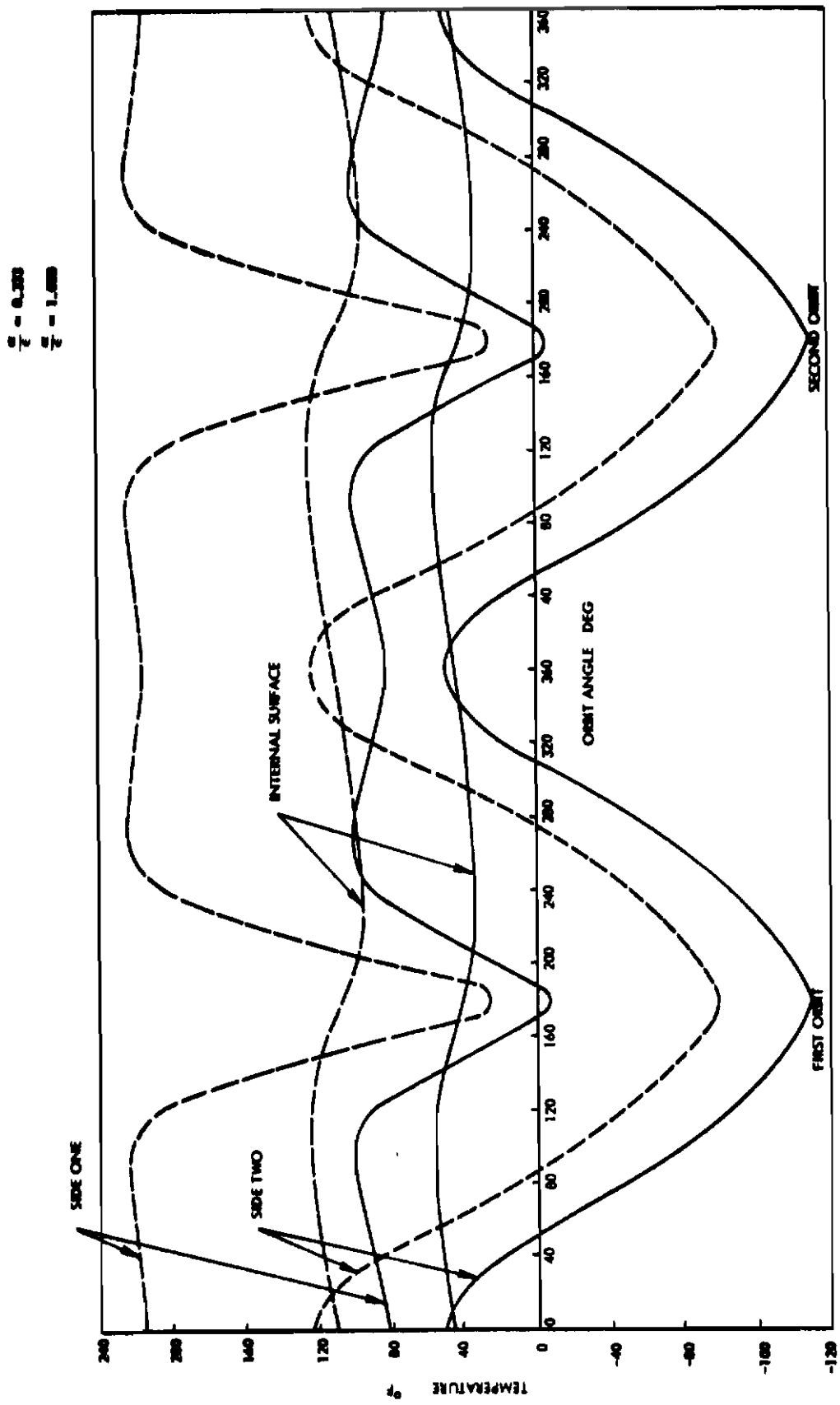

Figure 6-2. Preliminary Estimate of Airlock Temperature

A more advanced analysis will show the temperatures to lag the orbit period by some amount and the temperature range to be less extreme; i. e., the heat capacity of the wall would tend to dampen out the amplitude of the temperature history curve. An advanced analysis should be made for an exact design orbit, and should consider the attitude of the MSL and account for thermal interchanges between the MSL and the airlock. The airlock itself should be broken down into a thermal model and radiant interchange factor should be computed between internal surfaces, and between the outside surface and the MSL by means of the Monte Carlo Radiation Interchange Factors program. Also, the conduction paths between each node, and the heat capacities of each node, should be calculated. The necessary number of different α/ϵ ratios should be investigated so that the proper finish or combinations of finishes can be selected to produce the desired temperature ranges. It appears that an α/ϵ of between 0. 33 and 1. 0 would be satisfactory.

Consideration should be given to all heat sources and sinks, including the following:

a. Direct solar insolation

b. Earth albedo

c. Earth shine

d. Spacecraft

e. Active heat source if used

f. Astronaut rejected heat

g. Space (heat sink)

The performance of the thermal control surfaces could be affected by the rubbing and scuffing of the surface when the airlock is folded into the stored position. An investigation should be made to determine the effect of this folding on the quality of the thermal control surfaces.

6. 1. 2 PARABOLIC STRUCTURES THERMAL ANALYSIS

Limited thermal analysis was made of parabolic structures because a specific design must be defined before a definitive analysis can be made, and

because the analysis is complex and extensive. A definitive analysis is therefore beyond the scope of the contract.

6.1.2.1 THERMAL CONSIDERATIONS

Proper selection of materials, coatings, and fabrication techniques will minimize the effects of the thermal environment. The parabolic structure requires considerable attention in the area of thermal analysis, as surface distortions are of great concern.

Random orientation of the parabola with respect to the sun is an additional complication, in that nonsymmetric thermal gradients across the disk can cause local distortions and should be considered more thoroughly than the case of simple thermal loading. The analysis is further complicated if the surface is considered in discretely supported modules as opposed to a continuous shell of revolution.

One of the most straightforward ways of controlling thermal gradients is with properly selected surface treatments to obtain an optimum α/ϵ ratio. This method of combating thermal distortion is generally more successful than attempting to select structural material having a low coefficient of expansion, as the accompanying thermal conductivity usually varies to offset any optimization.

6.1.2.2 THERMAL ANALYSIS OF HONEYCOMB STRUCTURE

A preliminary analysis has been made of the thermal performance of aluminum honeycomb used as a solar collector or an antenna. The results are shown in Table 6-1. The transverse temperature gradient (ΔT) is based on a 0.30-inch overall thickness aluminum sandwich construction consisting of 0.003-inch skins, 0.29-inch core weighing 3.1 lb/ft^3, and 0.002-inch epoxy cement at each skin-core interface.

The surface finish optical properties used in this analysis are shown in Table 6-2 as well as the maximum temperature if the convex surface of the parabola faced the sun.

Table 6-1

RESULTS OF THERMAL PERFORMANCE PRELIMINARY ANALYSIS

Config. No.	Front Surface Finish	Rear Surface Finish	Front Surface Max Temp *	Max. Steady Steady ΔT**	Thermal Shock	Weight	Fabrication Complexity
1	Chem Polished Alum	Chem Pol Aluminum	402°F	6°F	C	D	B
2	Chem Polished Alum	Optical Black Paint	15°F	12°F	C	C	B
3	Back Surfaced Mirrors	Chem Pol Aluminum	-88°F	0.25°F	D	A	A
4	Silver on Plastic Coat	Chem Pol Aluminum	253°F	3°F	D	A	A
5	Optical Black Paint	Optical Black Paint	155°F	37°F	A	B	C
6	Optical White Paint	Optical White Paint	-16°F	9°F	B	B	C
7	Alzak Aluminum***	Alzak Aluminum	-33°F	7°F	C	C	B
8	Silver on Plastic Coat	Alzak Aluminum	-76°F	4°F	D	A	A

* Front surface normal to sun.

** Measured in a direction parallel to the honeycomb cores with front surface normal to sun.

*** 303 Aluminum base with 99.9% clad electrically brightened and coated with clear anodizing (α_s = .15 ϵ = 077 ρ = .85).

Table 6-2

OPTICAL PROPERTIES OF SURFACE FINISHES AND MAXIMUM TEMPERATURES

Config No.	Front Surface		Rear Surface		Rear Surface	Max Steady
	I-R Emiss	Solar Absorb	I-R Emiss	Solar Absorb	Max Temp *	State ΔT **
1	0.04	0.17	0.04	0.17	402°F	6°F
2	0.04	0.17	0.85	0.85	253°F	3°F
3	0.77	0.06	0.04	0.17	24°F	12°F
4	0.02	0.06	0.04	0.17	465°F	4°F
5	1.00	1.00	1.00	1.00	155°F	37°F
6	0.80	0.24	0.80	0.24	-16°F	9°F
7	0.70	0.18	0.70	0.18	-33°F	7°F
8	0.02	0.06	0.70	0.18	45°F	0.4°F

* Rear surface normal to sun.

** Measured in a direction parallel to honeycomb core with the rear surface facing sun.

The selection of the "best" configuration must be done from a systems standpoint, so no attempt has been made to do this. However, the data in Tables 6-1 and 6-2 would be required inputs to such a selection process.

The maximum temperatures listed in Tables 6-1 and 6-2 are based on the assumptions that the altitude is sufficiently high that the effects of planetary albedo and emission are negligible, and that albedo and emission from the focal plane are negligible. Also, it was assumed in each case that the parabolic surface can be represented approximately as a flat plate. The condition normal to the sun's rays was the only condition considered (Table 6-1).

The column in Table 6-1 labeled "thermal shock" is based on the initial temporal temperature gradient when the reflector is eclipsed by the earth. The configuration with the "A" has the most severe gradient and the configurations with the "D" have the least severe gradient.

The columns labeled "weight" and "fabrication complexity" in Table 6-1 are relative values where the "A" indicates the heaviest and most complexity and "D" the least weight and least complexity.

The painted surfaces will be most subject to degradation over a given time span.

6.2 METEOROID SHIELDING

One of the most critical design considerations imposed by the space environment is the meteoroid hazard. The environment used here is consistent with Air Force and NASA meteoroid environments, and all three are harmonious with meteor, meteoroid, and space microphone data. Cometary stoney, and earth-orbiting meteoroid masses are obtained from this environment, confidence limits on velocity are also given.

The principle of the mechanism of bumper-foam shielding is for the bumper fabric to vaporize the incoming meteoroid; the foam subsequently absorbs the energy of the expanding gas. The foam thickness for 0.9999 probability of no penetration is based on a 7.10^{-3}-gram meteoroid impacting between

36 and 38 km/sec; a proposed design can furnish the required shielding for less than 0.2 lb/ft^2.

The bumper fabric thickness is not determined by the largest expected meteoroid (cometary), but by the densest and slowest. A $1.7 \cdot 10^{-4}$-gram stone impacting at 13 km/sec requires more than 0.1 lb/ft^2 bumper; to meet the requirements for both stones and cometaries, Space-General selects 0.15 lb/ft^2. However, slower earth-orbiting meteoroids could dictate a still greater thickness and may in fact require a relaxation of the 0.9999 probability of no penetration of the shield (to perhaps 0.999). The extreme problem posed by these particles is given in detail in this section.

Special caution must be taken to avoid two pitfalls: (1) application of recent hypervelocity metal penetration experiments in space to define the environment for bumper-foam shielding would yield nearly an order of magnitude false sense of security; (2) meteoroids less numerous than cometaries (and hence unimportant for design of metal shielding) must not be neglected here. To do so would result in a bumper fabric too thin by more than a factor of 2 with at least an order of magnitude real increase in the probability of penetration of the foam. Micrometeoroid testing should be performed to validate the composites shielding effectiveness to verify past test results and prove the supporting analysis.

6.2.1 METEOROID ENVIRONMENT

The meteoroid environment was the subject of considerable hypothesizing and investigation in the early 1960's. Out of this work a semblance of agreement has been attained as to the total meteoroid flux in the range of 10^{-5} to 1 gram.

The Air Force standard flux rate density in this range was worked out by V. C. Frost in 1964 (Reference 2). Frost's integrated flux in mass in grams is given by:

$$\frac{U}{A_s T} = \left(K + F \frac{A_p}{A_s}\right) S_E N \qquad (6\text{-}1)$$

where:

$$\log N = -1.34 \log m - 10.423 \qquad (6\text{-}2)$$

For 30 days in a 200 n.m. orbit K = 1.75, F = 0.92 and S_E = 0.64. In Equation (6-1) Frost takes into account meteoroid showers (F), seasonal variations in the flux (K, F), and earth-shielding effects (S_E). A_s is total surface area, and A_p is projected area. The symbols are discussed in some detail in Reference 2. The NASA standard flux rate density (Reference 3) is essentially the same (but neglects seasonal variations in the sporadic flux).

Parkinson separates the environment into its component parts in Reference 4. The cometary particle flux is:

$$\log N_c = 13.68 - \frac{5}{3} \sqrt{|\log m + 12|^2 + 8^2} \qquad (6\text{-}3)$$

The (extrapolated) earth-orbiting flux at 200 n. m. is:

$$\log N_E = -12.66 - \frac{5}{3} \log m \qquad (6\text{-}4)$$

And the (extrapolated) stoney flux is:

$$\log N_s = -11.21 - \log m \qquad (6\text{-}5)$$

where each flux is given per ft^2 day. Then $N = N_c + N_E + N_s$. Equations (6-3), (6-4), and (6-5) have taken into account effects of earth-shielding, gravitational concentration and orbital decay of earth-orbiting meteoroids, but have neglected showers (letting F = O) and seasonal variations (letting K = 1).

It should be mentioned that in the neighborhood of 10^{-7} to 10^{-8} particles/ft^2 day, both the earth-orbiting and stoney fluxes have been extrapolated. The earth-orbiting flux above 10^{-6} gram has been measured by Explorer 8 (Reference 5), and is produced by an orbiting collision process for which the theoretical mass exponent is negative 5/3 (Reference 6). Accurate extrapolation of this earth-orbiting flux to regions less than the cometary flux either follows the straight line of Figure 6-3 or falls below it. To date, no experiments have been capable of isolating this component for measurement below 10^{-6} gm. The stoney flux follows Hawkins (Reference 7). Its extrapolation to 10^{-3} gram is probably good. In fact, Mariner 4 may have extended it to 10^{-11} gram.

The environments of Frost and Parkinson are compared in Figure 6-3 and are seen to be in excellent agreement. See Cautionary Note.

CAUTIONARY NOTE

There is a temptation to look for data supporting a less severe environment. The Pegasus meteoroid experiments have been interpreted by some to mean the total meteoroid flux is much lower than indicated in Figure 6-3. Figure 6-3 is based on photographic meteor data with additional inputs extrapolated from meteorite finds, space microphone experiments, and even zodiacal light. (Tentative

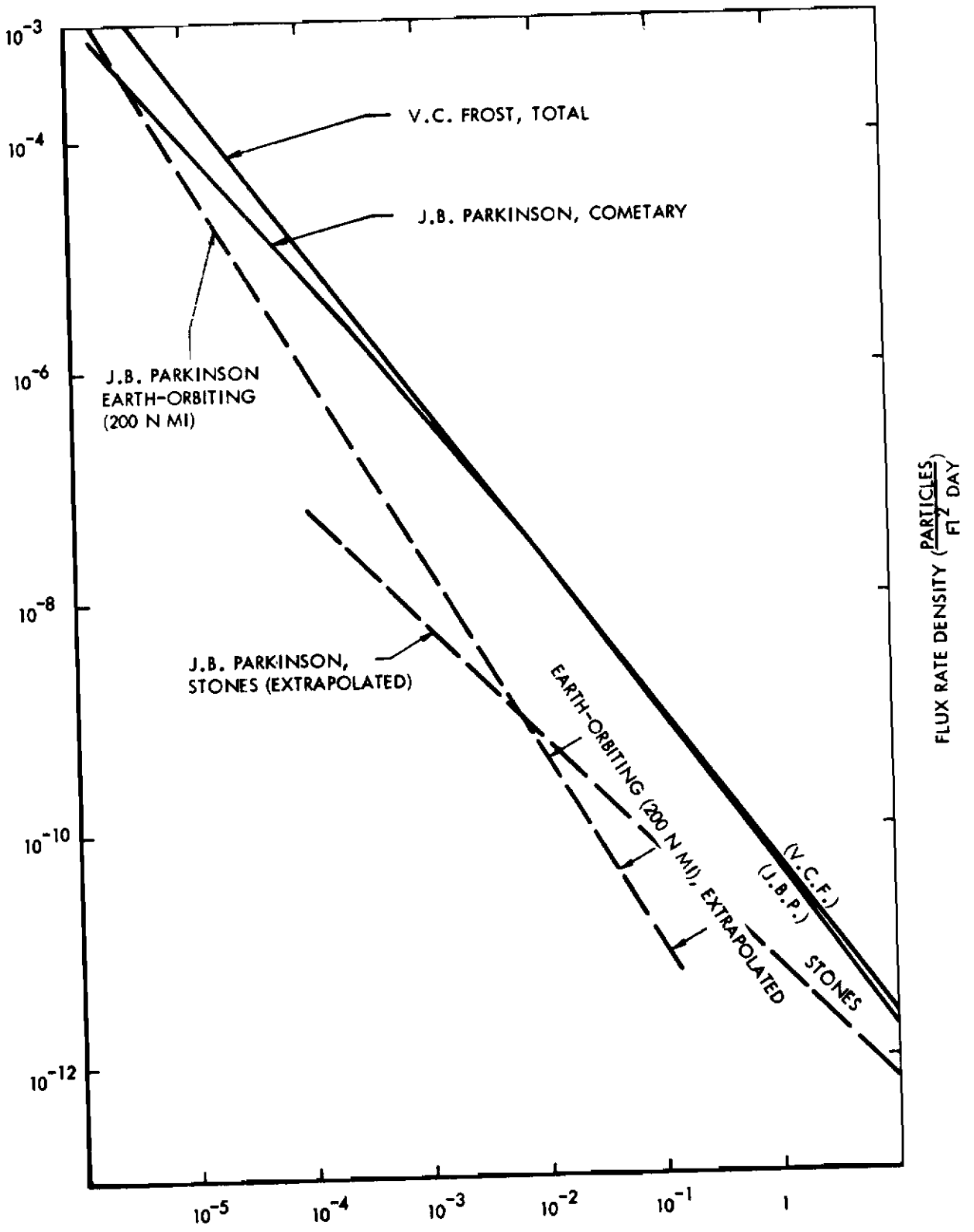

Figure 6-3. Meteoroid Environments

reports of radiometer data around 10^{-4} gm are somewhat higher than Figure 6-3.) There is a special temptation here to use lower data (Pegasus) where the meteoroid design is so critical. However, the Pegasus data today represent two inseparable experiments: (1) flux rate density and (2) hypervelocity penetration of polycrystalline metal. Laboratory hypervelocity testing has not yet been able to simulate the densities and velocities of cometary meteoroids. And the hypersonic-supersonic-crystal lattice mechanism of cratering in polycrystalline solids is entirely different from the vaporize-and-absorb mechanism for bumpered foams. Therefore, Pegasus data are very useful for designing metal shielding, but are not yet applicable to defining the meteoroid environment for foam shielding. (However, combining the environment of Figure 6-3 with the Pegasus data implies that porous cometary meteoroids are less destructive to metals than metal projectiles of the same size and velocity.) An attempt to substitute some recent interpretations of the Pegasus data for photographic meteor data will yield a false sense of security - by nearly an order-of-magnitude.

6.2.2 IMPACT PROBABILITIES

The airlock is to be 30 days in a 200 nmi circular orbit. The spherical configuration has a 65 ft^2 exposed area plus 24 ft^2 of hatch. The meteoroid hazard calculations will be based on about 90 ft^2. The airlock exposure is therefore 30 x 90 = 2700 ft^2 days.

The probability of no penetration is to be 0.9999. Thus, the desired mean flux rate density is no greater than:

$$N = \frac{2700\ ft^2\ day}{1.0-0.9999} = 2.7 \cdot 10^7\ ft^2\ day \qquad (6\text{-}6)$$

From Figure 6-3 it may be seen that $2.7 \cdot 10^{7}$ ft^2 days corresponds to a $7 \cdot 10^{-3}$ gram cometary particle, or an earth-orbiting particle no larger than $7 \cdot 10^{-4}$ gram, or a $1.7 \cdot 10^{-4}$ gram stoney particle.

The mean velocity of cometary particles at 200 nmi is about 22 km/sec with a 1σ interval of 18-35 km/sec, a 2σ interval of 14/61 km/sec, and a 3σ interval of 12.5-75 km/sec. The velocity of earth-orbiting particles at 200 nmi is 8-9 km/sec, with a 1-sigma interval of perhaps 15-25 km/sec. In no event will cometary or stoney particles have less than the 11 km/sec escape velocity. These velocities do not, however, represent the impacting velocity with an orbiting satellite.

The probability that an omnidirectional meteoroid flux with velocity Vm and vehicle orbiting with velocity V_o will impact with relative velocity less than V_r is

$$P_{3x} = 1/2 - \frac{V_o}{4 V_m} \left[1 + \frac{V_m^2}{V_o} - \frac{V_r^2}{V_o} \right] \qquad (6\text{-}7)$$

which may be obtained by straightforward integration over solid angle and vector velocity relations. The same probability in two dimensions (more nearly applicable to Earth-orbiting particles and circular-orbiting vehicles) is

$$P_{2x} = \frac{1}{\pi} \cos^{-1} \frac{V_o}{2 V_m} \left[1 + \frac{V_m^2}{V_o} + \frac{V_r^2}{V_o} \right] \qquad (6\text{-}8)$$

Using Equations (6-7) and (6-8) one may obtain probabilities of impact velocity extremes.

Orbital velocity in a 200 nmi circular orbit is 7.6 km/sec. There is a 1-sigma confidence that a 35 km/sec cometary particle will not impact with a velocity higher than 38 km/sec. There is a 10% chance each that an 18 km/sec cometary (or stoney) meteoroid will impact with a velocity as low as 12.7 km/sec, and there is no chance of impact as low as 10 km/sec. There is a 1-sigma confidence that an Earth-orbiting meteoroid will impact with a velocity no lower than 8 km/sec; there is a 10% chance as low as 3 km/sec.

6.2.3 PUNCTURE ANALYSIS

The principle for shielding against meteoroids with organic foams is a two-step process. An outer fabric is used to first break up the meteoroid (whether by vaporization, or merely by melting) and then the foam absorbs the kinetic energy of the expanding debris (whether gas or liquid). When the ability of the shield to protect against meteoroids is compared with the meteoroid environment a suitable shield can be designed for any desired degree of confidence. In contrast to design of metal shielding, the calculation of organic foam shielding is simple in principle and straightforward in practice.

An Experimental Penetration Test

A Space-General 1.15 lb/ft^3 (0.018 gm/cm^3) polyurethane foam with a 6 mil (0.0152 cm) dacron cloth bumper has been tested at WPAFB with a $7 \cdot 10^{-4}$ gram mylar slug at 10.065 km/sec. For purposes of comparison, the anticipated penetration is calculated here. The mylar slug would have had an equivalent diameter of at least

$$d_{eq} = \left(\frac{6}{\pi} \frac{m}{\rho}\right)^{1/3} = \frac{6}{\pi}\left(\frac{7 \cdot 10^{-4} \text{ gm}}{1.38 \text{ gm/cm}^3}\right)^{1/3} = 0.10 \text{ cm}$$

The energy of the slug was

$$Ep = \frac{1}{2} mv^2 = \frac{7 \cdot 10^{-4} \text{ gm } (1.0065 \cdot 10^6 \text{ cm/sec})^2}{2} = 3.5\ 10^8 \text{ erg}$$

$$= 0.0087 \text{ kcal}$$

The slug must impact with a mass of dacron at least equal to the projected area, of

$$M_b \geq \frac{\pi}{4} \rho_t d^2 \Delta Z \geq \frac{\pi}{4}\ 1.38 \text{ gm/cm}^3\ (0.10 \text{ cm})^2\ \ 0.0152 \text{ cm}$$

$$= 1.6 \cdot 10^{-4} \text{ gm}$$

The energy lost by the slug on impact is, therefore, at least*

$$\frac{\Delta E_p}{m} = \frac{v^2/2}{\left(\frac{m}{M} + 1\right)^2} = \frac{1/2\ (1.0065 \cdot 10^6\ \text{cm/sec})^2}{\left(\frac{7 \cdot 10^{-4}}{1.6 \cdot 10^{-4}} + 1\right)^2}$$

$$= 1.7 \cdot 10^{10}\ \frac{\text{erg}}{\text{gm}}$$

Now assume the slug vapor expands in a cone of 45° half-angle (quite typical). For a given mean penetration, p, a volume, V, is removed

$$V = \frac{2}{3}\ \pi\ p^2 \left(1 - \frac{\sqrt{2}}{2}\right) p = 0.614\ p^3$$

The energy to melt polyurethene foam is about 0.2 kcal/gm, while the additional energy to decompose it is at least 1.0 kcal/gm (and possibly as high as 1.5 kcal/gm). Therefore, as the expanding slug vapor decomposes the foam, the foam will absorb at least 1.2 kcal/gm. If now the penetration, P_{in}, is expressed in inches or energy E it will be absorbed

$$E = 1.2\ \rho V\ \frac{\text{kcal}}{\text{gm}} = 0.22\ p_{in}^3\ \text{kcal/in}^3$$

Therefore, (neglecting energy losses in passing through the bumper) the mean penetration should be

$$P_{in} = \left(\frac{E_p\ \text{in}^3}{0.22\ \text{kcal}}\right)^{1/3} = \left(\frac{0.0087}{0.22}\ \text{in}^3\right)^{1/3} = 0.34\ \text{inch}$$

---

*This equation represents the kinetic energy lost by the projectile (in a projectile coordinate system) and therefore gained by it as thermal energy. Since the momentum balance is $mv = (M + m)\ v_2$,

$$\frac{\Delta E_p}{m} = \frac{1}{2}\ (\Delta v)^2 = \frac{1}{2}\ \left(v - v_2\right)^2 = \frac{1}{2}\ \left(v - \frac{mv}{M \pm m}\right)^2$$

$$= \frac{v^2/2}{\left(\frac{m}{M} + 1\right)^2}\ .$$

The experimental result was penetration varying from 1/4 to 3/8 inch, which certainly represents excellent agreement with the calculated 0.34 inch.

6.2.4 METEOROID PROTECTION DESIGN

To obtain a 0.9999 probability of no penetration with 50 percent confidence for 30 days, it has been shown that one must design for a $7 \cdot 10^{-3}$ gram cometary particle. The impact velocity will be no greater that 38 km/sec for a 1 sigma confidence level. However, other kinds of particles must be considered.

The first step is the design of the fabric bumper. As above, a meteoroid impacting a fabric bumper gains a thermal energy per unit mass* of

$$\frac{\Delta E}{m}_p = \frac{v^2/2}{\left(\frac{m}{M} + 1\right)^2} = \frac{12}{\left(\frac{m}{M} + 1\right)^2} \left(\frac{v}{10 \text{ km/sec}}\right)^2 \frac{\text{kcal}}{\text{gm}} \qquad (6\text{-}9)$$

where

$$\frac{m}{M} = \frac{2}{3} \frac{\rho_p d_p}{\rho_t Z_t} \quad \text{and} \quad dp = \left(\frac{6\, m}{\pi \rho_p}\right)^{1/3} \qquad (6\text{-}9a)$$

m is projectile (meteoroid) mass

M is mass cored out of the bumper (fabric)

ρ_p is projectile (meteoroid) density

ρ_t is bumper fabric density

d_p is projectile (meteoroid) diameter

Z_t is bumper (fabric) density

v is impact velocity

---

* Note: Effects due to the divergence of bumper fragments are usually more than compensated for by the effective increase is bumper thickness due to oblique impact. Both effects are therefore neglected here.

The bumper will successfully vaporize the meteoroid if the specific energy of Equation (6-9) is much greater than the vaporization energy of the meteoroid. Vaporization energies for meteoroids are: cometary particles (ρ = 0.4 gm/cm^3), no greater than 0.7 kcal/gm; stones and earth-orbiting particles (ρ = 3 gm/cm^3), 1-2 kcal/gm (Z).

It is evident from Equation (6-9) that the low velocity particles determine the bumper fabric thickness (i.e., they are harder to vaporize). Also, the thickness of the bumper fabric will be determined not by the heaviest impacting particle cometary) but by the densest impacting particle (stone or earth-orbiting). This is illustrated in the following calculation (design) for cometary and stone particles. The largest cometary particle to be designed against is $7 \cdot 10^{-3}$ gm; its impact velocity certainly should not be expected less than 12.7 km/sec. Thus, from Equation (6-9)

$$\frac{12}{\left(\frac{m}{M} + 1\right)^2} \left(\frac{12.7}{10}\right)^2 \frac{\text{kcal}}{\text{gm}} > 0.7 \frac{\text{kcal}}{\text{gm}}$$

from which

$$\frac{m}{M} < 4.26, \text{ and therefore}$$

$$\rho_t Z_t = \frac{2}{3} \frac{\rho_p d_p}{m/M} = \frac{2}{3} \frac{\rho_p}{m/M} \left(\frac{6}{\pi} \frac{m}{\rho_p}\right)^{1/3}$$

$$> \frac{2}{3} \frac{0.4}{4.26} \left(\frac{6}{\pi} \frac{7 \cdot 10^{-3}}{0.4}\right)^{1/3} = 0.02 \frac{\text{gm}}{\text{cm}^2} = 0.04 \frac{\text{lb}}{\text{ft}^2} \qquad (6\text{-}10)$$

The largest stoney particle to be designed against is $1.7 \cdot 10^{-4}$ gm; its impact velocity will be not less than 12.7 km/sec, to a 1 sigma confidence. Thus, repeating the above procedure

$$\frac{12}{\left(\frac{m}{M} + 1\right)^2} \left(\frac{12.7}{10}\right)^2 \frac{\text{kcal}}{\text{gm}} > 2 \frac{\text{kcal}}{\text{gm}}$$

from which $\frac{m}{M} < 2.11$ and therefore

$$\rho_t Z_t > \frac{2}{3} \frac{3}{2.11} \left(\frac{6}{\pi} \frac{1.7 \cdot 10^{-4}}{3} \right)^{1/3} = 0.045 \frac{gm}{cm^2} = 0.09 \frac{lb}{ft^2} \quad (6\text{-}11)$$

which is more than twice the bumper thickness required by cometary meteoroids.

Thus far, the influence of earth-orbiting meteoroids on bumper-design has not been discussed. A calculation based on the largest earth-orbiting meteoroid consistent with P = 0.9999 ($7 \cdot 10^{-4}$ gm) at the most probable impact velocity (11 km/sec) yields a bumper thickness

$$\frac{m}{M} < 1.7, \ \rho_t Z_t > \frac{2}{3} \frac{3}{1.7} \left(\frac{6}{\pi} \frac{7 \cdot 10^{-4}}{3} \right)^{1/3}$$

$$= 0.09 \frac{gm}{cm^2} = \frac{lb}{ft^2} \quad (6\text{-}12a)$$

If the same calculation were based on the 1 sigma minimum velocity of 8 km/sec

$$\rho_t Z_t = 0.16 \frac{gm}{cm^2} = 0.33 \frac{lb}{ft^2} \quad (6\text{-}12b)$$

If it were based on the 90 percent confidence velocity of 3 km/sec no bumper thickness is sufficient to vaporize the particle. Around (1/2) gm/cm^2 $\left(1 \frac{lb}{ft^2}\right)$ of solid dacron shielding would be required to stop the particle.

It is proposed to make the dacron bumper 0.15 lb/ft^2 thick- sufficient to insure complete vaporization of all stoney and cometary particles to allow the full 0.9999 probability of success. However, if earth-orbiting meteoroids should prove as numerous as an extrapolation of known data indicates (Explorer 8, etc. - see previous discussion), it is proposed that the probability of no penetration through the bumper and foam (alone) be relaxed. Should the earth-orbiting meteoroids be so dense, and should the criterion be relaxed, a 0.999 probability of no penetration of the airlock is still in prospect.

Assuming all particles are successfully vaporized, the most energetic particle will penetrate deepest. Thus, the foam thickness will be based on a 7.10^{-3} gm cometary meteoroid. There is a 1-sigma confidence its impact velocity will not exceed 38 km/sec (50% confidence is 36 km/sec).

The total energy of all debris leaving the bumper is equal to the kinetic energy of the incident meteoroid:

$$E = 1/2\ 7\cdot10^{-3}\ \text{gm}\ (3.8\cdot10^{6}\ \text{cm/sec})^2 = 5.1\cdot10^{10}\ \text{erg}$$
$$= 1.2\ \text{kcal} \qquad (6\text{-}13)$$

We continue to use the 45 degree spherical sector for the volume of foam consumed in absorbing the energy of the gas cloud:

$$V + 0.614\ p^3 \qquad (6\text{-}14)$$

so that the total energy absorbed is

$$E = 1.2\ \rho V\ \frac{\text{kcal}}{\text{gm}} = 0.74\ \rho p^3\ \frac{\text{kcal}}{\text{gm}} \qquad (6\text{-}15a)$$

If we choose to express ρ in lb/ft^3 and p in inches, Equation (6-15a) becomes

$$E = 0.193\ \rho p^3\ \text{kcal} \qquad (6\text{-}15b)$$

Thus the product $\rho^{1/3}p$ to absorb the 1.2 kcal (Equation (6-13)) becomes

$$\rho^{1/3}p = \left(\frac{1.2\ \text{kcal}}{0.193\ \text{kcal}}\right)^{1/3} = 1.84\left(\frac{\text{lb}}{\text{ft}^3}\right)^{1/3}\ \text{inch} \qquad (6\text{-}16)$$

For a 1.2 lb/ft^3 foam the thickness must be

$$p = 1.74\ \text{inch} \qquad \left(\rho p = 0.174\ \frac{\text{lb}}{\text{ft}^3}\right) \qquad (6\text{-}17)$$

Or, to maintain a 1.5 inch thickness, the density must be

$$\rho = \left(\frac{1.84}{1.5}\right)^3 = 1.85\ \frac{\text{lb}}{\text{ft}^3} \qquad \left(\rho p = 0.174\ \frac{\text{lb}}{\text{ft}^2}\right) \qquad (6\text{-}18)$$

(There is therefore a weight savings in using minimum foam density.)

There is another device available to reduce total foam thickness with some increase in weight and complexity. Material density far from the bumper fabric is more effective than near it, as is to be inferred from Equation (6-16). Density increases in the last 20-30% of foam are very effective. One method for reducing total foam thickness of 1.74 inch in Equation (6-17) to 1.5 inch is to insert a 0.04 lb/ft^2 polyurethane film about 1.3 inch behind the bumper fabric. Another is to use 1.2 lb/ft^3 polyurethane foam for 1.25 inch behind the bumper fabric, and 3 lb/ft^3 foam in the final 0.25 inch. Either approach yields a 0.19 lb/ft^2 foam thickness.

The hatches are to be made of about 0.030 inch of aluminum. There is about 10% chance of penetration of the bare outer hatch during the 30-day exposure. Since foam-bumper shielding can be made much higher than metal shielding, the hatch should also be protected by foam-bumper shielding to provide an equal probability of no penetration.

6.2.5 SELECTED OTHER PENETRATION TESTS

The Air Force contractor on the MOL Crew Transfer Tunnel (Reference 8) has run several tests on a 2 inch, 1.2 lb/ft^3 foam with and without a 0.041 lb/ft^2 (0.02 gm/cm^2) bumper; the projectile was estimated at $4.81\ (\pm 1.38)\cdot 10^{-3}$ gm with velocities in the range 7-10 km/sec. They claim "the specimen with the bumper wall removed showed barrier penetration similar to the specimens with bumper walls" (although their pictures on Page 104 of Reference 8 appear to show more material removed from the unbumpered foam by the particle). A quick calculation reveals the reason: For the expected mylar particle ($5 \cdot 10^{-3}$ gm) mass ratio of particle to the bumper cored out by it is

$$\frac{m}{M} = \frac{2}{3}\frac{\rho_p d_p}{\rho_t z_t} = \frac{2}{3}\frac{1.38\ \frac{gm}{cm^3}}{0.02\ \frac{gm}{cm^2}}\left(\frac{6.5\cdot 10^{-3}}{1.38}\right)^{1/3} = 8.7$$

Thus at the mean velocity (9 km/sec) the particle leaving the bumper has gained thermal energy

$$\frac{E_\rho}{m} = \frac{12}{\left(\frac{m}{M} + 1\right)^2} \left(\frac{v}{10\ \text{km/sec}}\right)^2 \frac{\text{kcal}}{\text{gm}} \frac{12}{(8.7 + 1)^2} (0.9)^2 = 0.10 \frac{\text{kcal}}{\text{gm}}$$

Since the vaporization energy for mylar is also about 0.1 $\frac{\text{kcal}}{\text{gm}}$ it is likely that some (if not all) of each incident particle was not vaporized by the bumper. (Divergence of bumper fragments could account for it.) Hence, the anomalous result is not surprising. A thicker bumper (0.05-0.1 lb/ft^2) should certainly have vaporized the particle and exploited the fuller shielding capability of the foam. It is therefore unfortunate they draw from the tests the conclusion that "it is questionable whether or not the bumper wall would be necessary from a micrometeoroid protection standpoint."

For an easily vaporized particle such as mylar ($\Delta Hv \sim 0.1$ kcal/gm) the bumper may or may not make an enormous difference. But to extrapolate to meteoroids with vaporization energies of order 1 kcal/gm (10 times larger) is unsound and will lead to questionable results. The projectile mass and velocities in these tests are certainly in the range of interest, but the test specimens were inadequate to exploit the potential of foam-bumper shielding.

One Air Force contractor analyzing rigidized fluted core systems has taken an intelligent approach to the foam-bumper shielding problem, in building an open truss-structure bumper in front of the foam shield. This allows considerable dispersion of the spray leaving the bumper before the foam stops it. Holten (Reference 10) found that this structure was penetrated only 0.43 lb/ft^2 by a 5 mg mylar slug near 9 km/sec, as opposed to 0.6 lb/ft^2 or lighter for other structures tested. (Note that the above-mentioned test of the Space-General specimen, for a meteoroid of half the diameter at 10 km/sec, penetrated only 0.08 lb/ft^2; this is equivalent to 0.15 lb/ft^2 for a 5 mg mylar slug at 9 km/sec.)

6.3 RADIATION

The radiation hazard for 30 days in a low inclination 200-nautical miles orbit is essentially negligible. The maximum ionizing radiation hazard is from solar flares (ca 1970) and is still much less than 100 rads. A dose of 100 rads is not enough to make a healthy man ill, much less damage the airlock. Trapped radiation at low magnetic latitudes does not reach down to 200-nautical miles, as the atmosphere is too dense. Ultraviolet radiation, atmospheric particle collisions, and the neutron albedo are all unimportant also.

The trapped radiation (Van Allen) belts constitute no hazard to the airlock in a 200-nautical mile low inclination orbit. The expected electron and proton dose environments for 1968 (Reference 11) are given in Figures 6-4 and 6-5, based on the environments of James I. Vette of Aerospace (Reference 12). It will be noted that for 3.4 mg/cm^2 shielding (about 1 mil dacron-essentially no shielding) the 300-nautical mile equatorial orbit suffers only 1 rad/day from electrons and still less from protons. Therefore it is safe to conclude that at 200-nautical miles, essentially no trapped radiation will be encountered.

Ionizing radiation from solar flares and cosmic rays will also not be a problem. If the orbital inclination is less than 50° the magnetic latitude can be no greater than 65° at any time. Particles of less than 100 Mev cannot penetrate below 65° magnetic latitude and therefore can never be a problem. Reference 13 suggests an equation for the annual flux of protons above 100 Mev, based on the compilations of McDonald (Reference 14) and Lewis, et. al. (Reference 15), from which in 1970 about $5 \cdot 10^8$ proton/cm^2 could be expected. It is worthy of note that 10^9 proton/cm^2 above 100 Mev has never been recorded in any year (References 14 and 15). The conversion to dose is $1\text{-}2 \cdot 10^7$ rads per proton/cm^2 (Reference 1, Figure 6), depending on spectral distribution above 100 Mev. Therefore, the dose of protons received by the airlock from solar flares is certainly less than 100 rads. The 30-day primary cosmic ray dose will be much less than the solar flare dose, and its maximum is during solar minimum and vice versa.

Radiation damage suffered by most organic materials is dependent upon total energy absorbed, and only slightly dependent on the type of ionizing

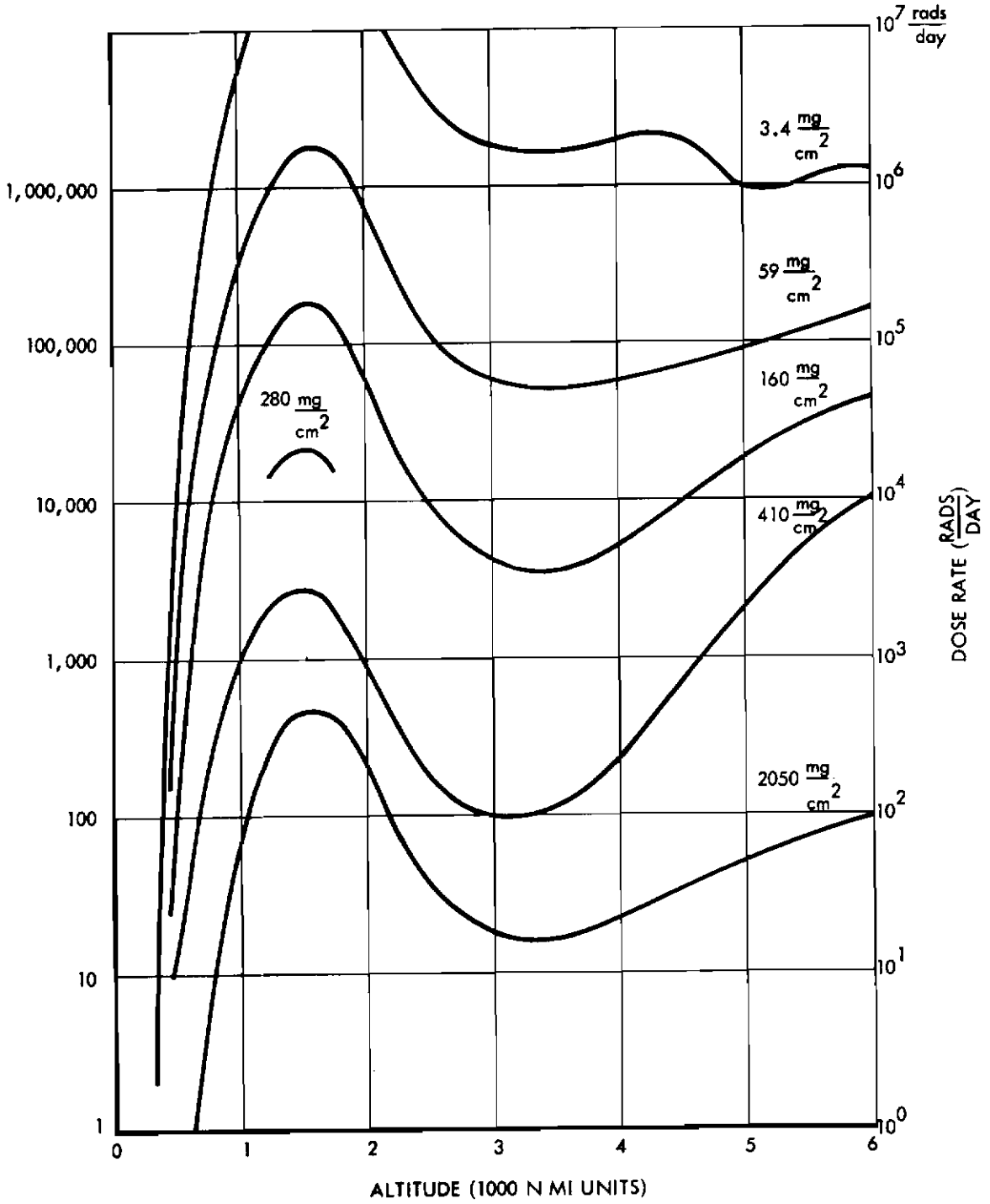

Figure 6-4. Electron Dose Rates, 1968

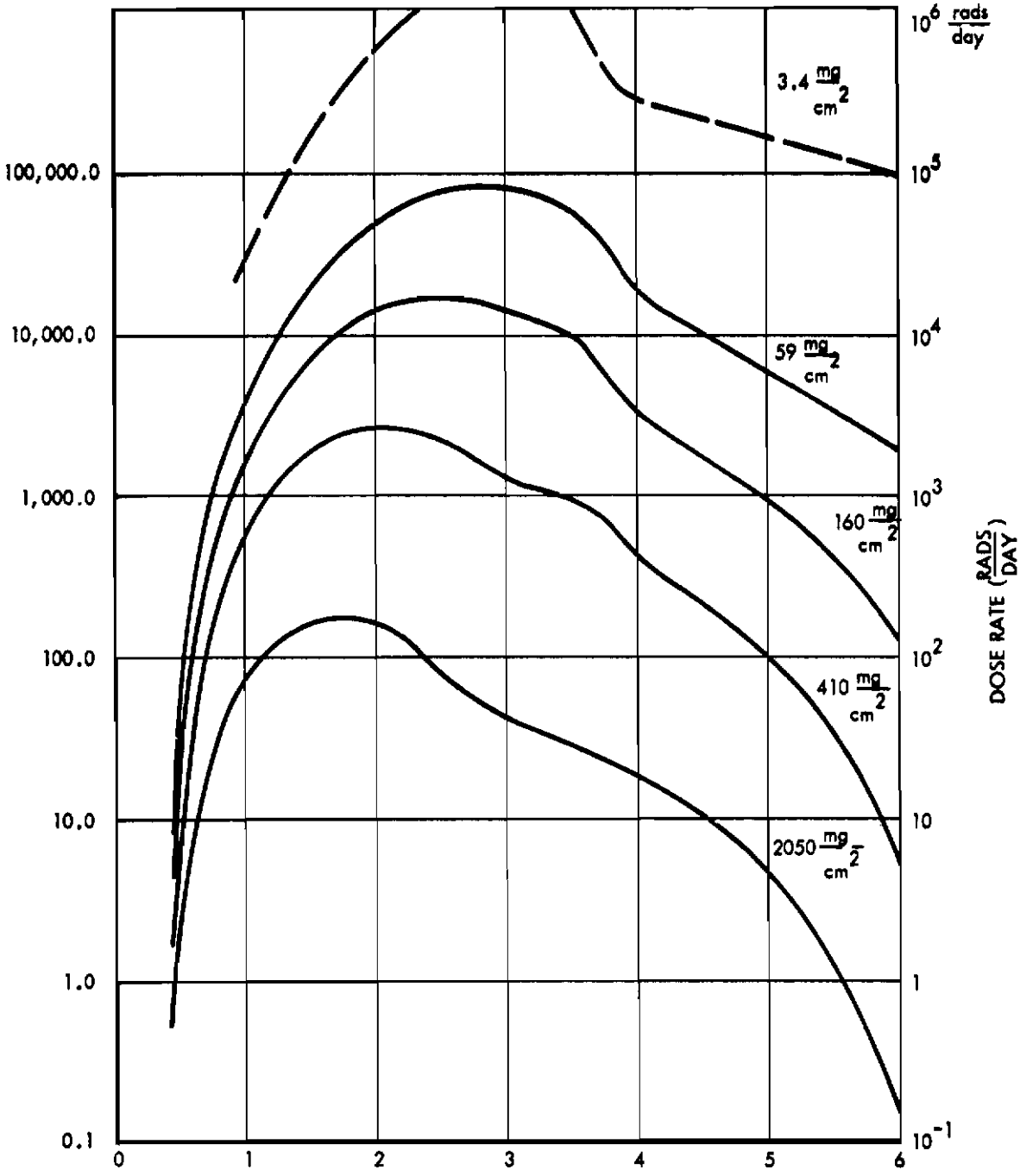

Figure 6-5. Proton Dose Rates, 1968

radiation, because damage is by destruction of the chemical bonds. J. W. Gordon (Reference 16) is an investigation of materials for extreme environments and gives 10^5 rads as a minimum damage threshold for a class of organic insulations, specifically including both polyurethane and mylar (which is dacron when produced as a fibre). Human beings do not even get nauseated from as little as 100 rads. Therefore it is safe to conclude that ionizing radiation is no problem to any part of the airlock system for 30 days in a low-inclination 200-nautical mile orbit.

Ultraviolet radiation effects during 30 days will be small or negligible. Effects of collisions with atmospheric (exospheric) particles will be completely negligible during 30 days (except perhaps in terms of orbital decay). The neutron albedo flux will contribute less than 0.01 rad over the 30-day period, and is also negligible.

6.4 VACUUM COLD WELDING CONSIDERATIONS

The behavior of materials exposed to the vacuum existent in a 160 to 300-nautical mile (10^{-7} to 10^{-9} torr) orbit results in various unique phenomena, including "cold welding". Cold welding can occur when the normally protective contact films or interfacially absorbed gaseous layers between mating surfaces, which are relative motion to each other, are no longer present. (Although this is principally a metallic problem, certain plastics display a tendency toward this effect.) The movement of mating surfaces in this experiment extend from rotating joints (booms) to mechanical connections, such as tongue-and-groove joints and canister latches to electrical connections (sliding contacts, relays, and switches). Typically, the surfaces of these items are microscopically rough so that the area of true contact is only a small fraction of the apparent contact area. High localized temperatures (frictional heating) and contact pressures are therefore generated at the points of contact (to the extent that the surfaces are "clean" -- to gaseous or fluid interface). The increase in temperature aids the removal of such interfaces. The force necessary to shear these welded joint junctions also increases. Thus, for example, a heavier duty motor would be required to extend or rotate the boom.

The "clean" surface results when there is sufficient vacuum to remove and prevent the return of surface contaminants (lubricants, coatings, dirt, etc.) and, subsequently, the surface metallic equilibrium vapors. Thus, a layer of gas one molecule thick will form on a metal surface in about one second at 10^{-6} torr. The "monolayer time" increases to about 20 minutes at 10^{-9} torr. Automatically, clean surfaces can be achieved when the total pressure due to absorbable gases is lowered to approximately 10^{-10} torr or less (Reference 17).

This entire process (outgassing) is a function of three other processes: evaporation, sublimation, and desorption. The rate of outgassing of a pure material can be approximated by the classical Knudsen-Langmuir equation (Reference 18). A more precise determination of most engineering materials must also consider the effects of diffusion rates, barrier layers, e.g., oxides), and changing composition as outgassing proceeds.

The metal's oxide will prevent the sublimation of the metal itself. Therefore, presence of oxides minimizes cold welding. Since, as in the case of the metals (Reference 19), the oxides vary in their rates of outgassing, a different oxide can often be chosen which has a lower vapor pressure (Reference 20).

The following precautions will also minimize cold welding for 10^{-7} to 10^{-10} torr environment.

a. Moving mating surfaces should be kept at a minimum.

b. Select bearing surfaces which are dissimilar, mutually insoluble, and with maximum hardness and lowest volatility.

c. A minimum use of tight tolerances for all moving parts should be maintained where possible.

d. Use tenacious but soft (low shear stress) surface films (not stripped away by the vacuum) which reduce the coefficient of friction.

e. If loading permits, the use of metallic-to-nonmetallic mating surfaces is indicated, such as steel Teflon. Where the loading does not permit this type of mating surface, phosphate or chromate passivating coatings should be used when these specific moieties are Thermodynamically and/or Vacuum Stable.

f. Use solid lubricants, such as molybdenum disulfide, tungsten, disulfide, or niobium diselenide. The latter material possesses the best combination of electrical conductivity and high-vacuum/high temperature stability. Graphite lubricants should not be used below 10^{-4} torr.

g. For single time movements as with a tongue-and-groove interconnect joint, the requirements are not as stringent as for the duty cycle movements, and the use of a solid lubricant coating between the mating parts should suffice. Care must be exercised, however, in avoiding collection of dust on the moving parts.

h. For duty cycled moving parts, additional precautions are indicated:

   (1) Use filled, porous metal surfaces (e.g., Teflon, Kel-F, or niobium diselenide in porous steel or brass metal bearing surfaces) to minimize metal surface contact areas.

   (2) Provide sufficient protection to eliminate collection of dust where long interval transient duty cycle is involved.

i. Provide provisions for dissipating any heat generated during extended duty cycles, if necessary, for operational efficiency and reliability.

Although the above discussion has been devoted to cold welding, it should be noted that the significance of this particular effect of a vacuum upon the materials themselves is often overshadowed by the deposition of outgassed products upon other materials and/or components in their vicinity. These could readily include other moving mating surfaces.

6.5 ATMOSPHERIC DRAG

In order to examine the effects of employing large diameter parabolas on orbiting vehicles, a preliminary analysis was conducted to indicate the magnitude of atmospheric drag imposed to a hypothetical vehicle for a 10-foot and 100-foot diameter parabolic antenna or solar collector. While this analysis is based on a vehicle mass of only 3000 pounds, it serves to indicate a relative order of magnitude of the drag effect on orbit degradation. It will be noted that the drag effect is largely dependent on the solar cycle as it affects the upper atmospheric density by a considerable amount.

Atmospheric drag causes orbital attitude to decrease in time. Orbital decay rates have been calculated from the equation.

$$\frac{\Delta r}{r-1} = \frac{2\pi\rho r}{(w/C_D A)} \frac{r}{r-1} \text{ per orbit}$$

$$= \frac{39,115\,\rho}{(w/C_D A)} \frac{r^{1/2} R_E^{3/2}}{r-1} \text{ per year} \qquad (6\text{-}19)$$

Atmospheric densities vary as a function of the solar cycle and of the local Earth time. The Harris-Priester models (NASA TND-1444) have been adopted here, because they are believed accurate within a factor of two. The Harris-Priester "S" as a function of the solar cycle is (range of monthly averages, and yearly average).

1975	95-115, 100	1979	160-280, 225	1983	100-150, 110
1976	100-180, 135	1980	130-260, 180	1984	95-110, 100
1977	130-300, 210	1981	100-210, 145	1985	95-105, 100
1978	170-300, 250	1982	100-180, 125		

The atmospheric densities at various altitudes averaged over circular orbits are given in Table 6-3. The orbital decay rates thus calculated are given in Table 6-4, and in Figures 6-6 and 6-7. A few simple examples will illustrate their use:

Consider a 3000-pound satellite with a 100-foot diameter antenna perpendicular to the velocity vector in an 800 km polar orbit. Then we may read directly its decay rates for various years between 1975 and 1985.

1975	1.2% per year
1978	88% per year
1981	7.5% per year
1985	1.2% per year

For the years in between, interpolation is required. (1975-1985 represents exactly one solar cycle.) Note that where the decay rate is greater than 5-10%, new values should be taken from the graphs; e.g., the 800 km orbit in 1978 would actually last for only one or two months (one month if the orbit is in the noon-midnight plane, and two months if in the dawn-twilight plane).

Table 6-3

ATMOSPHERIC DENSITIES

(gm/cm^3)

	1975	1978**	1981	1985	11-year Average
150 km	$2.9 \cdot 10^{-12} \pm 1\%$	$3.0 \cdot 10^{-12} \pm 1\%$*	$2.9 \cdot 10^{-12} \pm 1\%$*	$2.9 \cdot 10^{-12} \pm 1\%$*	$2.9 \cdot 10^{-13}$
200	$2.4 \cdot 10^{-13} \pm 2\%$	$4.9 \cdot 10^{-13} \pm 1\%$	$3.4 \cdot 10^{-13} \pm 2\%$	$2.4 \cdot 10^{-13} \pm 2\%$	$3.4 \cdot 10^{-13}$
300	$1.1 \cdot 10^{-14} \pm 10\%$	$6.3 \cdot 10^{-14} \pm 4\%$	$2.5 \cdot 10^{-14} \pm 10\%$	$1.1 \cdot 10^{-14} \pm 10\%$	$3.0 \cdot 10^{-14}$
500	$1.9 \cdot 10^{-16} \pm 30\%$	$44 \cdot 10^{-16} \pm 10\%$	$8.4 \cdot 10^{-16} \pm 20\%$	$1.9 \cdot 10^{-16} \pm 30\%$	$17 \cdot 10^{-16}$
800	$3.6 \cdot 10^{-18} \pm 35\%$	$260 \cdot 10^{-18} \pm 20\%$	$22 \cdot 10^{-18} \pm 40\%$	$3.6 \cdot 10^{-18} \pm 35\%$	$80 \cdot 10^{-18}$
1100	$6.4 \cdot 10^{-19} \pm 15\%$	$285 \cdot 10^{-19} \pm 35\%$	$20 \cdot 10^{-19} \pm 30\%$	$6.4 \cdot 10^{-19} \pm 15\%$	$87 \cdot 10^{-19}$
1600	$1.1 \cdot 10^{-19} \pm 25\%$	$21 \cdot 10^{-19} \pm 35\%$	$3.5 \cdot 10^{-19} \pm 15\%$	$1.1 \cdot 10^{-19} \pm 25\%$	$7.4 \cdot 10^{-19}$
2050	$3.1 \cdot 10^{-20} \pm 35\%$	$60 \cdot 10^{-20} \pm 15\%$	$12 \cdot 10^{-20} \pm 25\%$	$3.1 \cdot 10^{-20} \pm 35\%$	$22 \cdot 10^{-20}$

* Maximum seasonal variation for polar orbit (add for orbit in noon-moonlight plane; subtract for dawn-twilight plane). No seasonal variation for equatorial orbit. Seasonal variations average out over one year for all orbits.

** Values depend strongly upon solar activity; expected average is given. Values will vary temporarily by factors from 1.0 to 10.

Table 6-4

ORBITAL DECAY RATES

$$\frac{\Delta r}{r-1} = \frac{\Delta h}{h} \quad \text{per year}$$

w = 3,000 lb d = 100 ft C_D = 3.0

	1975	1978	1981	1985	11-year Average
150 km	50,000 ± 1%*	52,000 ± 1%*	50,000 ± 1%*	50,000 ± 1%*	50,500
200	3,100 ± 2%	6,400 ± 1%	4,400 ± 2%	3,100 ± 2%	4,500
300	100 ±10%	500 ± 4%	200 ±10%	100 ±10%	200
500	1.0 ±30%	24 ±10%	4.6 ±20%	1.0 ±30%	8.6
800	0.012 ±35%	0.88 ±20%	0.075 ±40%	0.012 ±35%	0.27
1100	0.0015 ±15%	0.072 ±35%	0.0050 ±30%	0.0015 ±15%	0.022
1600	0.0022 ±25%	0.0038 ±35%	0.0006 ±15%	0.0002 ±25%	0.0015
2050	0.00005 ±35%	0.0009 ±15%	0.0002 ±25%	0.00005 ±35%	0.0003

*Maximum seasonal variation for polar orbit (add for orbit in noon-moonlight plane; subtract for dawn-twilight plane). No seasonal variation for equatorial orbit. Seasonal variations average out over one year for all orbits.

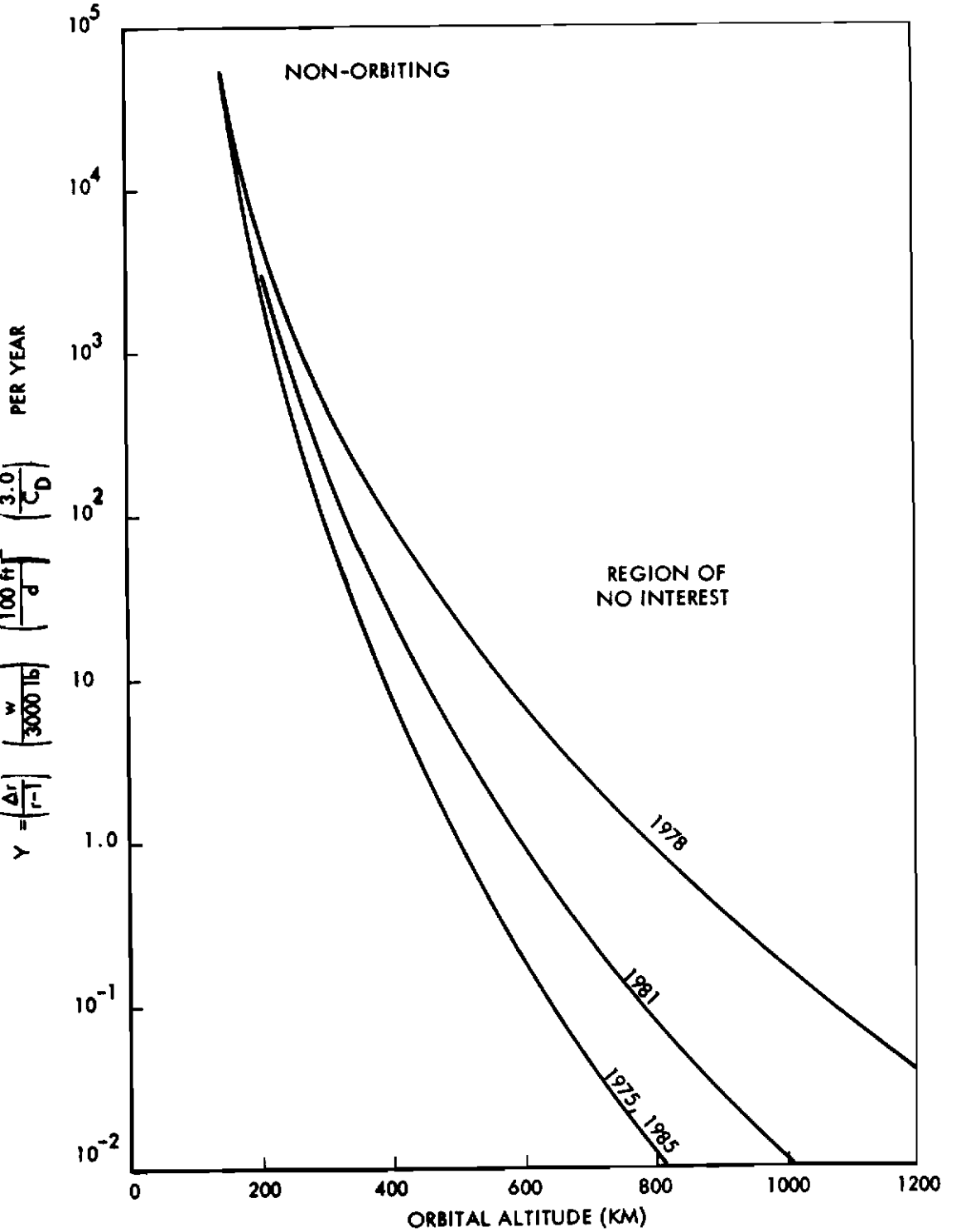

Figure 6-6. Orbital Decay Rates, 1975-1985

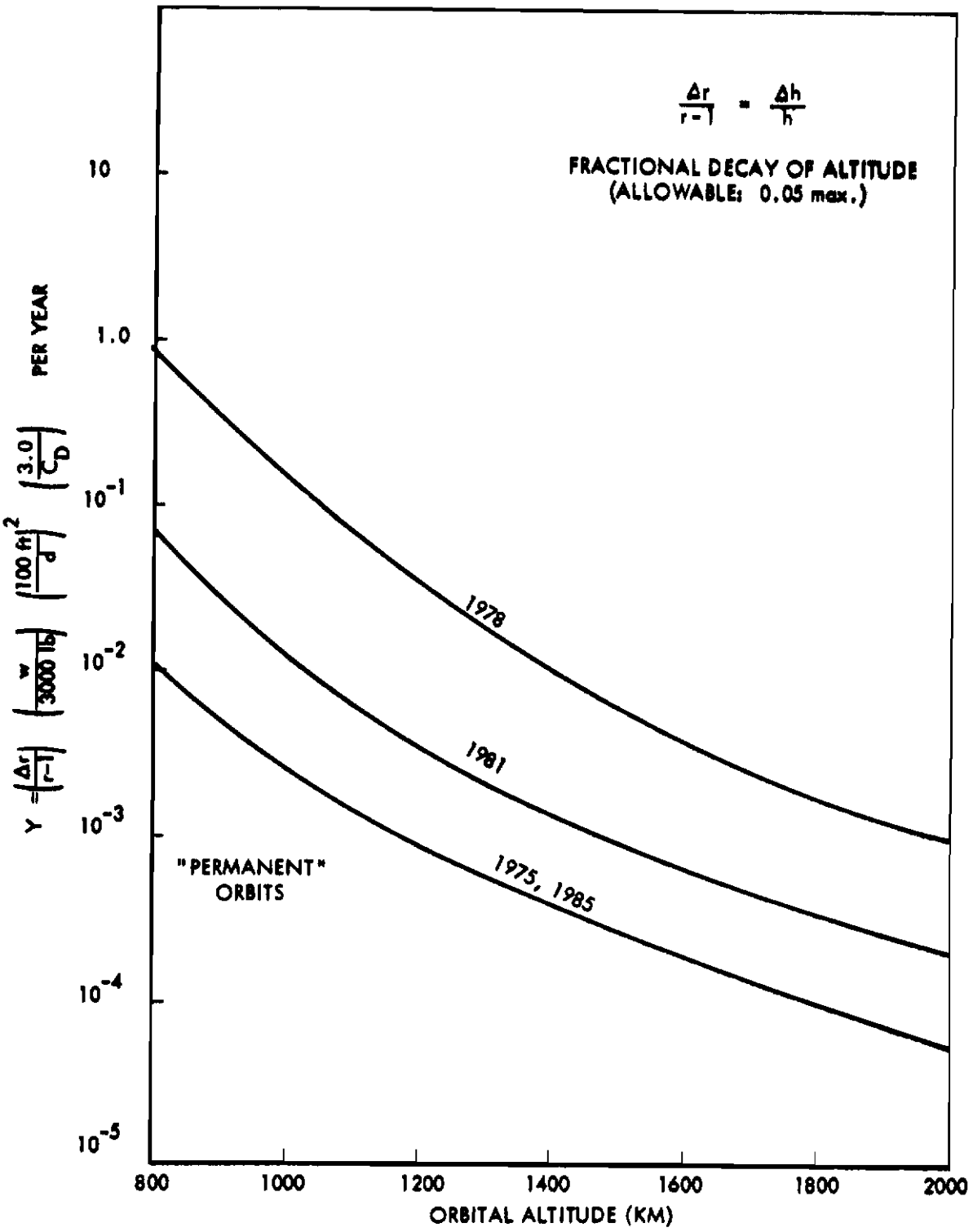

Figure 6-7. Orbital Decay Rates, 1975-1985

If instead the antenna is only 10 feet in diameter, the figures above must be multiplied by $\left(\frac{10\text{ ft}}{100\text{ ft}}\right)^2$ or

1975	0.012% per year
1978	0.88% per year
1981	0.075% per year
1985	0.012% per year

Averaged over 11 years time, the decay rate is roughly the average of the 1975, 1978, and 1981 values, or 0.3% per year.

If there were no (or a negligibly small) antenna, a 3000-pound satellite might be a sphere 4 feet in diameter. For this case, let $C_D = 2.4$. Then in 1978, the decay rate would be

$$\frac{\Delta r}{r\text{-}1} = 0.88\left(\frac{4\text{ ft}}{100\text{ ft}}\right)^2\left(\frac{2.4}{3.0}\right)\text{ per year}$$

$$= 0.0011\text{ per year} \approx 0.1\%\text{ per year}$$

which for all practical purposes is a permanent orbit.

6.6 REFERENCES

1. "R. J. Chesner, "Incident Thermal Radiation and Horizontal and Vertical Cylinders and 15° Half-Angle Cones in Noon Orbits", Lockheed Missiles and Space Co., TXA129, January 12, 1960.

2. Wright-Patterson Air Force Base Purchase Request 22583, Attachment B, 13 August 1964, and reprinted many times since.

3. Paige B. Burbank, Burton G. Conr-Palais, and William E. McAllum, "A Meteoroid Environment for Near-Earth, Cislunar, and Near-Lunar Operations"; NASA TND-2747, April 1965.

4. W. Jenisch, Jr., and J. B. Parkinson, "Space Environment Criteria"; Aerojet-General Report 3147, January 1966, Contract NAS 8-11285.

5. C. W. McCraken and W. M. Alexander, "The Distribution of Small Interplanetary Dust in the Vicinity of the Earth"; NASA TND-1349, July 1962.

6. J. B. Parkinson, "Notes on Geocentric Meteoroids" (unpublished).

7. Gerald S. Hawkins, "Interplanetary Debris Near the Earth"; Annual Review of Astronomy and Astrophysics 2, pp. 149-164 (1964).

8. A Prototype Lunar Meteoroid Detector; Space-General Corp., P-6745, 20 July 1966.

9. T. L. Hoffman, "Utilization of Elastic Recovery Materials for the Development of Crew Transfer Tunnels, Airlocks, and Space Maintenance Hangars, Part II"; Wright-Patterson Air Force Base, Technical Report AFAPL-TR-66-2, Part II (June 1966).

10. Andre J. Holten, "Simulator of Meteoroid Impact Effects"; 2nd Aerospace Expandable Structures Conference, Minneapolis, 25-27 May 1965, AFAPL-TR-65-108.

11. J. B. Parkinson, "Environment and Radiation Dose Rates", Space-General internal correspondence to L. B. Wilker, 5140:vt:MO950 of 29 April 1966.

12. James L Vette, "Environments AP1-AP4, and Orbital Integration for Projected 1968 Electron Environment" (unpublished).

13. W. Jenisch, Jr., and J. B. Parkinson, "Space Environment Criteria", Aerojet-General Corp., Report 3147, January 1966. Contract NAS 8-11285.

14. Solar Proton Manual, ed. Frank B. McDonald, NASA X-611-52-122 (Goddard Space Flight Center), 1962.

15. L. R. Lewis, G. M. Brown, J. Gabler, and R. M. Magee, "Solar Flares Radiation Survey," RTD-TDR-63-3044 under Contract AF 29-5224 (December 1963).

16. J. W. Gordon, "Radiation Effects Considerations on Materials in Cryogenic Systems of Nuclear Rockets", in IRE Transactions on Nuclear Science, NS-9, 1 January 1962.

17. "An Ultra-High Vacuum Chamber for Space Simulation", J. C. Simons, Jr., National Research Corporation, Sixth National Symposium on Vacuum Technology, 7-9 October 1959.

18. "A Preliminary Report on Behavior of Materials in a Vacuum", MM-65-11, S. L. Lieberman, Space-General Corp., 4 June 1965.

19. "Evaporation Effects on Materials in Space", L. D. Jaffe and J. B. Rittenhouse, JPL TR No. 32-161, 30 October 1961.

20. "Space Environment on Materials", WADD TR-60-721, J. H. Atkins, et al. National Research Corporation, December 1960.

Section 7

EXPERIMENT DEFINITION SUMMARY

7.1 PRELIMINARY EXPERIMENT DEFINITION SUMMARY (EDS) FOR A MSL TYPE VEHICLE

The original intent of this program was to provide experiment definition summaries in the first, fifth, and final reports. Each of these summaries were to be subsequently up-dated as the program progressed, and appear in the final report reflecting only the most recent data. However, as the latter portion of this program effort was concentrated primarily on a revised experiment configuration, specifically for the Saturn SIVB vehicle, much of the earlier generated experiment definition work for an MSL was not applicable. The preliminary version of the EDS for the MSL is reported in this section.

The following information is a summary of the experiment definition, to date (5/15/66), of the modular parabola and the elastic memory airlock experiment for a MSL vehicle. However, the chemically rigidized structures are also dealt with in the latter sections and the development program schedule.

7.1.1 WEIGHT AND DIMENSIONS (STOWED AND DEPLOYED)

a.	Modular Parabola, Boom, Mechanism and Work Station (less electrical)		85.35 lb
	(1)	Volume-stowed	5.97 c.f.
	(2)	Dimensions-stowed	
		Panel canister and work station	32 x 25 x 12 in.
		Boom	2 x 72 in.
		Hub	14 in. dia x 7 in.
	(3)	Dimensions-deployed	10 ft dia x 45° rim angle

b.	Elastic Memory Airlock, Boom, and Retract Mechanism		123.95 lb
	(1)	Volume, stowed (canister)	9.7 c.f.
		Boom	.036 c.f.
		Support Structure	2.0 c.f.
	(2)	Stowed dimensions (overall)	4 ft dia x 2 ft
	(3)	Deployed dimensions	7 ft long x 4 ft dia
c.	Experiment Subsystems		
	(1)	Control consoles, instrumentation data acquisition and cables	40 lb
		(a) Volume	1.8 c.f.
		(b) Dimensions	3.0 x 30.0 x 10.0 in.
	(2)	Pressurization system	34.5 lb
		(a) Volume	3.4 c.f.
		(b) Dimensions	Integral
d.	Provisions for MSL Structure Mod		10.0 lb
e.	Total Experiment System (Both Airlock and Modular Parabola)		
	(1)	Weight	293.8
	(2)	Volume	22.9 c.f.

7.1.2 POWER REQUIREMENTS

The experiment power loadings are illustrated in Figures 7-1 and 7-2. These charts are based on the experiment structural system requirements of elastic memory airlock and modular parabola components.

7.1.3 STOWAGE LOCATIONS AND ATTACHMENT EXPERIMENT/VEHICLE

The MSL installation study indicated that the best location for mounting the two canisters is on diametrically opposite sides of the MSL, at the

OPERATIONAL SEQUENCE

A.	INSTRUMENTATION WARMUP	CONTINUOUS (20 MIN)	5 WATTS
B.	CONTROL CONSOLE POWER "ON"	CONTINUOUS (10 MIN)	4 WATTS
C.	TELEMETRY POWER "ON"	CONTINUOUS (5 MIN)	10 WATTS
D.	INSTRUMENTATION READOUT	OBSERVATION PERIOD	8 WATTS
E.	FAIRING RELEASE	.1 SEC (SURGE)	125 WATTS
F.	CANISTER RELEASE	.1 SEC (SURGE)	125 WATTS
G.	BOOM CONTROLS	1 MIN MAX DUTY CYCLE	53 WATTS - TRANSIENT - 42W 2 WATTS
H.	CANISTER VENT	.5 SEC	12 WATTS
I.	CANISTER OPEN	.1 SEC (SURGE)	125 WATTS
J.	STRUCTURE CONTROLS	1 MIN DUTY CYCLE	3 WATTS - TRANSIENT - 42W 4 WATTS
K.	PRESSURE CONTROLS	DUTY CYCLE	12 WATTS

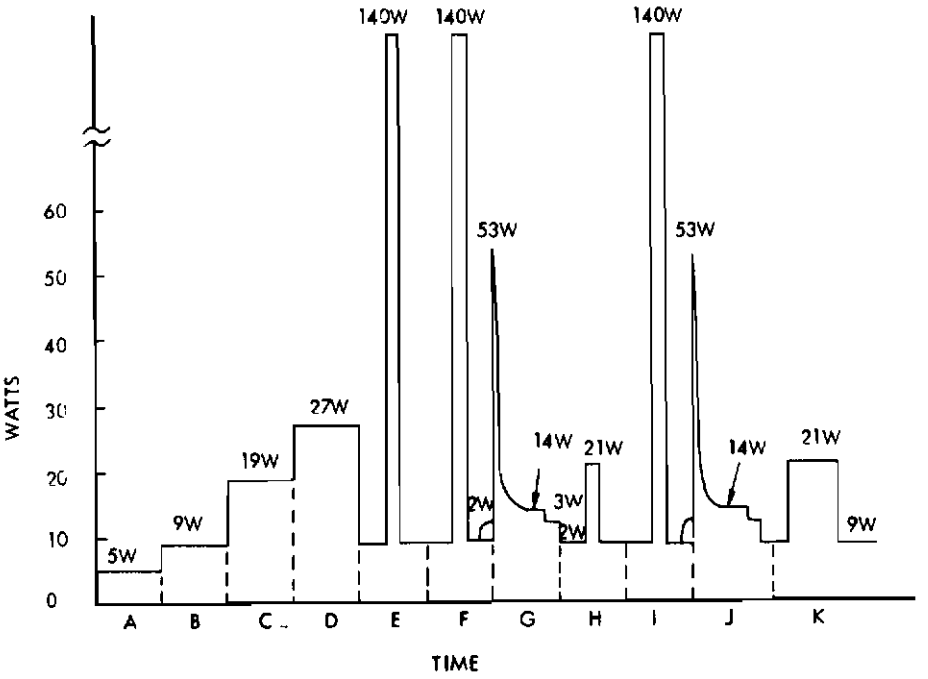

Figure 7-1. Elastic Memory Airlock Power Requirements

OPERATIONAL SEQUENCE

A.	INSTRUMENTATION WARM-UP	CONTINUOUS	5 WATTS (3 PANEL LIGHTS, SENSORS)
B.	CONTROL CONSOLE POWER "ON"	CONTINUOUS	4 WATTS (3 PANEL LIGHTS, ELECTRONICS)
C.	BOOM FAIRING RELEASE	.1 SEC	125 WATTS (PYRO)
D.	BOOM RELEASE	.1 SEC	125 WATTS (PYRO)
E	BOOM ERECTION	1 MIN (CONTINUOUS)	42 WATTS SURGE, 3 WATTS OPERATE (MOTOR) 4 WATTS (LIGHTS)
F	CANISTER RELEASE	.1 SEC	125 WATTS SURGE (PYRO)
G	EXTERNAL CONTROLS	CONTINUOUS	1 WATT, MOTOR CURRENT (PANEL LIGHT)
H	INSTRUMENTATION - TELEMETRY	CONTINUOUS	10 WATTS (ELECTRONICS)
I	INSTRUMENTATION - MANUAL READOUT	CONTINUOUS	8 WATTS (PANEL INDICATOR)

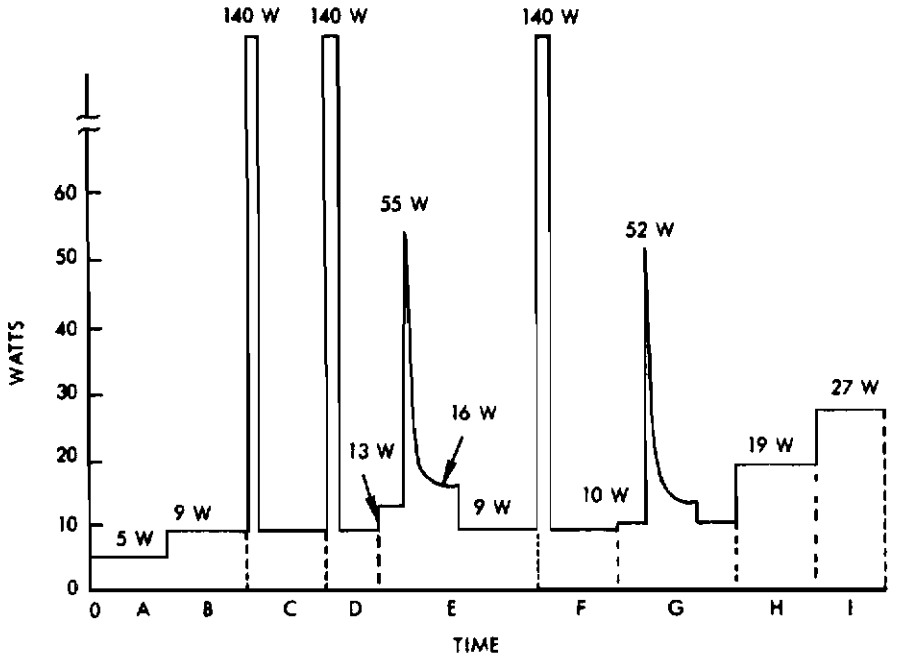

Figure 7-2. Modular Parabola Power Requirements for a Remotely Deployed, MSL Vehicle Experiment

forward end of the unpressurized compartment as shown in Figure 7-3. An alternate acceptable installation geometry is with the experiment canister systems stowed internal to the vehicle in the unpressurized compartment of the MSL and extracted by the astronaut through an EVA hatch and manually attached to the vehicles outer surface for deployment. An example of the operational locations of the experiment's components is shown in Figure 7-4.

The configuration and installation concepts were developed to permit a maximum of astronaut visual control through view ports and a minimum of interference with the MSL structure, ACS plumes, and surface radiators. The two expandable structures for each flight are proposed to be diametrically installed on MSL to minimize asymmetry of drag and center of gravity changes.

The experiment was designed to permit flexibility of installation, simplicity of checkout, and a minimum of interfaces with MSL subsystems. The structure is designed to survive the Titan IIIC launch environment as well as typical handling and shipping loads.

The subexperiments are packaged in canisters that protect the expandable structures system from the ground, launch, and orbital environment until deployed. The expandable structure is encased within a canister; this permits containment of the experiment in a conditioning environment during stowage. Evacuation of internal pressures prior to launch eliminates imposing large pressure loads or sealing requirements on the canisters. The canister design permits installation by flush mounting in the unpressurized MSL compartment or internal mounting if desired.

The experiment is designed as a completely integrated system. Prior to launch of the MSL, the experiments will be stowed within the experiment canister. Installation on the MSL would require only the connecting of electrical and pneumatic lines, installation of canister fasteners, arming of pyrotechnics, and last minute prelaunch checkout of the electrical systems.

Alternate considerations of an elastic memory airlock suggest the system could be recessed over the MSL pressurized compartment EVA hatch. This would provide immediate operational status on deployment and testing.

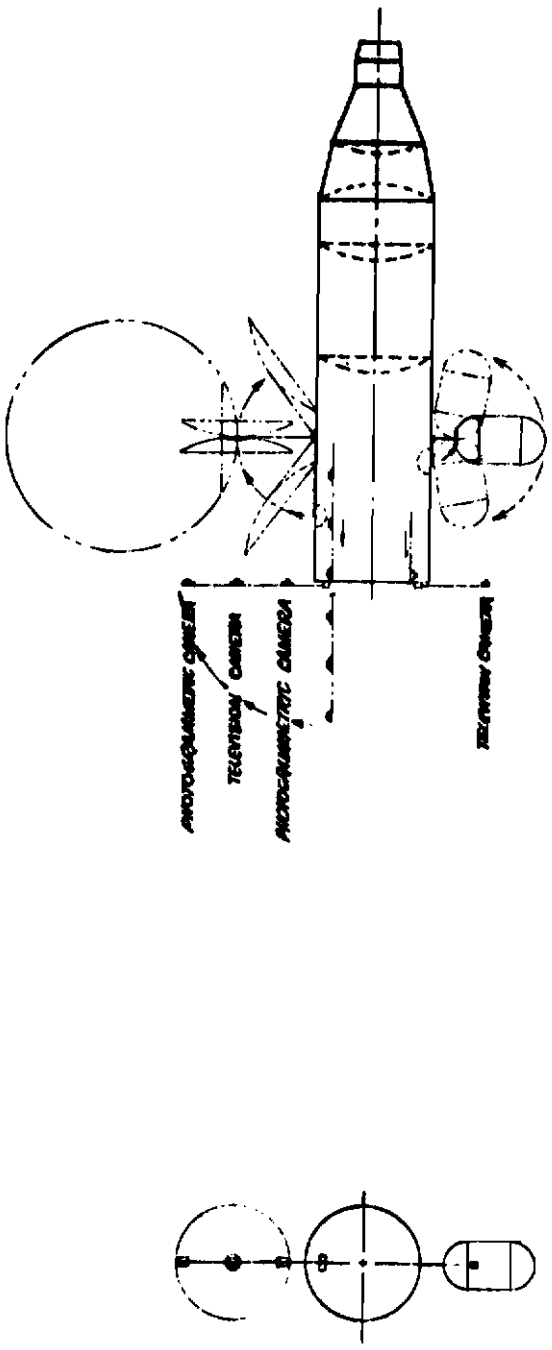

Figure 7-3. Experiment Components Located Forward and on Opposite Sides of the MSL

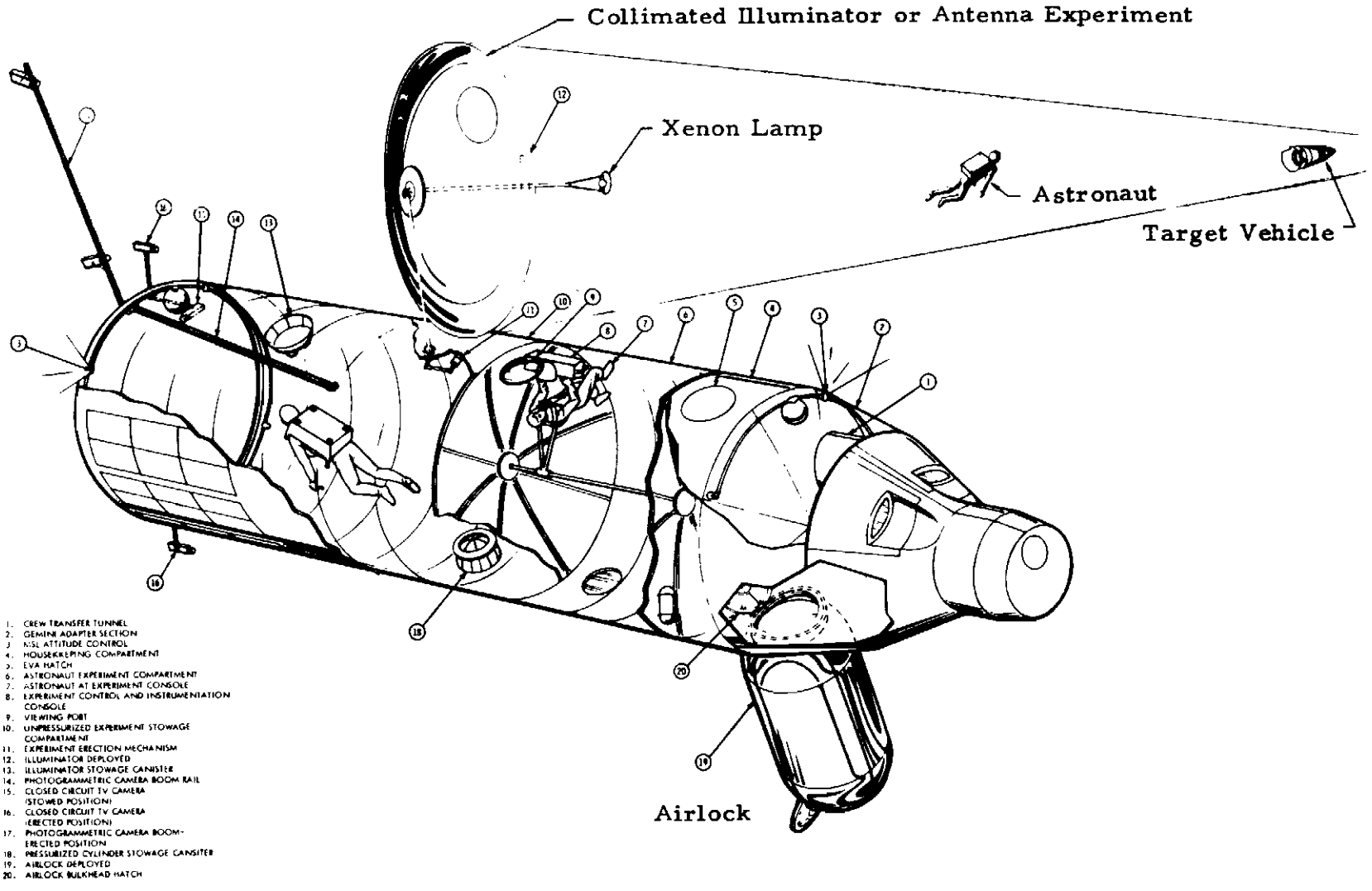

Figure 7-4. MSL Experiment Operational Locations

In the event of an MSL subsystem failure, the airlock could be jettisoned to facilitate use of the MSL EVA internal compartment airlock.

In the case of the manually assembled modular type parabola, boom and hub assembly mechanisms may be faired to the external vehicle surface, but with the contoured panel canister located in any convenient work station area accessible to the EVA astronaut. Such a work station is depicted in Figure 7-5 with the assumption that the aft end of the unpressurized MSL is not obstructed with a transstage. A foldable work station is also presented to facilitate almost any convenient installation location.

7.1.4 ORBITAL TEST OBJECTIVES

Progress in the development of large boosters required for the exploration of space has been rapid and the Air Force now has the capability to inject very large payloads into orbit. To fully exploit these manned and unmanned orbit system capabilities, large space structures are required that exceed the volumetric and geometric limitations of the launch vehicles. The expandable airlock and modular parabola experiment is planned to demonstrate the feasibility and efficiency of the construction of large structures in space utilizing the technology of expandable structural-material systems and manned assembly of a precontoured modular parabola.

This preliminary design study defines an experiment to demonstrate the deployment in space of small-scale parabolic mirrors of high geometric accuracy, and pressure vessels characteristics of those required for airlocks and larger manned space station work compartments. The man-machine relationship and integration characteristics and requirements for testing on the Manned Space Laboratory were investigated. The study indicates that parabolic solar concentrator mirrors and illuminators larger than 50 feet in diameter, and large pressure vessels suitable for environmentally controlled manned compartments can be constructed in space from flexible materials or modules stowed in small high-density packages in current booster payload compartments.

Small-scale expandable parabolic reflectors for solar concentrators, search and tracking illuminators, or antennas will be manually deployed

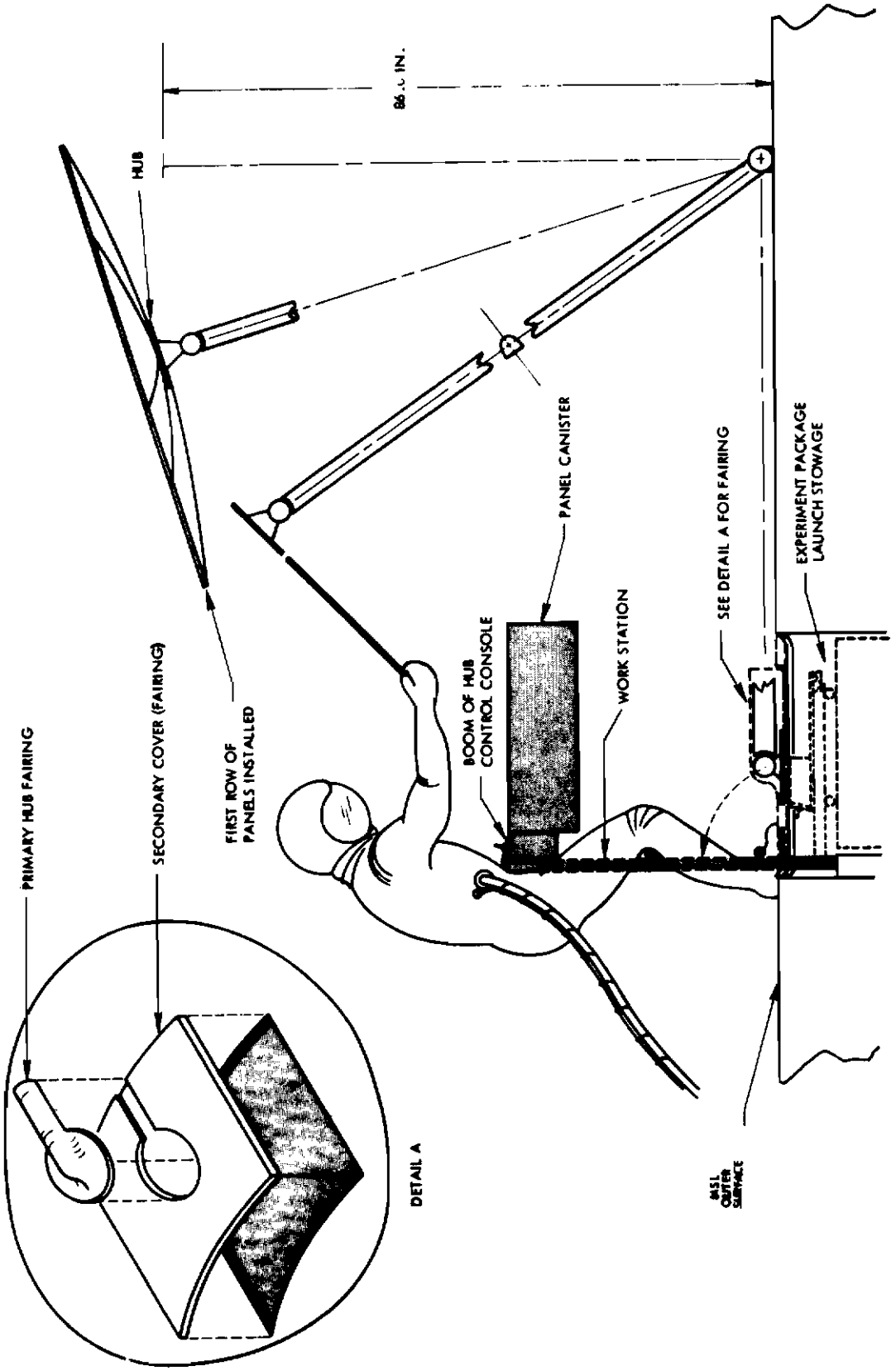

Figure 7-5. Modular Parabola Work Station

in space. Final assembly and operational demonstration will be accomplished by the astronaut. Erectable and operational airlocks will also be demonstrated.

7.1.5 ORBITAL TEST DURATION

This experiment evaluation period is designed to satisfy the test objectives in a 30 to 90-day orbit, although a service life greater than one year is anticipated for these structural systems.

7.1.6 ORBITAL DATA REQUIRED AND RETURNED TO EARTH

Orbital flight tests are required to evaluate the effects of zero-g and hard vacuum on:

a. Deployment and erection system characteristics.

b. Parabolic accuracy achieved.

c. Airlock assembly, structural integrity, and utility.

d. Illuminator efficiency for search and tracking aid of EVA astronauts or rendezvous targets.

e. Thermal distortions of the parabolic surface during orbit, and degradation with time by means of contour mapping techniques.

f. Periodic measurements of temperature, pressure, and airlock leakage rates.

At the end of the MSL flight, small material samples and the photographic film will be returned to earth for laboratory analysis.

7.1.7 SEQUENCE OF EXPERIMENTAL EVENTS

The experiment checkout control and instrumentation system will include instrumentation and controls for the following subsystem functions:

a. Checkout

(1) Circuit continuity

(2) Safe and arm condition

(3) Canister atmosphere (pressure, temperature, etc.)

(4) System power

b. Deployment

(1) Canister pressure vent (if applicable)

(2) Canister ordnance arming

(3) Closed-circuit TV and motion picture camera erection

(4) Deployment sequence initiation

(5) Ordnance firing

(6) Experiment erection

(7) Erection rate regulation

(8) Deployment pressurization initiation

(9) Operational pressure testing

(10) EVA inspection of structure

(11) Transfer of airlock to operational location

7.1.8 TASK AND TIME LINE ANALYSIS OF SEQUENCE OF EXPERIMENTAL EVENTS

7.1.8.1 TASK DESCRIPTION FOR ELASTIC MEMORY AIRLOCK AND MODULAR PARABOLA STRUCTURES

a. Prepare for experiment

(1) Retract any other movable structures which may interfere with or be damaged by expandable structures erection.

(2) Check out equipment.

(a) Crewman takes place at control console.

(b) Crewman erects photographic camera and TV camera booms (if so mechanized)

(c) Check out photo and TV camera control circuitry.

(d) Check out and calibrate instrumentation and recording circuitry.

(e) Check temperature, pressure, and humidity of Experiment canisters, and monitor temperature for acceptable erection temperature zone.

NOTE 1: In event of failure of any tasks or steps, enter corrective maintenance for the appropriate MSL subsystem. If maintenance time takes longer than allotted preparation time, the experiment may have to be rescheduled. If pressure is too high, vent storage area for required pressure differential.

b. Erect Structures

(1) Expandable airlock

(a) Deploy expandable airlock structure.

1 Verify that pressure in canister is safe for erection and arm cover-removal circuitry.

2 Deactivate ACS.

3 Activate TV cameras and adjust display for optimum picture of structure erection area.

4 Activate recording instrumentation for structure.

5 Initiate deployment sequence, and monitor erection on TV, making verbal recording of deployment process.

6 Photograph or video tape record significant aspects of deployment.

NOTE 2: In the event of failure of any deployment event, the experiment may be deactivated until the problem is resolved.

(b) Inflate expandable airlock structure.

1 Verify that structure is in position for inflation.

2 Monitor inflation process on TV display and/or through viewing port, making verbal recordings of the process.

3 Photograph significant aspects of inflation process.

NOTE 3: In the event of failure of the forming sequence, the astronaut will provide manual override to stop or adjust any step that had been initiated.

4 Verify that structure has the designated form and that strain and pressure gages indicate acceptable structural stability.

(c) Pressure test airlock at 7.5 or 5.5 psig.

1 Increase pressure inside cylinder by 0.5-psig increments every two minutes.

2 Verify and monitor recording of temperature, pressure, and stress during pressurization.

(2) Modular Parabola Experiment (Externally Stowed) Task Description

(a) Activate parabola control and instrumentation console.

(b) Verify that canister pressure is within limits for opening.

(c) Arm pyrotechnics and release boom fairing.

(d) Erect boom until limit is indicated.

(e) Release secondary canister fairing.

(f) Proceed EVA and raise work station and panel canister assembly from stowed compartment.

(g) Assume position at work station and open panel canister.

(h) Position boom and hub angles by actuation of work station control switches.

(i) Sequentially remove panels from canister and insert into hub; continue assembly until parabola is complete.

(j) Extract bolt rope from canister and attach circumferentially to parabola.

(k) Remove contour evaluation template from stowed position and install on hub of parabola.

(l) Place "Hub Rotate" switch "ON" so that probes on template scan surface of parabola. (remove stow after measurement)

(m) Install xenon light sting.

(n) Retract work station and canister into recess.

(o) Reenter vehicle and deactivate remote control console.

c. Monitor both Experimental Structures for Five Hours (Every 90 Minutes)

(1) Orient MSL so that airlock and parabolic structure face sun when emerging into sunlight side of orbit.

(2) Monitor parabolic structure during emergencies into sunlight.

(a) Record temperature and strain until stability is reached.

(b) Record time required to stabilize.

(3) Monitor leak rate of airlock.

NOTE 4: Observe slope of pressure; record mean average line to calculate leak rate.

(4) Record temperature, pressure, and strain.

(a) Calibrate instrumentation recorders.

(b) Record parameters

(5) Inspect surface of structures.

(a) Rotate parabola to view all sides and photograph any unusual surface characteristics.

(b) Rotate airlock and photograph any unusual surface characteristics.

(6) Evaluate data and store significant information for transmittal to ground.

(7) Position booms so that structures do not interfere with other experiments.

d. Monitor Structures Every Five Days

(1) Orient MSL so that airlock and parabolic structures face sun when emerging into sunlight.

(2) Monitor parabolic structure during emergence into sunlight.

(3) Monitor leak rate of airlock.

(a) Note slope of pressure; record mean average line.

(4) Record temperature, pressure, and strain.

(a) Calibrate instrumentation recorder.

(b) Record parameters.

(5) Inspect surface of structure.

(a) Repeat step c (5) (a).

(b) Repeat step c (5) (b).

(6) Evaluate data and store significant information for transmittal to ground.

(7) Position booms so that structures do not interfere with other experiments.

e. Retrieve Samples and Photographic Records

(1) Prepare for EVA

(a) Depressurize expandable airlock structure.

(b) Orient parabola to "secure" position so focus will not impinge on crewman or MSL structure.

(c) Don pressure suit.

(d) Obtain camera, knife, and tethers for EVA.

(e) Deactivate ACS.

(2) Retrieve samples of structures.

(a) Exit MSL and anchor tethers.

(b) Translate to airlock.

(c) Using attached locomotion aids, translate over surface of airlock to examine for defects and verbally record condition of surface.

(d) Photograph significant areas of airlock either on basis of own evaluation or on request from ground.

(e) Use knife or scissors to cut out 4 x 4-inch sample of most significant area, and seal specimen in plastic bag.

(f) Translate to parabolic structure.

(g) Using attached locomotion aids, examine face and back of parabola for degradation of surface, and verbally record observations.

(h) Photograph significant areas of parabolic structure.

(i) Detach 4 x 4-inch specimen panel and seal specimen in plastic bag.

NOTE 5: Other crewman monitors performance of EVA.

(3) Retrieve photographic cameras.

(a) Translate to camera.

(b) Remove film and place in tethered pouch.

(c) Translate to airlock, enter, and release tethers.

(d) Doff spacesuit.

f. Perform Post-Experiment Activities

(1) Gather experiment data for transfer to Gemini B.

(2) Evaluate data gathered during EVA and store significant information for transmittal to ground.

7.1.8.2 MAXIMUM WORK PERIODS

The preparation phase should not take longer than 20 minutes and is limited to one occurrence. It is principally a one-man activity.

Structure erection of the airlock will require a maximum of 15 minutes during which constant monitoring of the deployment and pressurization

process is required. During pressurization, it is necessary to monitor the instrumentation for periods of 2 minutes every 5 minutes. Structure erection is principally a one-man activity; however, the other crewman may be required for MSL attitude control. Evaluation and storage of significant data will not require more than 30 minutes.

Monitoring the structures periodically during a 5-hour period of orbit time will require approximately 20 man-minutes. The major performance variable is monitoring the parabolic structure for stability during emergence from the occulated to the sunlit side. To orient MSL, the second crewman will be required for 5 minutes.

Monitoring the structures every 5 days will require approximately 60 man-minutes. To orient the MSL, a second crewman will be required for 5 minutes.

Retrieving the specimens and photographic records will require approximately 30 minutes (plus suit donning time) with both crewmen involved in standard EVA and supporting procedures.

The post-experiment activities will require approximately 30 man-minutes.

The total time requirement for one man is approximately 205 minutes, with the other crewman being required for a maximum of 75 minutes, over the 30-day period.

7.1.9 CREW TRAINING REQUIREMENTS

The crewman should be able to classify the anticipated surface characteristics such as orange peel, wrinkle, pittings, etc., and such structural characteristics as leakage and creep.

The crewman should acquire proficiency in the function of the temperature, pressure, and stress instrumentation so he can evaluate the relationships between readings. This will also involve the basic laws of gases.

For the modular parabola experiment, the astronaut training requirements consist mainly of experiment familiarization and procedural task

training. The zero-buoyancy tests indicate a typically short learning curve of two to three assembly trials for the assembly tasks. Allocation of pre-flight time may be as listed below. It would also be desirable to conduct a zero buoyancy assembly test exercise that would require an additional eight man-hours of astronaut time, and zero-g tests in the KC-135 aircraft that will require another eight hours for one astronaut.

Preflight Indoctrination Schedule

First Day:

0800	Indoctrination; experiment purpose and objectives
0830	Discussions; experiment plan and procedure
1000	View movies of zero buoyancy and zero-g tests
1100-1200	Examine experiment hardware
1300	Trial neutral buoyancy assemblies and disassemblies of structure
1600-1700	Discuss problem areas and procedural changes

Second Day:

0800	Explanation of contour measurement
0900	Examine equipment and typical data
0930	Demonstration of measurement procedure
1000	Test Exercise
1100-1200	Discussion of results
1300-1600	Dress rehearsal of total experiment tasks.

Post-Flight Time Requirements

The post-flight requirements of the astronaut will involve one day on discussion of in-orbit experiment results. The astronaut will observe the film history taken during the space assembly and will dictate his observations, with particular emphasis on difficulty encountered, and any recommendations for the improvement of the technology under evaluation.

7.1.10 AGE AND GSE REQUIREMENTS

A minimum of AGE or GSE is required; it consists principally of simple dollies and circuit continuity checkout equipment for the consoles and instrumentation.

7.1.11 DATA DISPLAY REQUIREMENTS

The displays required in the pressurized section of the MSL include the two subsystem control consoles and the instrumentation console. These preliminary console panel layouts are shown in Figures 7-6, 7-7, and 7-8. The instrumentation system considered assumes no data aquisition is provided on MSL vehicle.

7.1.12 DEVELOPMENT AND SCHEDULE

The planned Development Program Schedule is shown in Figure 7-9.

7.1.13 DEVELOPMENT TESTS

The primary objectives of the current and proposed test program is to demonstrate the feasibility, structural characteristics, efficiency, and typical operational applications of expandable airlock structural-material systems and manually assembled modular parabolas. A secondary objective of the test program is to evaluate the astronaut's capabilities, limitations, and EVA procedural problems relative to the conduct of final assembly and operational procedures.

Maximum utilization of laboratory test equipment is planned to minimize the space test program costs and to maximize the probability of successful in-orbit test and data retrieval. The majority of environmental conditions can be evaluated in environmental test facilities. However, the zero-g conditions cannot be evaluated, especially in combination with vacuum environment. These tests, and astronaut EVA tasks, must be conducted on the MSL program. KC-135 zero-g flight tests can evaluate certain astronaut EVA tasks:

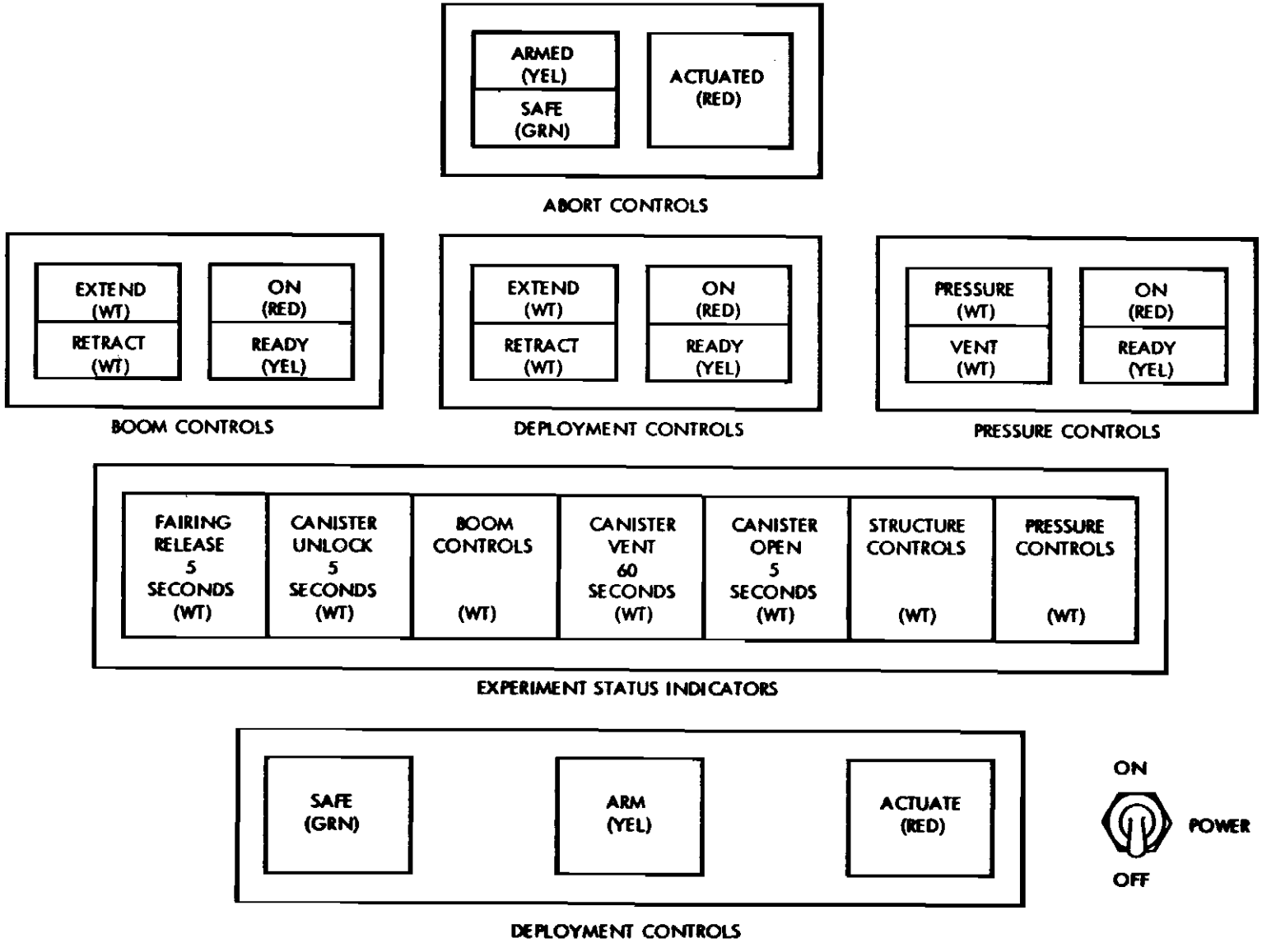

Figure 7-6. Revised Elastic Memory Airlock Control Console Panel Layout

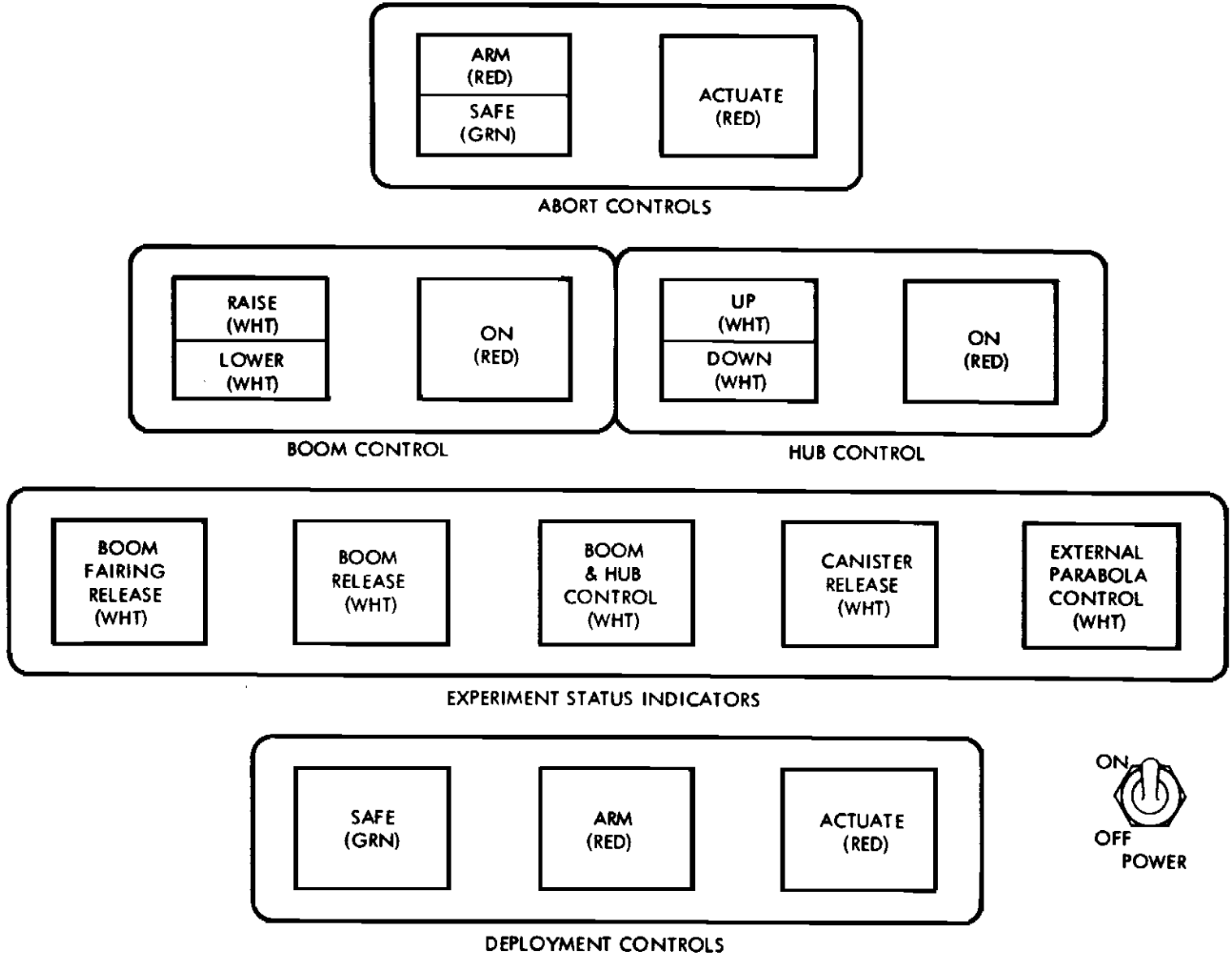

Figure 7-7. Parabola Control Console

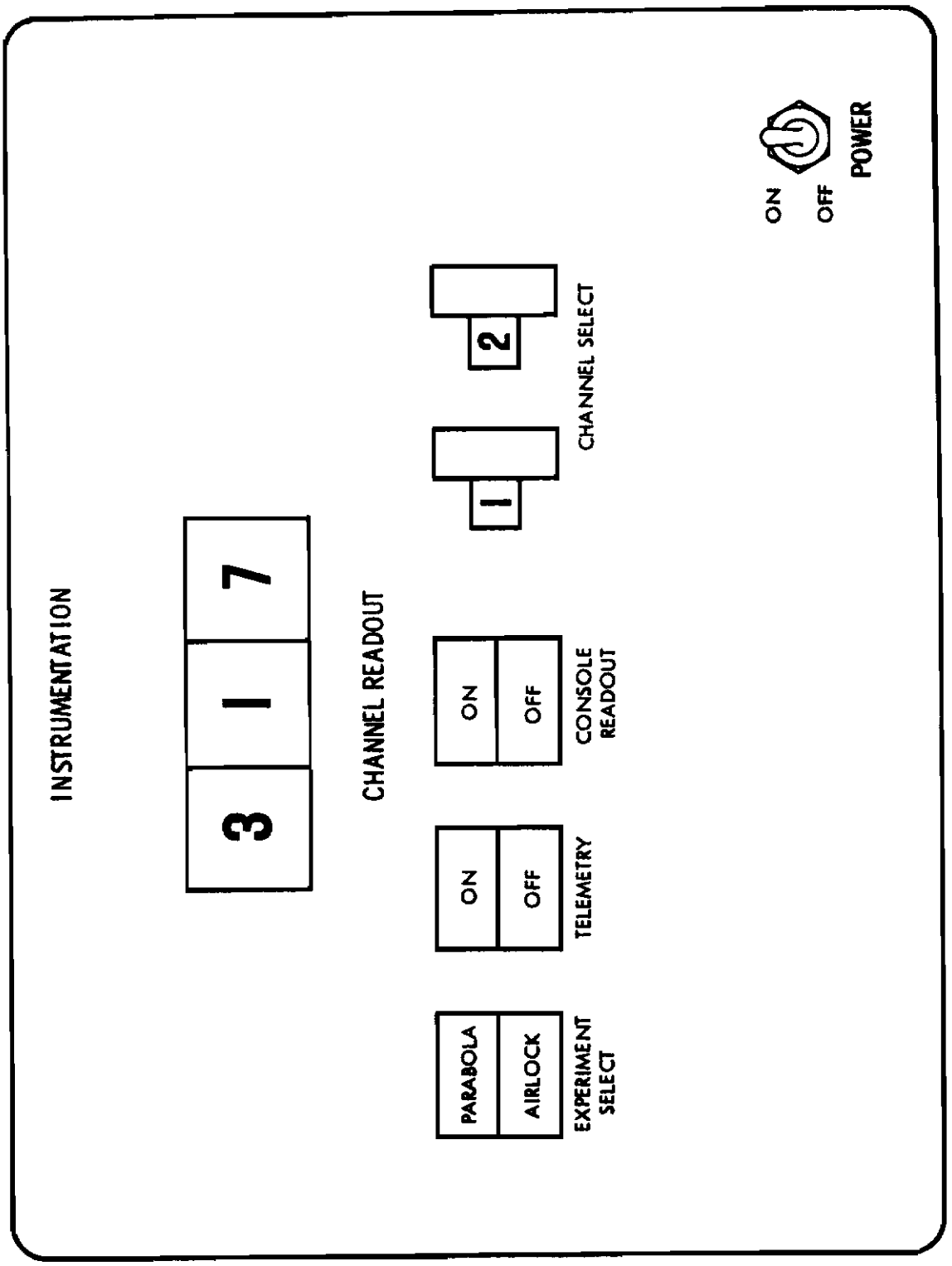

Figure 7-8. Instrumentation Console

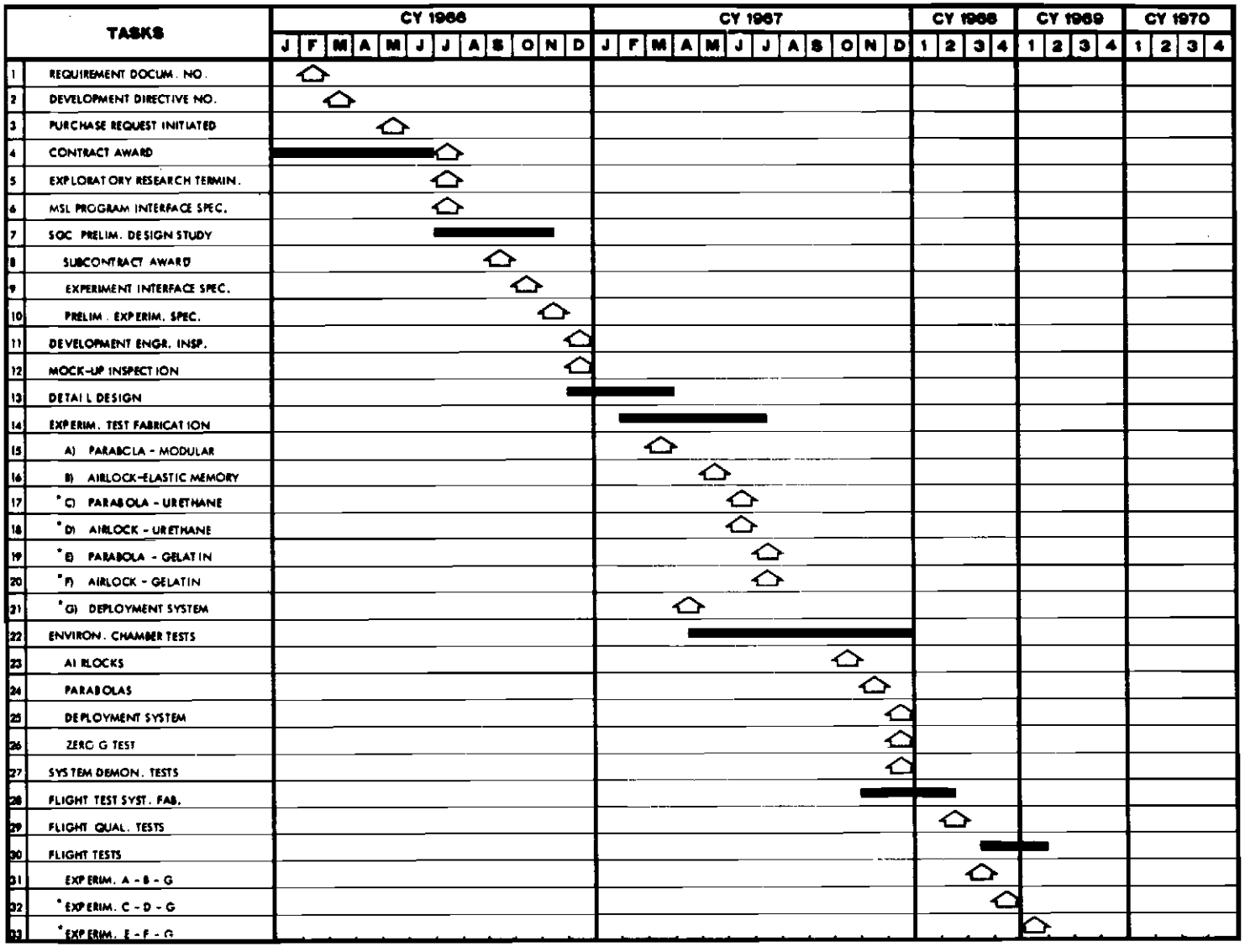

* SUBJECT TO EXPLORATORY DEVELOPMENT PROGRESS REVIEW

Figure 7-9. Development Program Schedule

a. Approximately five experimental and prototype structural-material experiment hardware sets are required for each of the sub-experiment tests for functional mock-ups, development tests, and system tests.

b. Approximately five experimental and prototype experiment mechanization systems (canister, booms, control panels, etc.) will be required for functional mock-ups, development tests, and system tests.

c. Two or three complete sets of flight hardware are required for each of the experiments.

The primary laboratory test effort is related to the evaluation of the deployment and structural and surface accuracy characteristics of the subexperiments. The parabolas have been sized for zero buoyancy testing in General Electric facilities. The airlock was configured for minimal astronaut operational maneuverability requirements and can be tested in a number of environmental facilities.

The mechanical and electronic experiment subsystems and components are relatively small and will be tested in Space-General's laboratory facilities.

The elastic memory airlock and modular parabola structural-material systems will be evaluated in the laboratory for:

a. Shelf life characteristics.

b. Sensitivity to stowage environment.

c. AGE requirements.

d. System preflight checkout procedures.

e. Effects of boost environment on stowed experiment.

f. Folding and packaging tests.

g. Canister release characteristics.

h. Expandable structures deployment in vacuum.

i. Structural characteristics of material sections including tension strength, modulus, deflection characteristics, etc.

j. Geometrical accuracy of the parabolic mirror face and thermal deflections.

k. Specular reflectivity of the mirror surfaces.

l. Micrometeoroid penetration damage.

m. Functional degradation in a simulated space environment, including UV, IR, hard radiation, temperature, and vacuum, as a function of time.

n. KC-135 zero-g flight tests and zero buoyancy tests to evaluate simulated astronaut EVA final assembly and inspection tasks and special tool requirements.

7.1.14 DEVELOPMENT COSTS

7.1.14.1 FY 1967 WORK DESCRIPTION

a. Task 1 - Preliminary Design - Contract will be awarded to the Space-General Corporation for the completion of the MSL Experiment preliminary design, MSL system integration and installation studies in coordination with the General Electric Corp., Space Laboratory Contractor, and the MSL Program Office, and analysis of industry state-of-the-art and capabilities to develop the components of the experiment system.

Space-General will develop the Experiment Interface Specification and the Preliminary Experiment Specification documentation from SGC preliminary design data. DEI and mock-up inspections will be conducted prior to start of detail design. Prior Exploratory Development analysis and test data will be reviewed to insure that the SGC proposed design utilizes designs and techniques sufficiently developed to insure the successful completion of the program.

b. Task 2 - Detail Design - The Space-General Corporation project team will detail design the test components of each of the subexperiments and the subsystems required for the installation, stowage, and deployment of the experiment in MSL orbit. Design and performance specifications will be provided to the MSL Program contractors for development of the experiment control and display consoles.

c. Task 3 - Experiment Test Fabrication - Four of the six subexperiments, and the deployment mechanization subsystem, will be fabricated for laboratory testing. It is planned to make maximum use of government facilities for testing, although specimen and other laboratory tests will be conducted in existing Space-General owned laboratories and subcontractor facilities during this task period.

7.1.14.2 FY 1968 WORK DESCRIPTION

a. Task 1 - Experiment Test Fabrication - The two remaining subexperiments will be fabricated and all test instrumentation completed in the first quarter of the year.

b. Task 2 - Laboratory Tests - Vacuum chamber tests of the full scale subexperiments will be conducted in the WPAFB and AEDC chambers starting at the first of the year. Each test can be completed in less than ten days of facility schedule time with one subexperiment scheduled approximately every 22 calendar days.

WPAFB KC-135 zero-g aircraft will be utilized for modular parabolic mirror assembly task by pressure-suited astronauts. Other tests will include installation and ingress-egress tests through the airlock. Zero-buoyancy tank tests will be conducted in General Electric Aquarama tank test facility for the modular parabolic assembly.

Material samples of the experiments will be tested in the WPAFB micrometeoroid test facility.

Complete system demonstration and function tests will be conducted at the Space-General Corporation facility.

c. Task 3 - Flight System Fabrication - Two experiment subsystems will be fabricated for each experiment; one system will be used as a back-up article. Design changes indicated by the laboratory testing will be incorporated as required.

d. Task 4 - Qualification and Flight Test - Qualification tests of the flight hardware will be conducted, including canister and plumbing leakage, circuit and component functions under simulated launch dynamic environment, and instrumentation calibration.

The first MSL Experiment system will be available for factory or launch pad installation on or before the second quarter of 1968.

The schedule has been planned with built-in contingency factors to accommodate unforeseen development problems. Nominal contract performance, and no critical problem developments, could permit first launch in early 1968.

The second MSL Experiment is scheduled for launch within three months or less after the first launch and will be ready for installation in the second quarter of FY 1968.

The contractor will conduct astronaut training briefings, support installation tasks, and accomplish prelaunch system checkout and technical support of the command control center during orbit.

Retrieved material specimens and data will be analyzed in government or SGC laboratories as required.

7.1.14.3 BY NEW OBLIGATION AUTHORITY (NOA)

	FY 67	FY 68	FY 69	FY 70
Task 1:	1,000	600	2,000	600
Task 2:	1,200	400		
Task 3:	900	700		
Task 4:		400		
INDUSTRIAL FACILITIES	0	0	0	0
TOTAL	3,000	2,100	2,000	600

7.1.15 TECHNICAL RISKS

7.1.15.1 PARABOLIC ILLUMINATORS

The rigid modular illuminator experiment, assembled by an astronaut, offers a simple assembly method to produce a highly efficient mirror from very accurately prefabricated components. Prepreliminary studies of this concept do not reveal any significant technical problem areas. Detail joint configuration design and concentricity control device studies are complete. The metal honeycomb sandwich structures are relatively fragile; therefore, the EVA astronaut must be restrained properly to permit simple but precise assembly tasks. Technical risks appear to be very small.

The expandable, rigidized, resin-impregnated structures pose a number of unsolved problems related to contour accuracy and mirror surface finish. Techniques to store, deploy, and rigidize the structures do not present serious technical problems. However, achievement of the required contour accuracy has not been demonstrated in the laboratory to date. These problems are generated primarily by resin shrinkage, distortion of relatively elastic laminates under pressure, and incompatability of laminates and adhesives. The technical risk is therefore relatively high for the predictable solution of these problems within the allowable MSL schedule period.

7.1.15.2 AIRLOCKS

Several structural-material concepts and preliminary designs of airlocks have been developed that offer a high probability of success with small associated technical risks. The elastic memory material system offers predictable deployment and structural characteristics, and requires only investigation of stability requirements in the unpressurized mode. If stabilization is required, several simple solutions to this problem are available. The gelatin-impregnated sandwich structure presents no critical technical problems, with the possible exception of resin distribution control as a function of packaging configuration and extruding pressures (this problem is common to all rigidized resin systems). The gas-cured urethane resin system is also considered to present a relatively low technical risk but does require solution of an additional problem related to the perfection of a manifolding system to insure that high-density resin areas are cured prior to depletion of catalytic gases.

7.1.16 LOGISTICS

No critical logistics requirements are apparent at this time, as standard transportation and handling procedures will suffice.

7.1.17 ATTITUDE CONTROL REQUIREMENTS

Stabilization is noncritical with the following exceptions:

a. During deployment ACS should be off.

b. The thermal balance of the deployed structures require at least some heat input during the orbit. This preferrably can be accomplished by periodic (1/2 orbit) exposure to the sun.

7.2 ELASTIC RECOVERY AIRLOCK EXPERIMENT DEFINITION SUMMARY FOR A SATURN SIVB

A review of the Experiment Definition is presented in this section oriented toward application on the Saturn SIVB vehicle. Only the main topics are discussed either for brevity or because they have not been firmly established.

7.2.1 ORBITAL TEST OBJECTIVES

The experiment has two objectives. The basic objective is to demonstrate an expandable Elastic Recovery System which can be utilized as a serviceable space structure in the launch and space environments for extended periods of time. The second objective is to demonstrate that such an expandable structural system can, through proper design, provide an operational expandable airlock for use on future manned missions requiring extra vehicular activity.

7.2.2 DESCRIPTION OF THE EXPERIMENT EQUIPMENT

The experiment equipment will be a self-contained system package (Figure 7-10), consisting of the following subsystems:

a. Expandable airlock canister, complete with integral controls.

b. Integral oxygen gas pressurization system for three pressurization phases.

   (1) One cycle at 5.5 psig for deploy and test

   (2) Three cycles at 3.5 psig for ingress/egress and leak tests

   (3) One cycle at 3.5 psig for revisitation pressurization

c. A remote control console (not integral with airlock package)

d. Instrumentation for airlock pressure and temperature gradients with readouts:

   (1) Internal airlock readout

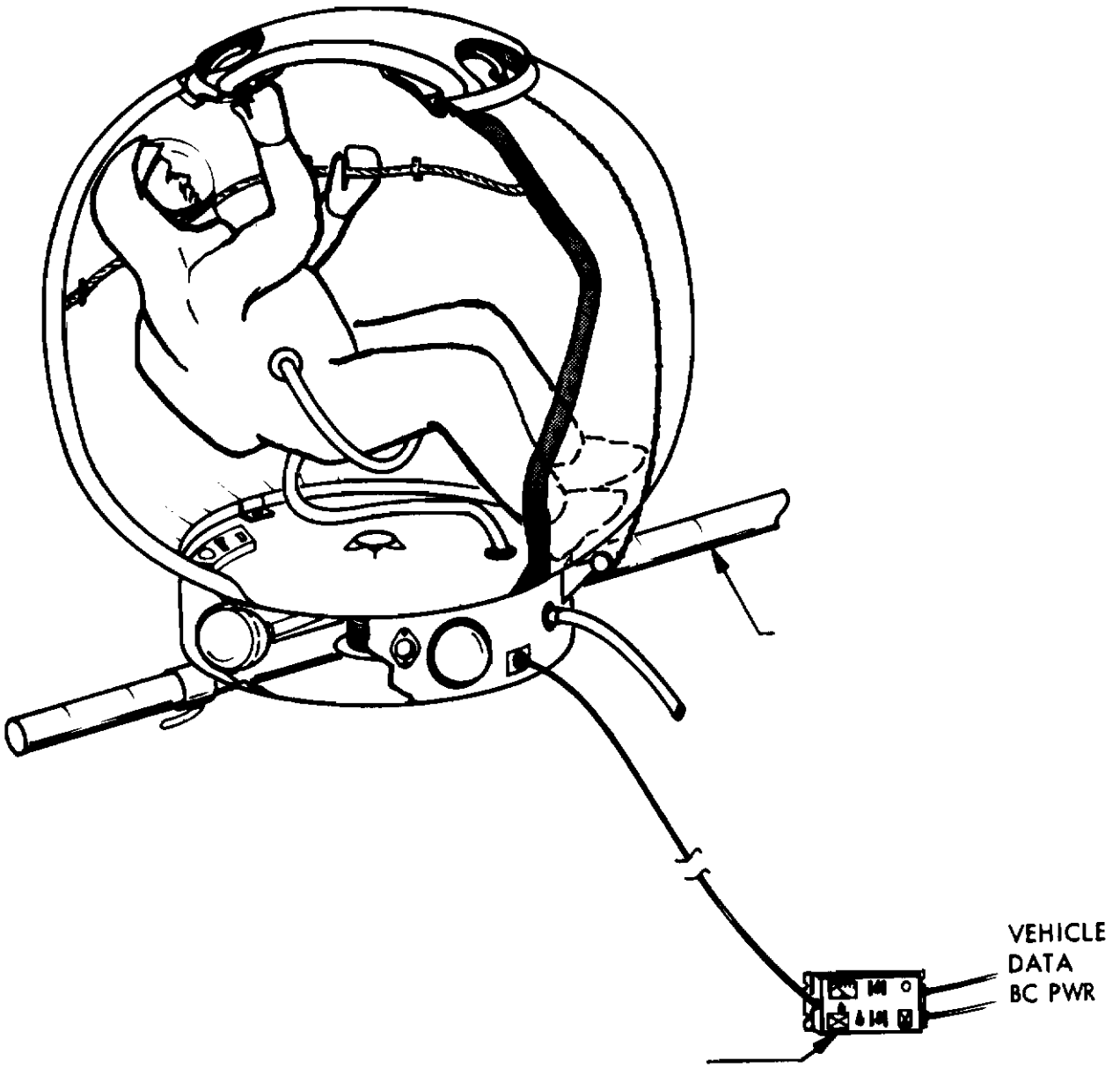

Figure 7-10. Airlock Experiment Package Configuration

(2) Remote console readout

(3) To SSESM record and/or telemetry.

e. The experiment will interface with the SSESM vehicle in the following areas:

(1) Experiment structural attachment (location to be determined)

(2) SSESM vehicle electrical power, (28-Vdc unregulated)

(3) SSESM vehicle data acquisition and recording

(4) Auxiliary pressurization line for extra pressure cycles if required

(5) Astronaut oxygen and communications umbilical

(6) The astronaut himself.

7.2.3 WEIGHT AND DIMENSIONS

a. Total Experiment System

(1)	Stowed Dimensions	Height	24 inches
		Diameter	39 inches
(2)	Deployed Dimensions	Height	56 inches (inside)
		Diameter	60 inches (inside)
(3)	Deployed Volume (airlock internal)		92 ft^3
	Total Weight (including Retraction Mech)		135.37 lb

b. Subsystem Weight Breakdown

Airlock entity	71.62 lb
Base support structure	16.14 lb
Pressurization system	35.54 lb
Retract system	4.07 lb
Remote control console and instrumentation	5.00
Cabling	3.00

7.2.4 POWER REQUIREMENTS

The electrical power requirements from the SSEM vehicle are as follows:

26-Vdc to 34 Vdc operating

18-Vdc to 36 Vdc no damage

Electrical power requirements for this experiment are not continuous. Various phases of the experiment sequence have different power requirements. This is depicted as a power demand profile in Figure 7-11.

7.2.5 STOWAGE LOCATIONS AND VEHICLE ATTACHMENT INTERFACE

The exact stowage locations have not been established, but candidates in order of their preference are as follows:

a. On SSESM vehicle forward tubular superstructure so that deployment is possible from the launch location. Instrumentation and control cabling could be preconnecting, minimizing the astronaut's preparatory EVA tasks.

b. On the SSESM vehicle tubular superstructure near a supported tie-point for launch, but on a tubular member so that by loosening simple clamp straps the package may be slid and rotated into a suitable deployment attitude. Again, all cabling and connection are made prior to launch, minimizing the astronaut's EVA tasks.

c. Against the H_2 forward tank structure - requiring EVA to reinstall in deployment location.

d. Internal to the SSESM H_2 tank attached to the 10-32 threaded holes on the waffle structure. This mounting will be accomplished by the astronaut after retrieving the experiment package from its stowed or deployed position.

The precise attachment interfaces cannot be designed until coordination has been made with the various associated agencies, such as McDonnell. The experiment base structure design is flexible so that the addition of simple attachment fittings will permit mounting on virtually any surface.

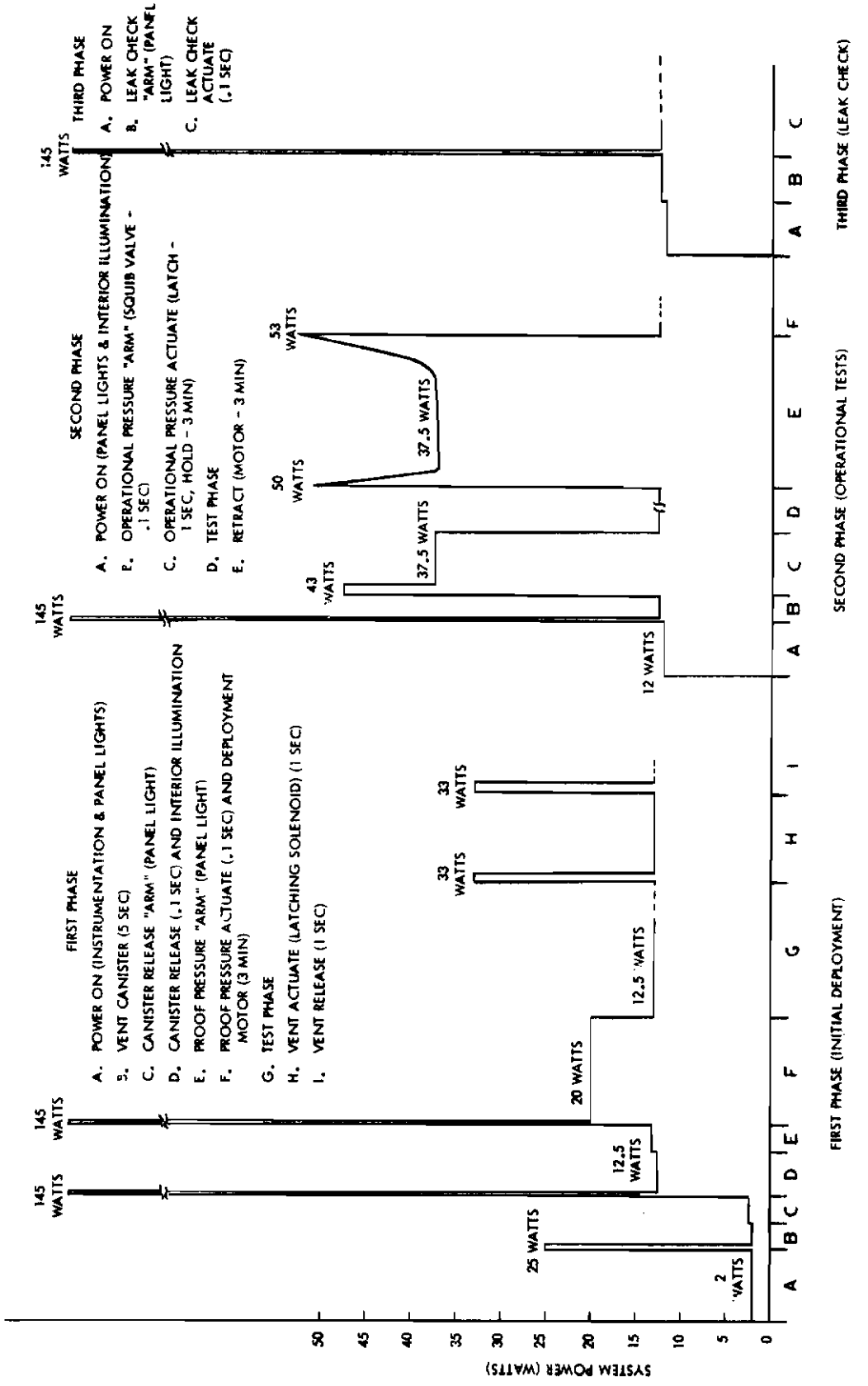

Figure 7-11. Power Demand Profile

7.2.6 ORBITAL TEST DURATION

An orbital test duration of 30 days is anticipated, except for the lapsed time for the revisitation phase. This is not known at present.

7.2.7 DATA RETURN REQUIRED

The data planned for the evaluation of the Elastic Recovery Airlock experiment is classified in five major areas:

a. Pressure and temperature gradients from recorded or telemetered data sensors affixed to the experiment package. These channel requirements are as follows:

   (1) Pressure 1 channel

   (2) Temperature 4 channels

b. Photographic records (movie film obtained by second astronaut) returned to earth via the Apollo vehicle. These films will be of the:

   (1) Deployment and pressure test

   (2) Astronaut EVA activities with the experimental procedure (ingress/egress, etc.)

   (3) Retraction (if used)

c. Verbal recordings of the astronaut's comments during the airlock experiment activities.

d. Post-flight debriefing interviews with the astronauts.

e. Elastic Recovery composite samples exposed to the environment retrieved by the astronaut and returned by the Apollo vehicle.

   (1) One sample at the end of the 30-day mission.

   (2) A second sample subsequent to revisitation.

7.2.8 SEQUENCE OF EXPERIMENTAL EVENTS

As this section cannot be accurately defined until a definite experimental procedure has been established, a preferred sequence of events will

be presented, assuming vehicle location of the experiment allows it to be deployed from its launch location. The orbit has been obtained and the airlock experiment begins:

Phase I

(1) Astronaut proceeds EVA to inspect package for visual damage during launch. Checks cables, attachments and closes manual vent on hatch.

(2) Astronaut returns to SSESM airlock to location of Remote Control console.

(3) Second astronaut positions self at window of either Apollo vehicle or Gemini hatch window on SSESM airlock with movie camera.

(4) First astronaut turns on console power.

(5) Reads experiment package pressure (0) and temperature (within deployment limits).

(6) Arms canister release function.

(7) Movie camera is started by second astronaut.

(8) Releases canister deploy mechanism.

(9) Airlock deploys partially.

(10) Arms deployment pressure function.

(11) Actuate squib valve on deployment pressure bottle.

(12) Airlock slowly pressurizes and fully deploys.

(13) Read pressure and temperature observing stability.

(14) Stop camera.

(15) Observe pressure and temperature periodically to determine airlock initial leak rate (duration of first leak test not yet determined).

End of Phase I

Phase II

(1) Astronaut vents airlock pressure from remote console.

(2) Proceed EVA and inspects airlock for any apparent anomaly. (Second astronaut starts camera.)

(3) Open manual vent and release hatch latch mechanism.

(4) Inspect interior of deployed airlock.

(5) Ingress into airlock and close hatch and lock.

(6) Second astronaut arms ingress/egress pressure system.

(7) First astronaut pressurizes airlock to 3.5 psig, (automatic) checking internal pressure on gage provided.

(8) First astronaut (in airlock) vents airlock, opens hatch and latch closes vent.

(9) Repeat the ingress/egress procedure a second time.

(10) Astronaut returns from EVA to SSESM vehicle tunnel.

(11) Actuate ingress/egress pressure control on remote console in SSESM airlock for long term leak test (14 days).

(12) Periodically taking pressure and temperature recording on SSESM data system.

(13) Proceed EVA (near end of mission) and retrieve material samples (previously secured to the exterior of the airlock).

(14) Place sample in bag provided and seal.

(15) Return from EVA to SSESM airlock.

End of Phase II

Phase III (Upon revisitation to SSESM)

(1) Proceed EVA and inspect airlock.

(2) Arm revisit pressure switch and actuate last bottle squib valve. (Remotely on console if power available or manually at airlock.)

(3) Read pressure and temperature and observe leak rate by pressure decay if any.

(4) Retrieve second sample from airlock exterior and return from EVA.

End of Phase III

7.3 EXPERIMENT DEFINITION SUMMARY FOR A MODULAR PARABOLA EXPERIMENT FOR A SATURN SIVB TYPE VEHICLE

7.3.1 WEIGHT AND DIMENSIONS

Modular Parabola Experiment Package	92.2 lb
Volume	5.80 ft^3
Dimensions (a) Deployed	10 ft dia. x 45° rim angle
(b) Stowed (Launch)	
Canister	32 x 25 x 12 inches
Boom (dia)	72 x 2 inches
Work station	36 x 24 inches

7.3.2 POWER REQUIREMENTS

The experiment system is designed to operate on SIVB supplied electrical power of 28-Vdc $\pm$ 4 volts. The power demands are transitory as the system is deployed primarily manually, therefore the average power consumed is low. A power demand profile was shown in Figure 7-11.

7.3.3 STOWAGE LOCATIONS AND ATTACHMENT TO THE VEHICLE

The experiment package (Figure 7-12) is designed for launch storage behind the thermal curtain of the SIVB and forward of the hydrogen fuel tank. The exact location has not been determined, but is noncritical providing launch compatibility exists with the package dimensions. A suggested launch location is seen in Figure 7-13.

Attachment to the SIVB structure wll be under two conditions: (1) launch stowage involving simple quick-release brackets and (2) internal to the SIVB living quarters which will involve attachment of the boom and work station bases to the inner structural tank walls via the metal tongs or the 10-32 tapped holes provided by the vehicle contractor. An illustration of the Modular Parabola set up in the SIVB SSESM tank is shown in Figure 7-14.

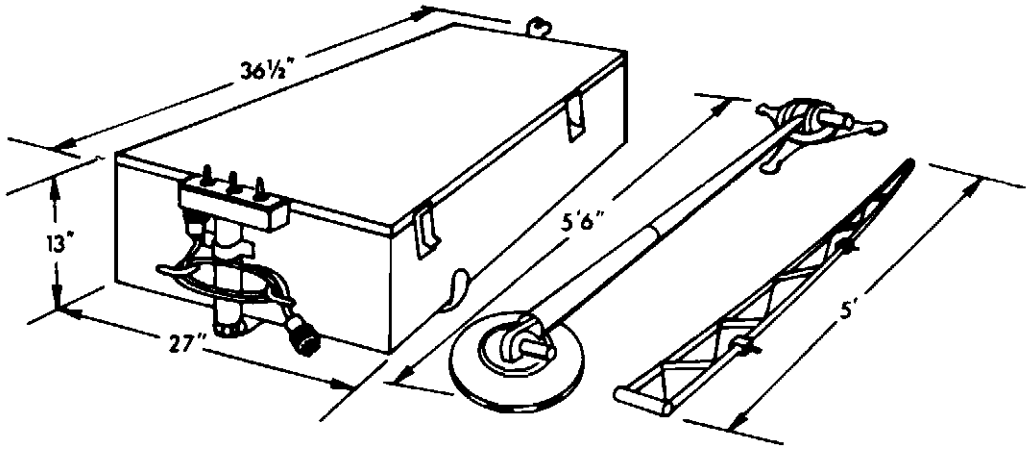

EXPERIMENT PACKAGE CONFIGURATION

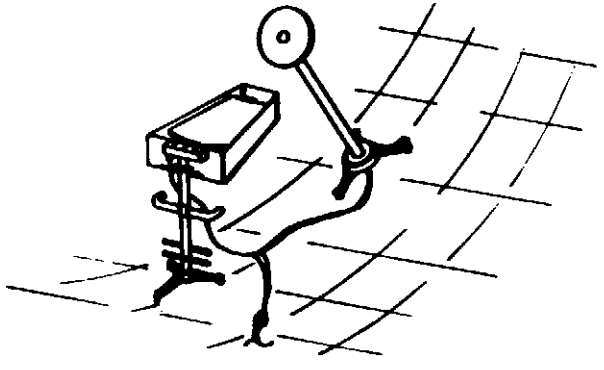

SETUP CONFIGURATION

Figure 7-12. Experiment Package Configuration

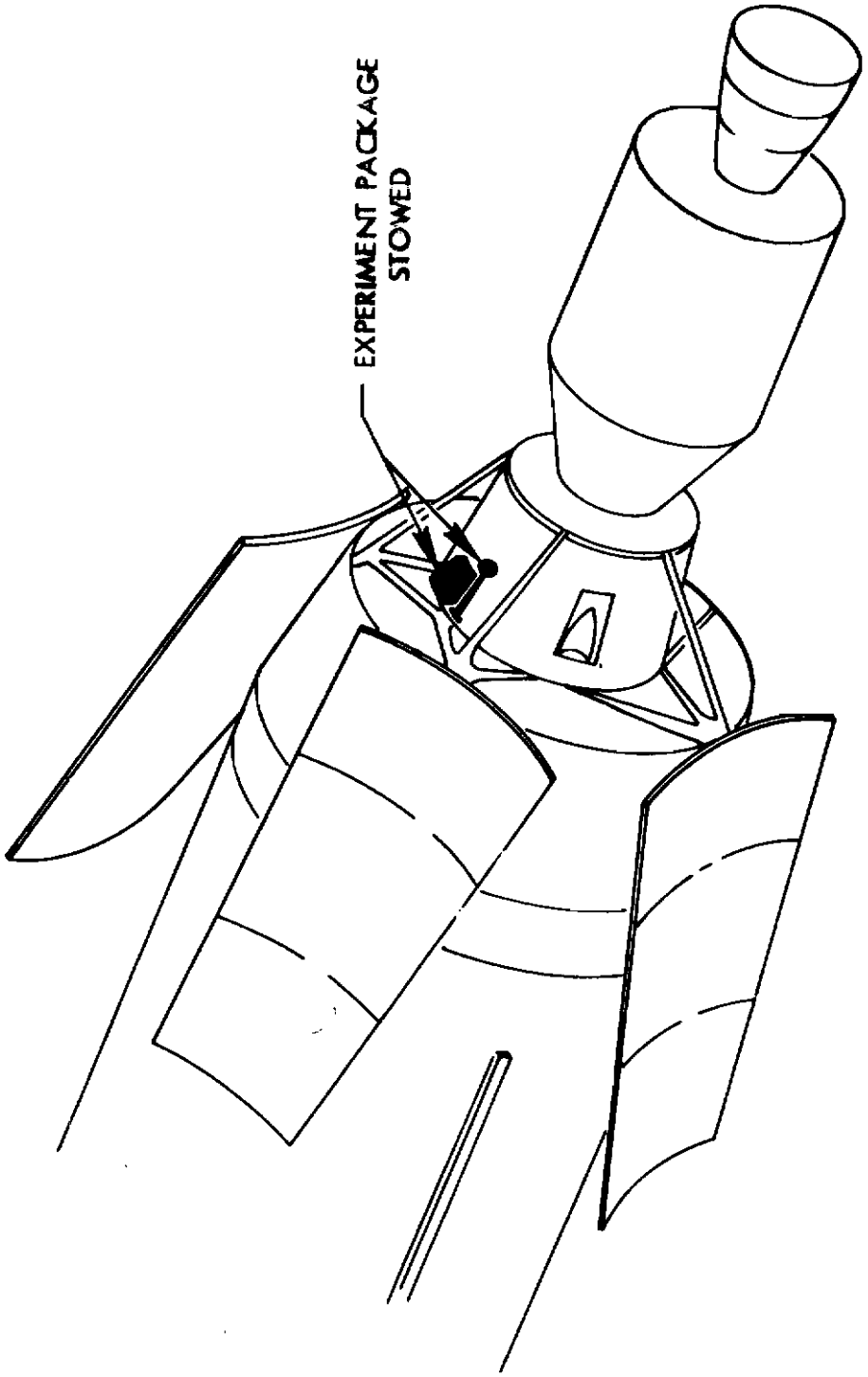

Figure 7-13. SIVB Experiment Launch Position

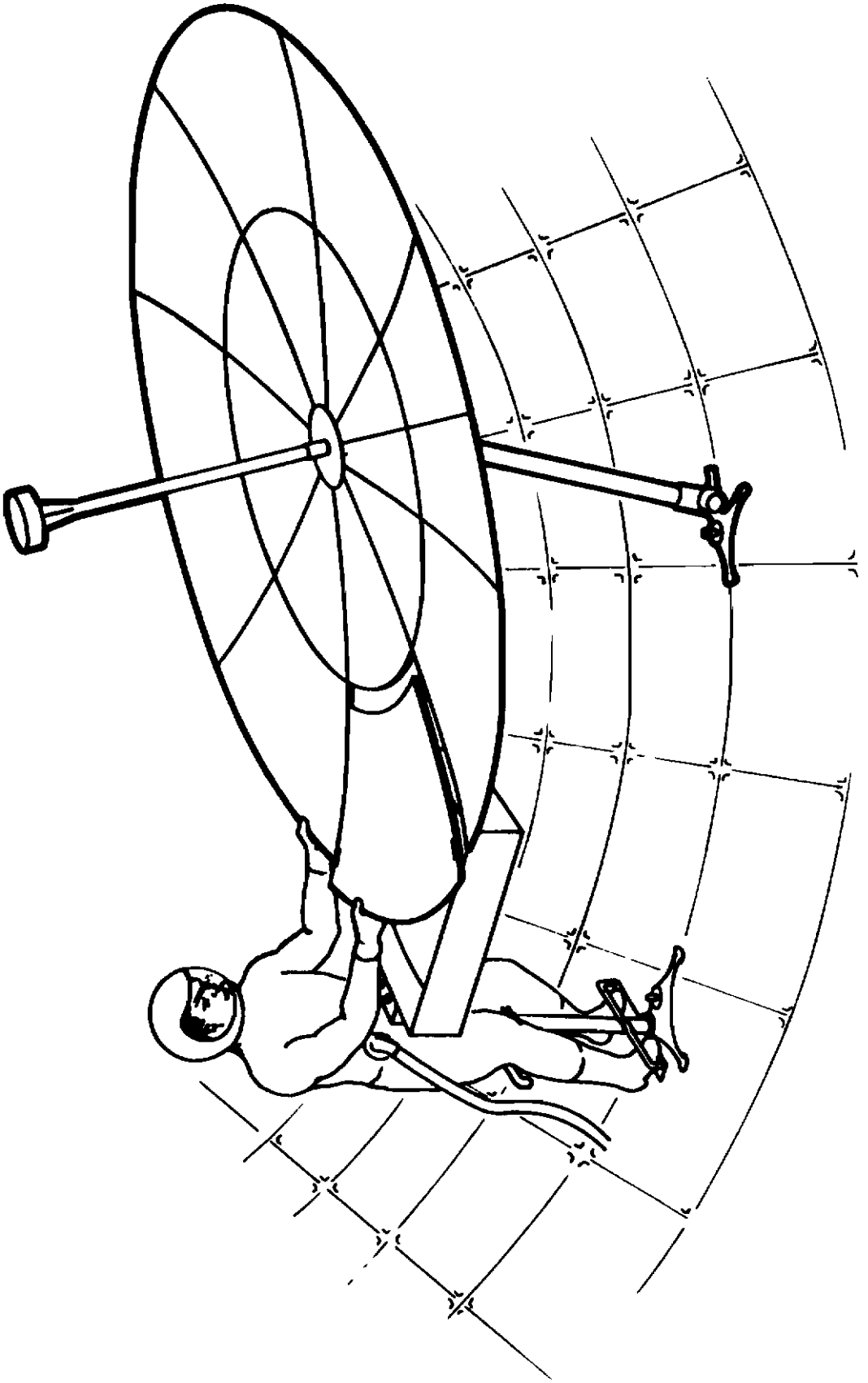

Figure 7-14. Experiment Setup and Assembly in the SIVB Workshop

The precise location of the experiment manual assembly task is noncritical and attach may be made at nay convenient vehicle station which provides sufficient clearance for the assembly of the 10-foot diameter parabola.

If during the course of advanced mission planning it becomes desirous to perform the assembly of the modular structure exterior to the SIVB Vehicle tank for possible application evaluation as an antenna or illuminator, the contoured modules may be disassembled and restacked into the canister. The experiment system may be refolded or packaged and transported through the SSESM airlock hatches and secured to the desired extravehicular location, where it may be reassembled for any desired purpose. Although electrical power is not an absolute necessity for the experiment assembly it provides a substantial aid in manipulating the boom and hub for simplication of the astronaut's assembly tasks.

7.3.4 ORBITAL TEST OBJECTIVES

Progress in the development of large boosters has advanced rapidly in the last few years. Capabilities to inject large and heavy payload into orbit has been amply demonstrated. To fully exploit these manned and unmanned system capabilities, large space structures are required that exceed the volumeter and geometric limitations of the launch vehicles. The expandable modular parabola experiment has been designed to demonstrate the feasibility of a technological concept to manually assemble large precision structures in space for use as antennae, illuminator, or solar collectors.

This design study defines an experiment to demonstrate the assembly of a subscale parabolic structure of high geometric accuracy by the use of lightweight precision-contoured aluminum honeycomb panels. In this experiment, an astronaut will extract the experiment package from its launch location and carry it into the SIVB Vehicle tank. There it will be set up and assembled from a high density canister into a 10-foot diameter, 45° rim angle parabola. A work station is provided to allow the astronaut to react the low faces required in the assembly task. This experiment has been designed to reflect the same tasks and assembly concepts which are applicable to parabolic structures up to 100 feet in diameter. This assembly

concept has been successfully evaluated by neutral buoyancy testing techniques using pressure suited subjects. In this test the 10-ft diameter structure was assembled from 24 contoured modules in approximately 10 minutes of low metabolic effort.

7.3.5 ORBITAL TEST DURATION

Although the SIVB Vehicle experiment will be on the order of 30 days duration, this experiment may be evaluated in a short period of approximately one hour. With the exception of a specimen module undergoing the full 30-day space environment exposure.

7.3.6 ORBITAL DATA REQUIRED AND RETURNED TO EARTH

Orbital flight tests are required to evaluate this technological concept in the space environment and zero-gravity conditions. The data to be accumulated from this experiment is as follows:

a. The ability of a pressure-suited astronaut in zero "g" to efficiently assemble a large precision parabolic structure from precontoured, lightweight modules. The data will be obtained from:

   (1) Photographic movies of the assembly task

   (2) Voice recordings of the subject astronaut during the assembly

   (3) Debriefing interviews with the astronaut on return to earth.

b. The contour accuracy achieved by the assembled structure, which can be compared with:

   (1) The theoretical accuracy predicted, and

   (2) The accuracy obtained in prior laboratory assemblies of the structure

c. The behavioral characteristics of the material and mechanical concepts used in the design and construction to the environments imposed by man in zero "g" and the space conditions of hard vacuum and radiation.

d. A much needed comparison will be achieved by a single test subject to evaluate the effectiveness of other earth-bound simulation techniques of neutral buoyancy and Keplerian aircraft trajectories to the actual space-orbital conditions. At the end of the flight a small material sample will be retrieved along with the voice recordings and photographic movie films. These will be returned to earth in the Apollo Vehicle.

7.3.7 SEQUENCE OF EXPERIMENTAL EVENTS

After the SSESM has attained orbit and the Apollo Spacecraft has rendezvoused and the initial housekeeping tasks have been accomplished, the sequence of experimental events for the modular parabola can commence. These are summarized below as follows:

a. Astronaut proceeds EVA and extracts experiment package from stowed location on the forward SSESM structure, behind the thermal curtain.

b. The modular parabola canister, boom and work station is brought through the Gemini hatch on the SSESM airlock and into the SIVB workshop area.

c. The boom assembly and work station/canister assembly is attached at its base to the interior wall of the hydrogen tank via the 10-32 tapped holes and metal tangs provided on the wall's inner surface.

d. The astronaut takes his position on the work station and one by one extracts the contoured parabolic modules from the canister and inserts them into the hub provided on the boom. The hub is rotated as each module is attached until the 24 panels have been successively placed into place. This procedure is recorded by a photographic movie camera operated by a second astronaut.

e. A bolt rope is then extracted from the canister and attached circumferentially about the back surface of the completed 10 foot diameter parabolic structure. This bolt rope is then tightened to cause all of the interconnecting, tongue-and-groove joints on the panels to seat themselves to the full precision of their original alignment.

f. A contour evaluation template affixed with displacement transducers is then inserted into the center of the hub and the surface scanned to record the contour accuracy achieved by the assembly.

g. The assembly procedure may then be revised, stowing the modules back into the canister until the structure is completely disassembled.

h. A subsequent assembly trial will be attempted in order to measure the effects of learning.

7.3.8 TASK TIME ANALYSIS

Task time presented in Table 7-1 were actual measurements of the steps in the modular parabola assembly in a neutral buoyancy test as performed by a Test Engineer in a Mark IV pressure suit.

Subsequent improvement in the hardward design which resulted from this neutral buoyancy test program should reduce these task times even further.

7.3.9 CREW TRAINING REQUIREMENTS

For the modular parabola experiment, the astronaut training requirements consist mainly of experiment familiarization and procedural task training. The zero-buoyancy tests indicate a typically short-learning curve of two to three assembly trials for the assembly tasks. Allocation of preflight time may be as listed below. It would also be desirable to conduct a zero buoyancy assembly test exercise that would require an additional eight man-hours of astronaut time, and zero-g tests in the KC-135 aircraft that will require another eight hours for one astronaut. These results could then be compared with the results of the actual flight assembly tasks. There by providing a much needed correlation to evaluate test methods effectiveness.

7.3.9.1 PREFLIGHT INDOCTRINATION SCHEDULE

<u>First Day:</u>

0800	Indoctrination; experiment purpose and objectives
0830	Discussions; experiment plan and procedure
1000	View movies of zero buoyancy and zero-g tests
1100-1200	Examine experiment hardware
1300	Trail neutral buoyancy assemblies and disassemblies of structure

Table 7-1

ASSEMBLY TASK TIME STUDY

Event		Time (secs) Elapsed	Incremental
Inner Annulus	Start	0	0
	Panel #1 installed	10	10
	#2	35	25
	#3	55	20
	#4	70	15
	#5	95	25
	#6	115	20
	#7	133	18
	#8 (closure	178	45
Readjust Boom Position		245	67
Outer Annulus	Panel #9 installed	258	13
	#10	286	28
	#11	318	32
	#12	350	30
	#13	380	30
	#14	398	18
	#15	421	23
	#16	445	24
	#17	465	20
	#18	493	28
	#19	528	35
	#20	573	45
	#21	600	27
	#22	622	22
	#23	640	18
	#24 (closure)	700	60
Total Time = $11^{\underline{m}}$ $40^{\underline{s}}$			

First Day: (Continued)

1600-1700 Discuss problem areas and procedural changes

Second Day:

0800 Explanation of contour measurement

0900 Examine equipment and typical data

0930 Demonstration of measurement procedure

1000 Test Exercise

1100-1200 Discussion of results

1300-1600 Dress rehearsal of total experiment tasks.

7.3.9.2 POST-FLIGHT TIME REQUIREMENTS

The post-flight requirements of the astronaut will involve one day on discussion of in-orbit experiment results. The astronaut will observe the film history taken during the space assembly and will dictate his observations, with particular emphasis on difficulty encountered, and any recommendations for the improvement of the technology under evaluation.

The remaining topics in the Experiment Definition Summary were not expanded beyond that described in the EDS in Section 3.4 and for the most part are generally applicable.

7.3.10 AGE AND GSE REQUIREMENTS

A minimum of AGE or GSE is required; it consists principally of simple dollies and circuit continuity checkout equipment for the consoles and instrumentation.

7.3.11 TECHNICAL RISKS FOR PARABOLIC ILLUMINATORS

The rigid modular illuminator experiment, assembled by an astronaut, offers a simple assembly method to produce a highly efficient mirror from very accurately prefabricated components. Prepreliminary studies

of this concept do not reveal any significant technical problem areas. Detail joint configurations design and concentricity control device studies are complete. The metal honeycomb sandwich structures are relatively fragile; therefore, the EVA astronaut must be restrained properly to permit simple but precise assembly tasks. Technical risks appear to be very small.

7.3.12 LOGISTICS

No critical logistics requirements are apparent at this time, as standard transportation and handling procedures will suffice.

7.3.13 ATTITUDE CONTROL REQUIREMENTS

Stabilization is noncritical with the following exceptions:

a. During deployment ACS should be off.

b. The thermal balance of the deployed structures require at least some heat input during the orbit. This preferably can be accomplished by periodic (1/2 orbit) exposure to the sun.

Section 8

PROGRAM COORDINATION

Space-General was required to coordinate the experiment with appropriate agencies on consent of and as scheduled by AFAPL. In addition to the normal coordination with General Electric as a subcontractor and potential subcontractors for material systems, several coordination meetings were held involving Air Force and NASA personnel. These are reviewed in this section.

On August 29, 1966, E. G. Blackwell gave a program presentation at Space-General Corporation to Fred Forbes and the following Air Force personnel from USAF Headquarters, SSD and WPAFB:

Major William E. Smith, RTD (RTTP)
Major G. Lewis Jr., AFSC (SCTR)
Lt. Col. C. F. Toler, Jr.
Major T. J. Borgstrom
1/Lt. D. J. South

Mr. J. E. Crawford, SGC Program Manager, at the request of Fred Forbes, coordinated and supported preparation of the SIVB modular parabola Experiment Definition and program plan at WPAFB during the week of August 30, 1966.

At an SIVB Experiment requirement coordination meeting with Mr. J. E. Crawford and Dr. Wm. Fedderson, NASA/MSC, the week of 3 October, Dr. Fedderson was critical of an airlock experiment which would not represent an operational configuration if only one hatch was operational. It was recommended that in the interest of minimizing weight, a dual hatch simulation could be achieved by a dummy mechanism on the other end of the experiment, thereby more accurately simulating actual operation of the airlock. This was considered by Dr. Fedderson to be an acceptable and desirable approach.

MSC personnel were not aware of any SIVB mission plans for the astronaut to go EVA outside of the interstage thermal blanket, and stated that several experiments had been rejected because of this requirement. It is SGC's understanding that the Air Force has proposed an airlock experiment plan requiring EVA beyond the thermal blanket and that approval has been granted by NASA/MSC personnel.

Another point of discussion was the availability of attachment lugs on the inner surface of the SIVB hydrogen tank. The attachment lugs on the internal side wall of the tank were designed and located by NASA/MFSC personnel and have already been installed by Douglas. These lugs were identified as 3-inch-long metal tangs attached to the tank walls by single 10-32 screws on a random pattern, averaging approximately 5 feet (or greater) on centers. Some areas of the tank, however, have these lugs only on 25-foot centers.

Gerome Seemans NASA/MSC was also contacted regarding human factor restraint for SIVB astronauts. He stated that the astronaut would wear a backpack PLSS which would protrude 10.5 inches from his back. The absolute minimum hatch which an astronaut so equipped could clear is 29.0 inches, and the preferred opening would be 37 inches in diameter.

It was also stated that floodlights would be installed for astronaut task illumination under the thermal blanket and that approximately 1000 watts of electrical power would be available, on a time-sharing basis, for the SIVB experiments.

Of particular importance, Ken Hecht (NASA-MSC Airlock Project Coordinator) stated that the proposed elastic memory airlock experiment could use SSESM oxygen for pressurization if the requirement was transmitted to MSC and approved prior to Final Experiment Definition. A 90 psi oxygen umbilical is available for such purposes in the interstage area.

At the request of the Air Force Project Engineer, the neutral buoyancy test configuration of the 10-ft. diameter modular parabola was shipped to WPAFB to familiarize Air Force personnel with the experiment assembly procedure. During the week of 16 September 1966, E.G. Blackwell, Space-General Project Engineer, made a trip to WPAFB to demonstrate the setup and assembly of the zero buoyancy modular parabola.

This demonstration was performed in cooperation with Capt. J. B. Catiller of the Research and Technology Division of AFPL. The modular parabola experiment was set up in the USAF Aeromedical Research Laboratory's pool facilities, and several trial assemblies were made by Capt. Catiller and E. G. Blackwell.

The pool, 8 to 9 feet deep, was too shallow to allow complete assembly of the outer annulus, so complete structural closure was not effected. Therefore, the structural integrity and rigidity could not be demonstrated with only a partially assembled parabola.

A trial assembly test was conducted by an Air Force test subject, with zero "g", KC-135, experience who had also been associated with other WPAFB underwater neutral buoyancy testing. The subject was in a Gemini pressure suit at 3.5 psig air pressure. Time did not permit pretraining, so he was totally unfamiliar with the assembly task. The trial assembly was further complicated as the subject wore a chest pack (the SSESM astronaut will wear a backpack) which interfered with his position, and vision, at the work station. No consideration was included in the work station configuration for subjects with chest packs.

Assembly of the neutral buoyancy modular parabola was carried as far as the pool depth allowed. Discussion between the pressure-suited test subject and the writer after the assembly test revealed the following problem areas during the assembly.

a. The work station foot bar was not large enough to accept the large pressure suit boot.

b. The work station upper end interfered with the chest pack, thereby not allowing the subject to position himself comfortably at the station.

c. The "astronaut" was positioned too high on the work station due to the abnormal foot restraint and chest pack problem, so he began to have difficulty in reaching the last few panels during the latter assembly phases. His abnormal position also required a greater reach and therefore generated a higher metabolic work rate in the pressurized suit.

d. The subject was unable to operate the special zipper type panel joint which used a split tube for joining the two panel edges. This problem apparently was due to his inability to reach across his chest pack to hold the joint closed with one hand while slipping the split tube on with the other hand. (This agreed with SGC's earlier conclusion about this particular joint concept). Capt. Catiller, who was standing by in SCUBA, completed that joint connection for the test subject.

In general, the subject thought the assembly concept quite workable, and was particularly pleased with the reaction restraint offered by the work station. It is the intent of Capt. Catiller to write a critique of the assembly task conducted by the zero "g" test subject, so that future designs may incorporate suggestions arising from the critique.

Present at the demonstration were Capt. J. Scholfield, Capt. J. Catiller, Fred Forbes, Chester May, Adam Cormier, Steve Shook, and several other WPAFB personnel. Also present were E.G. Blackwell and Bruce Hansen of Space-General Corporation.

Section 9

BIBLIOGRAPHY

Boast, W. B., Illumination Engineering, McGraw-Hill, 1953.

Brink, N. O., et al, Development and Evaluation of the Elastic Recovery Concept for Expandable Space Structures, Whittaker Corp., NASA CR-121, 1964

Brink, N. O., Research on an Expandable Airlock Utilizing the Elastic Recovery Principle, Whittaker Corp., NASA CR-351, 1965

Carnsweet, T. N., and D. Y. Teller, Relation of Increment Thresholds to Brightness and Luminance, Journal of The American Optical Society, Oct. 1965

Harshbarger, J., and J. Basinger, Test and Evaluation of Electronic Image Generation and Projection Devices, AMRL-TR-65-116, Vol. III, 1965

Hoffman, T. L., Utilization of Elastic Recovery Materials for the Development of Crew Transfer Tunnels, Airlocks, and Space Maintenance Hangars, Goodyear Aerospace Corp., AF APL-TR-66-2, Parts I and II, 1966

Jemisch, W. Jr., and J. B. Parkinson, Space Environment Criteria, Aerojet-General Corporation, Report No. 3147, 1966

Keesey, U. T., Visibility of a Stabilized Target as a Function of Rate and Amplitude of Luminance Variation, Journal of The American Optical Society, Nov. 1965

Liddell, R. B., et al, Expandable Structures Design Handbook, Spacecraft Organization, Lockheed-California Co., ASD-TDR-63-4275, Part II, 1965

Luchiesh, M., Light, Vision and Seeing, D. Van Nostrand Co., 1944.

Moon, P., The Scientific Basis of Illuminating Engineering, Dover 1961

Parcel and Maucy, Statically Indeterminant Stresses

Nelms, F. W., Vacuum Deployment Test of a Large Expandable Aerospace Shelter, ARO, Inc., AEDC TR-66-123, August 1966

Roark, Formulas for Stress and Strain

Schjeldahl, G. T., Gelatin Rigidized Expandable Sandwich Solar Energy Concentrators and Space Shelters, Monthly Progress Reports No. 21, 22 and 23, Contract AF33(615)-2058

Sears, F. W., Optics, Addison - Wesley 1949

Sharpe, Louis H., Assembly with Adhesives, Pg. 178-200, Machine Design, August 18, 1966

Stacy, J., Research and Experimentation on Space Applications of Millimeter Waves, Electronics Research Laboratory for CSSD, USAF, Feb. 1964, Report No. TDR-169(3250-41) TN-1 and TN-2

Vaughan, V. L., and E. L. Hoffman, Self Erecting Flexible Foam Structures for Space Antennas, La RC, NASA, TN D-1610, 1963

ADM - Expandable Self-Rigidizing Honeycomb Aerospace Shelters and Solar Collectors, Progress Reports for Months of Sept, Oct, Nov, Dec. 1966

Aviation Week and Space Technology, Mars Flight Goal of Bio-Science Research, Page 80, Aug 15, 1966

Lighting Handbook, Second Edition, Illumination Engineering Society 1952

NARMCO Research and Development Division, Research on an Expandable Airlock Utilizing the Elastic Recovery Principle, Final Report No. NAS7-283

UNCLASSIFIED
Security Classification

DOCUMENT CONTROL DATA - R&D
(Security classification of title, body of abstract and indexing annotation must be entered when the overall report is classified)

1 ORIGINATING ACTIVITY (Corporate author)
SPACE-GENERAL CORPORATION
9200 East Flair Drive
El Monte, California

2a REPORT SECURITY CLASSIFICATION
Unclassified

2b GROUP

3 REPORT TITLE
Project AHT

4 DESCRIPTIVE NOTES (Type of report and inclusive dates)
Final Report 14 December 1965 to 14 December 1966

5 AUTHOR(S) (Last name, first name, initial)
Crawford, James E.
Blackwell, Earl G.

6 REPORT DATE	7a TOTAL NO OF PAGES	7b NO. OF REFS
March 1967	458	23

8a CONTRACT OR GRANT NO.
AF33(615)-3469
b PROJECT NO
8170
c
Task No.: 817004
d

9a ORIGINATOR'S REPORT NUMBER(S)
SGC 965-8(FR)

9b OTHER REPORT NO(S) (Any other numbers that may be assigned this report)
AFAPL-TR-67-30

10 AVAILABILITY/LIMITATION NOTICES
This document is subject to special export controls and each transmittal to foreign governments or foreign nationals may be made only with prior approval of Air Force Aero Propulsion Laboratory(APFT), Wright-Patterson AFB, Ohio 45433.

11 SUPPLEMENTARY NOTES

12 SPONSORING MILITARY ACTIVITY
Air Force Aeropropulsion Laboratory
Wright-Patterson Air Force Base, Ohio

13 ABSTRACT

Current booster vehicles have the capability to inject heavy payloads into orbit, but the geometry requirements of the payloads for manned missions are larger than the vehicle compartment dimensions. To fully exploit these manned and unmanned vehicle system capabilities, an experiment is planned to demonstrate the feasibility and efficiency of the construction of large structures in space utilizing the technology of expandable structural-material systems.

This design study defines the detail configuration of an experiment to demonstrate the deployment in space of small scale parabolic structures of high geometric accuracy which may be manually assembled by an astronaut. An experiment will also demonstrate the applicability of expandable structural-material systems to an airlock which has been designed to exhibit the operational characteristics for use on future manned vehicle missions. This study indicates that parabolic structures up to 100 ft in diameter can be assembled by man in space, and that an Elastic Recovery Airlock can be designed to provide the manned mission requirements. These structures can be constructed of flexible materials and modular components which can be stowed in small high density packages in current booster payload compartments.

DD FORM 1 JAN 64 1473

UNCLASSIFIED
Security Classification

14 KEY WORDS	LINK A		LINK B		LINK C	
	ROLE	WT	ROLE	WT	ROLE	WT
Expandable Space Structures						
Airlocks						
Parabolas - Large						
Manually Assembled Space Structures						
SIVB Experiments						
Antennae, Expandable						

INSTRUCTIONS

1. ORIGINATING ACTIVITY: Enter the name and address of the contractor, subcontractor, grantee, Department of Defense activity or other organization *(corporate author)* issuing the report.

2a. REPORT SECURITY CLASSIFICATION: Enter the overall security classification of the report. Indicate whether "Restricted Data" is included. Marking is to be in accordance with appropriate security regulations.

2b. GROUP: Automatic downgrading is specified in DoD Directive 5200.10 and Armed Forces Industrial Manual. Enter the group number. Also, when applicable, show that optional markings have been used for Group 3 and Group 4 as authorized.

3. REPORT TITLE: Enter the complete report title in all capital letters. Titles in all cases should be unclassified. If a meaningful title cannot be selected without classification, show title classification in all capitals in parenthesis immediately following the title.

4. DESCRIPTIVE NOTES: If appropriate, enter the type of report, e.g., interim, progress, summary, annual, or final. Give the inclusive dates when a specific reporting period is covered.

5. AUTHOR(S): Enter the name(s) of author(s) as shown on or in the report. Enter last name, first name, middle initial. If military, show rank and branch of service. The name of the principal author is an absolute minimum requirement.

6. REPORT DATE: Enter the date of the report as day, month, year, or month, year. If more than one date appears on the report, use date of publication.

7a. TOTAL NUMBER OF PAGES: The total page count should follow normal pagination procedures, i.e., enter the number of pages containing information.

7b. NUMBER OF REFERENCES: Enter the total number of references cited in the report.

8a. CONTRACT OR GRANT NUMBER: If appropriate, enter the applicable number of the contract or grant under which the report was written.

8b, 8c, & 8d. PROJECT NUMBER: Enter the appropriate military department identification, such as project number, subproject number, system numbers, task number, etc.

9a. ORIGINATOR'S REPORT NUMBER(S): Enter the official report number by which the document will be identified and controlled by the originating activity. This number must be unique to this report.

9b. OTHER REPORT NUMBER(S): If the report has been assigned any other report numbers *(either by the originator or by the sponsor)*, also enter this number(s).

10. AVAILABILITY/LIMITATION NOTICES: Enter any limitations on further dissemination of the report, other than those imposed by security classification, using standard statements such as:

(1) "Qualified requesters may obtain copies of this report from DDC."

(2) "Foreign announcement and dissemination of this report by DDC is not authorized."

(3) "U. S. Government agencies may obtain copies of this report directly from DDC. Other qualified DDC users shall request through _____."

(4) "U. S. military agencies may obtain copies of this report directly from DDC. Other qualified users shall request through _____."

(5) "All distribution of this report is controlled. Qualified DDC users shall request through _____."

If the report has been furnished to the Office of Technical Services, Department of Commerce, for sale to the public, indicate this fact and enter the price, if known.

11. SUPPLEMENTARY NOTES: Use for additional explanatory notes.

12. SPONSORING MILITARY ACTIVITY: Enter the name of the departmental project office or laboratory sponsoring *(paying for)* the research and development. Include address.

13. ABSTRACT: Enter an abstract giving a brief and factual summary of the document indicative of the report, even though it may also appear elsewhere in the body of the technical report. If additional space is required, a continuation sheet shall be attached.

It is highly desirable that the abstract of classified reports be unclassified. Each paragraph of the abstract shall end with an indication of the military security classification of the information in the paragraph, represented as *(TS)*, *(S)*, *(C)*, or *(U)*.

There is no limitation on the length of the abstract. However, the suggested length is from 150 to 225 words.

14. KEY WORDS: Key words are technically meaningful terms or short phrases that characterize a report and may be used as index entries for cataloging the report. Key words must be selected so that no security classification is required. Identifiers, such as equipment model designation, trade name, military project code name, geographic location, may be used as key words but will be followed by an indication of technical context. The assignment of links, rules, and weights is optional.